Activation of Elemental Sulfur *via* Multicomponent Reactions for more Sustainable Organocatalysts and Sulfur-containing Polymers

Zur Erlangung des akademischen Grades eines

DOKTORS DER NATURWISSENSCHAFTEN

(Dr. rer. nat.)

von der KIT-Fakultät für Chemie und Biowissenschaften

des Karlsruher Instituts für Technologie (KIT)

genehmigte

DISSERTATION

von

M. Sc. Roman Nickisch

aus Bruchsal

1. Referent: Prof. Dr. Michael A. R. Meier

2. Referent: Prof. Dr. Joachim Podlech

Tag der mündlichen Prüfung: 26.10.2022

Für meine Eltern,

Renate und Kai Nickisch

“Ich habe fertig“-Giovanni Trapattoni

Declaration of Authorship

Die vorliegende Arbeit wurde von Dezember 2018 bis September 2022 unter Anleitung von Prof. Dr. Michael A. R. Meier am Institut für Organische Chemie (IOC) des Karlsruher Instituts für Technologie (KIT) durchgeführt.

Erklärung

Hiermit versichere ich, dass ich die Arbeit selbstständig angefertigt, nur die angegebenen Quellen und Hilfsmittel benutzt und mich keiner unzulässigen Hilfe Dritter bedient habe. Insbesondere habe ich wörtlich oder sinngemäß aus anderen Werken übernommene Inhalte als solche kenntlich gemacht. Die Satzung des Karlsruher Instituts für Technologie (KIT) zur Sicherung wissenschaftlicher Praxis habe ich beachtet. Des Weiteren erkläre ich, dass ich mich derzeit in keinem laufenden Promotionsverfahren befinde, und auch keine vorausgegangenen Promotionsversuche unternommen habe. Die elektronische Version der Arbeit stimmt mit der schriftlichen Version überein und die Primärdaten sind gemäß Abs. A (6) der Regeln zur Sicherung guter wissenschaftlicher Praxis des KIT beim Institut abgegeben und archiviert.

Karlsruhe, 09.09.2022

Roman Nickisch

I. Danksagung

Auf meinem Weg zur Promotion wurde ich von vielen Menschen unterstützt und motiviert mein Ziel zu erreichen. Im Folgenden folgt eine Danksagung an die Personen, ohne die es diese Thesis vermutlich nicht geben würde.

Zunächst möchte ich Mike danken, der mich schon in meiner Vertieferarbeit bei sich aufgenommen hat und mir auch meine Masterarbeit bei sich in der Arbeitsgruppe ermöglichte. Mike ich danke dir für dein konstruktives und stetiges Feedback. Ich habe es immer sehr geschätzt, mit dir über Chemie diskutieren zu dürfen. Als Chef kommst du uns Mitarbeitern immer auf Augenhöhe entgegen und sorgst für ein optimales Arbeitsklima in der Gruppe! Auch abseits der Chemie, sei es bei der Kaffeepause, beim Tischtennis oder bei einem Feierabendbier, warst du immer für ein nettes Gespräch zu haben.

Dem ganzen Arbeitskreis möchte ich natürlich auch danken, der mich so herzlich aufgenommen hat und in dessen Umfeld ich fachlich, sowie menschlich enorm wachsen konnte. Ihr habt es geschafft, dass meine Arbeit sich oft nicht wie Arbeit angefühlt hat, sondern eher wie ein netter Tag unter Freunden. Unsere gemeinsamen Grillabende und Ausflüge waren immer Highlights der Woche für mich. Abschließend bleibt mir nur zu sagen, dass ich jedem einzelnen Doktoranden für seine Promotion eine Arbeitsgruppe wie euch wünschen kann!

I would also like to thank Wiebe and his working group who allowed me to stay in Enschede for three months. Thank you for the amazing time in the Netherlands, because of you I was able to not only learn a lot about membranes, but also enjoy my stay to the fullest. Wiebe you have created a pleasant and supportive atmosphere for your employees and science in your MSuS group and, not surprisingly, as a result, obtained a group with only great people! I am looking forward to see you guys once again in person.

At this point, a special thanks goes to Irshad. Thank you for all the time, you were helping me with membrane science, as far as I can tell, you are an amazing scientist. You are able to explain complex topics to people with ease, so they will understand. On top of that and more importantly, you are a great person, and I really enjoyed the discussions with you, also besides work-related themes!

Ich möchte mich des Weiteren bei Dr. Maximiliane Frölich und Dr. Michael Rhein bedanken. Maxi du bist für mich die netteste und herzlichste Seele unter dieser Sonne und manchmal einfach zu gut für diese Welt! Danke, dass du dich auch neben der Arbeit immer so gut um mich gekümmert hast und mir in jeder Lebenslage zur Seite standest. Egal wie es gerade um mich stand, du warst immer da und verwandeltest jede Stimmungslage im Nu in eine Bessere.

Michi, rückblickend ist einer der wenigen Dinge, die ich an meiner akademischen Karriere wirklich bereue, dass ich dich erst während der Masterarbeit kennen gelernt habe. Ich habe

noch nie einen Menschen getroffen, der mich immer direkt so versteht wie du! Es tat mir immer unglaublich gut zu wissen, dass es neben mir noch einen Rucksack gab, der den gleichen, schlechten Humor an den Tag legte, wie ich. Deinen pragmatischen, charmanten, fairen und doch oft direkten Charakter habe ich immer stets nur bewundern können und in vielerlei Hinsicht gereichtest du mir als Vorbild, auch wenn ich dir das vielleicht noch nie gesagt habe.

Maxi, Michi, ich habe es von Anfang an als großes Privileg angesehen, nicht mit Kollegen, sondern mit guten Freunden arbeiten zu dürfen. Keine Sekunde, in der ich mit euch im Labor stand, fühlte sich wie Arbeit an. Über die letzten vier Jahre habe ich mit euch gearbeitet, gefeiert, gelacht und geweint und für mich ist eine Freundschaft entstanden, die man wohl nur selten im Leben findet. Ich wünsche jedem einzelnen Doktoranden von ganzem Herzen, dass er auf seinem Weg seine Maxi und seinen Michi findet, denn das macht jede anstrengende Strapaze, jede harte Aufgabe tausendfach leichter… und jedes Fest tausendmal geiler.

Nun zu meinem Lieblings-HiWi-/Bachelor-/HiWi-II-/Masterstudenten: Pete, ich wurde zu Beginn meiner Promotion gefragt, ob ich früher anfangen könnte, da noch händeringend (wie eig. immer) Doktoranden für die Praktikumsbetreuung gesucht wurden. Bis heute bin ich dankbar, dass ich mich darauf eingelassen habe, denn so haben wir uns letztlich kennen gelernt. Ich durfte mit ansehen wie (mein kleiner) HiWi-/Bachelor-/HiWi-II-/Masterstudent alle Aufgaben, die ein Chemiestudium so mit sich bringt, mit Pauken und Trompeten bestand und das durch nichts geringeres als pures Können gepaart mit unzerstörbarem Arbeitseifer. Ich bin unheimlich stolz auf deine Leistungen und deine Fortschritte, die du gemacht hast. Doch am meisten erfüllt mich mit Stolz, dass ich dich inzwischen als guten Freund gewinnen konnte!

Ein weiterer Dank gebührt meiner Vertieferbetreuerin und geschätzten Arbeitskollegin Frau Dr. Katharina Wetzel. Katha, vielen Dank für alles was ich von dir lernen konnte! Du warst in vielerlei Hinsicht ein Ideal, das ich versucht habe anzustreben, wenn es darum ging Studenten oder Azubis zu betreuen. Ich danke dir für die vielen netten Gespräche, die ich mit dir führen durfte. Du hattest immer ein offenes Ohr für meine Anliegen und ich hoffe du weißt, dass ich das immer zu schätzen wusste.

Ich habe das einmalige Glück im Leben, neben all diesen tollen Menschen, die ich durch meine Zeit am KIT kennen gelernt habe, noch weitere großartige Freunde um mich zu haben, die mir so viel Kraft und Freude gebracht haben und ohne die ich sicherlich nicht so weit gekommen wäre:

Celine und Jan, mein Traumpaar, das so gut zusammenpasst wie eine Arztpraxis und eine Apotheke! Was ich ohne euch beide machen würde, will ich gar nicht erst wissen. Ihr zwei erduldet meine ausschweifenden und oft die Wahrheit beugenden Geschichten von Drachen und Löwen nun schon seit gefühlten Äonen und, dass ihr dabei noch nicht einmal eingeschlafen seid, betrachte ich als das größte Kompliment, das man mir machen kann.

Euch zwei als Freunde zu haben ist für mich das beste Rezept für ein glücklicheres Leben, denn bei euch kann ich Energie tanken und meine Batterien wieder voll aufladen. Ich danke euch dafür, dass ich mit euch all die Jahre so viel Spaß haben durfte, denn bei euch kann ich so sein, wie ich bin.

Nino, gefühlt kenne ich dich, seit ich auf dieser Erde wandle und dafür bin ich schon lange sehr dankbar. Ich danke dir dafür, dass du mich immer verstehst und das oft, ohne darüber reden zu müssen. Du hast bis jetzt jede meiner Lebensphasen miterlebt und mit mir geteilt und ich kann und will mir, um ehrlich zu sein, auch keine kommende Phase ohne dich vorstellen. Also mach dich auf was gefasst, denn die unzähligen und unvergesslichen Abende mit dir zusammen will ich mindestens noch verdoppeln!

Dominik, du bist einer der cleversten Personen, die ich kenne und nach all den Jahren bin ich immer wieder fasziniert, mit wie viel Ruhe und Gewissenhaftigkeit du Dinge angehst. In gewisser Weise warst du für mich immer ein Leitbild an rationalem und durchdachtem Handeln! Ich danke die für die vielen schönen Abende, die ich mit dir verbringen durfte und hoffe das es weiterhin so bleiben wird.

Marcel, ich danke dir für die vielen großartigen Stunden, in denen wir bei dir Brettspiele spielten, auch wenn ich meistens den Kürzeren zog. Ich habe es immer bewundert mit welchem effizienten Pragmatismus du deine Ziele verfolgst! Daran will ich mir immer ein Beispiel nehmen. Ich hoffe, dass wir auch in Zukunft noch viele schöne Momente zusammen erleben können, damit ich meine Siegquote gegen dich weiter verbessern kann.

Darüber hinaus danke ich dem hiesigen (manche sagen den Großen) Fußballverein FSV Büchenau. Jungs, ich hatte immer Spaß im Training, sowie im Spiel mit euch alles zu geben. Der FSV ist für mich eine Ansammlung an großartigen, manchmal etwas schrulligen und cholerischen, Charakteren, die durch ihr Einbringen und Engagement den Verein so weit gebracht haben. Ich bin froh, dass ich weite Strecken meiner fußballerischen Karriere beim FSV verbringen durfte! Ich hoffe das ich weiterhin aktiv am Vereinsleben teilnehmen kann, um mit euch gemeinsam weiter Erfolge feiern zu dürfen.

Ein besonderes Dankeschön geht an Anna-Lena. Über die letzten knapp acht Jahre standest du immer zu 120% hinter mir, auch wenn es für dich hieß, dass du zurückstecken musstest. Niemand gab mir so sehr das Gefühl etwas Besonderes zu sein wie du! Du hast in mir immer ein Potential gesehen, dass ich nie in mir gesehen habe, und konntest mir daher an wichtigen Stellen im Leben immer einen Schups in die richtige Richtung geben. Ich danke dir von Herzen dafür, dass du mich durch Aufgaben begleitet hast, die mir allein als unüberwindbar erschienen, denn mit dir an meiner Seite war alles gleich halb so wild. Unsere gemeinsame Zeit bleibt für mich immer ein unvergleichlicher Teil meines Lebens.

Wie üblich kommt das Beste zum Schluss und mir bleibt noch meine Eltern zu danken. Mama, Papa es ist für mich nicht leicht in Worte zu fassen, wie sehr ihr mich in meinem Leben schon unterstützt habt. Eltern wie euch zu haben erfüllt mich mit purem Stolz! Mit euch hatte und habe ich immer zwei Vorbilder im Leben, die mir zeigen, was es heißt ein

guter Mensch zu sein, der auf seine Mitmenschen achtet. Ich sehe es als eins der größten Privilegien im Leben an, Eltern zu haben, die für mich gleichzeitig auch sehr gute Freunde sind, mit denen ich gerne Zeit verbringe, lachen und weinen kann. Ihr habt mich nie zu etwas gedrängt, standet immer hinter mir und wart immer stolz auf mich, egal wie gut oder schlecht ich es auch gemacht habe. Eure Fürsorge und Unterstützung hat es mir erst erlaubt zu studieren und auch dafür bin ich euch unendlich dankbar, dass ich diese Chance wahrnehmen dufte. Da ich es sonst auch viel zu selten sage: ich liebe euch!

II. Abstract

A more sustainable isocyanide synthesis was established for non-sterically demanding aliphatic isocyanides using *p*-toluenesulfonicacid chloride (*p*-TsCl) as dehydrating agent, which is, compared to typical reagents like phosgene derivatives or phosphorous oxychloride, less toxic and easier to handle. In addition, *p*-TsCl is a waste product of the saccharin synthesis. The synthesis protocol was used to synthesize 11 isocyanides from the respective mono- and di-*N*-formamides in moderate to excellent yields (up to 98%). The E-factor was strongly decreased by using simple extraction as sole purification step after quenching. Considering the degree of sustainability of this procedure, the burden of using isocyanide in synthesis routes can be strongly decreased.

Using the greener access to isocyanides, a multicomponent reaction (MCR) between isocyanides, amines and elemental sulfur yielding thioureas was introduced as more sustainable approach for the synthesis of thiourea-based organocatalysts. These compounds are typically formed using toxic reagents like thiophosgene derivatives or carbon disulfide, which can be avoided employing the reactivity of base activated sulfur with isocyanides. The use of elemental sulfur is further desired, since it is a waste product from the petroleum industry and the storage of the annual generated surplus leads to safety and environmental issues. A broad investigation of different activating motifs to obtain catalytically active thiourea catalysts showed that typically used electron-poor aryl moieties had to be introduced *via* the isocyanide component in the MCR. The use of the more sustainable isocyanide approach introduced in this work for these compounds was proven to be inapplicable. In addition, two novel activation motifs, *i.e.* isophthalicacid ester and *p*-(alkyl)sulfonyl phenyl, were introduced exhibiting similar catalytic activities as the widely used bis-3,5(trifluoromethyl)phenyl motif in an Ugi-reaction and a ring-opening of carbonates. Furthermore, the tailorability of the ester and sulfonyl groups bore the potential to adjust the solubility of the thiourea organocatalysts, since the often exhibit low solubilities in classic organic solvents.

The transfer of such catalytically active thiourea groups into polymers was further investigated to obtain recyclable organocatalysts by step-growth (polycondensation and poly-Thiol-Ene reaction) and living polymerization (ring-opening-metathesis polymerization (ROMP)). The ROMP approach proved to be the most promising one, since nearly full conversion of a norbornene thiourea compound was achieved in only two hours at 44 °C depicting the potential of a high tailorability to adjust the solubility of the obtained polymers. Furthermore, by using a *co*-ROMP approach of the thiourea norbornene with norbornene or cyclooctene, an additional parameter to alter the solubility was introduced leading to a faster reaction rate of the thiourea monomer and full conversion after one hour. Nevertheless, no sufficient purification procedure could be established that allowed the isolation of the formed polymers. Still, the thorough evaluation of all three approaches showed that a ROMP approach could lead to the formation of the desired polymeric organocatalysts by addressing the solubility issues in the work-up.

Mechanistic studies of the above-mentioned MCR between isocyanides, amines and sulfur led to the establishment of a more sustainable isothiocyanate synthesis, which is the key intermediate in this reaction. By using tertiary amines, amidines or guanidines as amine component in the reaction, elemental sulfur was sufficiently activated yielding isothiocyanates instead of thioureas. Using this procedure, 20 mono- and diisothiocyanates were synthesized in moderate to excellent yields (34-95%) bearing aliphatic, cyclic, benzylic and aromatic moieties, underlining the broad applicability of this procedure. Comparison of the E-factors with typical synthesis procedures showed the advantages of this method. In addition, substitution of solvents in this reaction like DMSO that are

needed to dissolve the base-activated sulfur with greener ones like Cyrene™ or GBL was achieved and the purification method was optimized in terms of sustainability.

Further mechanistic investigation on the reaction of base-activated elemental sulfur with carbene-like functional groups such as isocyanides led to the introduction of a novel synthesis of tetra substituted aryl olefines using tosylhydrazones as starting material. The mechanistic pathway was hypothesized to proceed *via* a carbene formation after nitrogen extrusion of the tosylhydrazone and a subsequent Barton-Kellogg-like reaction. The optimized reaction procedure led to a feasible protocol for tetraarylethylenes in excellent yields, exemplified on two compounds in a proof of concept. In addition, test experiments for the evaluation of the reaction pathway were suggested and thoroughly discussed.

Thiosemicarbazides were obtained using hydrazine as amine component in the MCR with isocyanides and elemental sulfur, extending the scope of this MCR. Using a step-growth polycondensation between dithiosemicarbazides and aryl dialdehydes, 13 novel (*co*-)poly(thiosemicarbazone)s were obtained and fully characterized by NMR, IR; SEC, DSC and TGA analysis. High molecular weights up to 38 kDa were obtained and the polymers reached their decomposition temperatures at roughly 200 °C. In general, the polymers exhibited no T_g unless a certain amount of bulky thiosemicarbazide moieties were introduced leading to high T_gs (162-182 °).

The application of these polymers as complexation ligand for metals was shown by formation of a membrane in a non-solvent induced phase separation process (NIPS). Membranes with permeabilities in the range of ultrafiltration (UF) to reverse osmosis (RO) were obtained (32-0.3 $Lm^{-2}h^{-1}bar^{-1}$) using DMSO and NMP as solvent in NIPS, while high molecular macromolecules like *bovine serum albumin* (BSA) were completely retained. No salt rejection or removal of micropollutants was observed, most likely due to defects in the membrane. Complexation of copper and silver ions was shown in a batch removal experiment and a dead-end dynamic set-up was performed in a proof of concept for the sufficient removal of silver ions from a water stream.

III. Zusammenfassung

Eine nachhaltigere Synthese für nicht sterisch anspruchsvolle aliphatische Isocyanide, die *p*-Toluolsulfonsäurechlorid (*p*-TsCl) als Dehydratisierungsreagenz verwendet, wurde eingeführt. Dieses Reagenz ist im Vergleich zu klassischen Dehydratisierungsreagenzien, wie Phosphoroxychlorid, weniger toxisch und leichter handhabbar. Zudem ist *p*-TsCl ein Abfallprodukt aus der industriellen Saccharinsynthese. Dieses Syntheseprotokoll wurde verwendet, um 11 Isocyanide aus den jeweiligen Mono-und Di-*N*-formamiden in moderater bis exzellenter Ausbeute (bis zu 98%) herzustellen. Durch einfaches Extrahieren als einzigen Aufarbeitungsschritt wurde der E-Faktor im Vergleich zu gängigen Syntheseprotokollen deutlich reduziert.

Mit dem optimierten Zugang zu Isocyaniden konnte die Multikomponentenreaktion (MCR) zur Bildung von Thioharnstoffen aus Isocyaniden, Aminen und elementarem Schwefel für einen nachhaltigeren Zugang zu Thioharnstoff-basierten Organokatalysatoren verwendet werden. Durch die Reaktivität von mit Basen aktiviertem Schwefel können so Thioharnstoffe hergestellt werden, wobei typischerweise verwendete, giftige Chemikalien, wie Thiophosgenderivate oder Kohlenstoffdisulfid, vermieden werden. Des Weiteren ist die Verwendung von elementarem Schwefel wünschenswert, da er ein Abfallprodukt der Ölindustrie ist und die Lagerung des jährlichen Überschusses an Schwefel zu Sicherheits- und Umweltproblemen führt. Eine weitreichende Untersuchung der Aktivierungsmotive, die zu katalytisch aktiven Thioharnstoffen führen, zeigte, dass häufig verwendete elektronenarme aromatische Reste über die Isocyanidkomponente in der MCR eingeführt werden müssen. Zwei neuartige Aktivierungsmotive, genauer der Isophthalsäureester- und der *p*-(Alkyl)sulfonylphenylrest, die eine ähnliche katalytische Aktivität wie der weitläufig verwendete 3,5-Bis(trifluoromethyl)phenylrest in einer Ugi- und einer Ringöffnungsreaktion von Carbonaten aufwiesen, wurde aufgezeigt. Die neuen Aktivierungsgruppen haben des Weiteren das Potential die Löslichkeit der, in gängigen organischen Lösemitteln oft schwerlöslichen, Thioharnstoffkatalysatoren anzupassen. Zusammenfassend bietet der in dieser Arbeit vorgestellte Syntheseweg mittels MCR von elementarem Schwefel einen nachhaltigeren Zugang zu katalytisch aktiven Thioharnstoffen.

Der Transfer solcher katalytisch aktiven Thioureagruppen in ein Polymergerüsts mittels Stufenwachstums- (Polykondensation und Poly-Thiol-En Reaktion) und lebender Polymerisation (Ringöffnungsmetathese Polymerisation (ROMP)) wurde weiterführend untersucht, um recycelbare Organokatalysatoren zu erhalten. Die ROMP erwies sich als der vielversprechendste Ansatz, da fast vollständiger Umsatz eines Thioharnstoffnorbornens nach nur zwei Stunden bei 44 °C erreicht wurde. Darüber hinaus zeigte der Ansatz das größte Potential für eine Anpassung der Löslichkeit der erhaltenen Polymere. Mittels eines *co*-ROMP-Ansatzes des Thioharnstoffnorbornens und Norbornen oder Cycloocten konnte ein weiterer Paramater zur Steuerung der Löslichkeit eingeführt werden, wobei zudem ein schneller Umsatz des Thioharnstoffmonomers erreicht wurde (vollständiger Umsatz nach einer Stunde). Nichtsdestotrotz konnte kein adäquates Aufreinigungsprotokoll etabliert werden, dass die Isolation der hergestellten Polymere erlaubte. Im Allgemeinen konnte durch die Evaluierung aller drei Ansätze gezeigt werden, dass über den ROMP-Ansatz die gewünschten polymeren Organokatalysatoren erhalten werden könnten, wenn die Löslichkeitsproblematik in der Aufarbeitung adressiert wird.

Mechanistische Untersuchungen der oben erwähnten MCR zwischen Isocyaniden, Aminen und Schwefel führten zu der Etablierung einer nachhaltigeren Isothiocyanatsynthese, welches das Schlüsselintermediat dieser Reaktion darstellte. Durch die Nutzung von tertiären Aminen, Amidinen und Guanidinen als Aminkomponente wurde der aktivierte, elementare Schwefel mit dem Isocyanid zum Isothiocyanat statt dem Thioharnstoff umgesetzt. Mit diesem Protokoll konnten 20 Mono- und Diisothiocyanate in moderater bis exzellenter Ausbeute (34-95%) hergestellt werden. Die breite Anwendung des Syntheseprotokolls wurde durch die Umsetzung von aliphatischen, zyklischen, benzylischen und aromatischen Isothiocyanaten unterstrichen. Ein Vergleich der E-Faktoren von typischen Syntheserouten zeigte die Vorteile dieser Methode (Einfachheit, Minimierung von Abfall). Zudem konnten Lösungsmittel, wie DMSO, die für das Lösen von Basen-aktiviertem Schwefel unabdingbar sind, durch nachhaltigere Lösungsmittel, wie Cyrene™ oder GBL, ersetz werden, während die Aufarbeitungsmethode im Sinne der Nachhaltigkeit optimiert wurde.

Weitere mechanistische Untersuchungen zu der basischen Aktivierung von Schwefel mit carbenartigen funktionellen Gruppen, wie Isocyaniden, führte zum Erhalt einer neuen Synthese von tetrasubstituierten Arylolefinen startend von Tosylhydrazonen. Der hypothetische Reaktionsmechanismus wurde postuliert, ausgehend von einer Carbenbildung unter Stickstoffextrusion mit nachfolgendem Barton-Kellogg-ähnlichem Reaktionsverlauf. Die optimierte Reaktion führte zu einem einfachen Syntheseprotokoll für Tetraarylethylene in exzellenten Ausbeuten, beispielhaft gezeigt an zwei Tosylhydrazonen. Darüber hinaus wurden weitere Testexperimente vorgeschlagen und konkret diskutiert, die den vorgeschlagenen Reaktionsmechanismus bestätigen könnten.

Durch die Verwendung von Hydrazin als Aminkomponente in der MCR mit Isocyaniden und elementarem Schwefel konnte die Anwendungsbreite der Reaktion erweitert und Thiosemicarbazide erhalten werden. Über eine Polykondensation von Dithiosemicarbaziden und Aryldialdehyden wurden 13 neuartige (*co*-)poly(thiosemicarbazon)e hergestellt und vollständig über NMR, IR, SEC, DSC und TGA Analysen charakterisiert. Die Polymere zeigten Molekulargewichte bis zu 38 kDa und Zersetzungstemperatur ab ca. 200 °C. Generell zeigten sie keinen T_g, sofern nicht ein gewisser Anteil an sterisch anspruchsvollen Thiosemicarbazidresten verwendet wurde, der wiederum zu hohen T_gs führte (162-182 °C).

Die Anwendung dieser Polymere als komplexierender Ligand für Metalle wurde anhand von Membranen gezeigt, die über den Anti-Lösungsmittel induzierte Phasenseperationsprozess (non-solvent induced phase separation, NIPS) hergestellt wurde. Für die Herstellung *via* NIPS wurden DMSO und NMP als Lösungsmittel verwendet und die Membranen zeigten Permeabilitäten im Bereich der Ultrafiltration bis zur Umkehrosmose (32-0.3 $Lm^{-2}h^{-1}bar^{-1}$). Hochmolekulare Makromoleküle, wie Bovines Serumalbumin (BSA), wurden komplett zurückgehalten. Salze oder Mikroschadstoffe wurden nicht zurückgehalten, vermutlich durch Defekte in den Membranen. Komplexierung von Kupfer und Silber wurde in einem Batch-Absorptionsexperiment gezeigt und ein dynamisches dead-end set-up wurde durchgeführt, um zu zeigen, dass Silberionen auch in einem Wasserfluss zurückgehalten werden können.

Table of Content

1 Introduction

Nowadays, humanity still heavily relies on fossil resources, leading to several environmental issues like the Green House effect. More recently, additional problems have arisen due to our high consumption of these resources. For instance, elemental sulfur is accumulating in sulfur deposits in tremendous amount, because it is mainly produced as a waste product by the reductive desulfurization of crude oil in the petroleum industry.[1,2] Thus, over 80 million tons of sulfur were produced in 2021.[3] On the other side, there is currently only one main application for sulfur on industrial scale, namely the synthesis of sulfuric acid, leaving a great annual surplus.[1,4–6] This might sound harmless at first, considering that sulfur is a non-toxic, unreactive solid.[4] However, due to the shear amount of sulfur being stored, issues such as the acidification of soil and water by oxidation of sulfur, for instance by bacteria or the risk of a fire, which would ultimately release a high amount of toxic sulfur dioxide, arose.[1,7] Therefore, more applications for elemental sulfur, especially on large scale, are highly desired.

In the last decades, research was sparked in the field of elemental sulfur chemistry and several methods were introduced to activate this unreactive compound, unlocking its versatile reactivity for organic and polymer chemistry. For instance, one of the most common activation methods is based on the activation by a base, which allows the use of sulfur not only as starting material in a reaction but also as oxidant, reductant and as catalyst.[8] Due to its various reactivity, sulfur was also introduced for several multicomponent reactions (MCR)s and the numbers of new reactions with sulfur as key component are increasing annually. Among these MCRs, sulfur also shows a unique reactivity towards carbene-like functional groups such as isocyanides forming C=S double bonds.[9] Thus, thioureas can be obtained by an isocyanide and sulfur based-MCR in the presence of an amine base.[10]

One of the main applications of thioureas is the field of organocatalysis. This concept was already established in the early 2000s and the importance of this idea, especially for asymmetric guided reactions, was underlined in 2021, when the Nobel prize was awarded to David MacMillan and Benjamin List for their groundbreaking work on this field. Nowadays, thiourea-based organocatalysis is widely applied and various approaches for an increased catalytic activity of the functional group were established.

Despite the long establishment of thiourea-based organocatalysis and its potential for many applications, it is surprising that the incorporation of thiourea organocatalysis in the framework of Sustainable Chemistry is still lagging in several points and most often only focus on the recyclability of a catalyst. Still, the synthesis routes of these compounds rely heavily on noxious reagents like isothiocyanates, thiophosgene its derivatives or carbon disulfide.[11–17]

2 Theoretical Background

2.1 Concept of Sustainable Chemistry

Due to the ongoing depletion of fossil resources and the growing awareness of the population concerning the limits of our planet, sustainability is one of the most important topics of this century and found its way irreversibly into all sectors of politics.

The first report of the term "sustainability" in the German language area can be dated back to 1713 by Hans Carl von Carlowitz,[18] where it was used as an economic term in forestry describing a resource-protecting way of logging of trees. However, it took until the second half of the 20th century to get global public attention for this subject. In 1972, Meadows *et al.* published their book "*The Limits to Growth-A Report for THE CLUB OF ROME`s Project on the Predicament of Mankind*", in which they concluded that if the growth trends at that time considering world population, industrialization, depletion of resources, food production and pollution continued unchanged, the limits of growth on earth would be reached within in the next one hundred years. In the following an uncontrolled collapse would most likely appear.[19] Having arrived at that severe prediction, they asked to strive for a sustainable global equilibrium of not only economic but also ecological stability. In 1987, the UN World Commission on Environment and Development published the Brundtland Report ("*Our Common Future*") defining the word "*sustainability*" as "*meeting the needs of the present generation without compromising the ability of future generations to meet their own needs*".[20]

During that time, political movements were sparked leading to the Rio Conference (Earth Summit), in which the Agenda 21 for sustainable development was adopted as a means to mediate between ecological and economic interests.[21] In the following years, the interdisciplinary character of sustainability was further extended to incorporate not only economic and ecological but also social aspects. This was visualized by the introduction of the "*3-column model* of sustainable development" by the Enquete-commission of the German Bundestag see Figure 1).[22] This model states that all three aspects are equally balanced and can only be optimized mutually to secure sustainable progress. In 2015, the UN renewed and extended their goal for sustainable development in the universal Agenda "*Transforming our world: The 2030 Agenda for sustainable development*" calling it "a plan of action for people, planet and prosperity".[23]

With the production from bulk to fine chemicals to pharmaceuticals, chemical industry contributes in a large part to the worldwide emission of CO_2 and thus, to global warming, as well as waste.[24,25] For instance, 923 million tons CO_2 were produced due to the production of primary chemicals like methanol, ammonia, ethylene, propylene, benzene, toluene and mixed xylene in 2020.[26] Because of this tremendous impact on our planet, the term sustainability was implemented in the following years into chemistry giving birth to the subject "Sustainable Chemistry", which represents the subcategory for sustainability in the chemistry sector.[27] Therefore, it was urgent to adopt and incorporate suitable guiding principles to address all aspects of Sustainable Chemistry. Consequently, metrics were established that allowed to quantify the sustainability factor of synthesis and processing. In 1991, Trost introduced the so-called atom efficiency (AE, also called atom economy),

which describes the number of atoms of the starting materials incorporated in the final product and can be directly obtained from the reaction equation.[28] To obtain a minimal amount of waste the value should be close to the ideal value of 100% (see chapter below for more details).

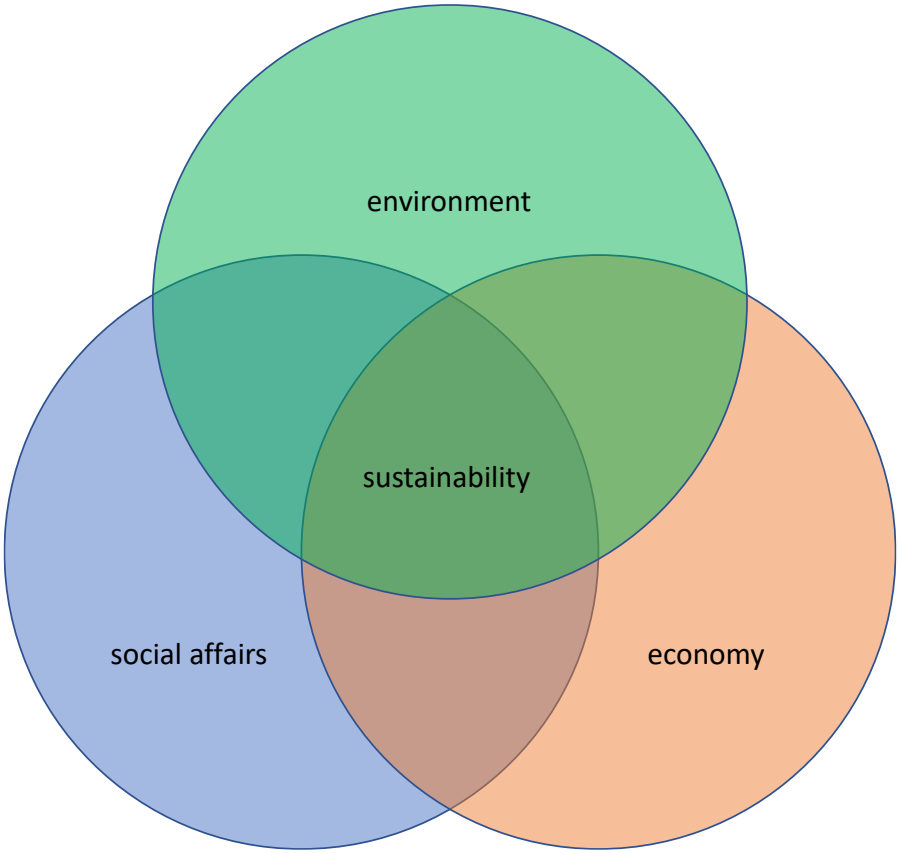

Figure 1: 3-column model of sustainable development.[22]

A milestone for Sustainable Chemistry was achieved in 1998, when Anastas and Warner introduced their *Twelve Principled of Green Chemistry* depicted in Table 1.[29] According to Anastas *et al.*, the main aim of these principles is to provide a cohesive framework for sustainable design.[30] All stages of a chemical life-cycle should be considered and adjusted towards a more sustainable one. Thereby, hazards occurring due to the use of chemicals or processes should be reduced. This means that prevention of waste and maintenance of safety in chemistry for people and the environment is the highest goal.

The Twelve Principles were summarized as the acronym PRODUCTIVELY, as shown in Table 1.[31] As one important aspect of the Twelve Principles, the waste of a reaction should be minimized (principles **P** and **E**). This includes the avoidance of by- and side products, *i.e.* a high degree of selectivity of the reaction. Typically, catalytic reagents can help to achieve this demand (principle **C**). To further reduce the production of waste, derivatizations and auxiliaries like protection/deprotection, blocking groups and temporary modification of physical/chemical process as well as the use of solvents should be avoided (principles **O** and **V**). Since high energy consumption is another factor that contributes to the low sustainability of many chemical processes, overcoming the need for harsh conditions (high and low temperatures and pressures) is another important principle of Green Chemistry. This can at the same time reduce the potential hazard of chemical processes (principle **T**). In addition, starting materials should be obtained from renewable feedstock to avoid depletion of resources (principle **R**). The aspects of safety are addressed mainly be reducing

the toxicity of chemical compounds, for instance by using less toxic, at best innocuous, chemicals (principle **Y**).

Table 1: Twelve Principles of Green Chemistry listed with short explanations ordered to depict the acronym "PRODUCTIVELY" as a straightforward mnemonic. Adopted from ref.[29,31]

	Principle	Explanation
P	Prevent waste	It is better to prevent waste than to treat or clean up waste.
R	Renewable materials	A raw material or feedstock should be renewable rather than depleting whenever technically and economically practicable.
O	Omit derivatization steps	Unnecessary derivatization should be minimized or avoided, if possible.
D	Degradable chemical products	Chemical products should be designed so that at the end of their function they break down into innocuous degradation products and do not persist in the environment.
U	Use safe synthetic methods	Substances and the form of a substance used in a chemical process should be chosen to minimize the potential for chemical accidents, including releases, explosions, and fires.
C	Catalytic reagents	Catalytic reagents (as selective as possible) are superior to stoichiometric reagents.
T	Temperature, pressure ambient	Energy requirements of chemical processes should be recognized for their environmental and economic impacts and should be minimized. Synthetic methods should be conducted at ambient temperature and pressure.
I	In-Process monitoring	Analytical methodologies need to be further developed to allow for real-time, in-process monitoring and control prior to the formation of hazardous substances.
V	Very few auxiliary substances	The use of auxiliary substances should be made unnecessary whenever possible and innocuous when used.
E	E-factor maximize feed in product	Synthetic methods should be designed to maximize the incorporation of all used materials into the final product.
L	Low toxicity of chemical products	Chemical products should be designed to preserve efficacy of the function while reducing toxicity.
Y	Yes, it is safe	Reagents and products should carry little or no toxicity for humans or the environment.

It was further clarified that the reduction of toxicity should be considered for the whole life cycle of a process, not only for the synthesis or the processing. Thus, a product should not be intrinsically toxic or lead to the emission of noxious derivatives into the environment by degradation. Moreover, even if non-toxic, chemicals should not be persistent in the environment (principles **L** and **D**). Besides the toxicity of compounds, a major aspect of security is also addressed by the demand to use safe synthetic methods, minimizing the potential for accidents like fire, explosions, or release of chemicals

should (principle **U**). Ultimately, analytical monitoring should be employed to allow real-time control of the whole process preventing the formation of hazards before they arise (principle **I**).

Over the years, these principles became the fundamental guidelines to optimize the sustainability of a chemical synthesis or process.[32] In addition, the term *Green Chemistry* became an integral part of the field of Sustainable Chemistry, which was often misleadingly used since the excessive use of the words "*sustainable*" and "*green*" in media eventually blurred their definitions.[33,34] Thus, Warner *et al.* defined both terms more clearly: *Sustainable Chemistry*, as discussed above, can be seen as subsystem of sustainability representing all kind of aspects involving materials and chemical compounds in the artificial world like safety and risk policy, remediation technologies, water purification, alternative energy, and Green Chemistry evaluating them in a cost-benefit analysis.[27,35] In turn, *Green Chemistry* was defined as the part of Sustainable Chemistry which can be used as application focusing on the transfer of starting materials to their final technology".[27,35,36] However, it must be mentioned that achieving all twelve of these principles is idealistic and thus, the overall aim for chemists should be to address as many of these principles as possible, understanding them more as guidelines and consequently making their synthesis process holistically more sustainable.[37,38]

As a result of the interplay between scientific research and political involvement, the field of Green Chemistry experienced a tremendous growth starting from 1998.[38] The establishment of a scientific platform for the community, namely the journal Green Chemistry by the RSC, contributed majorly to the growth by allowing to publish greener chemical investigations in a journal designed especially for that purpose.[30,38,39] The importance of social aspects as the third pillar of sustainability was also well addressed in the latest twenty years, as nowadays, for instance, universities offer Green Chemistry and Green Engineering classes, Green Chemistry research centers have been established and government funding has been multiplied.[30,40]

2.1.1 Quantifying Sustainable Chemistry

As mentioned in the previous section, the need for a quantification of sustainability led to the introduction of different metrics. However, since the term sustainability is a complex concept involving several different aspects, no metric can assess sustainability completely. Instead, several metrics were established over the years, highlighting and balancing different aspects of Green and Sustainable Chemistry, which will be discussed in the following. As already mentioned above, Trost introduced the atom efficiency (AE, also called atom economy) in 1991, which is depicted in equation 1:[28]

$$AE = \frac{M(product)}{\sum_i M_i(starting\ material)} \quad (1)$$

It is defined as the ratio between the molecular masses of the atoms of starting material and those incorporated in the final product and is ideally equal to one (100%). The AE is straightforward to calculate and gives a first impression about the mass balance of a reaction. However, stoichiometric amounts and quantitative yield are assumed, ignoring other aspects like excess of reagents and use of auxiliaries that do not appear in the reaction equation as well as conversion. The purification process is furthermore neglected completely. Another widely applied metric is the Environmental impact factor (short E-factor), introduced by Sheldon in 1992 (see equation 2):[41]

$$E - factor = \frac{m(waste)}{m(product)} \quad (2)$$

The E-factor is calculated dividing the obtained amount of waste by the amount of product obtained. Ideally, when no waste is produced at all, the E-factor is zero. This metric allows to also consider the yield of a reaction, since it is connected to the amount of product obtained. In addition, the recycling of compounds like catalysts, non-reacted starting materials and solvent can be considered as well. It must be mentioned that a theoretical E-factor only considering the reaction equation will deliver the same information as the AE comparing reactions, which is depicted in Scheme 1.[32]

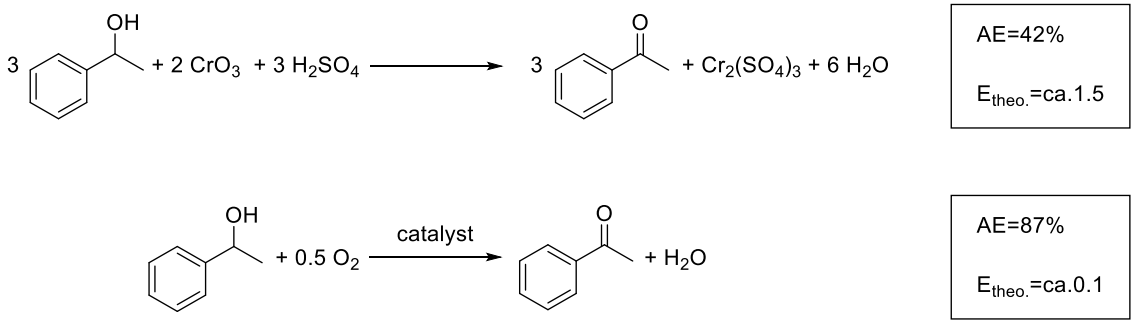

Scheme 1: Comparison of AE with a theoretical E-factor, exhibiting the same information exemplarily shown on the oxidation of 1-phenylethanol. Note that actual E-factor values will probably be considerably higher.

Stoichiometric oxidation of 1-phenylethanol to acetophenone with chromium oxide under treatment with sulfuric acid leads to chromium sulfate and water as by-product, resulting in an AE of 42% and a theoretical E-factor of ca. 1.5. In contrast, the aerobic oxidation of the alcohol leads to a higher AE of 87% of and a lower E-factor of ca. 0.1. In practice, the E-factor will probably be much higher since all

the other forms of waste, as discussed above, are considered as well. Thus, an outstanding AE does not automatically correlate to an excellent E-Factor.

Since the E-factor refers to the actual amount of waste and is easy to calculate, it is used also in the chemical industry.[32] Table 2 depicts typical E-factors of chemical industry segments and underpins why a sustainable development in chemistry is an urgent matter. Some sectors, like the fine chemical industry, generate high E-factors.

Table 2: Overview of chemical segments and their respective tonnage and E-factors. Adapted from ref.[42].

Industry segment	Product tonnage	E-factor
Oil refining	10^6-10^8	<0.1
Bulk chemicals	10^4-10^6	<1-5
Fine chemicals	10^2-10^4	5-50
Pharmaceuticals	10-10^3	25->100

While oil refining and bulk chemicals are strongly optimized processes, the E-factors are low (E-factor <5). The E-factors are considerably higher for more complex chemicals and pharmaceuticals (up to 100 for drugs). When publishing the calculation of E-factors, Sheldon challenged the chemical industry to change their solely economic ambitions towards more holistically sustainable concepts.[32]

Still, several aspects of the Twelve Principles of Green Chemistry are not considered in the E-factor. For instance, the toxicity of compounds, the energy consumption and the wastewater produced (not to be confused with water produced by the reaction, which is included) also play a major contribution to overall sustainability.[32,43] If the amount of wastewater is known though, it can add up to the amount of waste and thereby be included in the E-factor as well.[44]

Several other metrics were introduced optimizing the idea of quantifying sustainability, sparked by AE and E-factor. For instance, the reaction mass efficiency (RME) builds up from the AE but at the same time considering the yield of the reaction.[45,46] Further, the actual applied ratio of compounds (stoichiometric factor SF) is considered, *i.e.* excess of reagents, and also the recovery of compounds that can be reused (solvents, catalysts, etc.), including all solvents and reagents used in the work-up (mass recovered factor MRF, see equation 3).[47]

$$RME = Yield \times AE \times \frac{MRF}{SF}; SF = 1 + \frac{\sum masses\ excess\ of\ reagent}{\sum masses\ reagents\ without\ excess} \quad (3)$$

The Process Mass Intensity (PMI) is the most common metric used in pharmaceutical industry.[48] It is the ratio of total mass used in the process divided by the mass of product. Thus, it is closely related to the E-factor as in fact the PMI is the respective E-factor plus one (see equation 4).

$$PMI = \frac{\sum total\ mass\ used\ in\ process}{m(product)} = \frac{m(product) + \sum mass\ of\ waste}{m(product)} = E - factor + 1 \quad (4)$$

Reasons for using the PMI over the E-factor can be related to the fact that the focus in the PMI is set on the input of the materials rather on the produced waste, the former of which is in general the bigger contribution to the life cycle assessment (LCA, for explanation see below). In addition, waste water is considered in the PMI.[49]

Reflecting on the fact that sometimes additional waste is considered inconsistently in the E-factor with different estimations of recovery of wastewater or solvent making the metric less comparable, Sheldon suggested subtypes of the metric, which are defined as follows: i) the simple E-Factor (sEF), which does not consider solvent and water and is useful for an early stage evaluation of a synthesis route, and ii) the complete E-factor(cEF), which takes solvent and water into account assuming no recycling and is useful for evaluation of the total amount of generated waste.[42,50] Recently, Hollmann *et al.* introduced the E^+-factor, which includes an energy term, demonstrating that energy waste like greenhouse gases should not be neglected as they can bear a major contribution to the overall sustainability.[51]

As prevention of toxicity and hazards is the second major pillar of the Twelve Principles of Green Chemistry besides the prevention of waste, metrics quantifying these parameters were needed as well. This led to several interesting concepts, since toxicity and hazard could not simply be measured by absolute or relative values.

A semi-quantitative analysis for sustainability was introduced by Van Aken *et al.* the so-called Eco Scale.[52] This concept uses a score system rating the processes with a maximum of 100 points in the categories yield, cost, safety, technical setup, temperature/time and ease of work-up and purification. Thus, it also considers the properties of the compounds used and the toxicity and hazards of the methods applied. Further, energy consumption is considered. The concept is clearly defined and easy to apply. However, the drawbacks of Eco Scale are the missing evaluation of the use of solvents and of the waste formation, both factors with tremendous impact, and the inherently arbitrary character of the scoring system.[43] Nevertheless, the Eco Scale evaluation allows to add further factors into its calculation and the scoring system can be adjusted freely and is therefore potentially a good foundation for more holistic, qualitative metrics for sustainability.[43,52]

To account for the toxicity of the used chemicals, the E-factor can also be multiplied by an unfriendliness quotient Q which takes the nature of the compounds into account taking the role of an arbitrary weighing factor, resulting in the Environmental Index (EI).[53] For instance, NaCl, a nontoxic salt, can be assigned to the factor one, while heavy metal salts are assigned to factor 100-1000 depending on their toxicity, their annual production and the location of their production site.[54] Several classification aspects, *e.g.* water and air pollution, toxicity, availability of raw materials, complexity of synthesis, in which the raw materials are used, can be included in the determination of Q by scoring them with certain values.[55] EATOS (*Environmental Assessment Tool for Organic Syntheses*), a free accessible software, was introduced to allow an easy calculation of the EI.[56,57]

The attempt to obtain a holistic evaluation of sustainability further led to the incorporation of life cycle assessments (LCAs) in Sustainable Chemistry.[43] Ideally, LCAs consider every step needed for and caused by one product. Lancaster defined these steps as the production of raw materials, manufacturing, the use and disposal and the distribution by transportation.[43,58] While such a LCA considering every step of a product would be called cradle-to-grave type, the scope of a LCA can be chosen freely to look at a partial life cycle as well.[43] It is important to mention that the application of Green Chemistry is connected inherently to a positive influence in all aspects of a LCA.[59] The use of renewable raw materials reduces the impact of the starting materials, processing and manufacturing benefits from the evaluation by sustainable metrics, the use of a catalyst and waste reduction as well as biodegradable products and recycling can lower the burden of the disposed product in the environment.[43]

In addition, LCAs are able to expose the effects of the so-called burden-shifting, meaning that the optimization of one life-cycle step of a product can lead to worsening of one or several other steps.[43] For instance, the use of alternative, environmentally more friendly starting materials might include toxic reagents for their synthesis, or a more efficient synthesis procedure decreasing waste might consumes more energy.

Still, several drawbacks come with the use of LCA like expensiveness and time consumption of the evaluation as well as the lacking availability of the needed data. In addition, LCAs often miss transparency due to their complex nature. Thus, simplifications are needed to address one or several of their downsides. Also, various software tools were developed to allow a faster and easier access to LCAs like the *Fast Life Cycle Assessment of Synthetic Chemistry* (FLASC^{TM}) from GlaxoSmithKline (GSK).[60] With increasing interest in LCAs, more and more user-friendly LCAs have been introduced allowing a fast and understandable evaluation of one compound.

Such feasible LCAs are for instance represented by solvent selection guides as the impact of the used solvent is tremendous.[61,62] Since the amount of solvent typically makes up 70-80% of the reaction medium, it overshadows the effect of the use of more sustainable starting materials or reagents in a synthesis.[63,64] Moreover, the use of solvents is not limited to chemical reactions but contributes also to a low sustainability of other processes, such as membrane formation in chemical engineering.[65] Thus, increasing the greenness of the solvent can already lead to an immense improvement of the overall degree of sustainability of a synthesis process, which makes solvent selection guides an essential tool for Sustainable Chemistry and Engineering.

Concluding, many useful metrics to determine the degree of sustainability of a process were introduced over the last three decades and all of them have their own advantages and disadvantages. In the end, it is crucial to be aware of their benefits and limitations to allow an optimal evaluation of a process. Often more than one metric should be taken into account to evaluate compromises between sustainability, expensiveness, efficiency, accuracy and transparency.

2.1.2 Sustainable toolbox for chemists

With the introduction of Green Chemistry, reactions and methodologies were developed which are intrinsically address several principles of Green Chemistry. Nowadays, chemists can rely on a broad sustainability toolbox, which constantly keeps growing. In the following, some important representatives of this repertoire are introduced briefly, accompanied by specific examples. However, it has to be mentioned that, whereas all of this examples definitely exhibit inherent potential for sustainable applications, their use will not automatically result in an overall greener process but has to be implemented into the framework of Green Chemistry.

Sharpless *et al.* introduced the term Click Chemistry, which describes reactions known for their high thermodynamic driving force (above 20 kcal mol^{-1}) in one direction, usually leading to hetero-bond formation (C-X).[66] Consequently, they will lead to very high yields, while being regio- and/or stereospecific. Other criteria for click reactions are simple reaction conditions and readily available starting materials and reagents. Further, this group of reactions is defined by its modularity, its wide scope and generation of, if at all, only inoffensive by-products. Solvents should be avoided or at least benign and a stable product should be isolated easily avoiding chromatographic purification methods. Since these characteristics will unavoidably lead to reduction of waste, safer process conditions and less hazardous and toxic products, click reactions are prone to be used in sustainable chemical processes.

Multicomponent reactions (MCR), which convert three or more starting materials in an one-pot procedure, attracted a lot of attention recently for being useful reactions in the toolbox of Green Chemistry.[67,68] Typically, high atom economies and high conversions are obtained.[68] In addition, they often show a synergetic effect with other green methodologies (*e.g.* green solvents, flow reactions). Since MCRs embedded in a sustainable context are a major part in this thesis, they are discussed in more detail in chapter 2.3. An example of the usefulness of MCRs in greener approaches is depicted in Figure 2A. By using an Ugi-four-component reaction (see chapter 2.3.1), praziquantel, a drug for treatment of parasitic worm infections, can be obtained in only two steps than in five steps as in the commercial synthesis route.[69] Further, the AEs of both steps are higher than the ones from the commercial route and, like this, the overall yield was increased considerably to 74% (before 48%).

Besides reactions that are prone to be more sustainable, also reaction conditions that increase the sustainability of reactions have been developed over the last decades. For instance, microwave assisted reactions can lead to a reduction of waste and energy since they often show high yields and selectivities in short reaction times and easier work-up.[70] Further, microwave irradiation can be combined with other aspects of sustainability like performing reactions under flow conditions and the use of green solvent or solvent-free conditions. Tran *et al.* introduced a Friedel-Crafts benzoylation of several aryl compounds with bismuth triflate as catalyst under microwave heating. This led to a considerable decrease in reaction time (from 6 hours to 15-40 minutes) and slightly better yields and selectivities (see Figure 2B).[71]

Similarly, the application of ultrasonic irradiation (sonochemistry) can lead to greener synthesis procedures by reducing the reaction times and increasing yields and selectivities.[72] Li *et al.* underlined this by synthesizing bis(indolyl) methanes using dodecyl benzenesulfonic acid (ABS) as catalyst in an aqueous medium at 25 kHz obtaining slightly increased yields after shorter reaction times (see Figure 2C).[73]

Mechanochemistry, which includes for instance ball-milling and twin screw extrusion, is also closely connected to Green Chemistry due to the use of solvent-free conditions.[74] Also several other principles of Green Chemistry are usually fulfilled when using mechanochemical activation, such as the access of challenging products under benign reaction conditions, the simplification of synthetic routes and the operational simplicity. The latter is complemented by the recent introduction of real-time monitoring (Raman spectroscopy, synchrotron powder X-ray diffraction).[74–76] Applying ball-milling conditions on the four steps synthesis of the receptor antagonist PZ-1361, the product was obtained in a yield of 64% after only 5.5 hours instead of 34% after 60 hours using classic chemistry in solution (see Figure 2D).[77] In addition, no flash column chromatography was needed. The E-factor was lowered vastly from 1932 to 715, making it not a green synthesis *per se*, but highlighting the positive effect of mechanochemical methods towards reduction of waste. In addition, the overall toxicity and energy consumption was reduced.

In photochemistry, sunlight can be used as green energy source allowing access to different reactivities of molecules under mild conditions. In the excited states, molecules show different electronic distributions.[78–80] Light can therefore be seen as "*traceless*" reagent, thus increasing the AE. Waste is also reduced, since ideally no reagent is employed compared to reactions using stoichiometric or even catalytic amounts of reagents.[79,81,82] Using a photochemically approach with sun light, Monnerie *et al.* were able to photooxidize citronellol in the presence of rose bengal quantitatively (see Figure 2 E).[83] It is also worth noting that this reaction was performed on an eight liter scale, showing that photochemistry can be applied also to bigger scales.

Biocatalysis uses enzymes to perform very regio- and stereoselective reactions yielding complex molecules. Like this, synthetic routes are shortened and at the same time waste production is reduced as stochiometric amounts of reagent are substituted with catalytical ones.[84] In addition, enzymes can be immobilized as to allow recycling and facilitate cascade reactions with different enzymes, lowering the produced waste even further.[85] For instance, Weiß *et al.* established a greener process for the synthesis of enantiomerically pure β-amino acids, which are key building blocks for many pharmaceuticals. They used immobilized *Candida Antarctica* lipase B (CALB) in a two-step one-pot reaction (see Figure 2F).[86,87] Thus, they avoided column chromatography with organic solvent as complete purification of only one intermediate was needed which resulted in a considerable decrease of the E-factor to 41 from 359 (an E-factor of 41 is typical for pharmaceuticals, compare Table 1 in chapter 2.1.1.).

Another possibility to achieve benign reaction conditions is by using electrochemistry obtaining high AEs and reducing energy consumption.[88,89] The used electrodes can be considered as heterogenous catalyst that can be regenerated electrochemically, therefore preventing the formation of heavy metal redox reagent waste.[88,90] Moreover, electrons flowing as current are often the only regents added, resulting in low amount of waste. However, as typically different reactions take place at the cathode and anode at the same time, it has to be ensured that both sides will yield desirable products out of an economic and ecological point of view. In certain cases, the same product can also be produced on both sides.[90] Also, synergetic effects can be achieved by combining electrochemistry with other green principles or approaches like the use of renewable feedstock or less toxic starting materials.[89,90]

Further, Combinational Chemistry is a concept which can be adapted to greener processes. Originally, it was introduced to produce large compound libraries and perform high-throughput

screenings quickly using robotics and efficient methodologies, synthesis and work-up procedures like the above-mentioned MCRs, solid-phase synthesis or immobilization techniques.[91] Due to its ability to perform a large number of processes efficiently, this approach leads to increased AE and energy efficiency as well as to a reduction of waste.[92] For instance, Wolf *et al.* established a deconvolution strategy for discovering the most suitable catalyst for a reaction, in which they put together a complex mixture of several precatalysts and ligands in a small number of reactions.[93] When observing superior catalytic activity in one batch, it can be iteratively deconvoluted by successively splitting the compounds contained in the batch into smaller batches. Thus, the actual catalyst is identified, reducing not only time but also waste and energy.

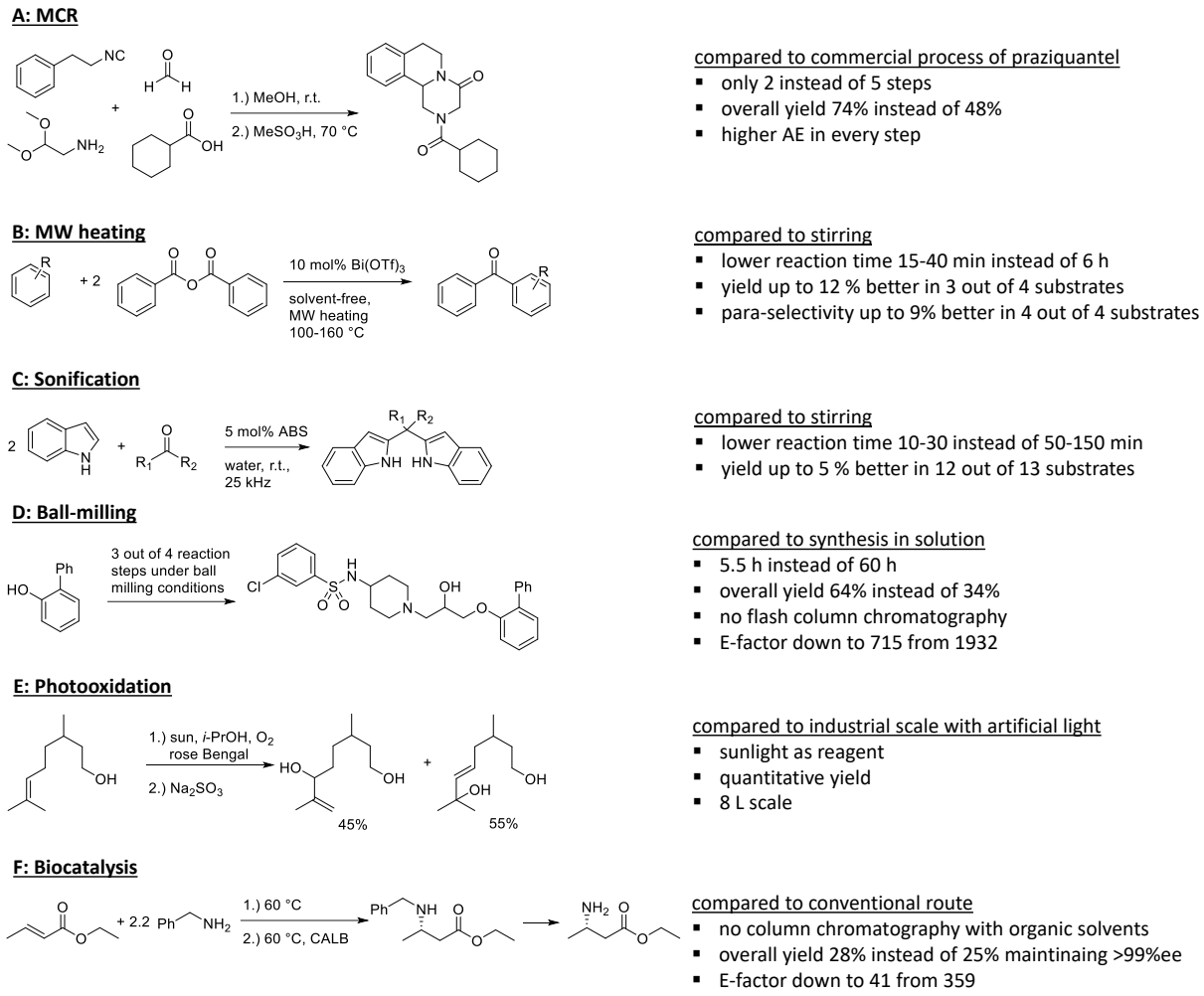

Figure 2: Collection of synthesis procedures in which the sustainability was improved using various methodologies (left side). Improvements are summarized for each approach by suitable comparison with classic synthesis protocols (right side).

Concluding, several aspects of chemical synthesis have been a subject to development towards more sustainability over the last decades. This involves the choice of reaction types, reaction conditions and handling as well as analysis. Consequently, the number of greener processes is constantly increasing, facilitating the interest of Green Chemistry and driving the frontier of sustainable research further. This will probably lead to the establishment of new methodologies and reactions that are greener in the future. Right now, the focus of Sustainable Chemistry should be set on the transfer of as many of its concepts as possible to industrial scale since the positive trends are lagging in this sector.[70,74,79] Ultimately, it needs to be highlighted that probably the most astonishing feature

of all the mentioned concepts is the ability to yield synergetic effects when several concepts are combined which reflects on the interdisciplinary character of sustainability.

2.2 Elemental sulfur

Sulfur belongs to the group of chalcogens and is, with 0.035%, the 16th most abundant element in the earth crust.[94] It is benign and in general unreactive in elemental state at room temperature and has a broad range of oxidation states from -II to +VI.[4,95] Further, it is the element with the highest number of known allotropic forms, which come in cyclic S_n(n=5-30) and chain like structures.[4,96] However, only the S_8 ring yields stable modifications, while all other forms are meta stable and can be obtained from the melted or gas phase as well as from solution or *via* chemical reactions.[96] At room temperature, sulfur is a yellow, brittle solid consisting of S_8 rings in orthorhombic structure, called α-sulfur.[4] Upon reaching 95.6 °C, it changes reversibly to β-sulfur, which is monocline containing only S_8 molecules. Starting from 100 °C, sulfur can be sublimed, while it reaches its melting point at 119.6 °C forming an inviscid, yellow solution. In this form, called λ-sulfur, an equilibrium between smaller sulfur rings is present, while the majority is still S_8 rings (S_7 and S_6 are formed with a ratio of less than 5%). Increasing the temperature, several different S_n cycles are formed (n=6-26), yielding π-sulfur. At the same time, μ-sulfur is formed, which consists of polymeric S_n chains (n=10^3-10^6), which is the dominant species at increasing temperature. As a result, the viscosity of sulfur increases suddenly at 159 °C and reaches a maximum at 187 °C due to most sulfur molecules being polymeric chains. The color of sulfur changes from yellow to dark red. Further heating results in a decrease in viscosity as polymeric sulfur is thermally cleaved more frequently. The boiling point is reached at 444.6 °C, at which it is a dark red, inviscid liquid. In the gas phase, a temperature-depending equilibrium between S_{1-8} molecules is present, whereas above 2200 °C sulfur is present in atomic form. Cyclic sulfur molecules S_{5-30} are corrugated, while the polymeric chains come in several conformations. The S_4 molecule is red and has a chain like structure, while S_3 is blue and has an angled structure analogous to ozone. S_2 is violet blue, paramagnetic and exhibits a double bond analogous to O_2. Targeted sulfur cycles S_n (n=6, 7, 9, 10, 11, 12, 13, 15, 18, 20) can be obtained synthetically by using bicyclopentadienyl titanpentasulfid and sulfur chlorides.[96] The S-S bond has an average length of 206 pm. However, this value varies by 10 pm, since several allotropic forms of sulfur show different conformations leading to variations in the bond length because of hyperconjugation and Pauli-repulsion like for instance in S_7. The bond angle is in general between 101-110° and the torsion angle between 75-100°. Sulfur is naturally found in several oxidation states:[95] Sulfide salts like pyrite (FeS), sphalerite (ZnS) and galena (PbS) as well as hydrogensuflide (-II), amino acids (-I), sulfur dioxide (+IV) and sulfates (+VI) like anhydrite ($CaSO_4$), kieserite ($MgSO_4$*H_2O) and barite ($BaSO_4$).[95,97] Sulfur in neutral form is also found due to reduction of bacteria or originated from volcanic activity.[95,97]

A straightforward process of harvesting elemental sulfur is the Frasch process.[4,98] Hot water vapor is pumped into the rocks containing elemental sulfur until it has melted. Then, air pressure is applied to transport it to the surface, where it is obtained in high purity (99.5-99.9%).[4] However, the major part of the annual production of elemental sulfur is obtained from hydrogen sulfide in the Claus process (see Scheme 2).[4,99,100]

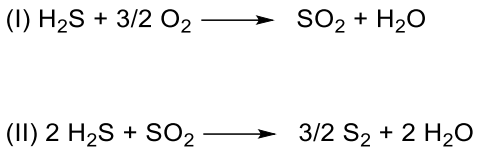

Scheme 2: The two reaction steps of the Claus-process. Both reactions take place in the same reactor vessel. The Claus reaction (II) is then again repeated at catalytical conditions in a cascade of reactors to remove residual hydrogen suflide.[100]

The needed hydrogen sulfide comes from acidic natural gas, of which it is washed off with aqueous aminoalcohols or from the petroleum industry due to the reductive desulfurization of crude oil.[2,100] First, sulfur dioxide is obtained by oxidizing parts of the hydrogen sulfide thermally at 950-1200 °C. In a second step, sulfur dioxide and hydrogen sulfide comproportionate to elemental sulfur and water, which takes place in the same reactor where the hydrogen sulfide is oxidized.[4,100] Sulfur is obtained as gaseous S_2 molecules by this reaction.[100] Since the temperature is so high, thermal decomposition of hydrogen sulfide to hydrogen and S_2 takes place as well as side-reaction. Subsequently, the reaction mixture is cooled down by a heat exchanger and the liquid sulfur is removed at ca. 200-300 °C. The remaining gas mixture contains still a certain amount of hydrogen sulfide and is thus transferred to a cascade of several reactors in which the same reaction sequences are repeated at lower temperatures (170-350 °C) using heterogeneous catalysts. Since the reaction between hydrogen sulfide and sulfur dioxide is highly exothermic, the catalytic synthesis of elemental sulfur can only be performed with the residual gas mixture exhibiting lower hydrogen sulfide content and therefore the thermally oxidation as first step is unavoidable.[4,100]

In 2021, 80 million tons of elemental sulfur were produced mainly as a by-product of the petroleum industry (97% of produced elemental sulfur was accounted to petroleum by-product in 2003).[1,5] Compared to ten years ago, the amount of produced sulfur has more than doubled (35 million in 2011).[4,95,101] On the other hand, there is only one major application on industrial scale in which elemental sulfur is applied, *i.e.* synthesis of sulfuric acid.[4] In 2021, 90% of the overall produced elemental sulfur was consumed by sulfuric acid formation.[101] Nevertheless, further application areas are for instance vulcanization of rubber, gunpowder, polymeric materials, and Li-S-batteries.[2,102–105] However, the worldwide demand of sulfur is no longer on par with its annual production and thus, sulfur deposits started to grow rapidly.[1,5,6] Considering that sulfur is a non-toxic and innocuous compound, this did not lead to safety issues directly. However, nowadays, enormous amounts of sulfur are stored in forms of powder or huge blocks, several hundred meters of length and width, and above 20 meters high (see Figure 3 **A**).[1,2] Such deposits achieve sizes which can be seen from outer space (see Figure 3 **B**-**C**). Now, the actual accumulation of this tremendous quantities ultimately resulted in several safety issues. For instance, aside the fact that sulfur is non-toxic, it is flammable and thus, a fire of such a deposit would result in a massive release of noxious sulfur dioxide.[1] However, the more likely issue related to storing tremendous amount of sulfur is its ability to being oxidized under aerobic and moist conditions for instance by bacteria. This results in formation of sulfuric acid, which ultimately leads to acidification of water and soil.[1,7] Therefore, more applications for the use of elemental sulfur are highly desired on industrial scale decreasing the annual surplus of elemental sulfur. In 2011, Rappold *et al.* suggested an environmentally friendly storage concept for sulfur by mineralization, in which complete oxidation towards sulfuric acid is followed by sulfate formation with abundant alkaline silicates.[1] The formed sulfate salts could be then simply discarded on land or sea, while the vast amount of energy produced by the mineralization could add up to the regional energy supply.

Sulfur is inert at room temperature towards water or non-oxidizing acids like hydrogen chloride.[4] Nevertheless, at elevated temperatures, it reacts with many metals and other elements. Among all its known allotropes, S_7 is the most reactive form due its high ring strain, whereas S_8 depicts the lowest reactivity. It is nearly insoluble in typical organic solvents or water but shows high solubility in carbondisulfide.[4] Nevertheless, it shows some solubility in polar solvents like methanol or acetonitrile in which S_7 and S_6 rings are formed in an equilibrium, however only in small amounts (about 1%).[106] Even though several important reactions revolving around elemental sulfur are now known for several decades, like the Asinger or the Willgerodt-Kindler reaction (see chapter 2.3.2.), research around elemental sulfur in organic chemistry was scarce for a long time.

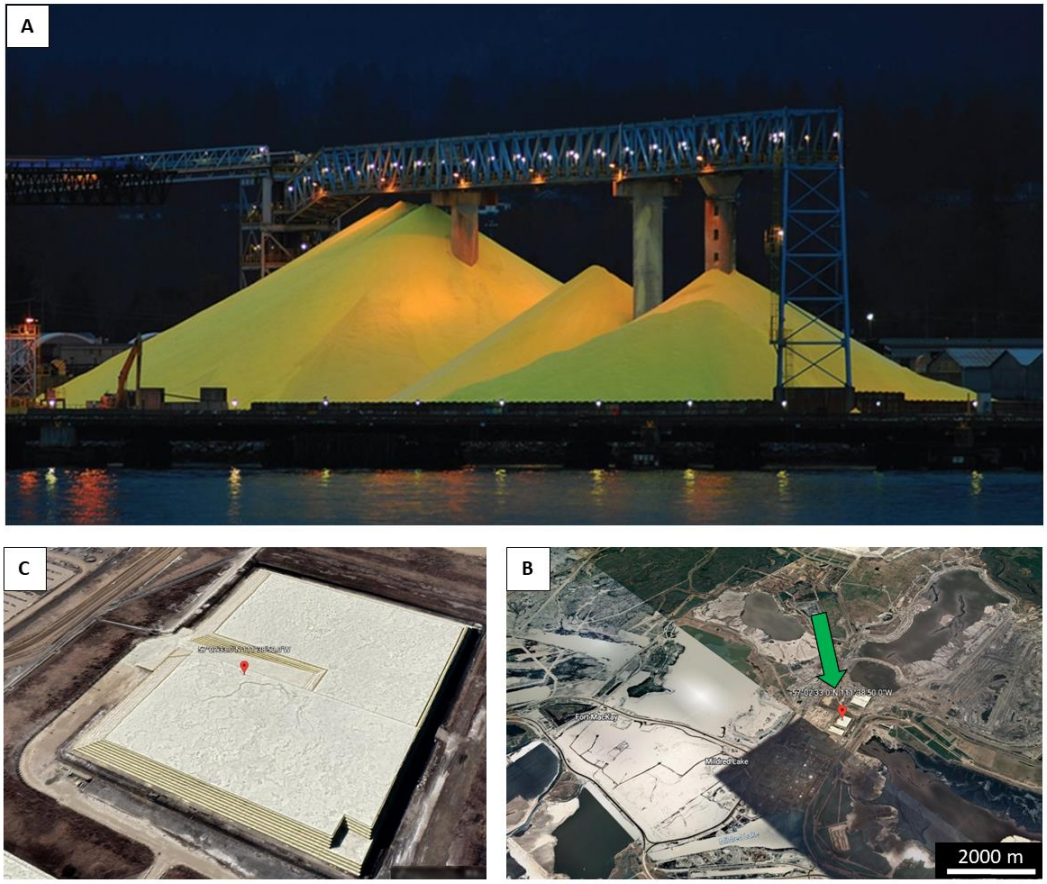

Figure 3: Images of deposits of elemental sulfur. A) deposit with elemental sulfur in powder form (adapted with permission from Nature Chemistry).[2] B-C) Screenshots of satellite images on Google Earth of deposit of elemental sulfur in block form, Canada, at 57° 02`33 N, 111° 38`50 W.[1] B) close-up. C) Zoom-Out, sulfur deposit is highlight by the green arrow. The images B-C) have been edited to color the sulfur gray, probably since sulfur exhibits a high albedo.[1]

Recently, elemental sulfur has attracted increasing interest in organic chemistry, which can be seen by the increasing numbers of papers published about this topic annually (see Figure 4). In 2021, the number of publications (197) were nearly three times as high as they were two decades ago (71) and the trend seems to continue (after ca. six months in 2022, already 126 papers have been published). This is probably a result of the fact that, when activated, sulfur exhibits an astonishingly versatile potential as a reagent in a reaction, which has finally come to the attention of many working groups. It can participate in a reaction as oxidizing or reducing agent, catalyst or building block while at least one sulfur atom is being incorporated into the final product.[8] Thereby, the reactivity is strongly depending on the reaction conditions (temperature, irradiation, etc.) or external activation agents, which are numerous in types as well, ranging from acid and bases to metal complexes to precursors

of radicals. In addition, sulfur is, as discussed above, a highly abundant, cheap, non-toxic easy to handle solid, which is a waste product of petroleum industry making its utilization in chemistry favorable in terms of sustainability. In the following, an overview over the different kinds of roles played by sulfur in a reaction is given on brief examples to highlight its versatility as reagent as well as starting material. In addition, the different activation condition or reagent applied is mentioned.

No notes about the reaction mechanisms are made since they are, in all cases, still under discussion and vary strongly by the role sulfur has in the respective reaction. Exception is the activation of elemental sulfur by bases, which is discussed thoroughly in the following chapter, including current opinions of tentative reaction pathways, due to its importance for the work of this thesis.

The use of elemental sulfur in multi component reactions, a group of reactions in the toolbox of Green Chemistry (compare chapter 2.1.2.), is discussed separately in more detail as well (see chapter 2.3.2) as this synergy can lead to an increased degree of sustainability, which was harvested for this thesis as well.

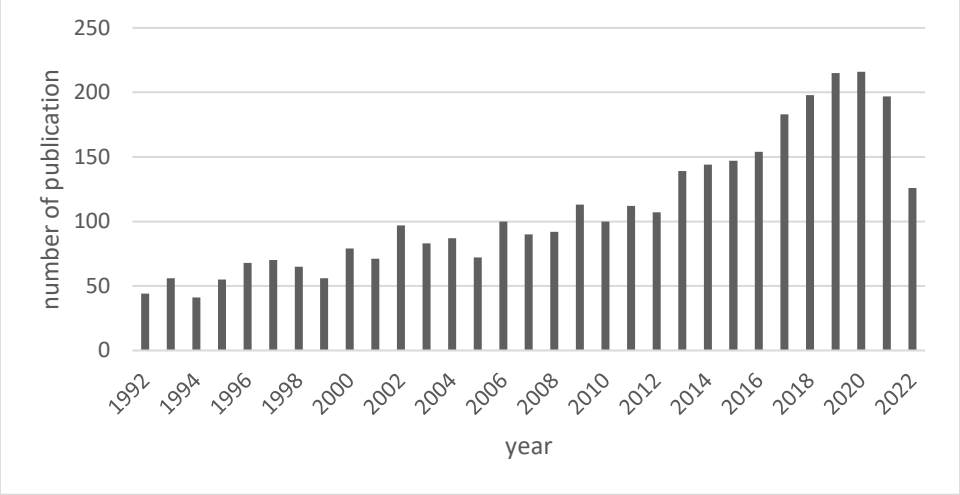

Figure 4: Scopus search of the fixed term "elemental sulfur" in the field of chemistry, extracted at the 23.06.2022.

Sulfur can be implemented in various ways as starting material, which is depicted in Scheme 3. For instance, it can be used for thiiranes synthesis from alkenes or allenes by utilization of molybdenum or rhodium catalysts at elevated temperature.[107–109] More commonly, thiophenes can be obtained by reacting alkylidyne aryl moieties or Glaser-coupling products by applying high temperatures with or without basic activation.[110–112] Also sulfur-based MCRs (SMCRs), like the Gewald reaction, yield thiophenes (see Scheme 16 **C** and Scheme 17 **E**). Besides thiophene, several other sulfur-containing heterocycles can be accessed like thiazolines, thiazoles, oxathiolanes, thiazolidines, benzothiazoles and aromatic thiolocarbamates (see Scheme 16 **B** and Scheme 17 **B-D**, **F**). Thioethers can be obtained applying oxidative coupling conditions with aryl boronic acids or reductive coupling of carboxylic acids with tetramethyldisiloxanes.[113,114] Thioamides are obtained by Willgerodt-Kindler reactions and its many modifications (see Scheme 16 **A** and Scheme 17 **A**). With carbenes or carbene-like structures, for instance carbon monoxide, *N*-heterocyclic carbenes or isocyanides, sulfur forms C=S double bonds in the presence of basic activation agents or metal catalysts already at room temperature.[9,115,116] Moreover, sulfur can also act as multiple sulfur donor yielding disulfides or polysulfur cycles like thiepins or dithiolans with various compounds using metal catalysts at basic conditions, strong basic conditions, or elevated temperature, respectively.[117–120] Finally, sulfur can form polymers by donating multiple sulfur atoms. For instance, in the inverse vulcanization, glassy and dark red polysulfane *co*-polymers were obtained with divinyl compounds at 185 °C using

elemental sulfur as *co*-monomer and solvent at the same time in a radical polymerization since sulfur chains are mainly present as liquid biradical at this temperature.[2] In the synthesis of a triazine network at 400 °, elemental sulfur was used as cross linking agent and inserted forming a polysulfane-triazine-*co*-polymer.[121]

Further, sulfur can act as an oxidant. For instance, the reaction of benzaldehydes and aryl-2-pyridiylmethylamines led first to an imine condensation, which is then followed by cyclization due to the sulfur oxidizing the aldehyde carbon, yielding imidazo[1,5-α]pyridines in up to 83% (see Scheme 4**A**).[122] The oxidative property of sulfur was further confirmed as hydrogen sulfide was verified to be formed in the reaction by a lead(II) acetate test. The reaction was performed in DMSO at 80 °C without any additional activating agent. However, as one of the starting materials was a basic amine component which was employed in slight excess (1.10 eq.) this can probably be related to a basic activation of the surplus of the amine (see also the following chapter).

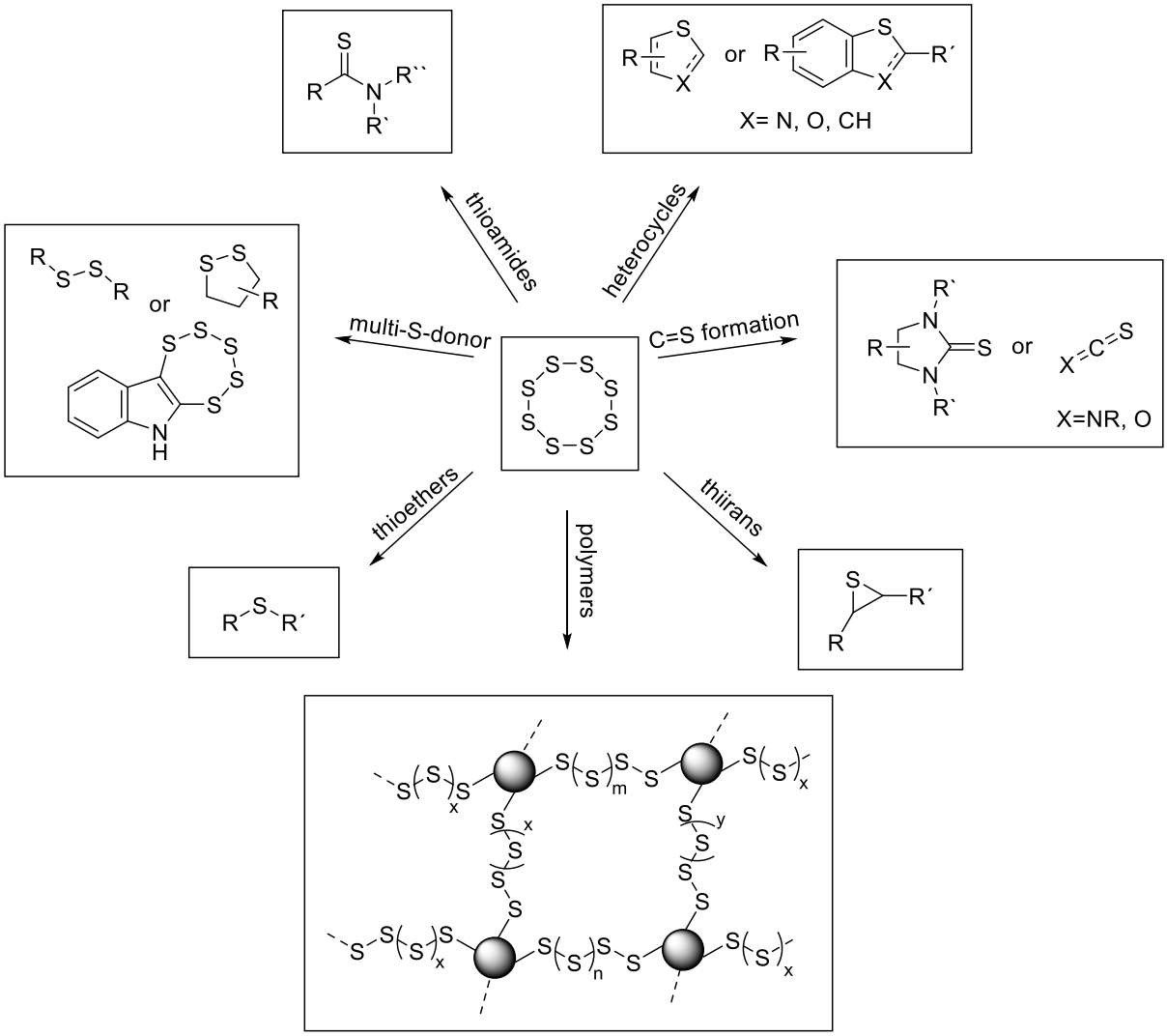

Scheme 3: Overview of the scope of different products and functional groups obtained by incorporation of one or more sulfur atoms using elemental sulfur (S_8) as starting material. In the examples of sulfur incorporated in polymers, the organic moieties are abbreviated with black balls and polysulfane chains of different length are obtained.

Moreover, benzyl chloride derivatives could be converted to 2-aryl benzoxazoles and benzothiazoles by reacting it with o-amino phenols and thiophenols in the presence of sulfur (see Scheme 4**A**).[123] Sulfur oxidizes the benzylic CH_2 group under evolution of hydrogen sulfide and the formation of the heterocycle. The reaction is performed in pyridine, acting as solvent and activating base, at 130 °C obtaining yields up to 96%.

On the other hand, sulfur can act as reductant. Nitroarenes can be reduced using three equivalents of elemental sulfur (in this case three equivalents of S_8 molecules) using various bases like K_2CO_3, NaOH, primary, secondary and tertiary amines (see Scheme 4**B**).[124] Ultimately, $NaHCO_3$ as mild base was used in the general synthesis protocol, while DMF was applied as solvent at 130 °C. The reaction exhibited high selectivity and yields, which was underpinned by comparison of the application of the reduction protocol with sulfur against Raney-nickel and hydrogen in the synthesis of a certain thienopyrimidine. Reduction of the nitro group containing precursor with sulfur led to the targeted compound in a yield of 93%, while Raney-nickel and hydrogen led to a yield of only 76% and by-products due to unselective reduction of other functionalities. No comment was made about the oxidized sulfur species, which was obtained in the report. However, gas formation was reported, which could be related to carbon dioxide formation due to the use of $NaHCO_3$ or formation of sulfur dioxide, or similar.

Benzofuroxanes could be reduced selectively to benzofurazans using elemental sulfur in moderate yields (28-58%, see scheme 4 **B**).[125] The reaction was performed at high temperatures (145-160 °C) in ethylene glycol without any additional reagent. Nevertheless, morpholine was reported to accelerate the reduction reaction. No comment on the oxidized sulfur species was made. Compared to typical deoxygenation agents like trialkyl- and triarylphosphines, trialkyl phosphites, hydrazine, hydroxylamine, and sodium azide, sulfur is the safer reagent in terms of toxicity and hazardousness.

Finally, elemental sulfur was reported to be a sole catalyst or assistant reagent for some reactions.[8,126,127] However, since at least one equivalent of sulfur was applied for the reactions and no report of full recovery of the sulfur was made, sulfur probably deserves the labelling of “assistant reagent” or “stoichiometric auxiliary reagent mediating the reaction without being consumed” rather than “catalyst”. Nevertheless, symmetric and unsymmetric 1,3-disubstituted ureas could be obtained by using 30 mol% of sulfur catalyzing carbonylation of carbon monoxide which was then reacted with a nitroaryl and an aminoaryl (see Scheme 4**C**).[128] The reaction was performed at 150 °C at 30 bar carbon monoxide pressure adding five equivalents of the base triethyl amine in an ionic liquid obtaining yields up to 96%. As mentioned above, sulfur and carbon monoxide yield carbonyl sulfide which was hypothesized to reduce the nitroaryl compound under release of elemental sulfur forming an isocyanate which reacted to the final product with the arylamine.

Heteropropellanes were obtained using two equivalents *o*-amino phenol with cyclohexanones using 50 mol% of elemental sulfur (see Scheme 4**C**).[129] The reaction was performed in DMSO at 80 °C under acidic conditions applying acetic acid with yields up to 85% and complete regio- and stereoselectivities. Sulfur probably took part in the reaction as an oxidant forming hydrogen sulfide, which then reacts with DMSO yielding dimethyl sulfide and elemental sulfur making DMSO the terminal oxidant of the reaction. Using these oxidative conditions of sulfur in DMSO, disulfides can yield either thioamides or aza heterocycles as well while down to 5 mol% of elemental sulfur was applied. [130]

Concluding, elemental sulfur is a highly versatile compound, which can be used either as starting material or reagent yielding a multitude of different substance classes and even polymers. Sulfur is nowadays mainly produced as a waste product especially in the petroleum sector. On the other hand, a high annual surplus of sulfur is produced, since the main applications do by far not consume the produced amount completely. As a result, sulfur depots are increasing in sizes, developing threats for humans and environment like acidification of soil and water. Thus, sulfur can be considered as an abundant, cheap and non-toxic feedstock and its utilization in chemistry exhibits a high potential of sustainability. The recent increase in sulfur related research shows that working group have finally realized the value of this compound. Nevertheless, sulfur related chemistry is still

in its infancy, especially in terms of mechanistic understanding of the reaction pathways, and it can be anticipated that this research field will keep growing in the next years.

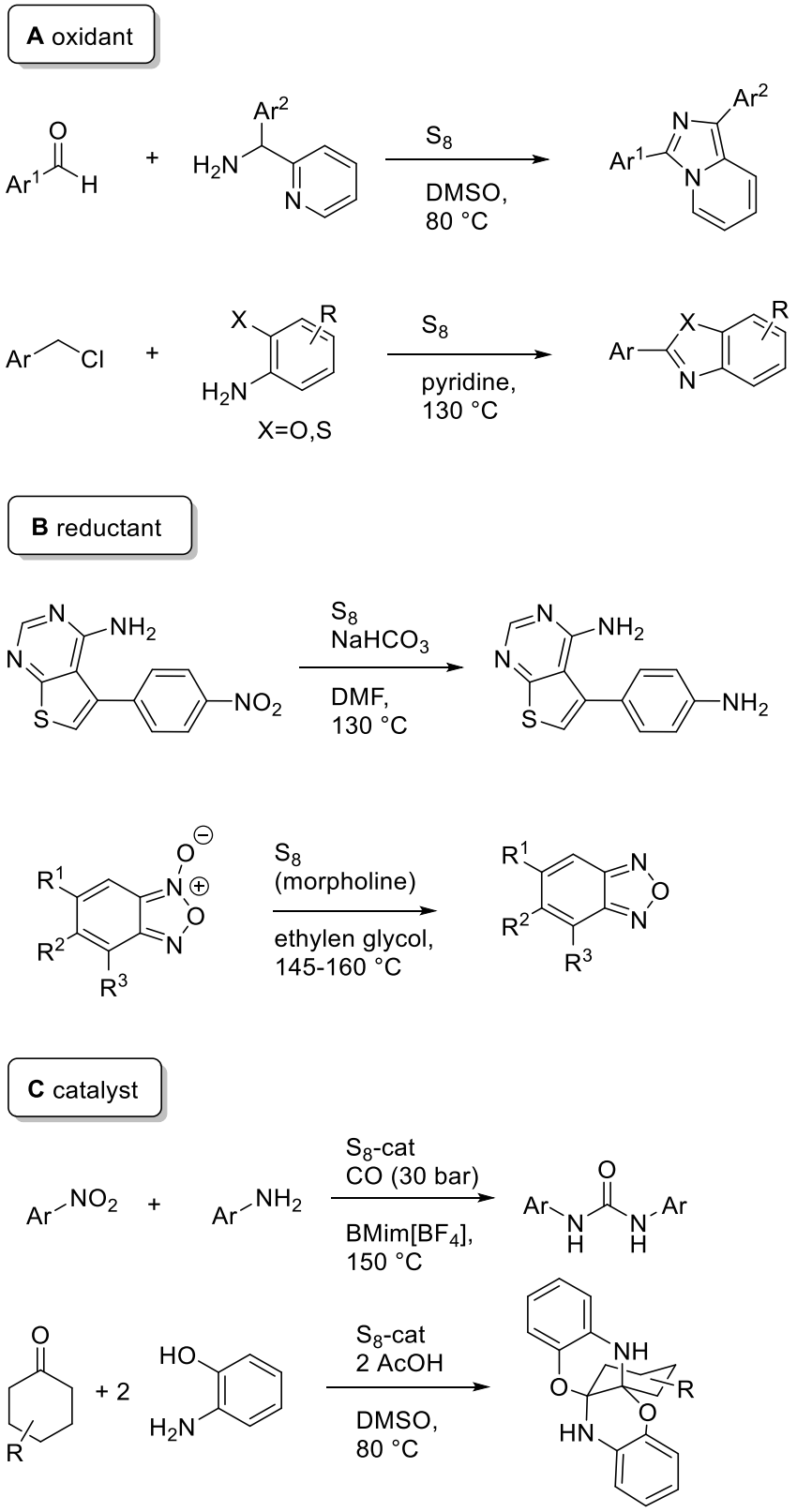

Scheme 4: Overview of the different roles of sulfur while participating in reactions as reagent.

2.2.1 Activation of elemental sulfur under basic conditions

As discussed in the previous chapter, elemental sulfur is inherently inert towards the most compounds at room temperature and thus, an activating agent or condition like metal-catalyst or high temperature is usually required to unlock its versatile reactivity (see previous chapter). Nowadays, the activation under basic conditions is one of the most common approaches for the activation of sulfur. Since the key reaction of this work, *i.e.* the synthesis of thioureas by the use of a sulfur and isocyanide based MCR (AM-3CR, see Scheme 5**A**), relies on the basic activation of sulfur involving C-S formation, this chapter discusses the mechanistic aspects and reaction conditions in detail.[10] However, the mechanistic understanding of this type of sulfur reactivity is, like other sulfur containing reactions, not fully understood yet and discussions are ongoing. Thus, the current most accepted reaction pathway involving polysulfane anions is depicted and discussed thoroughly providing information about credibility obtained by test experiments, analyses and calculations. Other less reported pathways are discussed briefly as well. The chapter concludes with a qualitative evaluation of the degree of sustainability in this kind of reactions. Therefore, typical reaction parameters (like solvent, stoichiometry, temperature, concentration) were extracted from more than forty synthesis protocols in literature using basic activation of sulfur and compared thoroughly.

All commonly applied pathways start by opening of the octasulfur ring forming an octasulfane chain **I** (see Table 3, for references see Table 4). Thereby, the base acts as nucleophile attacking the sulfur ring. The respective pathway is determined by the properties of the base used for activation. For instance, nucleophilic bases like amines (primary, secondary and tertiary ones like morpholine, *N*-methyl piperidine, TEA, PMDETA, DABCO),[10,131–135] amidines,[136–139] guanidines,[138], thiolates,[120,140] sodiumsulfide[141,142] and hydrides[143–146] are hypothesized to open the ring nucleophilically (see Tables 3 and 4). In addition, reactions using basic starting materials like amines, enamines or enhydrazines have no need for an additional activation agent, since a small excess of the starting material can already activate sulfur sufficiently.[10,132,147,148] On the other hand, the base can deprotonate the starting material forming a more nucleophilic species like a carbanion. Thus, less nucleophilic bases like carbonates, *tert*-butanolates, butyl lithium and hydroxides can be utilized as well (*e.g.* deprotonation of a terminal alkyne or a benzyl CH_2 group).[144,149,150] It is noteworthy that, even though nucleophilicity is increasing with degree of basicity, both properties are not inherently depending on each other, for instance high nucleophilicity can arise from stereoelectronic effects like the α-effect in hydrazones or other electron-donating effects like in DMAP or NMI.[151,152] However, several examples are found in literature which show that a certain degree of basicity is crucial for the reaction and has to be exhibited by the activation agent to obtain a successful activation.[153,154] No investigation was reported so far, in which an overall comparison of the nucleophilicity and basicity of the successfully applied bases for sulfur activation in several reactions is made to shed more light on the actual importance of this properties. This is further underlined by the multitude of synthesis protocols reported over the last decades using activation agents with a certain degree of basicity (see comparison of 43 synthesis protocols in Table 4) while outliners are scarce (three publications were found relying on less basic compounds, i.e. *N*-alkyl imidazoles, DMAP and HMPA).[155–157] Thus, this works refers to this activation approach as “activation of elemental sulfur under basic conditions”.

In a next step, the octasulfane chain **I** attacks other sulfur molecules in an anionic ring-opening polymerization like pattern, forming polysulfane chains **II** (see Table 3). The intermediate octasulfane chain **I** and the final polysulfane chain **II** formed by nucleophilic attack exhibit a negatively charged terminal sulfur atom, while the other chain end consists of the base moiety, which is now attached to the sulfur chain by a covalent bond. Depending on the utilized base, the overall charge of the octasulfane chain can be divalent negative (sodium sulfide),[141,142] monovalent negative (thiolates, hydrides, carbanion)[120,140,143,144,146,149,150] or neutral (amines, amidines and guanidines).[10,132,134,136–

[139,158] The neutral octasulfane chains are described as inner salts, since the base moiety bears a positive charge besides the negative charge of the terminal sulfur atom.[10] An additional equilibrium is expected from tautomerism if a proton transfer between the base moiety and the terminal, anionic sulfur atom is possible forming a non-charged octasulfane chain bearing a terminal thiol functional group (compare primary and secondary amines against tertiary ones in Table 3). No reports were made about the direct verification of these polymers so far. GPC analysis would be a reasonable approach to obtain data about the molecular weight of this polymers, since typical eluents like DMF or DMAc are able to dissolve activated polysufanes as discussed below.

Table 3: Currently most used reaction pathway to describe the activation of elemental sulfur (S_8) under basic conditions forming polysulfane chains. Different kind of bases or basic starting materials (Nu) lead to a different overall charge of the polysulfane which is depicted in the table providing examples as well. [10,120,132,134,136–144,146,149,150,158]

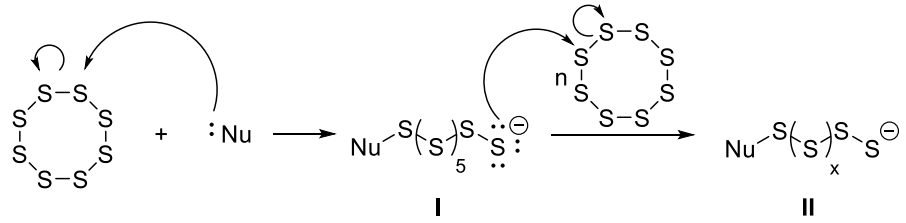

base	Na_2S	thiolates, hydride salts, carbanion	amines, amidines, guanidines, ammonia, hydrazones
charge	divalent	monovalent	neutral (zwitterionic)
example	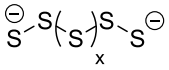	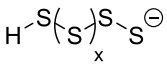	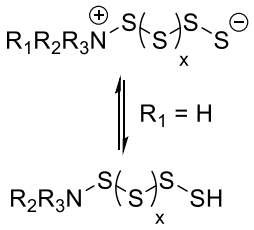

In addition, a characteristic color change of the reaction mixture is obtained after activation of the sulfur by base.[153] The obtained reaction mixture is usually described to have a dark red to deep brown color, which is typical for poylsulfanes (see previous chapter: i) color of µ-sulfur, ii) color of polymers obtained by inverse vulcanization, see also pictures in Table 4), at least indicating the presence of these polymers. Furthermore, the color change of the reaction mixture is usually accompanied by partial or complete dissolution of the, in general insoluble, elemental sulfur clearly indicating its conversion (see pictures in Table 4).[138,153] However, even though this color change is consistently reported, it can arise from other compounds and thus, the presence of this color should not be considered as sole proof for the formation of polysulfane chains.

No review about the activation of elemental sulfur under basic conditions was published up to the point when this chapter was written and thus, to obtain the general reaction parameters for this kind of basic activation of sulfur, data from 40 publications was extracted. In all cases, the authors reported reaction pathways *via* polysulfane chain formation (in addition, three publications were considered applying similar reaction conditions but do these three did not report a more detailed activation step of sulfur). The results are summarized in Table 4:

Table 4: Overview of reaction parameters for the activation of elemental sulfur (S_8) under basic conditions. The data was extracted out of 43 publications (from 2003 to 2021) reporting sulfur conversion under basic conditions referring mostly to formation of polysulfane chains.[10,120,131–150,153–173]

Number in brackets show how often the compound was reported. In addition, the color change upon dissolution of sulfur by polysulfane formation is depicted (left: insoluble S_8 in DMSO at 100 °C and right: upon addition of K_2CO_3 solubilized polysulfanes). Pictures were adapted from Journal of American Chemical Society ref.[153] *(SI-Figure S2).*

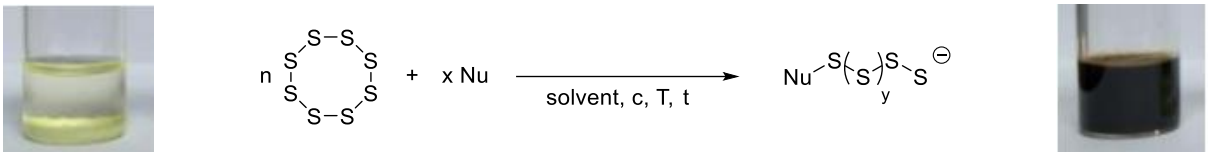

base	amines (16), *tert*-butanolate salts (6), carbonate salts (6), amidines (4), hydride salts (4), sodium sulfide (2), hydroxide salts (2), thiols (2),
base equivalents	0.1-29
solvent	DMF (11), DMSO (10), THF (5), water (5), bulk (5), dioxane (4), toluene (4), DMAc (2)
S_{atomar} equivalents	1-24
$c(S_{atomar})$	0.05 M - bulk
T	room temparture-140 °C
t	0.5-72 h

Typical bases for the mentioned groups were already discussed above. Mostly amines were applied as base for the activation, providing a vast scope of applicable basic reagents or starting material. The equivalents of bases differ from 0.1 to 29 equivalents. [10,120,131–150,153–173] Most importantly, the successful use of substoichiometric amounts of the base underlines the role as activation agent for sulfur (substoichometric amounts are only applicable if the used base is no starting material at the same time).[135,140–142,145,148,154,165] As solvents, mainly polar aprotic solvents like DMSO and DMF were used but less polar solvents like THF, dioxane or toluene were reported as well. [10,120,131–150,153–173] The solubility of the (ionic) polysulfane chains in these solvents is depicted in the pictures in Table 4 compared to non-activated elemental sulfur.[153] In some cases, the use of no solvent was reported. Nevertheless, at least a small excess of a liquid base or ionic liquid was used in these cases and it can be assumed that the polysulfane were soluble in these compounds.[10,148,160,166] Only one report was made using no excess of base or any other additive allowing the labelling as bulk reaction.[155] Thus, the concentration of the sulfur (per atom) ranges in general from nearly bulk conditions (>20 M) to 0.05 M. [10,120,131–150,153–173] The basic activation of sulfur can be already performed at room temperature, as several examples show.[10,140,159,169] However, most of the synthesis protocols use elevated temperatures up to 140 °C. [120,131–139,141–150,153–158,160–168,170–173] Surely, it can be expected that the certain reaction temperature initiating the activation of sulfur differs from the type of base and solvent used but most likely the following reaction steps in the respective synthesis need more energy than the sulfur activation. In addition, it has to be mentioned that the application of temperatures above 120 °C will lead to λ-sulfur, which consists in small portions of S_7, the most reactive modification of sulfur, which could enable a ring opening in cases where S_8 proves to be unreactive (see previous chapter). Ultimately, the time scales for the reaction ranges from half an hour to 3 days. [10,120,131–150,153–173] Again, this parameter is a result of all reaction steps including follow up reaction converting the polysulfane chains and it can be assumed that at least for some cases the activation of sulfur is quite fast (for instance a suspension of elemental sulfur in DMSO will immediately result in a dark brown solution upon addition of DBU at room temperature under stirring (experiment was performed in the scope of this thesis).

Nearly every reported mechanism relies on the formation of a polysulfane chain. The formed poylsulfane is a strong nucleophile, since it consists of a thiolate like end-group attached to other sulfur atoms resulting in an α-effect. Thus, it will react with a multitude of electrophiles resulting in different reaction pathways, depending on the nature of the starting materials and the nucleophilic attack. Therefore, typical reaction behavior of the polysuflane chain is discussed in the following on chosen examples.

For instance, carbene like groups such as isocyanides can be attacked forming a C-S bond and transferring the negative charge to the carbon.[10,143,145,155] As a result, the sulfur chain is hypothesized to act as a leaving group, whereby the former terminal sulfur atom, now attached to the former carbon isocyanide, remains at the starting material under formation of a C=S double bond. This is exemplified by the multicomponent reaction AM-3CR, since this reaction was crucial for the investigation in this thesis (see Scheme 5**A**, also see chapter 2.3.1 and 2.3.3 for further information).[10]

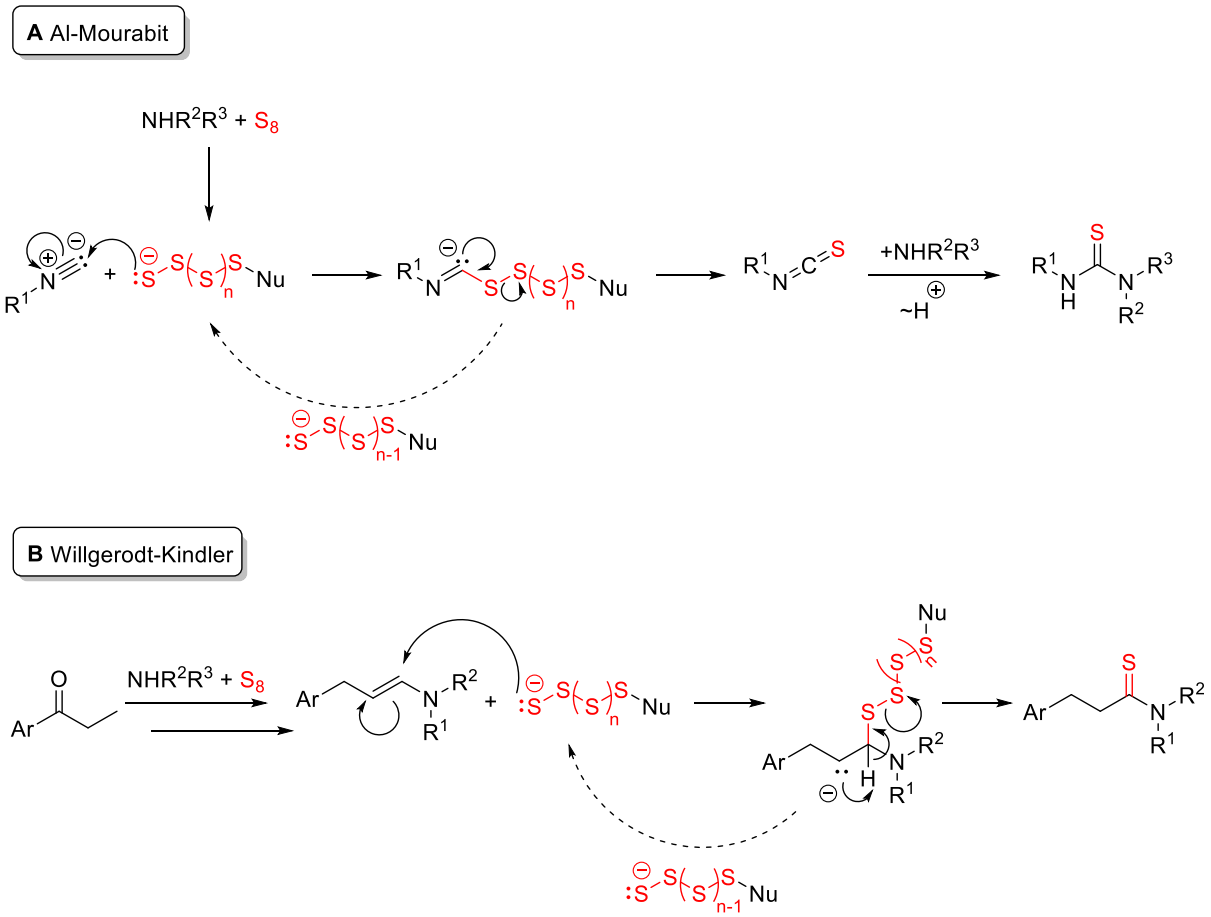

*Scheme 5: Possible mechanistic pathways forming C=S double bonds. The steps involving polysulfane are depicted in detail. The polysulfane attacks first in a nucleophilic addition step, followed by a subsequent elimination of the polysulfane with one sulfur atom less which can start the sequence again (dashed lines). Ultimately, a C=S double bond is formed. Examples are given for the starting material isocyanide (**A**) and enamine (**B**).*[10,174,175] *The base is abbreviated with Nu when attached to the polysulfane, sulfur is colored red.*

Sulfur, amine as base and starting material, as well as isocyanide as carbene like functional group was used forming thiourea as final product. In the case of an isocyanide, the C=S double bond formation is assumed to yield an isothiocyanate, which was not detected in the scope of the reported work. However, Ábrányi-Balogh *et al.* reported a modification of this reaction with alcohols or thiols and sodium hydride, instead of an amine component, and a test experiment yielded the respective isothiocyanate.[143] Thus, an indirect prove of isothiocyanate as intermediate was provided. Since

isothiocyanates are prone to react with suitable nucleophiles, it is probably immediately consumed after formation by the reaction with the amine component (or in the modification with the alcoholate or thiolate), leading to the final product (thiourea, thionocarbamate or dithiocarbamate respectively).[10,143]

Another example following a similar pathway leading to a C=S double bond formation is assumed in the final reaction sequence for the Willgerodt-Kindler reaction (see Scheme 5**B**), forming a thioamide.[174,175] First, sulfur mediated imine migration takes place yielding the terminal imine (see also Scheme 16**A** for further information about the initial steps of this reaction). Finally, the enamine is hypothesized to act as an electrophile and is attacked by the polsulfane chain under formation of a C-S bond. Subsequent proton shift leads to a polysulfane carbanion, the same intermediate hypothesized in the previous examples. Ultimately, a C=S double bond is formed under the extrusion of a polysulfane consisting of one sulfur atom less.

Other electrophiles will lead to a completely different reaction path, for instance in the benzo thiazole synthesis of Nguyen *et al.* (see Scheme 6).[134] First, the poylsulfane is formed standardly by the attack of a base, here *N*-methyl morpholine. In a second step, an aldehyde is attacked nucleophilically in an addition-elimination reaction. A hydride is eliminated subsequently forming an acylpoysulfane. The protonated base is released by the attack of the eliminated hydride yielding again a polysulfane. This is assumed to attack a second electrophile in this case *o*-chloro nitrobenzenes in a nucleophilic aromatic substitution reaction. The obtained aryl acyl polysulfane reacts further in a cascade of base mediated redox reaction steps to reduce the nitro group, which is not completely understood at this point. The final oxidized sulfur derivative is proposed to be SO_3. This assumption was strengthened by the isolation and XRD analysis of the sulfonated benzothiazoles obtained as side product in this reaction. The respective regioisomer obtained can be typically obtained by sulfonation of benzothiazoles with SO_3.[134]

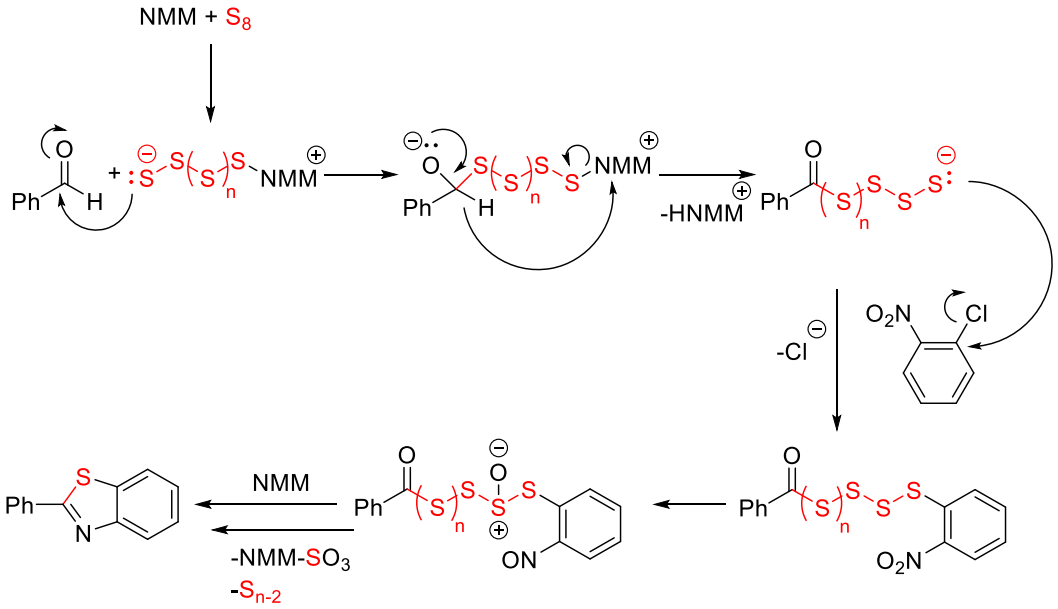

Scheme 6: Possible mechanistic pathway yielding benzothiazoles by use of sulfur (red) and a base (N-methyl morpholine (NMM)). The steps involving polysulfane are depicted in detail. Polysulfanes react first in an addition-elimination step, followed by a nucleophilic aromatic substitution. Subsequently, sulfur reduces the nitro group. Ultimately, a benzothiazole is obtained after several redox reaction steps not clear to this point.[134]

In cases where sulfur acts not as starting material but as oxidant, reductant or catalyst, similar reaction steps were proposed. However, often the final reaction steps differ, since sulfur is ultimately eliminated from the product compound. An example is the benzoxazole synthesis of Ngo and Nguyen

using o-aminophenol, arylaldehydes and sulfur in the presence of catalytic amounts of sodium sulfide (see Scheme 7).[142] Here, the polysulfane, formed after ring opening sulfur with sulfide, attacks the formed imine of the aldehyde and the aminophenol nucleophilically. Hydride shift is assumed under ring closing by the attack of the hydroxy groups releasing polysulfane with one sulfur atom less. A thiolo benzthiazolidine is obtained forming the product in a final step by aromatization under release of hydrogen sulfide. No gas formation was observed indicating hydrogen sulfide however, it is known that hydrogen sulfide reacts with DMSO (the solvent in this reaction), yielding dimethyl sulfide and elemental sulfur in return. The fact that dimethyl sulfide was found in the reaction mixture by NMR-analysis strengthened the assumptions made for this mechanism.

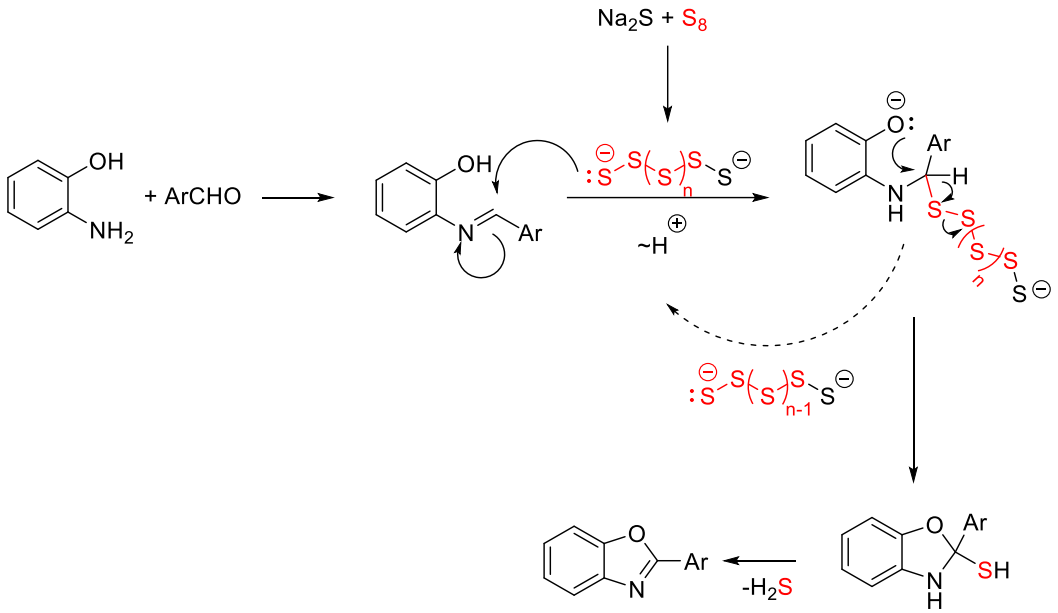

Scheme 7: Possible mechanistic pathway yielding benzoxazoles by use of sulfur (red) and sodium sulfide as base. The steps involving polysulfane are depicted in detail. Polysulfanes reacts first in an addition-elimination like step yielding a thiol group releasing a polysulfane with one sulfur atom less which can start the sequence again (dashed lines). Ultimately, the product is obtained by release of hydrogen sulfide thus, sulfur acts as oxidant in this reaction.[142]

In turn, other mechanisms were proposed in cases were the formation of the polysulfane is performed by attack of a starting material acting as base like a carbanion. For instance, the reaction pathway of the Gewald reaction (see Scheme 8 and also Scheme 16**C**) was described by Tinsley to form a poylsulfane chain with an anionic Michael adduct and then reacts further *via* ring closing to a thiophene.[161] Interestingly, the five membered heterocycle is assumed to be formed by the attack of the sulfur atom attached to the carbon, in contrast to the previous discussed approaches, in which the terminal anionic sulfur is the nucleophilic species. In a second step, the remaining sulfane chain is hypothesized to release the thiophene precursor under elimination of a sulfur ring consisting of one sulfur atom less.

Due to several reasonable approaches present in literature leading to polysulfane intermediates, exhibiting different follow-up reaction behavior, some recent syntheses are described with more than one pathway. For instance, Yu and Zhang proposed three mechanisms for their reaction between aryl amines, sulfur and carbon dioxide yielding benzothiolocarbamates (see Scheme 9).[162] In all cases, an aryl isocyanate is assumed to be formed as key intermediate underpinned by several control experiments. In addition, several other control experiments indicated that indeed all three pathways seem equally reasonable while a radical proceeding of the reaction could be ruled out in test experiment using TEMPO. The first one proceeds *via* addition reaction of the polysulfane chain to the isocyanate forming polysulfane carboxamide. As mentioned before, the polysulfane moiety

can act as a leaving group and is released in an electrophilic aromatic substitution reaction forming the final product.

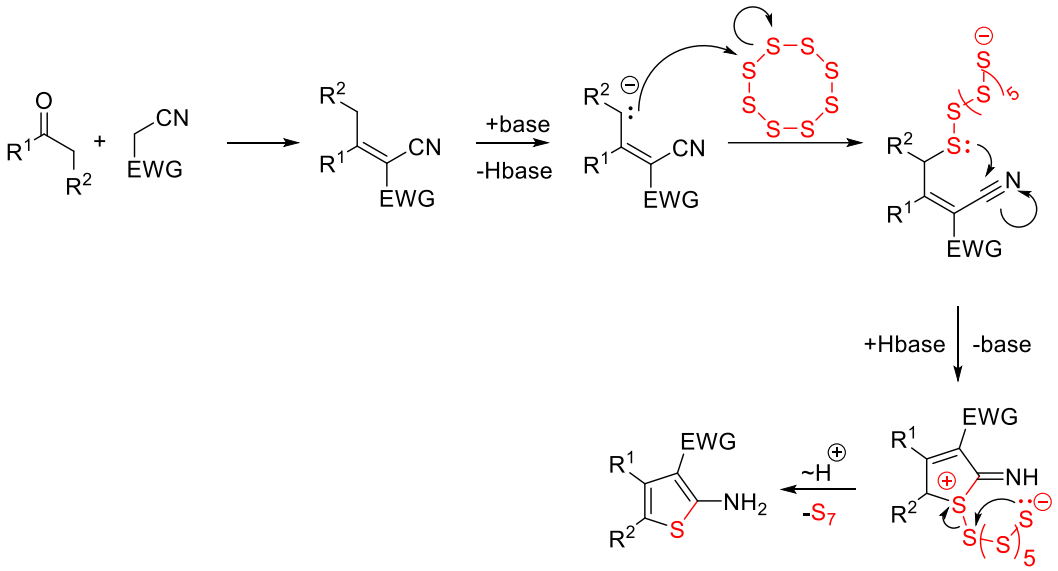

Scheme 8: Possible mechanistic pathway of the Gewald reaction. The steps involving polysulfane are depicted in detail. Polysulfanes are formed by attack of sulfur (red) by a deprotonated Michael system. Subsequently, the sulfur atom attached to starting material moiety reacts under cyclization. Ultimately, the 2-amino thiophene is obtained by release of S_7 in this reaction.[161] *The reaction is assumed with an octasulfane chain however, it seems reasonable that longer polysulfane chains can be formed since the reaction conditions are similar to previously discussed reactions.*

On the other hand, the second proposed pathway proceeds initially by the electrophilic aromatic substitution of the aryl isocyanate opening the S_8 ring. Subsequent elimination of a sulfur ring consisting of one sulfur atom less yields the *o*-thiolo isocyanate which reacts to the product by intramolecular cyclization. Finally, the third pathway, introduced the thiol functional group like the second pathway but prior to the formation of the isocyanate by electrophilic aromatic substitution of the aryl amine.

Ultimately, the polysulfane will act as a one sulfur donor or reagent (oxidant, reductant, or catalyst) and is thereby reduced in its chain length by one atom in all proposed publications. Considering the reaction parameters, especially the often stochiometric amount of sulfur applied, it can be assumed that the smaller polysulfane chain can react again with several other starting materials stripping of one sulfur atom of the chain at a time until the chain is fully consumed. On this explicit step, literature does not provide any detailed hypothesis when a polysulfane chain is labelled as “completely consumed”. Two options can be assumed: first, every sulfur atom can be transferred resulting in the release of the base, which explain its substoichometric nature and ultimately allow the assignment of the term catalyst to the base. The utilization of sulfur without any excess (one equivalent) in several approaches is in accordance with this assumption. However, no recovery of the base was reported so far for any reaction using this approach. Second, as the chain length decreases, the reactivity of the polysulfane could lead to inactivity. The highest difference in reactivity would be most likely a chain consisting of only one sulfur atom, since the α-effect of the polysulfane will be lost decreasing, the nucleophilicity of the thiolate group. Furthermore, the nucleophilic attack could be impeded at smaller chain lengths. Since the respective nucleophilic sulfur atoms would be in the surrounding of the terminally attached base of the chain, this might lead to steric hindrance. At the same time, it seems reasonable that longer polysulfane chains can be again obtained by the transfer of sulfur atoms from one polysulfane chain to the other, thus decreasing the impact of this

assumption unless high conversion of stochiometric amount of sulfur is reached. No side product was reported so far indicating a remaining base-sulfur intermediate or by-product.

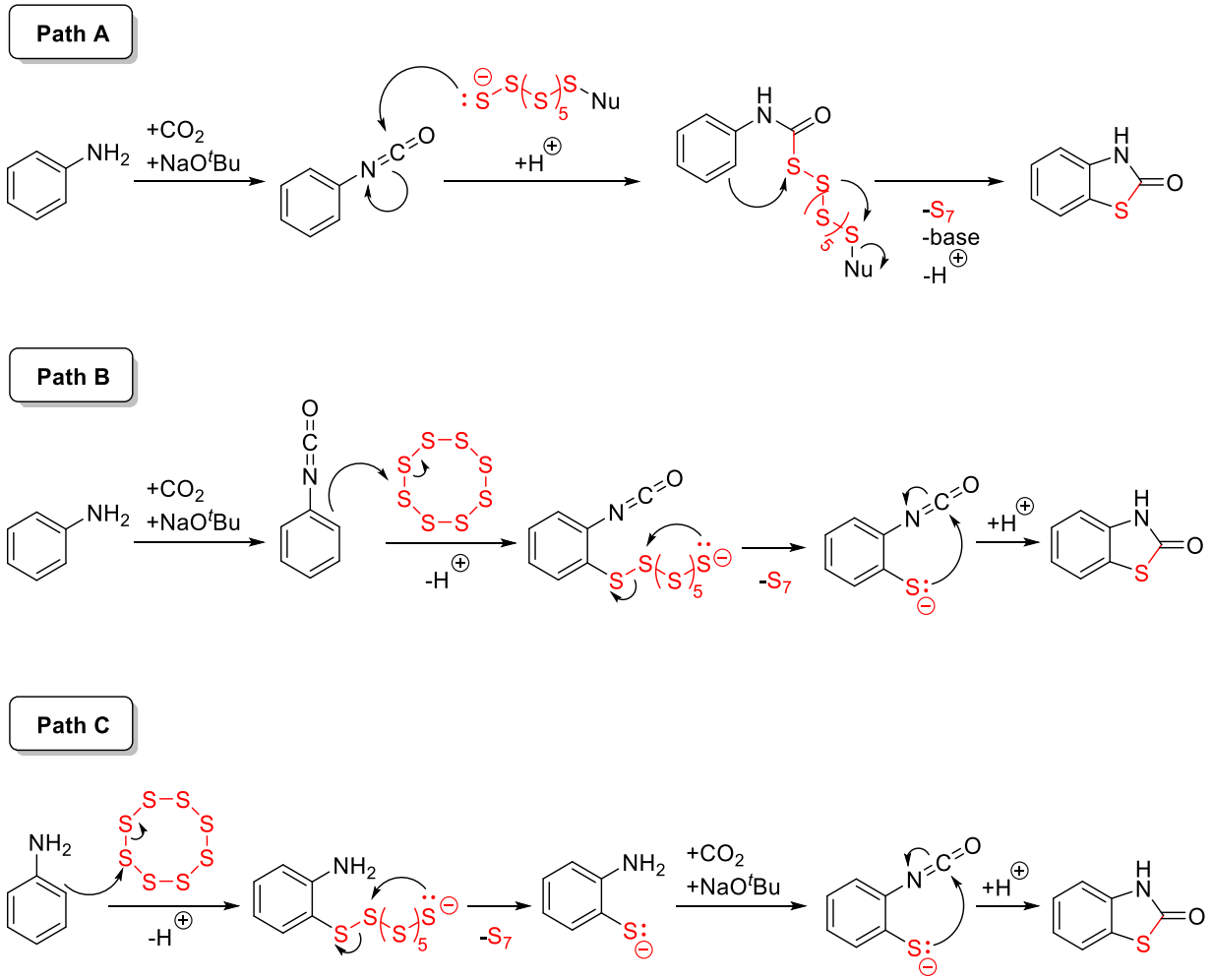

*Scheme 9: Three possible mechanistic pathways for the synthesis of benzothiolocarbamtes using sulfur (red) under basic conditions.[162] The steps involving polysulfane are depicted in detail. In path **A** the polysulfane is formed with sulfur and a base attacking the formed isocyanate nucleophilically. Subsequently, electrophilic aromatic substitution releases S_7 ultimately yielding the product. For path **B**, the sulfur is transferred to the polysulfane by electrophilic aromatic substitution of the isocyanate. Under release of S_7 a thiolate is formed resulting in the product after cyclisation. Path **C** exhibits same reaction steps as path **B** but in reverse order (first thiolate formation than isocyanate formation) yielding the product again after cyclisation. The reaction is assumed with an octasulfane chain however, it seems reasonable that longer polysulfane chains can be formed since the reaction conditions are similar to previously discussed reactions.*

All discussed reactions were proposed with polysulfanes as key intermediate being accepted so far as most likely compound for reactions involving activation of sulfur under basic conditions. Nevertheless, some other mechanisms can be found, even though in small numbers. For instance, Zhang and Zhang introduced a synthesis protocol for the formation of bisisothiazole-4-yl disulfides by reacting two equivalents of alkynyl oxime ethers with sulfur under activation by DBU (see Scheme 10**A**).[176] In contrast to the discussed reactions, elemental sulfur acts not only as mono sulfur atom donor yielding isothiazole moieties but also as di sulfur atom donor forming disulfides. For the incorporation of the disulfide functional group, the authors assume that formation of divalent disulfide anions taking place by oxidation of DBU (see Scheme 10**A**). This anion attacks both alkyne functions with one anionic sulfur each in the following yielding the disulfide group. In case of the isothiazole function, an attack of a carbanion intermediate is assumed which opens the S_8 ring leading to a thiolate group. Even though this step is not further described, it is in accordance with typical mono sulfur atom transfer mediated by a polysulfane chain. A radical pathway was ruled out

by control experiments with radical scavengers (TEMPO and BHT). No more detailed comment was made about the reaction between DBU and sulfur for instance the stoichiometry (equivalents of formed divalent disulfide anion per S_8 ring) is unclear. Since the reaction applied a huge excess of sulfur (16 equivalents of atomic sulfur or two equivalents of S_8 molecules) the proposed mechanism seems to be reasonable.

Polysulfanes are also known to dissociate in polar aprotic solvents like DMSO, DMF and HMPA besides reacting to divalent disulfide anions.[177] An agreed mechanism starts from the S_8 ring, which is reduced in a two electron transfer to the S_8 dianion (see reaction of Wang and Phan in Scheme 10**B**). Under extrusion of diatomic sulfur, the divalent S_6 anion is formed. The spontaneous homolytic scission of the chain results in the formation of the blue chromophore S_3 radical anion, which is for instance responsible for the color of the pigment ultramarine blue. It is assumed that the S_8 dianion can also react with other sulfur molecules to polysulfane, which could dissociate to yield sulfur radical anions with different chain length. The radical species can be detected using EPR-analysis.

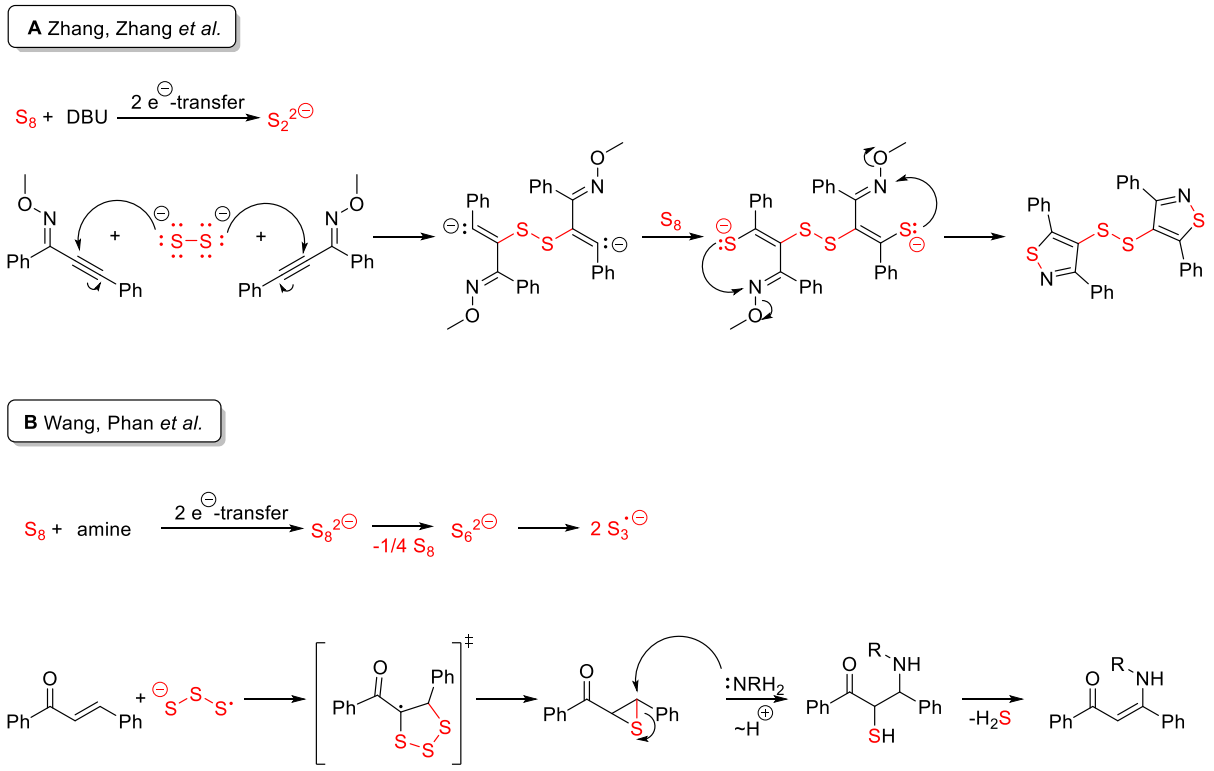

Scheme 10: Two examples of mechanisms of reactions using base-activated sulfur proceeding without a polysulfane as a key intermediate. First, isothiazole disulfide synthesis with divalent disulfur anion as key compound.[176] *Second, β-aminoenones formation by reaction with S_3 radical anion.*[177]

In several synthesis approaches with sulfur and bases, the importance of these sulfur radicals was ruled out by the fact that control experiments with radical scavengers did not affect the conversion and yield considerably (see above). Thus, polysulfane seems to be the reasonable key intermediate in this kind of reaction. However, some reports about a tremendous effect of radical scavengers in reaction of elemental sulfur under basic conditions can be found. For instance, Wang and Phan found that the β-C(sp^2)-H amination of a Michael system with an amine and sulfur yielding β-aminoenones was significantly influenced by radical scavengers.[178] Thus, no polysulfane-based mechanism was assumed but the reaction of the double bond of the Michael system with a S_3 radical anion forming a thiirane (see Scheme 10**B**). This thiirane is subsequently opened by the amine and elimination of hydrogen sulfide provides the final product. The mechanism was further underpinned, since the thiirane was verified as intermediate by GC-MS and the characteristic adsorption peak of the S_3 radical anion at 550-700 nm was found in the reaction mixture by UV/VIS-analysis. In addition, DFT

calculations agreed with the proposed pathway. Lei *et al.* also reported the S_3 radical anion as key reagent in the formation of thiophenes from sulfur, sodium *tert*-butanolate and 1,3-diynes.[110] Radical scavengers nearly completely inhibited the reaction and EPR-analysis proved the presence of the radical anions under typical reaction conditions. Lan and Song reacted 1,3-enynes with sulfur and potassium carbonate to disulfide thiophenes. In this reaction, one S_3 radical anion ultimately yielded a mono and two sulfur transfer resulting in the thiophene and disulfide functional group respectively. Verification as key intermediate was provided by UV/Vis and radical scavenger experiments as well as DFT calculations.[179] In addition, a trapping experiment of the radical with norbornene was conducted yielding *exo*-3,4,5-trithiatricyclo[5.2.1.02|6]decane determined by ESI-MS further underlining that the S_3 radical anion is not merely a side product of the reaction but a crucial intermediate.

Concluding, even though polysulfanes are the most accepted key intermediate in reactions of activation of sulfur under basic conditions, other pathways were also reported. In case of the pathway involving the S_3 radical anion, the importance of this compound as intermediate was further underpinned by immersive control experiments, analyses like EPR and UV/VIS as well as DFT calculations. Nevertheless, both discussed mechanisms (disulfur anion and S_3 radical anion approach) proceed under typical conditions for the polysulfane formation and the assumption that polysulfanes are also present in the reaction mixture seems to be reasonable. Thus, further investigations are needed to completely validate that in these cases polysulfanes do not participate in the reaction proceeding entirely.

Since this work was performed in the framework of sustainable chemistry, a brief evaluation of the reaction conditions and parameters of a basic activation of sulfur seems to be appropriate: Often high boiling and toxic solvents like DMSO and DMF are applied, since the polysulfane chain exhibit a good solubility in these solvents. As already mentioned in chapter 2.1.2., the solvent can be a considerable amount of the overall waste and is a major parameter for the E-factor. Thus, the question arises: is the positive effect of the use of elemental sulfur as waste product in terms of sustainability reduced or maybe even dwarfed by the use and amount of such solvents?

Many syntheses listed in Table 4 apply high concentration or nearly bulk conditions, allowing a considerable decrease of the overall amount of solvent resulting in a lower E-factor. Ultimately, the negative impact of waste and its energy consumption originating from solvents can be kept minimal. Nevertheless, nontoxic substitutions, ideally obtained out of renewable feedstock, like GBL or Cyrene™ would be desirable for the often-used polar aprotic solvents. Therefore, the stated question can be answered by no, the solvent does not overrule the positive effects of elemental sulfur qualitatively speaking. Further, the use of bases in substoichemtric amounts results only in low amount of waste. The applied bases typically exhibit low molecular weights (like morpholine, sodium carbonate or sodium hydride), decreasing the amount of waste further. The toxicity for some bases that were applied for the activation of sulfur is also low, for instance sodium carbonate is labeled with “warning” being only irritating to the eyes (H319).[180] Considering several approaches use high temperatures up to 140 °C, it might be beneficial for this, or subsequent reaction steps to apply a more sustainable transfer of energy like microwave irradiation or sonochemical approaches (even though several cases report that sulfur can be activated already at room temperature). Since the presence of solvent is important, a mechanochemical reaction set-up seems to be unlikely to bear beneficial impact in general. Nevertheless, in cases of nearly bulk conditions, where the amount of base itself exhibits the ability to dissolve polysulfane chains to a sufficient degree (*e.g.* a reaction in which excess of base is applied because it acts as activation agent and starting material), it might be still a reasonable approach for increasing the sustainability.

Concluding, the use of elemental sulfur under basic activation bears a potential to have a sufficient degree of sustainability, which is mainly depending on the used solvent and its concentration. Many different products can be obtained using this approach, which is straightforward and feasible considering its typical reaction conditions and set-ups. The activation itself is postulated to proceed *via* ring opening of sulfur forming polysulfanes, which can react as strong nucleophile subsequently in various ways depending on the applied starting materials. Further studies are needed to shed more light on the actual mechanism for this activation of sulfur to increase the understanding of the reactivity of elemental sulfur as starting material and reagent. It is expected that sulfur bears still unknown potential in chemistry and more research has to be conducted to pave the way for multitude of novel applications.

2.3 Multicomponent reactions (MCRs)

In multicomponent reactions (MCRs), three or more compounds react to form a product consisting of most of the atoms of the used starting materials (typically high AEs, >80%, are obtained).[68,181,182] Thereby, the used compounds break and form more than one covalent bond yielding a complex structure.[183] MCRs are one-pot reactions, which have considerable advantages over multistep synthesis, since no intermediate needs to be separated or purified, resulting in an overall more efficient synthesis.[182] Furthermore, the nature of these reactions are often modular, meaning a vast scope of different moieties is allowed, leading to a broad variety of potential products, while the starting materials are often easy to obtain or commercially available.[183,184] Due to their mentioned properties, MCRs are often labelled as green reactions (see also chapter 2.1.2.), for instance due to high AE and decreased waste, while renewable compounds can be employed as well.[68,185–187] By exploiting MCRs, pharmaceuticals can be evaluated since large compound libraries are easily and quickly accessible.[182,188,189] MCRs can also be used in polymerizations following a step-growth mechanism, which will be discussed in more detail in chapter 2.3.3. due to the importance of this topic for this work. Furthermore, high yields are often obtained making them ideal candidates in the field of sequence-definition. Uniform macromolecules can be obtained for instance by iterative synthesis.[190–193] In general, MCRs can be divided in three subtypes, which are depicted in scheme 11.[182]

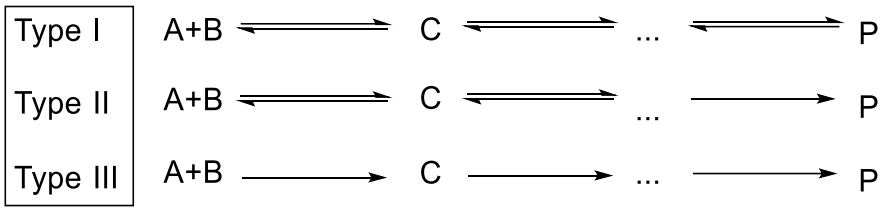

Scheme 11: Subtypes of MCRs which differ in the number of irreversible steps. A, B are assigned as starting material, C as one example of an intermediate and P stands for product. Note that in theory any number of intermediates can be obtained as highlighted by "…".[182]

Type I is a reaction in which every component, intermediate and product is in an equilibrium. As a result, it is typically difficult to obtain high yields, since there is no driving force towards the product side and the reaction mixture can contain considerable amounts of intermediates and starting materials.

On the other hand, type II reactions profit from their last reaction step, which is irreversible and draws the equilibrium towards the product side, thus increasing the yield. Typical examples for type II reactions can be for instance strongly exothermic reactions like ring closing reaction as well as aromatization.

Type III reactions consist of only irreversible steps, which makes the type II and III MCRs preferrable over type I. However, type III reactions are very rare in synthetic chemistry but can be found in biochemical processes in nature. The transition of these three subtypes of MCRs are often very smooth and thus, the classification can be blurred. In the following, an overview of important MCRs is given in which the order is chronologically, highlighting the impact of MCRs exemplarily (see Scheme 12). The first MCR was reported in 1850 by Strecker, reacting an aldehyde, ammonia and cyanic acid (see Scheme 12**A**).[194] The formed α-aminonitrile could be hydrolyzed to obtain α-amino

acids.[182,194] In 1882, Hantzsch was able to form dihydropyridines by the reaction of two equivalents of β-ketoesters, ammonia and an aldehyde (see Scheme 12**B**).[195] Nifedipin a drug of this compound class, which is treated for high blood pressure, could thus be obtained in one step.[196] Further oxidation of the dihydropyridines led to pyridines by aromatization. Several years later, Hantzsch was able to obtain pyrroles using β-ketoester, amines and α-haloketone (see Scheme 12**C**).[197] Biginelli established the synthesis of dihydropyrimidone in 1891. Therefore, urea, β-ketoester and an aldehyde (see Scheme 12**D**) were used.[198] Later, Mannich reacted enolizable carbonyl groups (aldehyde or ketones) with amines and aldehydes to obtain a β-amination reaction (see Scheme 12**E**).[199] This reaction found its way in Robinsons Tropinone synthesis and was the first example of the application of MCRs in the synthesis of natural compounds.[200] In 1993, Petasis published a modification of the Mannich reaction using boronic acids instead of enolizable carbonyl groups as nucleophiles to alkylate, vinylate or arylate imines, which can be considered a distinct MCR nowadays (see Scheme 12**F**).[201,202]

So far, only three or four component reactions were mentioned but also five and up to seven component reactions were investigated (*e.g.* an Ugi reaction with alcohol and carbon dioxide as acid yielded a five-, the combination of an Asinger and an Ugi-reaction resulted in a seven component reaction, respectively, both MCRs are described in the following chapters).[203,204]

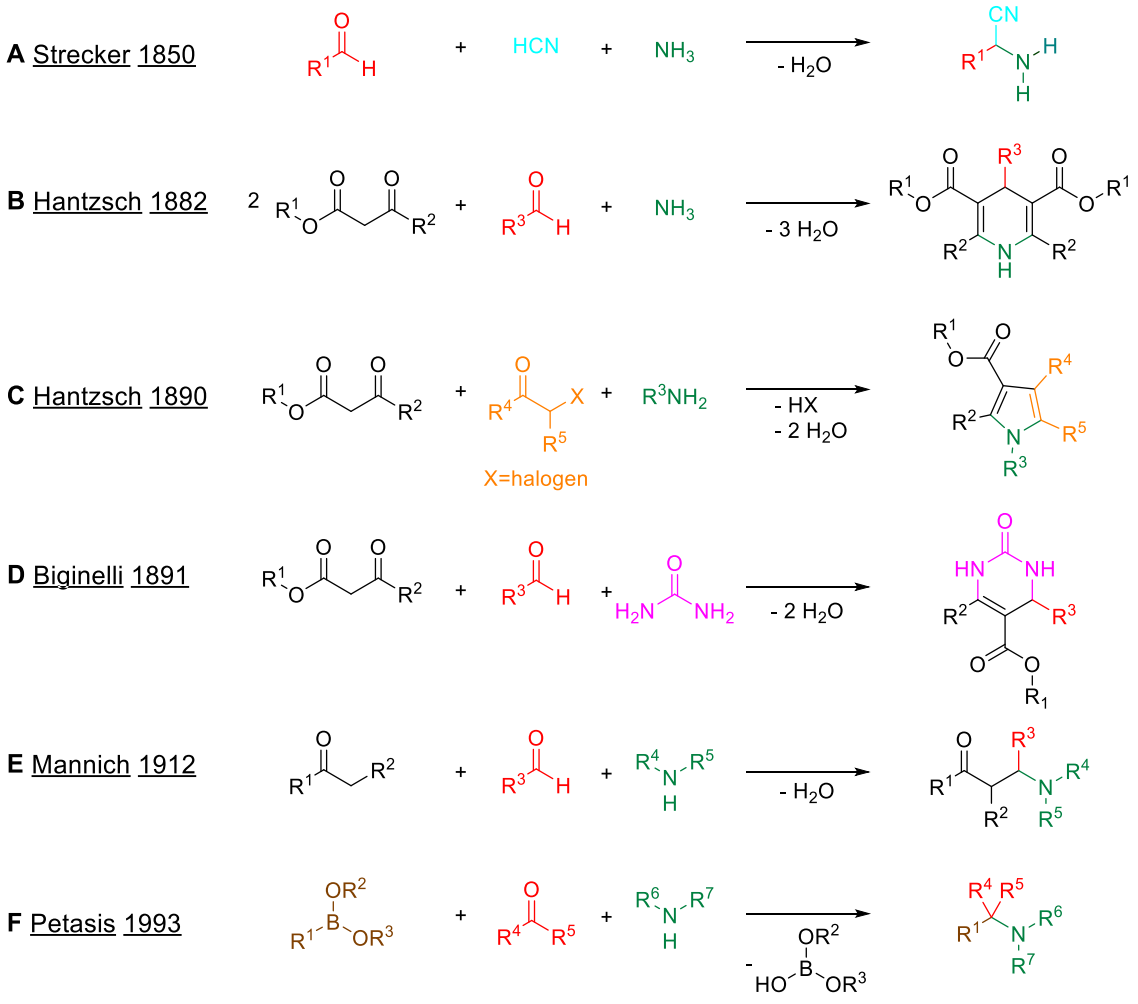

Scheme 12: Chronological overview of important MCRs. The starting materials are colored to highlight their implementation into the final product. Enolizable carbonyl groups are colored in black, aldehydes in red, amines and ammonia in green, halogenaldehydes in orange, urea in purple, cyanic acid in turquois and boronic acids in brown.

Thus, a variety of MCRs are well established in which several rely on the reactivities of the same compounds. Therefore, subgroups for MCRs can be introduced like the metal-catalyzed as well as isocyanide-and sulfur-base MCRs. In the metal-catalyzed MCRs, the key-step is mediated by a metal atom, which forms an organometallic intermediate triggering a following reaction sequence. Finally, the catalyst is released under formation of the product. Often transition metals like ruthenium or palladium are exploited as catalyst due to their ability to catalyze several different reactions.[205–208] Moreover, isocyanide- and sulfur-based MCRs rely on the inherent reactivities of the respective compounds and due to their importance for this work, they are discussed in the following chapters independently.

2.3.1 Isocyanide-based Multicomponent reactions (IMCR)

Isocyanide-based Multicomponent reactions IMCRs rely on the inherent and unique reactivities of isocyanide functional groups, like α-additions, α-acidity and carbene-like character (see chapter 4.1.). In this chapter, an overview of important IMCRs is given based on three reaction pathways, which can be only obtained by exploiting isocyanide groups. Finally, a brief evaluation of IMCRs is given in the view of Green Chemistry, since this was the overall framework of this work.

Most commonly, IMCRs proceed with an α-addition as key reaction step (in the following labelled as IMCR type-I). Thereby, the isocyanide group acts first as a nucleophile attacking a suitable electrophile. As a result, the isocyanide group is transformed to a nitrilium ion, which is a strong electrophile and thus react with an additional nucleophile (see Scheme 13), leading to the respective product. This sequence can also proceed in a concerted manner, in which the bond formation between the electrophile and the nucleophile proceeds simultaneously. This reaction step is applicable to a variety of different electrophiles and nucleophiles and thus, several IMCRs of type I have immerged over the last century. In the following, the most important ones are discussed according to their mechanism and provided details about their compound variety. Moreover, some examples of their application are given.

The first IMCR, discovered in 1921, is the so-called Passerini reaction.[209] A carboxylic acid and an aldehyde react with the isocyanide under step wise α-additions. According to recent DFT calculations, an acylimidate is formed that is not stable and undergoes an irreversible Mumm-rearrangement, immediately forming an α-acyloxycarboxamide (see Scheme 13**A**).[210] The overall driving force of the reaction was reported to be the oxidation of the isocyanide carbon from (+II) to (+IV),[182] however it has to be noted that the isocyanide carbon is transformed to an amide group with usually has an oxidation state of +III. One of the most astonishing features of the Passerini reaction is the variety of compounds that can be used. For instance, instead of the aldehyde component, other oxo-compounds like ketones, ketenes as well as acylcyanides and -isothiocyanates can be employed.[209,211–213] For the carboxylic acid, a broad scope of other acidic compounds is applicable as well as hydrazoic acid, hydrogen chloride, hydroxylamines, phosphinic acids and silanols.[214–218] Electron-poor phenols can also participate in this reaction as acid component, leading to the Passerini-Smiles reaction, since the irreversible rearrangement as last reaction step is a Smile-rearrangement.[219] By using alcohol and carbon dioxide, forming carbonic acid, a four-component Passerini reaction can be achieved.[185] Thus, a manifold of different substance classes can be obtained by the Passerini reaction (*e.g.* α-acyloxycarboxamides, hydroxytetrazoles, *N*,*N*-diacyloxamides, α-hydroxycarboxamides, α,γ-oxocarboxamides, α-cyanoarboxamides, α-aminoxycarboxamides, α-siloxycarboxamides). These products can be applied in several research fields like sequence-definition, Medical, Green Chemistry as well as polymer chemistry, further described in chapter 2.3.3.[186–188,193]

Adding an amine to the Passerini reaction results in the four component Ugi reaction (see Scheme 13**B**) that follows a similar reaction pathway compared to the Passerini reaction (see Scheme 13**A**). Here, an imine condensation takes place prior to the α-addition, leading to an α-acylaminocarboxamide.[182,220] The α-addition can take place in concerted manner in non-polar or in step wise manner in polar protic solvents, while again the overall driving force is the oxidation of the carbon isocyanide.[221] Like the Passerini reaction, the Ugi reaction allows a variety of different oxo and acid components for instance ketones, carboxylic acid, water, hydrazoic acids, phenols, salts of

secondary amines, cyanates, thiocyanates, hydrogen sulfide as $Na_2S_2O_3$ and hydrogen selenide.[182,222–226]

α-addition reaction step

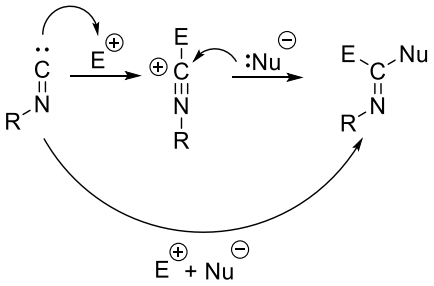

A Passerini

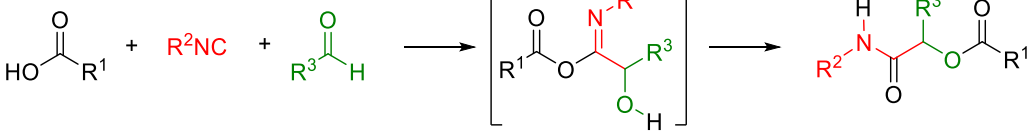

B Ugi

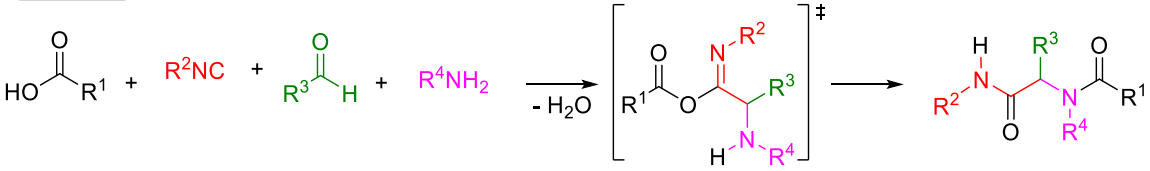

C Groebke-Blackburn-Bienaymé

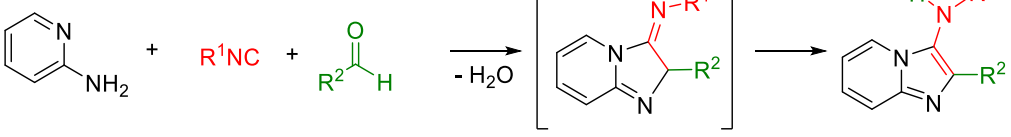

D Ugi-Dömling

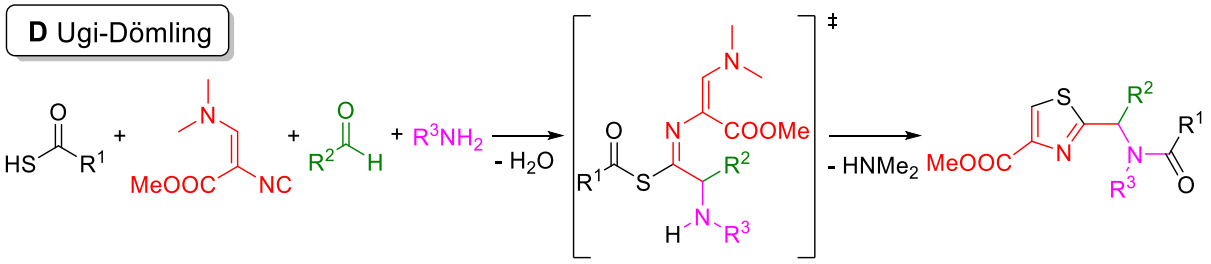

Scheme 13 Mechanistic pathway of the IMCR type-I in which an α-addition of the isocyanide functional group with an electrophile (E) and a nucleophile (Nu) is performed. The rection step can proceed step-wise or concertedly. In addition, an overview of important IMCR type-I is given while the key intermediates after the α-addition reaction are depicted as well. The starting materials are colored to highlight their implementation into the final product, isocyanides are red, aldehydes green, acid components black, and amines purple.

The Joullié-Ugi reaction is a three component modification of the Ugi reaction in which a cyclic imine is used.[227,228] Using α-amino acids in presence of an alcohol, a four-component five center Ugi reaction can be achieved yielding α-aminoacylcarboxamid esters.[229] By applying an alcohol and CO_2, COS or CS_2 as acid component a five component Ugi reaction is obtained.[203] Moreover, applying an Asinger product as imine component, a seven component Ugi-reaction can be performed.[204] In addition, the amine component holds further versatility, since besides primary and secondary amines also hydroxylamines, hydrazines, hydrazides and urea derivates can be used.[182] The application area of the Ugi reaction is vast and reaches from sequence-definition, Medical Chemistry to synthesis of organic compounds as well as polymer chemistry, further discussed in chapter 2.3.3.[230–235]

Grobke, Blackburn and Bienaymé discovered simultaneously the reaction of heterocyclic amidines like 2-amino pyridine, pyrazines or pyrimidines with aldehydes and isocyanides, leading to 3-amino imidazo[1,2-a]pyridines, pyrazines or pyrimidines (see Scheme 13**C**).[236–238] The reaction can be considered a derivation of the Ugi-reaction, in which the 2-amino *N*-heterocycle reacts as the amine group and later on with its endocyclic nitrogen as nucleophile. The acid compound is not incorporated in the final product and is typically a Lewis or Brønsted acid catalyst.[239] However, also other catalysts were reported including bases, ionic liquids and the absence of catalysts.[240–243] Formally, the reaction is considered a [4+1] cycloaddition reaction between the imine, formed prior by 2-amino heterocycles and the aldehyde component, and the isocyanide. Herein the oxo compound must be an aldehyde, since after the cyclisation step an aromatization takes place by a tautomerism of the former aldehyde proton. Compared to the Ugi and the Passerini reaction, aromatization is the last step of this cycloaddition rather than oxidation of the isocyanide carbon.[239] The imidazo-*N*-heterocyclic compounds have several applications, for instance there are widely used in Medical Chemistry due to their broad pharmacological effects but they can be also applied for Combinatorial Chemistry and formation of fluorescent compounds.[239,243–245]

In 2000, Dömling used a vinyl isocyanide bearing a tertiary amin and an ester group, which was reacted with an aldehyde, amine and a thiolocarboxylic acid in an Ugi-like reaction (see Scheme 13**D**).[246] However, due to the attached Michael system and its leaving group (tertiary amine group), the product after Mumm-rearrangement, α-acylaminocarboxthionoamide (compare the oxo analogue in Scheme 13**A**), further reacted in a 5-exo-trig cyclization reaction forming α-acylaminothiazoles. The cyclization was possible, since the thionoamide is inherently nucleophilic at the sulfur atom.

A second type of IMCR (in the following labelled as IMCR type-II) uses the reactivity of the acidic α-CH_2 group of the isocyanide group as well as the isocyanide carbon (see Scheme 14). The acidity of the α-CH_2 group is thereby increased by additional electron-withdrawing groups (EWG) like tosylates or esters that are attached to the group. In the presence of an imine, the carbanion is formed by deprotonation and, subsequently reacts as a nucleophile attacking the imine in a Mannich reaction like fashion. Subsequently, the formed amine attacks the isocyanide carbon in return, nucleophilically. The final step is usually a proton transfer towards the negatively charged, former isocyanide carbon. The overall reaction can be considered a formal [2+3] cycloaddition reaction.

The first reported reaction according to this mechanism is a derivation of the Van-Leußen oxazole reaction, in which an aldehyde, amine and tosylmethyl isocyanide react forming imidazoles (see Scheme 14**A**). It was first reported in 1977 by Van-Leußen but as a two-component reaction using an aldimine, which was prepared beforehand.[247] Later on, the three-component reaction was established as well.[248–250] The reaction was performed in presence of an external base besides the

imine.[247] After the formation of 2-imidazoline, an elimination reaction of the proton of the former aldimine takes place, mediated by the base resulting in the extrusion of the tosylate group under aromatization. Nowadays, this reaction is used for instance in Medical Chemistry due to the importance of the imidazole moiety exhibiting pharmacological and biological activities.[248–250]

α-acidity+isocyanide as electrophile

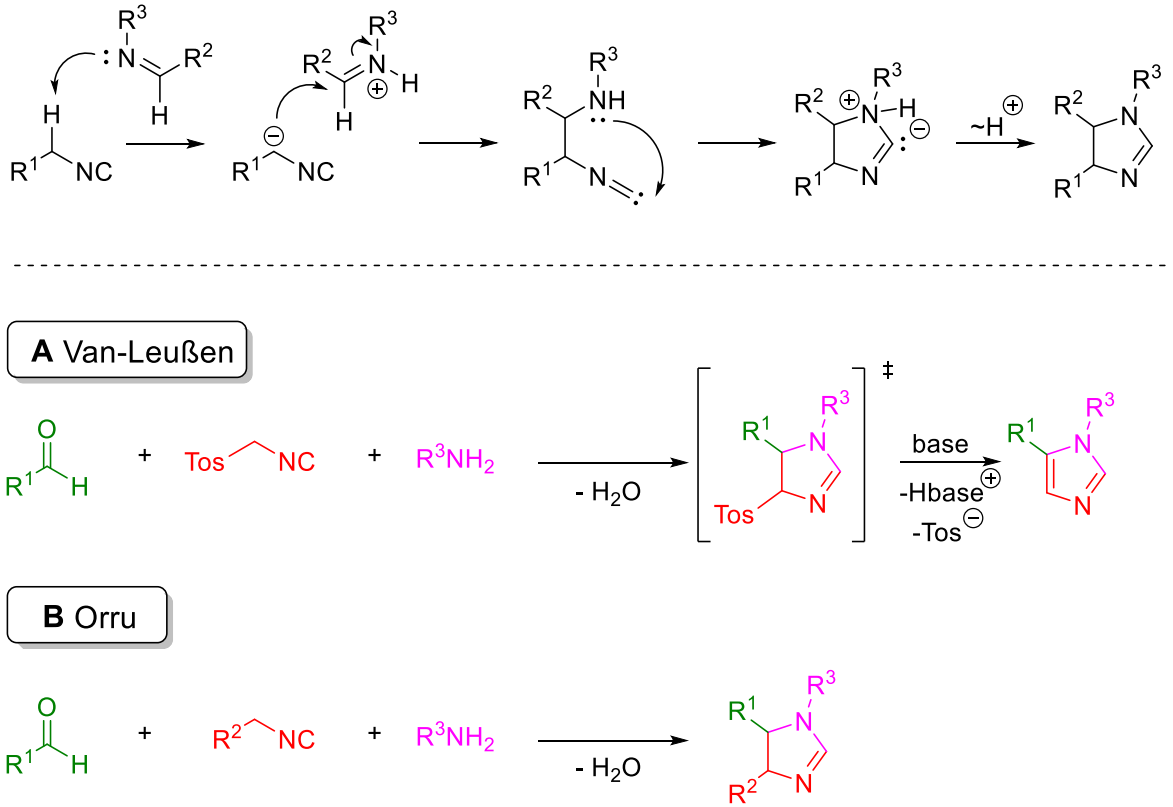

*Scheme 14: Mechanistic pathway of the IMCR type-II, in which high α-acidity of the α-CH_2 group of the isocyanide functional group is needed. In the presence of a good leaving group like toluenesulfonyl group (Tos) and an external base the Van-Leußen reaction can be performed (**A**) while without an external base the Orru reaction can proceed (**B**). The starting materials are colored to highlight their implementation into the final product, isocyanides are red, aldehydes green and amines purple.*

In 2003, Orru *et al.* used the same three components to form 2-imidazolines but this time no additional base was employed. The isocyanides were in α-position to ester and 9-fluorene groups instead of tosylate functionalities (see Scheme 14**B**).[251] Later, also ketones were successfully reacted as substituents for the aldehydes.[252] Moreover, Zhu *et al.* reported that with isocyanides bearing additional ester or amide groups, oxazoles rather than imidazolines can be obtained following an α-addition pathway (IMCR type-I, see above). In the following year, reaction protocols were established to selectively chose the final product by altering the catalysts and using amide groups instead of ester groups.[252,253]

Finally, IMCRs of type-III procced by double bond formation of the isocyanide carbon with a chalcogen like sulfur or selenium. This reaction type was first reported nearly a decade ago and the mechanism is not fully understood yet, but it is usually assumed for sulfur that the chalcogen is activated by a base beforehand and forms an oligo-or polymeric sulfur chain. This sulfur compound attacks the isocyanide nucleophilically and subsequently, it is stripped of one of its atoms by elimination due to the attack of the formed carbanion (see Scheme 15, for further detail of the

activation of sulfur see also chapter 2.2.1.). Here, the product is an isoseleno- or isothiocyanate, which is subsequently attacked by a third component that serves as additional nucleophile.

C=S double bond formation-reaction step

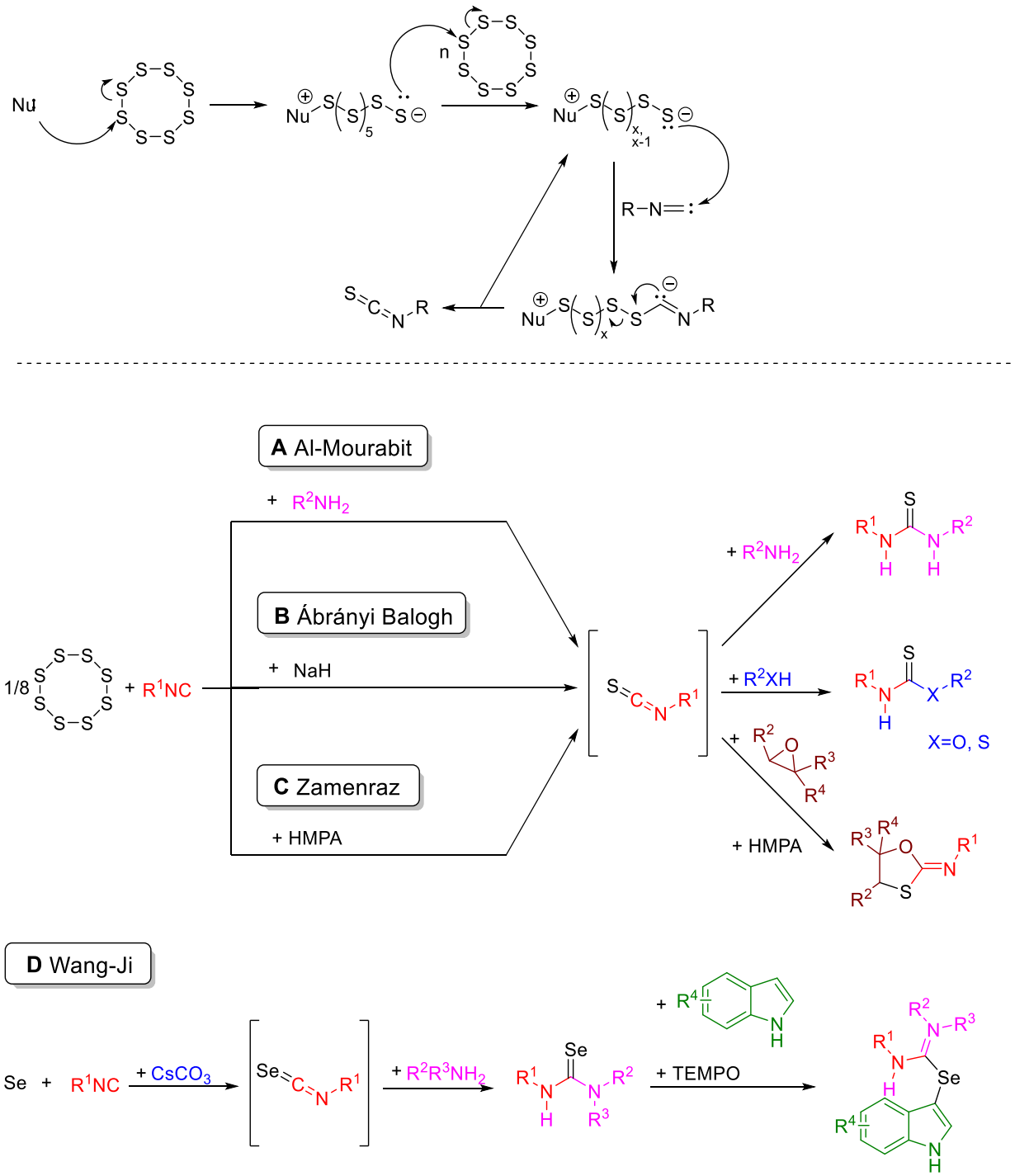

Scheme 15: Mechanistic pathway of the IMCR type-III in which a C=S double bond is formed (top). The chalcogen (here elemental sulfur, S_8) is activated by a base (Nu) forming a sulfur chain derivative which attacks the isocyanide carbon nucleophilically. In the folowing it is stripped off of its terminal atom yielding the isothiocyanate as well as the polymeric chain reduced by one atom, which can reacts again with another isocyanide and so on. In addition an overview of several IMCR type III reactions is given (bottom). The first reaction step is always the formation of the iosthio or isoselenocyanate initiated by the external base (amine, NaH or HMPA). Starting materials are colored to hihghlight their implementation in the final product, sulfur and selenium are black, isocyanides red, amines purple, alcohol and thiols blue, epoxides brown and indols green.

The first IMCR type III was reported already by Lipp *et al.* in 1959 using isocyanide, sulfur and aromatic amines forming thioureas.[254] Decades later, in 2014, Al-Mourabit *et al.* established the conversion of primary and secondary amines for this MCR (in the following labelled as AM-3CR).[10] Since this reaction was crucial for this thesis, see chapter 2.2.1. for a detailed discussion about the reaction mechanism. In 2021, Ábrányi-Balogh *et al.* reported a modification of the AM-3CR, in which 2-bromoacetophenone is added after conversion of the isocyanide to react with the formed thioureas to 2-imino and 2-aminothiazoles.[133] In the same year, the same group could show that if DBU, DBN or TBD was used as amine component for this reaction in aqueous conditions, a ring opening of the amidines and guanidines took place, resulting in thiourea bearing additional lactam or cyclic urea groups.[138,139]

Furthermore, Ábrányi-Balogh *et al.* reported that amines could be substitutes by either an alcohol or a thiol yielding thiono- or dithiocarbamates if an external base like sodium hydride was used (see chapter 2.2.1).[143] Using isocyanides, sulfur and an epoxide mediated by HMPA Zamenraz *et al.* could obtain 1,3-oxathiolane-2-imines.[157]

Recently, Ji and Wang introduced a four component IMCR between isocyanides, selenium, secondary amines and indoles under basic and oxidative conditions to form isoselenothiocyanate *in situ*, which was reacted to the selenourea compound and finally to the isoselenourea product.[255]

To sum up, IMCRs are not only a small niche group of MCRs, they are rather a multitude of different reactions offering a variety of different complex scaffolds as products, which can be easily obtained in one-step. This variety originates directly from the diverse reactivity of the isocyanide functionality, *i.e.* α-addition, α-acidity and carbene-like reactions (excluding the intrinsic variety of the Ugi and Passerini reaction due to their long list of suitable acid, amine and oxo components). However, the fact that MCRs have a positive impact of the degree of sustainability and are often used in Green Chemistry as a toolbox reaction, as discussed in chapter 2.1.2., should still be briefly evaluated. Principles of Green Chemistry should always be considered prior, meaning just because MCRs are nowadays considered to be “in general” sustainable reactions, does not hold true for all of them or that none of them can be further improved in terms of sustainability. This counts also for IMCRs. While starting materials of MCRs are usually easily accessible, including commercially available functional groups, which are also abundantly present in renewable feedstock, isocyanides are not.[68,256] They need to be prepared typically from the respective amines involving an excess of often toxic reagents like phosphoryl chloride, thionyl chloride, phosgene or its derivate (for a more detailed overview over the synthesis of isocyanides see chapter 4.1.).[68,257,258] Justifiably, Ruijter and Orru stated that “this is unequivocally the most valid argument holding down the expansion of isocyanide multicomponent reactions as truly green methods”.[68] Dömling *et al.* established an *in situ* protocol in which *N*-formamides were converted to isocyanides and then applied to an IMCR in the same pot, reducing waste and time as well as obtaining similar or superior yields than usual procedures.[259] More recently, the same group reported a superior synthesis protocol for isocyanide synthesis with the toxic compound phosphoryl chloride.[260] Thereby, the work-up was minimized to a one-step short silica plug/filter column filtration, reducing contact time with the toxic reagents and waste whereas yields were increased. Furthermore, highly sensitive isocyanides, which could not be isolated with other methods, were obtained with this method as well. The overall improvement was visible in the strong decrease of the E-factor (*e.g.* E-factors for the synthesis of phenylethyl isocyanide ranged from 60-83 while the optimized method led to an E-factor of 8.4). Concluding, a greener isocyanide synthesis would probably allow the IMCRs to obtain the rank of a sustainable reaction, while this labelling should never be taken for granted and a reevaluation according to the principles of Green Chemistry is highly recommended. While highly efficient procedures are nowadays available allowing

a considerable decrease in waste, a less toxic replacement for the dehydrating reagents like phosphoryl chloride is highly desired.

Finally, if a more sustainable isocyanide synthesis approach is ensured, the combination of IMCRs with the use of elemental sulfur as starting material exhibits a high potential for sustainable chemistry. This is highlighted for instance by the thiourea synthesis starting from isocyanides, sulfur and amines, for which several modifications are already established increasing its potential even further.

2.3.2 Sulfur-based multicomponent reaction (SMCR)

Elemental sulfur has the potential to mediate and undergo several different reaction steps, like oxidation, reduction, sulfanylation or thionylation (see also chapter 2.2 and 2.2.1.). Therefore, it is not surprising that several MCRs harvest this versatile reactivity by using sulfur as one of its starting materials, like the IMCR using isocyanides (see previous chapter). Considering that sulfur is a highly abundant waste product of the petrochemistry (80 million tons in 2021),[101] which keeps accumulating since no large process on industrial scale rely on this compound apart from sulfuric acid production, its utilization *per se* goes in hand with Green Chemistry (see also chapter 2.1).[261] In the following, the most important sulfur-based MCRs (SMCRs) are discussed and complemented by more recently discovered reactions, highlighting the increasing progress of this research area of sulfur chemistry. Mechanistic investigations of the reactivity of elemental sulfur for several reaction steps are still in their infancy. Thus, the mechanism of the following reactions is still under debate and being only discussed briefly as far as it is reported (for the activation of sulfur by base, see chapter 2.2.1. for a thorough discussion).

The first reported SMCR is the Willgerodt-Kindler reaction, in 1887. Willgerodt discovered the MCR without the use of elemental sulfur, but ammonium sulfide, which was reacted with acetophenone and ammonium hydroxide to form 2-phenyl acetamide.[262] Later in 1923, Kindler established a modification using elemental sulfur and ammonia together with acetophenone to obtain 2-phenyl thioacetamide, decreasing the reaction temperature from 160 to 100 °C (see Scheme 16**A**).[263] Nowadays, the scope of the starting material for the Willgerodt-Kindler reaction has increased immensely. Instead of ammonia, primary and secondary amines can be applied as well.[263,264] Substitution of the ketones can be obtained by using aldehydes, alkynes, acetals, alkenes, thiols, imines, benzyl halides and cinnamic acids.[264–268] The most astonishing feature of this SMCR is the migration of the carbonyl function if a ketone is used towards the terminal alkyl chain like in a Zipper reaction.[264] However, with increasing chain lengths, the yield of the conversion decreases and it is considered that reasonable yields can be obtained with alkyl chain consisting of two to three carbons.[264,269] Furthermore, the obtained thioamides can be easily converted to the respective thioesters and carboxylic acids, increasing the versatility of this SMCR even further.[270,271] However, today the reaction can be seen as underutilized compared to its potential.[264] It is still used in Medical Chemistry, heterocycle synthesis and for crop protection products.[272–275]

Since the scope of the starting materials in the Willgerodt-Kindler reaction is so large, it is hard to evaluate one mechanism for all of them. Nowadays, the mechanism of Carmack *et al.* is widely accepted for the case of ketones.[174,175] The first reaction step is an imine condensation with the amine component, followed by tautomerization to the enamine. Due to the mediation of an *in situ* formed aminopolysulfane compound, regioisomerism towards the terminal alky group takes place, reducing the formed carbonyl carbon. After the terminal enamine compound is formed, an oxidation of the terminal carbon is performed by attack of an aminopolysulfane species followed by a [1,2]H-shift forming the thioamide (see chapter 2.2.1. for more details). Substitution of sulfur with selenium was also reported, yielding the respective selenothioamide.[276]

The probably most known SMCR is the Asinger reaction, which was discovered in 1956.[277] It consists of elemental sulfur, ammonia and two equivalents of a ketone, which makes it a four-component reaction (see Scheme 16**B**). Thereby, 3-thiazolines are usually obtained as the main product, which are an important substance class exhibiting pharmacological and biological activity.[277–279] Compared

to other SCMRs, the reaction is conducted at room temperature.[279] One of the major applications of the Asinger reaction is the synthesis of D-penicillamine a non-proteinogenic amino acid, which is used for instance against rheumatoid arthritis, Wilson´s disease and heavy metal poisoning.[278,280–283] The reaction mechanism is not fully understood yet, but a reasonable pathway is considered to start with an imine formation of the ketone and ammonia.[279] Then, tautomerization to the enamine allows the sulfanylation of the former α-CH_2 group, followed by the cyclization with the second ketone, which has formed its respective imine, under extrusion of ammonia. Different ketones can be used for this reaction, however if both are enolizable, a mixture of products is obtained.[278] Aldehydes are in general not applicable, besides isobutyraldehyde that is used for the synthesis of D-penicillamine. Ammonia can be replaced with aziridine to react with a ketone, such as pentan-3-one to obtain 5,6-dihydro-1,4-thiazines. In this case also the substitution of sulfur with selenium was reported. Besides, a modified three-component Asinger reaction called “resynthesis” can be performed without elemental sulfur using an α-sulfanylketone, ammonia and a second oxo component.[279]

In 1966, Gewald reported a reaction between nitriles bearing a second EWG in α-position like ester, amide or nitrile reacting with an oxo compound (aldehydes, ketones, 1,3-dicarbonyl compounds) and sulfur using a secondary amine obtaining 2-aminothiophenes (see Scheme 16**C**).[284]

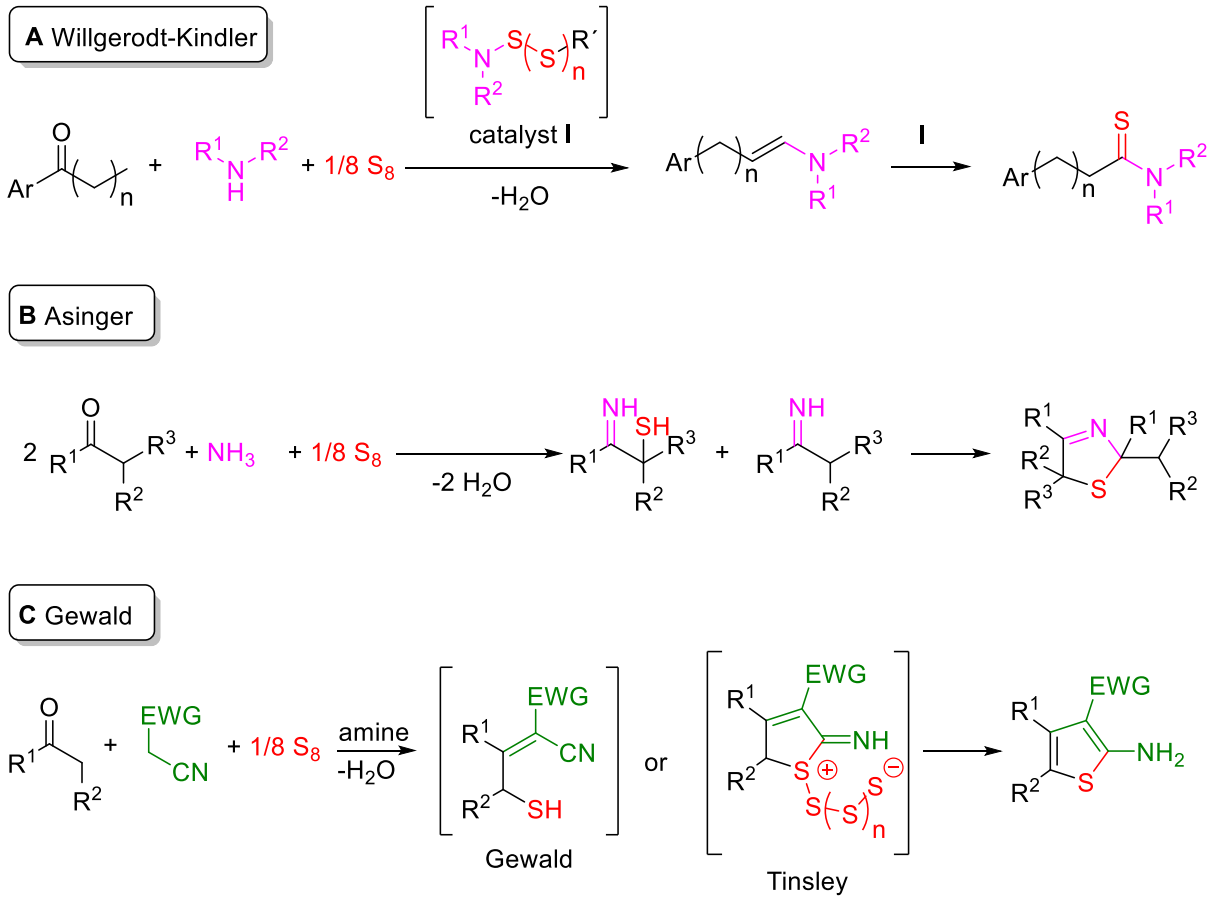

Scheme 16: Overview of classic SMCRs. Important intermediates are depicted while the starting materials are colored to highlight their implementation in the final product. Carbonyl compounds are black, amine purple, 1,3 carbonyl derivatives are green and sulfur red.

In this reaction, a Knoevenagel condensation is believed to be the first reaction step.[285,286] The following reaction steps are not yet identified, hence discussed differently in literature. Gewald proposed sulfanylation of the obtained Michael system in γ-position (α-CHR group of the former oxo compound), comparable with the pathway of the Asinger reaction.[284] Subsequently, the thiol attacks

the nitrile in a 5-exo-dig ring closing reaction. Tinsley assumed that instead of the formation of a thiol functional group, a polysulfide chain is formed, which ultimately results in ring closing upon extrusion of a one atom smaller sulfur ring.[161] In both pathways the final thiophene is obtained after tautomerization.[161,284] Application of this reaction is found in Combinatorial and Medical chemistry, for instance as low molecular weight inhibitors.[286]

Since recently the reactivity of elemental sulfur has gained more interest, several new SMCR have been reported. In the following, no reaction mechanism is discussed since no pathway could be fully proven so far. Nevertheless, all reports propose mechanisms following the reaction pathway of the formation of a polysulfane chain intermediate by the ring opening of the octasulfur ring using a base as nucleophile (detailed examples of this mechanism are given in chapter 2.2.1.). Several modifications of the Willgerodt-Kindler reactions were reported, as listed in the following: the reaction between i) sulfur, primary/secondary amine and a benzylic amine, ii) sulfur, primary/secondary amine and terminal alkyne, iii) sulfur, aryl/alkyl chlorides and formamide and iv) sulfur, benzylic/cinnamic acids and primary/secondary amines.[132,150,160,166] The latter reaction protocol is special in the sense that a decarboxylation of the benzyl and cinnamic carboxylic acid takes place, resulting in an aryl and benzylthioamide, respectively, meaning the carbonyl compound is migrating towards the phenyl ring (see Scheme 17**A**, compare Scheme 16**A**).[166] Moreover, Peng and Fu established a Willgerodt-Kindler modification with sulfur, acetophenones and cyanamide as amine component resulting in heterocycle formation yielding 2-amino-4-arlythiazoles (see Scheme 17**B**).[287]

Not only new modifications of already known SMCRs were reported. In 2015, Samzadeh-Kermani studied reactions of terminal alkynes with sulfur and epoxides or tosyl aziridines to obtain 1,3-oxathiolane- and 1,3-thioazolidin-2-alkylidenes. Here, sodium hydride was present, while performing the reaction at elevated temperature leading to yields of 67-92% (see Scheme 17**C**).[144] In 2017, Nguyen *et al.* was able to obtain 2-aryl benzothiazoles by reacting *o*-nitro halobenzenes with aryl aldehydes and elemental sulfur in the presence of morpholine in a redox cyclization (see Scheme 17**D**).[134] Electron-rich and poor moieties were tolerated for either the aldehyde or the halobenzene, yielding 61-80% of the products at a reaction temperature of 130 °C. To obtain the thiazole, the nitro group was reduced by oxidation of one sulfur atom to SO_3 which was proven by the isolation of the sulfonated thiazole product as side product. Further, two equivalents of acetophenones and sulfur can form 2,4-diaryl thiophenes under the mediation of aniline and *p*-toluoenesulfonic acid with yields up to 88% at temperatures above 100 °C (see Scheme 17**E**).[288] Also tetrasubstituted tricyclic thiophenes could be obtained with non-aromatic ketones, such as cyclopentanone, while other aliphatic ketones resulted in complex mixtures. By C-H bond functionalization of anilines with sulfur and carbon dioxide using sodium *tert*-butanolate, Zhang and Yu were able to obtain thiazolidine-2-ones in moderate to good yields (up to 87%) at 140 °C (see Scheme 17**F**).[162] By using naphthalene-1-amines, it was further possible to obtain thiazinan-2-ones as well.

Recently, also the combination of isocyanides and sulfur have yielded new MCRs by the *in situ* formation of isothiocyanates. Three important examples of this sulfur and isocyanide-based MCR type were already discussed in the previous chapter and are depicted in Scheme 15**A-C**.

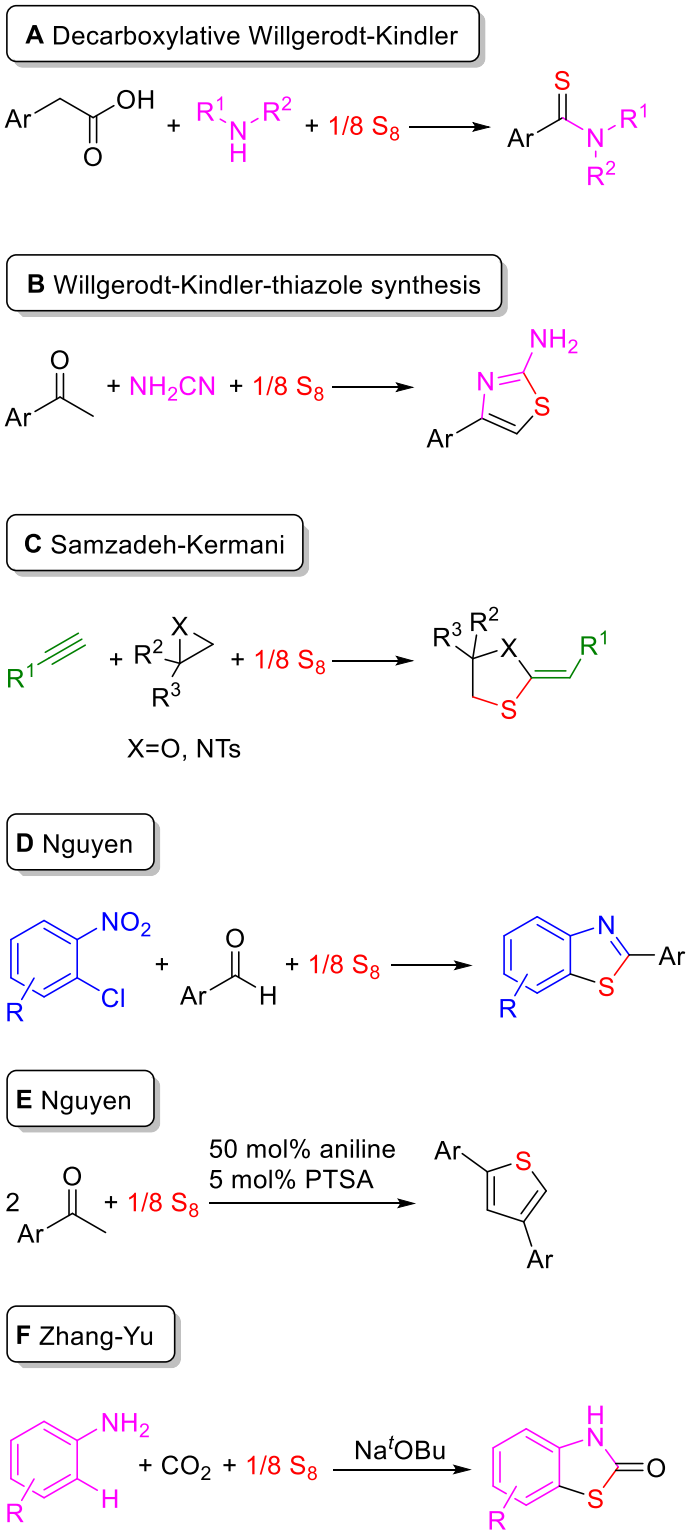

Scheme 17: Overview of recently introduced SMCRs. Starting materials are colored to highlight their implementation in the final product. Oxo compounds are black, amines purple, sulfur red, nitroaryls blue and alkynes green.

Nowadays, more and more new SMCR are reported, as sulfur is a highly versatile reagent of increasing interest, broadening the scope of the already well applied long known reactions (Asinger, Gewald, Willgerodt-Kindler). Moreover, the more frequent utilization of sulfur, an abundant and non-toxic waste product, is desired from a sustainability point of view. Thus, research in SMCR is expected to further grow in the following years.

2.3.3 IMCRs and SMCRs in Polymer Chemistry

Only a decade ago, the manifold opportunities of MCRs were realized in the field of polymer chemistry.[289–291] Today, many different MCRs are frequently applied in polymer chemistry, including, for instance, the Biginelli reaction[292,293] or the Hantzsch reaction.[294] The most efficient and versatile MCR for polymer chemistry, and especially for step-growth polymerizations, are IMCRs. Considering these IMCRs, especially the Passerini three- (see Scheme 13**A**) as well as the Ugi four component-reaction (see Scheme 13**B**) are now frequently used tools in polymer science and can be applied for monomer synthesis, grafting reactions, as well as step-growth polymerizations.[295] To provide an overview, the most relevant developments in IMCR-based polymerizations will be described in this chapter. Furthermore, suitable examples of SMCRs are given as well.

In 2011, Meier *et al.* introduced a polymerization protocol using the Passerini three-component reaction. For the first time it was shown that MCRs are not only suitable for monomer synthesis but also for highly efficient and structurally versatile step-growth polymerizations as well as grafting-onto approaches.[296] Carboxylic diacids (AA-type monomers) and dialdehydes (BB-type monomers) were reacted with various isocyanides to yield α-amide substituted polyesters with molecular weights up to 56 kDa (see Scheme 18**A**). In the following, Li *et al.* reported the Passerini polymerization of a carboxylic diacid and a diisocyanide with different aldehydes on the one hand, and the reaction of a dialdehyde and a diisocyanide with various carboxylic acids on the other hand.[297,298] Poly(ester amide)s with molecular weights up to 15 kDa and polyamides with ester side chains with molecular weights up to 17 kDa were obtained, respectively. Both groups also contributed to the development of Passerini polymerizations employing AB-type monomers containing an aldehyde or ketone and a carboxylic acid moiety.[299–301] Similar early developments were achieved using the Ugi four-component reaction for polycondensation reactions to yield diversely substituted polyamides under mild reaction conditions.

Initially, Meier *et al.* investigated optimized polymerization conditions for the combination of two bifunctional and two monofunctional components (six combinations are possible: diisocyanide + dialdehyde, diamine + diisocyanide, dialdehyde + diamine, diamine + carboxylic diacid, dialdehyde + carboxylic diacid and diisocyanide + carboxylic diacid, see Scheme 18**B**).[302] Precipitated polymers with molecular weights above 10 kDa were obtained for all six combinations, while operating under mild polymerization conditions. Subsequently, the same group demonstrated that the acid component can be replaced by CO_2 and an alcohol, leading to non-isocyanate polyurethanes *via* the Ugi five-component reaction.[303] Luxenhofer *et al.* also investigated the six above-mentioned possible component combinations of the Ugi reaction bearing aromatic moieties in the backbone and side chain of the polymers, revealing that in nearly all cases the polymer backbone is formed during the Mumm rearrangement.[304] After these initial trend-setting reports on Ugi- and Passerini-based step-growth polymerizations, both polymerizations are nowadays broadly applied for the synthesis of structurally diverse polymers offering different application possibilities.

For instance, Li *et al.* demonstrated photo or redox degradable Passerini type polymers bearing an *o*-nitro benzylic moiety (cleavable by irradiation with UV light), a disulfide group (cleavable by reduction with DTT), or a pinacol boron ester benzylic moiety (cleavable by oxidation with hydrogen peroxide).[305,306] Such degradable Passerini-derived polymers bearing disulfide groups were later applied in the field of drug delivery.[307] Furthermore, the group of Li demonstrated the synthesis of Passerini polymers with tertiary ester linkages with M_n of up to 30.6 kDa and promising material properties by applying several electron deficient ketones as reactants.[308] Recently, Barner-Kowollik *et al.* introduced the visible light-induced formation of poly(amide thioester)s, prepared by the *in situ* generation of thioaldehydes, which were subsequently applied as oxo components in a Passerini

polymerization. These polymers were shown to be cleavable by aminolysis as well as chain-extended by insertion of thiiranes due to the reactivity of the thioester group.[309] In 2016, Becer *et al.* used the renewable platform compound levulinic acid in an Ugi polymerization with several diamines and diisocyanides to prepare polyamide lactams with M_ns of up to 12.3 kDa.[310] In the same year, Wang *et al.* synthesized polypeptoids *via* an Ugi polymerization using amino acids as starting materials and demonstrated their biocompatibility, antibacterial activity as well as their application possibility in the field of drug delivery.[311] Further examples are countless, as a new research direction in polymer synthesis was established. This new field ranges from polypeptoids and other functional bio(medical)-materials *via* self-healing hydrogels to various macrocyclic systems, clearly demonstrating the synthetic versatility of IMCRs, which translates into designed application possibilities.[312–316]

Compared to the multitude of applications of IMCRs for polymer synthesis, examples for SMCRs for the synthesis of sulfur-containing polymers are scarce in literature, especially in which the MCR itself is the step-growth reaction. An example is the Willgerodt-Kindler reaction of sulfur, dialdehydes and diamines, which was applied for the synthesis of polythioamides in yields up to 96% and molecular weights up 38 kDa (see Scheme 18**C**).[317] Another variation using sulfur, dialkynes and diamines was also reported for the synthesis of polythioamides emitting fluorescence under UV irradiation.[318]

Finally, the most relevant development of MCR chemistry for polymer science for this thesis is the recent report of Tang *et al.* on the one-step conversion of elemental sulfur with primary or secondary diamines and diisocyanides to yield polythioureas (see Scheme 18**D**).[169]

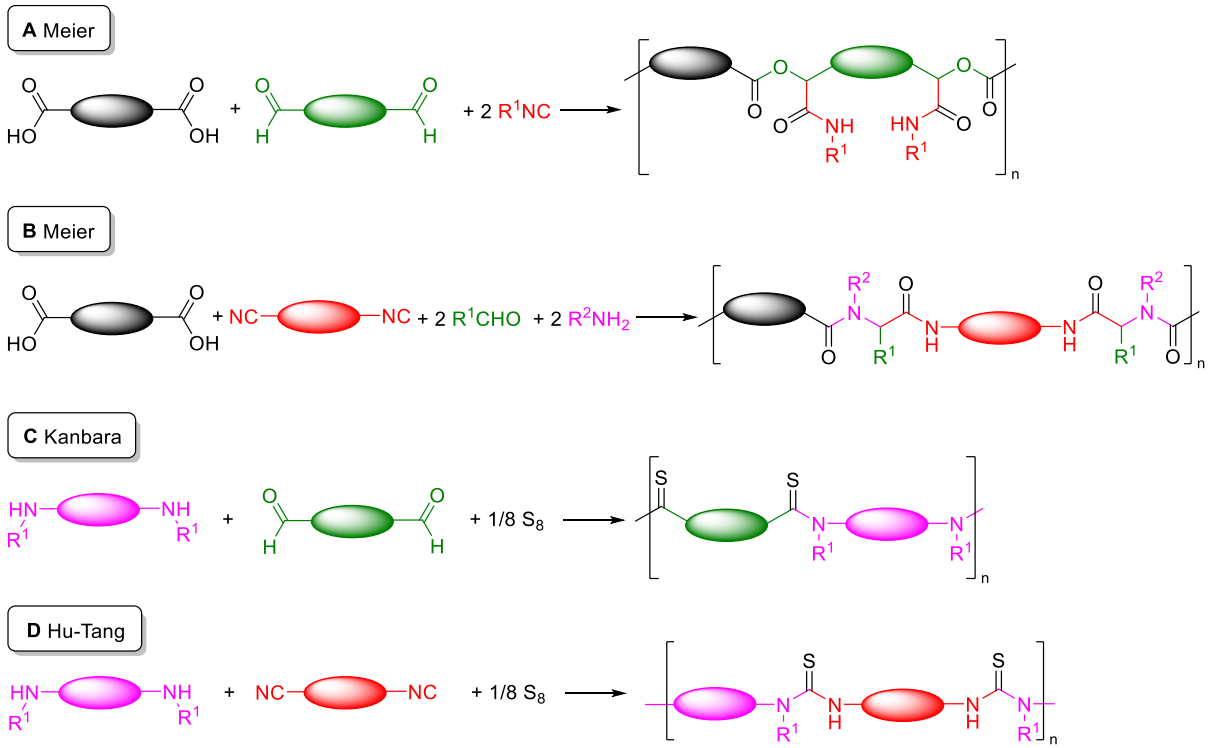

Scheme 18: Overview of IMCR and SMCR based step-growth polymerizations. The starting materials are colored to highlight their implementation in the final polymer. Carboxylic acids and sulfur are black, isocyanides red, aldehydes green and amines purple.

This polymerization approach used the AM-3CR (see Scheme 15**A**).[10] For the polymerization approach, aliphatic primary and secondary diamines were combined with aliphatic and aromatic diisocyanides to yield high molecular weight polymers that were suitable for Hg^{2+} binding and removal from water.[169] Some very basic material properties were described, while sustainability was,

apart from using elemental sulfur and potentially renewable diamines, not addressed. For instance, unfavorable DMF/toluene mixtures were used for polymerizations and the overall strategy related to large amounts of generated waste (for instance during monomer synthesis). Catalytic activity of either the poly(thiourea)s or defined low molecular weight organic compounds were not reported. The modification of this MCR by Ábrányi-Balogh *et al.* was later also transferred to polymer chemistry obtaining poly(thionocarbamate)s exhibiting a high refraction index and could be used as mercury sensor.[143,146]

Concluding, IMCRs show a broad spectrum of applications in polymerization reactions for the synthesis of a variety of useful materials. On the other side, SMCRs are rarely applied for the preparation of polymeric materials. Considering the straightforwardness of implementing sulfur-atoms into polymers, more research on this area should be expected as the interest in elemental sulfur is constantly growing. In addition, it must be mentioned that optimization in terms of Green Chemistry often stops with the use of a MCR for the polymerization. Seldomly, the typically used toxic solvent like DMF are tested for possible substitution by more benign alternatives, nor the amount of waste is further decreased in additional optimizations of the reaction or the work-up. Nevertheless, renewable feedstocks are frequently applied as starting material which facilitates the overall degree of sustainability of the MCR polymerization.

2.4 Thioureas

The thio analogues of urea are called thioureas, while additionally lending its name to the respective functional group and the group of substituted thioureas. this chapter focuses on substituted thioureas (TUs), which can be generally divided into four subtypes with respect to their degree of substitution of both nitrogen atoms, namely mono-, 1,1- and 1,3-di-, tri- and tetra substituted TUs (see Scheme 19).

TUs can be found in many applications due to their intrinsic properties and reactivities. For instance, TUs are known to exhibit a broad spectrum of biological activities and can thus be used in agriculture (*e.g.* antifungicidal,[319] herbicidal agent,[320] or rodenticide)[321] or in medicine (*e.g.* anti-thyroid,[322] anti-tumor,[11] anti-epileptic,[323] anti-hypertonic agent,[324] or antioxidant).[11] Furthermore, they are used in dyes, photographic films, textiles or in plastics.[13] More recently, corrosion inhibition properties were reported as well.[325] In chemistry, TUs are widely used as intermediates for heterocycle,[326–330] amidine[331] or guanidine synthesis,[332–334] or as ligands in the formation of metal complexes.[335–339] In addition, TUs are prone to form hydrogen bonding with many electron-donating substrates, especially the 1,3-disubstitued TU derivatives.[340,341] Due to these supramolecular interactions, they have emerged as a strong tool in the field of organocatalysis in the last decades, which is discussed more thoroughly in the following chapter. The ability to work as a receptor for anions by host-guest complexation[342–345] is also used frequently.

Due to the excessive use of these compounds, several routes for the synthesis of TUs were reported over the last century. However, typically toxic compounds like isothiocyanates (ITCs) and carbon disulfide are exploited for their syntheses, while other more sustainable and less toxic synthesis protocols seem to be rather scarce. In the following, typical procedures for TU synthesis are discussed, while sustainable progress and synthesis are emphasized.

Typically, a one-step procedure is applied by using an amine and an ITC to obtain TUs (see Scheme 19**A**). This addition reaction is straightforward, since usually the compounds are simply stirred in solution at elevated or room temperature, while tolerating a broad scope of moieties. Even less reactive arylamines can be converted under these conditions by addition of a base[15] or applying increased pressure (0.6 GPa).[346] Thus, mono,[347] 1,3-di[11,348,349] and tri substituted[12,350,351] TUs can be obtained easily, while 1,1-di and tetra substituted ones can intrinsically not be formed. In 2000, Kaupp and *co*-workers established a more sustainable modification of this synthesis route by applying gas-solid reactions using volatile amine components like (methyl) ammonia or solid-solid reactions applying a ball-mill or grinding with a mortar.[352] Thus, no solvent had to be applied and several TUs were obtained in quantitative yield, reducing the waste drastically. The advantages of mechanochemical techniques was then further elaborated by Friščić and *co*-workers who synthesized 49 symmetric and unsymmetric 1,3-aryl/aryl and aryl/alkyl TUs in a rapid fashion.[16]

On the other hand, carbon disulfide is often exploited, converting one or two amines to the desired TU. This reaction proceeds *via* the formation of a dithiocarbamate salt, which is further transformed to the respective TU under heating[13,353] or the use of a base.[14,354–356] The latter proceeds *via* addition of a second amine component under the elimination of hydrogen sulfide or its salt (see Scheme 19**B**). In contrast to the before mentioned approach *via* ITCs, 1,1-di[357] and tetra[356] substituted TUs can be obtained as well. Zhang and co-workers reported that ball-milling under basic conditions was found to facilitate the reaction in a more sustainable fashion, resulting in several 1,3-disubstituted

unsymmetric TUs.[358] However, an increased excess of carbon disulfide (5.00 eq) had to be applied. In contrast, symmetric TUs were obtained using only one equivalent of carbon disulfide. Another environmentally more benign procedure was reported by Dalal and *co*-workers, who obtained 1,3-TUs bearing aryl or benzylic moieties performing the reaction in water without stirring while exposing the mixture to sunlight.[359] After simple filtration and recrystallization, the products were obtained avoiding additional waste.

The use of other thionylation reagents, *i.e*. thiophosgene[15] or its derivatives (*e.g.* bis(1-benzotriazolyl) methanethion,[16] phenyl chlorothionoformate)[17] is common as well (see Scheme 19**B**). Symmetric 1,3-TUs can be obtained in one step by two consecutive addition elimination reactions of two amine molecules.[15] Converting only one equivalent of the amine component with the respective thionylation reagent usually yields the respective ITC but in some cases a different intermediate is present. For instance, converting secondary amines permits the formation of an ITC.[355] Stable thiocarbamyl derivatives can be isolated in these cases, which can be further reacted to an unsymmetric TU in a second step (see Scheme 19**B**).[16,17] With this approach, mono,[360] 1,1-[355] and 1,3-di,[16] and tetra[361,362] substituted TUs can be obtained as well. In 2016, mechanochemical and gas-solid reaction techniques were reported for this approach as well by Štrukil and *co*-workers using bis(benzotriazolyl) methanethione.[360] Thus, several mono TUs could be obtained in excellent yields (87-99%), while aqueous work-up was performed decreasing additional formation of waste.

The use of inorganic thiocyanate salts was reported to yield mono[363] and symmetric 1,3-disubsituted TUs upon heating with an amine (see Scheme 19**C**).[364]

Recently, Sharma and co-worker converted isocyanides with ditertbutyldisulfide in a radical pathway to dithiocarbamates *via* ITC formation, which could be reacted to the corresponding TU by addition of an amine (see Scheme 19**D**).[365] This reaction yielded 1,3 and tri substituted TUs in high yields in one step avoiding the use of solvent or catalysts.

Al-Mourabit and *co*-workers established a multicomponent reaction between an isocyanide, elemental sulfur and an amine towards 1,3 and tri substituted TUs in a more sustainable fashion (AM-3CR) using sulfur as sulfurization reagent, while only a minimum of solvent or no solvent at all had to be used (for further discussion of this reactions see chapter 2.2.1 and 2.3.1).[10]

Further, TU derivatives can be obtained by derivatization of easily accessible or commercially available TUs (see Scheme 19**E**). Thus, unsymmetric TUs can also be obtained by transamidation of a symmetric TU, like the commercially available diphenylthiourea with aliphatic amine or ammonia.[366]

All so far discussed approaches rely on amines, which is certainly an abundantly present functional group but it can be anticipated that in several synthesis routes its access might be not possible. Thus, Ciszewski and *co*-workers reported a synthesis protocol, in which mono or 1,3 di substituted TUs could be obtained by reacting thiourea or mono TUs with an aldehyde and trimethyl chlorosilane, forming an imine adduct which was subsequently reduced with sodium borhydride.[367] Recently, Wang, Yu and *co*-workers extended this reductive alkylation approach by using ketones, reducing them in the same step with trichlorsilane catalyzed by HMPA.[368] In this context, the Biginelli reaction has to be mentioned as well, since this reaction allows the easy formation of complex cyclic thioureas, *i.e.* 3,4-dihydro pyrimidine-2-thiones. This multicomponent reaction can be conducted in

one-pot using thiourea or mono substituted TUs, β-ketoester and an aldehyde under acidic catalysis (see Scheme 12**D**).[369,370]

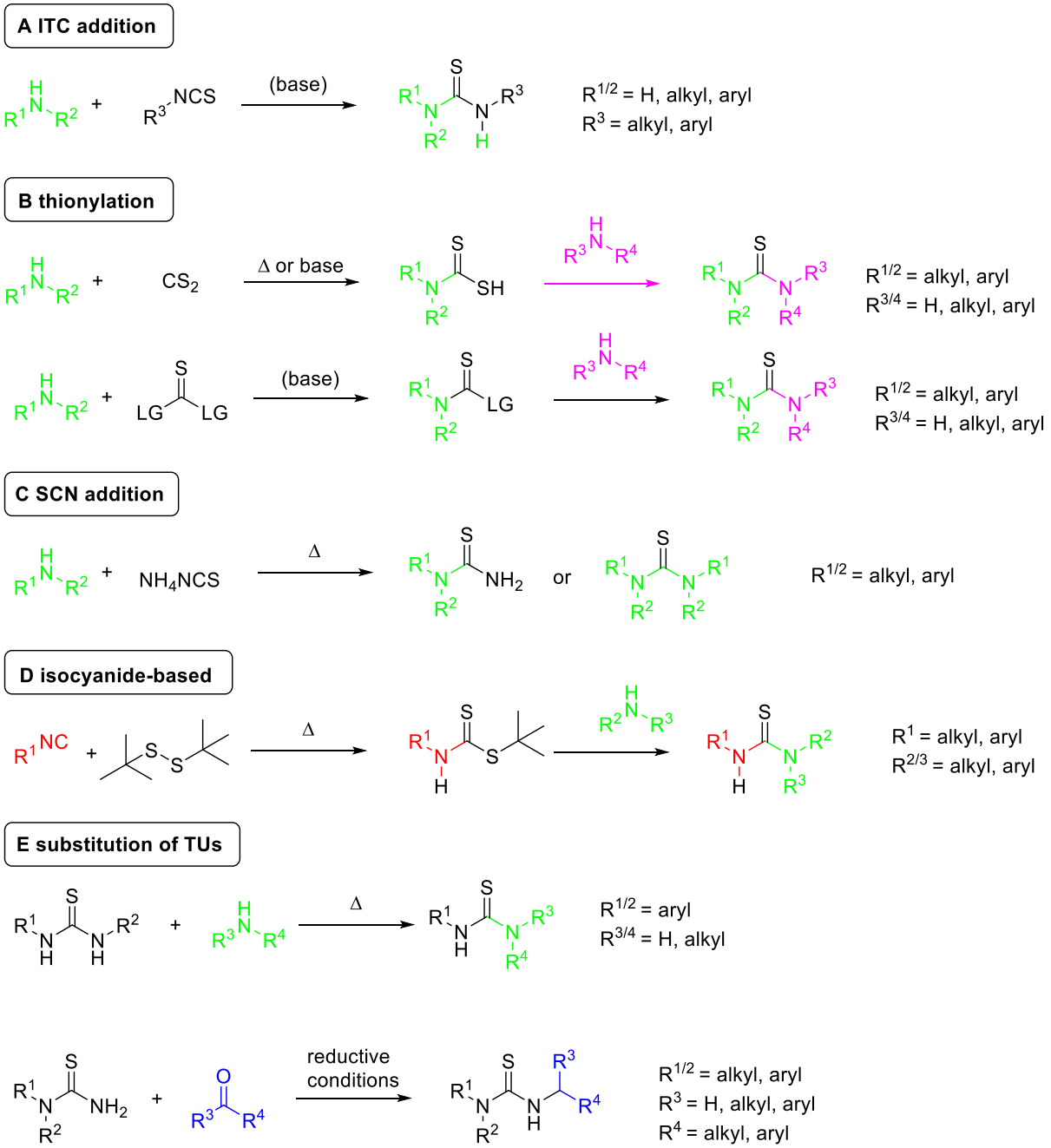

Scheme 19: Overview of typical and more recently reported syntheses of TUs yielding the product in one or two steps. Key intermediates and reaction conditions are depicted. Starting materials are colored to highlight their incorporation in the TU motif: amines are green, isocyanides red and aldehydes or ketones blue. If a second amine is used in the synthesis, it is colored in pink to underline the formation of an unsymmetric TU. LG=Leaving group

In conclusion, TUs are a versatile functional group with applications in laboratory and industry. Several well-established procedures are known for their synthesis. Most of them rely on amines at some point, which is in general an easily accessible reactant (compare number of amines used as components in Scheme 19). Furthermore, amines can be accessed from renewable feedstock *via* sustainable routes like using reductive amination.[371] However, often toxic compound like thiophosgene, its derivatives or carbon disulfide must be applied, making the thiourea synthesis a highly unsustainable process. Still, several improvements were achieved more recently to establish

more sustainable synthesis protocols, like *in situ* formation of toxic ITCs or solvent-less methods. The use of waste products like elemental sulfur and multicomponent reactions complements the pursuit of greener syntheses for TUs, which should be applied more vastly.

2.4.1 Application of thioureas as organocatalysts

Organocatalysts are known for more than 100 years, yet they have only received increased attention over the last three decades. In 2021, the Nobel prize was awarded to Benjamin List and David MacMillen for their contribution to the establishment of asymmetric organocatalysis, further highlighting the importance of this research field.

Organocatalysts were originally defined as “a small organic molecule having no metal as part of the ´active principle´“ ,thereby catalyzing chemical reactions *via* the formation of covalent or non-covalent bonds.[372–374] Compared to metal-containing catalysts and enzymes, organocatalysts possess advantages regarding stability, comparably low cost, low sensitivity to oxygen and moisture as well as straightforward preparation in several cases.[373,375] Typically, these catalysts act *via* their lone electron-pairs as nucleophiles or Lewis bases (*i.e.* nitrogen- or phosphorous-based catalysts)[374,376] or *via* hydrogen bonding (*i.e.* urea derivatives, bisphenols, bisamidines, squaramides, or croconamides).[377–382] Bifunctional catalysts combining Lewis base activity and hydrogen bonding are particularly attractive.[374] Generally, organocatalysts offer broad application possibilities, including numerous aldol type reactions (*e.g.* Morita-Baylis-Hillmann reaction, Michael addition, Henry reaction, Pictet-Spengler reaction)[383–389] and MCRs (*e.g.* Strecker, Biginelli and Mannich reaction),[390–392] among others (*e.g.* Claisen rearrangement, polycyclization, acetalization, ring-opening polymerization).[15,393–395]

In the following chapter, the application of thioureas as organocatalysts will be discussed more thoroughly. Since this research area has grown incredibly, the focus was set on the mechanistic explanation of the catalytic activity (mostly relying on the 3,5-bis(trifluoromethyl) phenyl moiety) by a chronological introduction of successful types of thiourea catalysts. Having obtained an overview of the vast scope of different catalysts, more specialized ones are being discussed introducing several entirely different activation modes. Again, the thiourea group is fascinatingly versatile in its application and thus, the aim of the second part of this chapter was not to give a holistic sequence of all majorly used catalysts. This was simply not possible in the scope of a thesis and thus, the focus was set to highlight the versatility of this catalytically active group by suitable examples (historical and recently relevant ones). In a third part, the privilege of the 3,5-bis(trifluoromethyl) phenyl moiety as activation motif is discussed, presenting thiourea catalysts exhibiting catalytic activity due to different activator groups.

Urea derivatives are one of the most common structural motifs in organocatalysis (see Scheme 20).[374,375] This development started in 1988 by Etter, who investigated the hydrogen bonding (HB) of ureas by cocrystallizing them with different guest acceptors,[396] as well as 1994 by Curran, who, for the first time, applied a urea derivative to activate sulfoxides in a radical allylation and later on also in a Claisen rearrangement.[397]

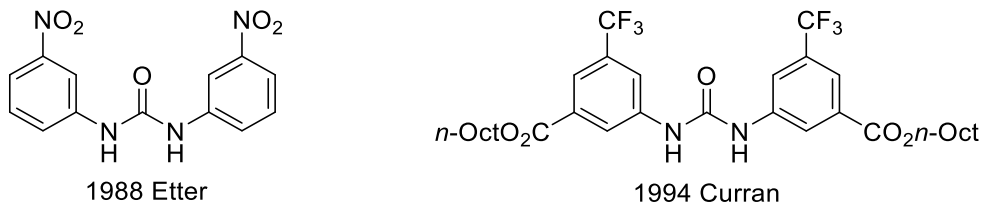

Scheme 20: First two described urea derivatives that were investigated in terms of hydrogen-boning and catalytic activity.

Another milestone in the development of these catalysts was their introduction to the field of asymmetric catalysis in 1998 by Jacobsen, who described the first chiral bifunctional thiourea catalyst bearing an imine functionality (see Scheme 21).[398] Thus, catalysis of several imine-based MCRs, such as the Strecker or Mannich reactions, were reported to proceed asymmetrically.[391,392] Attachment of this catalyst to a solid support offered the possibility of catalyst recycling (up to ten times) in an asymmetric Strecker synthesis.[399] Later on, Jacobsen introduced chiral organocatalysts that were able to provide excellent enantioselectivities by combining covalent with non-covalent interactions between catalyst and substrates (see Scheme 21).[384] Here, the urea group activates the electrophile, as typical for such catalysts, and, at the same time, the nucleophile is activated in an imine-enamine tautomerism, resulting in up to quantitative yields and ee values of up to 92%.

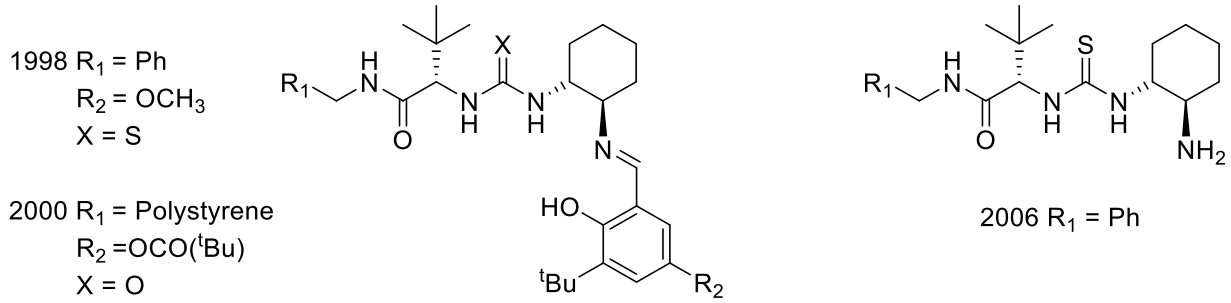

Scheme 21: First thiourea motif exploited in asymmetric catalysis and its later modification to be used on a solid support as well as the modification to achieve synergy of covalent and non-covalent catalysis due to an additional primary amine group.

In 2002, thioureas were investigated for the first time as organocatalysts in a crucial study by Schreiner, explaining the activation mechanism of the thiourea moiety thoroughly. Moreover, the highly active 3,5-bis(trifluoromethyl) phenyl moiety was introduced to urea catalysis, marking the beginning of a long-lasting era of the development of (thio)urea catalysts bearing this moiety (see Scheme 22).[377]

First, a urea or thiourea group acts as dual HB donor with its two N-H bonds (if available) and thereby is in general able to bind HB acceptors, like carbonyl, carboxylic acid, sulfuric acid and nitrate groups supramolecularily.[375] Due to this binding the electron density of the HB acceptor is shifted to the direction of the thiourea protons, resulting in a higher partial positive charge at the acceptor.[400] For instance, considering an aldehyde as HB acceptor, the electron density shift results in a higher electrophilicity of the carbonyl carbon as the partial positive charged is increased and thus, the aldehyde will be more reactive towards suitable nucleophiles.[375] Therefore, the activation mechanism of thiourea can be labeled as Lewis-acid like.[375,400] However, typically this HB is not strong enough to already facilitate a vast scope of different reactions (for instance the complexation of a carbonyl compound with a thiourea is only modestly strong with ca. 7 kcal mol^{-1} at room temperature in dichloromethane) and entropic effects could outnumber the binding exothermicities.[377,400] Thus, Schreiner made use of several other beneficial enthalpic and entropic effects by attachment of aryl moieties adjacent to the thiourea functional group, which are visualized in Scheme 22. First, the use of electron-withdrawing groups (EWGs) like fluoro or trifluoromethyl-groups attached to the aryl moieties were investigated.[400] Particularly, their -M and -I-effect, respectively, led to a further decrease of the electron-density of the N-H bond, thus leaving the protons with a higher partially positive charge and the HB strength increased. Schreiner could show that the EWG effects of the aryl moieties in *meta* positions with respect to the urea group led to the strongest HB abilities and thus, to the strongest catalytic activity of the respective thiourea.[400] This

constitution was beneficial as i) less sterically hindrance with the thiourea group will arise compared to the *ortho* position and ii) two EWG can be employed compared to only one at the *para* position, while the difference in steric hindrance of *meta* and *para* position are of minor magnitude. Second, an additional electron-withdrawing effect was achieved by exploiting thioureas that show higher polarizability compared to the urea homologues (negative charge can be better accommodated at a sulfur atom than in an oxygen atom intrinsically due to the decrease in lone pair-lone pair interaction in the larger sulfur anion). In addition, the lower electronegativity of sulfur decreases the self-association.[400,401] Thus, the N-H bond of the thiourea group was strongly polarized, leading to an increase of the HB donor activity. To this enthalpic driving force, an entropic effect is added lowering the Gibbs free energy of the catalyst substrate complex during complexation of the HB acceptor: Since aromatic hydrogens in *ortho* position to the thiourea functionality are more polarized due to the EWG effect of for instance the trifluoromethyl groups, stronger intramolecular HBs are formed with the sulfur atom. The rotational barrier for the aryl moieties is increased and the favored conformation of this thiourea compound is planar. Due to this preorganization effect, the entropic penalty for the complexation of a substrate was decreased.

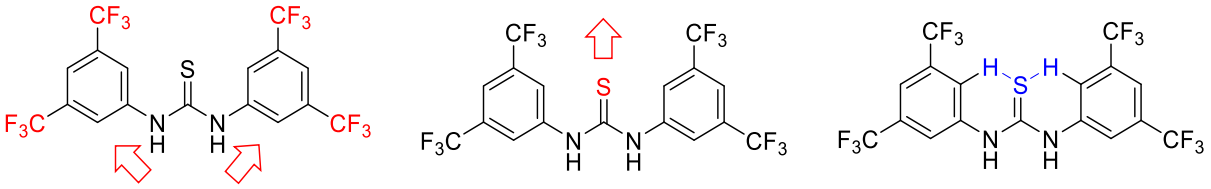

Scheme 22: Enthalpic and entropic effects observed in the Schreiner catalyst, leading to activation of the thiourea as HB donor (enthalpic effects enhancing the polarization of the N-H bond by electron-withdrawal are colored in red, while the red arrows qualitatively indicate the polarization showing the direction in which the electrons are withdrawn; entropic effects lowering the entropic penalty, which occur during substrate complexation, are colored in blue).

Application examples of this catalyst include Diels-Alder reactions of dienophiles that act as a HB acceptors.[400] However, compared to conventional Lewis acids like $AlCl_3$ or $TiCl_4$, the catalytic activity was clearly weaker. On the other hand, a typical benefit using organocatalysis, *i.e.* no product inhibition was indicated as catalytic activity was still present after 80% conversion.[375,400] It has to be mentioned that the catalytic effect is also strongly dependent on the solvent, as polar protic solvents like methanol can compete in the complexation due to their ability to also form HB with the starting materials. Nevertheless, application of strong HB donor solvents like water can still lead to high catalytic activities, since also hydrophobic effects have to be considered as well.[400] In the following years, a manifold of optimization possibilities were described. Most of them still relied on the activation of the thiourea catalyst by the 3,5-bis(trifluoromethyl) phenyl motif. A collection of several important catalysts of this class is shown in Scheme 23.

In 2003, Takemoto investigated Michael-Addition reactions of malonates with nitro-olefins using a chiral TU catalyst bearing an additional tertiary amine for dual activation. Thus, he demonstrated the advantageous activation and pre-coordination of malonates and nitro-olefins to the amine base and the thiourea moiety, respectively, leading to high yields and enantioselectivities (up to 95% yield and up to 93% ee).[385] Only one year later, Nagasawa demonstrated asymmetric Morita-Baylis-Hillman reactions of cyclohexanone with various aldehydes, also using a chiral dithiourea catalyst that provided, in combination with DMAP, a significant rate enhancement and up to 90% ee.[387]

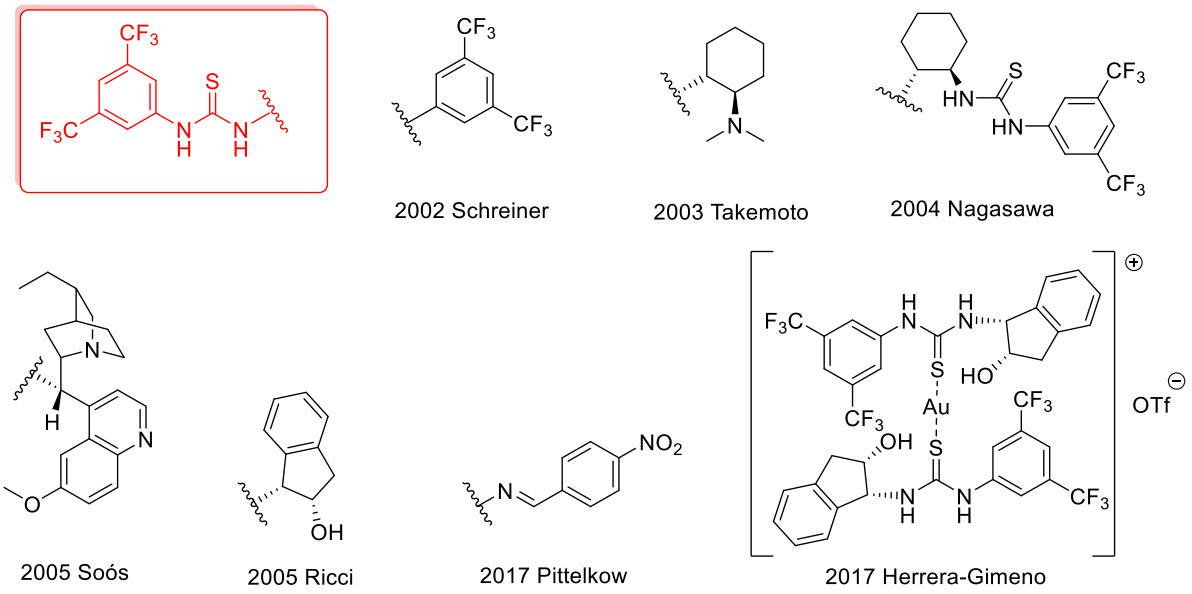

Scheme 23: Collection of several important thiourea catalysts listed in chronologic order. The Schreiner motif is partially present in every catalyst (see red colored inset).

In 2005, Soós demonstrated the catalytic activity of quinine-based thiourea derivatives as organocatalysts for an enantioselective Michael-Addition of nitromethane to chalcones, providing yields up to 94% and ee values of up to 98%.[386] In the same year, Berkessel extended the potential uses of bifunctional urea derivatives for asymmetric catalysis by demonstrating the dynamic kinetic resolution of azlactones with allylic alcohol.[402] Ricci was able to perform, for the first time, an enantioselective Friedel-Crafts alkylation of indoles with nitroalkenes by attaching an (1*R*,2*S*)-*cis*-1-amino-2-indanol moiety onto a thiourea. It was proposed that the reaction was mediated by additional hydrogen bonding interaction of the hydroxyl group of the indole motif in addition to the typical thiourea activation.[403] More recently, Pittelkow demonstrated the catalytic activity of thiosemicarbazone derivatives, which are closely related to thioureas, for instance for tetrahydropyranylation reactions.[404] Herrera and Gimeno used Au(I) salts to coordinate to the sulfur atoms of chiral thioureas, thus activating the HB donor ability *via* intermolecular Lewis pair formation.[405] Further, diversity of applications for thiourea catalysts contains more recent reports in rotaxane catalysis, dearomatization reactions, electro- and photochemistry.[406–411]

With the increasing structural variety of different thiourea catalysts, their application in different organic transformations increased as well and this eventually led to the development of catalysts showing substrate activation differing entirely from the conventional ones. A small collection of this types of catalysts is shown in Scheme 24. So far, the thiourea functionality was used as a HB donor, thus activating the substrate in a Lewis acid-like fashion directly. However, in 2008, Jacobsen took advantage of the ability of thiourea catalysts to bind anionic species, like chlorides. He then applied a chiral thiourea catalyst for enantioselective nucleophilic addition reactions to 1-chloroisochroman.[412] The substrate was activated indirectly by abstraction of the chlorine anion, leading to the formation of a highly reactive oxocarbenium ion that underwent asymmetric substitution with a silyl ketene acetal. In 2021, Tao and Wang highlighted the efficiency of anion abstraction by thiourea catalysts by performing a ring-opening polymerization of *O*-carboxyanhydrides, obtaining high molecular weights of 150 kDa while maintaining high selectivities and suppressing side-reactions like back-biting, chain-transfer and epimerization.[413] In 2011, Schreiner introduced his catalyst as a chelating ligand for silicon halides to form weak silicon-based Lewis acids, which are able to catalyze the

rearrangement of epoxides to aldehydes or ketones.[414] In the same year, Herrera used this anion-binding mechanism to increase the Brønsted acidity of different carboxylic acids by stabilizing the carboxylate anion with a thiourea compound, achieving yields up to 96% and ee values up to 89% in a Friedel-Crafts alkylation of indoles with nitroolefins.[415]

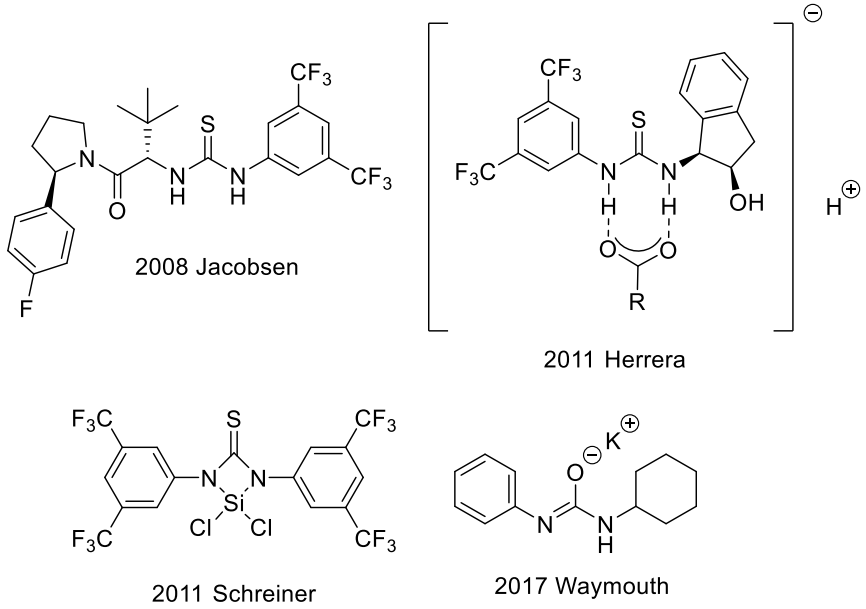

Scheme 24: Collection of four (thio)urea catalysts showing different activation modes compared to conventional Schreiner or Jacobsen catalysts. Jacobsen showed the application of indirect activation by anion abstraction, Herrera the use as co-catalyst to activate Brønsted acids, Schreiner the application as ligand for activation of Lewis acids, while Waymouth used the urea anion as bifunctional catalyst.

In the latter case, the thiourea compound should be labelled as co-catalyst, since the cooperative catalytic complex is formed *in situ* with the carboxylic acid, while the asymmetric behavior of the reaction can be tuned by the application of either a chiral thiourea or a chiral acid or both. Later on, Varga and Pápai. could show by computational-experimental studies that the Schreiner catalyst exhibits sufficient Brønsted acidity itself to catalyze the protection of an alcohol with 3,4-dihydro-2*H*-pyran.[416] The moderate Brønsted acidity of Schreiner´s catalyst (pKs of 10.7) was also shown to be disadvantageous when Lewis-acid like activation conditions were applied in a ring-opening reaction of cyclic carbonates with amines.[417]

In 2020, Seidel *et al.* introduced a bifunctional thiourea catalyst bearing a benzoic carboxylic acid group which can be considered the first use of thiourea catalysts as sole Brønsted acid catalyst for formation of oxa-Pictet-Spengler products.[418] In the same year, the same group established Brønsted catalysis activity also by applying a selenourea-thiourea catalyst in a Michael addition reaction.[17]

So far, all the discussed catalysts rely on the Schreiner´s motif and it remained important for these developments due to its outstanding performance in all different activation modes. However, in 2017 Waymouth *et al.* reported a catalyst not relying on the 3,5-bis(trifluoromethyl)phenyl moiety by using deprotonated urea catalysts as bifunctional catalysts.[419] Due to this Umpolung reaction, they were able to activate the electrophile as well as the nucleophile simultaneously, showing similar activation behavior as the organic superbase TBD (1,5,7-triazabicyclo[4.4.0]dec-5-en). Applying them in a ring opening polymerization of different lactones full conversions was obtained within seconds reaching molecular weights of up to 39.8 kDa.

As it can be clearly seen from the broad overview given so far, the 3,5-bis(trifluoromethyl) phenyl moiety seems to be a highly versatile moiety when it comes to the activation of thiourea catalysts and is not only overemphasized by poor choice of herein given examples. In 2012, Schreiner could show that "the privileged 3,5-bis(trifluoromethyl)phenyl group" also interacts with its *ortho* C-H bond besides its two N-H bonds with Lewis-basic binding sites *via* HB facilitating the complexation.[420]

Nevertheless, over the decades other catalysts were developed without exploiting Schreiner´s motif while relying on the classic activation by Lewis-acid like activity (see Scheme 25). In 2007, Ellman was able to introduce *tert*-butyl sulfonamide as moiety for thioureas to activate them by electron-withdrawing, while simultaneously bearing a stereocenter for chiral induction, leading to high yields of up to 92% and excellent selectivities with ee values of up to 96% and diastereomeric ratios of up to 93:7 in aza-Henry reactions of nitroalkanes with Boc-protected imines.[421] One year later, Seidel used cationic aryl motifs to activate the thiourea by ionic interactions.[422] This concept was further modified by Kass by exploiting ionic interactions of *N*-methylated pyridinium moieties.[423] In 2009, Smith showed that thioureas can also be activated by using a second urea functionality, reaching yields of up to 97% and ee values higher than 99% in a Mukayama-Mannich reaction.[424] In 2017, Pápai and Pihko described similar urea-thiourea catalysts with excellent yields and selectivities, ascribed not to urea-thiourea activation but to the formation of a foldamer catalyst bearing an active site pocket adjusted for the substrate, while suppressing undesired side reactions.[425]

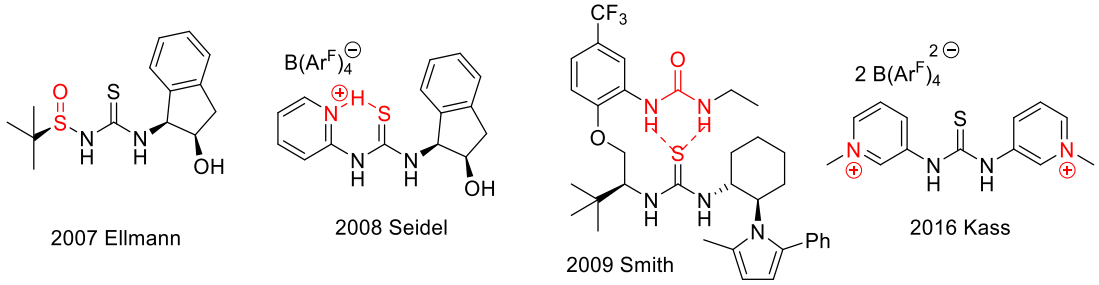

Scheme 25: Four types of thiourea catalysts that do not rely on the 3,5-bis(trifluoromethyl) phenyl EWG group. Ellmann used a chiral sulfonamide moiety for electron-withdrawing, while Seidel and Kass exploited ionic interactions. Smith was able to activate the thiourea with a second urea group. EWG are marked in red.

Concluding, thioureas can be used as organocatalysts in an astonishingly versatile fashion, mainly because of their ability to catalyze reactions *via* several different activation modes. The reactivity originates in all cases from the fact that the N-H bond has an increased partially positive charge, which is usually achieved by attaching EWG like the often exploited 3,5-bis(trifluoromethyl) phenyl moiety to the adjacent thiourea group. Since there is a manifold of applications for such catalysts, it would be of great interest to create a more sustainable synthesis route for its kind as typically toxic compounds are being used (compare previous chapter). This topic was a major point of this thesis and is discussed in the following chapter.

2.4.2 Organocatalysis, an approach for the sustainable toolbox?

Thioureas are often applied as organocatalysts, as discussed in the previous chapter, and since this thesis was written in the context of Sustainable Chemistry the question might arise: Are thiourea catalysts sustainable? It has to be mentioned that sustainability issues related to thiourea catalysis are far less frequently discussed compared to investigation about their mechanistic pathways or the scope of reactions, which they are able to be catalyzed. Thus, a thorough overview about this topic is presented in the following.

Looking carefully at the discussed advantages of organocatalysis (see previous chapter), several principles of Green Chemistry are fulfilled when using organocatalysts as they are insensitive to moisture and oxygen, avoid the use of transition metals and are relatively inexpensive.[373] Moreover, typical reactions are performed at room temperature and the moieties for potentially enantiomeric reaction pathways can be obtained from natural resources like amino acids (*e.g.* proline).

Still, organocatalytic approaches using thioureas are in general not considered as typical examples for greener synthesis procedures and thus, they were not listed in chapter 2.1.2. summarizing important reactions and their conditions for a greener synthesis. The reason for that is the synthesis of the thiourea organocatalyst, which is in general connected to several elaborate reaction steps.[373] This expense is generally needed for the introduction of complex, chiral moieties to achieve the desired stereoselectivities. In addition, for catalysts relying on supramolecular bonding mechanism like thioureas, low concentrations are often applied to hamper self-aggregation of the catalysts. Due to the amount of reaction steps needed for thiourea synthesis as well as the often-applied high amount of solvent for the catalysis reaction, a tremendous amount of waste is generated.

Historically, organocatalysis started growing rapidly in the same decade as Sustainable Chemistry but there were no mutual roots connecting both subjects and therefore, little focus was usually set on the reduction of waste or toxicity in the synthesis of organocatalysis.[426,427] This is again an example that displays the complex nature of sustainability evaluation: the application of an organocatalyst fulfilling several green principals may result in an overall non-green synthesis route, as the potentially small E-factor and low overall toxicity of the reaction is outnumbered by the immense E-factor of the synthesis of the catalyst.

Another drawback of organocatalysis is the fact that, compared to metal catalysts, often higher catalyst-loadings (up to 20-30 mol%) are applied to reach sufficient catalytic activities.[383,428,429] This leads ultimately to more waste.

In the following, typical effects of the synthesis of organocatalysts on the E-factors of the reaction in which they are applied are underlined using two examples of a complex organocatalyst on the one hand and a simple-structured one on the other hand. A brief overview of the impact of the catalysts´ moiety in the context of sustainability is given. In addition, the focus is also set on the application of the thiourea organocatalyst in the framework of Green Chemistry. Subsequently, thiourea catalysts are discussed in terms of their potential as sustainable catalyst considering the effect of recyclability as well.

The problem of organocatalyst synthesis was well displayed by Antenucci and Renzi in the synthesis of the second generation Maruoka catalyst, which is used as chiral phase transfer catalyst (see Scheme 26).[373,430] The synthesis route starts from 1,1'-bi-2-naphthol (BINOL) and consists of twelve steps, all with excellent yields resulting in a very good overall yield of 49%. However, several

principles of Green Chemistry are clearly disregarded. Acetal (methoxymethyl, MOM) and ether groups were introduced as protecting groups and a combination of extraction and column chromatography was needed in seven steps. This led to an enormous amount of waste, depicted in the overall E-factor of 2872. It has to be noted that the herein discussed E-factors are in the typical order of magnitudes of organocatalysts and are not purposely chosen to overemphasize their negative effect (E-factor ranges roughly between 10 and 10^4, however also E-factors of up to 12500 are reported for *e.g.* chiral sulfoneimides).[373,431,432] The second, sixth and ninth step of the synthesis involve a lithiation with *n*-butyl lithium and acylation with triflate anhydride, respectively, which have a high energy demand due to very low reaction temperatures.

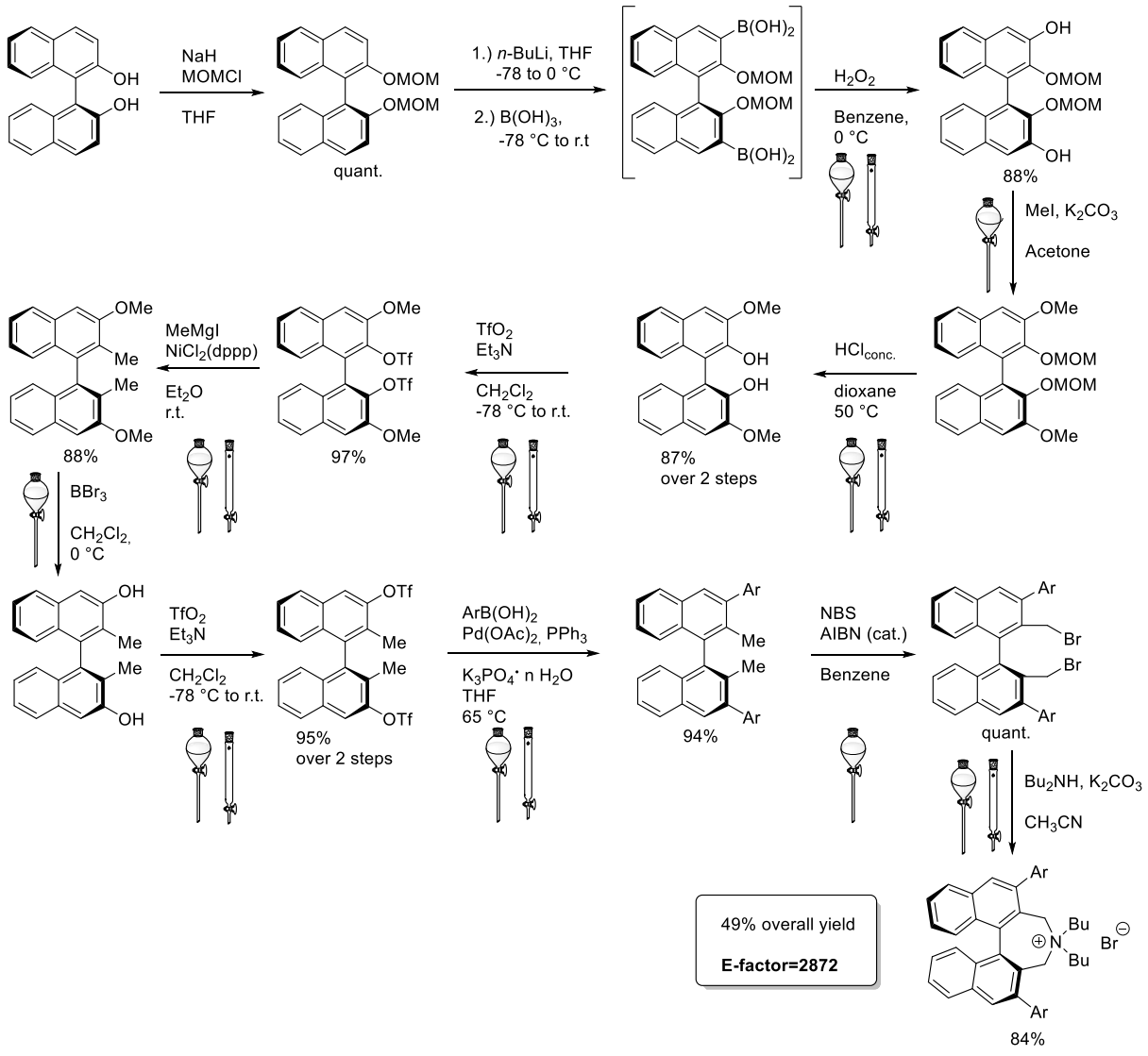

Scheme 26: Overview of the synthesis of the 2nd generation Maruoka catalyst starting from BINOL. Yields are given for the purified intermediates as well as the overall yield and the E-factor. Work-up and purification of a reaction step by extraction and/ or column chromatography is labelled with the respective images of the used glassware.[373,430]

Several reagents that are used are carcinogenic, reprotoxic or noxious, *i.e.* chloromethyl methyl ether, nickel chloride, methyl iodide, boron tribromide, triphenylphosphine and dibutylamine. Also, the used solvents include several volatile organic compounds (VOCs), *i.e.* THF, diethyl ether, DCM, acetone, and even carcinogenic benzene. Since solvents contribute usually to a considerable amount to the generated waste, the use of toxic or VOCs should be avoided (see chapter 2.1.1.).

This example shows that by applying an organocatalyst an overall negative effect on sustainability can arise, which clearly originates from the need of a complex, often chiral, scaffold. Due to the performance of several reaction steps a large amount of waste is generated and often several toxic compounds are used. The reduction of the reaction steps of an organocatalyst would most likely reduce the amount of waste thereby formed, which will ultimately lead to a decrease in the E-factor. However, this holds true only when talking about the exact same catalyst. A decrease of the E-factor is not automatically granted by using a catalyst produced by less steps than another catalyst, since obviously the applied reaction conditions and yields for each catalyst must be compared. This was highlighted by Antenucci and Renzi comparing an unmodified *L*-proline catalyst compared to *L*-proline derivatives which needed to be synthesized first on the example of the aldol addition reaction of cyclohexanone and 4-nitrobenzaldehyde (see Table 5).[373]

Three different reaction protocols using *L*-proline on the one hand and two different derivatives of *L*-proline on the other hand are compared. Approach **A** uses ball-milling conditions, which is generally considered a green methodology (see chapter 2.1.2.) without solvent as well as 10 mol% of the available proline catalyst, obtaining nearly quantitative yield (99%) and excellent stereoselectivities (95%ee, 89:11 d.r.).[433,434] Approach **B** uses water as a solvent, applying 4 mol% of a silylether derivative of proline and a four-fold excess of the ketone. In this case, a lower yield of 80% and a higher ee of 99% were obtained, while the d.r. remained lower (20:1).[435] Approach **C** uses two equivalents of the ketone and no solvent as well as 5 mol% of a thioamide derivative of proline to obtain the product in 99% yield and the best overall selectivity (96%ee, 98:2 d.r).[436] All reactions were performed at room temperature and an overview of the three approaches with the overall E-factors is depicted in Table 5.

Comparing the catalyst-loading, approach **A** was with 10 mol% higher than for **B** and **C**, which were 4 and 5 mol%, respectively. Nevertheless, approach **B** and **C** should exhibit the negative impact of the catalysts synthesis as it is not present in approach **A**. In addition, approach **A** uses the lowest excess of cyclohexanone and no solvent, yet the E-factor is with 227 the highest.[373] The reason cannot be extracted from the given data, but reveals itself upon evaluating the amount of waste created due to the work-up. Interestingly, the amount of solvent for removing the product from the ball-milling apparatus is considerably higher than the amount of solvent used in the work-ups of the other approaches and completely overturned the before-mentioned positive effect on the E-factor. Compared to that, approach **C** shows a lower E-factor of 95, even though the synthesis of the catalyst needed three steps. This is due to the low waste production during the work-up of the catalyst as it does not need a purification by column chromatography.[373,436] The possibility to recover the catalyst by acid/base extraction followed by crystallization after the aldol reaction decreased the E-factor further. The best E-factor of 10 is obtained surprisingly by approach **B**, which showed the lowest yield while using solvent conditions and a high excess of cyclohexanone.[373] This is a result of the minimal impact of the synthesis of the catalyst compared to approach **C** as it is a one-pot, two step procedure with good yield (80%).[437]

Concluding, when comparing different organocatalysts synthesized *via* a different number of reaction steps, the catalysts with the least number of steps will not necessarily exhibit a superior E-factor. Since the reaction protocols (reaction conditions, work-up, yield, selectivity) will differ depending on the used catalysts, the lowest E-factor and thus, the superior catalyst can only be determined by a thorough evaluation of the generated waste.

*Table 5: Comparison of three different proline-based catalysts for the stereoselective organocatalytic aldol reaction of cyclohexanone **A** and 4-nitro benzaldehyde **B**.*[373]

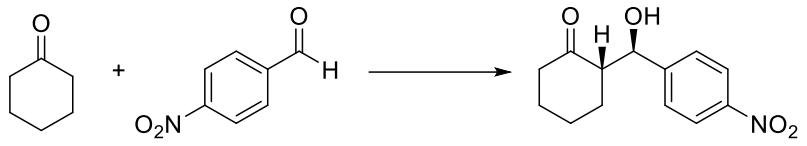

A **B** **P**

	Approach A	**Approach B**	**Approach C**
catalyst (cat.-loading)	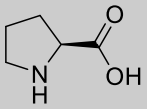 10 mol%	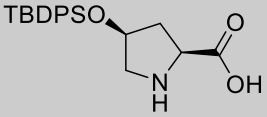 4 mol%	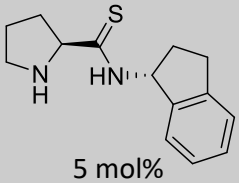 5 mol%
stochiometry (**A**:**B**)	1:1.1	1:5	1:2
reaction conditions	r.t., ball-milling, 24 h	r.t., 5 h	r.t., 5 h
solvent	none	water	none
yield/%	99	80	99
selectivities	95%ee (89:11 d.r.)	99%ee (20:1 d.r.)	96%ee (98:2 d.r.)
reaction steps	-	2 (one-pot)	3
work-up	washing with huge amount of solvent	washing with solvent	no column chromatography
E-factor	227	10	95

The synthesis of thiourea catalysts also often suffers from high E-factors. In addition, as already mentioned in chapter 2.4., thioureas are mainly synthesized from isothiocyanates, which are usually toxic themselves and are formed using toxic, flammable and volatile reagents like thiophosgene, its derivatives, as well carbon disulfide and a stochiometric amount of desulfurization agent. An evaluation of a sufficiently precise E-factor starts from the respective amine that is converted to the isothiocyanate first and then to the thiourea in a second step. For instance, the introduction of the majorly employed 3,5-bis(trifluoromethyl) phenyl moiety, increasing the hydrogen bonding activity of the catalyst as discussed in the previous chapter. The respective isothiocyanate is typically obtained from the corresponding amine and thiophosgene with nearly quantitative yield. However, due to purification by flash column chromatography the E-factor is 364.[407] Recently, Schoenebeck *et al.* introduced an procedure that generated less waste using the bench-stable solid tetramethylammonium trifluoromethanethiolate, resulting in an E-factor of 83.[438] For asymmetric thiourea catalysts amino acids are often used as precursors for the chiral moiety as seen in the Jacobsen catalysts (see Scheme 21), which usually involves the use of protecting group, thus increasing the synthesis steps and the E-factor.[373] Subsequently, the thiourea is formed by a simple addition reaction with a second amine, this reaction is typically performed at room temperature and the product is purified by column chromatography. This is exemplified by the synthesis of the Takemoto's and the Soós' catalyst in Scheme 27.

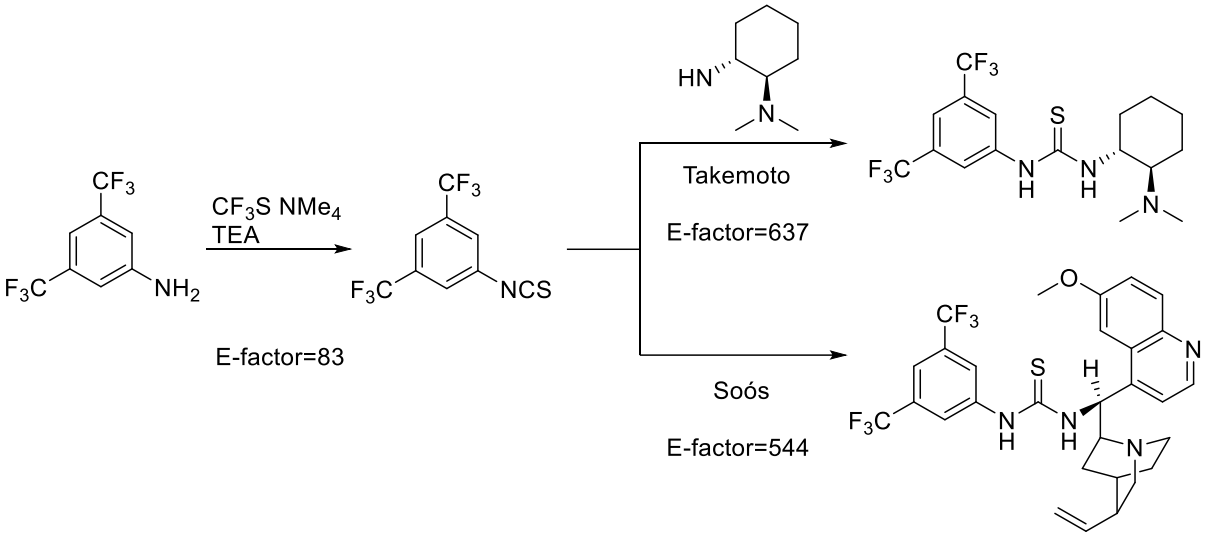

Scheme 27: Synthesis routes of the Takemoto (upper part) and the Soós (lower part) thiourea catalyst starting from the respective amine. E-Factors are given for all synthesis steps.[373]

Takemoto's catalyst can be obtained by reacting the isothiocyanate and the 1,2-diamine with a yield of 65% and an E-factor of 637.[385] The diamine is obtained from *trans*-1,2-diaminocyclohexane by reductive amination. During this, the second amine group is maintained by attaching protecting groups. This increased the overall E-factor additionally, although similar derivatives of this bifunctional thiourea bearing a primary amine group instead of the ternary one still have E-factors above 400.[439–441]

The cinchona alkaloid moiety implemented in Soós catalyst is inexpensive and obtained from renewable feedstock, both of which beneficial for the overall degree of sustainability of syntheses using this catalyst. To obtain the desired quinine bearing a primary amine group, from the respective feedstock an E-factor of 150 is assumed.[373,442,443] Ultimately, a good yield of 81% was obtained for the thiourea synthesis but the overall E-factor was still high (544) due to unavoidable purification by column chromatography.

Concluding, even though thiourea synthesis often involves only two straightforward steps if commercially available amines are used, the obtained E-factors are high, for instance due to purification by column chromatography or use of protecting groups to introduce chiral scaffolds (E-factors are typically higher than 500).[373] In addition, toxic compounds used for their synthesis have further negative impact in terms of sustainability. Less hazardous chemicals like Schoenebeck's reagent still yield moderate E-factors. Another factor that should also be considered in the calculation of the E-factor for thiourea catalysts is the synthesis of the widely used 3,5-bis(trifluoromethyl) phenyl group. The introduction of the CF_3-groups for moieties and reagents further decreases the degree of sustainability. For instance, a commercial process for the preparation of the trifluoromethyl aryl moiety is the halogen-fluor exchange with a chlorinated methylaryl compound and toxic hydrogen fluoride.[444]

Thiourea catalysts have also been synthesized from renewable feedstock, for instance the Soós motif. However, reported literature of this subject is scarce. Ma *et al.* used saccharides as renewable building blocks for the synthesis of chiral thiourea catalysts bearing additional primary amine moieties. Michael additions to nitro olefins showed yields of up to 99% and ee values of up to 98%.[445]

The catalyst could be obtained in three steps from β-D-glucopyranose, while elaborate purification methods like column chromatography could not be avoided.

To summarize, the synthesis of organocatalysts often comes with several synthesis steps due to the need of specific and partly very complex moieties. The impact of the catalyst synthesis will increase the E-factor for the overall synthesis it is used for. This is also the reason why industrial applications for organocatalysts are currently still considered to be inconvenient.[446,447] For future investigations, not only applying (organo)catalysts, but also keeping its synthesis route straightforward and short is a crucial point to obtain synthesis protocols with overall lower E-factor of a synthesis protocol.[373] But as it was shown, also the reaction conditions in which the catalyst will ultimately be used have to be considered as well. Sustainability always has to be evaluated in a holistic manner to avoid potential negative burden-shifting.

To develop new strategies, it is not possible to only rely on commercially available and easily accessible organocatalysts, since they will not always meet the desired yields or selectivities. Finally, elaborately synthesized tailored catalysts come back into consideration when recyclability of the catalyst is applicable, since the negative effect of the catalyst synthesis on the sustainability will be decreased.[427,448–452] As the aspect of recyclability of organocatalysts was an important part of the investigations performed in this thesis, a more detailed overview of thiourea-based, recyclable organocatalysts is given in the following.

Thiourea catalysts were reported to be recyclable using column chromatography but this is an approach related with high waste production, thus contributing strongly to a higher E-factor.[453] Another approach uses the attachment of tags that alter the solubility parameters of the catalyst, enabling post-reaction extraction and filtration of the catalysts. For instance, in 2006, Takemoto *et al.* described recyclable chiral PEG-functionalized dithioureas as homogeneous catalysts that showed better catalytic activity in Michael reactions than TentaGel- or polystyrene-bound analogues (see Scheme 28**A**).[454] The catalysts could be easily recovered by precipitation in diethyl ether, showing the same activity and selectivity in subsequent catalytic reactions.

In a second example, Zhang *et al.* introduced a Soós type thiourea catalysts bearing a quinine and a *p*-(perfluorooctyl) aryl moiety. These catalysts were used in an asymmetric one-pot Michael/aldol cyclization for the formation of spirooxindoles obtaining 99%ee for the major diastereomer and yields of up to 82%. After the reaction, the catalyst could be recovered by fluorous solid-phase extraction due to a fluorous tag with a yield of 93% and 98% purity (see Scheme 28**A**).[455] The same perfluorinated tag was used for a bifunctional thiourea catalyst exhibiting a primary amine group which was applied in a Michael reaction of aldehydes and maleimides.[456] Recovery was performed three times by a simple precipitation-filtration process. Yields and selectivities were maintained (yield 86-91%, 99%ee) while the recovery rate was moderate to good with 60-100%.

Moreover, also hydrophobic tags could be applied for thiourea catalysis (see Scheme 28**A**). For instance, Otaka *et al.* used alkylated gallic acid moieties attached to a Takemoto type bifunctional thiourea catalyst.[457] The catalyst could be recovered at least four times after an aza-Henry reaction with nitromethane and *N*-Boc benzaldimine, maintaining a recovery rate of 99% and constant yields and selectivities by adding acetonitrile to the mixture after the reaction was finished.

Furthermore, other tags could be applied as well. Pedrosa *et al.* used a [60]Fulleren tag for a bifunctional thiourea catalyst. This led to the fivefold recovery of the catalyst with only a slight decrease in yield (from 99 to 87%) while maintaining selectivity.[458]

The second common approach to regain organocatalysts efficiently is the immobilization onto existing supports, such as soluble polymers or cross-linked resins (see Scheme 28**B**). This immobilization allows the filtration of the catalyst after the reaction. Heterogenous thiourea catalysts immobilized on a resin support like polystyrene, PVC or on Merrifield and Wang resins were reported in several cases.[459–464] The approach of polymer-supported immobilization was already interwoven with thiourea catalysis by Jacobsen *et al.* in 2000, as already mentioned in the previous chapter (recycling of a thiourea catalysts for Strecker reaction up to 10 times).[399] Later on, Pedrosa *et al.* applied a bifunctional thiourea catalyst bound on a polystyrene resin in an aza-Henry reaction with *N*-Boc aldimines and nitroalkanes. The catalysts could be recycled at least five times, maintaining high yields (71-80%) and high selectivities (80-82% ee).[465] Besides, less common supports for immobilization were also reported. Poly(methylhydrosiloxane)-supported Takemoto-type catalysts were able to catalyze a nitro-aldol reaction of diethyl malonate and nitrostyrene, while modest recyclability was described.[466]

A combination of renewable feedstock and recyclability was reported in one example by Pedrosa *et al.* using a chitosan support for a bifunctional thiourea catalyst.[467] The catalyst could be recycled five times by filtration in an aza-Henry reaction of *N*-Boc benzaldimine and nitromethane maintaining yield and selectivity (yield 64-74%, 84-86%ee).

Further, also metal-organic frameworks were reported to be a suitable support to bind thiourea catalysts (see Scheme 28**B**). Wang et al. performed acetalization and Morita-Baylis-Hillman reactions using this type of immobilized thiourea catalyst, achieving good to excellent yields (up to 98% and 81%, respectively).[468] In the acetalization reaction, the catalysts could be reused five times efficiently without loss of activity.

So far, there is only one report for a poly(thiourea) structure used as a catalyst, which does not rely on a support. Li *et al.* used tris(4-aminophenyl) amine and 1,4-phenylene diisothiocyanate to form a porous heterogenous catalyst for the Michael addition of nitrostyrene and diethylmalonate (see Scheme 28**C**).[469] The catalyst showed high turnover numbers (TON) up to 2700 and could be recycled at least four times with a negligible loss in yield of 2%.

All approaches can lead to a high degree of recyclability of the catalyst. Nevertheless, to attach the catalytic active thiourea group to a tag moiety or to immobilize it, usually exploits classic synthesis procedures that rely on toxic compounds and generate large amounts of waste. The approaches that were shown in this chapter are important steps towards more sustainability in thiourea orgnaocatalysis. Still improved synthesis protocols, straightforward catalyst design and catalyst recycling need to be developed further in order to set a framework for a possible sustainable toolbox based on thiourea organocatalysts.

A Tag-bound-homogeneous catalysis followed by extraction or filtration

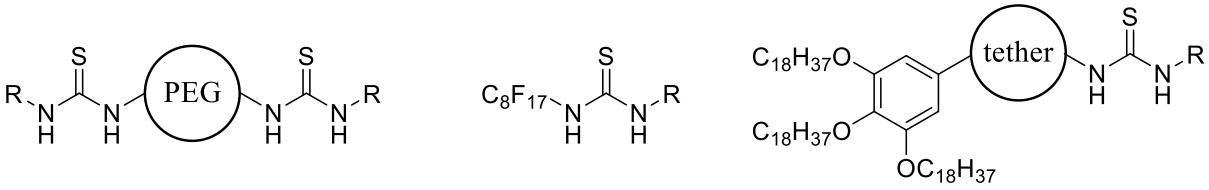

B support-bound-heterogeneous catalysis followed by filtration

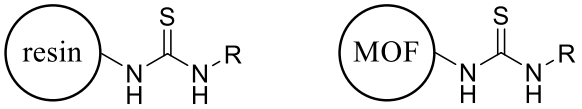

C polymer-heterrogeneous catalysis followed by filtration

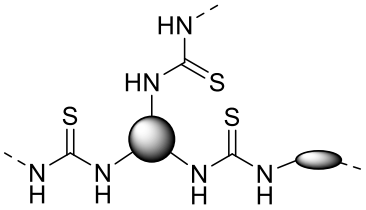

Scheme 28: Schematic overview of different approaches for the recycling of homogeneous and heterogeneous thiourea catalysts. The respective recycling step is given. Moiety R stands either for an activation group of the thiourea function or for a chiral scaffold for application in asymmetric catalysis. Black balls and ellipsoids stand for moieties in the polymer.

3 Aims

The aim of this work is the synthesis of recyclable organocatalysts and novel sulfur-containing polymers using the activation of elemental sulfur by a base. Therefore, the MCR introduced by Al-Mourabit *et al.* between isocyanides, amines and elemental sulfur (in the following AM-3CR) is used as key reaction to obtain thiourea or other sulfur containing functional groups (see Scheme 5**A** and Scheme 15**A** for detailed reaction scheme).[10] In addition, this investigation is conducted in the framework of sustainability and principles of Green Chemistry are addressed as far as possible.

This work is divided into four work packages:

First, an approach towards recyclable thiourea organocatalysts is addressed. A schematic overview of the project is given in Figure 5, highlighting the factors contributing to a more sustainable approach.

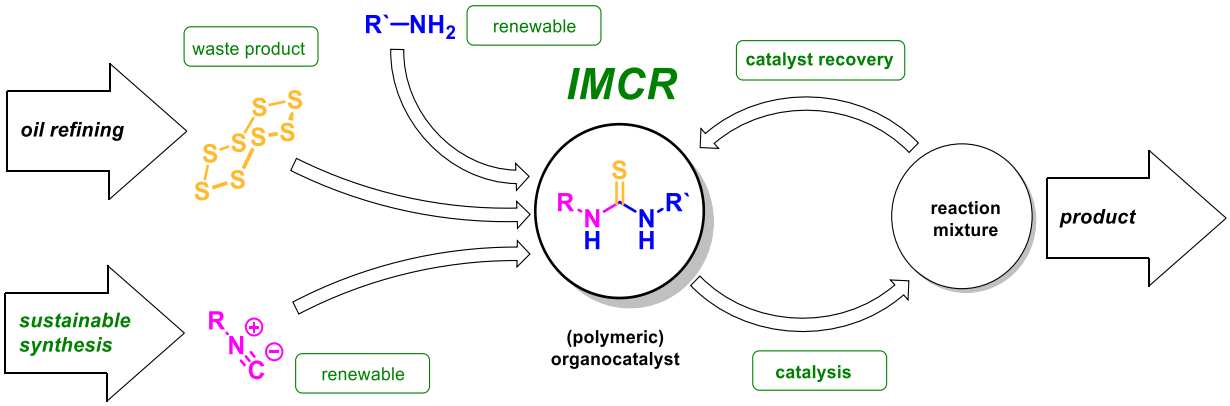

Figure 5: Schematic summary of the aimed project – the most important factors contributing to sustainability are highlighted in green: sulfur is a waste product of the oil refining industry, storing of which gets increasingly problematic,[1] the use of renewable platform chemicals fosters the required transition away from depleting fossil reserves,[470,471] MCRs are highly atom economic;[68] recycling, sustainable synthesis as well as catalysis contribute to waste reduction.

Initially, the degree of sustainability of the concept was a focus. A main downside of the MCR is the isocyanide-based nature, since these compounds were typically synthesized in an unsustainable fashion. Thus, a more sustainable synthesis for the isocyanide starting material is needed.

Second, potential catalytic active thiourea motifs need to be determined and their synthesis established *via* the mentioned MCR. In terms of recyclability, their solubility properties are important as well.

Third, the obtained catalytically active TU bearing the established or further modified activating motifs is transferred and incorporated into a polymer. In a proof of concept, the recyclability of the obtained novel poly(thiourea)s is investigated.

Finally, mechanistic studies of the AM-3CR are conducted to elucidate its reaction pathway by the activation of elemental sulfur with a base. Thus, the obtained understanding is envisioned to improve the overall sustainability of this work and further lead to establishment of other reaction yielding sulfur-containing molecules and polymers.

4 Results and Discussion

4.1 More sustainable synthesis of isocyanides

The first part of this work focused on the improvement of the sustainability of the starting materials of the AM-3CR forming thioureas (see chapter 2.3.1. for reaction equation), *i.e.* isocyanide synthesis. Thus, an overview of the typical synthesis protocols for isocyanides is given as mostly toxic compounds like phosgene and its derivatives or phosphorus oxychloride are applied, while generating a considerable amount of waste (several extraction steps followed by flash column chromatography, see below). Thus, it was assumed that the high degree of sustainability of the AM-3CR resulting from the low amount of solvent, low overall toxicity of the components, ambient temperature, and the use of non-toxic elemental sulfur, a waste product of petroleum, could be reduced or even dwarfed by the preceding synthesis of isocyanide.

Parts of this chapter and the associated parts in the experimental part have been published before:

"A more sustainable and highly practicable synthesis of aliphatic isocyanides"-

K. A. Waibel, R. Nickisch, N. Möhl, R. Seim, M. A. R. Meier, *Green Chem.* 2020, **22**, 933–941.

(The author contributed to the writing (introduction and supporting information of the publication) co-supervised N. Seul, a "Vertieferstudent", who was also involved in the synthesis of the compounds. In addition, the author contributed to planning and evaluation of the experiments in a minor extent. K. Waibel conducted the planning and evaluation of the experiments and contributed to the writing (results and discussion part, abstract, conclusion of the publication). C. Rieker conducted first experiments (Bachelor thesis under the co-supervision of K. Waibel),[472] N. Möhl carried out the GC screening (Bachelor thesis under the co-supervision of K. Waibel),[473] whereas R. Seim applied the improved conditions to synthesize an isocyanide library under the co-supervision of the author and K. Waibel.)

Abstract

Three different dehydration reagents (typically used phosphoroxy chloride ($POCl_3$), the combination of triphenylphosphane (PPh_3) and iodine as well as p-toluenesulfonyl chloride (p-TsCl) were evaluated in their performance transferring N-formamides into isocyanides. Following the Principles of Green Chemistry, more sustainable solvents were tested for all candidates while p-TsCl was optimized more thoroughly (base, stoichiometry, reaction time). After comparison of yields and E-factors the optimized reaction protocols, the approach using p-TsCl seemed to be superior for converting aliphatic non sterically demanding mono or di-N-formamides (yields up to 98% and lowest E-factor 6.45). In addition to the reduction of the E-factor, the application of p-TsCl is recommended since it is less toxic than other dehydration reagents while the synthesis protocol and work-up is more feasible. Ultimately, a greener approach for aliphatic isocyanide functional groups was established using p-TsCl.

Isocyanides represent a unique type of functional group due to their α-acidity and their ability to perform α-addition as well as radical reactions.[182] Except for a few examples, most derivatives exhibit

low toxicity and interestingly, many natural isocyanides show antibiotic, fungicidal, antineoplastic, or antifouling effects.[182,474] Most commonly, they are used in isocyanide-based multicomponent reactions (IMCRs),[68,182,475,476] which have manifold applications ranging from organic synthesis[182] to drug discovery[189,477] and polymer science.[290,478–480] Multicomponent reactions (MCRs) are generally considered as a sustainable synthesis tools, as they fulfil many of the Twelve Principles of Green Chemistry,[68] it is important to further consider the synthesis of their starting materials in the scope of green chemistry. Since the first known isocyanide synthesis by Lieke in 1859, many synthesis routes starting from different precursors were described. While Lieke and Meyer were able to obtain isocyanides by reacting allyl or sugar halides with silver cyanide, Hoffmann obtained them by converting amines with *in situ* formed carbenes of chloroform and potassium hydroxide, or by heating isothiocyanates with PPh_3.[481–485] Gassman and Kitano introduced trimethylsilyl cyanide as cyanide transfer reagent, which forms isocyanides with alcohols and epoxides in the presence of zinc salts.[486,487] However, these procedures suffer from major drawbacks, for instance low to moderate yields and the lack of general applicability, since they are restricted to specific moieties. Nowadays, *N*-formamides are most often used as starting materials to form isocyanides by addition of a dehydration reagent under basic conditions. Ugi first described this procedure using phosgene and later its surrogates (di- and triphosgene) as dehydration reagents.[477,488–492] Afterwards, other reagents were introduced, for instance the Burgess reagent, Appel reagent, trifluoromethyl sulfonic acid anhydride, or *p*-TsCl.[493–496] Nowadays, the commonly used reagent is $POCl_3$ due to its suitability for different structural motifs.[193,230,497–499] Generally, isocyanide synthesis still heavily relies on laboratory preparation, since the number of commercially available isocyanides is limited to a few examples, and even small amounts are relatively expensive.[256] Bienaymé, Bossio and Armstrong focused their isocyanide synthesis work on feasible derivatization routes, which eventually led to more easily accessible isocyanides.[492,500,501] However, most of the dehydration reagents, which are used for converting the formamides into the targeted isocyanide, are either highly toxic or were synthesized by employing toxic precursors (see Figure 6). In addition, large amounts of waste are produced during the synthesis and thus, typical isocyanide syntheses cannot be considered as sustainable. Recently, Wang *et al.* introduced a less toxic dehydration reagent using PPh_3 and iodine obtaining good yields of up to 90% for mainly aromatic formamides.[502] Porcheddu *et al.* were able to improve the approach initially reported by Hoffmann to a more sustainable procedure by applying mechanochemical activation via ball-milling, reducing the required amount of chloroform to a stoichiometric amount. Thus, they were able to obtain isocyanides with a broad spectrum of aliphatic, benzylic and aromatic moieties in yields up to 71%.[503]

In this work, we investigated various synthesis procedures in order to develop a more sustainable and generally applicable route to convert aliphatic *N*-formamides into isocyanides. Therefore, we optimized the isocyanide syntheses employing $POCl_3$, *p*-TsCl, and the combination of PPh_3 with iodine and compared not only the yields but also the E-factors as well as several other parameters such as waste in purification steps and energy consumption.

Results and discussion

Considering the discussed syntheses of isocyanides, this work aimed to improve the sustainability of the dehydration of *N*-formamides. Thus, three commonly used dehydration reagents, *i.e.* $POCl_3$, PPh_3 in combination with iodine, and *p*-TsCl were investigated.[496,502,504] Furthermore, the focus was set on the introduction of more sustainable solvents since often DCM is used for this kind of reaction which is hazardous like many other halogenated solvents. Following solvent selection guides, suitable

candidates were determined.[61,505,506] Typically, highly reactive reagents like $POCl_3$, phosgene, phosgene surrogates, or *p*-TsCl are employed for the synthesis of isocyanides.

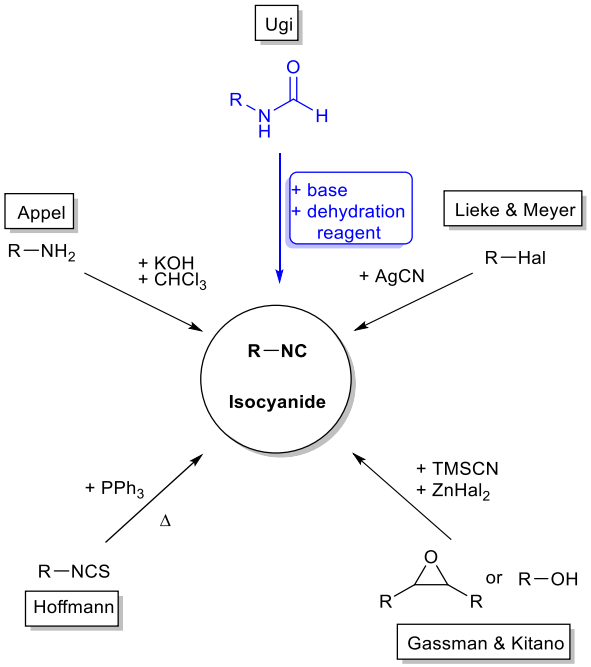

Figure 6: Summary of described isocyanide synthesis procedures. The most widely applied procedure employs N-formamides as starting materials and various dehydration reagents in combination with a base (highlighted in blue). Adapted from ref.[258]

Therefore, the solvent has to be inert towards these reagents excluding alcohols, water, amines and ketones. Nevertheless, several suitable sustainable solvents fitted the conditions applied and could be used in the optimization study (see Table 6-8). *N*-octadecyl formamide **1** was chosen as model compound for the solvent evaluations due to its easy handling and the absence of other functionalities which could interfere in the reaction proceeding (see Table 6-9). To compare the sustainability of the different approaches, E-factors were calculated according to Sheldon[507] considering all reactants, the solvent used for the reaction as well as waste generated through quenching (reagents and solutions). Waste obtained during work-up of the crude product (*i.e.* solvent used for extraction and washing or column chromatography) was not considered for the herein reported E-factors. For the comparison a synthesis E-factor was calculated exclusively.

Formamide dehydration utilizing *p*-TsCl

In 1979, Schuster *et al.* reported a procedure to synthesize isocyanides employing quinoline and *p*-TsCl as dehydrating reagent.[496] The protocol was superior to the Ugi-approach for small isocyanides like methyl or ethyl isocyanides. Since these compounds exhibit decent solubility in water excluding an aqueous work-up the reaction was performed under simultaneous distillation. Main advantages of the use of *p*-TsCl are, compared for instance with $POCl_3$, the easier operation and significantly lower toxicity. Furthermore, *p*-TsCl is a waste product obtained in the industrial saccharine synthesis by the Remsen-Fahlberg procedure increasing its sustainable potential and economical benefit.[508,509]

In a first attempt to optimize the isocyanide synthesis using *p*-TsCl, the Ugi-approach reaction parameters were applied.[504] Since *p*-TsCl exhibited the highest potential in terms of sustainability, the conditions for this reaction were optimized by GC-screening.

GC-screening for optimized conditions utilizing p-TsCl

In general, the dehydration consists of two reaction steps, first an adduct between formamide and dehydration agent is formed which is followed by an elimination. Thus, at least two equivalents of a base are needed to obtain full conversion since both reaction steps require basic mediation.

In a first series of test experiments, different bases were tested. According to the globally harmonized system, amine bases are typically listed as toxic with the exception of pyridine which is listed as only health hazardous. This was underpinned by further toxicity and sustainability studies validating this classification.[510] As a result, we chose diisopropylamine (DIPA), diisopropyl ethylamine (DIPEA), triethylamine (TEA) and pyridine (Py) since they can be obtained sustainably and are commercially available (see Table 6).[511–516]

*Table 6: Optimization of the dehydration of formamide **1** using p-TsCl and a base to obtain isocyanide **2**. In addition to the yield, the E-factor of the respective conditions are given.*

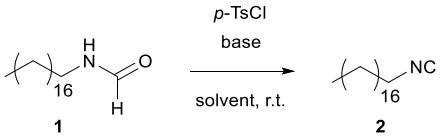

1 **2**

entry	solvent	base	c/M	t/h	yield/%[a)]	E-factor
1	DCM[a)]	DIPA	0.33	21	35[b)]	54.3
2	DCM[a)]	DIPEA	0.33	7.8	14[b)]	132
3	DCM[a)]	TEA	0.33	1.5	25[b)]	72.2
4	DCM[a)]	Py	0.33	2	66[b)]	26.4
5	Me-THF[a)]	Py	0.33	2	12[c)]	106
6	DMC[a)]	Py	0.33	2/18	7/85[c)]	217/31.8
7	ACN[a)]	Py	1.0	4/18	70/56[c)]	8.20/10.5
8	Cyrene™ [a)]	Py	1.0	1/2	10/2.4[c)]	80.2/324
9	GBL[a)]	Py	1.0	1/2	28/22[c)]	26.5/34.8
10	DCM	Py	1.0	2	96[c), d)]	7.76
11	DMC	Py	1.0	18	89[c), d)]	7.41

a) Yields determined by GC applying a calibration curve of isocyanide **2**. b) The respective solvent, 5.00 mmol formamide (1.00 eq.), *p*-TsCl (1.30 eq.) and the base (2.60 eq.) were used. c) The respective solvent, 5.00 mmol formamide (1.00 eq.), *p*-TsCl (1.50 eq.) and the base (3.00 eq.) were used. d) Values are yield after work-up and isolation.

With 14% and 25%, tertiary amines (DIPEA and TEA) led to the lowest yields (see Table 6, entries 2 and 3). DIPA showed an increase yield of 35% (see Table 6, entry 3) while the highest yield could be obtained using pyridine (66%, see Table 6, entry 4) in two hours reaction time. Not the degree of basicity but the steric influence of the base seemed to be the main factor leading to a successful transformation towards isocyanide **2** since the yield increased with utilization of less demanding bases. Next, solvents were investigated while conventional and sustainable ones were considered. In addition, the stoichiometry of the starting materials was altered increasing the amount of applied dehydration reagent and base to 1.50 and 3.00 equivalents, respectively. The concentration was also increased in the course of the screening to 1 M to decrease the amount of waste and increase the reaction rate. The excess amount of *p*-TsCl had to be applied to compensate partial hydrolysis to *p*-toluenesulfonic acid (PTSA) by water during the reaction. Since isocyanides are sensitive to acidic milieus, the amount of base was increased as well to maintain the alkaline conditions as the reaction proceeded. γ-Butyro lactone (GBL) and dihydrolevoglucosenone (Cyrene™) resulted in low yields after two hours (22% and 2.4%, respectively, see Table 6, entries 8 and 9). Side reactions were indicated since yields started to decrease after one hour. In case of 2-methyltetrahydrofuran

(Me-THF) the respective ammonium salt precipitated shifting the equilibrium to the product side. Nevertheless, a yield of only 12% was obtained after two hours (see Table 6, entry 5). Utilization of acetonitrile (ACN) resulted in a good initial yield of 70% after four hours which started to decrease afterwards leading ultimately to a yield of 56% after 18 hours (see Table 6, entry 5). The least toxic solvent of this series, dimethyl carbonate (DMC) led to a good yield of 85% after 18 hours (see Table 6, entry 6) which consistently gave the lowest E-factor of 31.8. Reevaluation of DMC at 1 M and comparison with DCM, the conventionally used solvent for this reaction, revealed that DMC led to a very good yield of 89% which was nearly as high as the one obtained using DCM (96%, see Table 6, entry 10 and 11). While the reaction in DMC is slower and provided a slightly lower yield its advantages were clearly the non-toxicity of the solvent and the slightly lower E-factor. Furthermore, DMC can be synthesized from renewable sources.[517,518] Subsequently, different purification methods (washing and column chromatography) were evaluated. We remained to use the initially applied work-up procedure, *i.e.* quenching with sodium carbonate solution and aqueous work-up, being the most promising one. Moreover, DMC proved to be superior in the work-up steps as DCM formed often stable emulsions which were time-consuming in their separation. The obtained results seemed very promising as *p*-TsCl was the least toxic dehydration reagent investigated in this work and further, it depicted the lowest exothermy in the dehydration reaction. Thus, a safer and easier reaction handling could be applied while intense water cooling was only needed for large reaction scales (isocyanide **6** was synthesized in batch sized up to 100 mmol).

Ugi-approach utilizing ($POCl_3$)

The procedure of Ugi employing $POCl_3$ as dehydration reagents is a well-established synthesis procedure which is reported to yield consistently good yields.[230,479,519–521] Thus, the yield of the initial reaction in DCM led to an excellent yield (96%, see Table 7, entry 1). Substitution of the solvent by ethyl acetate (EA) or Me-THF resulted in lower yields of 90% and 94%, respectively (see Table 7, entries 2 and 3). DMC showed again good but lower yields compared to DCM which was similar to the other tested, sustainable solvents (see Table 7, entry 4). It has to be mentioned that the reaction needed constant cooling due to the high reactivity of $POCl_3$ making the reaction set-up more elaborate and more unsustainable since cooling consumes energy. E-factors of the reaction ranged from 12.6 to 17.8. Nevertheless, this value does not include the hazardousness of $POCl_3$ due to its toxicity, high reactivity and corrosive properties and thus, its use should in general be avoided with high priority.

*Table 7: Dehydration of formamide **1** with $POCl_3$ and DIPA in different solvents. Yields as well as the E-factors are given.*

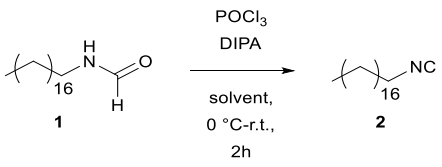

Entry	Solvent	Yield/%[a)]	E-factor
1	DCM	96	17.8
2	EA	90	13.9
3	Me-THF	94	12.6
4	DMC	90	15.9

a) he respective solvent, formamide **1** (3.00 mmol, 1.00 eq., 0.33 M in solvent,), $POCl_3$ (1.30 eq.) and DIPA (2.60 eq.) were mixed under ice-bath cooling and subsequently, the reaction was stirred for two hours at room temperature.

Wang procedure utilizing (PPh_3) and iodine (I_2)

More recently, in 2015 Wang et al. reported a dehydration protocol for formamides using PPh_3 and iodine similar to the Appel reagent.[502] Their work was sparked initially due to the fact that $POCl_3$ is not easily available in China. Compared to $POCl_3$ both reagents (PPh_3 and iodine) are less toxic and in addition, PPh_3 is an easy to handle bench stable solid. On the other hand, iodine sublimes at room temperature and is skin irritating as well as hazardous when inhaled.

Like for the other two dehydration reagents, a solvent screening was conducted for the dehydration reaction following the protocol of Wang *et al.* adapted for formamide **1** (see Table 8). While DCM, EA and DMC only yielded moderate yields (33-42%, see Table 8, entries 1,2 and 4), Me-THF resulted in a very high yield of 93%. The E-factors were thus consistently higher with the lowest value of 18.4 for Me-THF.

*Table 8: Dehydration of formamide **1** with PPh_3, iodine and TEA in different solvents. Yields as well as the E-factors are given.*

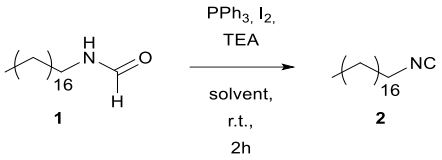

Entry	Solvent	Yield/%[a)]	E-factor
1	DCM	42	54.3
2	EA	37	49.2
3	Me-THF	93	18.4
4	DMC	33	60.8

a) The respective solvent, formamide (3.00 mmol, 1.00 eq., 0.33 M in solvent), PPh_3 (1.50 eq.), iodine (1.50 eq.) and TEA (3.00 eq.) were used and stirred for two hours at room temperature.

Comparison of the three approaches

In a next step, the three approaches were compared in their effectiveness (yield) and sustainability (E-factor, see Table 9).

*Table 9: Overview of the dehydration of formamide **1** using $POCl_3$, PPh_3 and iodine as well as p-TsCl in the optimized solvent and reaction conditions. Yields and E-factors are given to allow comparison.*

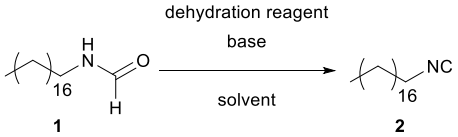

Entry	method	Solvent	Yield/%[a)]	E-factor
1	Ugi[a)]	Me-THF	94	12.6
2	Wang[b)]	Me-THF	93	18.4
3	*p*-TsCl[c)]	DMC	89	7.41

a) see table 7. b) see table 8. c) see table 6.

The most toxic reagent is clearly $POCl_3$ being toxic, highly reactive and thus, needed constant cooling as well as being corrosive. On the other hand, the least hazardous dehydration reagent, *p*-TsCl, allows an easier reaction set-up (cooling only in large scale, see Figure 7) and the use of less solvent (higher concentration of 1 M) ultimately generating less waste.

Figure 7: Left top side: transformation of tert-butyl formamide (11.6 mmol in 35 mL DCM, (0.33 M)) to the respective isocyanide. To add $POCl_3$ the dissolved formamide has to be cooled by an ice-water bath. Left bottom side: The same reaction mixture after $POCl_3$ was added (internal temperature was 0 °C). Nevertheless, the evolution of HCl vapor is visible. Right top side: transformation of tert-butyl formamide (35 mmol in 35 mL DCM, 1.00 M) to the respective isocyanide. To add p-TsCl a water bath was applied for cooling. Right bottom side: The same reaction mixture after p-TsCl was added. An exothermic reaction could not be detected by visible indicators but in some dehydration reactions, a slightly increased temperature was observed. Adapted from ref.[258]

Using PPh_3 and iodine higher E-factors were obtained compared to the other approaches (18.4 kg waste per kilogram isocyanide, see Table 9, entry 2). Thus, the use of the less toxic reagents, compared to $POCl_3$ is dwarfed by the additional 5.07 kg of waste per kg of isocyanide **2**. Moreover, avoiding column chromatography as purification method was one of the main aims of this work since it contributes to a considerably part to the overall generated waste (silica gel as well as solvent used as eluent). After simple extraction, the isocyanide can be obtained in sufficient purity by applying $POCl_3$ because all by-products are water soluble. However, this was not possible for Wang´s procedure since triphenylphosphine oxide was formed exhibiting a poor solubility in water and thus column chromatography had to be performed adding to the E-factor. By using *p*-TsCl and pyridine the purification of the isocyanides could be conducted easily by extraction and washing since the pyridinium salt is soluble in water (*vide infra*).

In addition, the investigation of the solvent screening showed that non-toxic, renewable DMC is an ideal solvent for the dehydration of formamides with *p*-TsCl. Further Me-THF was found to led to good yields however, compared to DMC it is also renewable but health hazardous. Applying DMC and less toxic dehydration reagent *p*-TsCl for formamide **1** resulted in a low E-factor of 7.41 and a high yield of 89%. Concluding, this approach was the most promising one considering degree of sustainability as well as practicability and thus, was applied in the following investigations.

Isocyanide syntheses with optimized reaction conditions

In a next step, the scope of the synthesis protocol using *p*-TsCl (see Scheme 29) was evaluated by synthesizing a library of twelve isocyanides **2-13** (see Table 10).

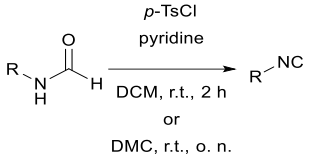

Scheme 29: Isocyanide synthesis starting from N-formamide applying p-TsCl and pyridine at optimized conditions (room temperature in DCM for two hours or in DMC overnight (o.n.)).

Since DMC led to high yields comparable to the ones obtained by the typical solvent DCM, but showed longer reaction times (DMC reaction were performed overnight, while DCM reaction took only two hours) the syntheses were performed with both solvents. For a good comparison of the synthesis protocol with a conventional one, isocyanides were chosen that were already reported to be synthesized by the Ugi-approach or were commercially available (isocyanide **10-12**).

Formamides bearing long alkyl chains as moieties, *i.e.* isocyanides **2-4**, were obtained in both solvent in high yields (DCM (96/90/97%) and DMC (89/94/98%), respectively) comparable to reported ones in literature (87/94/no literature (n. l.)%).[519] However, comparing the E-factors the herein reported method resulted in a 75 and 80% lower value for compound **2** and **3**, respectively highlighting the improvement towards a more sustainable isocyanide synthesis using *p*-TsCl. Furthermore, diisocyanides **8**, **9** as well as benzylated isocyanide **5** were obtained in better yields using the more sustainable approach.[230,302,522] It also has to be mentioned that isocyanides **4**, **8** and **9** have an increased degree of sustainability as they are all obtained from renewable feedstock, whereas isocyanide **5** was chosen, since it can be employed for sequence-defined macromolecule synthesis.[193] In the case of isocyanide **5** the three-step synthesis was optimized in terms of sustainability leading to an overall E-factor of 16.8 and a yield of 94% clearly improving its synthesis since the former procedure resulted in a yield of 63% and an E-factor of 33.2.[230] A conversion of a formamide group was possible while simultaneously tosylating a free hydroxyl obtaining moderate yield and enabling post-functionalization, which is depicted on the example of isocyanide **6**. Nevertheless, synthesizing commercially available isocyanides (**10-12**), the limits of the more sustainable approach for isocyanides was determined as only moderate yields were obtained (44-79%). The yields seem to be affected by water solubility and steric hindrance. The latter reason could also explain the lower yield obtained for benzylic and aromatic formamides (**11** and **13**). On the other hand, a decreased nucleophilicity of the deprotonated formamide adjacent to an aromatic system seemed also a reasonable explanation for lower yields. Still, in case of isocyanide **10** and **12** the new procedure led to decreased E-factors compared to literature (28.8-14.7 instead of 62.0-24.9).[523,524] Isocyanide **11** could be obtained with comparable yields but the E-factor was higher 25.6 instead of 22.2 in literature.[479] Kim *et al.* reported a convenient isocyanide synthesis in 2013 using a continuous-flow microreactor obtaining excellent yields for **10** and **11**.[521] However, the general access to such reactors is not given and toxic $POCl_3$ was used, which was substituted by *p*-TsCl due to above mentioned reasons. Ultimately, aromatic isocyanide **13** underlined the restriction of the more sustainable protocol as it was obtained in a poor yield of 13% and an E-factor of 109. Concluding, the dehydration of formamides with *p*-TsCl is a promising method to obtain non-sterically hindered isocyanides in a greener fashion.

Column chromatography was used in all cases to determine the yields, but it has to be mentioned that a simple flash column chromatography was already sufficient to obtain pure products.

Furthermore, increasing the washing steps, many isocyanides could also be obtained in satisfying purity avoiding column chromatography completely, which is depicted on the example of the ^{1}H-NMR-spectrum of isocyanide **9**after purification by either washing or column chromatography in Figure 8.

*Table 10: Library of isocyanides **2-13** obtained by dehydration of N-formamides applying p-TsCl and pyridine in either DCM or DMC at optimized reaction conditions (see above).*

substrate	procedure A-yield/%[a)]	E-factor A	procedure B-yield/%[b)]	E-factor B	literature-yield/%	E-factor-literature[c)]
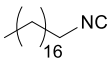 **2**	96	7.76	89	7.40	87[54]	36.9
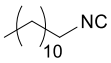 **3**	90	11.9	94	9.93	94[54]	48.8
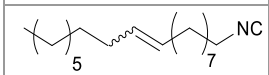 **4**	97	7.73	98	6.68	n. l.	-
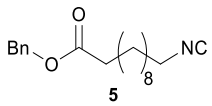 **5**	97	7.11	97	6.45	66[60]	22.3
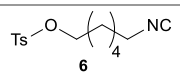 **6**	53	15.0	68	11.0	n. l.	-
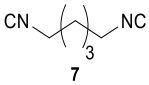 **7**	48	49.0	82	25.7	n. l.	-
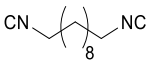 **8**	93	15.8	89	15.0	71[59]	33.6
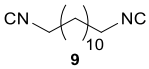 **9**	87	14.8	97	12.0	75[56]	33.6
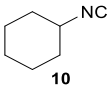 **10**	67	28.8	68	24.9	76[61]	62.
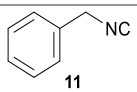 **11**	44	41.5	62	25.6	64[9]	22.2
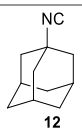 **12**	79	16.5	78	14.7	93[62]	28.9
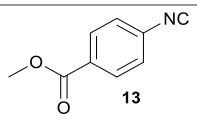 **13**	13[d)]	109	-	-	96[57]	12.9

n. l. = no literature available. a) Formamide (5.00 mmol, 1.00 eq.) in DCM (1 M), 1.50/3.00 eq. *p*-TsCl/pyridine at r.t. for 2 h. b) Formamide (5.00 mmol, 1.00 eq.) in DMC (1 M), 1.50/3.00 eq. *p*-TsCl/pyridine at r.t. overnight. The doubled amount of reagents was used for diformamides (3.00/6.00 eq. for *p*-TsCl/pyridine respectively). c) E-factors were calculated using the values in the respective literature. d) Adjusted equivalents: Formamide (5.00 mmol, 1.00 eq.) in DCM (1M), 1.70/3.40 eq. p-TsCl/pyridine at r.t. for 2 h.

Passerini-three-component polymerization reaction (P-3CPR)

To prove that the herein obtained isocyanides exhibited a high purity and could be reacted without further purification by column chromatography, a step-growth polymerization *via* P-3CR was

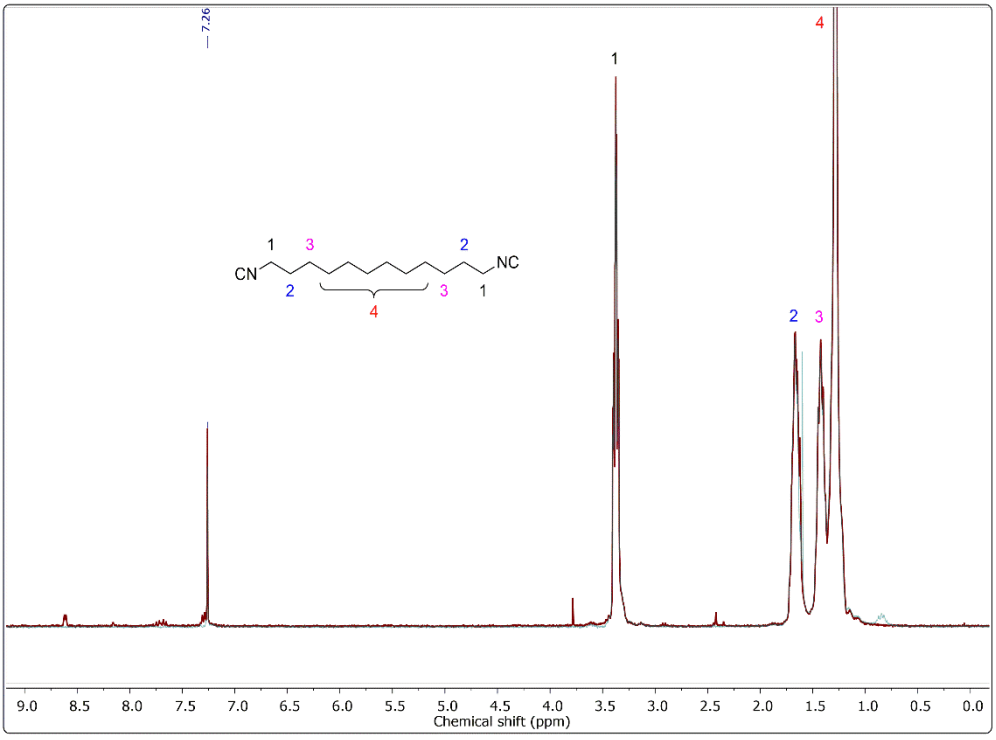

*Figure 8: Overlay of two ^{1}H-NMR spectra both depicting diisocyanides **9** in $CDCl_3$. The red line shows the spectrum after several washing step, the blue line after purification by flash column chromatography. Adapted from ref.*[258]

performed. Since a step-growth polymerization will only yield high molecular weights if equimolar stoichiometry of the respective monomers is applied, even small impurities will alter yield and conversion of the polymerization greatly (see Scheme 30). Sebacic acid **14** and heptanal **15** were thus converted with 1,12-diisocyanododecane **9** to Passerini-polymer **16** without using solvent. This reaction was performed twice, once with the isocyanide **9** purified by flash column chromatography and one with the respective isocyanide purified by washing septs. Comparison of the purified polymers **16** after precipitation was conducted by SEC (see Scheme 30).

Using isocyanide **9** purified by column chromatography, polymer **16** was obtained exhibiting a number average molecular weight (M_n) of 10.5 kDa. Compared to that, polymer **16** was obtained with an M_n of 8.4 kDa applying isocyanide **9** after purification by washing steps. This result was sufficiently proving that the simplified and more sustainable work-up procedure was superior. While both polymers were obtained as waxy solids, the polymer obtained from the isocyanide purified by washing showed a darker coloration.

Conclusions

Evaluation of the degree of sustainability for the utilization of $POCl_3$, PPh_3 in combination with iodine, and *p*-TsCl for the dehydration of *N*-formamides was performed. *p*-TsCl led to the highest yields (up to 98%) and on the same time to the lowest E-factors (down to 6.45) for non-sterically demanding aliphatic *N*-formamides. Furthermore, DCM was shown to be substituted sufficiently using the more sustainable solvent DMC by the synthesis of ten different aliphatic isocyanides. All products were obtained in high yield and excellent purity. In addition, the E-factors obtained were lower compared to already established synthesis procedures. Using only extraction as purification step, isocyanides in sufficient purity were obtained as underlined by their utilization in a P-3CPR yielding adequate

molecular weights. Restrictions of this more sustainable approach were shown as well since only low conversion were obtained for sterically demanding and aromatic formamides.[1] Still, this new procedure depicts a significant improvement in terms of sustainability for aliphatic isocyanide syntheses providing an easier access to more sustainable isocyanide-based chemistry like IMCRs.

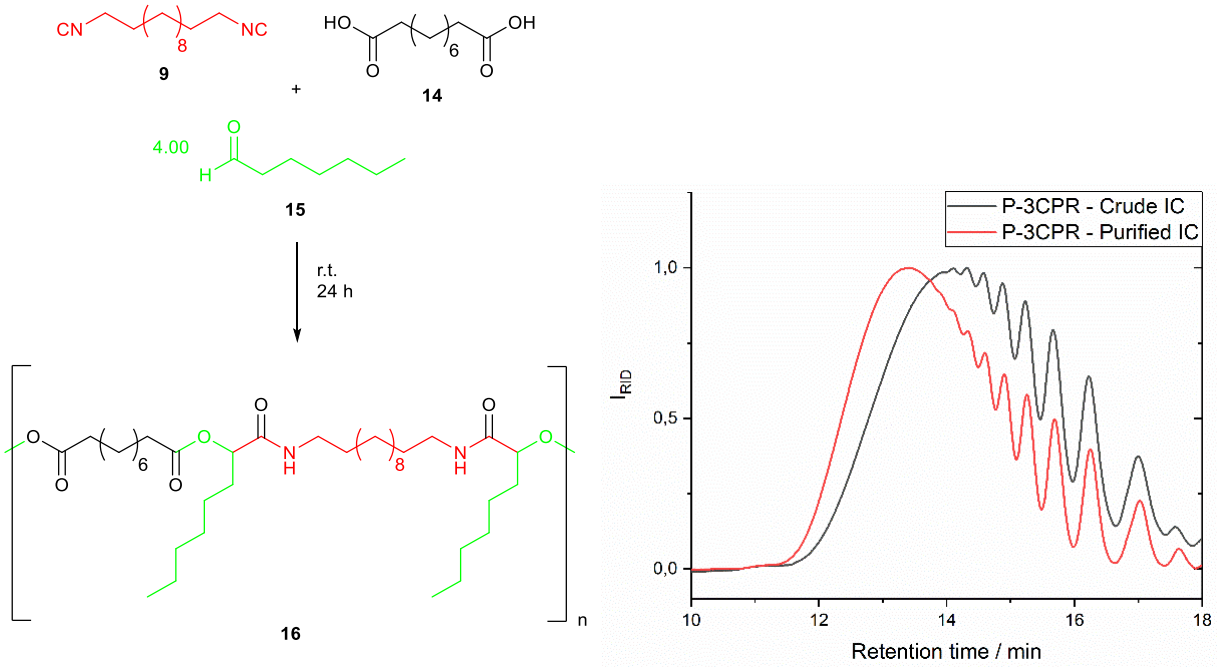

*Scheme 30:Left: Solventless P-3CPR of diisocyanide **9** (red), sebacic acid **14** (black) and heptanal **15** (green). To proof that the isocyanides (ICs) were obtained in sufficient purity after several washing steps, the polymer **16** was synthesized twice. One time with diisocyanide **9** purified by column chromatography and another time purified by several washing step. Right: SEC-curves of the two polymers **16**. Higher molecular weight was obtained with the column chromatography purified diisocyanide (polymer **16a**) while the crude isocyanide led still to sufficient molecular weight (polymer **16b**). Adapted from ref.*[258]

[1] It was hypothesized that aromatic formamides bear lower nucleophilicity compared to their aliphatic analogous and thus, the electrophilicity of *p*-TsCl is too low to yield reasonable conversions while more reactive dehydration reagents like $POCl_3$ lead to high yields. It can be envisioned that the use of more reactive surrogates of *p*-TsCl like its anhydride or *p*-TsI would result in high yields as well, however the degree of sustainability would probably be decreased due to an additional use of reagents or even an additional reaction step.

4.2 Synthesis of thioureas *via* AM-3CR and evaluation of their catalytic activities depending on their moieties

Having obtained a more sustainable synthesis protocol for aliphatic isocyanides the overall sustainability of the AM-3CR could be considerably improved. As a next step of this work, the catalytical activities of thioureas were investigated. As thoroughly discussed in chapter 2.4.1 the catalytic activity of thioureas arises from the attachment to an electron-withdrawing group, mostly bound to an electron-poor aryl motif. For this purpose, the vast majority of thiourea catalysts bear the privileged 3,5-bis(trifluoromethyl) phenyl group. However, this motif was insufficient for the concept of this work, since its synthesis is highly unsustainable (*vide infra*). In addition, the solubility of the final catalysts should be considered as well and the 3,5-bis(trifluoromethyl) phenyl group usually does not lead to compounds which are easily soluble in a vast range of organic solvents (for instance the Schreiner catalyst sometimes only dissolved upon addition of the starting material that is a hydrogen bond acceptor). Thus, the focus of this section was to establish a more sustainable activating motif for thiourea catalysis by altering the electron-withdrawing group and improving the reaction conditions in terms of sustainability. Furthermore, the newly introduced group should also yield better solubility in general for organic solvents.

Parts of this chapter and the associated parts in the experimental part have been published before:

"Novel Access to Known and Unknown Thiourea Catalyst *via* a Multicomponent-Reaction Approach"-

R. Nickisch, S. M Gabrielsen, M. A. R. Meier, *ChemistrySelect* 2020, **5**, 11915-11920.

(The author planned and evaluated the experiments as well as wrote the publication. Furthermore, he established the optimized synthesis protocol, ^{31}P-NMR-analysis and GC-screening method. In addition, the author co-supervised L. Wildersinn together with M. Frölich, who was involved in the investigation of the catalysis of an Ugi reaction by thiourea compounds (Bachelor thesis).[525] M. Gabrielsen carried out the synthesis of the library of thiourea compounds (under supervision of the author). Moreover, GC screening and ^{31}P-NMR analysis was performed together with the author.)

Abstract

Thioureas are frequently used in organocatalysis and typically rely on 3,5-bis(trifluoromethyl) phenyl moieties motifs to enhance their catalytic activity. In this work, these common motifs were replaced with tailorable functional groups, such as ester or sulfone aryls, applying elemental sulfur in a multicomponent reaction (MCR) strategy for the first time for thiourea catalyst synthesis. First, several thioureas bearing aryl, benzylic or aliphatic moieties were synthesized and tested for their hydrogen bonding strength by evaluating thiourea phosphine oxide complexes *via* ^{31}P NMR and their catalytic activity in an Ugi four-component reaction (U-4CR). Finally, ester and sulfone aryl thioureas were tested in the aminolysis of propylene carbonate, leading to conversions similar to those previously reported in the literature using the 3,5-bis (trifluoromethyl)phenyl moiety, proving that these groups are suitable alternatives for the trifluoromethyl group.

Results and discussion

Synthesis of thioureas via MCR (AM-3CR)

To obtain various catalytically active thioureas *via* the above mentioned MCR pathway, we synthesized several *N*-cyclohexyl thioureas (see Figure 9) varying the second moiety. We changed the solvents for AM-3CR from high-boiling DMF, and toluene, or bulk,[10,169] to methanol

(*c*(isocyanide)=1 M), since bulk reaction conditions turned out to be troublesome in some cases due to restricted stirring. Using a minimal excess of sulfur (1.12 eq. corresponding to the amount of sulfur atoms) and amine (1.10 eq.) proved to be sufficient for achieving high yields. Elevated reaction temperature (up to 80°C) was sometimes needed to achieve full conversion or obtain higher yields. In many cases column chromatography could be avoided, and purification was performed by simple precipitation.

Since Curran *et al.* had shown that the trifluoromethyl groups of an aryl moiety adjacent to the thiourea group can be partially replaced by an ester group to increase the solubility of the thiourea, while maintaining catalytic activity,[397] we decided to investigate the impact of aromatic ester moieties on the hydrogen bonding ability (compound **25**). Following this idea, a thiourea bearing an aromatic sulfone moiety (compound **26**) was prepared, expecting similar features. In addition, several other moieties (aromatic, benzylic and aliphatic) were investigated for their suitability of the new synthesis approach as well as for their hydrogen bonding activity, bearing the potential of an easier access *via* sustainable resources (see Figure 9). Commercially available cyclohexyl isocyanide was first reacted with cyclohexyl-, furfuryl-, and benzyl amine, as well as with ammonia and hydrazine to obtain the corresponding thioureas **17-**21 in one step in good yields (70–89%). Since aromatic amines are less nucleophilic and basic, thus preventing the formation of the desired thiourea (see chapter 4.1), aryl moieties had to be introduced *via* the isocyanide component, resulting in products **22-27** in yields between 26 and 82%. In the case of thioureas **26** and **27**, the corresponding isocyanides were found to be sensitive to moisture, as they started to decompose to the respective *N*-formamide when column chromatography was performed or remaining dehydration reagent ($POCl_3$) was quenched with aqueous sodium hydrogen carbonate solution. This observation was attributed to their higher electrophilicity resulting from the electron-withdrawing groups (EWG). In the case of the aromatic thiourea derivatives **22-27**, the isocyanide starting component could not be synthesized *via* our recently reported more sustainable synthesis protocol using *p*-TsCl as dehydration reagent (compare previous chapter),[258] as test reactions to obtain methyl 4-isocyanobenzoate **13** (corresponding to thiourea **24**) led to very low yield (13%).[258] Instead, the toxic $POCl_3$ had to be used in this case for the dehydration step. In summary, the synthesis of the thioureas depicted in Figure 9 is achieved in a straightforward one step reaction with acceptable to good yields, clearly demonstration the advantage of the MCR approach for the synthesis of structurally diverse organocatalysts.

Hydrogen bonding strength of thiourea compounds

In 2014, Hilt *et al.* showed that the hydrogen bond donor ability of thioureas can be quantified by ^{31}P-NMR analysis of a suitable hydrogen bond acceptor (tri-*n*-butylphosphine oxide) and further correlated with their catalytic activity.[526] Formation of a thiourea phosphine oxide complex led to a downfield shift of the ^{31}P signal with increasing hydrogen bonding strength of the thiourea compound. The hydrogen bonding ability of the thioureas **17-27** was thus determined *via* ^{31}P-NMR measurements following a protocol adapted from Franz *et al.* using triethyl phosphine oxide ($POEt_3$) as analytical reagent (chemical shift δ in ^{31}P-NMR was 51.40 ppm in CH_2Cl_2/$CDCl_3$ 4:1).[527] Table 11 shows the chemical shift δ of the respective thioureas and the difference compared to pure $POEt_3$ ($\Delta\delta$). The thioureas derived from ammonia and hydrazine (**18** and **19**) show negligible downfield shifts, as expected due to an increased electron density of the thiourea motif. Similar observations were made for **23**, bearing two thiourea groups connected by an aromatic system, but the solubility of this compound was very low and thus, these shift values should be considered with caution. Dicyclohexyl thiourea **17** showed a small downfield shift of 1.54 ppm, while benzylic moieties, as present in **20** and **21**, resulted in moderate shifts of 3.06 and 2.54 ppm, respectively, which were higher compared to the shift of phenyl thiourea **22** (2.06 ppm). While aryl ester thiourea **24** led to a

moderate chemical sift of 2.86 ppm, the other electron-deficient aryl thioureas **25-27** exhibited higher downfield shifts, thus indicating stronger hydrogen bonding.

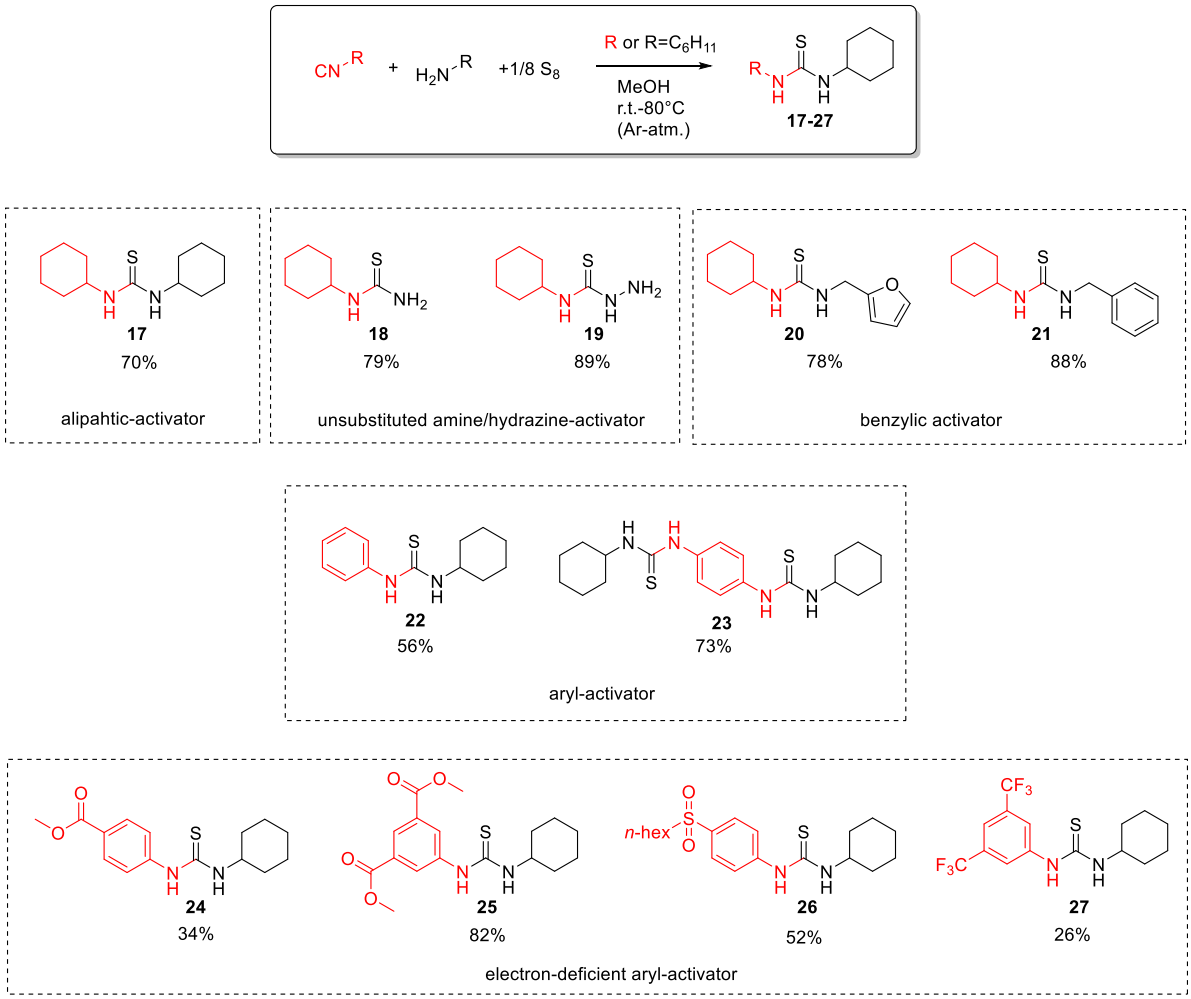

*Figure 9: Overview of the synthesized N-cyclohexyl thiourea derivatives **17-27** using AM-3CR (isocyanide is the red moiety in the final catalyst). Cyclohexyl isocyanide and the corresponding amine component were used to prepare non-aryl thiourea derivatives, while aryl thioureas were prepared using cyclohexyl amine and the corresponding isocyanide. Since the respective isocyanide of compound **27** was sensitive to moisture, it was converted immediately after it had been formed and the given yield is referenced to the used N-formamide which was dehydrated to the isocyanide.*

Compared to aryl thiourea **24** bearing one ester group in *para*-position, thiourea **25** showed considerably stronger hydrogen bonding due to two ester groups in meta position of its aromatic system, being consistent with the early findings of Schreiner that two electron-deficient substituents attached in meta position of the aryl thiourea group resulted in the most efficient catalyst.[400] Applying the stronger electron-withdrawing sulfone group, hydrogen bonding was further increased based on the Δδ-value of 4.82 ppm of thiourea **26**. Even though only one sulfone group is attached to the *para*-position, sulfonaryl thiourea **26** showed stronger hydrogen bonding than both ester aryl thioureas, which was attributed to the intrinsically higher electron-withdrawing-strength of the sulfone moiety. Compound **27** was considered as a benchmark for the typically used 3,5-bis(trifluoromethyl)phenyl moieties in thiourea catalysis to determine the magnitude of chemical shift required for a thiourea compounds to be a suitable candidate as catalyst in this investigation (thiourea **27** itself was already reported as potent catalyst in aminolysis of carbonates,[417] also *vide infra*). Comparing the Δδ value of thiourea **26** and **27** (4.82 ppm and 5.14 ppm) showed that one sulfone group attached in *para*-position of the aromatic moiety resulted in a slightly lower shift than

two trifluoromethyl groups at each meta position, suggesting that compound **26** could act as an organocatalyst with a similar potential as thiourea **27**.

*Table 11: Relative hydrogen bonding strength of the thioureas **17-27** determined by ^{31}P-NMR measurement of a complex of $POEt_3$ and the respective thiourea. The corresponding chemical shift δ and Δ δ-values of the supramolecular complexes are listed.*

thiourea	chemical shift δ /ppm	Δδ /ppm
17[c)]	52.94	1.54
18[c)]	52.76	1.36
19	52.13	0.73
20	54.49	3.09
21	53.94	2.54
22[d)]	53.42	2.02
23	52.44	1.05
24[b), c)]	54.26	2.86
25[c)]	55.72	4.33
26	56.21	4.82
27	56.53	5.14

a) Each thiourea compound (2.40 eq.) was added to $POEt_3$ (1.00 eq.) in a mixture of CH_2Cl_2/$CDCl_3$ (4:1). The experiments were performed three times and the average values are given. b) The experiments were performed two times and the average is given. c) Catalyst was not entirely soluble under the applied conditions. d) Thiourea showed very low solubility even when the amount of solvent was doubled.

Investigations of catalytic activity in an U-4CR

Using the results of the quantification of the hydrogen bonding strength as a guide, thioureas **17-27** were evaluated for their catalytic activities. First, we sought to investigate the potential use of thioureas as catalysts in the U-4CR, as the mechanistic pathway of the reaction shows several steps that might profit from thiourea hydrogen bonding. For instance, thioureas are expected to increase the Brønsted acidity of the carboxylic acid component by anion stabilization and enhance the electrophilicity of the aldehyde or acylimidate by complexation (see Table 12 and Scheme 31).

Thus, the synthesis of Ugi-product **28** was followed by ^{1}H-NMR, as conversion can easily be evaluated in this case (see Table 12). Bisamide **28** was synthesized using acetic acid **29**, *p*-toluidine **30**, *p*-methoxy benzaldehyde **31** and tert-butyl isocyanide **32** in dry $CDCl_3$ in the presence of 10 mol% of the respective thiourea compound. The Schreiner catalyst (bis(3,5-(trifluoromethyl)phenyl) thiourea) was tested as a reference for its catalytic activity in the U-4CR and the conversion of acetic acid was determined using the singlet signal of its CH_3 group compared to the respective signal in product **28**. Conversions were recorded at two reaction times (66 hours, and 6 days) and are listed in Table 12. We set out to investigate the catalytic activity in rather dilute, non-optimal conditions (0.10 M corresponding to acetic acid) to enable the observation of possible catalytic effects. We note that the herein reported yields are thus lower than those obtained under commonly employed conditions (0.50 M concentration of acetic acid **29** in methanol yielded 58% of **28**).[182528] Importantly, no

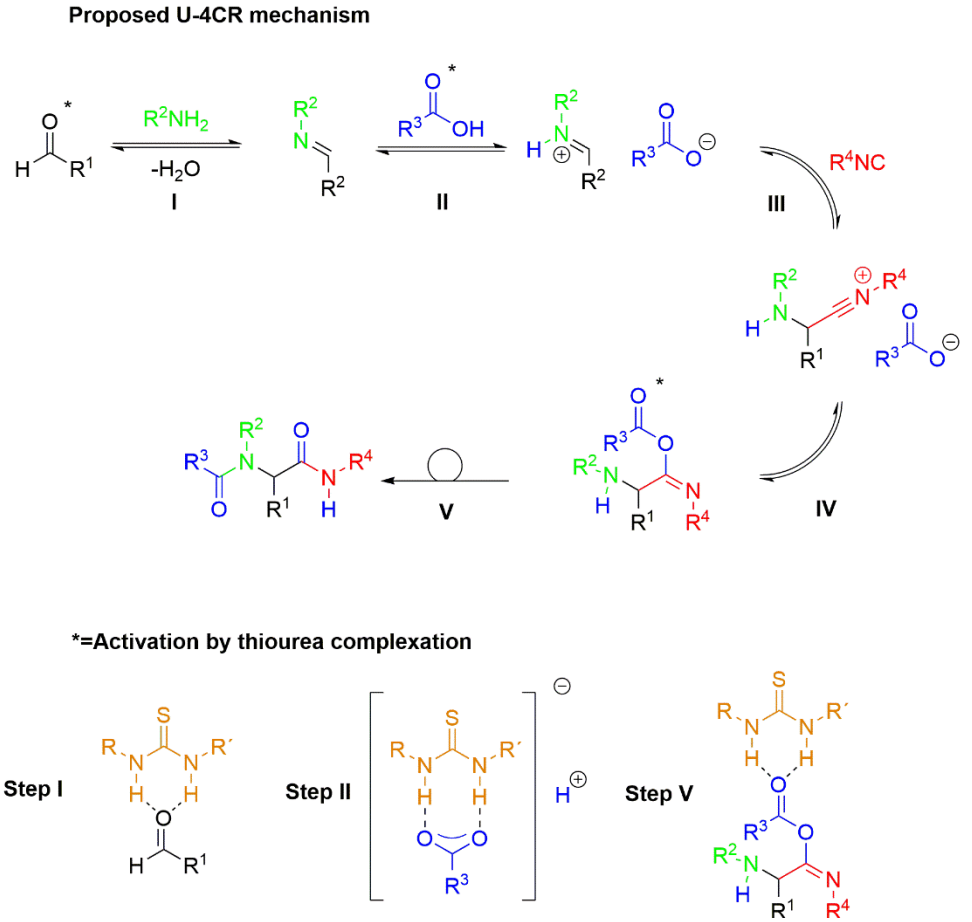

Scheme 31: Proposed reaction pathway for the U-4CR of an aldehyde (black), an amine (green), a carboxylic acid (blue) and an isocyanide (red). By enhancing the electrophilicity of an aldehyd, a thiourea (orange) might catalyze imine formation (step I). On the other hand, stabilizing the carboxylate anion would increase the Brønsted acidity of the carboxylic acid, resulting in an equilibiurm shift towards the protonated imine (step II). In addition, Mumm-rearrangement might be fostered by enhancing the electrophilicity of the ester carbon (step V). The corresponding proposed thiourea complexes are shown below. Adapted from SI of the authors publication.[591]

Passerini or other side-products were detected. When thioureas **17-22**, all showing low to moderate hydrogen bonding according to Table 11, were used as catalysts in U-4CR, the conversion did not increase compared to the respective blind test (19% conversion, all within expected error margin). Since polar protic solvents are known to improve the conversion of Ugi-4CR reactions,[182] the addition of methanol as catalytic species (40.0 mol%) was also tested without notable effect. Aryl ester thiourea **24** did show a minimal positive effect, while aryl diester thiourea **25** led to a slightly increased conversion of 22%. Finally, sulfonaryl thiourea **26**, showing the highest observed chemical shift in Table 11, led to an increased conversion of 28% after six days, which was similar to reference compound **27** (27% after six days). These results further confirmed the obtained data of the NMR-investigation, *i.e.* that compound **26** shows similar catalytic properties than compound **27**. The highest conversion of 31% after six days was obtained by the Schreiner catalyst, which was ascribed to its two activating moieties. Increasing the catalyst-loading to 20 mol%, catalyst **26** achieved same conversion than the Schreiner catalyst (33% conversion after six days). The improved performance of catalyst **26** in higher concentrations is most likely due to better solubility of this compound, since the Schreiner catalyst was not completely soluble under this condition. Although this catalytic enhancement seems small (absolute increase in yield 14%, relative increase in yield ~73%), it shows that an Ugi-4CR can be positively influences using thiourea catalysts, opening new possibilities in the field of multicomponent reactions.

*Table 12: Investigations of catalytic activity of thiourea compounds and methanol in an U-4CR leading to Ugi product **28**. Conversions were determined by measuring ^{1}H NMR-spectra of the respective reactions after 66 hours, and 6 days.*

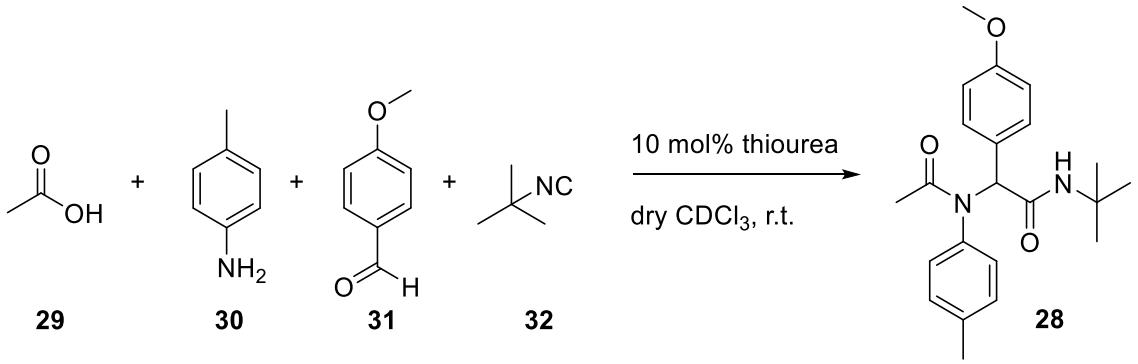

thiourea	conversion after 66 h/%[a)]	conversion after 6 d/%[a)]
-	14	19
17	12	17
18	14	20
19	12	16
20	14	19
21	11	17
22	16	19
23[b)]	15	20
24	14	20
25	16	22
26	21	28
26[c)]	n. d.	33
27	22	27
Schreiner catalyst	26	31
Schreiner catalyst[b), c)]	n. d.	33

a) Reactions were performed with carboxylic acid (1.00 eq.), amine (1.50 eq.), isocyanide (1.50 eq.), aldehyde (1.38 eq.) and 10 mol% of the respective thiourea compound in dry $CDCl_3$ (c(carboxylic acid)=0.10 M) at room temperature (r.t.). Each experiment was performed three times and the average values are given. b) was not completely soluble. c) 20 mol% catalyst was used.

Catalysis of aminolysis of propylene carbonate

In order to further explore the potential of thiourea **26** as a catalyst, we sought to use it in another reaction where its previously reported analogue, thiourea **27**, exhibited high organocatalytic activity. Therefore, the aminolysis of propylene carbonate **33** with cyclohexyl amine **34** was chosen and two carbamates **35a** and **35b** as regioisomers were obtained, as previously reported by Caillol and Andrioletti.[417] The reaction is known to be effectively catalyzed by urea and thiourea compounds like thiourea **27**, among others (see Table 13). In addition, thiourea **25**, which showed minimal catalytic activity in U-4CR, as well as thiourea **17**, **22** and **23**, were tested in this aminolysis reaction. While only 7% of conversion (9% reported in literature) was observed after one hour in the absence of any catalyst for this reaction, thiourea **27** was reported to show 66% of conversion. In our experiments, the conversion was slightly higher, obtaining 70%. Sulfonylaryl thiourea **26** yielded similar results with a conversion of 68%, confirming the similar activating effect of sulfonylaryl thiourea and aryl-CF_3 moieties already observed for the Ugi-4CR reactions. Interestingly, the conversion of the reaction using isophthalic acid ester thiourea **25** as catalyst reached 65% conversion after one hour, thus indicating that diester aryl motifs are also suitable candidates for organocatalysis.

*Table 13: Aminolysis of propylene carbonate **33** with cyclohexyl amine **34** catalyzed by several thiourea compounds.*

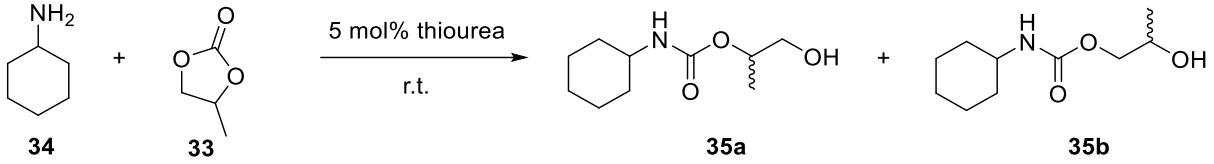

34 **33** **35a** **35b**

catalyst	conversion after 30 min/%[a)]	conversion after 60 min/%[a)]
none	3 (5)	7 (9)
thiourea 17	12	25
thiourea 20	16	30
thiourea 22	27	38
thiourea 23[b)]	21	33
thiourea 25	55	65
Thiourea 26	59	68
thiourea 27	64 (55)	70 (66)
Schreiner catalyst	47 (28)	58 (41)

As the viscosity of the reaction mixtures increased with conversions, we added ethyl acetate to obtain a homogeneous solution before taking a GC-sample. Values in brackets were reported in the literature. a) Each experiment was performed three times and the average is given. Biphenyl (12 mol%) was used as internal standard. b) Catalyst was not completely soluble.

Comparing benzylic thiourea **20** with aromatic thiourea **22**, the aromatic catalyst showed a higher but still moderate activity (38% conversion after one hour). These results are contradictory to the determined hydrogen bonding strength of thiourea **20**, which was higher compared to thiourea **22** (Δδ-value was 3.09 ppm for **20** and 2.02 ppm for **22**) underlining that hydrogen bonding strength obtained by ^{31}P-NMR measurements is a good first indicator for catalytic activity of thiourea catalyst, but performance in the actual catalytic system may vary. Furthermore, dithiourea **23** showed improved performance if compared to thioureas **17** and **20**, while showing the lowest hydrogen bonding strength (Δδ-value 1.05 ppm), which was attributed to the fact that the concentration of catalytically active thiourea functional groups was doubled due to its bis-functionality. Compared to thiourea **25-27**, Schreiner catalyst yielded slightly lower conversions after one hour (58%), being consistent with the results reported previously. However, the reported conversion of the Schreiner catalyst (41%) differed from our observations, most likely due to adjusted reaction conditions compared to the literature (see Table 13).

Conclusions

Various differently functionalized thiourea compounds were synthesized using a straightforward and a less hazardous synthesis protocol via an MCR of an amine, an isocyanide and elemental sulfur. The hydrogen bonding strength of the thiourea compounds was evaluated using ^{31}P-NMR measurements. Subsequently, their catalytic activity was verified by applying them as catalysts in an U-4CR, revealing that sulfonylaryl thiourea moieties lead to catalysts with similar activities as catalysts bearing aryl-CF_3 groups. Subsequently, the aminolysis of propylene carbonate was evaluated, confirming that *p*-(alkylsulfonyl)phenyl and dialkylisophtalic acid ester moieties are suitable activating functional groups for thioureas in organocatalysis. Especially the sulfone group showed comparable results to the commonly used 3,5-bis(trifluoromethyl) phenyl group in all tests. The herein introduced functional groups are promising moieties for thiourea catalyst design, since they are tailorable and thus allow to increase the solubility of the respective catalyst compared to commonly applied

catalysts. They furthermore broaden the scope of suitable EWGs, paving the way for a wider scope of application of thiourea compounds in organocatalysis.

4.3 Transferring catalytically active thiourea motifs to polymers

Since one aim of this thesis was the access to more sustainable TU organocatalysts, in a final step of this project it was investigated if thiourea functional groups with activation motifs discussed and introduced in chapter 4.2. could be introduced into polymeric structures. The recyclability of these poly(TU)s were investigated subsequently to obtain first insights if a potential application as recyclable organocatalyst might be reasonable. Thus, potential catalytically active thiourea groups were synthesized using the AM-3CR and transferred into a polymeric structure by several approaches. As less reaction steps reduce the amount of produced waste, the focus was set on straightforward approaches, especially for the synthesis of suitable TU containing monomers. In the following, these approaches are discussed and evaluated thoroughly followed by a brief comparison and final discussion.

As activating motifs for the thiourea compounds, (*p*-alkylsulfonyl) aryl and isophthalic acid ester groups were chosen, since they proved suitable catalytic activities (see chapter 4.2.). Furthermore, they allowed the introduction of moieties that could increase the overall solubility in organic solvents, like DCM and toluene, which are typically used for organocatalyzed reactions. Thus, it was hypothesized to obtain a catalyst capable of homogeneous catalysis. In addition, every approach was envisioned to be conducted with the 3,5-bis(trifluoromethyl) phenyl group to obtain a benchmark catalyst, since this group had proved its potential for broad application in organocatlaysis for more than two decades (see chapter 2.4.1.).

Since electron-deficient thiourea motifs are needed, they can only be introduced *via* the isocyanide compound (as discussed in chapter 4.2.), leading to highly reactive isocyanides. These compounds have to be handled with care and usually result in low yields for the corresponding thiourea (compare yield of thiourea **26** and **27** in chapter 4.2.). Moreover, as discussed in chapter 4.1., the desired aryl isocyanides cannot be obtained by the herein reported more sustainable synthesis protocol. Thus, the $POCl_3$-based method had to be employed for their synthesis. The final hypothetical poly(TU) catalyst will have an increased overall E-factor as a result of the low yield of its precursor (isocyanides and/or thiourea), while the overall use of toxic compounds will be increased as well.

4.3.1 Poly(thiourea)s *via* step-growth AM-3CPR

Initially, a step-growth polymerization approach was envisioned to obtain poly(TU)s using the AM-3CR as a polyaddition reaction (AM-3CPR) between diisocyanides, diamines, and elemental sulfur. This reaction was already successfully reported for poly(TU) synthesis by Hu, Tang *et al.* which were used for application in mercury pollution.[169] No investigation or evaluation of catalytic activities of the obtained poly(TU)s were reported. Using the AM-3CPR for the synthesis of poly(TU)s as organocatalysts is beneficial, as the catalytically active TU motifs are formed during the polymerization reaction decreasing the overall reaction steps for these compounds. In a first investigation, it was evaluated if this polymerization approach is applicable for TU motifs bearing electron-deficient aryl activating motifs.

Thus, the introduced activation motifs, *i.e.* (*p*-alkylsulfonyl) aryl and isophthalic acid esters groups had to be implemented in a suitable diisocyanide (as mentioned before, only the isocyanide component can introduce these moieties, see chapter 4.2.). The most reasonable candidates envisioned for the AM-3CPR are shown in Scheme 32.

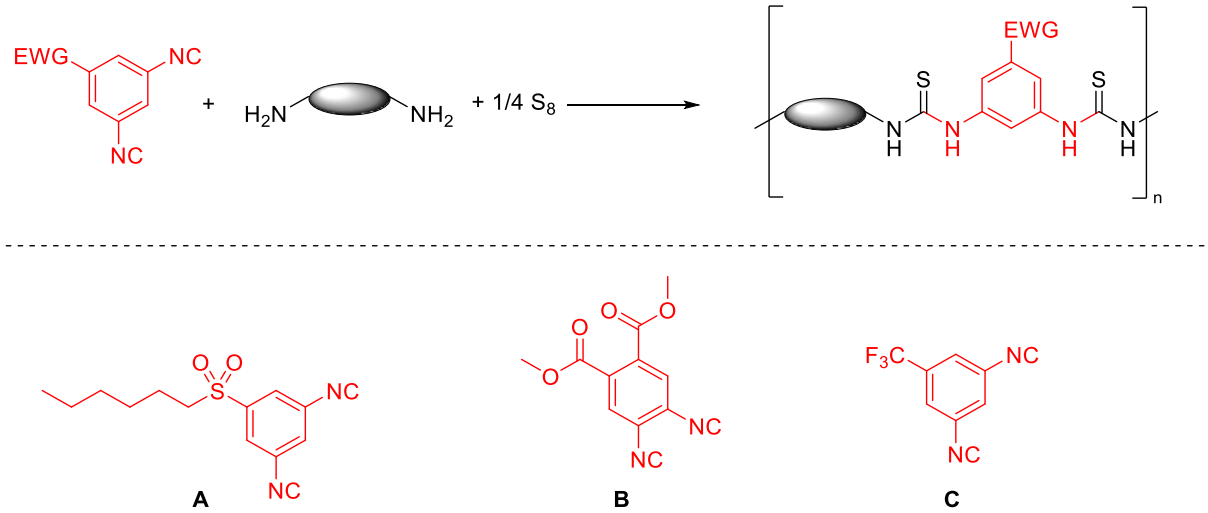

*Scheme 32: Overview of the poly(thiourea) synthesis by step-growth approach using the AM-3CPR between electron-deficient diisocyanide (red), diamine, and elemental sulfur. In addition, two reasonable diisocyanides are depicted bearing the alkylsulfonyl aryl or ester aryl groups, respectively (**A** and **B**) as electron-withdrawing groups (EWGs). To yield reference poly(TU)s compound **C** was hypothesized. Note that the polymeric structure depicted is obtained using diisocyanide **A** and **C**.*

The alkylsulfonyl group does not necessarily need to be attached to the aryl isocyanide in *para* position, but can also be attached in *meta* position, probably resulting in similar activation of the later formed TU (see chapter 2.4.1.). Thus, a 3,5-diisocyano arylsulfone **A** was hypothesized as a suitable candidate for the AM-3CPR. However, as no appropriate precursor for this compound was commercially available nor a straightforward synthesis protocol was reported, only an elaborate synthesis was envisioned, starting for instance from halogen benzene being very time-consuming.[2]

[2] Hypothesized synthesis protocol for diisocyanide **A** in Scheme 32:

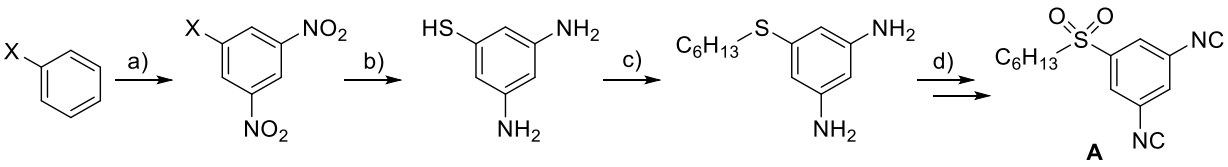

X= Cl, Br, I; a) H_2SO_4, HNO_3; b) i.) Na_2S, ii.) S_8, $NaHCO_3$;[124] c) alkylation, and subsequent steps d) (oxidation, formylation, isocyanide synthesis) following the procedure of thiourea **26**.[592]

Therefore, this approach was inapplicable for the alkylsulfone aryl activation group in the time scale of this thesis. Nevertheless, compound **A** could probably yield poly(TU)s exhibiting catalytic abilities.

On the other hand, the isophthalic acid ester moiety bears two ester groups, which also can be attached either at the *para* or *meta*-position as discussed above maintaining a certain level of activation ability. To avoid the occupation of the adverse *ortho*-position (see chapter 2.4.1.) of one of the two needed isocyanide groups on the same aromatic ring, only phthalic acid ester **B** is a possible candidate. However, as for compound **A**, only a time-consuming synthesis protocol was found for compound **B**, for instance, 4,5-dimethyl-2-nitroanilin can be converted in three step[3] and thus, this approach was also not applicable in the remaining time of this work.[4]

Finally, as mentioned in the previous chapter, a benchmark polymer was envisioned bearing a 3,5-bis(trifluoromethyl) phenyl group. Since no compounds were determined to compare the benchmark, the purpose of the molecule was redundant. However, since this moiety is often depicted as a guarantor for catalytic activity, the step-growth approach by AM-3CPR was still applied to further validate if poly(TU)s could be obtained by this approach. Following the above-mentioned points, the removal of one CF_3 group allows the utilization of 5-(trifluoromethyl) benzene-1,3-diisocyanide **C** which is easily accessible by the respective commercially available diamine. The loss of the second CF_3 group will probably reduce the catalytical activation properties, but it can be assumed that it will not lead to inactivation as shown by Schreiner *et al*.[400] However, in this case, the synthesis of the diisocyanide **C** from the respective 5-trifluoromethylphenyl-1,3-di-*N*-formamide failed and a glassy insoluble black solid was obtained after purification with column chromatography.[5]

Concluding the initially envisioned step-growth approach is not suited for the formation of poly(TU)s bearing electron-deficient aryl groups as the synthesis of reasonable monomers would result in a very elaborate and time consuming synthesis involving several steps. As these moieties are typically used nearly exclusively for the activation of thioureas, no alternative substituents could be imagined. Thus, it was envisioned that different approaches to incorporate catalytically active thiourea motifs in polymers exhibit a higher potential, since they were more feasible involving starting materials that are less time consuming to synthesize and can be accessed using already established synthesis procedures of this work.

---

[3] One example of a synthesis protocol for diisocyanophthalicacid ester **B** with the least amount of steps reported:[638]

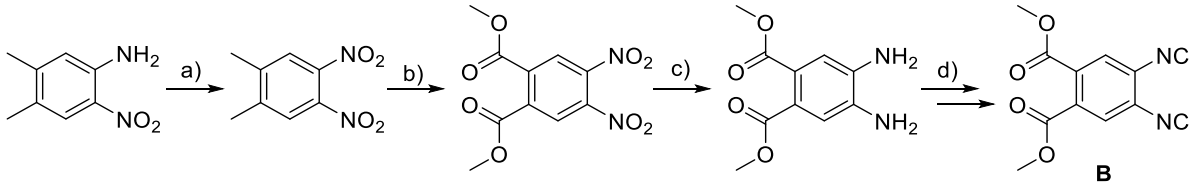

a) H_2O_2, AcOH; b) i.) HNO_3, ii.) $SOCl_2$, MeOH; c) H_2, Pd/C, d) formylation, isocyanide synthesis) following the procedure of thiourea **26**.[592]

[4] Note that the use of only one ester group attached to the phenyl ring, *i.e.* the 3,5-diisocyano aryl ester, similar to compound **A**, would be a candidate that is easily accessible, since the respective acid is cheap and commercially available. However, the absence of the second ester group would result in an inactivation of the TU compound (compare one to two ester moieties in the catalytic activity studies in chapter 4.2.).

[5] Isocyanide vibration was confirmed by IR-analysis of the obtained insoluble solid. It was assumed that the highly reactive isocyanide underwent polymerization.

4.3.2 Poly(ester)s bearing thiourea functions in side chains by polycondensation

Some experiments of this chapter were performed by a student (Peter Conen) working as a research assistant and an apprentice for chemical technical assistant (Benjamin Felker) under the supervision of the author. The respective experiments are highlighted with footnotes.

As the direct incorporation of TU functional groups into a polymer backbone by a step-growth approach with the AM-3CPR, was not considered a suitable approach, another approach was investigated yielding poly(ester)s bearing the organocatalytically active thiourea moiety in the side chain.

In order to incorporate the thiourea moiety in the side chain of a polymer, a monomer has to be designed, which can reliably be polymerized and furthermore contains the thiourea functionality which is stable under the applied polymerization conditions. It was assumed that a suitable polymer reaction exhibiting the mentioned features was a polycondensation reaction, since i.) the reaction set-up is usually straightforward and can be tailored to fulfill several demands of Green Chemistry (no solvent, no additional toxic reagents), ii.) a suitable TU monomer was already synthesized in chapter 4.2, *i.e.* isophthalic acid ester thiourea **25** (see scheme 33), iii.) the second moiety of the TU can be tailored to adjust solubility in a later stage of this research and iv) the TU moiety was expected to be inert under typical conditions applied for a polycondensation. In the following, the investigation of the polycondensation reaction of thiourea diester compounds is discussed.

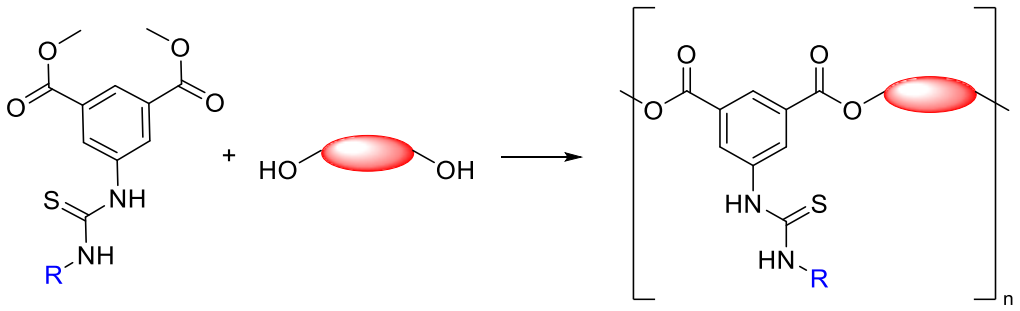

*Scheme 33: Overview of the envisioned polycondensation reaction to introduce TU functional groups into a polymer in the side chain. The moiety of the dialcohol (red ellipsoid) and the second moiety of the thiourea component (blue) can be tailored to adjust the solubility of the resulting polymer. A representant of the herein depicted group of isophthalicacidester thiourea was already synthesized in chapter 4.2. (compound **25**).*

Establishing a synthesis protocol for the polycondensation reaction

To optimize the reaction conditions of the polycondensation reaction and allow for a broad range of analysis, especially in solution analysis, a transesterification reaction with mono alcohols was initially investigated as a model reaction. It was assumed that the obtained parameters can be transferred to a polymerization reaction with dialcohols. Instead of the utilization of compound **25** bearing a cyclohexyl moiety, another isophthalicacidester thiourea **36** (see figure 10) was synthesized bearing a *n*-dodecyl moiety, since it was hypothesized that a long, non-branched aliphatic chain could increase the overall solubility of the starting material and the product. Therefore, the respective isocyanide was converted with *n*-dodecylamine and sulfur to thiourea **36**in an AM-3CR following the protocol in Figure 9 (yield 63%, r.t., overnight). Second, dodecanol **37** was chosen as a suitable alcohol component exhibiting a high boiling point (T_b = 260-262 °C), allowing the evaluation of elevated temperatures, necessary for a polycondensation, without loss of the starting material.[529]

The rection set-up allowed the monitoring of the reaction *via* ^{1}H-NMR-spectroscopy for a rapid determination of the conversion. Figure 10 shows an example of a ^{1}H-NMR-spectrum of the reaction mixture at t=0 hours and after two days.

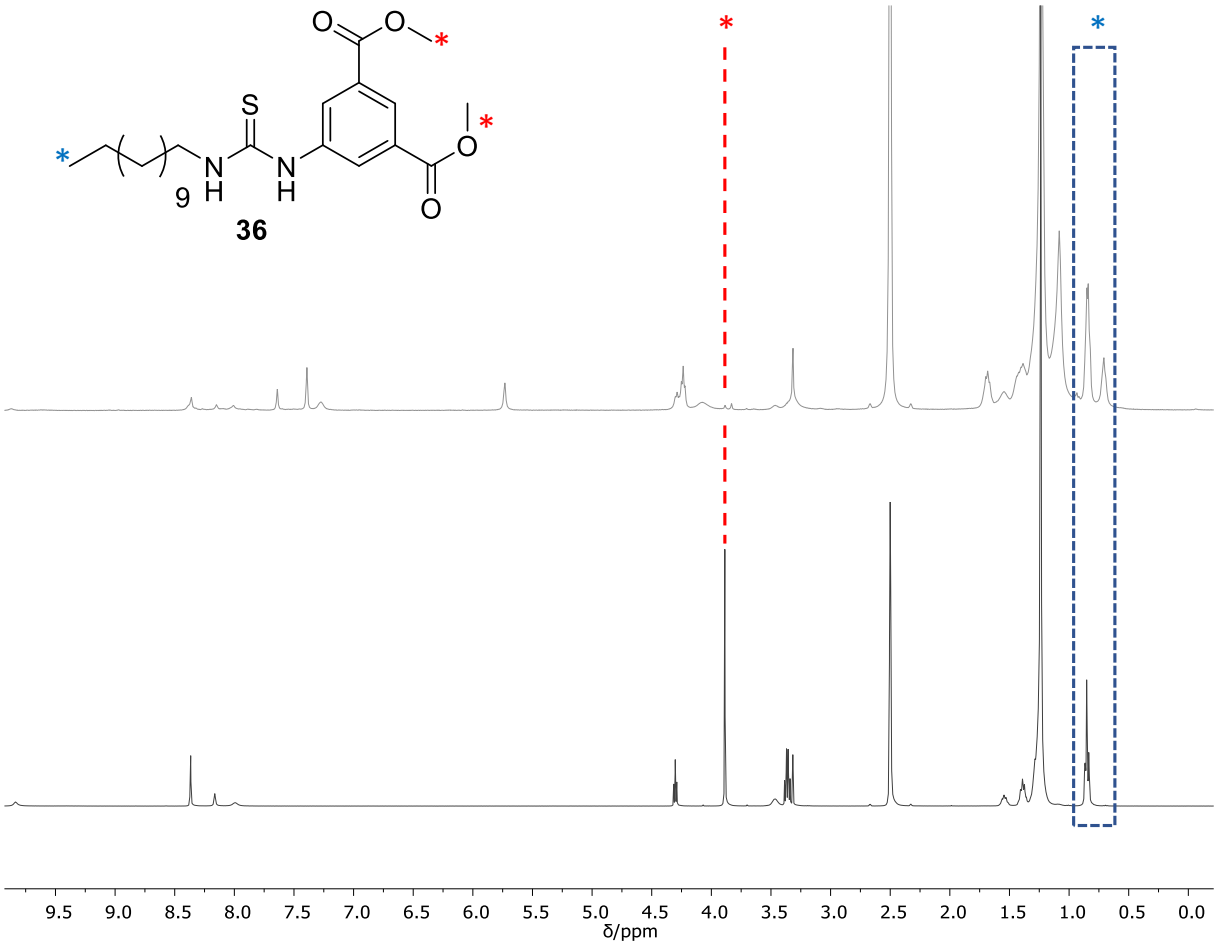

*Figure 10: Stacked ^{1}H-NMR-spectra. Top: reaction mixture of thiourea **36** and dodecanol **37** after two days (100 °C, 10mol% Ti(O^{i}Pr)$_4$, bulk. Bottom: pure thiourea **36**. Conversion of the transesterification reaction could be monitored by following the decrease of the CH_3 signal of the methyl ester group (red, at 3.89 ppm, integral of 6.0 at t=0 h since two ester groups were present in compound **36**) while referencing on all terminal CH_3 of the dodecyl chains, i.e. the one of the thiourea **36**and both equivalents of dodecanol **37** (blue, at 0.85 ppm, integral of 9.0).*

The CH_3 signal of the methyl ester groups was an ideal candidate to follow the reaction, since the singlet signal decreases during the reaction and no other signal overlaps in this range. On the other hand, no internal or external standard was needed, because the terminal CH_3 groups of the dodecyl chains (one present in thiourea **36** and two equivalents in dodecanol **37**) could be used as a reference as their value does not change over the course of the reaction. Since the chemical surrounding of both terminal CH_3 groups was very similar, only one signal was obtained (the signal consists of two triplets resulting from each of the two CH_3 species, which can only be seen in a zoom-in as their chemical shift is nearly identical, see Figure 10, bottom). In addition, both signals did not overlap with other signals of the starting materials (see Figure 10, bottom), or signals formed during the reaction (see Figure 10, top). Therefore, the starting point of the reaction at t=0 h can be set to a ratio of integrals 2:3 for CH_3 of esters compared to CH_3 of dodecyl chains. However, in the following described experiments, it was found that the actual value of a t=0 h-sample showed a slightly lower value for the CH_3 ester group (*e. g.* 5.7 instead of 6.0) when referenced on the terminal CH_3 groups. This probably occurred due to the base line error of the NMR-instrument as well as the fact that intensities of signals in the deep field region are often slightly lower compared to signals in the high field region. Thus, the actual ratio of the CH_3 groups was used for the determination of the conversion and was always determined by the respective t=0 h-measurement.

In addition, at a certain level of conversion of the ester groups, it was observed that the terminal CH_3 signal of the dodecyl chains at 0.85 ppm start to split up (one remained at 0.84 ppm and one appeared at 0.71 ppm). It was not clear which species is formed resulting in a CH_3 group with a signal shifted more towards the highfield. Both signals could be integrated together and used as reference signals for determination of the conversion, but a certain degree of uncertainty arose due to the increased error of the base line. Since the aim of this experiments was not to quantify the conversion at a certain time scale with the highest accuracy, but rather determine the highest (ideally full) conversion, monitoring by ^{1}H-NMR-spectroscopy was assumed to be still a reasonable analysis method for the transesterification reaction due to it feasibility. It has to be noted that the utilization of an internal standard, *i.e.* 1,3,5-trimethoxy benzene, was envisioned to further increase the resolution of the monitoring, but upon higher conversion solubility was not maintained. Other monitoring possibilities like GC-analysis, was not possible due to the decomposition of thiourea **36** at elevated temperature (*vide infra*) leading to inconsistent sets of data.

With the monitoring in hand and having chosen both starting materials, a first reaction was performed at 100 °C in DMF (*c*(thiourea)=2 M). The stoichiometry of the reaction was held at equimolar conditions (2.00 eq. of dodecanol **37** per thiourea **36**), since this condition would lead later to the highest molecular weights in a step-growth.[6] In addition, 10 mol% of a catalyst, *i.e.* $Ti(O^iPr)_4$ was applied to facilitate the conversion (see Table 14, entry 1).

Since only a low conversion of 32% was achieved after two days, in a next step, the reaction was performed without any solvent (Table 14, entry 2) while sufficient stirring was ensured at the beginning of the reaction (dodecanol **37** was a liquid at the applied temperature which was able to dissolve thiourea **36** completely). The obtained conversion increased to 82% after two days. Subsequently, several other catalysts were tested including Lewis and Brønsted acids (see Table 14, entry 3-6) but $Ti(O^iPr)_4$ remained to be superior. As the titaniumalkoxide seemed to provide decent conversion, also $Ti(OBu)_4$ was tested obtaining nearly full conversion (95% after two days, see Table 14 entry 7).

Even though the titaniumalkoxides yielded high conversions, it was noted that side products were formed, as indicated by additional signals in the ^{1}H-NMR-spectrum. To ensure that these side-products would not alter the reaction conditions in a later applied polycondensation reaction (for instance, formation of chain stoppers) analysis of these compounds was attempted.[7] A list of determined and indicated side products of the reaction is depicted in Scheme 34 First, TLC evaluation

[6] The degree of polymerization (DP) in a step-growth polymerization between functional group **A** and functional group **B** can be described by Carothers equation, in dependance of conversion p and stoichiometry parameter r:[639]

$$DP = \frac{r+1}{r-2rp+1}$$

Whereas r is defined as: $r = \frac{N_A}{N_B}$ and $r \leq 1$; N_A and N_B are defined as the molar amount of the respective functional group. The equation describes an exponential growth and thus results in an infinite DP as conversion p reaches one. If the conversion p is held constant, the highest DP will be obtained at $r = 1$ and the equation transforms to:

$$DP = \frac{1}{1+p}$$

[7] For instance, assuming 5 mol% of a chain stopper would be formed and then react with monomer **A** which was applied initially in equimolar ratio to monomer **B** while conversion would be assumed to be 94% resembling the conversion obtained in the optimized transesterification conditions. Thus, the degree of polymerization (DP) would be calculated by Carothers equation (see previous page) using $r = 0.95$ resulting in a DP of 11.9 (ca. 12-mer). Comparing, 10 mol% chain stopper ($r = 0.9$) would only yield a 9-mer. A 16 to 17-mer is obtained in the absence of chain stopper for this example.

of the reaction mixture using titaniumalkoxide as catalyst with a vanillin staining solution yielded six spots of which were three dark green and three yellow in color. Dark green coloration is typical for thiourea compounds and seldomly obtained by other compounds. Thus, it could be assumed that the mixture consisted of three different thiourea compounds, namely the starting material **36**, the mono substituted dodecyl ester thiourea **39** and the desired product **38** (see Scheme 34).

*Table 14: Screening of different catalysts for the transesterification reaction of thiourea **36** and dodecanol **37**. The reaction has ceased after two days.*

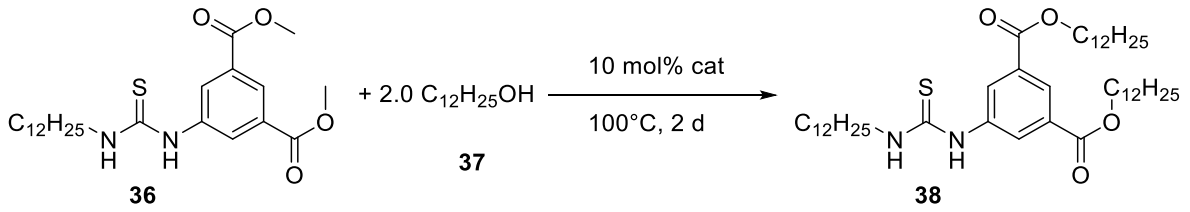

entry	catalyst	conversion of 36 after 1 d/%	conversion of 36 after 2 d/%
1	$Ti(O^iPr)_4$[a)]	24	32
2	$Ti(O^iPr))_4$	72	82
3	$Bi(OTf)_3$	n. d.[b)]	n. d.[b)]
4	$VO(O^iPr)_3$	52	n. d.[c)]
5	H_2SO_4	-	-
6	H_2SO_4[d)]	28	27[b)]
7	$Ti(OBu)_4$	93	95

a) reaction was performed in DMF (*c*(thiourea **36**=2 M). b) ^{1}H-NMR spectrum of the respective reaction mixture depicted the formation of several other species indicating unselective nature of the catalyst and no clear conversion could be determined. c) A dark resin was obtained which could not be dissolved anymore, thus no NMR-sample could be taken. d) 1.00 eq. of H_2SO_4 and 20 mol% $B(OH)_3$ were used.

On the other hand, yellow coloration is quite typical for several functional groups, among them for instance amines and *N*-formamides. It was assumed that a decomposition of thiourea **36** might lead to formation of such side products in this reaction. Most likely, the thiourea functionality will be cleaved forming an isothiocyanate and an amine, whereas the amine compound probably bears the moiety which is the better leaving group (in this case the isophthalic acid moiety).[530] Comparison of the ^{1}H-NMR spectrum of the reaction mixture and a spectrum of pure isophthalicacidester amine **40** revealed that it was indeed formed by the reaction, fitting the TLC-results (see Scheme 34 and chapter 6.5.1.1. for ^{1}H-NMR-Spectrum). The respective dodecyl isothiocyanate **41** was observed by GC-MS-analysis and further, ASAP-MS depicted the mass of the dodecylamine, probably obtained by the further decomposition of the isothiocyanate function. A simple heating test series of thiourea **36** proved that decomposition already takes place in solution in absence of any reagent or additive starting at 70 °C. This was surprising, as for instance poly(TU)s exhibit in general decomposition temperatures above 170 °C (out of 42 poly(TU)s reported in literature, only two depicted a lower decomposition temperature; lowest was 107 °C).[169,531,532] The strong decrease of decomposition temperature probably originated from the activation motif (isophthalicacid ester motif), being a considerably good leaving group compared to typically applied moieties in the referenced poly(TU)s. Following this finding, it could be assumed that the other two compounds indicated by TLC-analysis are the respective amines of the mono substituted dodecyl ester **42** and product **43** (see Scheme 34). Their formation could not be detected in the NMR-monitoring, since the formed amine functional group had probably very similar chemical surrounding as the one of amine **40** and thus, all amine signals lead to one broadened signal (see Figure 24 in chapter 6.5.1.1.).

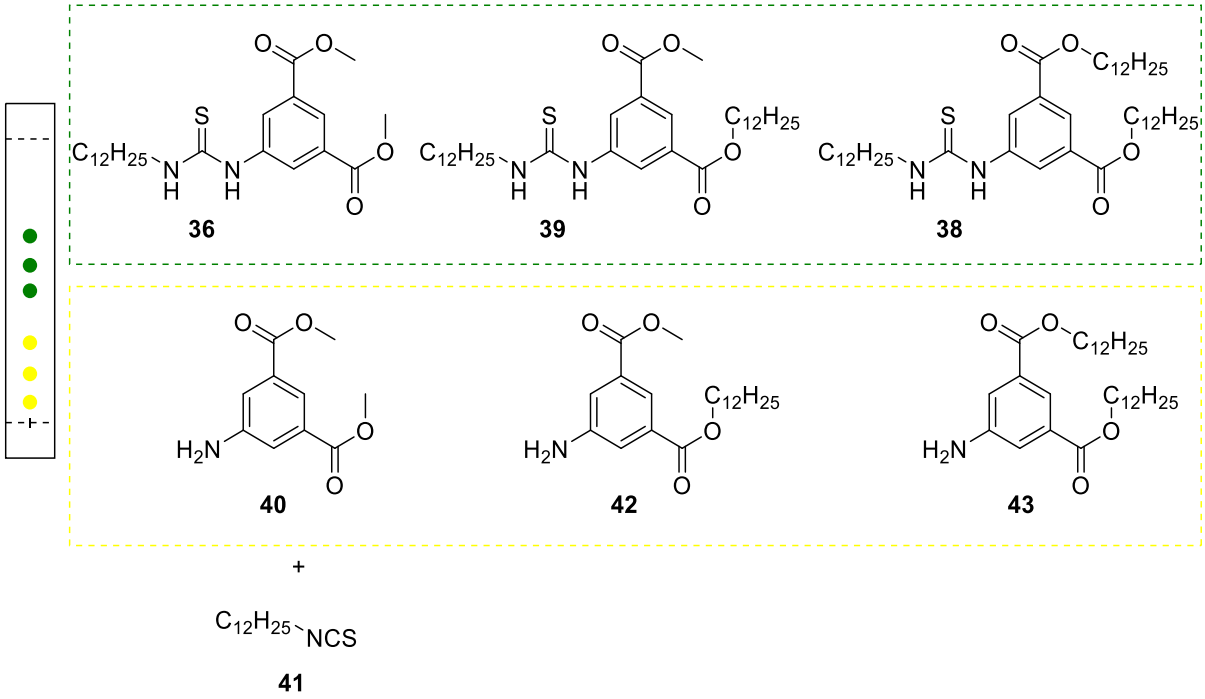

Scheme 34: Schematic of TLC analysis of the reaction mixture in 2:1 CH:EA and stained with a vanillin solution as well as the assigned amines **40**, **42**, **43** and thioureas **36**, **38**, **39**. In addition, dodecyl isothiocyanate **41** is displayed for starting material **36** which was the second decomposition product besides the amine and also indicated by GC-MS and indirect by ASAP-MS analysis.

Since no indication was found that amine **40**, **42**, **43** reacted further or decomposed, or that other side-products were formed in the NMR-monitoring, the degree of decomposition could be determined by ^{1}H-NMR-spectroscopy using the amine signal at 5.73 ppm (broad signal) referenced against the signals of the terminal CH_3 groups (see Figure 24, full decomposition to the respective amines would lead to a ratio of 2:9, NH_2 to terminal CH_3 signal).

Thus, the transesterification was performed using the optimized conditions of Table 14 ($Ti(OBu)_4$ in bulk), while lowering the temperature to suppress the decomposition of the TUs. The results are listed in Table 15:

*Table 15: Screening of different temperatures for the transesterification reaction of TU **36** and dodecanol **37** to suppress the decomposition of TU. The reaction has ceased after two days.*

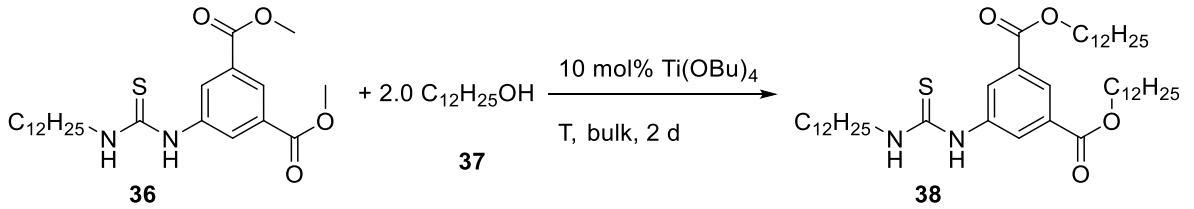

entry	*T*/°C	Conversion of 36 after 2 d/%	Decomposition of 36 after 2 d/%
1	100	95	45
2[a)]	100	82	40
3	90	94	31
4	80	77	10
5[b)]	70	73	15
6	60	-	-

a) $Ti(O^iPr)_4$ was used instead of $Ti(OBu)_4$. b) reaction time was six days.

Applying 100 °C resulted in the best conversion of 95% but also led to a considerable decomposition of the TU functions (45%, see Table 15 entry 1). $Ti(O^iPr)_4$ led to similar decomposition rates (see Table 15, entry 2). As the temperature was decreased to 80 °C, the decomposition rates dropped down to only 10% (see Table 15, entry 4). A higher decomposition rate of 15% was obtained at 70 °C due to the longer reaction time (six days), which were applied (see table 15, entry 5). The transesterification probably stops at some point, while the decomposition still proceeds slowly, ultimately leading to a higher degree of decomposition. Nevertheless, the conversion also decreased to 73% in case of 70 °C (see Table 15, entry 5). Since the reaction does not take place below 70 °C (see Table 15, entry 6), a compromise had to be made to obtain sufficiently high conversion, while maintaining only minor decomposition. Thus, the optimal temperature for the reaction was determined to be 90 °C since high conversion was maintained (94%, see Table 15, entry 3), while the decomposition was 31%.

To complement the obtained data, full characterization of didodecylester thiourea **38** was attempted, purifying the crude product by column chromatography after having applied optimized reaction condition. However, the pure product could not be obtained, because the separation by column chromatography was insufficient. Since the three thiourea compounds show very similar retention (see schematic TLC in Scheme 34), a very elaborate purification process was expected, and further purification was not further attempted. Nevertheless, an, until this point, not detected fraction was obtained in minor amounts, which could be assigned to the *N, O*-didodecyl thionocarbamate **44** (ca. 7% yield, see Scheme 35). The compound was indirectly assigned by comparing its very characteristic ^{1}H-NMR-spectrum to the one of the reference compound, *N*-dodecyl*, O*-hexyl thionocarbamte (see chapter 6.5.1.3.).[8] Two pathways could be envisioned leading to this side-product: i) addition reaction of dodecanol **37** with *in situ* formed dodecyl isothiocyanate **41** after decomposition of thiourea **36** (see Scheme 35, path **A**) or ii) addition elimination of the thiourea function of the starting material **36** by dodecanol **37** (see Scheme 35, path **B**). In both cases, $Ti(OBu)_4$ could mediate or foster the reaction as catalyst.[9]

Considering that this side-reaction would also occur in a polycondensation reaction, the resulting side product would be a thionocarbamte alcohol. This compound could in turn react with its second available alcohol function and an additional isothiocyanate to the dithionocarbamate, which would probably not impede or alter the polymerization process. However, more likely the thionocarbamate alcohol would react as a chain-stopper with the more abundant ester group of monomer thiourea **36** stopping the polymers in their growth, as no terminal alcohol group would be yielded. Therefore, it can be expected that the molecular weight of the hypothetically obtained polymers would be only small or moderate and rather oligomers were expected to be formed.

On the other hand, if thiourea **36** decomposes partly also to the isophthalic isothiocyanate instead of the dodecyl one **41** (which was found to be formed in minor extent for instance for typical heating conditions in a GC-analysis, T>200 °C) the reaction with the respective diol monomer would most likely yield cross linking, which is not necessarily impeding the further polymerization but decreasing

[8] The synthesis of this compound was performed by Benjamin Felker (apprentice for chemical technical assistant) under supervision, planning and evaluation of the author.

[9] For further investigation concerning the mechanistic pathway of the thionocarbamate **44**, a straightforward control experiment would be to perform the before mentioned reaction in the absence of the titanium-catalyst. Thus, it could be determined if the titanium-catalyst is thereby acting as catalyst for this reaction. Second, the reaction of dodecyl isothiocyanate **41** and dodecanol **37** could be tested under the before mentioned reaction conditions, one time with and one time without applying the titanium catalyst. Thus, it could be verified if path **B** (see Scheme 35) takes place and if titaniumalkoxides catalyze the reaction step. However, these experiments were not performed, since it did not affect the main aim of this work package.

the solubility of the polymer drastically.[10] Since no indication was found for the formation of such isothiocyanate under the applied reaction conditions, it was not further considered.

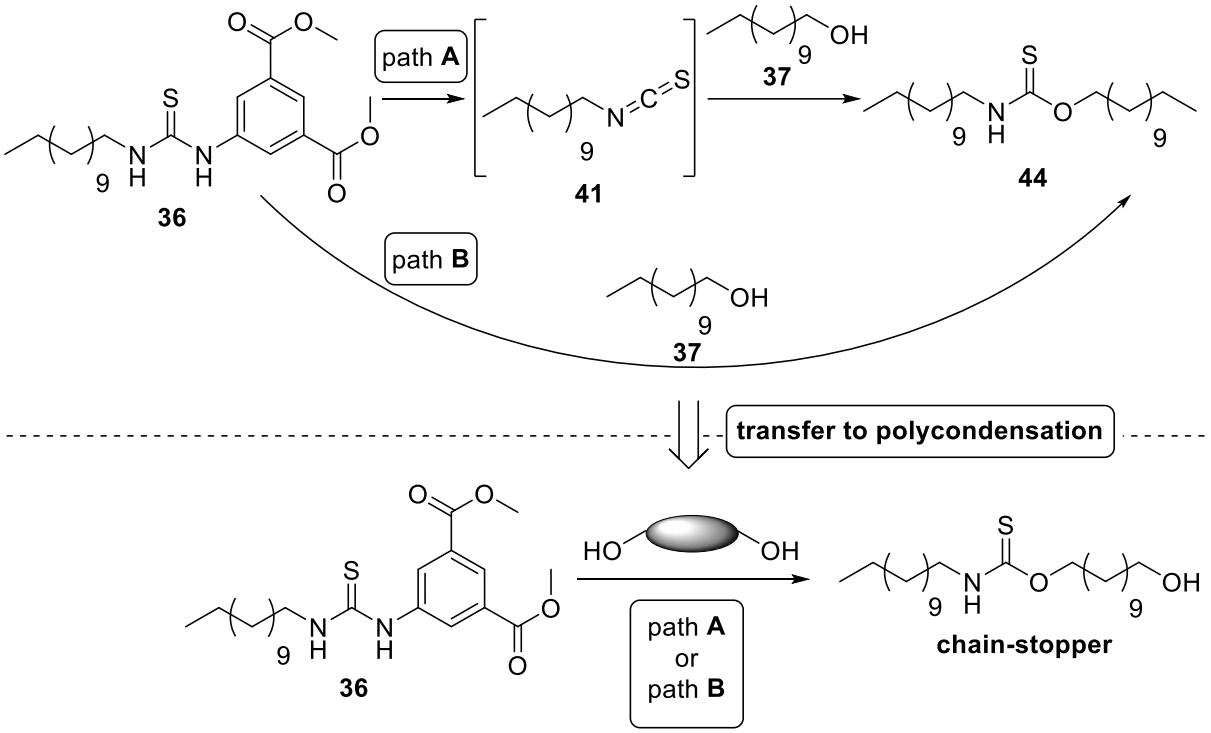

*Scheme 35: Top: Two possible reaction pathways for the formation of thionocarbamate **44** using 10 mol% Ti(OBu)$_4$ at elevated temperature in a transesterification of thiourea ester **36** and dodecanol **37**. Bottom: envisioned transfer to a polycondensation protocol would result in thionocarbamate monoalcohol (chain-stopper), which would act as a chain-stopper in a polymerization approach.*

The hypothesized path **B** for the thionocarbamate formation shown in Scheme 35, in which the alcohol component directly attacks a thiourea function, could also be hypothesized to occur in the polycondensation. Thus, besides the formation of the thionocarbamates from the starting materials, backbiting or chain transfer reactions of terminal alcohol groups would introduce thionocarbamate groups as well into the chain end of the polymers, stopping them from further growth.[11]

[10] Hypothetical formation of thionocarbamate alcohol groups as side chains as well as cross-linking due to formation of isophthalicacidester isothiocyanate under elevated temperature using 10 mol% of Ti(OBu)$_4$. The polymer backbone is only indicated by dashed lines to provide clear view of the structures.

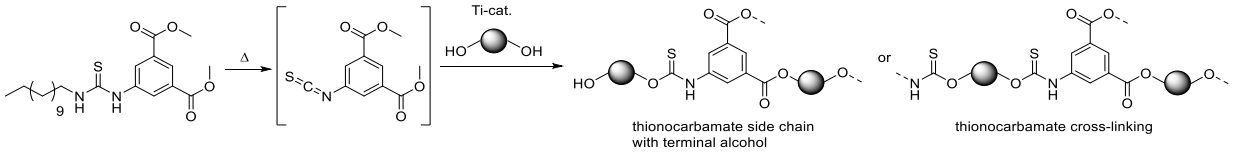

[11] Hypothetical formation of thionocarbamate groups due to backbiting or chain transfer reaction of the poly(ester), which would result in poly(ester-*co*-arylamine)s that are stopped in their growth due to a thionocarbamate capping the terminal alcohol group.

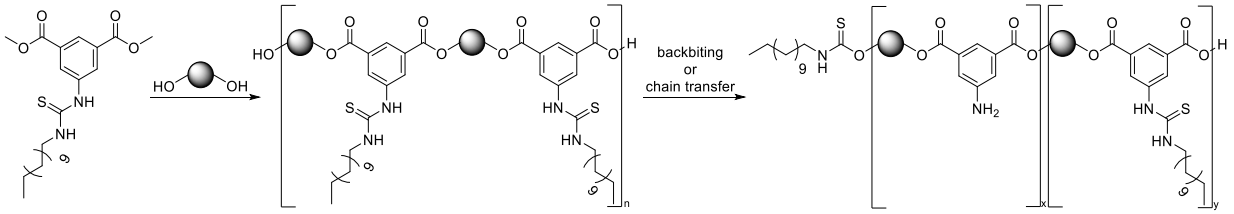

After having determined side products, this approach was reevaluated. First, nearly full conversions seemed to be promising for application in a polycondensation.[12] Still, further optimizations were expected to be applied in the actual polymerization, since the starting material and the type of reaction would be changed. The decomposition of the TU on the other hand led to a decrease of the TU functionality, which is expected to decrease the activity in its future application (organocatalysis *via* activated thiourea groups). However, since conditions were found ensuring a decent degree of TU groups were maintained after the reaction had finished, this decline of thiourea groups was deemed to be acceptable. The formation of thionocarbamte alcohols acting as chain-stopper during the reaction would indeed have a tremendous effect on the molecular weight of the obtained polycondensates. Since this reaction seemed to only occur to a minor extent, it still seemed reasonable to test the protocol for poly(TU-amine) synthesis.

Next, the reaction protocol was applied to a polycondensation reaction between TU **36** and a suitable diol. Poly(ester-*co*-arylamine)s bearing TU functions in their side chain were expected to be formed in small to moderate molecular weights, which were assumed to potentially exhibit the desired catalytic activity and solubility behavior.

Transfer of the synthesis protocol of the transesterification to a polycondensation reaction-poly(ester-*co*-arylamine)s with TU motifs in the side chains

With the optimized reaction conditions in hand, the protocol for the transesterification was applied to a polycondensation approach. TU diester **36** was therefore reacted with a diol to yield a poly(ester) or rather a poly(ester-*co*-arylamine) **45**, due to partial decomposition of the thiourea functionality during reaction (see Scheme 36).

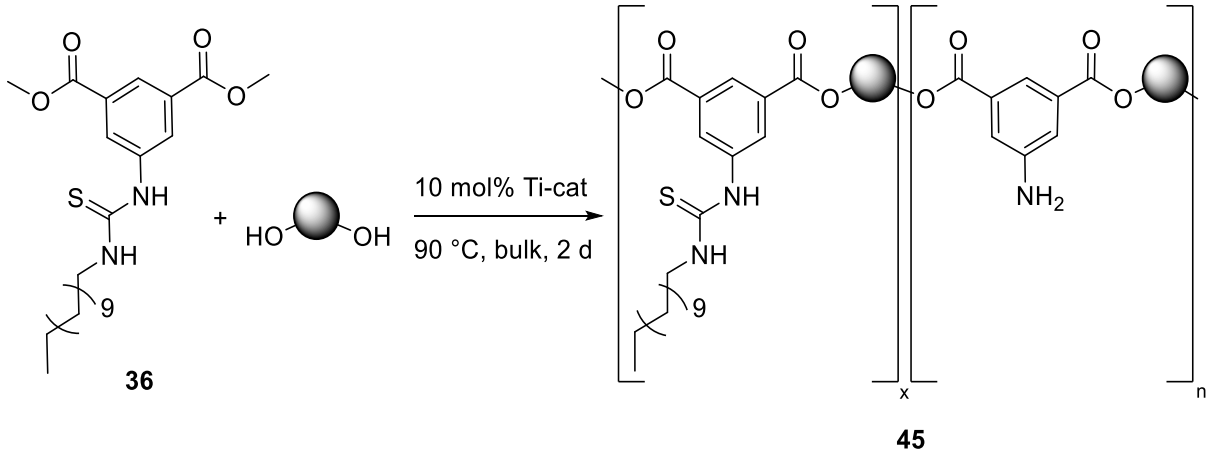

*Scheme 36: Reaction scheme of the formation of poly(ester-co-arylamine)s **45** bearing TU functional groups in their side chains.*

1,10-decanediol **46** was chosen as test dialcohol, since it exhibits a high boiling point of (T_b=297 °C) to ensure equimolarity of the monomers over the course of the reaction and a melting point lower than 90 °C, which was the reaction temperature (T_m=72-75 °C).[533] It was assumed that the alcohol component would start dissolving thiourea diester **36** upon melting, similar to dodecandiol **37** in the preliminary test experiments.

First, a brief reevaluation of the titanium alkoxide catalysts was conducted to adjust to the polymerization reaction. The conversion of the methylester groups and the partial decomposition of

[12] For instance, a 16-17-mer could be expected applying the Carothers equation for the degree of polymerization (DP), assuming 94% conversion p which was obtained in the optimized transesterification conditions:

$$DG = \frac{1}{1-p} = \frac{1}{1-0.96} = 16.7$$

the thiourea group were determined by ^{1}H-NMR monitoring, as described above, except that only one CH_3 group, *i.e.* the terminal CH_3 group of thiourea **36**, was present and used as the reference signal (the integral ratio of a t=0 h sample of methylester CH_3 groups to terminal CH_3 group was 2:1). In addition to the NMR-monitoring, SEC-analysis of the reaction mixture provided information about the obtained molecular weight of polymer **45**. The results are listed in Table 16.[13]

*Table 16: Screening of catalysts for the polycondensation between TU diester **36** and 1,10-decanediol **46** under equimolar stoichiometry. The conversion after one and two days are given as well as the decomposition of the TU group to arylamines. In addition, SEC-measurements using HFIP and 1w% KCF_3COO allowed insights about the obtained molecular weight and the dispersity Đ.*

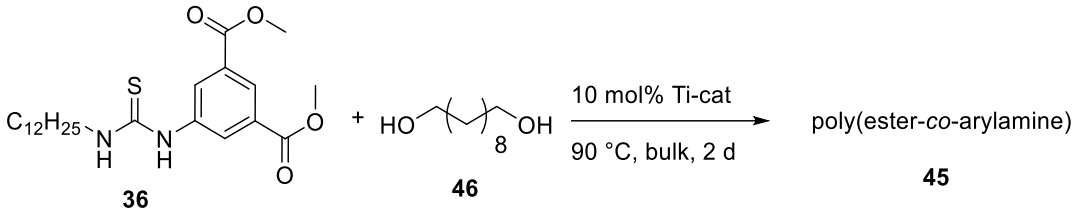

catalyst	conversion of 36 after 1 d/%	conversion after of 36 2 d/%	decomposition of thiourea of 36 (2 d)/%	M_n/kDa	M_w/kDa	Đ
$Ti(OBu)_4$	76	79	12	2.1	4.9	2.39
$Ti(O^iPr)_4$	81	n. d.[a)]	24[b)]	4.5[c)]	102	22.5
$Ti(OEt)_4$[d)]	82	n. d.[a)]	21[b)]	4.0[c)]	31.2	7.87

a) No NMR-sample could be taken, as the reaction mixture was not soluble in DMSO-d_6 anymore. b) Decomposition of TU groups after one day. c) SEC-sample was taken after one days, since the reaction mixture was not soluble in HFIP with 1w% KCF_3COO anymore. d) catalyst contained 5-15% isopropanol.

In addition to the previous tested titanium-catalysts, also $Ti(OEt)_4$ was considered. All three catalyst yielded similar conversion (79-82%). However, the reaction with $Ti(OBu)_4$ led to a slower reaction and the respective conversion was obtained after two days instead of one. On the other hand, $Ti(OBu)_4$ led to the lowest decomposition rates for the TU groups (12% after two days), while the other catalysts resulted in roughly the doubled amount of decomposition after only one day of reaction time. Compared to the preliminary experiments (transesterification with dodecanol **37**), lower decomposition rates were obtained (also considering the lower conversion obtained in the polycondensation). The obtained M_ns were low (2.1-4.5 kDa), fitting to 3- to 7-mers of polymer **45** (for exemplarily SEC-curves see chapter 6.5.1.2.). Following the Carothers equation using the conversions obtained by NMR-measurements, this value seemed reasonable.[14] On the other hand, the obtained dispersities differed tremendously depending on the employed catalyst from 2.39 to 22.5. Considering that the reaction with $Ti(O^iPr)_4$ and $Ti(OEt)_4$ led to an insoluble mixture, it seemed reasonable that the high dispersities (22.5 and 7.87, respectively) were obtained due to solubility and precipitation issues during the reaction proceeding. Considering the aimed application, namely recyclable organocatalysis, a lower dispersity is beneficial because the solubility parameters for several chain length are different, especially in lower molecular regime, where the impact of one monomer unit is not negligible. As a result, the recycling step of a future catalyst (either homogenous

[13] The screening of the catalysts for the polycondensation reaction leading to the data in Table 16 was performed by Peter Conen (student and research assistant at the time of this experiments) under the supervision, planning and evaluation of the author.

[14] Using equimolarity and a conversion of 79% as obtained applying the $Ti(OBu)_4$ catalyst after two days (see Table 16), the Carothers equation lead to a degree of polymerization(DP) of 4.76:

$$DP = \frac{1}{1 - 0.79} = 4.76$$

or heterogenous) gets more delicate, since a solvent system has to be found that fits for all polymer chains to ensure full recovery. Therefore, $Ti(OBu)_4$ depicted the best results.[15]

The herein attempted synthesis approach for poly(TU) catalysts did not need a certain high degree of polymerization, since it was assumed that the catalytic activity of the TU functional groups were intrinsically sufficient (as shown in chapter 4.2). Beneficial effects for the catalytic group arising from a respectively big polymer chain (*e. g.* intramolecular TU-TU activation or formation of active pocket sites, see also above)[424,425] could theoretically increase the activity, but were not focus of this work. Nevertheless, both effects could already appear for the above-described formation of oligo(TU)s (TU-TU activation would thereby be intermolecularly most likely). On the other hand, oligomers would probably exhibit higher solubility in classic organic solvents, which made this synthesis protocol still promising, even with incomplete conversion under the premise that a suitable work-up, like precipitation, was found.

However, attempts to precipitate and isolate the obtained oligomers were unsuccessful, as no suitable antisolvent could be determined. For instance, simple addition of water led to the formation of a suspension consisting of an aqueous liquid phase and a resin-like phase, which could not be further purified. Thus, the fastest way to obtain a suitable work-up procedure was hypothesized to further optimization of the reaction conditions, since full or nearly full conversion would lead to a mixture of polymers of higher molecular weights, probably being easier to precipitate. If this protocol was established, smaller oligomers could still be obtained if needed by altering the reaction conditions for instance, the stoichiometry.

Since the reaction protocol did not allow much deviation (stoichiometry, temperature, concentration, reaction time, and catalyst were already optimized) the most promising approach was envisioned to be improvement of the solubility of the reaction mixture. Thus, dialcohols exhibiting a higher solubility ability for TU diester **36** could be beneficial as the reaction proceeds, for a broader range of conversion, in solution. In addition, dialcohols leading to poly(TU)s that show a melting point lower than the applied temperature would be advantageous to obtain a homogenous reaction mixture. Thus, tetraethylene glycol (T_m=-5.6 °C, T_b=314 °C).[534] was tested as possible candidate as dialcohol component, since the ether groups were expected to result in different solubility conditions compared to 1,10-decanediol **46**. However, after the reaction was finished, only 62% conversion was obtained, while 20% of decomposition of the thiourea group was found.

Concluding, a transesterification protocol was established for TU diester **36** and dodecanol **37**. Several restrictions and issues related to the nature of the reaction were clearly investigated and proven by NMR-analysis (decomposition of thiourea groups to arylamines, formation of thionocarbamates which could act as chain-stopper in a step-growth polymerization). $Ti(OBu)_4$ was found to be the best catalyst in terms of conversion and lowest degree of decomposition of the TU functionality and 94% conversion was obtained. Since the conversions were sufficiently high, transfer of the protocol to a polycondensation approach with compound **36** and a dialcohol was attempted. Reevaluation of the titanium catalyst underpinned its performance and selectivity (lowest decomposition of TU group). However, only moderate conversion was obtained (up to 82%). Ultimately, further investigations were impeded by issues in the work-up, as no sufficient protocol could be established. The least time-consuming approach for optimization of the reaction and yielding an isolated polymer, *i.e.* alteration of the dialcohol component, was performed in order to

[15] Solving the Schulz-Flory equation for a step-growth polymerization, like the herein discussed polycondensation reaction, yields a theoretical dispersity of two approaching full conversion.[640] A higher dispersity can be an indication for less control over the reaction for instance, increase in viscosity and (partial) precipitation of growing polymer chains will alter the dispersity ultimately increasing it.

increase the conversion as well as establish a purification protocol. However, lower conversion was obtained. In the light of all the herein evaluated restrictions of this reaction, it was assumed that further investigation of this approach would not be productive. Table 17 summarizes the most important reaction parameters and compares the applied conditions with assumed ideal conditions, which could lead to successful polymer formation. In addition, the respective issues arising from deviation of the ideal conditions are given. Thus, the small space for improvement left for this synthesis protocol is underlined.

*Table 17: Comparison of ideal and applied parameters for the polycondensation of TU **36** with dialcohols.*

parameter	ideal condition	optimized conditions	related issue
stoichiometry	equimolar	equimolar	-
T	<70 °C	90 °C	thiourea decomposes at >70 °C
p	n. d.	n. d.	n. d.
t	n. d.	2 days	at T>70 °C as short as possible
solvent	dissolves starting material, oligo- and poly(TU)s	bulk	• viscosity • solubility
catalyst	n. d.	$Ti(OBu)_4$	• chain-stopper formation • decomposition of TU
polymer	solvent and anti-solvent available	no solvent and anti-solvent found,	work-up challenging
diol$_{(l.)}$	dissolves starting material, oligo-and poly(TU)s	dissolves TU but no bigger oligomers	• high T_b needed • viscosity • precipitation

Nevertheless, it has to be mentioned that decreased pressure could be beneficial for the conversion of the reaction, since methanol would be removed from the reaction vessel shifting the equilibrium to the product side. This approach would result in an elaborate investigation of pressure and temperature parameters, since the equimolarity has to be maintained or at least, stoichiometry should be ensured to lead to sufficient formation of oligomers. In addition, an elaborate and time-consuming catalyst screening on a broad scale (not only considering titaniumalkoxides) could reveal a catalyst, which shows improved activity and selectivity, especially in terms of C=O/C=S activation selectivity. Thus, the formation of thionocarbamtes could be reduced or prevented in both hypothesized reaction pathways if the catalyst was prone to take part in this reaction (see Scheme 35). It has to be mentioned that it was planned initially to use the deconvolution approach of Wolf *et al.* in the scope of this work.[93] This approach was reported to be a strong tool to determine suitable catalysts from a pool of multiple ones for a certain reaction in a rapid and straightforward fashion (see also chapter 2.1.2.). However, due to the restrictions of this reaction in the utilization of solvents, it could not be performed. If all these points would be addressed, the decomposition as well as the formation of potential chain-stopper molecules would be expected to be reduced or even impeded, which could lead to successful isolation of poly(TU)s.

4.3.3 Poly(thioether-ester)s bearing thiourea functions in side chains by poly-thiol-ene reaction

The experimental parts of this chapter were performed by Roxana Grömmer and Gia Trung Hoang due to their practical course (students, Organische Chemie für Fortgeschrittene, OC-F) under the supervision of the author. In addition, Alessandro Masini, a visiting researcher, performed practical experiments. The respective experiments are highlighted with footnotes.

Though the previous polycondensation approach did not result in the desired synthesis protocol for poly(TU)s, several important insights were obtained, like the decomposition of the TU diester **36** at elevated temperature (>70 °C) or the importance of selectivity for the reaction to prevent chain-stopper formation. Thus, a second approach was investigated based on the previous information by step-growth thiol-ene polymerization (see Scheme 37).

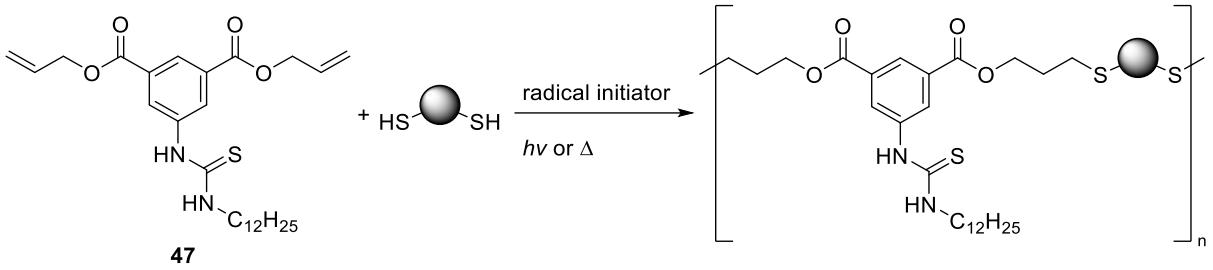

47

*Scheme 37: Thiol-ene polymerization approach for the formation of poly(thiourea)s using thiourea **47**.*

This approach was promising, as it tackled the most important issues which arose in the previous polycondensation approach. First, since thiol-ene reactions are typically performed under UV irradiation or thermally at mild conditions (<70 °C), decomposition of the thiourea group was expected to be prevented. Second, as the specific pathway for chain-stopper formation could not be verified completely in the previous approach (chapter 4.3.2.), it seemed reasonable that the applied catalysts could foster the formation and thus, a thiol-ene reaction approach was superior since no catalyst has to be applied. Nevertheless, radical starter agents are usually employed, which might react to a certain degree with the TU group. Still the direct formation of a chain-stopper would clearly depend on the nature of the respective reagent and it seemed reasonable that a thiol-ene reaction has the potential to prevent this side reaction or at least yield side reaction which do not impede the polymerization (for instance TU-radical starter agent adduct formation would not hinder the polymerization but decrease the amount of final TU functional groups by an acceptable degree). Third, the reaction protocol of the thiol-ene reaction could allow the use of a solvent, which would be beneficial by reducing the impact of precipitation and high viscosities. Lastly, while dithiols are commercially available, a suitable diene could be envisioned using again the thioureaisophthalicacid ester motif employed in the previous chapter (see Scheme 33). This compound **47** could be synthesized following the same straightforward four-step procedure as its methyl ester pendant **36** by using allylalcohol in the initial esterification instead of methanol.

Having thiourea diene **47** obtained in an overall yield of 18%, first test experiments were performed.[16,17] Since the ^{1}H-NMR monitoring approach proved to be useful in the polycondensation

[16] Main reason for the low overall yield was the isocyanide synthesis resulting in a yield of 31% while the prior esterification and formylation as well as the following thiourea synthesis gave yields of 79%, 95% and 77%, respectively.

[17] The synthesis of thiourea **47** was performed by Roxana Grömmer (first step, esterification) and Gia Trung Hoang (second, third and final step, formylation, isocyanide and thiourea synthesis) during both of their

approach (see chapter 4.3.2.), thiourea **47** was first tested in a reaction with a monothiol. Therefore, dodecanethiol **48** was chosen as the thiol component. Thus, the monitoring *via* ^{1}H-NMR-spectroscopy could be easily followed by the decrease of the double bond signals at 6.11-6.00 ppm and 5.45-5.27 ppm (see Figure 11), since there was no overlap with other signals present in the starting materials. Signals were referenced to the multiplett at 0.88-0.80 ppm, which could be assigned to the terminal CH_3 groups of thiol **48** as well as thiourea **47**.

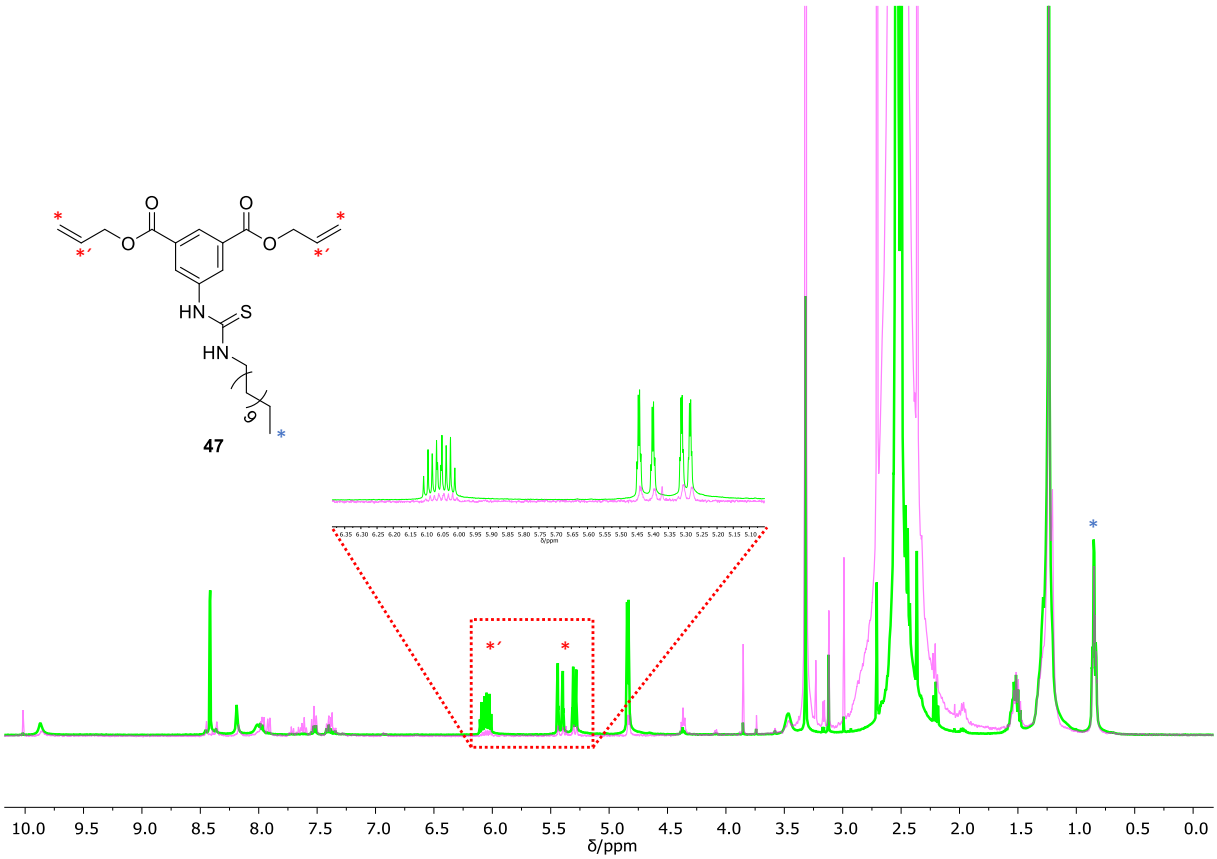

*Figure 11: Example of an overlay of ^{1}H-NMR-spectra in DMSO-d_6 of a thiol-ene reaction between thiourea diene **47** and dodecanethiol **48** using 50 mol% of DMPA in DMSO under UV irradiation (365 nm). Before irradiation (t=0 h, green) and after seven hours (see also Table 18) reaction time (pink) is depicted. Conversion could be determined by monitoring of the decrease of the double bond signals (red box) and respective zoom-in. Both spectra are normalized on the CH_3 signal at 0.88-0.80 ppm to highlight the decrease of the double bond signals. The multiplett of the signals of the terminal CH_3 groups of thiourea **47** and the dodecanthiol **48** were taken as reference signal (at t=0 h integral ratio of both double bond signals to CH_3 groups was 2:2:9).*

Equimolar conditions were applied, since this stoichiometry would lead to the highest molecular weight if the protocol was transferred to a polymerization approach as discussed before (see chapter 4.3.2.). Thus, the initial ratio at t=0 h between the signal of the double bonds and the CH_3 groups was 2:2:9.

DMSO was applied as a solvent, since TU **47** exhibited poor solubility in less polar solvents and 10 mol% of the respective radical initiator was applied. Finally, several different radical initiators were tested and the results are listed in Table 18:[18]

practical courses (Organisches Praktikum für Fortgeschrittene, OC-F) under the supervision, planning and evaluation of the author.

[18] The screening of radical initiators depicted in Table 18 was performed by Alessandro Masini, a visiting researcher, under the supervision, planning and evaluation of the author.

*Table 18: Screening of radical initiators in the thiol-ene reaction of TU diene **47** and dodecanethiol **48**.*

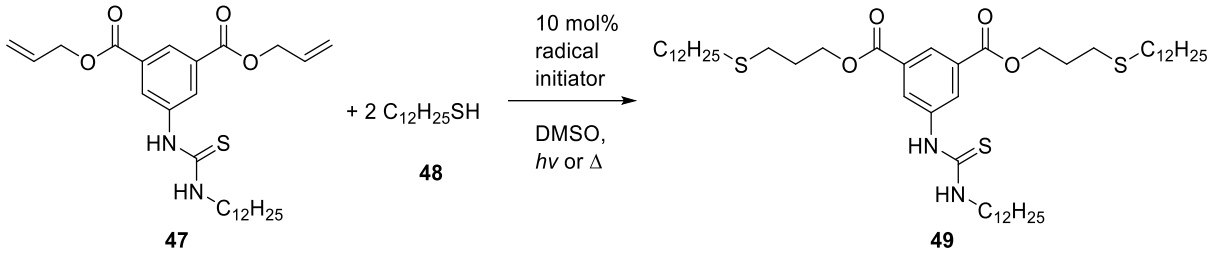

radical initiator	conditions[a)]	reaction time/h	conversion of 47/%
DMPA[b)]	A	24	0
DMPA[c)]	A	7	83
thioxanthone	A	24	40
thioxanthone[c)]	A	120	43
benzil	A	24	0
benzophenone	A	24	0
AIBN	B	24	0
TEMPO	C	24	0

Condition A: irradiation with a wavelength of 365 nm. Condition B: heating at 65 °C. Condition C: heating at 35 °C. a) TU **47** (1.00 eq.) and dodecanethiol **48** (2.00 eq.) were dissolved in DMSO (*c*(thiourea **47**)=0.25 M), the reaction mixture was purged with an argon balloon beforehand. b) reaction was also performed at *c*(thiourea **47**)=0.5 and 1 M. c) 50 mol% of radical initiator was applied.

Initially, DMPA was investigated since it is known to be a versatile radical starter for thiol-ene reactions. However, no conversion was obtained after 24 hours. Increasing the ratio of DMPA to 50 mol% resulted in a conversion of 83% after seven hours when the reaction had finished. Increasing the concentration of the thiourea compound **47** in the reaction to one molar did not improve the conversion. Other photoinitiated radical starters like thioxanthone, benzophenone and benzil were tested as well, since they were reported to be applied in thiol-ene reactions, but apart from thioxanthone no conversion was obtained.[535,536] In the case of thioxanthone only insufficient conversions of 43% were obtained, even when 50 mol% of radical starter was applied after 120 hours reaction time. As the photoinitiated reagents gave no sufficient conversion, thermally activated ones were tested as well, namely conventionally used AIBN and more recently reported TEMPO.[537] It has to be mentioned that the temperature for these protocols were typically under 70 °C and thus, no decomposition of the TU group was expected. Nevertheless, no conversion was obtained in both cases.

To summarize, the thiol-ene reaction of TU diene **47** and dodecanethiol **48** gave no sufficient conversions. DMPA was the only initiator resulting in higher conversion (83%), but 50 mol% of the radical initiator had to be used. As the conversion still needed improvement, the room for optimization was determined to be too narrow for further investigations as the choice of solvent and concentration was limited by the poor solubility of TU **47**. Further, polar aprotic solvents like DMSO were reported to be inadequate solvents for thiol-ene reactions using the photoinitiator phenylglyoxalic acid, which might be also disadvantageous for the herein investigated ones.[538] Also, the use of a large amount of radical starter seemed to be needed, at least for the tested reagents, and it was expected that a high concentration of radicals would foster side reactions like disulfide formation of the thiol. Thus, the stoichiometry of a polymerization approach using thiol-ene reaction

would be altered leading to smaller molecular weights.[19] This would be *per se* no exclusion criterion, but limits the control of the stoichiometry, which might by adverse for subsequent investigations like establishment of a work-up procedure. Furthermore, other side reactions might be not negligible anymore by using larger amounts of initiators, for instance radical reaction of the decomposed initiator with the TU group (this assumption is based on the common use of C=S double bonds in RAFT polymerization).[539] Considering all mentioned points still need to be addressed and the time frame of this work, this approach was not further investigated.

Nevertheless, a more extensive evaluation on the thiol-ene reaction might yield sufficient results. For instance, different wavelengths could be tested for the applied photo initiators, as the light with 365 nm could be also absorbed by the TU compound exacerbating or impeding the initiation step of the reaction (this was initially planned in the scope of this work, however no means to test other wavelengths were present). In addition, another double bond bearing moiety with a longer spacer attached to the isophthalicacid ester motif like 10-undecene-1-ol might result in a sufficient conversion due to negligible satiric hindrance arising from the presence of the aryl compound.

[19] For instance, assuming 5% consumption of thiol groups (r=0.95) by disulfide formation as side reaction in the thiol-ene reaction, the obtained degree of polymerization (DP) at 90% conversion p of the remaining thiol groups in the actual thiol-ene reaction would be:

$$DP = \frac{1 + r}{1 + r - 2rp} = \frac{1.95}{0.24} = 8.125$$

according to Carothers equation. For comparison a conversion of 95% of the thiol groups solely due to the thiol-ene reaction in absence of disulfide formation would yield a DP of 20.

4.3.4 Poly(norbornene)s bearing thiourea functions in their side chains by ring-opening metathesis polymerization (ROMP)

The experimental parts of this chapter were performed by Alessandro Masini, a visiting researcher, Gia Trung Hoang, a student performing his practical course (Organische Chemie für Fortgeschrittene, OC-F) and Fabian Schönle (student, research assistant) under supervision of the author. The respective experiments are highlighted with footnotes.

Since the stepgrowth polymerization approaches (polycondensation and thiol-ene reaction) described in chapters 4.3.2 and 4.3.3. with the isophthalicacid ester moiety did not lead to the desired results, a living polymerization approach by ring-opening metathesis (ROMP) was envisioned.[540] This kind of polymerization, like RAFT, NMP or ATRP, typically provides a high control over the polymerization process, yielding polymers with narrow molecular weights distributions.[541–543] While the low dispersity was not necessarily needed for the application as polymeric organocatalyst, it was hypothesized that the establishment of a suitable work-up procedure, like precipitation and filtration, for the TU containing polymers would be facilitated if the dispersity was lower. Especially in the regime of low molecular polymers, this would decrease the difference in the solubility parameters of the different chain lengths, facilitating purification by complete precipitation of the polymer and later complete recovery of the applied catalyst.

A ROMP approach was ultimately chosen for several reasons (see Scheme 38). First, the reaction is usually performed at room temperature, where no decomposition of TU groups takes place, while typically applied Grubbs-catalysts tolerate a broad range of functional groups.[544] Nevertheless, it has to be noted that no ROMP of a norbornene derivative bearing an additional TU group has been reported so far, while sulfur atoms *per se*, for instance in a thioacetal function, are tolerated.[545] Second, suitable norbornene amines were accessible from *exo* or *endo* *cis*-5-norbornene-2,3-dicarboxylicacid anhydride in an one step procedure from diamines. Third, the reactivity of *exo* and *endo* norbornenes in a ROMP differs tremendously and thus, an additional parameter for tuning the polymerization is obtained.[546] Fourth, the TU moiety will be located in the side chain of the produced polymer and its distance to the backbone is tailorable by the use of different diamines. This is an advantage over the previously tested approaches, where the TU was attached to the backbone of the polymer without any spacer (see chapters 4.3.2. and 4.3.3.). It has to be noted that none or short spacing of the TU functionality to the backbone is not intrinsically impeding either polymerization or the later catalytic applications. Yet it seemed reasonable that the resulting steric hinderance could result in a bulky polymer and thus, the catalytical centers are only accessible to a limited extent, while a low general solubility was assumed. Thus, attaching the TU to norbornene amines with long, flexible aliphatic spacers would increase their degree of freedom in solution. Moreover, if such a poly(TU) was insoluble in any typical organic solvent, it could still serve as a heterogenous catalyst, since the TU groups are easily accessible. For instance, Pedrosa *et al.* showed that a heterogenous, chitosan-based bifunctional poly(TU) catalyst bearing the TU groups in the side chain was inactive in an enantioselective aza-Henry reaction when the TU function is directly attached to the backbone, while longer spacers resulted in high yields and selectivities.[467] In the herein envisioned approach, the TU group is located at the end of the side chain and thus, the activation moiety can be freely chosen from all activation motifs established in chapter 4.2., *i.e.* the *p*-(alkylsulfonyl) aryl and isophthalicacid diester motif without further modification. In addition, the introduced motifs bear further potential for instance, adjustments in terms of solubility by introduction of different alkyl chains. Finally, the use of norbornene motifs will result in an unpolar poly(vinylcyclopentane) backbone, which exhibits typically good solubilities in less polar solvents, like DCM used generally in TU catalysis.

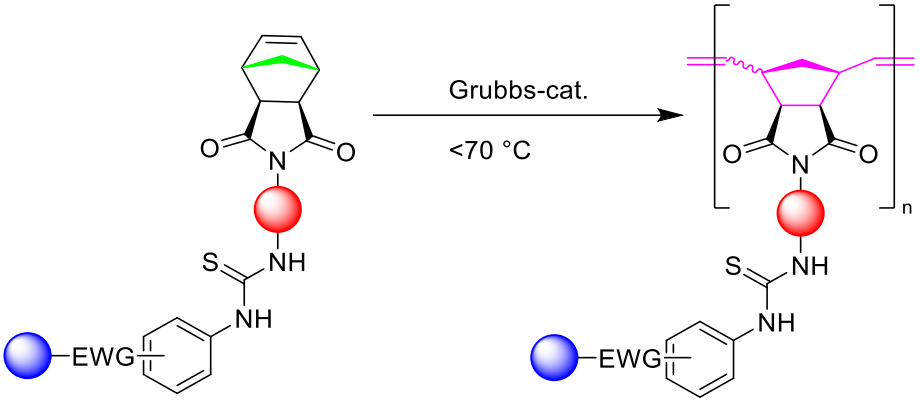

Scheme 38: Overview of the approach of poly(TU) synthesis by ROMP of norbornene TUs using room temperature. Advantages of this approach are highlighted by coloration. The solubility and accessibility of the thiourea group can be tailored by the tether between the norbornene and the TU function (red sphere). In addition, solubility can be altered by using different moieties attached to the EWG activating the TU group (blue sphere). The ROMP reactivity can be tuned by changing from exo norbornenes (starting material, green) to endo ones. Ultimately, an unpolar vinylcylopentane backbone motif is obtained (pink).

For this project, the focus was set solely on establishing poly(TU) synthesis by ROMP, as a proof of concept. Thus, the herein used TU monomer **50** (see Table 19) was not synthesized using the AM-3CR but using typical TU synthesis, since it was less time-consuming. Within this study, *exo* norbornene was chosen because it depicted in general the higher reactivity providing smaller reaction times.[546] On the other hand, the 3,5-bis(trifluoromethyl) phenyl group was considered as activation motif, since it proved its potential for catalytic activity not only in this work (see chapter 4.2.) but also in a broad range of different reactions and conditions being applied for two decades in thiourea organocatalysis as the privileged activation group (see chapter 2.4.1.). In addition, the presence of fluorine atoms in the molecule gave the option of analysis by ^{19}F-NMR-spectroscopy.

Thus, TU norbornene **50** was synthesized by reacting the respective amine with 3,5-bis(trifluoromethyl)phenyl isothiocyanate in dry DCM at 0 °C under argon and was obtained in a yield of 73% (overall yield of the two-step synthesis starting from *cis*-5-norbornen-*exo*-2,3-dicarboxylic acid anhydride was 52%).[20] Subsequently, different reaction conditions were tested for the ROMP, applying typical Grubbs catalysts. The results are summarized in Table 19:[21]

The reactions were performed in a Young-NMR-tube to allow determination of the conversion by ^{1}H-NMR-spectroscopy by following the transformation of the double bond of monomer **50** to the one of polymer **51** (see chapter 6.5.3.1. for details). Typical catalyst-loadings of 5 mol% were applied initially, aiming for a theoretical degree of polymerization (DP) of 20.[22] Use of Grubbs 2nd generation catalyst at room temperature in DCM led to ceasing of the reaction after roughly five hours with an insufficient conversion of 45%. Switching the solvent to THF, the temperature could be increased to 44 °C, leading to nearly full conversion after two hours (98%). The 3rd generation Grubbs catalyst

[20] The synthesis of TU norbornene **50** was performed by Gia Trung Hoang (first step, amin synthesis) during his practical course (Organisches Praktikum für Fortgeschrittene, OC-F) and Alessandro Masini who was a visiting researcher, under the supervision, planning and evaluation of the author.

[21] The screening of conditions for ROMP of TU norbornene **50** depicted in Table 19 was performed by Alessandro Masini a visiting researcher under the supervision, planning and evaluation of the author.

[22] The expected DP at 100% conversion for a living polymerization can be calculated by:

$$DP = \frac{[M]}{[I]} = \frac{0.1}{0.005} = 20$$

Where [M] is the monomer and [I] the catalyst concentration applied at the beginning of the reaction.[639] Thereby it is assumed that statistically every catalyst molecule will react with the same amount of monomers.

yielded slightly lower conversions (94% after two hours). Thus, suitable reaction conditions were obtained using 2nd generation Grubbs catalyst in THF at slightly elevated temperature (44 °C).

*Table 19: Screening of the reaction conditions for the ROMP of TU norbornene **50**.*

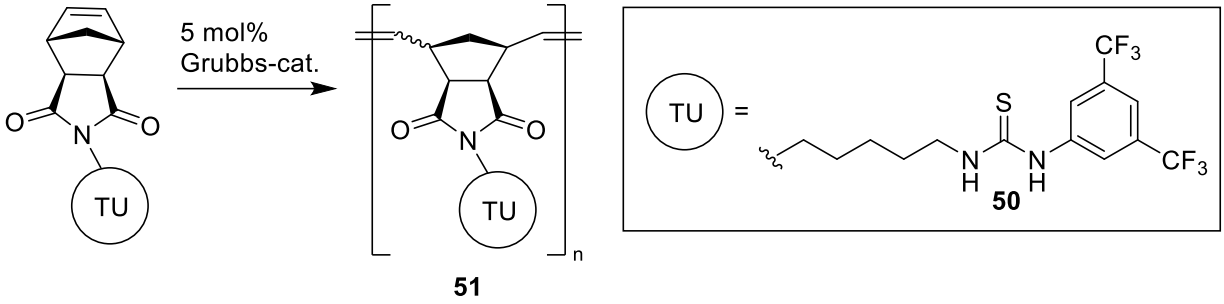

catalyst	solvent	*T*/°C	*t*/h	conversion/%
Grubbs 2nd	DCM	r.t.	1	36
Grubbs 2nd	DCM	r.t.	5	44
Grubbs 2nd	DCM	r.t.	o.n.	45
Grubbs 2nd	THF	44	1	94
Grubbs 2nd	THF	44	2	98
Grubbs 3rd	THF	44	1	90
Grubbs 3rd	THF	44	2	94

TU norbornene **50** (63.5 µmol) was dissolved in 318 µL DCM (dry, degassed) and a stock solution of the respective catalyst was prepared (5 mol%, 3.18 µmol) in 318 µL DCM (dry, degassed). Both solutions were mixed (final *c*(TU **50**)=0.1 M) in a Young-NMR-tube under argon atmosphere and let stay at the respective temperature for the respective time. r.t.= room temperature, o.n.= overnight.

Subsequently, solubility tests were performed to allow further work-up and characterization of the obtained poly(TU) **51**. The reaction applying optimized reaction conditions was quenched with ethyl vinyl ether and its excess as well as the solvent was removed under reduced pressure.[23] It was assumed that the obtained polymer **51** exhibited a high density of TU functional groups capable of intra- and intermolecular hydrogen bonding and thus, depicted a low solubility in typical solvents. Indeed, polar aprotic and protic solvents as well as less polar ones, *i.e.* DCM, THF, DMSO, DMAc and HFIP were all incapable of dissolving poly(TU) **51** and thus, no suitable purification method was found to purify polymer **51** to enable further characterization or investigations.

To address the solubility challenge and to allow analysis by NMR and SEC analysis, lower DPs were thus targeted by applying higher catalyst loading. In addition, a *co*-polymerization approach was envisioned, since a suitable *co*-monomer increases the solubility as well as the distance between the TU groups. The later point leads to a decrease of the overall amount of hydrogen bonding between the polymer chains probably increasing the solubility of the polymers further (see Scheme 39). To ensure solubility, the already discussed potential benefit of hydrogen bonding among thiourea groups forming highly catalytical active TU-TU complexes or foldamers with active pockets sites (see

[23] As all the monomer is consumed by the ROMP, the respective Grubbs catalyst is attached to the end of the polymer chain but still active. Side reaction already occurring during the proceeding of the ROMP like chain-transfer or backbiting reaction, can still take place since they do not depend on the amount of monomer but on the presence of double bonds. This number does not change during the reaction and the double bonds present in the polymer differ only in their reactivity towards olefine metathesis which does not mean they are inert. Thus, the terminal Grubbs moiety is usually quenched or transformed to inhibit further metathesis reactions. For instance, a common approach is the use of ethyl vinyl ether transforming the catalytically active Schrock-carbene of the Grubbs-catalyst in a less active/inactive Fischer-carbene.[641]

chapter 3) was thereby neglected, because the TU group by itself was already expected to exhibit sufficient catalytical activity. The catalytic potential of monomer **50** was thus investigated by its application as catalyst in the ring-opening reaction of propylene carbonate **33** with cyclohexlamine **34**, described in detail in chapter 4.2 resulting in an increased conversion of 46% after 30 minutes.[24]

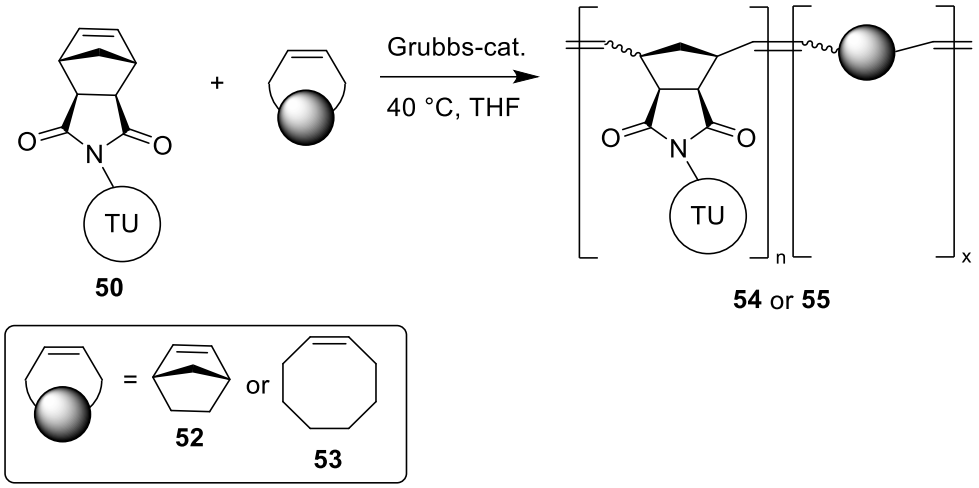

*Scheme 39: Overview of the optimized approach of the poly(TU) synthesis by ROMP using a co-polymerization approach with norbornene **52** or cyclooctane **53** yielding the respective* co-*polymers **54** and **55**.*

Thus, norbornene **52** and cyclooctene **53** were chosen as suitable co-monomers, since they were widely used in ROMPs. Norbornene is highly reactive in a ROMP and the formation of the vinyl cyclopentane motifs in the backbone decreases the density of the TU functional groups without introduction of an additional side chain or backbone moiety.[25] On the other hand, cyclooctene led to a partly linear aliphatic backbone that might be beneficial for the solubility compared to the aliphatic cyclic backbone obtained by norbornene derivatives.

Since the characterization by SEC and ^{1}H-NMR-analysis was crucial for a detailed investigation of the obtained polymers, the focus was set on the synthesis of soluble polymers. Therefore, a screening of different catalyst-loadings and ratios of TU monomer **50** to norbornene **52** or cyclooctene **55** was conducted and the obtained polymers **54** or **55** were tested in their solubility in THF, DCM, DMSO and DMAc. THF and DMAc were chosen since they were eluents used for SEC-analysis,[26] while DCM and DMSO were chosen as their deuterated pendants were typical solvents for NMR-spectroscopy. In addition, DCM was often applied for thiourea catalyzed reactions.

In case of the *co*-polymerization of norbornene **52** and TU **50**, the high reactivity of the norbornene ***52*** resulted in insoluble polymers if both monomers were dissolved in the reaction mixture prior to addition of the catalyst. Probably gradient like structures were obtained due to the large difference in reactivity, yielding first nearly poly(norbornene)s homopolymers that incorporate subsequently the TU derivatives. Thus, norbornene **52** was added dropwise to the reaction mixture

[24] The ring-opening reaction was chosen as suitable reaction since monomer **50** exhibited the 3,5-bis(trifluoromethyl) phenyl activation group like catalyst **27** leading to increased conversion of 64% after 30 minutes. For comparison 3% conversion were obtained without catalyst (see chapter 4.2 for more detail). The GC-screening of the ring-opening reaction was performed after the protocol established in chapter 4.2 and was performed by Fabian Schönle (student) who worked as research assistant at the time of this work under the supervision, planning and evaluation of the author.

[25] Under the optimized conditions norbornene was fully converted nearly instantaneously.

[26] By the time the screening was performed, the access to the mentioned SEC-instrument using DMAc and 0.3 w% LiBr as eluent was not possible anymore since the instrument was dismounted.

over the period of one hour immediately after the homo-ROMP of TU norbornene **50** was started by addition of the Grubbs-catalyst. Thereby, the concentration of norbornene **52** was kept low to decrease the formation of insoluble domains. The experiments with cyclooctene **53** were performed by dissolving TU **50** and cyclooctene **53** in THF, and adding the catalysts, afterwards, as cyclooctene **53** showed a similar reactivity compared to thiourea norbornene **50**.[27] It is notable that no Schlenk conditions had to be applied and simple purging of the dissolved starting materials with argon proved to be sufficient. The results of the solubility test are shown in Table 20 on the example of the poly(TU norbornene **50**-*co*-cyclooctene **53**)s **55** (for the results of the poly(TU norbornene **50**-*co*-norbornene **52**)s **54** see chapter 6.5.3.2.):[28]

*Table 20: Qualitative screening of solubility of a series of poly(TU norbornene **50**-co-cyclooctene **53**)s **55** in DCM, THF, DMSO and DMAc obtained by ROMP in dependance of the amount of catalyst used and the ratio between monomer **50** and **53**.*

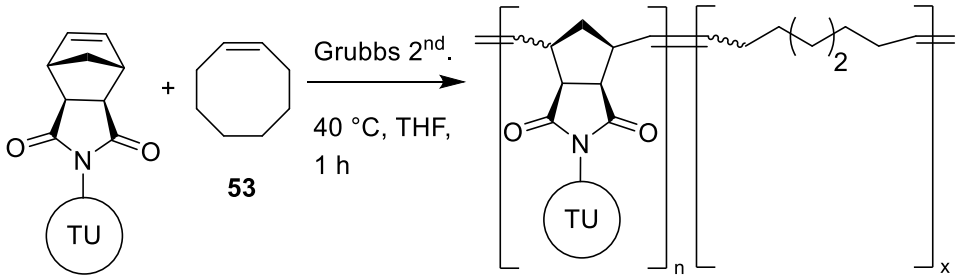

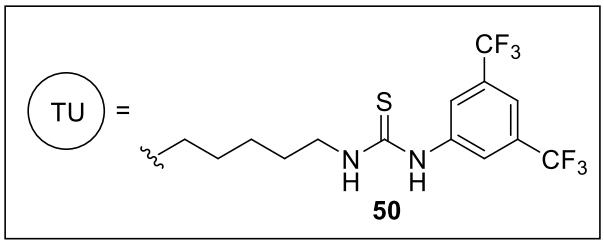

entry	cat.-loading/ mol%	$M_{n,\,theo.}$/ kDa[a)]	ratio 50:53	solubility in DCM[b)]	solubility in THF[b)]	solubility in DMSO[b)]	solubility in DMAc[b)]
1	10	1.5	1:9	✓	✓	-	-
2	5	4.3	1:3	-	✓	✓	-
3	3	7.1	1:3	-	✓	✓	✓
4	3	5.0	1:9	✓	✓	✓	✓
5	1	21.3	1:3	-	✓	✓	✓
6	1	15.1	1:9	-	-	✓	-

The respective ratio of the monomers were dissolved in THF (dry, *c*(TU **50**)=0.1 M) and the respective amount of Grubbs 2nd generation catalyst was added. a) Molecular weight of the respective *co*-polymers **55** were calculated according to their ratio dependent, averaged monomer molecular weight.[29] b) Qualitative determination by naked eye after quenching with ethyl vinyl ether and removal of its excess as well as the solvent.

[27] Using 5 mol% of Grubbs 2nd generation catalysts in a homo-ROMP of cyclooctene **53** at the optimized reaction conditions for TU **50** (40 °C, THF) led to a conversion of 96% after 30 minutes, determined by comparison of the starting material and polymer double bond signals in ^{1}H-NMR-spectrum.

[28] Synthesis of the series of *co*-polymers **45** and **55** using norbornene **52** as well as cyclooctene **53**, and the respective solubility tests were performed by Alessandro Masini a visiting researcher under the supervision, planning and evaluation of the author.

[29] Calculation is exemplified by entry 3 in Table 20 using 3 mol% of Grubbs 2nd generation catalyst and a ratio of monomers **50**:**53** of 1:3. The theoretical M_n was calculated as followed:

$$M_n = DP \times M_{av.} \quad (I); \qquad DP = \frac{[M]}{[I]} \quad (II); \qquad M_{av.} = xM(\mathbf{50}) + yM(\mathbf{53}) \quad (III)$$

A quantitative conversion of the double bonds was observed according to ^{1}H-NMR-monitoring after only one hour. Thus, the TU norbornene **50** was converted more rapidly into a polymer using *co*-monomer **54** or **55** (homo-ROMP of TU norbornene **50** resulted in 98% conversion after two hours, see Table 19). This was explained by the fact that the catalytically active Grubbs motif attached to the end of the growing *co*-polymer chain was more reactive when it was directly bound to the moiety of *co*-monomer **53** or **53** instead of TU **50** (either due to less steric hindrance or less coordination of the TU moiety to the catalyst altering its reactivity).

Two clear trends for the *co*-ROMP of TU **50** and cyclooctene **53** were observed. By increasing the amount of catalyst, lower DP polymers were obtained exhibiting higher solubility in THF and DCM (compare *e.g.* 1 mol%, 3 mol% and 10 mol% catalyst at a ratio of **50**:**53**, 1:9, Table 20, entry 1, 4 and 6). In addition, increasing the ratio of cyclooctene **53** resulted also in smaller, soluble polymers (compare in Table 20, entry 3 and 4 as well as entry 5 and 6). Furthermore, DMSO and DMAc were also suitable solvents for some compositions. As the amount of cyclooctene **53** increases and the molecular weight decreases, their ability to solubilize the polymers was insufficient (see Table 20, entry 1), probably because of the increasing impact of the unpolar octyl group. Concluding, THF and DMSO seemed to be the most suitable solvents for further analysis, for instance SEC-analysis and NMR-characterization after successful purification. The solubility screening of the respective series of poly(TU norbornene **50**-*co*-norbornene **52**)s **54** was performed with the solvents DCM and THF underlining the obtained results (see chapter 6.5.3.2.).

In a next step, the work-up protocol of the obtained polymers was attempted. Thus, several solvents were tested as suitable anti-solvent to precipitate the polymers. Methanol and *n*-hexane were chosen to test an unpolar and a polar protic organic solvent, while water was tested as well. However, no precipitation was obtained for the polymers **54** and **55** summarized in Table 20. Further, purification by DMT-column chromatography proved to be unsuccessful as well.[30] To evaluate why the purification proved to be troublesome, SEC-samples of both series of polymers **54** and **55** were taken after quenching, and removal of solvent and ethylvinyl ether. An example is depicted in Figure 12:

Whereas $M_{av.}$ is the average molecular weight of the monomer unit considering the applied ratio of monomers x and y, [I] and [M] are the concentrations of catalyst and the overall amount of double bonds in both monomers, respectively at the beginning of the reaction. Transferring (II) and (III) into (I) yield:

$$M_n = \frac{[M]}{[I]} \times (xM(\mathbf{50}) + yM(\mathbf{53}))$$

With M(**50**)=519.51 g mol^{-1} and M(**53**)=110.20 g mol^{-1} the M_n is obtained:

$$M_n = \frac{1}{0.03} \times (0.25 \times 519.51\ \frac{g}{mol} + 0.75 \times 110.20\ \frac{g}{mol}) = 7084\ \frac{g}{mol}$$

[30] DMT-column chromatography uses modified silica gel with dimercaptotriazine (DMT), which can be used as chelator for the Grubbs moiety after quenching with ethyl vinyl ether. Thus, the remaining catalyst is simply being retained by chelation and the pure polymer can be obtained by flushing the column with a suitable eluent. In this case DCM was used. This approach could be performed since full conversion was obtained otherwise the polymer would still be impure consisting residual unreacted monomers.

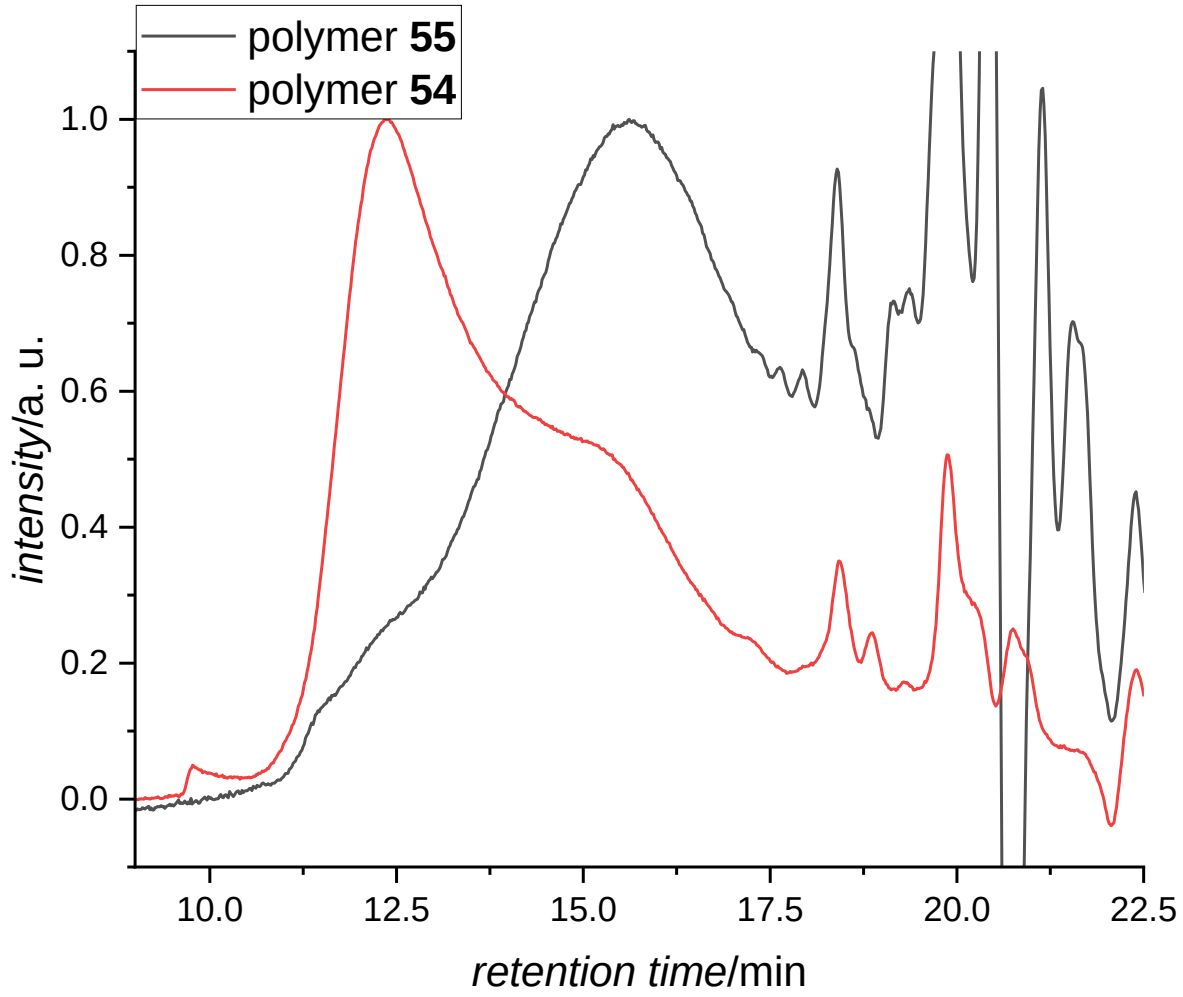

*Figure 12: SEC-results of the crude reaction mixtures of a ROMP of norbornene TU **50** and a co-monomer. The ratio of the monomers were **50**:**52** and **50**:**53**, 1:3 and 3 mol% 2nd generation Grubbs catalyst was applied (see Table 20, entry 3 and Table 33, entry 4). The reaction was performed in THF at 40 °C. The red curve depicts the co-polymer with norbornene **54**, the black one with cyclooctene **55**. Note that at around 20 min the solvent peaks are visible and that the exclusion limit of the column is reached at around 11 min altering the shape of the distribution.*

The same trend was observed for all SEC chromatograms: high or low molecular shoulders were clearly visible, indicating a bimodal distribution for the ROMP of TU norbornene **50** with norbornene **52** or cyclooctene **53**. Three factors were assumed to yield this distribution. First, with increasing amount of TU functional groups incorporated in the polymer, the polymer chain gets less soluble and thus, the proceeding in the ROMP is impeded. Second, side reactions like chain-transfer and backbiting were probably more pronounced in this reaction, since at least one of the three different double bond species formed in the polymer backbone were prone to react with the Grubbs catalyst motif of the growing chain ends.[31] Third, the TU functionality coordinates to the ruthenium center of the Grubbs motif, which eventually led to inactivation of some of the catalytical groups as they become less reactive or cannot be accessed anymore by the sterical hindrance of the coiled polymer chain. Either one of this points or an interplay of them seemed to be a reasonable hypothesis for the observed bimodal distribution.

As already mentioned in previous chapters, the aim was not to obtain highly controllable poly(TU)s, but ones which could be applied as recyclable catalysts. Thus, a different nature of distribution of the

[31] Double bond species of the two respective homo adducts of either TU norbornene **50** or the respective *co*-monomer can be formed, or the cross metathesis double bond species.

polymer was in general not an exclusion criterion *per se*, even if a bimodal shape was observed. As long as a work-up protocol could be established further investigation regarding the catalytical activity in a suitable reaction could be performed. However, this was not the case for the approach of poly(TU) synthesis by ROMP. It can be assumed that the bimodal distribution, even if not contradicting the actual concept of this work, is disadvantageous for the investigations of a suitable work-up procedure, since the reaction mixture is more complex in terms of solubility parameters.

To conclude, optimization of reaction conditions for a ROMP of TU norbornene **50** revealed that 2nd generation Grubbs catalysts is a suitable catalyst when applied at slightly elevated temperature (40 °C) for the conversion of TU-containing norbornenes. Compared to the two previously discussed approaches (polycondensation and thiol-ene polymerization of an isophthalicacid diester motif), the polymerization reaction led to nearly full conversion (98%) and thus, proved to be more promising. In addition, since this approach uses a living-polymerization technique instead of a step-growth polymerization, also lower conversion would yield polymers theoretically, since the polymer growth is linear and not exponential.[32] Nevertheless, the work-up procedure of the obtained polymers was not successful, as they proved to be insoluble in any applied solvent. Since the ROMP yielded nearly full conversion, an alternative approach was conducted, namely the *co*-polymerization of TU norbornene **50** with either norbornene **52** or cyclooctene **53**. Thus, additional parameters were unlocked to ultimately tailoring the solubility properties of the final poly(TU)s: i) *via* the ratio of the *co*-monomers, ii) *via* the solubility properties of the moieties introduced by the co-monomer and iii) by the difference in the reactivities of the two different double bond species, which could result in preferred formation of homo or cross bound double bonds depending on the interplay of the two monomers. Due to the versatile tailorability of this approach, it can be assumed that recyclable poly(TU)catalysts could be achieved. On the other hand, it has to be underlined that this concept is very complex at the same time. Further investigations on this approach are expected to be very elaborate and time-consuming, since only a holistic evaluation of all mentioned parameters seemed to be a reasonable approach for this concept to obtain sufficient overview and insights. For instance, choosing the ideal co-monomer would already exhibit a tremendous workload as not only low molecular weight norbornene derivatives, but also macromolecular ones can be considered for a ROMP.[547] In addition, it might be more promising to evaluate a different spacer for attaching the TU motif to the norbornene. The maleimide group present in norbornene TU **50**, even though allowing a straightforward synthesis of the monomer, might form additional hydrogen bonds with the TU groups and thus, decreasing the solubility and the overall flexibility of the TU groups.

Finally, a different synthesis approach for poly(TU)s might be more reasonable considering the straightforwardness and the time factor. Another concept could be for example the use of a TU norbornene **50** in a radical polymerization approach using radical starter like AIBN or simple heating (literature is scarce about the radical polymerization of norbornenes though).[548] While the final polymer side chains would be identical to the ones described in this approach, the polymer backbone would not consist of poly(vinylcyclopentane)s, but poly(norbornane)s, which could already exhibit different solubility properties allowing the establishment of a work-up procedure. Further, the purification steps are expected to be facilitated by the fact that no quenching step of a catalyst

[32] For instance, a step-growth polymerization yields a DP of two at a conversion p of 50% at ideal equimolar conditions after Carothers equation:

$$DP = \frac{1}{1-p} = \frac{1}{0.5} = 2$$

while a living polymerization applying 5 mol% of catalyst would yield a polymer with a DP of 10 after 50% conversion of the monomer.

$$DP = \frac{0.5 \times [M]}{[I]} = \frac{0.5}{0.05} = 10$$

and thus, no removal step of a catalyst has to be applied. The applied radical starter would be attached to the polymer chain end resulting in pure polymer after full conversion. As norbornenes are widely reported to be utilized in different polymerization techniques, further approaches by using TU norbornene **50** can be assumed to be based on ATRP, cationic or Ziegler-Natta-like insertion polymerization.[548–552]

4.4 More sustainable isothiocyanates

In a next step, the mechanism of the AM-3CR was investigated. Isothiocyanates **B** were hypothesized to be the key intermediate in this reaction by C=S double bond formation between an isocyanide and a polysulfane chain **A** (see Scheme 40). The reaction proceeding could successfully be blocked using sterically hindered secondary or tertiary amines. Thus, a more sustainable isothiocyanate synthesis was established using isocyanide as starting materials that were also accessible in a greener fashion due to the protocol introduced in chapter 4.1.

This chapter and the associated parts in the experimental part have been published before:

"A more sustainable isothiocyanate synthesis by amine catalyzed sulfurization of isocyanides with elemental sulfur"-

R. Nickisch, P. Conen, S. M Gabrielsen, M. A. R. Meier, *RSC Adv.* 2021, **11**, 3134-3142.

(The author planned and evaluated the experiments as well as wrote the publication. P. Conen established the synthesis protocol and synthesized part of the isothiocyanate compound library in his bachelor thesis[553] and as a research assistant under the supervision of the author. M. Gabrielsen carried out a major part of the synthesis of the library of isothiocyanate compounds and the polymerization reactions under supervision of the author.

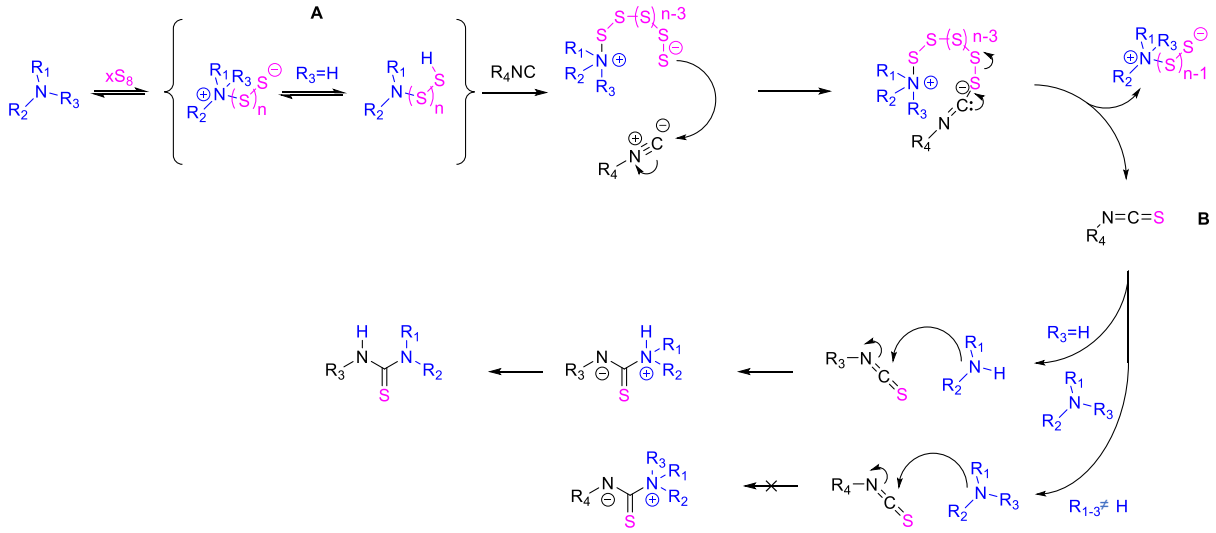

*Scheme 40: Possible mechanistic pathway of the MCR between isocyanide (black), elemental sulfur (purple) and an amine (blue), whereby the amine acts as reactant as well as catalyst to form polysulfur chains **A**. Applying primary or secondary amines leads to thioureas, while tertiary amines lead to isothiocyanates **B**. adapted from ref.*[9]

Abstract

Isothiocyanates (ITCs) are typically prepared using amines and highly toxic reagents such as thiophosgene, its derivatives, or CS_2. In this work, an investigation of a multicomponent reaction (MCR) using isocyanides, elemental sulfur and amines revealed that isocyanides can be converted to isothiocyanates using sulfur and catalytic amounts of amine bases, especially DBU (down to 2 mol%). This new catalytic reaction was optimized in terms of sustainability, especially considering benign solvents such as Cyrene™ or γ-butyrolactone (GBL) under moderate heating (40 °C). Purification by

column chromatography was further optimized to generate less waste by maintaining high purity of the product. Thus, E-factors as low as 0.989 were achieved and the versatility of this straightforward procedure was shown by converting 20 different isocyanides under catalytic conditions, while obtaining moderate to high yields (34–95%).

Results and discussion

Mechanistic investigation of sulfur activation

We initially evaluated the reactivity of various amines in the reaction of a model isocyanide (*n*-dodecyl isocyanide **3**) with elemental sulfur by reacting them in stoichiometric amounts in a suspension of DMSO, while monitoring the formation of the respective ITC **41** (see Table 21, entries 1-6). In every case, the instant formation of the polysulfane chains was visible, since the reaction mixture turned dark brown (same color change was observed in literature)[10,153] as soon as the base was added. As the reaction proceeded, the consumption of the suspended sulfur was also visually observed. GC monitoring of the test reactions revealed that equimolar amounts 1,8-diazabicyclo[5.4.0]undec-7-en (DBU) or 1,5,7-triazabicyclo[4.4.0]dec-5-en (TBD) led to quantitative conversion after 2 hours of reaction time (see Table 21, entries 3 and 6, respectively). Nucleophilic aromatic amines, like *N*,*N*-dimethylamino pyridine (DMAP) and N-methyl imidazole (NMI), were less efficient, both resulting in 38% of conversion, which was attributed to their lower basicity. In general, steric hindrance was deemed less important for the formation of the polysulfane chains, since the conversion of isocyanide **3** was observed using the sterically hindered triethylamine (TEA) and 1,4-diazabicyclo[2.2.2]octane (DABCO) were also high, 76% and 84%, respectively. Taking into account the basicity of the evaluated amines (see Table 21, entries 1–6), it was noted that the most basic amine (TBD) led to the highest conversion, which is consistent with previous reports in which elemental sulfur was activated by strong bases like NaH[143] or K2CO3.[153] However, DABCO, exhibiting the second lowest pKa-value, also showed good performance. Assuming both tertiary amine groups of DABCO are able to activate sulfur in this reaction, the amount of active groups present is doubled compared to the other bases, which might lead to higher conversions in this case. These results show that not only basicity defines the reactivity of the applied amine base, albeit a certain degree of basicity is certainly crucial to activate elemental sulfur. In a second step, we sought to apply the two best performing amines, *i.e.* DBU and TBD, in a sub-stoichiometric/catalytic amount, as no side products were detected, while monitoring the reaction with GC (see Table 21, entries 7-10). As a highly remarkable result, 10 mol% of DBU or TBD were able to convert isocyanide **3** after 22 hours at room temperature with high conversion (67% or 69%, respectively) and the corresponding ITC **41** was obtained. DBU showed better results, *i.e.* 57% conversion after only two hours, compared to 36% conversion for TBD after the same time.

Optimization of the reaction conditions

Having identified two amine bases (TBD and DBU) that can be applied in substoichiometric amounts, we optimized the reaction conditions addressing as many of the Twelve Principles of Green Chemistry[29] as possible and further minimized the E-factor[507] (not yet taking the purification steps into account). Initially, when screening the reaction temperature, higher conversions were obtained at higher temperatures, but in the context of sustainability a less energy-consuming procedure is desired and we thus considered moderate temperatures (40 °C) for further experiments. Next, we altered the solvents focusing on greener alternatives for commonly used solvents according to solvent selection guides[61,505,554] (for the complete screening, see chapter 6.6.1.).

*Table 21: GC-screening of various amine bases (bold) for the activation of elemental sulfur, leading to the formation of n-dodecylisothiocyanate **41**.*

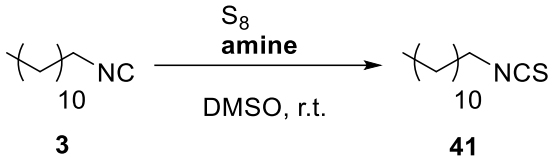

3 **41**

entry	amine (pK_a-value in H_2O)	eq. of amine base	reaction time/h	Conversion/%[a)]
1	DMAP (9.2)[555]	1.00	2	38
2	NMI (7.1)[556]	1.00	2	38
3	DBU (11.5)[555]	1.00	2	99
4	DABCO (8.9)[555]	1.00	2	84
5	TEA (10.7)[557]	1.00	2	76
6	TBD (14.5)[558]	1.00	2	100
7	DBU	0.10	2	57
8	DBU	0.10	22	67
9	TBD	0.10	2	36
10	TBD	0.10	22	69

a.) 1 mmol of *n*-dodecyl isocyanide **3** was reacted with elemental sulfur (2.00 eq. of sulfur atoms) and the respective amount of amine in 1 mL of DMSO at room temperature (r.t.). GC samples were taken after the respective time and conversions were calculated using biphenyl (0.25 eq.) as internal standard (IS).

A clear trend was observed, *i.e.* polar aprotic solvents like DMSO, GBL and Cyrene™ (dihydrolevoglucosenone) favored product formation, probably due to their ability to dissolve and stabilize polysulfane chains. Amongst them, Cyrene™ allowed full conversion of isocyanide **3** after two hours reaction time, while GBL and DMSO also led to high conversions (92 and 85%, respectively). Both GBL and Cyrene™ are greener alternatives if compared to DMSO and are synthesized from renewable resources (butane-1,4-diol[559] and cellulose,[560] respectively), thus decreasing the overall environmental impact. However, more volatile compounds would allow an easier removal and recycling of the solvent. Among the more volatile and sustainable solvents, only acetone was able to achieve good, yet lower conversions (69%). The contribution of the solvent for the proceeding of this reaction was further underpinned by testing the reaction in absence of any solvent, resulting in a low conversion of 8% after 30 minutes (see Table 22, entry 1). To decrease both reaction time and waste, we increased the concentration of isocyanide **3** up to 6 M in Cyrene™ (see Table 22, entries 2–4), which was the upper limit due to practical reasons (since elemental sulfur was only partially dissolved at the beginning of the reaction, a certain amount of solvent was needed to facilitate stirring). Thus, the E-factor could be reduced to 1.12 maintaining full conversion after 30 minutes (see Table 22, entry 4). Furthermore, we decreased the excess of elemental sulfur to 1.12 eq. of sulfur atoms, while maintaining high conversion (98% after 30 minutes). Since 10 mol% of catalyst performed excellent under the optimized conditions, we then evaluated lower catalyst loadings of DBU (see Table 23), since (i) higher conversions in less amount of time were obtained in prior tests and (ii) the stirring of the reaction is facilitated by DBU being a liquid. We note however that the toxicity of DBU is higher compared to TBD (DBU is labeled with GHS05, while TBD is labelled as GHS07). As a result of the high concentration of isocyanide **3** in the solvent (6 M), the catalyst loading of DBU could be further reduced to 1 mol% while still achieving nearly quantitative conversion after prolonged reaction times of 20 hours. Using 2 mol% of DBU at the same

concentration of **3** resulted in complete conversion after only four hours. For more diluted reaction mixtures (*c*(isocyanide) = 2 M), the amount of DBU had to be increased to 5 mol% to obtain full conversion after four hours, which is still a low catalyst-loading.

*Table 22: Optimization of reaction conditions (concentration) for the sulfurization of isocyanide **3** via GC-screening to decrease the E-factor*

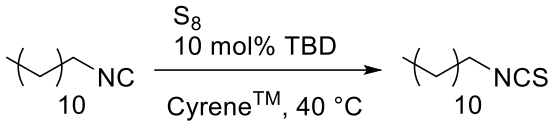

3 **41**

entry	solvent	*c*/M[a)]	conversion/%[b)]	E-factor[c)]
1	-	-	6.7	16.9
2	Cyrene™	1.0	85	5.71
3	Cyrene™	2.0	99	2.95
4	Cyrene™	4.0	100	1.58
5	Cyrene™	6.0	100	1.12

a) Concentration of isocyanide **3** in the solvent. b) 1.00 mmol of *n*-dodecylisocyanide **3** was reacted with elemental sulfur (2.00 eq. of sulfur atoms) and TBD (10 mol%) in the Cyrene™ at 40 °C. GC-samples were taken after 30 minutes of reaction time and conversions were calculated using biphenyl (0.25 eq.) as IS. c) E-Factor was calculated assuming conversion equals the yield, as no side-reaction was observed, not taking the purification steps into account.

The final optimized reaction conditions are depicted in Scheme 41. We note that when a liquid isocyanide was used, the conditions were 2 mol% of DBU in 6 M Cyrene™ solution, while for solid isocyanides 5 mol% of DBU in 2 M Cyrene™ was used, predominantly to facilitate stirring.

*Table 23: Optimization of reaction conditions (catalyst loading of DBU, bold) for the sulfurization of isocyanide **3** via GC-screening.*

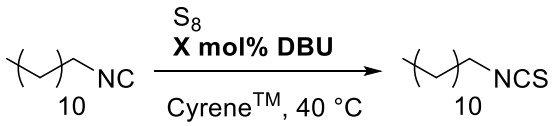

3 **41**

entry	catalyst-loading/mol%	*c*/M[a)]	reaction time/h	conversion/%[b)]
1	5	2.0	0.5	59
2	5	2.0	4	100
3	2	2.0	0.5	29
4	2	2.0	20	99
5	2	6.0	4	100
6	1	6.0	4	78
7	1	6.0	20	96

a) Concentration of isocyanide **3** in Cyrene™. B) 1.00 mmol of *n*-dodecylisocyanide **3** was reacted with elemental sulfur (1.12 eq. of sulfur atoms) and DBU (respective amount) in Cyrene™ at 40 °C. GC-samples were taken after the respective time and conversions were calculated using biphenyl (0.25 eq.) as IS

Evaluating the scope of the sulfurization of isocyanides

Having the optimized reaction conditions in hand, we synthesized several mono- and diisothiocyanates to evaluate the substrate scope of our new procedure (see Scheme 41). Aliphatic, benzylic as well as aromatic isocyanides were successfully converted to the respective

isothiocyanates. Comparing aliphatic isothiocyanates, steric hindrance was found to have minor impact on the yield, which varied from 34 to 94%. In the case of aromatic isothiocyanates, electron-rich and deficient as well as condensed aromatic isocyanides were successfully converted obtaining yields from 45 to 95%, whereby no trend related to electron density was observed.

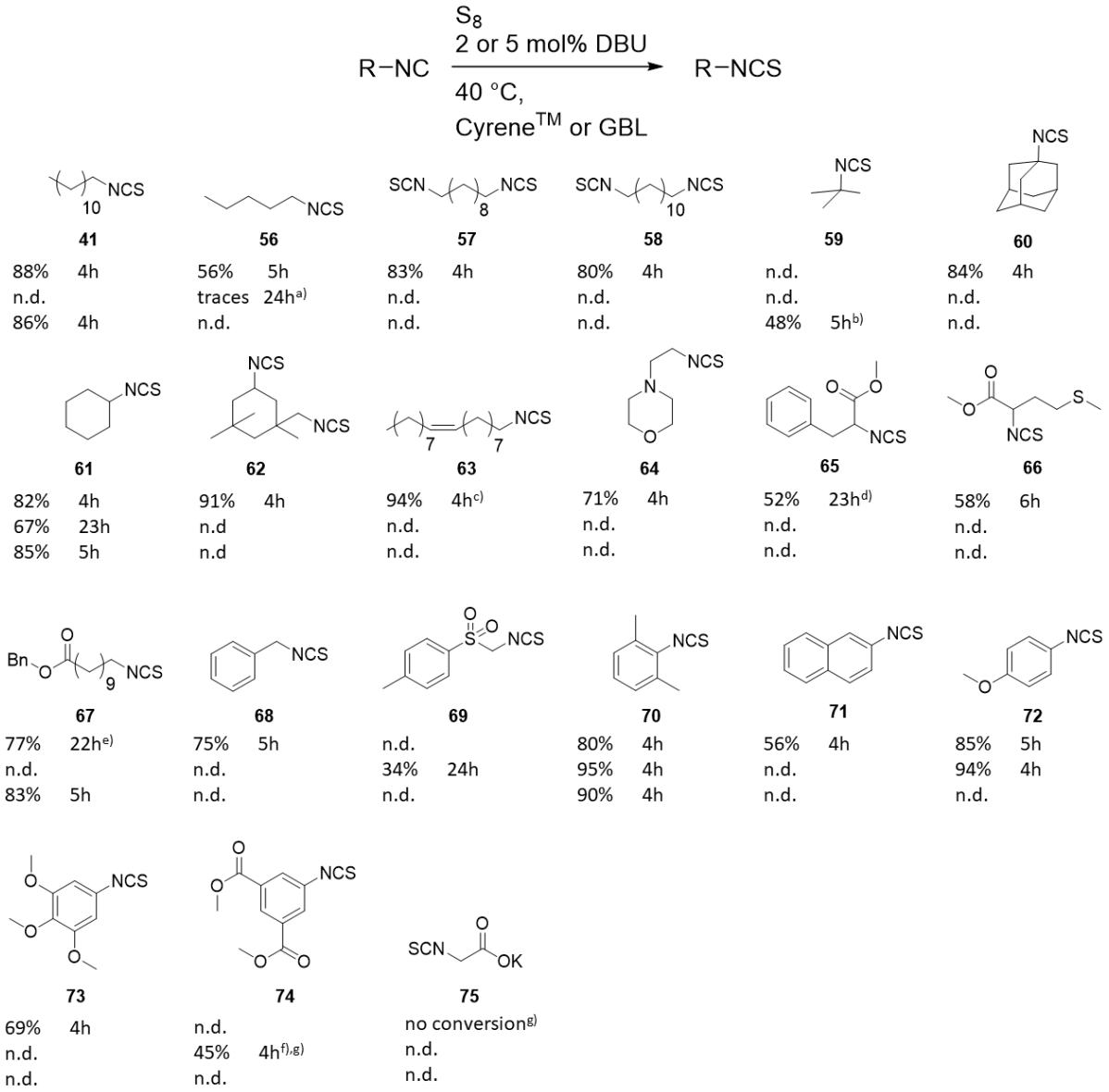

*Scheme 41: Herein synthesized ITCs **41**, **56-75** using the new procedure in a 2.5 mmol scale using elemental sulfur (1.12 eq. of sulfur atoms). If the isocyanide was a liquid at 40 °C, 2 mol% DBU and 417 mL solvent was used, if it was a solid, 5 mol% DBU and 1.25 mL solvent were used. For each compound, the yield and the reaction time are displayed. The first line corresponds to the reaction using Cyrene™ as solvent, the second line using GBL. The third line displays the reaction in Cyrene™ in a 15.5 mmol scale. GC-purities were in general >95% (see chapter 6.6.2). a) GC-purity was not determined (n.d.); b) pressure vial was used; c) GC-purity of the starting material **4** was 80% and of ITC **63** 83%; d) 2.31 mmol isocyanide **65** was used; e) 5 mol% DBU was used; f) 2.00 mmol isocyanide **74** was used; g) starting material was not/less soluble.*

In addition, the reaction had a high degree of chemoselectivity, since several functional groups (double bond (internal), ether (aliphatic and aromatic), thioether (aliphatic), tertiary amine, *p*-toluenesulfonyl, ester) were tolerated. However, the carboxylic acid salt **75** (85% purity) could not be converted, probably due to solubility issues. Considering the tertiary amine of 2-morpholinoethyl isocyanide **64**, an (auto-)catalytic effect might be anticipated, however it was ruled out by performing the reaction in absence of DBU (no yield after 3 hours). Since some isocyanide

compounds are volatile (**59**), a pressure tube was crucial to obtain the respective product. Besides Cyrene™, GBL performed very similar as solvent in this reaction, converting isocyanide **3** to ITC **41** and thus, we hypothesized that GBL could be a more suitable solvent for some ITCs. Therefore, we tested six substrates and as a result, better yields were obtained for aromatic ITCs **70** and **72**, while the yield of ITC **61** was lower. Synthesis of ITC **56** in GBL only resulted in minor traces of the product. Nevertheless, in the case of **69** and **74**, Cyrene™ exhibited similar retention time on silica gel and thus GBL was found to be more feasible for this reaction in the light of fast and more sustainable purification. These results showed that GBL can be superior to Cyrene™ in some cases, depending on the applied substrate. Purification of all herein reported compounds was performed by a modified ash column chromatography to reduce waste (*vide infra*). Furthermore, multigram scale reactions (15.5 mmol) were easily performed, generally resulting in similar or higher yields (*i.e.* **3**, **61**, **67** and **70** in Scheme 41). This increased yield was likely due to small amounts of sulfur sticking to the wall of the reaction flask, which is a negligible effect for larger scale reactions. All herein newly synthesized compounds were fully characterized by proton and carbon NMR-spectroscopy, IR-spectroscopy and high-resolution mass spectrometry. Purities of all synthesized ITCs were determined by gas chromatography (GC) and, for several substrates, elemental analysis (*vide infra*). Furthermore, E-factors were calculated for every ITC (see chapter 6.6.2. for characterization, purity and E-factor data).

Improving sustainability of purification

Purification of ITCs is commonly performed by (flash) column chromatography, thus adding a considerable amount of waste and resulting in poor E-factors. Therefore, we sought to optimize the purification procedure as well. Initial attempts to avoid column chromatography by applying several washing steps of the organic layers led to lower purities. Furthermore, excessive washing with aqueous layers was needed and thus, column chromatography was the purification method of choice, resulting in high purity and less waste (GC-purities in general over 95%, see chapter 6.6.2.). Ultimately, a dry loaded small column (5-8 cm, see Figure 40 in chapter 6.6.2.), similar to a silica plug, was applied as sole purification step directly at the end of the reaction. The amount of used silica, solvent and time was therefore minimized. Residual elemental sulfur was thus also removed, as confirmed by elemental analysis (elemental analysis was performed for several non-volatile ITCs, see chapter 6.6.2.). To further underpin the high purity of this less waste producing purification, we performed a polyaddition reaction of diisothiocyanates **58**, **59** and **62** with renewable 1,5-diamino pentane **76** (98% purity) in an equimolar stoichiometry. Since high purities of the monomers, here of the ITCs, are crucial to obtain high molecular weights via step-growth polymerization, a successfully polymerization is a good indication of the suitability of this more sustainable purification (see Scheme 42). In all three cases, high molecular weights (M_n of **77-79** were 18.6 kDa, 55.1 kDa and 58.1 kDa, respectively, for SEC-graphs see chapter 6.6.5.) were obtained, proving that this optimized purification step resulted in excellent purities. However, for compounds **69** and **74**, applying a classic common column chromatography could not be avoided, since the retention time of the substrate and the solvent were similar to the solvent (*vide supra*).

Overall sustainability

Combining the herein reported DBU catalyzed sulfurization of isocyanides with elemental sulfur and the optimized purification step, very low E-factors were obtained and the toxicity of the overall reaction was minimized by avoiding highly toxic starting materials. This is underpinned by comparison of the synthesis of compound **70** starting from the respective isocyanide **80** with several literature known procedures (see Table 24). For a better comparison of the synthesis protocols, we calculated the E-factor with and without the amount of solvent used (E-factor calculated without

respect to solvent was herein called synthetic E-factor), since some of these procedures would decrease their E-factors drastically by conducting the reaction in higher concentrations. Obviously, the use of a catalyzed reaction, compared to reactions using stoichiometric amounts of reagents, resulted in lower E-factors. Using the herein reported protocol with Cyrene™ resulted in the lowest yield of 80%, for which the synthetic E-factor was comparable to that of procedures using transition metal catalysts offering higher yields ($RhH(Ph_3)_4$ and $Mo(O)(S_2CNEt_2)_2$ obtaining 96 and 91%, respectively). On the other hand, the lowest synthetic E-factor of 0.129 was obtained using our procedure with GBL as solvent, obtaining an excellent yield as well.

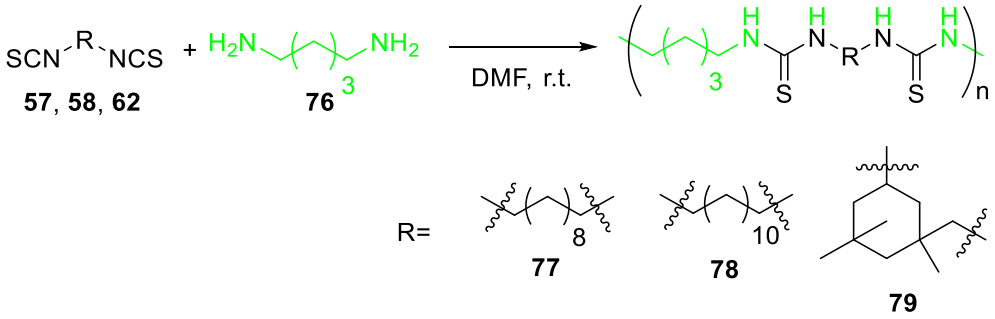

*Scheme 42: Synthesis of polythioureas **77-79** with 1,5-diaminopentane **76** (green) and herein synthesized ITCs **57**, **58** and **62** (black).*

*Table 24: Comparison of sulfurization approaches of isocyanide **70** considering E-factors, energy consumption and purification methods*

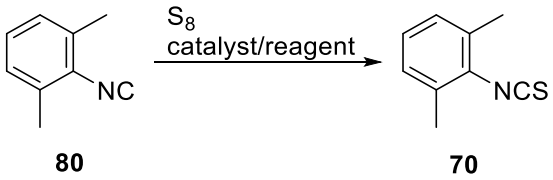

catalyst/reactant	conditions	yield/%	E-factor (syn.)[a)]	E-factor[b)]	purification	Ref.
5 mol% DBU	40 °C, 4 h	95	0.129	3.84	(1) optimized flash cc	this work[c)]
5 mol% DBU	40 °C, 4 h	80	0.349	5.30	(1) optimized flash cc	this work[d)]
2.00 eq. NaH	40 °C, 2 h, Ar-atm.	85	0.982	20.2	(1) dilution with EA, (2) filtration, (3) flash cc	[143]
1 mol% $RhH(PPh_3)_4$	56 °C, 2.5 h, Ar.atm.	96[e)]	0.353	10.4	(1) flash cc	[561]
1 mol% $Rh(acac)(CH_2=CH_2)_2$	56 °C, 2.5 h, Ar.atm.	91[e)]	0.412	11.0	(1) flash cc	[561]
1 mol% $Mo(O)(S_2CNEt_2)_2$	56 °C, 72 h, Ar.atm.	91	0.342	2.10	(1) dilution with petroleum ether, (2) filtration, (3) distillation	[562]
5 mol% Se, 2.40 eq. TEA	66 °C, 1 h	74	2.28	17.0	(1) filtration, (2) distillation	[563]

a) Synthetic E-factor involving reactants, catalysts and remaining starting material. b) E-Factor taking the used reaction solvent into account. c) GBL was used as solvent. d) Cyrene™ was used as solvent. e) Reference mentioned that high purity of isocyanide was very important. cc = column chromatography.

Taking the solvent into account, the E-factor of our new protocol for the synthesis of **70** remained very low with 3.84 and 5.30 for GBL and Cyrene™, respectively. Only the procedure reported by Bargon using a molybdenum catalyst resulted in a lower E-factor of 2.10 due to the use of acetone. Nevertheless, even lower E-factors, down to 0.989 (for **67**), were achieved with our method converting liquid isocyanides (for an overview of all E-factors see chapter 6.6.2.). In addition, this new procedure does not require inert atmosphere, while only moderate energy consumption is needed (40 °C for ca. 4 hours). Comparing the purification methods, we minimized the amount of waste produced by purification using an optimized flash column chromatography step as sole purification step. Furthermore, this procedure is metal-free and the overall toxicity of the reaction is minimized by using catalytic amounts of DBU. Nevertheless, the reader has to be reminded that ITCs intrinsically bear a certain degree of toxicity, which must be addressed by applying adequate safety measures.

Conclusion

Mechanistic investigations of a MCR between isocyanide, amines and elemental sulfur, leading to thioureas, confirmed isothiocyanates as intermediates, which could be trapped herein by using tertiary amines. As a result, a more sustainable synthesis protocol for the sulfurization of isocyanides towards isothiocyanates was established using DBU as greener catalyst in low loading down to 2 mol% and the green solvents Cyrene™ and GBL. E-Factors down to 0.989 were achieved while toxicity, energy and time consumption of the reaction was minimized obtaining moderate to excellent yields. The sulfurization method tolerates several functional groups and is easily applicable yielding the desired product in high purity. We hope that this procedure can pave the way for greener syntheses of isothiocyanates starting from the respective isocyanides and further the formamides and amines.

4.5 Reaction of activated sulfur with benzhydryl carbenes-unexpected alkene formation

The experimental parts of this chapter were performed partly by Peter Conen (student), who was a research assistant under the supervision of the author at the time the experiments were performed. The respective experiments are highlighted with footnotes.

As discussed already in chapter 2.2.1., activated sulfur was reported to form C=S double bonds with carbene-like structures, like carbon monoxide or *N*-heterocyclic carbenes. Further, isocyanides, which also bear a carbene-like structure, were shown in this work to yield isothiocyanates by C=S double bond formation (see chapter 4.4.). Only one report was found on the application of similar reaction approaches for carbenes without a heteroatom bound to the carbene center: Ishii *et al.* reported the synthesis of a C=S double bond from a diazo compound attached to a highly restricted dibenzobarrelene by heating in the presence of sulfur.[564] It was noted that classic approaches, like thionylation of the respective ketone using Lawesson´s reagent, did not lead to the desired product. Thus, further investigation on this topic seemed promising to establish a general synthesis procedure for the formation of thioketones and the Bamford-Stevens reaction was chosen as suitable starting point for this investigation, which is depicted in Scheme 43.

The reaction allows a defunctionalization of an enolizable ketone group, yielding a double bond.[565] Thereby the ketone is first transferred to a tosyl or Eschenmoser hydrazone. Upon heating, diazo compounds are formed using a base or a metal catalyst like rhodium acetate. Under extrusion of nitrogen, a carbene is formed in aprotic solvents, which yields the product after a [1,2]H-shift.[33] If the starting material allows the formation of more than one alkene as product, the thermodynamically more stable one is formed. This reaction seemed a promising starting point for further studies, as the typical alkaline conditions required for the decomposition of the tosylhydrazones in this reaction seemed to be suitable for the activation of sulfur as well.

Thus, it was hypothesized that performing a Bamford-Stevens reactions, while adding elemental sulfur to the reaction, would result in polysulfane formation that would attack the carbene intermediate, resulting in a C=S double bond (see Scheme 43). With this reaction pathway, thioketones could be obtained without relying on typically toxic and smelly reagents like Lawesson´s reagent or phosphorus pentasulfide.[566–569] Thioketones are compounds that show exceptional reactivities, for instance in several cycloaddition reactions (“superdienophiles”).[568,570–573] However, it has to be mentioned that the stability of thioketones is very variable and they might decompose.[574] In addition, they tend to tautomerize to their ene-thiol form, if enolizable thioketones are formed and they might degrade further due to their intrinsic nucleophilicity. Consequently, 4,4´-dimethoxybenzophenone **81** was chosen as starting material for this study as it had several advantages. First, the benzhydryl motif would lead to a non-enolizable thioketone, decreasing the side-reactions that can occur while working with thioketones (see Scheme 43). Second, due to the utilization of the non-enolizable ketone or tosylhydrazone derivative, respectively, the actual Bamford-Stevens reaction cannot proceed, as the [1,2]H-shift is not possible. Thus, if this condition would yield thioketones, no competitive reaction path would be present. This was important, since the last step of the Bamford-Stevens reaction is an intramolecular H-shift and it was assumed to be faster than an intermolecular addition reaction between carbene and polysulfane, probably resulting

[33] Note that the reaction can also proceed in polar protic solvents without the formation of a carbene.[565]

in a impeded thioketone formation. Third, electron-rich benzophenone derivatives were reported to yield stable thioketones and thus could be easier detected and fully characterized.[34]

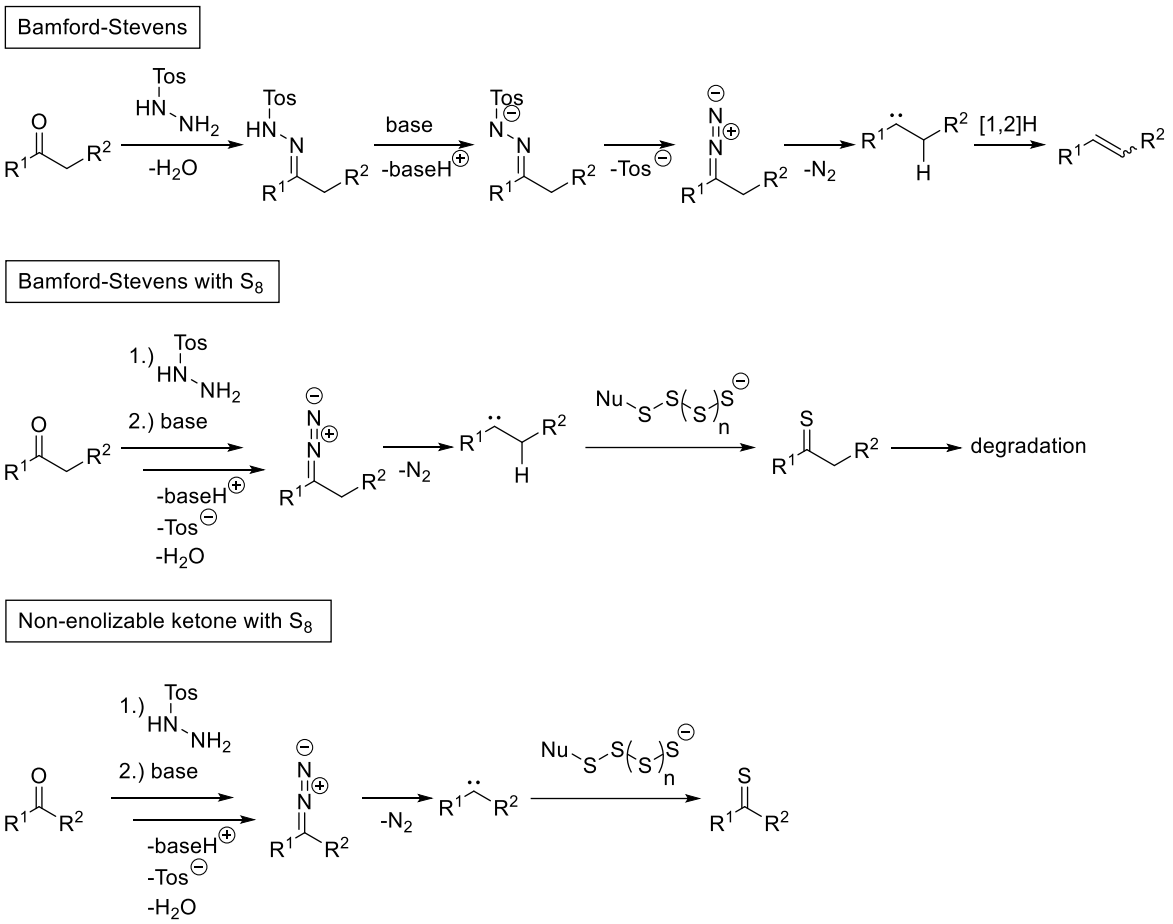

Scheme 43: Overview of the hypothesized modified Bamford-Stevens reaction with elemental sulfur. The reaction pathway of the classic Bamford Stevens reaction in aprotic solvent is given (top). In addition, the possible thioketone formation in the presence of sulfur is depicted (mid). Since the thioketones are typically unstable compounds, for instance when enolizable thiocarbonyl groups are formed, non enolizable aryl ketones (R^1, R^2 = aryl) were considered to allow the formation of more stable thioketones, while the actual defunctionalization reaction is impeded (bottom).

Finally, the methoxy groups of the benzophenone **81** allowed an easy reaction monitoring by ^{1}H-NMR-spectroscopy, as the singlet signal can be easily followed if converted (see also Figure 13).

A first reaction was performed using 4,4´-dimethoxybenzophenone tosylhydrazone **82**, which was obtained in one step from the respective ketone and tosylhydrazide in a yield of 83%.[35] To the starting material, two equivalents of sodium hydride and 0.25 equivalents of S_8 (corresponding to 2.0 equivalents of sulfur atoms) were added. The compounds were dissolved or suspended in DMSO and stirred at 130 °C, resulting in the typical dark brown solution indicating polysulfane formation (see Table 4). Sodium hydride was chosen, since it is typically used for activation of elemental sulfur (see Table 4), while no higher degree of reactivity is present towards the ketone or aimed thioketone,

[34] For instance, thionoxanthone could be stored in our laboratory at -17 °C under argon atmosphere and light exclusion for more than two weeks without notable impurities forming, as investigated by ^{1}H-NMR analysis. Further, Peter Conen (master student in our working group at the time this thesis was written) independently investigated from the work or contribution of the author that 4,4´-dimethoxythiobenzophenone showed no notable degradation for at least three weeks when stored in a brown-glass flask under argon atmosphere at room temperature.

[35] The synthesis was performed by Peter Conen, who was a research assistant at the time of this work under the supervision, planning and evaluation of the author.

which could result in side-reactions. After one hour, TLC indicated full conversion of tosylhydrazone **82** and in addition, a new spot was found exhibiting fluorescence properties when irradiated at 356 nm with an UV-lamp. Thus, column chromatography seemed reasonable as no other side products were indicated, allowing an easy separation of the product species **83** from salt or sulfur remainings of sodium hydride and sulfur, respectively. Interestingly, comparison of the ^{1}H-NMR-spectra of product **83** with the one of 4,4´-dimethoxybenzhydryl tosylhydrazone **82** and the respective thioketone **84**[36] showed that the chemical shifts were not fitting for either of the compounds (see Figure 13).

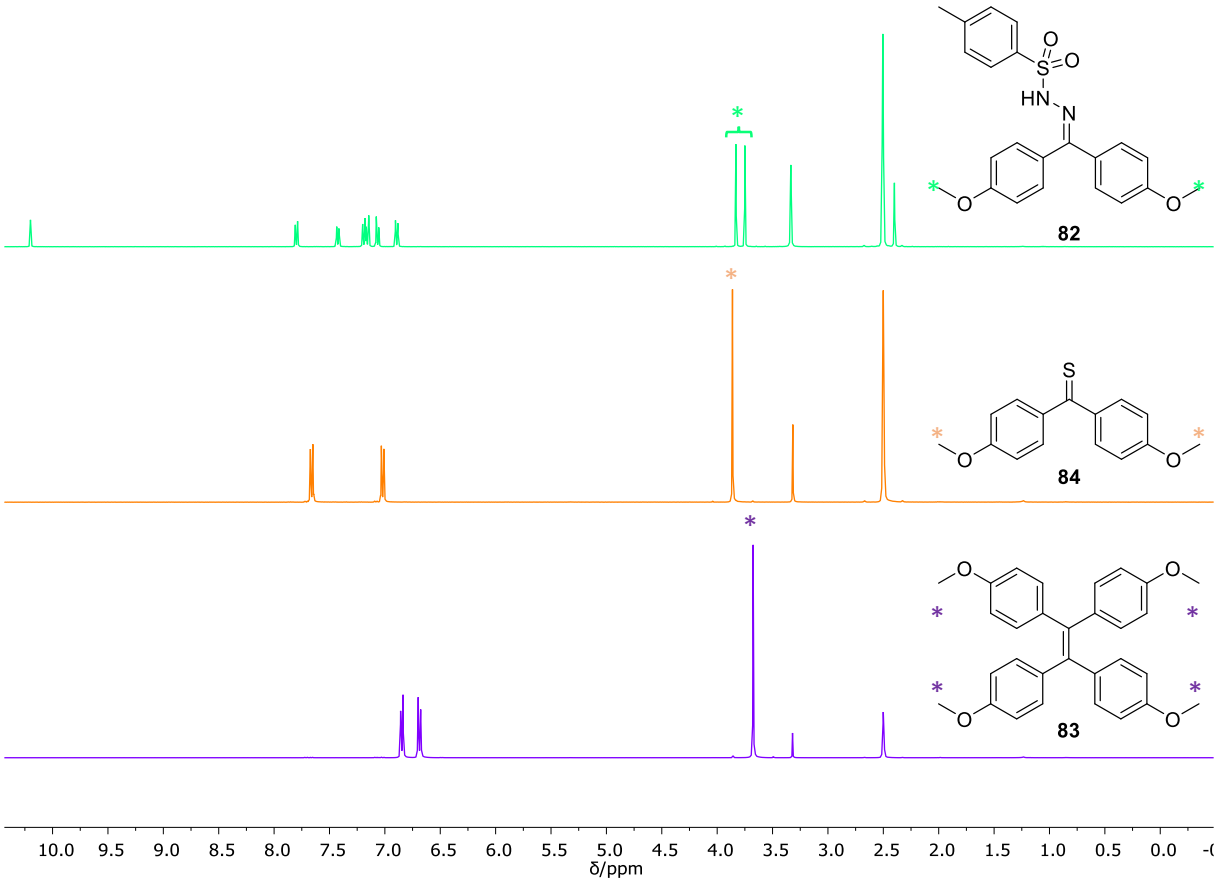

*Figure 13: ^{1}H-NMR-spectra of 4,4-´dimethoxybenzyhdryl tosylhydrazone **82** (green), the respective thioketone **84** (orange) and the obtained product **83** (purple) in DMSO-d_6. The respective singlet signals of the methoxy groups are highlighted by "*". Note that the proton signals of the benzhydryl moiety of the tosylhydrazone **82** are split up, since they have different chemical surrounding.*

All proton signals were shifted strongly towards the highfield, indicating an absence of electron-withdrawing heteroatoms like nitrogen, oxygen or sulfur (see Figure 13, purple spectrum). Ultimately, full characterization of the obtained product **83** proved that the coupling product of two benzhydryl moieties, *i.e.* the 1,1,2,2-tetra(4-methoxy)phenyl ethylene **83** was obtained (see Figure 13 for structure formula and chapter 6.7.2. for full characterization) with an excellent yield of 92%. This was further underpinned by comparison with the reported ^{1}H-NMR-spectrum of this compound.[575]

Since the unexpected formation of the tetraphenyl ethylene derivative seemed to be clearly the main reaction of this procedure, as underlined by the high yield, the initial aim of this work was

[36] The compound was provided by Peter Conen who performed his master thesis at the time this thesis was written, and the author did not contribute to the synthesis of this compound.

reevaluated. Thus, in a next step, it was aimed to optimize the reaction condition for the formation of compound **83**, which is depicted in Table X:[37]

*Table 25: Optimization of the reaction conditions for the alkene formation of tosylhydrazone **82** by base-activated sulfur.*

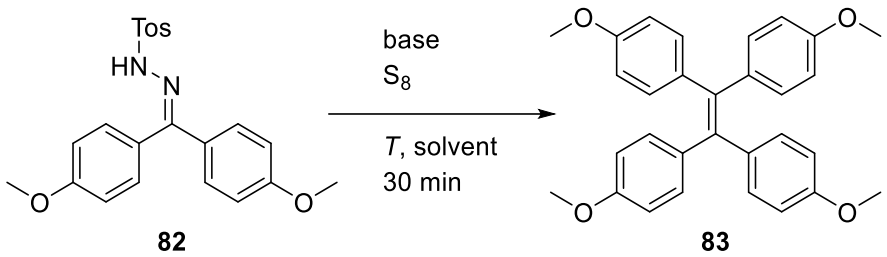

82 **83**

entry	base	*T*/°C	solvent	eq. of S_8	conversion of 82/%
1	NaH	80	DMSO-d_6	0.28	52[a)]
2	NaH	90	DMSO-d_6	0.28	70[a)]
3	NaH	100	DMSO-d_6	0.28	82
4	DBU	100	DMSO-d_6	0.28	54
5	K_2CO_3	100	DMSO-d_6[b)]	0.28	100
6	K_2CO_3	100	DMF	0.28	68
7	K_2CO_3	100	GBL	0.28	53[c)]
8	K_2CO_3	100	NMP	0.28	81
9	K_2CO_3	100	DMSO-d_6	0.188	97
10	K_2CO_3	100	DMSO-d_6	0.15	90
11	K_2CO_3	100	DMSO-d_6	0.138	91

Tosylhydrazone **82** (1.00 eq.) and the respective amount of elemental sulfur were suspended in the respective solvent (*c*(**82**)=0.5 M) and the respective base (1.20 eq.) was added. The reaction mixture was heated at the respective time and a ^{1}H-NMR-sample was taken after 30 minutes. a) ^{1}H-NMR-sample was taken after 4 hours. b) The same conditions at a concentration of *c*(**82**)=0.25 and 1.0 M led also to quantitative conversion. c) ^{1}H-NMR-sample was taken after 20 minutes at higher reaction times additional signals appeared were overlapping with the methoxy group of product **83**.

Due to the simple ^{1}H-NMR-spectra of tosylhydrazone **82** and product **83**, the conversion of the starting material could be monitored by ^{1}H-NMR-spectroscopy in DMSO-d_6. Conversion could be calculated by following the decrease of the methoxy group signals of **82** at 3.83 and 3.75 ppm, and the increase of the respective methoxy signal of the product **83** at 3.68 ppm. The equivalents of base was set to 1.20, since at least one equivalent was needed to fully deprotonate the tosyl hydrazone **82**. The reaction benefited from higher temperature, whereas the initial temperature of 130 °C could be reduced to 100 °C still yielding high conversion of 82% after only 30 minutes (Table 25, entry 3). Lower temperatures gave only insufficient conversion even after elongated reaction times (see Table 25, entry 1, 2). Subsequently, other typically used bases for the activation of sulfur, namely DBU and potassium carbonate, were tested. While DBU performed poorly (54%, see Table 25, entry 4) potassium carbonate led to quantitative conversion after 30 minutes (see Table 25, entry 5). Having found the ideal base, other solvents, *i.e.* DMF, GBL and NMP, were tested but DMSO proved to be superior (compare Table 25, entry 5-8). Finally, the equivalents of S_8 molecules were reduced from 0.28 to 0.138 (corresponding to 2.24 and 1.10 equivalents of sulfur atoms, respectively), leading to a conversion of 91% (compare Table 25, entry 5, 9-11). It seemed that a certain amount of excess of sulfur was beneficial for the reaction and thus, the optimized equivalents of sulfur were chosen to be 0.20 (corresponding to 1.60 eq. of sulfur atoms).

[37] The screening of the reaction conditions was performed by Peter Conen who was research assistant by the time these experiments were performed under the supervision, planning and evaluation of the author.

To prove that the optimized reaction protocol can yield tetraphenyl ethylene derivatives in high yields, the synthesis of **83** was repeated leading to quantitative yield. In addition, tetraphenylethylene **85** was also synthesized from benzophenonetosylhydrazone obtaining the pure product in a yield of 97% after column chromatography (see Figure 14).

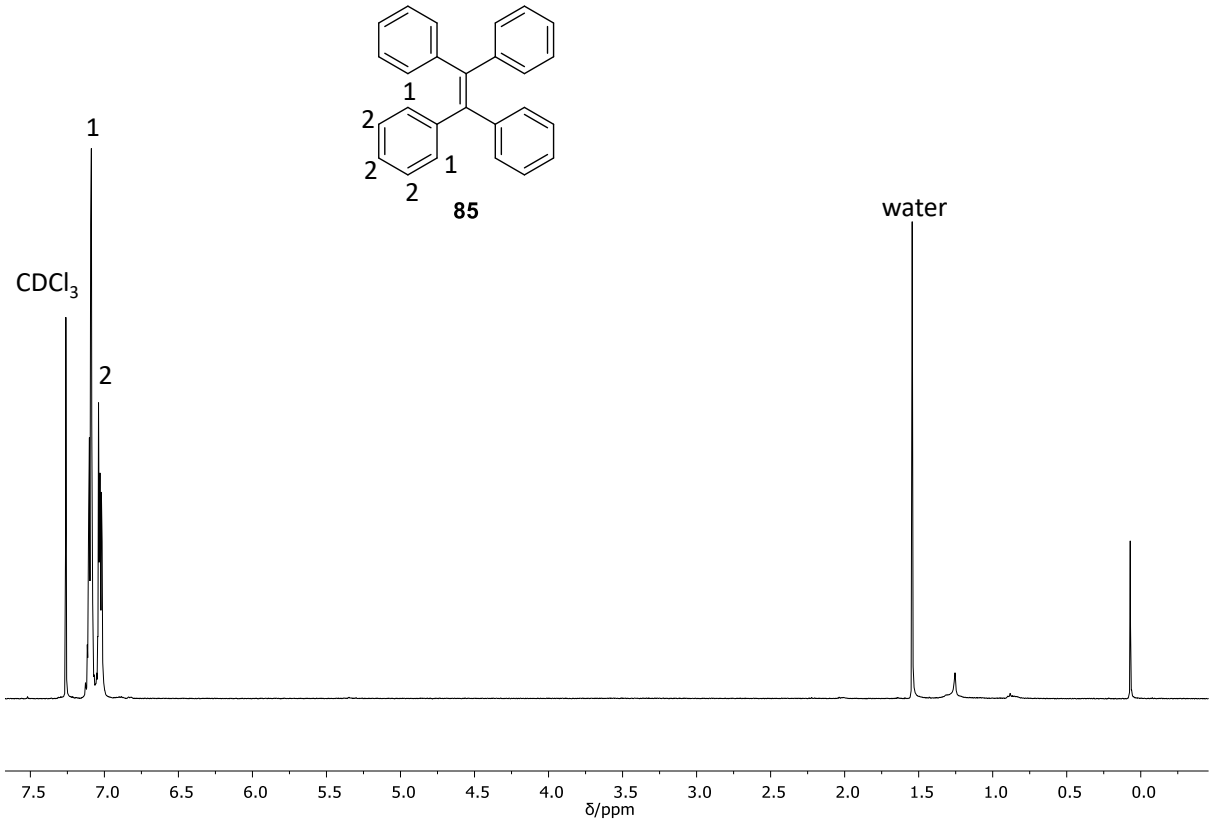

*Figure 14: ^{1}HNMR-spectrum of tetraphenyl ethylene **85** in $CDCl_3$ obtained from the reaction with respective tosylhydrazone, sulfur and potassium carbonate.*

Further investigations of the scope of these reactions could not be performed because of time issues. Nevertheless, the synthesis of the two compounds **83** and **85** showed that the synthesis protocol is a promising alternative for the double bond formation compared to typical reactions like the McMurry or the Barton-Kellogg reaction (see Scheme 44). While the McMurry reaction relies on widely commercially accessible carbonyl functions and the use of titanium trichloride that is reduced by an additional reagent like $LiAlH_4$, Zn/Cu or Mg to obtain alkenes by homo coupling, the work-up can be assumed to be challenging due to the presence of the metal salts, often in high excess.[576–579] For instance, Duan *et al.* reported the synthesis of tetraphenyl ethylene **85** using a McMurry reaction obtaining an excellent yield of 92%.[578] Therefore, they applied five equivalents of titanium tetrachloride and ten equivalents of zinc powder respective to benzophenone in a mixture of THF and pyridine under reflux and argon atmosphere for six hours, obtaining product **85** after extraction and subsequent column chromatography. Liu *et al.* were able to synthesize 4,4´-dimethoxybenzophenone **83** in a yield of 90% using stoichiometric amounts of titanium tetrachloride and zinc under reflux for two hours in THF and additional pyridine.[575] Product **83** was isolated by extraction and subsequent recrystallization. Compared to these conditions and the respective work-up, the herein described method can be more feasible (no Schlenk-conditions, probably faster work-up) and faster reaction rate (only 30 minutes), giving higher yields (97% and quantitative for **83** and **85**, respectively) as well as generating less waste, while being a metal-free approach. On the other hand, the Barton-Kellogg reaction uses a thioketone and a diazo compound,

both very sensitive and noxious starting materials, which have to be prepared beforehand in one or two steps, respectively.[38] The compounds react initially in a [2+3] cycloaddition, yielding a 1,3,4-thiadiazole, which can undergo extrusion of nitrogen, forming a thiirane.[580] In a last step, the alkene is obtained usually by applying a desulfurization reagent like PPh_3. It is thus one of the most efficient reactions to yield sterically demanding alkenes by cross coupling of carbonyl precursors.[581,582]

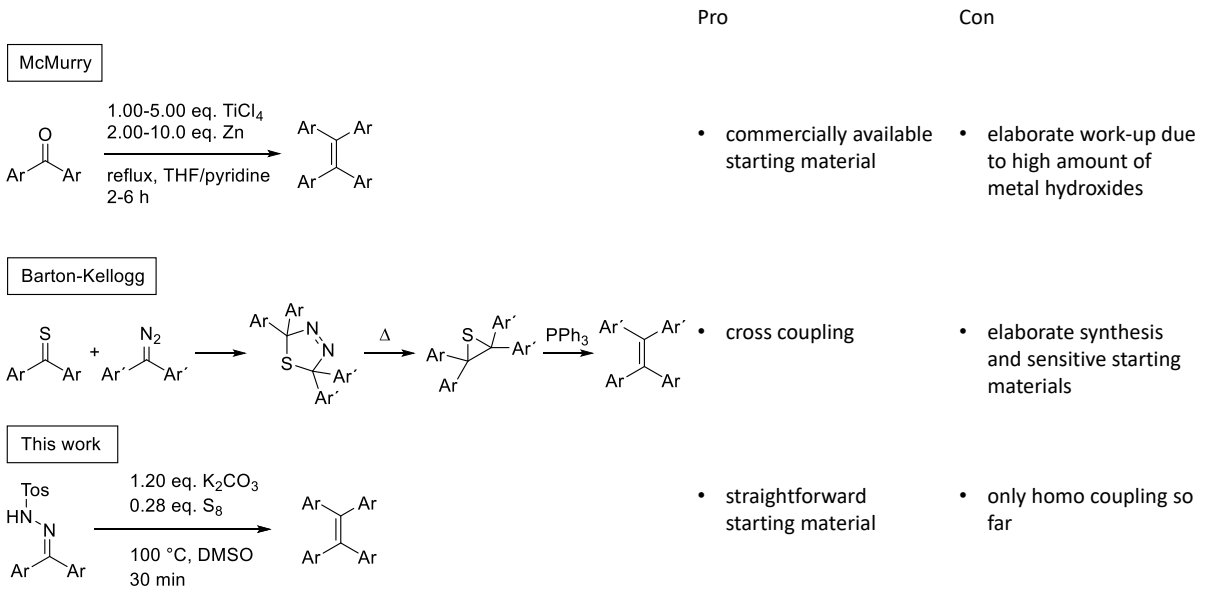

Scheme 44: Comparison of typical reaction conditions of the McMurry and Barton-Kellogg reaction with the herein reported alkene synthesis from tosylhydrazones. Pro and Cons for each reaction are given to provide a better overview of the potential of this novel C=C double bond formation.

Compared to the herein investigated double bond formation of tetraphenyl ethylene derivatives, advantages lie in the more easily accessible and bench-stable starting materials, namely tosylhydrazones. Moreover, only one step is needed to obtain the final product, while in a Barton-Kellogg reaction an additional desulfurization step of the obtained thiirane has to be applied typically (there are also cases reported where the desulfurization reagent can be applied in the same pot or none has to be applied at all).[582–584] However, a clear disadvantage of the herein established procedure is the fact that only homo coupling can be performed. Yet, further investigations on the reaction mechanism have to be performed to shed more light on the proceeding of the reaction. As a result, it could be possible to obtain alkenes by cross coupling of tosyl hydrazone moieties not relying on simple alteration of stoichiometry (high excess of one of the two starting materials would probably lead to challenging purification). For instance, it seemed reasonable that depending on the mechanism of the reaction that two different tosyl hydrazones might exhibit kinetic selectivity towards the cross coupled product instead of the two possible homo coupled products. Further, if isolatable intermediates of this reaction could be determined, the use of tosyl hydrazone and

[38] Typical syntheses of thioketones[566–569] and diazo compounds[564,642] for the use of a Barton Kellogg-reactions are:

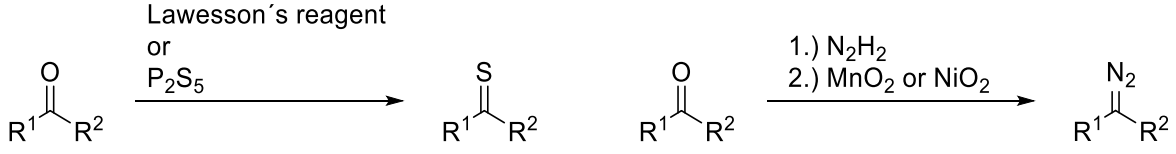

mentioned intermediate could also yield cross coupled alkenes, since the reaction kinetic of subsequent steps will be altered as a higher concentration of an intermediate is present from the start (*vide infra* for a concrete example).

Based on the herein obtained results, combined with the information from the thoroughly performed literature research conducted in chapter 2.2.1., a tentative mechanism of this reaction is suggested in Scheme 45. First, the formation of polysulfanes **I** is assumed, as the optimized reaction conditions like the substochiometric utilization of a base for the activation of sulfur, as well as the appearance of a dark brown solution indicated this compound as key intermediates for this reaction. Simultaneously, the tosyl hydrazone **A** follows the typical steps for the formation of a diazo compound **B** known to take place in the Bamford-Stevens reaction. It is first deprotonated by a base and subsequently eliminates *p*-toluenesulfinate to yield diazo compound **B**. Then, diazo compound **B** extrudes nitrogen forming the benzhydryl carbene **II**.

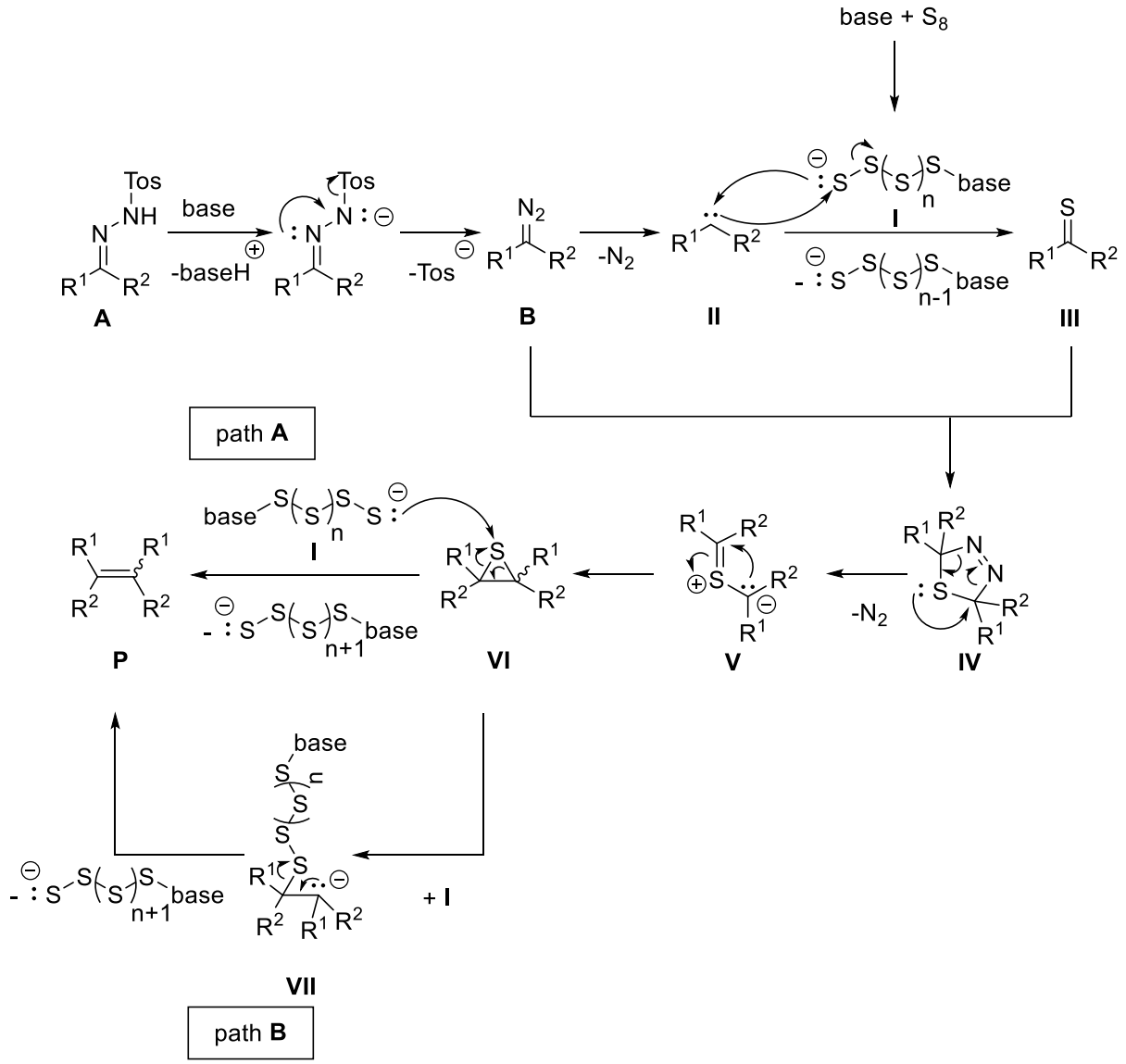

*Scheme 45: Tentative mechanism for the formation of tetraphenyl ethylenes **P** using base-activated sulfur as difunctional reagent, namely C=S double bond formation with carbene **II** and desulfurization of thiirane **VI**. In theory, no sulfur is consumed however, it is assumed that a slight excess of sulfur is needed to maintain a fast C=S double bond formation. Otherwise, the diazo compound **B** and carbene **II** might follow other reaction channels not leading to 1,3,4-thiadiazole **IV**.*

In a next step, the carbene **II** is attacked immediately by the polysulfane **I**, yielding the thioketone **III** following the mechanism for a C=S double bond formation, explained thoroughly in chapter 2.2.1. Thioketones usually exhibit a strong coloration due to their characteristic n-π* transition of the C=S double bond, absorbing light in the visible area.[570] For instance, the respective thioketones of tosylhydrazones herein used were reported to be dark blue, an unusual color for organic compounds.[585] Indeed, intense blue coloration was found during column chromatography of product **83**.

In addition, product **83** was obtained as slightly blue solid instead of being colorless,[586] even though high purity of product **83** was shown by NMR-spectroscopy (see Figure 13) indicating that the thioketone intermediate **III** seemed reasonable (for pictures see chapter 6.7.1.). As the thioketone **III** is formed, it is in return caught by the diazo compound **B**, undergoing a Barton-Kellogg reaction forming the 1,3,4-thiadiazole **IV**. Then, the reported extrusion of nitrogen takes place under the elevated temperature forming a sulfur ylide **V** that undergoes four-electron-electrocyclization yielding the thiirane **VI**. Finally, the polysulfane **I** was assumed to act as a desulfurization reagent by attacking the sulfur atom of the thiirane **VI** yielding the alkene **P**. This step could possibly proceed either in concerted fashion by retro [1+2] cycloaddition (path **A**, see Scheme 45) or stepwise under formation of a carbanion-polysulfane adduct **VII** (path **B**, see Scheme 45).

This reaction pathway might be very complex but reasonable indications are already present as the formation of the diazo compound and the proceeding of the Barton-Kellogg reaction are reported, as mentioned above, under similar conditions (elevated temperature, alkaline milieu). In addition, the dark brown coloration during the reaction and the intense blue coloration during work-up indicate the presence of polysulfanes and thioketones. Nevertheless, a thorough investigation of suitable test experiments would shed more light on this mechanism. Several hypothesized intermediates, like diazo compounds **B** or thioketones **III**, can be accessed by suitable alternative synthesis protocols, which allows an experimental approach for the mechanism investigation by control experiments. Since no time was left to further investigate the mechanism, some reasonable control reactions are presented in the following in Scheme 46, which could clearly identify the mechanism depicted in Scheme 45.

First it has to be mentioned that the reaction should not take place in the absence of elemental sulfur (see Scheme 46**A**). This is an important test reaction because it can also be hypothesized that the formed carbene **II** dimerizes to the product **P**, following the Wanzlick equilibrium without the participation of sulfur or polysulfane **I**.[39] This assumption has been confirmed by the time this thesis was written.[40]

Second, the respective diazo compound **B** applied as starting material in the reaction instead of the tosylhydrazone **A** should also yield the alkene **P** (see Scheme 46**B**).

[39] The Wanzlick equilibrium describes dimerization of two carbene species to form an alkene and was described for *N*-heterocyclic carbenes:[643]

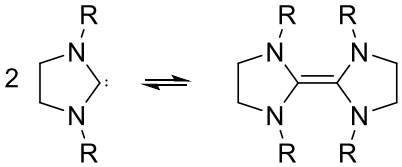

[40] The control experiment described, namely the reaction of tosylhydrazone **A** and a base at elevated temperature in DMSO without addition of elemental sulfur, was performed by Peter Conen in the scope of his master thesis and was independently investigated from the work or contribution of the author.

On the other hand, the most crucial control experiment would probably be applying thioketone **III** as starting material for this reaction instead of the tosylhydrazone **A** (see Scheme 46**C**). Since no diazo compound **B** would be present, no Barton-Kellogg reaction could take place and thus, no product could be formed.

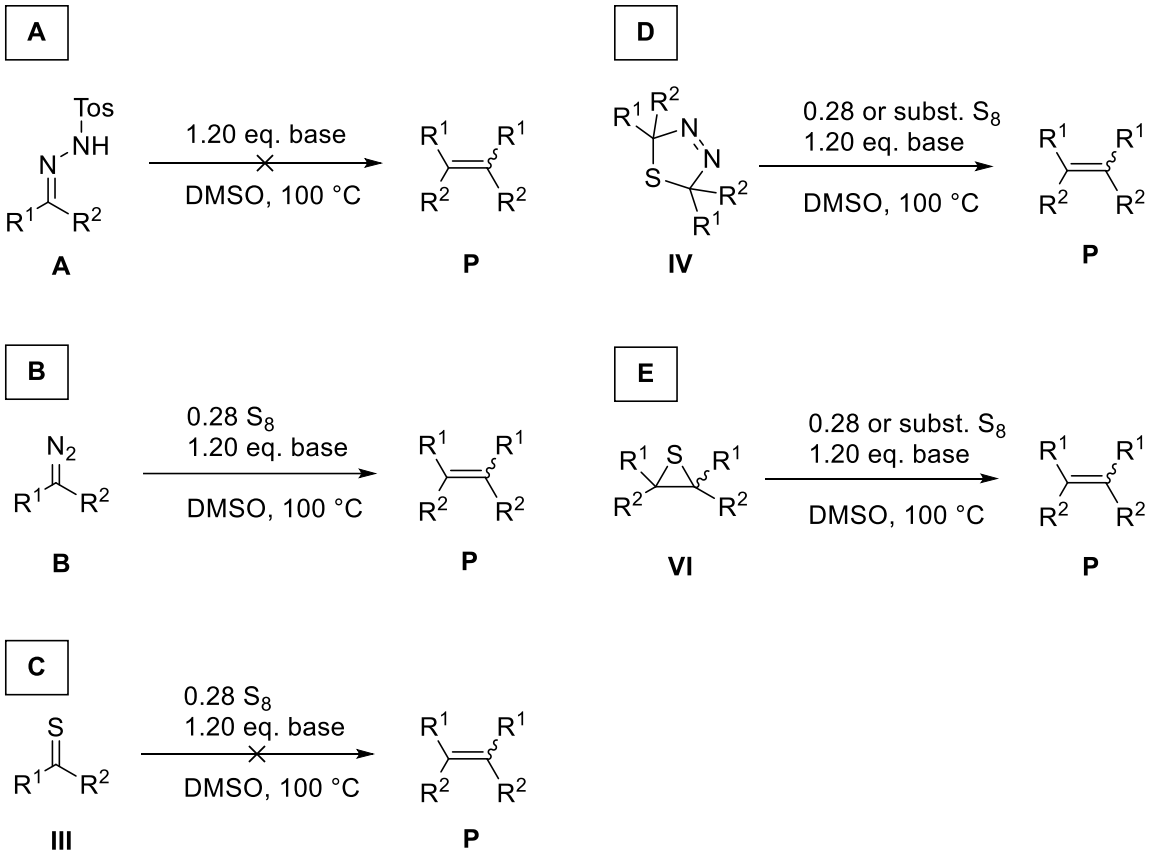

*Scheme 46: Envisioned control experiments to validate the herein proposed reaction mechanism of the formation of alkene **P** by conversion of tosylhydrazones **A** with base-activated elemental sulfur.*

It has to be noted that, assuming this mechanism, deliberate addition of thioketones to a tosylhydrazone might yield a synthesis protocol for an alkene obtained by cross-coupling. As the formation of the diazo compound is the first step of reaction sequence converting the tosylhydrazone, no further or only partial decomposition to the carbene intermediate **II** would take place in this case, since an additional thioketone starting material would immediately react with the formed diazo compound. Thus, the polysulfane **I** is not needed for the thioketone formation but is still relevant for the desulfurization step.

As some 1,3,4-thiadiazoles **IV** need elevated temperature for the extrusion[580] they could also be synthesized and then tested as starting material for the reaction forming alkenes **P** (see Scheme 46**D**).[41] This control experiment would clearly underpin the reaction proceeding *via* a Barton-Kellogg pathway, since also other formations towards the thiirane could be envisioned like by mediating of the polysulfane **I** or *via* a Büchner-Curtius-Schlotterbeck reaction pathway.[42]

[41] 1,3,4-thiadiazoles **IV** can be obtained by performing a Barton-Kellogg reaction with thioketones **III** and diazo compounds **B** in the absence of heat and a desulfurization reagent like PPh_3 (see Scheme 44). Alternatively, they can be obtained by formation of 1,3,4 thiazolidines from carbonyls, hydrazine and hydrogen sulfide followed by oxidation for instance with lead(IV) acetate.[580]

[42] For instance, the reaction of two carbenes **II** with polysulfane **I**:

Finally, the respective thiirane **V** should yield the product under the optimized reaction conditions (see Scheme 46**E**).[43] This would be the second crucial control experiment as it would clearly prove the participation of activated sulfur as desulfurization reagent, which was not reported before. Moreover, since this reaction step does not consume the polysulfane **I**, the conversion of thiirane **V** or 1,3,4-thiadiazole (see scheme 46**D** and **E**) should be tested also with substoichometric amounts of sulfur to obtain data about the catalytical character of polysulfane **I** in this reaction sequence.

In general, the hypothesized pathway for alkene formation by using tosylhydrazones does not consume sulfur because thioketone formation consumes one sulfur atom, whereas desulfurization releases one. Still, the screening experiments showed that an excess of sulfur is beneficial, which might be needed to convert formed carbene intermediates **II** fast enough into the thioketones **III** and thus, maintaining a low carbene concentration in the reaction mixture preventing side reactions like the Wanzlick-equilibrium.

Furthermore, information about the rate-determining step could be obtained from the above-mentioned control experiments. Two steps in the hypothesized mechanism are expected to need elevated temperature, namely the formation of diazo compound **B** and thiirane **V** and thus, could be potentially the rate-determining step. To verify if the diazo compound formation is the one, control experiment **B**, if successful, should be performed at lower temperatures (see Scheme 46**B**). Similarly, control experiment **E** using the thiirane **V** as starting material should be performed at lower temperatures as well (see Scheme 46 **E**). Further, using the deprotonated tosyhydrazone **A**, diazo formation was reported at lower temperature (40 °C) indicating that the deprotonation step might by the rate-determining step.[587] Thus, the deprotonated tosylhydrazone **A** should be tested as starting material for the reaction with sulfur and base at lower temperatures. In addition, deuterated tosyl hydrazide could be used to investigate the impact of the deprotonation step of **A** by a base for the overall reaction kinetic *via* primary kinetic isotope effect.[44]

Information about the stereoselectivity, *i.e. cis-trans* isomerism of the product, could be obtained by using a suitable starting material like 4-methoxybenzophenone comparing the ratio of the obtained

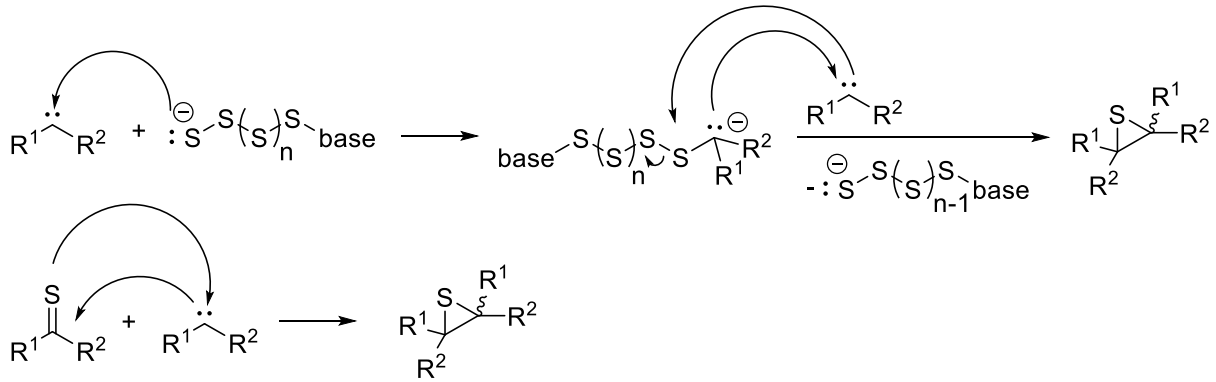

[43] Thiirane **V** can be obtained by performing a Barton-Kellogg reaction in the absence of a desulfurization reagent like PPh_3 (see Scheme 44).[580]

[44] Since the mass difference between hydrogen and deuterium is large (deuterium has roughly the doubled weight) a different kinetic behavior can be observed in a reaction comparing a X-H bond to a X-D bond.[644] A primary kinetic isotope effect describes thereby the direct formation or braking of such bond in the reaction pathway. In the mentioned reaction, the tosylhydrazone **A** is deprotonated hence the N-H and N-D bond would be broken, respectively. Since the N-D bond is stronger the reaction step would proceed slower and comparing the rates with the N-H bond braking would result in a primary kinetic isotope effect. This effect is rather small and is usually observed when the respective reaction step is rate-determining or at least contributes majorly to the overall reaction rate.

cis- and *trans*-product. This should be possible by ^{1}H-NMR-spectroscopy, since the methoxy groups of the products should exhibit different chemical shifts.

Indication for the chemoselectivity of this reaction, irrespective to the actual reaction pathway, could be obtained by the conversion of a ditosylhydrazone, since this would result in a step-growth polymerization. As a step-growth polymerization reaction only leads to high molecular weight when the conversion of the respective functional groups is high and selective, insights about the degree of side reactions could be extracted.[45]

Suitable analytic instruments further complementing the data that can be obtained out of the mentioned control experiments would be IR-techniques like ONLINE-IR. Thus, it could be possible to follow the *in situ* formation and conversion of intermediates like diazo compounds **B** as they exhibit very specific vibrational band.[46]

Concluding, a new reaction for the formation of tetraphenyl alkene derivatives was found by homo coupling of benzophenone tosylhydrazones, harvesting the versatile reactivity of sulfur activated by a base. The reaction was optimized and shown in a proof of concept on the example of two substrates, offering high yields while purification with flash column chromatography allowed fast isolation of the product. The reaction is a promising extension of the toolbox available for chemists to transfer carbonyl compounds and their derivatives into highly restricted alkenes like the McMurry or the Barton-Kellogg reaction. Further investigations are needed to fully understand the reaction mechanisms. For this case, suitable control experiments were suggested. In addition, the scope and limits of the reaction should be investigated as well. For instance, highly sterically demanding aliphatic tosylhydrazones, like the respective one obtained from adamantan-2-one, could be suitable starting materials for the reaction as well.[47] This reaction is envisioned to add a considerable

[45] Step-growth polymerization is described by Carothers equation:[639]

$$DP = \frac{1 + r}{1 + r - 2pt}$$

While DP is the degree of polymerization, p the conversion and r the ratio between the functional group A and B forming the polymer backbone, whereas $r \leq 1$. For instance, in a polycondensation of a dicarboxylic acid and a diol, functional group A would be the carboxylic acid and functional group B the hydroxy group.
In case of the up mentioned reaction the respective functional groups would be the diazo compound **B** and the thioketone **III** that react in a poly-Barton-Kellogg reaction of an AB-monomer:

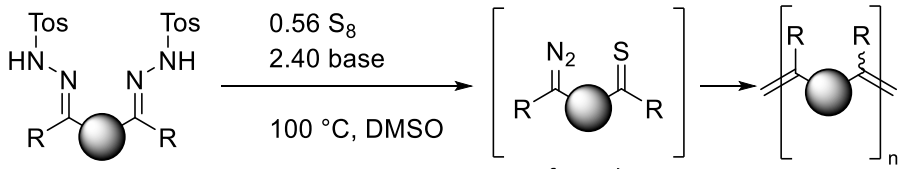

The Carothers equation describes an exponential growth for the DP and is maximal if the conversion p is quantitative and the ratio of functional groups r is one, meaning equimolar ratio of the functional groups are applied. This means for the up-mentioned reaction that the Barton-Kellogg reaction has to be very fast compared to the conversion of the diazo compound to the thioketone since pseudo equimolarity of the functional group would be obtained.

[46] For instance, the diazo compound from tosylhydrazone **82** is reported to exhibit a specific vibrational band at around 2028 cm^{-1} that can be probably related to the diazomethane group.[642]

[47] In case of an adamantyl motif, the thioketone intermediate could be kinetically stabilized by sterical hindrance while enolization is impeded as well due to the intrinsic stereoelectronic of the bridgehead atoms described by Bredt´s rule:[645] The conformation of a bridged multi-cyclic aliphatic system like an adamantyl scaffold depicts low overlap of its bridge headed sp^{3}-orbital of the C-H bond with an adjacent p-orbital. This p-orbital can for instance be present due to a carbonyl function and thus, enolization is impeded. This effect

contribution to the ongoing investigations on the topic of activation of sulfur by a base, increasing the potential application of polysulfane intermediates, while delivering important mechanistic insights. More generally, a new and efficient protocol for the synthesis of tetrasubstituted olefins describes an important contribution to general organic synthesis.

decreases with increasing ring size as the ring strain decreases as well and enolization is possible again for bigger rings.[646]

4.6 Polythisemicarbazones

The scope of the AM-3CR was extended in this work by using hydrazine monohydrate as the amine component yielding thiosemicarbazides as shown in chapter 4.2. on compound **19**. These thiosemicarbazides form imine groups with carbonyl groups such as aldehyde groups leading to thiosemicarbazones. Since the literature about poly(thiosemicarbazone)s was scarce, a possible step-growth polymerization approach between dialdehydes and dithiosemicarbazides, which has not been applied yet, was envisioned to access novel sulfur-containing polymers.

This chapter and the associated parts in the experimental part have been published before:

"Polythiosemicarbazones by condensation of dithiosemicarbazides and dialdehydes"-

R. Nickisch, P. Conen, M. A. R. Meier, *RSC Macromolecules.* 2022, **55**, 3267-3275.

(The author planned and evaluated the experiments, wrote the publication, established all synthesis protocols synthesizing all polymers and aldehydes. P. Conen contributed to this work as a research assistant by synthesizing the respective dithiosemicarbazides and performing the SEC-screening to optimize the polymer synthesis under the supervision of the author.

Abstract

An easy access to thermoplastic polythiosemicarbazones (polyTSCs) is presented by condensation of dithiosemicarbazides and aromatic dialdehydes, yielding eight polyTSCs and five co-polyTSCs, exhibiting Mns up to 38 kDa in good yields (58−93%). The polymerization proceeds at room temperature and is typically finished after 2−3 h. The monomer scope was investigated, revealing broad moiety tolerance (aliphatic, cyclic, benzylic, and aromatic groups). Full characterization was performed by proton and carbon NMR spectroscopy, IR spectroscopy, and size exclusion chromatography, confirming the anticipated chemical structure of polyTSCs. Thermal analysis of the polymers showed degradation starting at ∼200 °C by decomposition of the TSC function. Glass transitions were only observed for polymers derived from rigid monomers (162−198 °C). Further versatility of the reaction was underlined by the synthesis of five copolymers using different dithiosemicarbazide monomers.

Results and Discussion

Monomer synthesis

While dialdehydes are commercially available, dithiosemicarbazides are not.[588] Commonly, procedures rely on the use of isothiocyanates or thiocarbamoyl derivatives and hydrazine monohydrate, all of which are noxious themselves or require highly toxic reagents like thiophosgene and carbon disulfide.[404,530,589–591] To avoid such reagents as far as possible, we used a multicomponent reaction introduced by Al-Mourabit *et al*. using isocyanide, amine, and elemental sulfur, which forms the isothiocyanate in situ ultimately forming a thiourea.[10] We have recently shown that hydrazine monohydrate can be used as an amine component in this multicomponent approach to obtain the thiosemicarbazide function (see chapter 4.2 compound **19**).[592] We could not avoid using hydrazine, but we were able to obtain reasonable to good yields using this procedure for the monomers **86-90** (55−87%).[9] It is noteworthy that the applied approach for the isocyanide synthesis is an easy two-step synthesis protocol, which can be performed in a sustainable manner for

aliphatic derivatives, leaving hydrazine as the only major toxic burden.[258] Thus, the monomers can be obtained quickly in three steps with good overall yields (see Scheme 6.8.6.). The monomers bear a nucleophilic NH_2 group, which can react readily with suitable electrophiles, herein aromatic dialdehyde monomers.[593] To evaluate the influence of different monomer structures on this polycondensation reaction, five dithiosemicarbazides **86-90** were synthesized bearing short and long aliphatic chains, an aliphatic cycle, and benzylic as well as phenylic moieties (see Scheme 47).

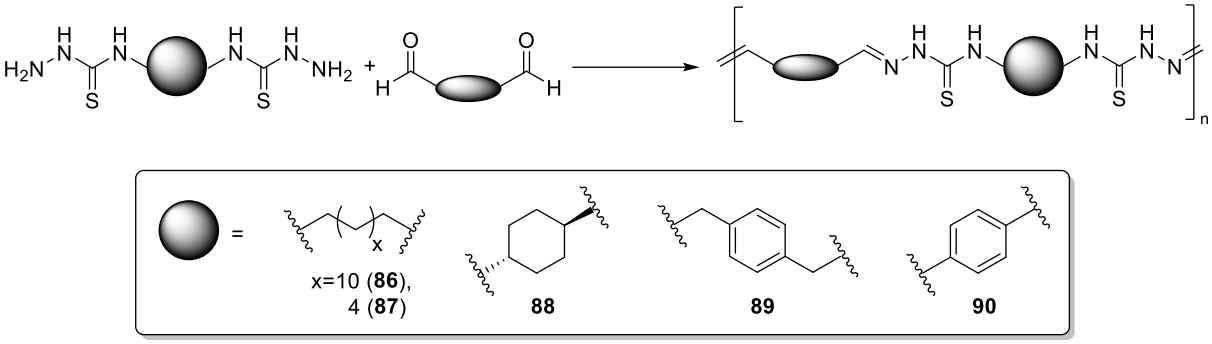

*Scheme 47: Overview of the herein investigated step-growth approach between dithiosemicarbazides and dialdehydes. Moieties that can be introduced by the herein introduced approach using dithiosemicarbazide monomers **86-90** are indicated by the black sphere and aldehyde moieties by the gray ellipsoid.*

The aliphatic monomers **86-89** were bench-stable, but benzene thiosemicarbazide **90** underwent rapid decomposition in solution, probably due to the phenyl group activating the electrophilic center of the thiosemicarbazide group, leading to an attack of the free NH_2 group (see chapter 6.8.7.). Consequently, no polymers could be obtained by using monomer **90**.

Optimization of Polymerization Conditions

As a test substrate for polymerizations, monomer **86** was reacted with terephthaldehyde **91** applying typical reaction conditions for the synthesis of low molecular weight TSCs (ethanol at 100 °C). A polymer was obtained after 2 h, as confirmed by SEC, with an Mn of 12 kDa and a dispersity of 1.73. Subsequently, we optimized the reaction conditions to obtain higher molecular weights. The most important observations are summarized in Table 26 (for the full screening results, see chapter 6.8.8.). Because ethanol was not able to sufficiently dissolve the polymers at an increasing molecular weight, other more polar aprotic solvents were tested since they were expected to show better solubility. DMF, DMAc (with addition of 0.3 wt % LiBr), and DMSO led to somewhat higher molecular weights up to 17 kDa, while maintaining a solution at high concentration (see Table 26, entries 2−5). Ultimately, DMSO was chosen as the ideal solvent, exhibiting the best solubility, allowing an increase in concentration up to 1.5 M. However, no higher molecular weights were obtained with the increased concentration. Performing the same reaction in bulk resulted in very low molecular weight with high dispersity, underlining the necessity of a suitable solvent for this type of polymerization (see Table 26, entry 6). In addition, higher temperature (120 °C) impeded the polycondensation, probably due to oxidation of the aldehyde group and thereby changing the 1:1 ratio of functional groups required to obtain high molecular weight. Thus, we decreased the temperature to room temperature. The monomers reacted rapidly to polymers at r.t., reaching an M_n of 18.9 kDa after 2 h (see Table 26, entry 7). The polymer was precipitated into water and dried at 100 °C and 500 mbar, yielding polymer **P1** with an M_n of 25.9 kDa and a dispersity of 1.73 (see Table 26, entry 8). The increase in molecular weight of the final polymer likely arose from an ongoing condensation reaction during drying at elevated temperatures. Besides SEC measurements, proton and carbon NMR

spectroscopy as well as IR spectroscopy were performed to confirm the chemical structure of the polyTSC **P1**.

*Table 26: screening of the polycondensation of monomer **86** and terephthalaldehyde **91**.*

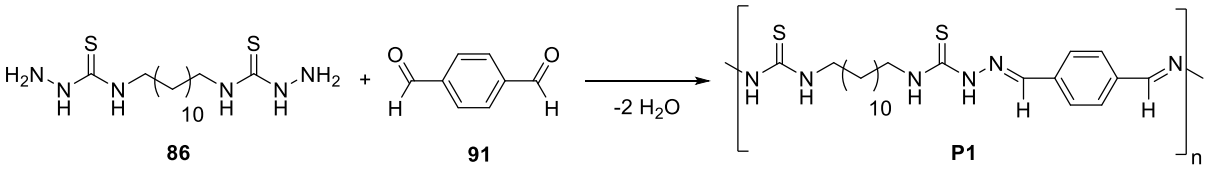

entry	solvent	*c*/M[a)]	*T*/°C	M_n/kDa[b)]	M_w/kDa[b)]	*Đ*[b)]
1	EtOH	0.083	100	12.4	21.3	1.73
2	DMF	1.0	90	15.0	32.4	2.16
3	DMAy	1.0	90	15.5	31.1	2.01
4	DMAy + 0.3w% LiBr	1.0	90	17.1	32.7	1.91
5	DMSO	1.0	90	16.5	34.4	2.08
6	-	-	90	2.20	6.00	2.73
7	DMSO	1.5	r.t.	18.9	29.6	1.56
8[c)]	DMSO	1.5	r.t.	25.9	45.0	1.73

a) Concentration of monomers **86** and , respectively. b) Determined by SEC using DMAc + 0.3 wt % LiBr as eluent after 2 h of reaction time. C) After work-up.

Figure 15 depicts the proton and carbon NMR spectra as well as the SEC curve of polymer **P1**. Furthermore, a comparison of the proton NMR spectra of the monomers is provided, showing that the aldehyde signal at 10.13 ppm and the NH_2 signal of the thiosemicarbazide group at 4.43 ppm were no longer observed for the polymer, indicating high conversion. Simultaneously, the characteristic NH signals of the thiosemicarbazone function at 11.49 and 8.54 ppm, and the imine proton at 8.05 ppm, appear in the polymer spectrum. In the carbon NMR spectrum, the imine carbon at 141.09 ppm and the thiosemicarbazone carbon (C=S) at 176.82 ppm were observed. Finally, the IR spectrum of **P1** shows the typical ν(C=N) vibration at 1530 cm^{-1} and bonds, which can be related to the participation of the C=S vibration at 1485, 1226, 1096, and 831 cm^{-1}.[594–596]

Monomer Variation

With the optimized reaction conditions in hand, we investigated the possible scope of monomer structures. Monomer **87** with C6 spacer reacted with **91** to polyTSC **P2** with M_n of 13 kDa after 2 h, allowing full characterization (for further information *vide infra*). However, because monomers **88** and **89** bear more rigid moieties, showing lower solubility in DMSO, the respective polycondensation reactions with **91** were considerably impeded. In the case of monomer **89**, only oligomers with M_n of 1.6 kDa could be obtained, even after an elongated reaction time of 6 h, while monomer **88** led to insoluble oligomers already after 2 h at lower concentration (SEC measurements after 1 h showed dimer formation). As oligomer formation was detected in both cases, we were able to react them further to polymers by applying 100 °C and 500 mbar for 17 h (in both cases oligomers were soluble in DMSO at 100 °C at first). Preformation of oligomers was crucial, since terephthaldehyde **91** sublimated under these conditions. However, the obtained sterically demanding polyTSCs **P3** and **P4** were not soluble, neither in DMAc + 0.3 wt % LiBr nor in DMSO, preventing SEC and NMR analysis. Thus, IR spectroscopy was first used for direct characterization of the chemical structure. In

Figure 16, a comparison of the IR spectra of polyTSC **P4**, monomer **89**, and **91** is shown exemplarily (for polyTSC **P3**, see chapter 6.8.9.).

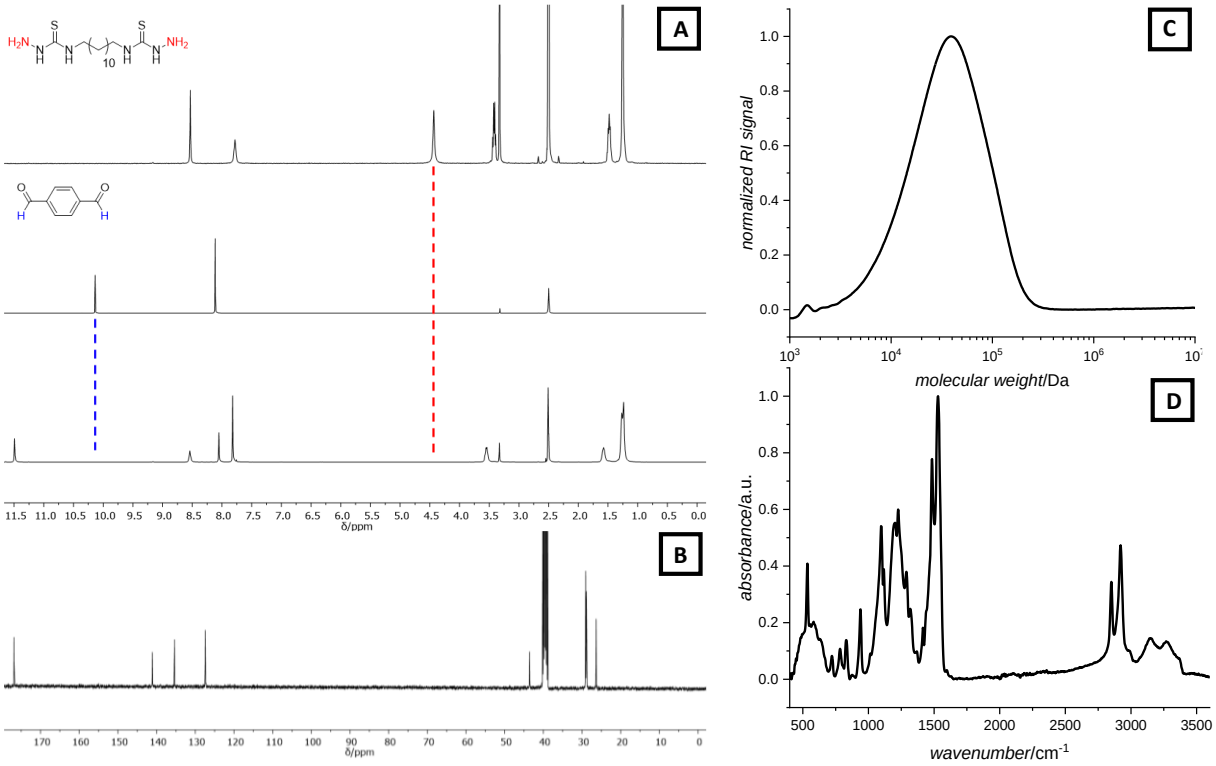

*Figure 15: (A) Comparison of proton NMR spectra of monomer **86** (top), terephthaldehyde **91** (middle), and polyTSC **P1** (bottom) in DMSO-d6. The protons of the aldehyde and thiosemicarbazide groups have vanished (blue and red dashed line). (B) Carbon NMR spectrum of polyTSC **P1** in DMSO-d_6. (C) SEC curve of polyTSC **P1** in DMAc + 0.3 wt% LiBr after purification. (D) IR spectrum of polyTSC **P1**. Adapted with permission from ref.*[597] *Copyright (2022) American Chemical Society.*

The formation of polyTSC **P4** is obvious, as the aldehyde function, exhibiting a strong ν(C=O) stretching vibration at 1685 cm^{-1}, has nearly vanished in the spectrum of polyTSC **P4**. The same is observed for the δ(NH_2) vibration of medium intensity of the thiosemicarbazide at 1615 cm^{-1}, proving that a considerable degree of polymerization was achieved (the end-group vibrations were of similar intensities than those of other polyTSCs; see chapter 6.8.10.). Furthermore, the typical bands of the polyTSC at 1520, 1273, 1100, and 827 cm^{-1}, as discussed before, were observed. However, as we aimed to establish a synthesis protocol of novel polyTSC accompanied by full analysis, the chemical structure needed to be confirmed besides IR spectroscopy. Thus, we performed two additional tests: (i) polycondensation of polyTSC **P3** and **P4** applying an excess of aldehyde **91** to obtain lower molecular weight and thus, higher solubility in the applied solvents allowing SEC and NMR analysis; (ii) copolymerization of monomers **88** and **89** each with well soluble monomer **86**, allowing full analysis of the respective high molecular weight copolymers containing a considerable amount of the rigid monomers. By applying an excess of 1.50 equivalents of the dialdehyde **91**, we obtained a soluble oligomer **O1** for monomer **89** (see chapter 6.8.11. NMR and SEC data), demonstrating the formation of polymer **P4**, while monomer **88** yielded insoluble oligomer **O2**.

Copolymerization of Rigid Monomers

To further verify the formation of polyTSCs **P4** and especially **P3**, as well as to evaluate the scope of our established synthesis protocol, an AA-A'A'-BB-type *co*-polycondensation, using well-soluble monomer **86** and aldehyde **91**, was investigated. Therefore, different ratios of monomer **88** or **89** to

monomer **86**, *i.e.* 70/30, 50/50, and 30/70, were used, while the amount of dialdehyde **91** corresponded to the overall amount of thiosemicarbazides applied, adjusting equimolarity of both functional groups.

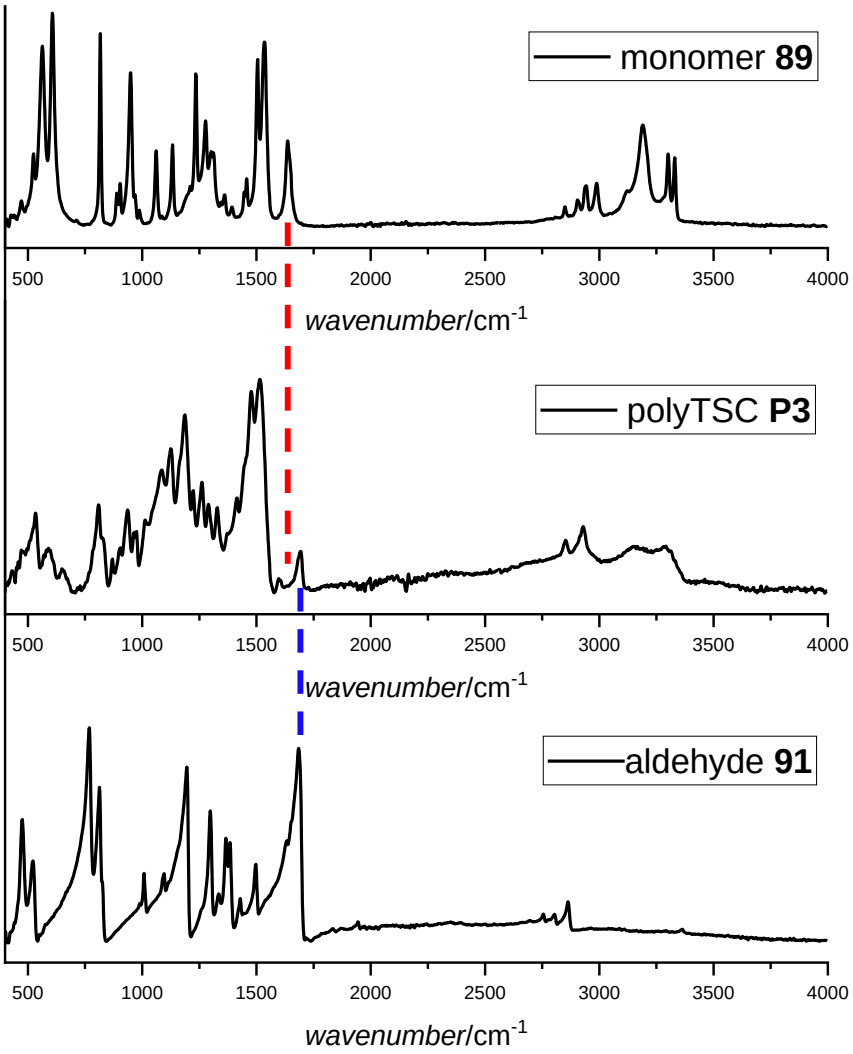

*Figure 16: Comparison of ATR-IR absorbance spectra of monomers **89**, **91**, and polyTSC **P4**. The red dashed line corresponds to the δ(NH_2) vibration of the thiosemicarbazide function and the blue dashed line to the ν(C=O) vibration of the aldehyde function. Adapted with permission from ref.[597] Copyright (2022) American Chemical Society.*

Table 27 shows an overview of the obtained molecular weights and dispersities determined by SEC analyses as well as the yields of all copolymers. The polymers **P5-P7** and **P8-P11** were in general obtained in moderate to good yields (58–84%). A clear trend was observed comparing the synthesized copolymers: the higher the amount of more soluble monomer **86**, the higher the molecular weight. All three copolymer **P5-P7** formed by using monomer **89** could be completely characterized, as they could be all dissolved yielding molecular weights up to 12.1 kDa. Considering the four copolymers of monomer **88**, **P8-P11** showed high dispersities because of a bimodal distribution, indicating an inhomogeneous polymerization (see Figure 6.8.12.). Nevertheless, by decreasing the amount of incorporated monomer **88**, we obtained a high molecular weight of 30.9 kDa for **P11**. One of the main aims of these copolycondensations was to provide further proof that bulkier thiosemicarbazides can form polyTSCs as well. Visual inspection showed that monomers **88** and **89** reacted in an early stage of the *co*-polymerization, resulting in a homogeneous reaction

mixture, while only a turbid solution or suspension was observed of the monomers in plain DMSO or during homopolymerization, respectively.

*Table 27: Co-polymerization of rigid monomers **88** and **89** with monomer **86** and terephthaldehyde **91** in different ratios of the dithiosemicarbazides*

***co*-polyTSC**	**Monomer feed ratio[a)]**	**Monomer composition[b)]**	M_n/kDa[c)]	$Đ^{c)}$	M_n/kDa[e)]	$Đ^{e)}$	**Yield/%[e)]**
P5	**89** to **86** 70/30	52:58	5.4	1.61	6.2	1.95	74
P6	**89** to **86** 50/50	56:44	10.1	1.43	10.0	1.88	59
P7	**89** to **86** 30/70	30:70	13.2	1.45	12.1	1.76	62
P8[d)]	**88** to **86** 70/30	-	8.6	13.3	-	-	-
P9[d)]	**88** to **86** 50/50	-	13.2	7.53	-	-	-
P10[d)]	**88** to **86** 30/70	29:71	20.4	6.64	22.4	5.53	58
P11	**88** to **86** 10/90	9:91	22.0	1.40	30.9	1.43	84

a) The amount of **91** was equal to the total amount of both thiosemicarbazides. DMSO, r.t., 3 h. b) Determined by ^{1}H NMR, as far as possible; see chapter 6.8.5. c) SEC sample taken out of reaction mixture. d) The polymer was not completely soluble in the eluent (DMAc + 0.3 wt % LiBr); however, an SEC sample was prepared of the soluble part. e) Value corresponds to the purified polymer.

Furthermore, proton as well as carbon NMR spectroscopy and IR spectroscopy were performed. Figure 17 depicts the comparison of co-polyTSC **P7** and polyTSC **P1** exemplarily, evidencing the successful incorporation of monomer **89** into the polymer backbone. The signals of polymer **P1** are clearly present in the NMR spectrum of **P7**. In addition, the respective signals arising from monomer **89** are visible (*e.g.* at 7.31 and 4.82 ppm). Furthermore, the ratio of incorporated monomer **88** or **89** to **86** could be determined by proton NMR, comparing two significant signals of each dithiosemicarbazide moiety. The observed ratios fitted well to the theoretical ratios used in the respective reactions (for **P10** with the 30/70 monomer ratio, NMR revealed a ratio of 29/71; see chapter 6.8.9. for respective copolymers). In the case of **P5**, a ratio of 52:48 was obtained which was addressed to the high amount of bulky monomer **89** probably leading to a deviation of the measured ratio due to restricted diffusion as well as solubility issues. These results underline the broad scope of this polycondensation reaction as it can be used for copolycondensation reactions adjusting a certain ratio of at least two different thiosemicarbazides precisely. Importantly, the copolymer characterization confirmed the results of the IR spectra, and the excess test of oligoTSC **O1** and **O2**, clearly verifying the tolerance of this reaction toward various moieties, *i.e.* aliphatic chains and cycles as well as benzylic moieties, introduced by dithiosemicarbazide monomers.

Scope of Dialdehydes

After having evaluated the scope of the dithiosemicarbazide monomers, we investigated the scope of dialdehyde monomers. Aldehyde functional groups tend to oxidize under air or undergo aldol addition and condensation reactions, if enolizable; nevertheless, there are several bench-stable aromatic dialdehydes accessible.[588] Such side reactions were indeed observed for aliphatic aldehydes, which were thus not further considered as suitable monomers. Thus, commercially available biphenyl-4,4'-dicarboxaldehyde **92** and 4,4'-(ethyne-1,2-diyl)dibenzaldehyde **93** were investigated. Because we wanted to obtain full characterization of the polyTSCs formed to clearly evaluate the scope of dialdehydes and to underline the potential of this reaction, we chose to react the aldehydes with monomers **86** and **87**, which yielded soluble polyTSC with aldehyde **91**. An overview of all obtained soluble polyTSCs **P1**, **P2** and **P12-15** is given in Table 28. While **P1** and **P2**

were formed rapidly at room temperature after 2 h, **P12-15** had to be further reacted at 100 °C and 500 mbar for 17 h before reaching higher molecular weights.

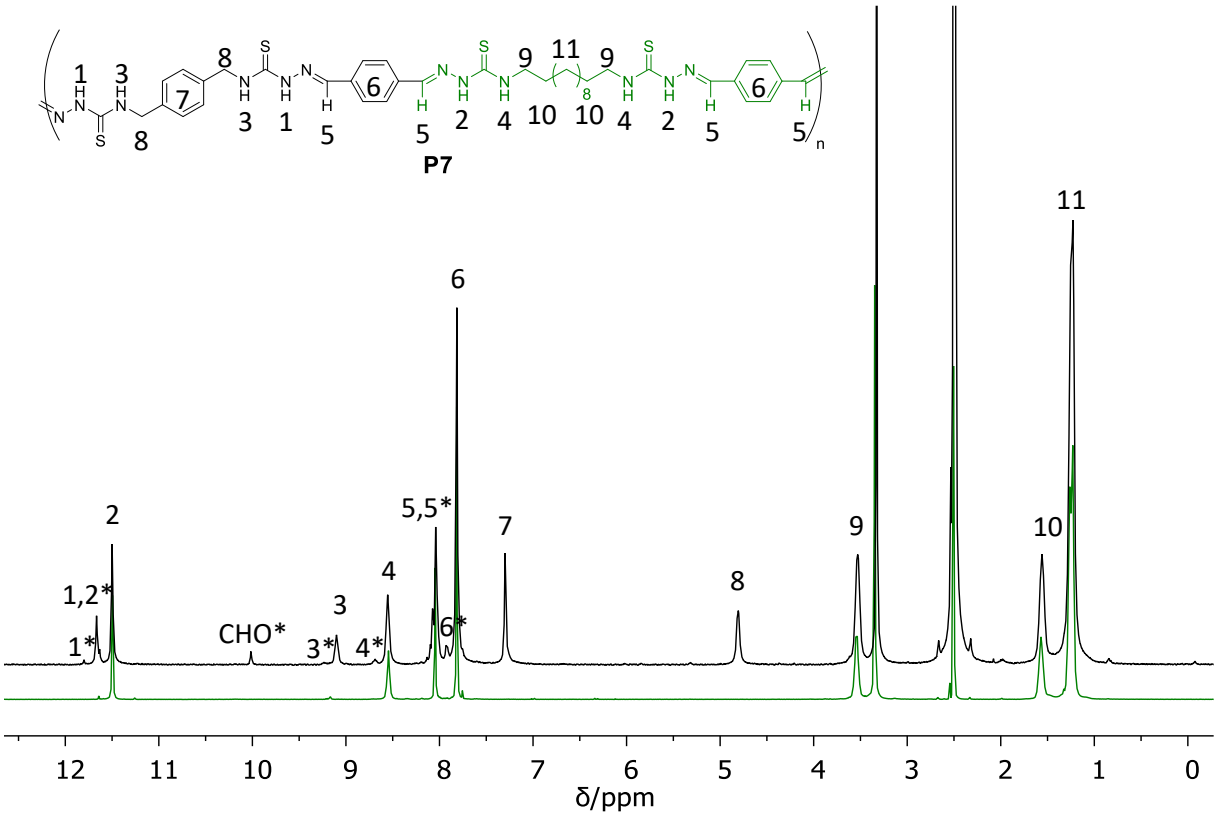

*Figure 17: Comparisons of proton NMR spectra of **P7** (black) and **P1** (green) in DMSO-d_6 (signal at 3.33 ppm is water). The signals arising from the **P1** domain (green colored in the structural formula) in the copolymer correspond to the respective signals of polyTSC **P1**. Signals arising from end-groups are marked with an asterisk (∗).Adapted with permission from ref.*[597] *Copyright (2022) American Chemical Society.*

Furthermore, the polymers had precipitated after completion of the reaction, and thus, an additional amount of DMSO was applied to redissolve them before following the before-mentioned work-up. Generally, all studied aldehydes polymerized well, thus significantly increasing the possible monomer scope. Interestingly, aldehyde **93** yielded the polymers with the highest M_ns. In general, good yields ranging from 74 to 93% were obtained by this polycondensation (quantitative yields were obtained for **P3** and **P4**). The loss in yield for some polymers could be related to (i) partial solubility of oligomers (especially when low molecular weights were obtained, *i.e.* **P6** and **P7**) and (ii) loss after filtration. The second issue was negligible applying larger reaction scale (1 g batch reactions were applied for polymers **P1** and **P12**, resulting in a yield of 98 and 92%, respectively; see chapter 6.8.5.). In the case of **P12-15**, proton NMR spectroscopy revealed that the polymers still contained a residual amount of DMSO; the largest amount, however, in **P15**, was below 4 wt %. Although several purification methods have been evaluated, washing the polymers with water under reflux is according to our experiments the most efficient purification method (see chapter 6.8.13. for full investigation of purification possibilities and overview of purities).

*Table 28: Overview of the molecular weight, dispersity, and yield of polyTSCs **P1**, **P2**, and **P12-15** obtained by using different dialdehydes. Adapted with permission from ref.*[597] *Copyright (2022) American Chemical Society.*

monomer AA \ monomer BB	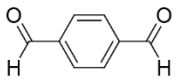 **91**	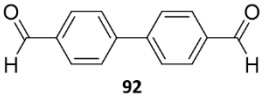 **92**	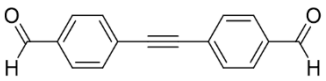 **93**
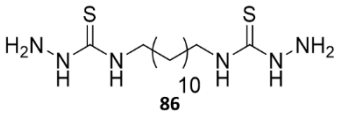 **86**	**P1** M_n=25.9 kDa M_w=45.0 kDa $Đ$=1.73 84%	**P12** M_n=17.0 kDa M_w=30.8kDa $Đ$=1.81 87%	**P14** M_n=38.1 kDa M_w=91.9 kDa $Đ$=2.41 93%
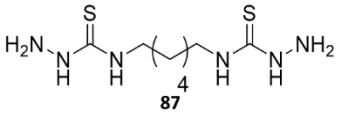 **87**	**P2** M_n=13.2 kDa M_w=24.1 kDa $Đ$=1.83 90%	**P13** M_n=16.8 kDa M_w=28.0 kDa $Đ$=1.67 90%	**P15** M_n=33.7 kDa M_w=76.7 kDa $Đ$=2.27 74%

Thermal Properties and pH Resistance of PolyTSCs

TGA experiments under nitrogen flow were conducted (see Table 29 and Supporting Information TGA curves of the respective polymer), revealing a clear trend: all polymers show a first decomposition step starting between 203 and 245 °C, resulting in a weight loss of ca. 5−26%. For polymers **P12-14**, a second decomposition step arises at slightly higher temperatures at 234−290 °C accompanied by a similar weight loss. Final decomposition started at 340−403 °C for all (*co*-)polymers except for **P3** (major decomposition step starts at 290 °C). In general, a considerable amount of mass was conserved after the measurements (up to 37 wt % at 600 °C for **P14**; for an overview of all decomposition steps see chapter 6.8.14.). Upon comparison of these results, the TSC functional group was likely to decompose first, since similar decomposition takes place in all polymers. To test this hypothesis, the decomposition of 4-methoxybenzaldehyde cyclohexyl TSC was investigated in a GC-MS measurement applying decomposition conditions (oven temperature 90−300 °C), resulting in the detection of only cyclohexyl isothiocyanate and 4-methoxybenzonitrile. This indicated an extrusion of one molecule of ammonia per TSC function. Indeed, ammonia extrusion was also detected for both decomposition steps by TGA-IR analysis of **P1** and **P13**, which were measured exemplarily (see chapter 6.8.15.). Contrarily, the corresponding diisothiocyanates and dinitriles, albeit being gaseous at the respective temperature, were not observed. The decomposition to the diisothiocyanate and dinitrile would result in quantitative weight loss, which does not match to the further degradation steps in TGA investigations.

Having the decomposition temperatures of all polymers in hand, we performed DSC analysis (see Table 29 and chapter 6.8.5. for DSC curves of respective polymer). Most of the polymers exhibited no phase transitions, underlining the strong supramolecular interactions present between the polymer chains, *e.g.* hydrogen bonding by the TSC groups. PolyTSC **P12** showed the lowest T_g at 166 °C, probably because of the more sterically demanding biphenyl group, impeding these intermolecular interactions. The use of a shorter spacer in **P13** seemed to increase the T_g to an extent that the decomposition temperature is reached first. Furthermore, **P2** exhibited a T_g at 198 °C whereas **P1**, bearing the longer spacer moiety, showed no T_g at all. For both series of copolymers, the same trend could be extracted: by decreasing the amount of the bulky monomers **88** and **89**, T_gs were observed (**P7** and **P11** showed T_gs at 166 and 162 °C, respectively; note that **P5**, albeit containing the largest

amount of bulky monomer **89**, has a lower experimentally determined content than **P6**; see also above).

Table 29: Overview of thermal properties of all synthesized polymers, i.e., T_gs Obtained by DSC and decomposition temperatures as well as residual weight by TGA analysis.

polymer	T_g/°C	1st decomp./°C	2nd decomp./°C	3rd decomp./°C	residual weight/w%
P1	-	228	403	-	15
P2	198	228	382	-	21
P3	-	224	290	-	24
P4	-	245	340	-	36
P5	182	237	360	-	34
P6	-	236	378	-	21
P7	166	238	391	-	15
P10	-	237	401	-	20
P11	162	234	399	-	13
P12	166	219	285	382	24
P13	-	226	290	369	30
P14	-	203	234	396	37
P15	-	224	380	-	33

The related homopolymers **P1**, **P3**, and **P4** did not show thermal transitions. Concluding, polyTSCs start decomposing at around 200 °C, bearing no T_g in general as the decomposition temperature is reached first. However, by implementing more rigid groups, polyTSCs with a high T_g can be obtained and tailored. The stability of polyTSCs was determined qualitatively by applying aqueous acidic and basic conditions for polymer **P1** (pH = 0 and 14, respectively), as hydrolysis might be expected, especially under acidic conditions. Interestingly, proton NMR analysis showed no degradation after 24 h, even when elevated temperature (50 °C) and sonification were applied (see chapter 6.8.16.).

Conclusion

Using dithiosemicarbazides and aromatic dialdehydes, polythiosemicarbazones (polyTSCs) could be obtained *via* polycondensation, reaching high molecular weights (M_n up to 38 kDa). The synthesis can be performed at room temperature, while more sterically demanding monomers require elevated temperatures and reduced pressure. A broad scope of moieties (aliphatic, cyclic, and benzylic) of the dithiosemicarbazide monomer is tolerated. The formation of eight polyTSCs was proven by full characterization (proton and carbon NMR spectroscopy, IR spectroscopy, and SEC) of the chemical structure. In the cases of two insoluble polyTSCs, additional experiments were performed to confirm the obtained IR data. Moreover, five *co*-polyTSCs incorporating two different dithiosemicarbazide monomers were synthesized and fully characterized, which allowed precise adjustment of monomer ratios as long as the amount of bulky moieties remained below a certain limit. Furthermore, thermal analysis (TGA and DSC) of the polymers was conducted, revealing that decomposition starts at around 200 °C in a two- to three-step process under extrusion of ammonia. In general, no T_gs were observed unless more bulky moieties were employed. The obtained co-polyTSCs allowed the introduction of T_gs by using small amounts of sterically demanding cyclic or benzylic monomers (T_g = 162−182 °C). Finally, this synthesis approach offers easy access to the often-used thiosemicarbazone functionality in a polymer backbone which is envisioned to be useful to many subjects of ongoing research as well as paving the way for new applications.

4.7 Poly(TSC)s derived membranes

In this work, the application of the novel poly(TSC)s introduced in the previous chapter for membrane formation and further the application of removal of transition metals from a water stream was investigated. Thus, a brief overview of membranes and their formation by non-solvent induced phase separation (NIPS) is given to provide the most important information about this process. Moreover, footnotes provide complementing information about the used analysis techniques that are uncommon in chemistry.

Membranes are materials that are able to separate particulate matter, colloidal particles, macromolecules, multicomponent solutions and gas mixtures from a liquid or gaseous stream.[598,599] Depending on the pore size, different separation mechanisms are in operation for instance by size exclusion or Donnan exclusion (repulsion of ions by fixed electric charges on the membrane).[598,600,601] Gas separation on the other hand relies on the solubility and diffusion parameter of gases.[602] Advantages of the utilization of membranes for separation are for instance that i) no phase change is needed in the process, ii) high selectivity and productivity is obtained and iii) no regeneration of the sorbent is needed.[603] They are thus used in several chemical, biological and environmental fields like electrodialysis, hemodialysis and membrane reactors.[603,604]

Membranes can be categorized according to their pore sizes and their respective permeability (water flux per transmembrane pressure, see Table 29).[603,605,606] Microfiltration (MF) membranes typically have a pore size range of roughly 0.1-10 µm and are used for instance for concentration of protein solutions, cell harvesting and clarification of fruit juice, beer and wine at high permeability of over 50 $Lm^{-2}h^{-1}bar^{-1}$.[603,607] Ultrafiltration (UF) membranes can have pore sizes in the range of 0.5 µm-1nm and a permeability of 10-50 $Lm^{-2}h^{-1}bar^{-1}$.[603,605,606] They are used in *e.g.*, pharmaceutical, chemical and textile industry. Pore sizes smaller than 2 nm are referred to as nanofiltration (NF) or reverse osmosis membranes (RO) which can be used for desalination of water or removal of micropollutants at low permeabilities (1.4-12 and 0.05-1.4 $Lm^{-2}h^{-1}bar^{-1}$, respectively).

Table 30: Types of membrane filtration processes and their respective pore size, pressure and flux range.[603,605,606]

membranes	pore size	pressure/bar	permeability/$Lm^{-2}h^{-1}bar^{-1}$
MF	10-0.1 µm	0.1-2.0	>50
UF	0.5-0.001 µm	1.0-5.0	10-50
NF	<2 nm	5.0-20	1.4-12
RO	<1 nm	10-100	0.05-1.4

Membranes can be made from ceramics, glass, metals or polymers using several different techniques like stretching, sintering, track-etching, template-leaching or dip coating.[603,608] One of the most common used methods for the formation of asymmetric membranes bearing a thin top layer, which determines the separation properties and a porous sub-structure, is phase inversion.[603,609] Precipitation of the membrane material and thus formation of the membrane can be achieved in a dry or a wet state by alteration of several parameters like temperature, solvent concentration by evaporation, precipitation from the vapor phase, or immersion in a coagulation bath.[603,608] Among these methods, the most used one is the immersion precipitation process, which is also called non-solvent induced phase separation (NIPS) and was used in this work for the formation of flat sheet membranes.[603]

NIPS was first introduced by Loeb and Sourirajan in the 1960s and allowed the controlled formation of a membrane from a polymer solution or dispersion (see Figure 18).[603,610] Therefore, a solution, consisting of at least one polymer (in general 15 to 25wt%),[611] one good organic solvent and possibly

additional additives, is casted on a mechanical support like a glass plate using a casting knife.[603] Subsequently, the mechanical support containing the casted solution is put in a coagulation bath consisting of a non-solvent that is miscible with the applied solvent of the polymer solution and possibly additional additives.[603,612,613] As a result, the solvent of the polymer solution starts to diffuse into the coagulation bath, while the non-solvent of the coagulation bath diffuses in the polymer solution layer but to a smaller extent resulting in a shrinkage of the film thickness.[609] Thus, the concentration of the non-solvent in the polymer domain is increased, which ultimately leads to phase separation, *i.e.* precipitation of the polymer, forming the final membrane. The precipitation allows the arrest of the polymer chains from this non-equilibrium process, which determines the obtained morphology of the membrane. It starts always at the interfacial layer between polymer solution and coagulation bath and the precipitation front then moves towards the mechanical support until the polymer is completely precipitated.

The mechanism of the phase separation is spatiotemporal dependent and due to the moving of the precipitating front and the ongoing solvent-non-solvent exchange, the densities of the polymer layer are altered, leading to an asymmetric membrane with thin, denser top and porous sublayer. Thereby, the rate of the precipitation process strongly influences the final morphology of the membrane.[614] Fast precipitation generally results in a rapid formation of a finely porous, thin top layer at the interface of polymer solution and coagulation bath, while macrovoids are formed in the sub-layer, which often exhibit a finger-like morphology.[614] Thus, a porous sub-structure is obtained that leads to a membrane with a high water flux and low salt rejection.[614] Contrarily, a low precipitation rate leads to slow formation of a top layer at the interface between polymer solution and coagulation bath, resulting in a denser, sponge-like morphology of the membrane exhibiting a very dense top layer.[614] Low water fluxes and high salt rejections are thus common for such membranes.[614]

Several parameters can be altered in a NIPS process to obtain a membrane with a completely different morphology. For instance, the precipitation process of a polymer strongly depends on the ternary system applied (polymer, solvent and non-solvent) and thus, the use of a different solvent or non-solvent will result in different precipitation rate and in a different morphology.[603] Further, the concentration of the respective components of the ternary system as well as the applied temperature will alter the precipitation. Finally, additives like pore forming agents or surfactants can be added to the polymer solution, yielding membranes with different morphologies and pore sizes.

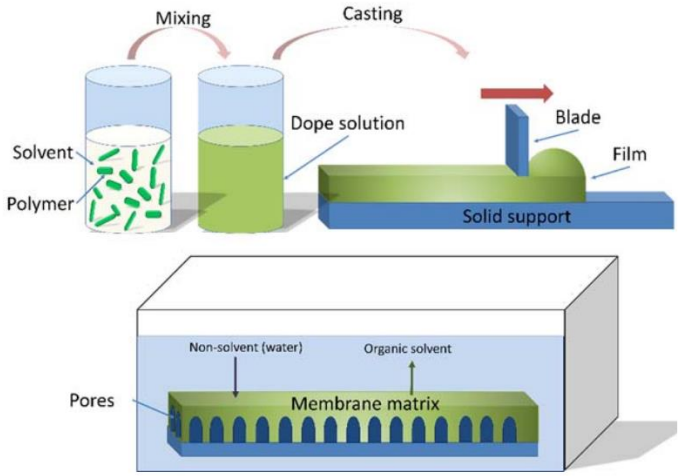

Figure 18: Schematic overview of the NIPS process on the example of forming a porous membrane adapted from ref.[615] *The polymer is first completely dissolved in a suitable solvent and then casted on a solid support using a casting knife. Then, the polymer film with support is immersed in a coagulation bath consisting of a non-solvent.*

Typical characterization of a membrane is obtained by determination of its water flux *J* (volume of water/solution *V* passed through the membrane per area *A* and time *t*) or permeability *P* (water flux *J* per transmembrane pressure *Δp*), measuring the amount of water passing through a membrane in a certain amount of time at a certain pressure (see equation 5).[603]

$$P = \frac{J}{\Delta p} = \frac{V}{A \times t \times \Delta p} \tag{5}$$

Furthermore, pictures of the top, bottom and cross-section of a membrane by scanning electron microscopy (SEM) provide valuable information of the morphology of the cross-section, thickness of the top layer, morphology of top layer and sub-structure and can reveal structural defects. In addition, atomic force and scanning force microscopy (AFM and SFM) yield similar information, also providing data on the friction force and surface roughness. Porosity and pore size distribution can be further determined by porosimetry, porometry or permporometry. Molecular weight cut off (MWCO) experiments analyzed by SEC-analysis also provide information about the pore size and which molecular weight is being fully retained.[616] Surface charge of the membrane can be determined by measuring the streaming potential.[617] Furthermore, analyses that are also used in chemistry like IR- and Raman-spectroscopy as well as secondary ion mass spectrometry (SIMS), transmission electron microscopy (TEM), energy dispersive X-ray spectroscopy (EDX), wavelength-dispersive X-ray spectroscopy (WDS), Auger electron spectroscopy (AES) and X-ray diffractometry (XRD) are applied to membranes to obtain important information, *e.g.* about the elemental composition, chemical structure and chemical state and structural order.[603]

Poly(TSC) membranes by NIPS

To obtain membranes from poly(TSC)s by NIPS, poly(TSC) **P1** was chosen since it offered the highest solubility in DMSO and NMP. Thus, polymer solutions (5 g) with different weight-percentages of **P1** (up to 20 wt% of polymer) were prepared in DMSO and NMP, and roughly half of the solution was used to cast a polymer film on a glass plate with a casting knife having a gap of 400 µm. Subsequently, the polymer film and the support were immersed in a coagulation bath consisting of Milli-Q® water (1 L), forming the final membrane. The obtained membranes were washed several times with water and their permeability was tested in a dead-end configuration using an Amicon cell set-up (for detailed information about the set-up see chapter 6.9.2.). A summary of the respective permeabilities of the obtained poly(TSC) **P1** membranes is depicted in Figure 19:

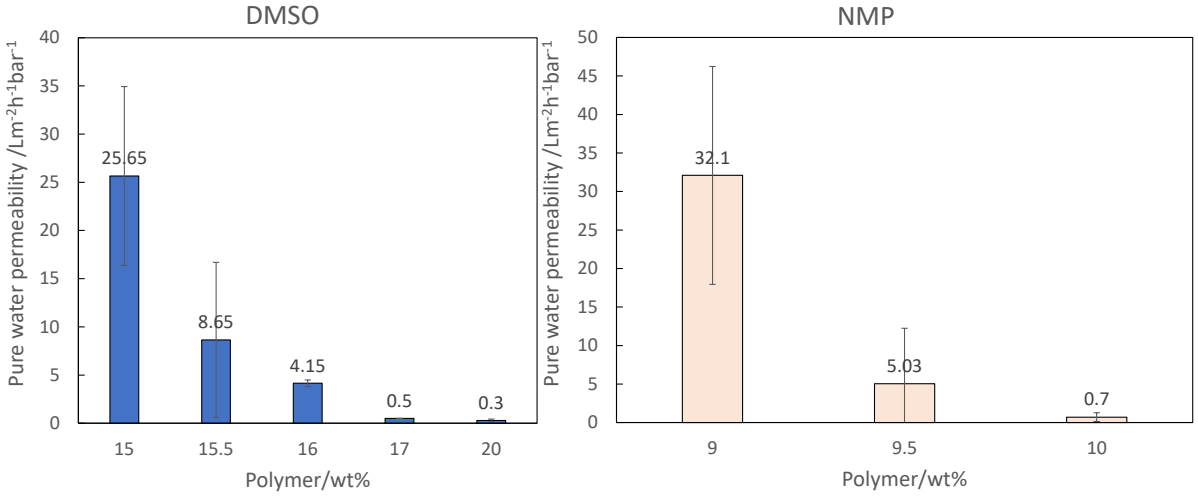

*Figure 19: Summary of membranes obtained by NIPS from polyTSC **P1** solutions in DMSO (left, blue bars) and NMP (skin color bars) at different weight percentages. In addition, their permeabilities and their respective error margins are depicted which were obtained by measuring at least two different samples.*

In general, a fast precipitation (usually <1-5 s) of the polymer was observed. Comparing the series of membranes prepared with DMSO and NMP, an expected trend is visible: with increasing weight-percentage of polymer content in the solution, denser membranes and thus, lower permeabilities were obtained. Using a 20wt% DMSO solution of polymer **P1** resulted in a low permeability of 0.3 $Lm^{-2}h^{-1}bar^{-1}$, while decreasing the polymer content to 15wt% yielded a permeability of roughly 29 $Lm^{-2}h^{-1}bar^{-1}$. Using NMP as solvent for polymer **P1** led to similar permeabilites (32-0.7 $Lm^{-2}h^{-1}bar^{-1}$) at lower polymer concentrations (9 to 10wt%) in comparison to DMSO. Membranes obtained from a polymer solution in NMP with a weight-percentage of the polymer higher than ten resulted in very dense membranes exhibiting no water permeability at all (15 and 20wt% polymer solutions were tested till 3 bar of applied pressure, see also below in Figure 20),[48] while lower weight-percentages (*e.g.* 7 and 5wt%) led to defective membranes. In addition, an uncommonly steep decrease of permeability was observed by increasing the polymer content by only one percent, namely from nine to ten weight percent. Considering the variability obtained from these measurements (see error bars), using NMP as a solvent led to considerable deviations. This was assumed to be a result of the very rapid precipitation in the NIPS process using NMP as solvent that was, compared to DMSO, even faster, which was assigned to a higher miscibility of NMP and water. Thus, only slight changes in the execution of the NIPS process, for instance different amount of time until the polymer film and support were immersed in the coagulation bath or tilting the support,[49] could have tremendous impact for the final membrane, leading to the observed high deviations in permeabilities. On the other hand, using DMSO as solvent led to reproducible results with the sole exception of the 15.5wt% solution. It has to be noted that TamiSolv® NxG (*N*-butyl pyrrolidone) was tested as solvent as well, but brittle membranes were obtained, which broke immediately.

SEM-analysis of the two series of membrane underlined the observations.[50] Figure 20 depicts the SEM images of the membranes obtained by using DMSO as a solvent exemplarily (for SEM-pictures of the membranes obtained by using NMP, see chapter 6.9.3.).

Dense top layers were obtained in all cases, while the layer was denser as the amount of applied polymer increased. The sub structure consisted of finger-like macrovoids, and with increasing amount of polymer used, the polymer domain increased in volume as well.

In the next step, MWCO experiments[51] were performed, as most of the membranes were in the range of UF to NF, which might allow the separation of proteins and micropollutants. Complete

[48] The permeability tests were run for at least 24 hours, resulting in no flux.

[49] The polymer casting solutions in either DMSO or NMP were found to phase separate also upon standing on air for a certain amount of time (several minutes), because the solvent exchange with water vapor from the air was already sufficient to induce precipitation. Since, only small amounts of non-solvent were enough to start precipitation, it seemed reasonable that a delay in the immersion of the casted polymer solution on a support and thus, longer solvent-non-solvent exchange with moist air could alter the final morphology of the membrane. Further, by tilting the support upon immersion, one part of the polymer film starts to phase separate earlier and thus, an additional precipitation front is formed, which moves not towards the support but towards the other side of the polymer film. Since the precipitation process is very fast, the impact of the induced, second precipitation front can be assumed to strongly influence the final morphology of the membrane.

[50] All SEM-pictures were taken by M. Irshad Baig, post-doctoral scientific researcher in the working group of Prof. de Vos at the University of Twente (Netherlands). The author evaluated the obtained data.

[51] MWCO is tested by pumping an aqueous solution of dissolved compounds with known molecular weight (*e.g.* PEGs or dextranes) through the respective membrane collecting the permeate and the retentate. SEC-analysis of the samples as well as the sample of the respective feed solution allows the evaluation of the MWCO by comparison of the SEC-traces. Usually, a constrained growth curve is obtained with a maximum of 100% rejection. The MWCO is thereby determined as the point where 90% of a sample compound is being rejected.

rejection of *Bovine Serum Albumin* (BSA, 66.5 kDa) was found for the membranes obtained using 15wt% **P1** and DMSO. The membrane made from a 16wt% solution of **P1** in DMSO was further tested for retention of smaller molecules with a mixture of PEGs (0.2-4 kDa, see chapter 6.9.5.), depicting an incomplete rejection of 80%.

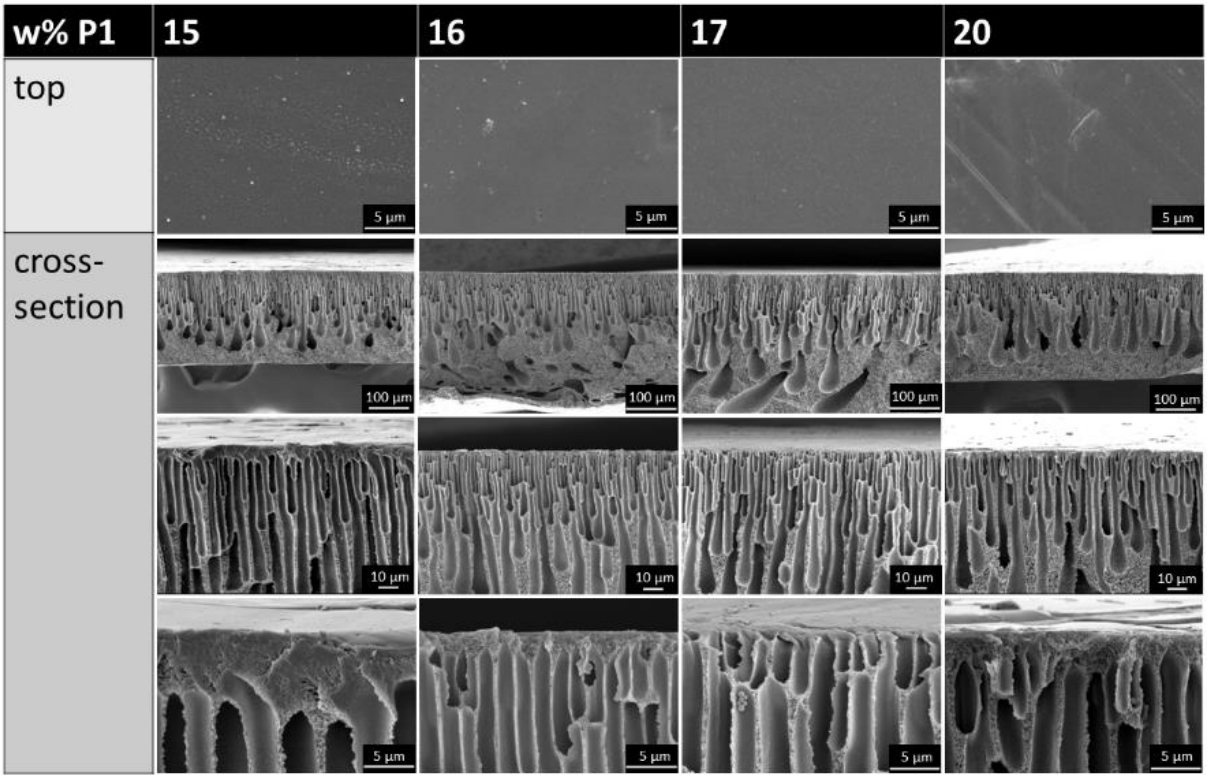

*Figure 20: SEM-images of the membranes obtained using different weight-percentages of poly(TSC) **P1** in DMSO as solvent. Top and cross sections as well as zoom-ins of the cross sections are depicted.*

In addition, the same membrane was applied for salt rejection tests[52] with NaCl, Na_2SO_4 and $MgCl_2$ since the permeability of roughly 4 $Lm^{-2}h^{-1}bar^{-1}$ was in the range of pore sizes which can separate salts by Donnan exclusion (such as NF membranes). However, no rejection was found and thus, streaming potential measurements were performed to obtain insights about the surface net charge density σ^d of the membrane.[53]

The membrane depicted a reasonable negative charge density (σ^d=-37.8 mV) that should allow the rejection of anions if the conditions for Donnan exclusion are given, *i.e.* pore sizes in the region of NF and no defects. This result was reasonable, since the poly(TSC) group exhibits an acidic proton attached to the hydrazide moiety of the TSC-group (chemical shift of the respective proton in a ^{1}H-NMR-spectrum in DMSO-d_6 was 11.50 ppm,[54] see also Scheme 48).

[52] Similar to the MWCO test, an aqueous solution containing the respective salt is pumped through the respective membrane and the permeate and retentate are collected. Comparing the conductivity of the samples and the feed solution yields the rejection of the respective salt since the conductivity shows linear dependency of the concentration of an ion.

[53] Streaming potential measurements was performed by the author together with M. Irshad Baig, post-doctoral scientific researcher in the working group of Prof. de Vos at the University of Twente (Netherlands). The author evaluated the obtained data.

[54] For comparison: an aryl carboxylic acid functionality like in benzoic acid exhibits a chemical shift of 12.96 ppm in DMSO-d_6.

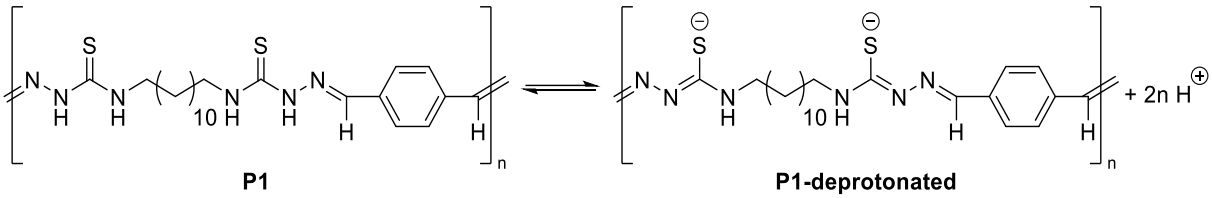

*Scheme 48: Schematic overview of the deprotonation equilibrium in poly(TSC) **P1**.*

Considering i) the incomplete rejection of the PEG solution, ii) the absence of salt rejection and iii) the negative charged surface, it was assumed that the membrane (16wt% polymer **P1** in DMSO) bore a certain degree of defects. Thus, smaller PEGs and salt ions cannot be retained, even though the negatively charged surface would facilitate the rejection in the latter case at small pore sizes. This was probably a result of the before-mentioned fast precipitation of the membrane in the NIPS process. Thereby, the polymer chains located in the top layer of the polymer film have nearly no time to relax and, when being arrested by precipitation, a conformation could be obtained exhibiting high mechanical stress that will ultimately lead to defects.[609] In addition, the sub-structure macro-voids are significantly close to the top layer and could easily act as stress concentration points near the surface. Such points where the beginning of a macro-void is very close to the top surface can lead to rupture and formation of a defect/pin-hole upon application in water pressure.

Water contact angle measurements showed a decent degree of hydrophilicity of the membranes (angles of 79.9 ° and 52.1 ° were obtained in NMP and DMSO, respectively, see also chapter 6.9.5.).[55]

To summarize, using DMSO and NMP as solvents and water as a non-solvent for a polymer solution of **P1**, membranes *via* NIPS were obtained depicting permeabilities in the range of UF to RO (32-0.3 $Lm^{-2}h^{-1}bar^{-1}$, compare Table 29). While NMP led to considerable deviation in the permeabilities, DMSO was a suitable solvent for the membrane formation. Full retention of BSA was obtained using a 15wt% solution of polymer **P1** in DMSO for membrane formation. Furthermore, streaming potential measurement revealed that a considerable negative surface charge is present due to the intrinsic acidity of the poly(TSC)s. Nevertheless, no complete rejection for small molecular weight compounds (*e.g.* micropollutants) or salts were obtained as most likely defects were present. By a thorough optimization of the NIPS process, slower precipitation could possibly be obtained, for instance by using a mixture of DMSO or NMP with water as non-solvent, instead of pure water. This might allow the formation of defect-free poly(TSC) membranes and could further lead to the application in the separation of micropollutants and salts.

Application of poly(TSC) membranes in the removal of transition metals

Compared to the separation of salts with membranes by Donnan exclusion in the NF-regime at low permeabilities (1.4-12 $Lm^{-2}h^{-1}bar^{-1}$, see Table 29), the removal of salts by complexation bears some advantages, since higher flux rates can be maintained as the separation process does not need small pore sizes relaying on a complexation sieving mechanism (for instance, permeabilities of 180 to 467 $Lm^{-2}h^{-1}bar^{-1}$ were reported with quantitative removal of metals).[618,619] However, on the other hand it is challenging to find a suitable polymer capable of sufficient complexation with metals, while delivering mechanically stability to allow application in a membrane process.[618] The TSC-group exhibits in general a strong affinity to several transition metal ions like Cu, Zn, Au, Hg and Ni *via* several different anionic and neutral binding modes.[594] These complexation reactions are reported to

[55] All water contact angle measurements were performed by M. Irshad Baig, post-doctoral scientific researcher in the working group of Prof. de Vos at the University of Twente (Netherlands). The author evaluated the obtained data.

already take place at room temperatures for several examples.[620–622] Furthermore, similar functional groups, like thioureas and thiosemicarbazides, are known to remove metal ions like Au or Hg with high sensitivities and selectivities from aqueous solutions.[169,618] Thus, it was envisioned to use the obtained poly(TSC) membranes for the removal of transition metal ions from an aqueous solution (see Figure 21).

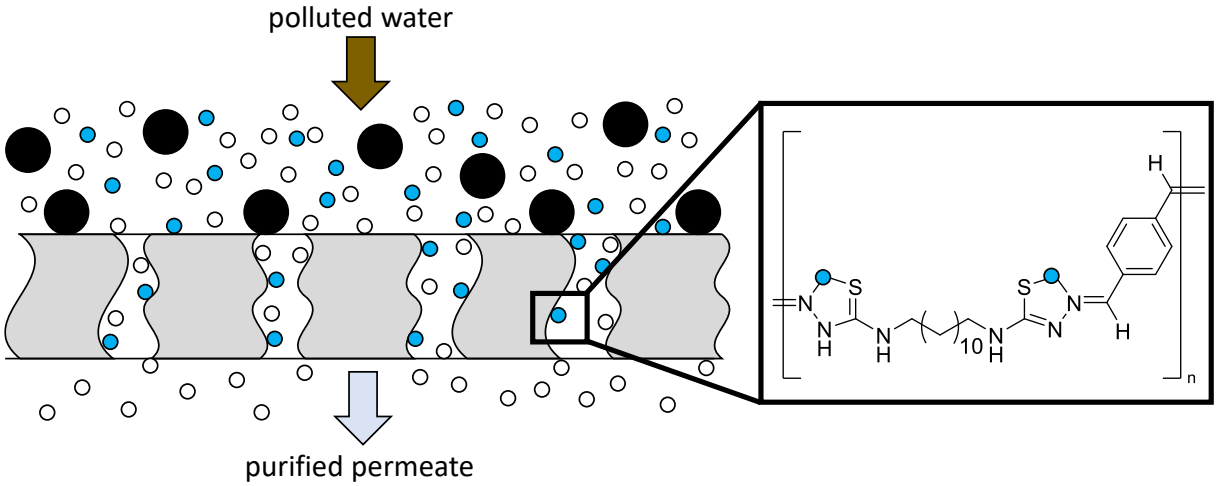

*Figure 21: Envisioned water purification using poly(TSC) **P1** membrane. Besides size separation (depicted by the bigger black spheres not able to pass through the membrane), complexation allows the removal of transition metals (blue spheres) as well, which would otherwise pass through due to their small size. Leaving only the pure water (white spheres) to pass through the membrane. In addition, the complexation of the metal ions by the TSC-groups is shown exemplarily by a neutral and anionic chelation on the righthand side.*

In a first batch removal experiment, 8 cm^2 of poly(TSC) **P1** membrane made from a 9.5wt% polymer solution in NMP was immersed in 5 mL of an aqueous solution of 1.25 mM salts.[56] Therefore, $ZnCl_2$, $CuCl_2$*$2H_2O$ and $AgNO_3$ were chosen as suitable test substrates and the membrane was put in the solution for five days under shaking. Subsequently, a sample was taken from the solution and ion concentration was determined by ion chromatography. The results are depicted in Table 30:

*Table 31: Removal rates of poly(TSC) membrane for $ZnCl_2$, $CuCl_2$*$2H_2O$ and $AgNO_3$ solutions measured by ion chromatography.*

salt	**cation-removal/%[a)]**	**anion-removal/%[a)]**	**removal rate µmol(cation)/cm^2**	**active TSC group/%[b)]**
$ZnCl_2$	5	0	0.04	0.3
$CuCl_2$*$2H_2O$	23	4	0.18	1.2
$AgNO_3$	45	34	0.45	2.3

a) 8 cm^2 of poly(TSC) **P1** membrane were immersed in 5 mL of an aqueous solution of the respective salt (*c*(salt)=1.25 mM) and were shaken for five days at room temperature. b) Value was determined by dividing the amount of removed metal cation by the amount of used TSC functional groups assuming successful complexation is obtained with one TSC group per metal ion.

[56] 8 cm^2 roughly equaled 25 mg of membrane material and thus depicted a considerable excess of functional groups which could potentially bind the metal ions:

$$n(TSC) = \frac{m(\boldsymbol{P1})}{M(\boldsymbol{P1})} \times 2 = \frac{25\ mg}{446.7\ \frac{mg}{mmol}} \times 2 = 112\ \mu mol$$

Where M(**P1**) is the mass of the monomer unit while the overall amount of salt was:

$$n(salt) = c \times V = 0.00125\ \frac{mmol}{mL} \times 5\ mL = 6.25\ \mu mol$$

Nearly no removal of zinc was obtained, while copper ions were removed to an extent of 23%. The highest removal rate was obtained by using $AgNO_3$ with 53%. Thus, 0.45 µmol of silver ions were removed per square centimeter of the membrane by complexation of 2.3% of the TSC moieties. Since not all TSC-groups present in the membrane are accessible for the metal ions, it can be expected that the percentage of the TSC-groups available for complexation is small. Furthermore, similar values were reported for membranes, which were applied for metal removal, while also higher values like 15% were reported.[57] Since the highest removal rate was obtained with $AgNO_3$, the kinetic of the batch adsorption experiment was monitored for membranes made from polymer casting solutions with different weight-percentages of polymer using DMSO or NMP as solvent (see Figure 22).

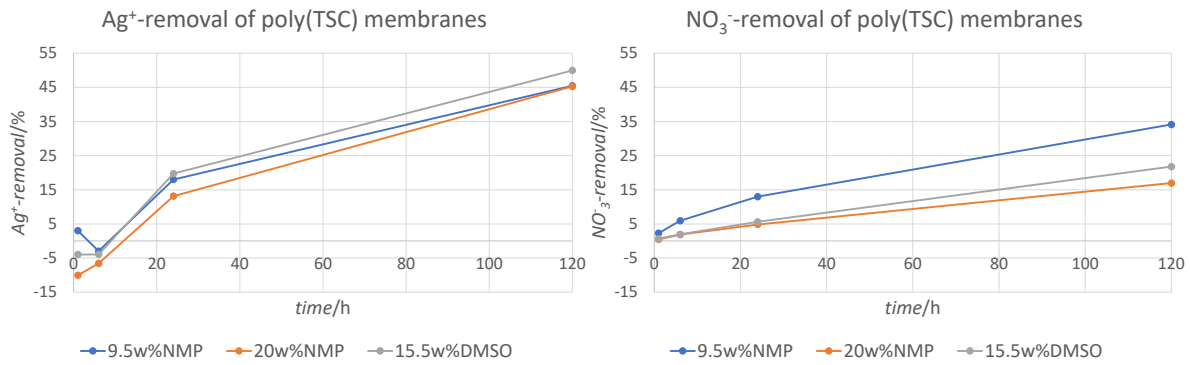

*Figure 22: Kinetic of the batch removal of $AgNO_3$ by poly(TSC) **P1** membranes made from different polymer casting solutions using DMSO or NMP as solvent. 20 cm^2 of the respective membrane was put in 20 mL of an aqueous salt solution ($c(AgNO_3)$=1.25 mM).*

Comparing the different membranes, the different morphologies seemed to have a minor impact on the overall removal rate for the silver ions. On the other hand, the removal of the NO_3-ions was more pronounced for the membrane obtained from a 9.5wt% polymer solution in NMP. The complexation rate of the silver ions was comparable over times, for instance after one day the membrane made from 9.5wt% polymer solution in NMP reached a removal rate for silver ions of 18%. Still, by comparing the removal rates of silver ions for smaller time frames, it can be seen that a certain error margin is present for the experiment, *i.e.* negative values obtained after six hours. This was because the ion chromatography analysis was performed at the lower resolution limit of the respective ion concentrations.[58] For more detailed investigations of the kinetics of the ion removal, different analysis like inductively coupled plasma optical emission spectroscopy should be applied.[618] Nevertheless, a clear trend can be obtained in the batch removal experiment analyzed by ion chromatography verifying metal ions that exhibit a high complexation affinity for TSC-groups.

Comparing the obtained results of the batch removal experiments, metal ions and their counterions were not removed in the same ratio. For instance, whereas silver ions were removed by 45% after five days using a membrane made from 9.5wt% polymer casting solution in NMP, the NO_3^-ion was only removed by 34% (see Table 30). This difference indicated the presence of anionic and neutral binding of the metal ion (see Scheme 49). A neutral complexation also leads to the stoichiometric

[57] For instance, Peinemann *et al.* reported the application of poly(thiosemicarbazide)s for the removal of copper and gold ions obtaining active groups of 1.7 and 15%, respectively (calculation were according to the calculation in Table 30, data was extracted from the respective paper).[618]

[58] The resolution limit for the respective salt was determined by measuring samples with the concentrations 5, 2.5, 1.25, 0.625 and 0.313 mM on the ion chromatography. Evaluation showed that linear dependency of the integral values of the chromatography signal and the concentration was maintained for concentration of 1.25 mM or higher.

removal of NO_3^-ion, since charge neutrality has to be maintained, while an anionic TSC-group substitutes the NO_3^--ion under release of nitric acid.

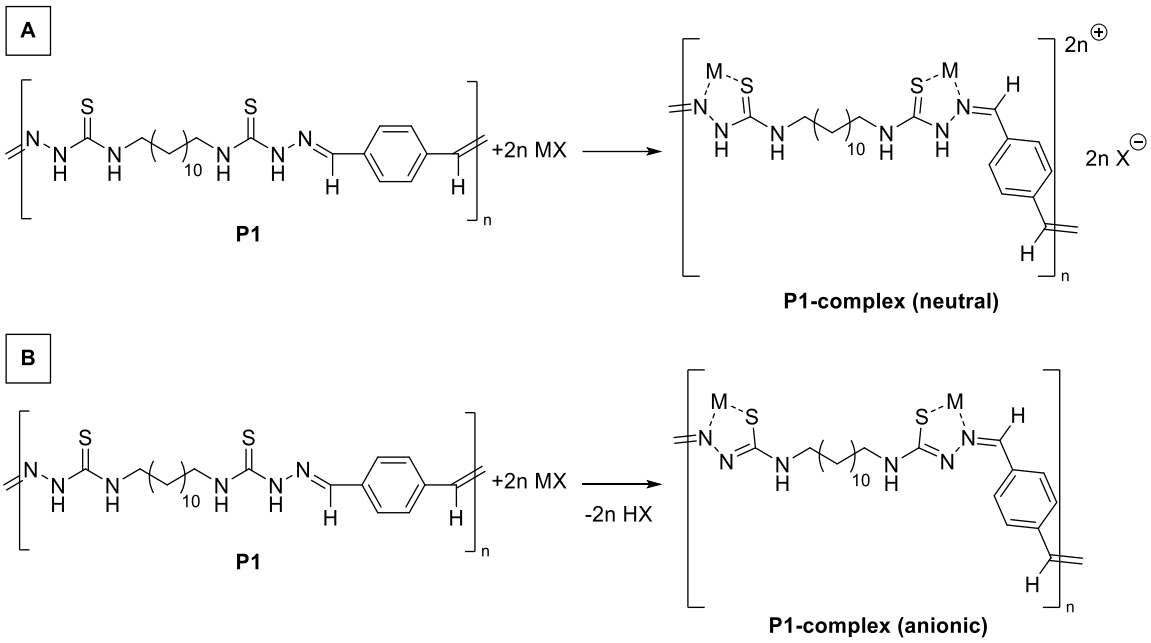

*Scheme 49: Schematic overview of the neutral (**A**) and anionic (**B**) chelation of a metal salt (MX) by poly(TSC) **P1**.*

Since the streaming potential of the poly(TSC) **P1** membrane revealed a negative surface charge, the presence of an anionic binding mode seemed reasonable. Furthermore, anionic binding should lead to a pH-drop of the aqueous solution since an acid is released. Indeed, a decrease of the pH-value from 6 (corresponds to the pH-value of Milli-Q® water) to approximately 3.5 for the batch removal of $AgNO_3$ and $CuCl_2*2H_2O$ was determined using pHpaper. This assumption was further underpinned by the reaction of poly(TSC) **P1** with $AgNO_3$, $ZnCl_2$ and $CuCl_2*2H_2O$ in DMSO. The resulting metallopolymer complexes were analyzed by IR-spectroscopy, depicting typical vibrational bonds for neutral and anionic TSC complexation (see chapter 6.9.7.).

In a next step, the removal of $AgNO_3$ was investigated in a dynamic flow set-up as a proof of concept. Therefore, the dead-end Amicon cell set-up used for determination of the permeabilities of the membranes was applied. Thus, 20 mL of a 1.25 mM $AgNO_3$ aqueous solution was pumped through a poly(TSC) membrane of 3.8 cm^2 made from a 16wt% polymer solution in DMSO. No drop in permeability was visible during the experiment. Successful, removal of silver ions could already be seen by visual observation, as the yellow membrane turned darker on the surface, while the bottom side remained yellow (see chapter 6.9.8. for pictures). Since the set-up did not allow application of a larger membranes the removed percentage of silver ions was too low to be detected by ion chromatography, because of the mentioned resolution limit.[59] Therefore, EDX and streaming potential analysis were chosen as suitable method to determine the content of silver ions after the experiments.

Due to the complexation of the cations by the TSC-group, it was expected that the surface charge of the membrane would be less negative after the filtration. Indeed, a reduced negative charge of -22.9 mV was obtained for a membrane casted by using a 15wt% polymer solution in DMSO (membrane not being exposed to $AgNO_3$ had a negative charge of -37.8 mV, *vide supra*). For

[59] For the batch kinetic rate experiment 20 cm^2 membrane were applied, thus since different membrane depicted similar removal rates, a removal rate of roughly 9% was expected for 3.8 cm^2 assuming that the contact time with the membrane was sufficient for the complexation.

comparison, immersion of a membrane made from a 16wt% polymer solution in DMSO in a high concentrated, aqueous $AgNO_3$ solution ($c(AgNO_3)$=17.9 mM) for two days yielded a similarly reduced negative charge of -24.2 mV, indicating that the contact time in the flow experiment allowed sufficient complexation of the silver ions. In addition, the EDX measurement clearly showed the presence of silver ions in the membrane (see Table 31).[60] Similar weight-percentages of silver were obtained for the top and bottom layer as well as in the cross-section (CS, 12.1, 7.9 and 14.3, respectively). As the top layer of an asymmetric membrane is the separation layer, compounds that pass this layer will also pass the more porous sub structure and thus, the presence of silver ions in the CS as well as the bottom layer proves that the removal of the salt proceeded not by size exclusion but complexation. For further comparison, the before-mentioned membrane, which was immersed in a $AgNO_3$ solution, depicted a higher amount of bound silver ions of 33-36 wt% (for further information about the EDX-spectra and the respective SEM-pictures see chapter 6.9.9.).

Table 32: Weight-percentages of the elements C, N, O, S and Ag obtained for poly(TSC) membranes exposed to silver in different procedures by EDX-analysis. Additionally, a membrane obtained by using a 16wt% polymer solution in DMSO is given as a reference that was not exposed to silver ions.

poly(TSC) membrane	layer	C/wt%	N/wt%	O/wt%	S/wt%	Ag/wt%
16wt% in DMSO	top	73	2	1	21	3
	CS	72	2	2	23	2
	bottom	71	4.	1	25	0
16wt% in DMSO-after removal of $AgNO_3$[a)]	top	55	13	2	18	12
	CS	58	7	3	18	14
	bottom	59	15	1	16	8
16wt% in DMSO-after immersion in $AgNO_3$[b)]	top	45	7	1	10	36
	CS	44	0	5	19	33
	bottom	46	0	2	18	35
15wt% in DMSO-exposed to $AgNO_3$ and immersed in water for desorption[c)]	top	69	1	1	19	9
	CS	77	0	1	22	0
	bottom	73	2	1	24	0

a.) Membrane was exposed to 20 mL of an aqueous 1.25 mM $AgNO_3$ solution in a dead-end Amicon cell set-up. b) Membrane was immersed in 1 L of an aqueous 17.9 mM $AgNO_3$ solution for two days. c) Membrane was exposed to 20 mL of an aqueous 1.25 mM $AgNO_3$ solution in a dead-end Amicon cell set-up. Subsequently, the membrane was put in ca. 5 mL of water for seven days. The water was exchanged three times over this period.

As the removal of silver ions was successful, a desorption experiment was performed to complement this proof of concept.

The desorption of the complexed silver ions is crucial for a reasonable application of the poly(TSC) membranes for the removal of silver ions from a water stream, allowing their repetitive utilization. Thus, a membrane obtained using a 15wt% polymer solution in DMSO was exposed to a 1.25 mM $AgNO_3$ solution in a dead-end Amicon cell set-up and subsequently put in ca. 5 mL of water for seven days. During this time, the water was exchanged three times and afterwards the amount of silver ions was determined by EDX-analysis (see Table 31). The top layer still depicted the presence of silver, while the bottom layer and the CS depicted no remaining silver. Thus, the desorption of the complexed silver ions could be partly performed by immersion in water. It seemed reasonable that the desorption rate of the sub-structure was higher than the one of the top layer, since the more open morphology allows an easier access of water by diffusion, while the dense top layer is more restricting. Concluding, the desorption studies should be further investigated to confirm the

[60] All EDX-measurements were performed by M. Irshad Baig, post-doctoral scientific researcher in the working group of Prof. de Vos at the University of Twente (Netherlands). The author evaluated the obtained data.

desorption of silver ions by immersion in water. In addition, different pH-values should be tested for the desorption experiment of the silver ions. Since, the complexation of the metal proceeded at least partly under release of a proton (*vide supra*), it seemed reasonable that a low pH-value (*e.g.* pH = 0 using an aqueous 1 M HCl solution) might lead to complete and/or faster desorption as the equilibrium of the complexion reaction is shifted towards the free metal ions (see Scheme 49**B**).

Lastly, it was attempted to obtain a poly(TSC)-$AgNO_3$ membrane by NIPS using 15 and 16wt% polymer solution in DMSO and an aqueous $AgNO_3$ solution ($c(AgNO_3)$=17.9 mM) as non-solvent, instead of Milli-Q® water. Thus, it was expected to obtain poly(TSC) membranes bearing a higher charge density on the surface (presence of anionic TSC-groups and the metal counterion) that could result in an improved retention of salts by Donnan exclusion. Furthermore, silver salts often depict antimicrobial properties, which could prevent biofouling.[61] The obtained membrane showed a different coloration (brown instead of yellow) and a surface net charge of only -10.2 mV, which was less negative than the membranes treated with $AgNO_3$ solutions (in batch or flow experiments). This seemed reasonable, since the silver ions can diffuse inside the polymer film during the precipitation process and thus, can access more TSC-groups in solution compared to a finished, solid membrane. However, the rigidity of the membrane strongly increased and zero permeability was obtained after two days in the Amicon cell setup at 3 bar water pressure. The altered properties were assigned to the complexation of the silver ions, which could also form cross linking by double-neutral or neutral-anionic bonding of two TSC-groups. Thus, the rigidity is increased and pore sizes of membranes with a certain weight-percentage of polymer are decreased, since the polymers are restricted in their separation during the precipitation by the cross-linking.

In conclusion, removal of copper and silver ions by the use of a poly(TSC) membrane was shown by batch removal experiments, while the affinity for silver was higher (2.3% active TSC groups for silver compared to 1.2% for copper). In additions, anionic binding of the TSC groups was proven by streaming potential, pH-value and IR measurements, while neutral binding modes were also indicated by IR and batch removal experiments. Finally, silver ion removal was successfully proven in a flow setup by streaming potential and EDX measurements confirming the use of complexation by TSC-functional groups as separation mechanism. Further applications of the poly(TSC) membranes can be envisioned in the field of transition metal ion removal from waste water, since several other metals could exhibit an even higher affinity for this functional group, while a first desorption experiment for reuse of the membrane was also promising.

[61] The performance of a membrane such as lifetime, permeability and removal capacity is highly influenced by the presence and degree of fouling taking place on the surface of the membrane.[647] Fouling can occur due to several mechanism and describes in general the fact that an inorganic, organic or biological compound will stick to the surface of a membrane, where it will alter the performance of the membrane. Ultimately, fouling can lead to rapid decline in flux of the membrane over time and thus, the membrane has to be cleaned or discarded. For instance, biofouling is a common fouling type due to the accumulation of microorganism on the membrane surface, which can be decreased by the use of antimicrobial membranes.[648]

5 Conclusion and Outlook

In this work, a more sustainable isocyanide synthesis was established using *p*-TsCl, a waste product from the saccharin synthesis, as dehydration reagent, which is less toxic than common ones like $POCl_3$, phosgene or its derivatives. Thus, non-sterically hindered mono- and di-*N*-formamides were converted to the respective isocyanides in high yields (up to 98%) using a feasible reaction set-up. The E-factor was thereby decreased strongly compared to common procedures (down to 6.45), since extraction and washing could be applied as sole purification step leading to a high purity underlined by the high molecular weights obtained from such isocyanides in a P-3CPR.

This synthesis protocol has a strong positive impact on the overall sustainability of isocyanide-based reactions like IMCRs, since their degree of sustainability is typically diminished by synthesis of the respective isocyanide starting material. As a result of the more sustainable isocyanide synthesis, the AM-3CR using isocyanides, amines and elemental sulfur allowed the synthesis of thioureas in a more sustainable fashion. Furthermore, the use of elemental sulfur, a waste product of the petroleum industry, as a starting material is desired and the purification of the product was typically performed by recrystallization and filtration.

Using the more sustainable AM-3CR approach for the synthesis of thioureas, a library of known and unknown thioureas was synthesized, investigating their catalytic activity and thus, their application as organocatalyst. It was shown that the AM-3CR allowed an easy access to several thiourea compounds bearing aliphatic, cyclic, benzylic and aromatic moieties. However, moieties that were prone to activate the thiourea functional group resulting in catalytic activity, *i.e.* electron-withdrawing aromatic motifs, proved to be challenging in their use in an AM-3CR. Due to the mechanism of the reaction, the electron-deficient aromatic moiety could only be introduced by the isocyanide component and thus, the use of toxic dehydration agents like $POCl_3$ was necessary for the isocyanide synthesis. In addition, the respective isocyanide is also activated by the moiety and thus, highly reactive to moisture decreasing the yield and impeding the purification. Still, two thioureas bearing novel activation moieties, *i.e.* isophthalicacid ester and *p*-alkylsulfonyl groups, were synthesized and depicted similar catalytic activity as thioureas with the often used 3,5-bis(trifluoromethyl)phenyl group in an Ugi reaction as well as a carbonate ring opening reaction. Compared to the latter activation motif, the isophthalicacid ester and the *p*-alkylsulfonyl groups can be tailored in their solubility by introduction of different moieties, for instance aliphatic chains in different length. This is advantageous considering that organocatalysts are used as homogenous catalysts, but most often exhibit low solubility parameters in typical organic solvents. Thus, the use of this motifs might allow organocatalysis of reactions that could not be catalyzed before due to solubility or concentration issues.

Novel polymeric thiourea catalysts were envisioned bearing the investigated activation motifs. A high overall sustainability was expected for such recyclable catalysts, even considering the drawbacks mentioned for the thiourea synthesis using an AM-3CR. Three different approaches were tested.

Firs,t a polycondensation approach with an isophthalicacidester thiourea compound was yielded insufficient conversions for a step-growth polymerization reaction. The reaction was thoroughly optimized and several side reactions (decomposition of the thiourea group and formation of

thionocarbamate acting as chain-stopper) were confirmed, which ultimately makes this approach non applicable.

A second approach using a poly-Thiol-Ene reaction relied again on the isophthalicacidester motif, but led to insufficient conversions as well. Typical photo- or thermally initiated radical starters like AIBN and DMPA were insufficient, even in high amounts (up to 50 mol% in case of DMPA). Since the proceeding of the radical reaction was highly depending on the used solvent but the scope of solvent was very limited due to the low solubility of the thiourea compound, this approach seemed to be less promising.

A third approach based on the ROMP of a norbornene thiourea compound depicted nearly full conversion of a thiourea containing norbornene using a Grubbs second generation catalyst after only two hours at 44 °C. Thus, this living polymerization approach was superior compared to the other two step-growth approaches. Furthermore, it was shown that several parameters of the starting material can be altered (chemical structure and length of the spacer between thiourea and norbornene, *exo/endo* reactivity of norbornene, activation motif for the thiourea compound) allowing a broad scope of optimization in terms of solubility and recyclability of the polymer. The use of *co*-monomers like norbornene and cyclooctene led to a faster conversion of the thiourea norbornene (full conversion after one hour), while in addition, the solubility could be further altered. Nevertheless, no purification process could be established in the time frame of this work to fully verify the proof of concept for the ROMP approach by obtaining a pure polymer. Still, the underlined high degree of tailorability of this approach is expected to have the potential for the synthesis of recyclable, homogenous and heterogeneous, polymeric thiourea organocatalysts.

An investigation on the reaction mechanism of the AM-3CR led to the clear identification of isothiocyanates as key intermediates for this reaction. By using DBU or TBD as amine component, the reaction proceeding from the isothiocyanate to the respective thiourea could be impeded obtaining isothiocyanates as main product in the reaction. Thus, a more sustainable synthesis protocol for the formation of isothiocyanates by sulfurization of isocyanides with elemental sulfur was established. The feasibility and functional group tolerance of the reaction was underpinned by the synthesis of 20 isothiocyanates in yields up to 95% and E-factors down to 0.989 (not including waste produced by the work-up). Furthermore, Cyrene™ and GBL were applied as greener solvents for the sulfur activation compared to typical solvents like DMSO and DMF. The purification was optimized in terms of sustainability using a short flash column chromatography as sole purification step obtaining the products in high purity (yield up to 95%). Considering that isocyanides were accessible *via* the more sustainable approach also presented in this work, the overall degree of sustainability for the three-step synthesis of isothiocyanates starting from amines (*N*-formylation, isocyanides and isothiocyanate synthesis) was highly increased avoiding toxic compounds like $POCl_3$, phosgene, thiophosgene and carbon disulfide. Finally, even though isothiocyanate are typically obtained in an one-step reaction from amines, it is expected that this new route is competitive compared to the classic approached concerning the lower overall toxicity.

Further mechanistical investigations on the C=S double bond formation of base-activated sulfur and carbene or carbene-like functional group were conducted using benzhydryl carbenes obtained from the respective tosylhydrazones. Even though thioketones were expected to be the obtained product in this reaction, two tetraarylethylenes were obtained in high yields after optimization of the reaction conditions due to formal homo coupling of two benzhydryl moieties (97 and 92%,

respectively). Thus, this reaction offers the access to tetra substituted olefines and is considered to extend the toolbox for the synthesis of such compounds besides reactions like the McMurry and the Barton-Kellogg reaction. Still, clear indications were found that a thioketone might be formed as an intermediate in this reaction by C=S double bond formation between a carbene and a polysulfane, leading to the assumption that a Barton-Kellogg-like reaction mechanism seemed to be reasonable. Besides, several further experiments were suggested to fully validate the proposed reaction mechanism. Full understanding of the reaction mechanism might also lead to the establishment of a hetero coupling of two different tosyl hydrazones.

Finally, novel sulfur-containing polymers, *i.e.* poly(TSC), were obtained by step-growth polymerization of dialdehydes and dithiosemicarbazides. The latter monomers were obtained by extending the scope of the AM-3CR using hydrazine monohydrate as amine component. Thus, eight poly(TSC)s and five co-poly(TSC)s were obtained by reacting two different dithiosemicarazides with dialdehyde components in good to excellent yields (58-93 %). In addition, high molecular weights were obtained (up to 38 kDa) and the polymers were fully characterized by NMR-, IR-, SEC-, DSC-, TGA-analysis. These polymers were envisioned to have a versatile potential of application, for instance due to the intrinsic complexation ability of the TSC-groups. Transition metals such as palladium that are prone to catalyze several different reactions, like coupling reactions, could be complexated yielding recyclable catalysts.

Thus, asymmetric poly(TSC) membranes were formed by using the NIPS process. Permeabilities in the range of UF to RO were obtained using DMSO and NMP as solvent (32-0.3 $Lm^{-2}h^{-1}bar^{-1}$). In addition, the membranes depicted full retention of high molecular weight compounds like BSA. No salt rejection of removal of micropollutants was observed, probably due to the presence of defects. Nevertheless, the removal of silver and copper ions was shown in a batch removal experiment and a proof of concept for the removal of silver ions in a dead-end dynamic flow set-up was also confirmed using a chelation mechanism. Furthermore, first experiments showed that desorption of the silver ions from the membrane seemed to be feasible. An optimized washing procedure for the membranes could yield a protocol that allows for a competitive use of the poly(TSC) membranes for the removal of transition metals in a water stream.

The several parts of this work clearly highlight the versatility of base-activated sulfur not only as starting material but also as mediating agents obtaining several different functional groups, while sulfur can be incorporated in small molecules but also polymers. It is expected that the potential of elemental sulfur is not completely exploited yet and that this research area will grow in the following years to obtain full understanding of the versatile reactivity of this compound. This is highly desired considering that this very abundant, non-toxic waste product is currently underused compared to its scope of application.

6 Experimental Section

6.1 Instrumentation

Nuclear Magnetic Resonance Spectroscopy (NMR):

^{1}H- and ^{13}C-NMR spectra were recorded on BRUKER Avance DPX spectrometers (Billerica, MA) with a 5-mm dual proton/carbon probe (300 and 400 MHz) and on a Bruker Avance III with a 5 mm z-gradient cryogenically cooled probe head (CPTCI, 600 MHz 1H/75.5 MHz). Unless otherwise stated, all spectra were measured at ambient temperature. The chemical shift for 1H-MR spectra was reported in parts per million (ppm) and referenced to characteristic solvent signals of partly deuterated solvents *e.g.* $CDCl_3$ at 7.26 ppm. 13C-MR spectra were reported in ppm relative to characteristic signals of partly deuterated solvents, *e.g.* the centroid peak of the $CDCl_3$ triplet at 77.2 ppm. The spin multiplicity and corresponding signal patterns were abbreviated as follows: s = singlet, d = doublet, t = triplet, q = quartet, quint. = quintet, sext. = sextet, m = multiplet and br = broad signal. Coupling constants *J* were noted in Hz. Furthermore, 2D-NMR methods, *e.g.* heteronuclear multiple quantum coherence (HMQC), heteronuclear single quantum coherence (HSQC), heteronuclear multiple bond correlation (HMBC) and correlated spectroscopy (COSY) were carried out, if necessary, for signal assignment and structure elucidation. If conformers (rotamers) of a substance could be observed due to restricted rotation, all species which could be assigned clearly were labelled with additional appendices (a, b, c. etc.). Hereby, the main conformer was labelled with the appendix “a”, the second conformer with appendix “b” and so on.

Mass Spectrometry (MS):

Fast-atom-bombardment (FAB) and electron ionization (EI) spectra were recorded utilizing a Finnigan MAT 95 mass spectrometer. A Q Exactive (Orbitrap) mass spectrometer (Thermo Fisher Scientific, San Jose, CA, USA) equipped with a HESI II probe was employed to record high resolution electrospray ionization–MS (ESI-MS). Calibration was carried out in the m/z range 74–1,822 using premixed calibration solutions (Thermo Fisher Scientific). A constant spray voltage of 4.7 kV and a dimensionless sheath gas of 5 were employed. The S-lens RF level was set to 62.0, while the capillary temperature was set to 250 °C. All samples were dissolved at a concentration of 0.05 mg mL−1 in a mixture of THF and MeOH (3:2) doped with 100 µmol sodium trifluoroacetate and injected with a flow of 5 µl min^{-1}.

Infrared Spectroscopy (IR):

Infrared spectra (IR) were recorded on a BRUKER Alpha-p instrument applying ATR-technology (ATR = Attenuated Total Reflection) in a frequency range from 3998 to 374 cm-1 . The band intensities were characterized in relation to the most intense signal as follows: s = strong, m = medium, w = weak. In addition, broad signals were expressed by the term: br = broad.

Fourier transform infrared (FTIR) spectroscopy was conducted using a Spectrum Two (Perkin Elmer, USA) in attenuated total reflectance mode in the wavenumber range 600 to 4000 cm^{-1}.

Gas Chromatography (GC):

Gas chromatography (GC) was performed on a Bruker 430 GC instrument equipped with capillary column FactorFourTM VF-5 ms (30.0 m x 0.25 mm x 0.25 µm), using flame ionization detection (FID). The oven temperature program was: initial temperature 95 °C, hold for 1 min, ramp at 15°C min^{-1} to 220 °C, hold for 4 min, ramp at 15°C min^{-1} to 300 °C, hold for 2 min, ramp at 15°C min-1 to 325 °C, hold for 3 min. Measurements were performed in split-split mode using nitrogen as the carrier gas (flow rate 30 mL min^{-1}).

Size Exclusion Chromatography (SEC):

A PSS SECcurity2 GPC system based on Agilent infinity 1260 II hardware. The system is equipped with a refractive index detector SECcurity² RI, a column oven “(Bio)SECcurity² column compartment TCC6500”, a “standard SECcurity²” autosampler, isocratic pump “SECcurity² isocratic pump”. THF (flow rate 1 mL/min) at 30 °C was used as mobile phase. The analysis was performed using the following column system: Two columns PSS SDV analytical (3 µm, 300 × 8.0 mm^2, 1000 Å) with a PSS SDV analytical precolumn (3 µm, 50 × 8.0 mm^2). For the calibration, narrow linear poly(methyl methacrylate) standards (Polymer Standards Service, PPS, Germany) ranging from 102 to 62200 Da were used

SEC measurements were performed on a SHIMADZU Size Exclusion Chromatography (SEC) system equipped with a SHIMADZU isocratic pump (LC-20AD), a SHIMADZU refractive index detector (24°C) (RID-20A), a SHIMADZU autosampler (SIL-20A) and a VARIAN column oven (510, 50°C). For separation, a three-column setup was used with one SDV 3 µm, 8×50 mm precolumn and two SDV 3 µm, 1000 Å, 3×300 mm columns supplied by PSS, Germany. Tetrahydrofuran (THF) stabilized with 250 ppm butylated hydroxytoluene (BHT, ≥99.9%) supplied by SIGMA-ALDRICH was used at a flow rate of 1.0 mL min^{-1}. Calibration was carried out by injection of eight narrow polymethylmethacrylate standards ranging from 102 to 58300 kDa.

SEC measurements were performed in HFIP containing 0.1 wt% potassium trifluoroacetate with Tosoh EcoSEC HLC-8320 SEC system. The solvent flow was 0.40 mL min-1 at 30 °C and the concentration of the samples was 1 mg min-1 . The analysis was performed on a three-column system: PSS PFG Micro precolumn (3.0 × 0.46 cm, 10000 Å), PSS PFG Micro (25.0 × 0.46 cm, 1000 Å) and PSS PFG Micro (25.0 × 0.46 cm, 100 Å). The system was calibrated with linear poly(methyl methacrylate) standards (Polymer Standard Service, Mp: 102-981 kDa).

SEC measurements were performed on a Polymer Laboratories PL-GPC 50 Plus Integrated System with an autosampler. The system was equipped with a PLgel 5 mm bead-size guard column (50 × 7.5 mm), which was followed by three PLgel 5 µm Mixed-C columns and one PLgel 3 µm Mixed-E column (300 × 7.5 mm), and a differential refractive index detector. For the measurements, DMAc was used as eluent containing 0.3 w% LiBr and a pressure of 1mL/min at 50 °C was applied. The number average molar mass (M_n), the weight average molar mass (M_w) and the mass distribution/dispersity ($Đ=M_w/M_n$) of the polymers were determined using a calibration of linear poly(methyl methacrylate) standards ranging from 476 to 2.5×10^6 g mol^{-1}. The polymer samples were dissolved at a concentration of 2 mg mL^{-1} in the eluent and filtered over a 0.2 µL filter prior to the measurement. Signals lower than 1000 g mol^{-1} correspond to solvent signal.

SEC measurements were performed on a Agilent 1200/1260 Infinity GPC/SEC series, Polymer Standards Service data centerand column compartment. Milli-Q ultrapure water containing 50 mg·L^{-1} NaN_3 was used as the eluent at a flow rate of 1 mL·min^{-1} through the SEC column (10µm Polymer Standards Service Suprema 8×300 mm 1000 Å and 10µm 30 Å, connected in series)

Dynamic scanning calorimetry (DSC):

DSC experiments were performed on a Mettler Toledo DSC 3 using a Huber Intracooler TC100 and aluminum crucibles (40 and 100 µL). Measurements were performed under nitrogen flow (50 mL min^{-1}) in three consecutive heating-cooling cycles from 25 °C up to 230 °C with a heating rate of 20-30 K min^{-1}. Each measurement was performed using 3-7 mg of substance for sample preparation. T_g values were determined as the onset of the transition in the second heating cycle.

Thermogravimetric analysis (TGA):

Thermogravimetric analysis was performed on a TGA5500 from TA instruments. 5-15 mg of a sample was placed in a aluminum pan and heated at a rate of 10 K min^{-1} from ambient temperature to 600-1000 °C under nitrogen flow. The onset was evaluated by Trios v5.0.044608 software.

Elemental analysis (EA)

EA was performed on an Elementar Vario Micro cube. O2-Dosage time: 70 s, Auto zero delay N: 10 s, Auto zero delay S: 10 s, Peak expectation N: 50 s, peak expectation C: 100 s, peak expectation H: 80 s, peak expectation S: 70 s, desorpt. CO2: 60 °C, desorpt. H2O: 140 °C, desorpt. SO2: 240°C

Thin Layer Chromatography (TLC):

For TLC analysis, precoated aluminium foils with fluorescence indicator from MERCK (TLC Silica gel 60, F254, layer thickness: 0.25 mm) were employed as stationary phase. The spots were firstly visualized by fluorescence quenching under UV-light (λ = 254 nm), fluorescence (λ = 365 nm), and by staining with Seebach reagent: solution of 2.50 g cerium(IV) sulfate tetrahydrate ($Ce(SO_4)_2 \times 4\ H_2O$), 6.25 g ammonium heptamolybdate tetrahydrate ($(NH_4)_6Mo_7O_{24} \times 4\ H_2O$), 225 mL water and 25.0 mL concentrated sulfuric acid. Or vanillin: solution of 15 g vanillin and 2.5 mL concentrated sulfuric acid in 250 mL ethanol.

UV/VIS spectroscopy

UV/VIS spectra were recorded using a UV-spectrophotometer (Shimadzu UV-1800, Jpan) at λ_{max} = 280 nm.

Ion chromatorgraphy (IC)

IC measurements were performed on an Ion Chromatography Eco IC (Metrohm, USA) equipped with a Cation column (Metrosep C 6 150/4.0), Anion column (Metrosep A Supp 17 - 150/4.0). The cation column eluent was 4 mM HNO_3 and the anion column eluent was 5 mM Na_2CO_3 + 0.2 mM $NaHCO_3$, while the anion suppressor solution was 0.3 M H_3PO_4.

Column chromatography

TLC silica gel F254 (Sigma Aldrich) and solvents, which had HPLC-purity, were used.

Scanning electron microscopy (SEM)

The surface and cross-sectional morphology of the membranes were analyzed using scanning electron microscopy SEM equipped with EDX (JSM-6010LA and JSM-7610F, field-emission electron microscope, JEOL, Japan). For cross-sectional images, the membrane samples were first immersed in liquid nitrogen before carefully fracturing them to preserve the pore structure. All the samples were dried at room temperature for at least 24 h before coating them with a 5 nm thick layer of platinum using a Quorum Q150T ES sputter coater (Quorum Technologies Ltd., UK).

Zeta potential

Zeta potential of the membranes was measured using a SurPASS electrokinetic analyzer (Anton Paar, Graz, Austria). Zeta potential values were calculated by measuring the streaming current versus pressure in a 5×10^{-3} M KCl solution using Equation 5:

$$\varsigma = \frac{dI}{dP} \times \frac{\eta}{\varepsilon \varepsilon_0} \kappa_B R \tag{5}$$

where ς is the zeta potential (V), I is the streaming current, P is the pressure (Pa), η is the dynamic viscosity of electrolyte solution (Pa s), ε is the dielectric constant of the electrolyte solution, ε_0 is the vacuum permittivity (F m^{-1}), κ_B is the bulk electrolyte conductivity (S m^{-1}), and R is the resistance (Ω) inside the streaming channel.

6.2 Materials

All chemicals were used as received, if not mentioned otherwise. All solvents used in HPLC grade or higher apart from dichlormethane and diethylether which were technical grade and thus, were distilled beforehand.

Acetic acid (technical grade), adamantly amine (Alfar Aesar 98 %), adamantylisocyanide (95%, Aldrich Chemistry), allyl alcohol (Sigma-Aldrich, ≥99%), 4-aminobenzoic acid (Alfar Aesar 99 %), amino decane (Alfar Aesar, 97 %), amino octadecane (TCI >85 %), 11-aminoundecanoic acid (Aldrich Chemistry, 97 %), anisaldehyde (98%, Alfar Aesar), Benzophenone (Sigma-Aldrich, 99%) benzyl amine (Merck kGaA, >99 %), benzylisocyanide (98%, Acros Organics), biphenyl (99%, Alfar Aesar), 4,4´-*bis*(dicarboxyaldehyde) biphenyl (Acros Organics 97%), 1,4-*b*is(methylamino) benzene (Sigma, 99%), bis-3,5-(trifluoromethyl) anillin (98% Acros Organics), bis-3,5-(trifluoromethyl)phenyl) thiourea (>98%, TCI), 4-bromo benzaldehyde (Maybridge, 98%), copper iodide (Sigma-Aldrich, 98%), *cis*-5-norboronene-*exo*-2,3-dicarboxylic anhydride (Sigma-Aldrich, 95%), cyclohexyl amine (Aldrich Chemistry, 99 %), *trans*-cyclohexyl-1,4-diamine (Aldrich 98%), cyclohexyl isocyanide (99%, Acros Organics), cyclohexyl isothiocyanate (98%, Sigma-Aldrich), Cyrene™ (Sigma-Aldrich), 4,4-´dimethoyxbenzophenone (Sigma-Aldrich, 97%), 1,4-diaminobenzene (Sigma-Aldrich, 98%), 1,12-diaminododecane (Aldrich Chemistry 98 %), 1,5-diamino pentane (ACROS Organics, 98 %), 1,4-diazabicyclo[2.2.2]octane (≥99%, Sigma-Aldrich), 1,8-diazabicyclo[5.4.0]undec-7-en (>98%, TCI), diisopropylamine (99%, abcr), 4-dimethylaminopyridin (99%, Acros Organics), 2,6-dimethylphenyl isocyanide (≥98%, Aldrich Chemistry), dodecylamine (Sigma-Aldrich, ≥99%), ethyl formate (ACROS 98+%), 4-ethynyl benzaldehyde (BLD Phram, 98%), formic acid (99%, Acros Orgaics), ethyl formate (ACROS 98+ %), formic acid (ACROS Organics 99 %), furfurylamine (≥99%, Aldrich Chemistry), heptanal (Aldrich 95 %), 1,1,1,3,3,3-hexafluro-2-propanol (HFIP) (fluorochem), hexylbromide (98%, Sigma-Aldrich), hexyl-1,6-diamine (Merck, >99%), hydrazine monohydrate (Merck KGaA ≥99%), 6-hydroxyhexyl amine (TCI >97 %), 2-isocyanonaphthalene (95%, Aldrich Chemistry), isophorendiamine (99%, TCI, mixtures of isomers), methanolic ammonia solution (7 M), 1-methylimidazole (NMI, ≥99%, Sigma-Aldrich), 4-methoxyphenyl isocyanide (97%, Aldrich Chemistry), 2-morpholinoethyl isocyanide (≥98%, Aldrich Chemistry), *para*-toluidine (99%, Aldrich), $Pd(PPh_3)_2Cl_2$ (Aldrich, ≥99.99% trace metal basis), pentylisocyanide (97%, Aldrich Chemistry), phosphorus oxychloride (99%, Aldrich), potassium 2-isocyanoacetate (technical grade (85%, Aldrich Chemistry), propylene carbonate (99.5%, Acros Organics), pyridine (Fisher Scientific UK, 99.9 %), oleylamine (Sigma-Aldrich, >98 %), *para*-toluenesulfonic acid monohydrate (Acros Organics, 99%), *para*-toluenesulfonyl chloride (Sigma-Aldrich ≥98 %), sebacic acid (Aldrich Chemistry 99 %), sodium sulphate (dry, Bernd Kraft), silica gel modified with dimercaptotriazine (0.50 $mmolg^{-1}$, Sigma-Aldrich ≥98 %), sulphur (elemental, technical grade), terephthaldehyde (Sigma-Aldrich, 99%), tetradecane (Sigma-Aldrich, ≥99 %), *tert*-butyl isocyanide (98% Aldrich), thionyl chloride (ACROS Organics 99.5+ %), tosylmethylisocyanide (Fluorochem), 3,5,7-triazabicylco[4.4.0]dec-5-en (TCI, >98%), triethylamine (99.5%, Fisher Chemical), triethylphosphor oxide (97%, Aldrich), 5-Trifluoromethly-1,3-dimaminophenylene (Sigma-Aldrich, 98%), 3,4,5-trimethoxyanilline (97%, Acros Organics)

6.3 More sustainable synthesis of isocyanides

6.3.1 Synthesis and characterization of *N*-formamides

General synthesis of aliphatic N-formamides

The corresponding aliphatic amine (30.0 mmol, 1.00 eq.) and ethyl formate (24.2 mL, 22.2 g, 300 mmol, 10.0 eq.) were heated under reflux overnight. Afterwards, remaining ethyl formate and ethanol were removed under reduced pressure and the crude product was used without further purification or analysis.

Exceptions:

Adamantyl *N*-formamide

Adamantyl amine, chloroform and ethyl formate were heated under reflux for 48 hours. Afterwards, remaining ethyl formate, chloroform and ethanol were removed under reduced pressure and the crude product was used without further purification or analysis.

N-(6-Hydroxyhexyl)formamide

6-Amino hexane-1-ol (5.00 g, 42.7 mmol, 1.00 eq.) and ethyl formate (34.4 mL, 34.6 g, 427 mmol, 10.0 eq.) were heated under reflux for 20 hours. Afterwards, remaining ethyl formate and ethanol were removed under reduced pressure, and the crude mixture was stored for two weeks at room temperature The product crystalized from the solution and was obtained as white solid (1.70 g, 11.7 mmol) in a yield of 27 % after filtration and washing with cyclohexane and ethyl acetate.

R_f = 0.16 (cyclohexane/ethyl acetate, 1:1) visualized *via* Seebach staining solution.

^{1}H-NMR (500 MHz, DMSO-d_6) δ/ppm = 7.98-7.91 (m, 2H, NH, CH, ^{1}), 4.34 (t, ^3J = 5.1 Hz, 2H, CH_2, ^{2}), 3.40-3.35 (m, 2H, CH_2, ^{3}), 3.07 (q, ^3J = 6.5 Hz, 2H, CH_2, ^{4}), 1.43-1.37 (m, 4H, CH_2, ^{5}), 1.31-1.25 (m, 4H, CH_2, ^{6}).

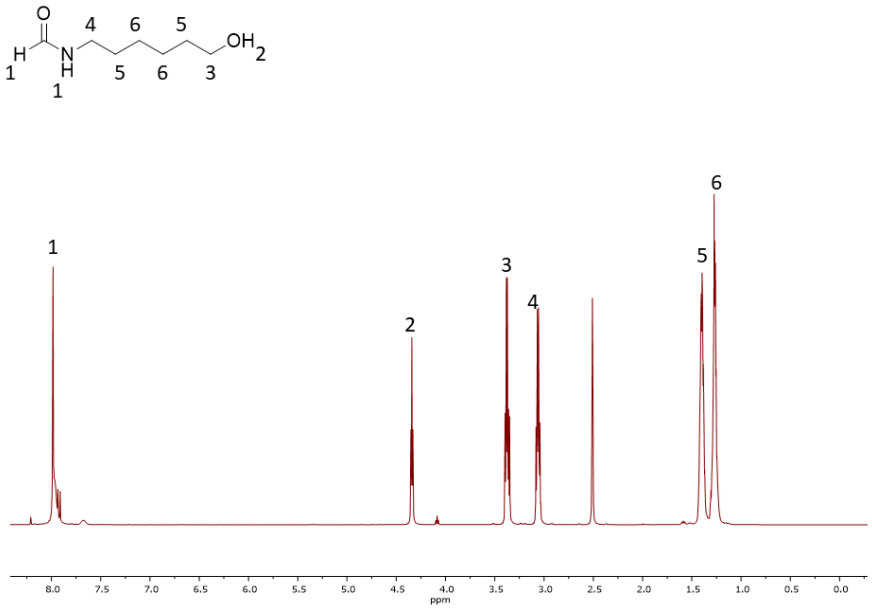

Figure 23: ^{1}H-NMR-spectrum of N-(6-hydroxyhexyl)fromamide.

^{13}C-NMR (126 MHz, DMSO-d_6) δ/ppm = 164.5, 160.9, 60.7, 40.8, 37.1, 32.5, 31.0, 29.1, 26.3, 25.8, 25.2.

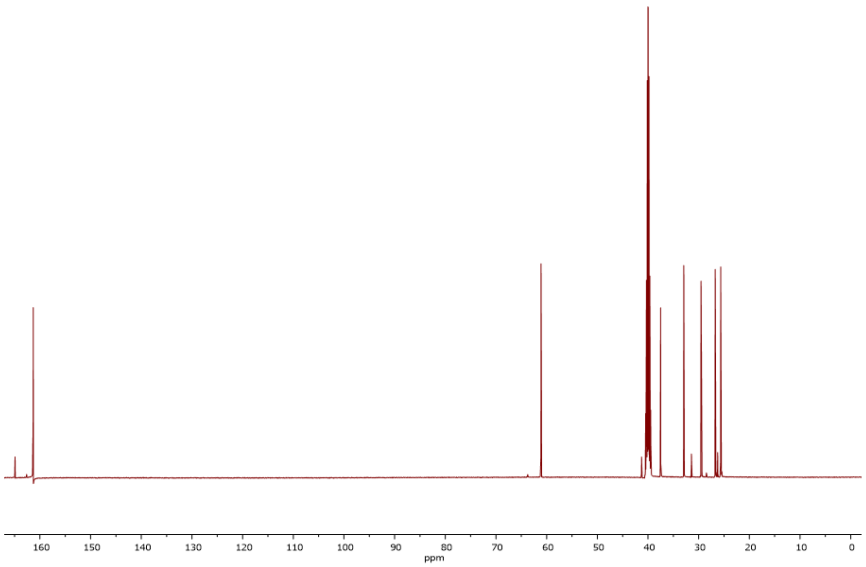

Figure 24: ^{13}C-NMR-spectrum of N-(6-hydroxyhexyl)fromamide.

EI-MS m/z: $[M-H]^+$ calculate for $[C_7H_{14}O_2N_1]^+$ = 144.1025, found: 144.1025, Δ = 0.0752 mmu.

IR (ATR platinum diamond): ν/cm^{-1} = 3374.0 (m), 3307.8 (s), 3035.1 (w), 2933.6 (s), 2854.5 (m), 1640.4 (s), 1523.9 (s), 1463.8 (m), 1362.9 (s), 1282.7 (m), 1240.9 (m), 1215.4 (w), 1107.2 (w), 1062,1 (m),1048.0 (s), 1024.8 (m), 1005.6 (m), 975.4 (m), 781.9 (m), 738.8 (w), 705.3 (s), 638.2 (s).

11-Formamidoundecanoic acid

11-Aminoundecanoic acid (25.1 g, 125 mmol, 1.00 eq.) was suspended in ethyl formate (101 mL, 92.6 g, 1.25 mol, 10.0 eq.) and DMF (50 mL), and was stirred at 75 °C until a clear solution was formed (mostly 20 – 26 h). After the reaction was finished, the solvent was removed under reduced pressure and the product was used without further purification. The product was obtained as white solid (28.7 g, 125 mmol) in quantitative yield.

^{1}H-NMR (500 MHz, DMSO-d_6) δ/ppm = 11.93 (br, 1H, COOH, ^{1}), 7.98 – 7.91 (m. 2H, CH, NH, ^{2}), 3.08 – 3.04 (m, 2H, CH_2, ^{3}), 2.19 (t, ^{3}J = 7.4 Hz, 2H, CH_2, ^{4}), 1.51 – 1.36 (m, 4H, CH_2, ^{5}), 1.25 (m, 12H, CH_2, ^{6}).

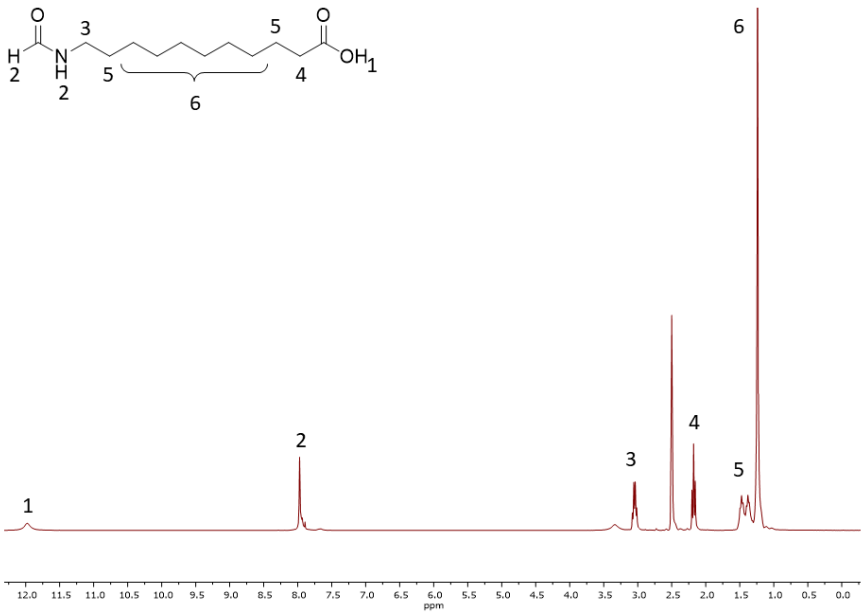

Figure 26: ^{1}H-NMR-spectrum of 11-formamidoundecanoic acid.

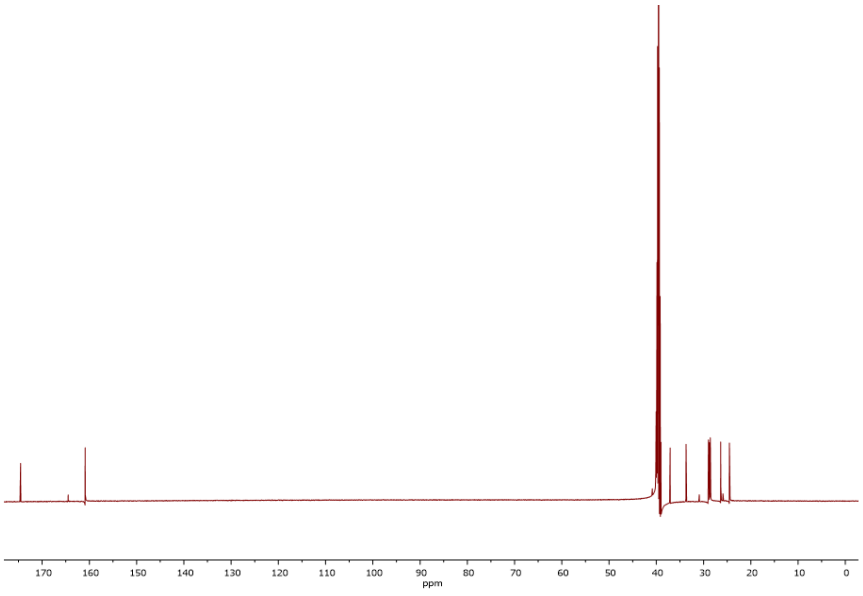

Figure 25: ^{13}C-NMR-spectrum of 11-formamidoundecanoic acid.

^{13}C-NMR (126 MHz, DMSO-d_6) δ/ppm = 174.6, 164.5, 160.9, 37.1, 33.7, 30.9, 29.0, 29.0, 28.9, 28.9, 27.8, 28.8, 28.7, 28.6, 28.6, 26.4, 25.9, 24.5.

FAB-HRMS m/z: $[M+H]^+$ calculated for $[C_{12}H_{24}NO_3]$ 230.1756, found: 230.1755 Δ = -0.107 mmu.

IR (ATR platinum diamond): ν/cm^{-1} = 3358.8 (w), 2938.6 (w), 2918.6 (s), 2849.3 (w), 2577.6 (w), 1720.9 (s), 1646.7 (w), 1626.3 (s), 1525.6 (m), 1470.7 (m), 1438.2 (m), 1409.8 (w), 1362.8 (s), 1319.3 (w), 1293.7 (w), 1273.4 (m), 1243.3 (m), 1206.6 (m), 1177.5 (s), 1108.8 (w), 1054.9 (w), 933.6 (m), 896.5 (w), 806.3 (w), 765.2 (w), 740.2 (w), 718.8 (s), 662.5 (m), 548.0 (w), 529.4 (w), 448.3 (s).

General Synthesis of Aromatic *N*-formamides

Methyl-4-formamidobenzoate

In a flask equipped with a Dimroth-cooler, methyl 4-aminobenzoate (9.82 g, 65.0 mmol, 1.00 eq.) was dissolved in formic acid (9.80 mL, 12.0 g, 260 mmol, 4.00 eq.) and was heated to 60°C for 24 h. Afterwards, formic acid and water were removed under reduced pressure and the product (11.0 g, 61.4 mmol) was obtained as white powder in a yield of 95 % without further purification.

R_f = 0.13 (cyclohexane/ethyl acetate, 2:1) visualized *via* UV quenching at 254 nm, vanillin and Seebach staining solution.

^{1}H-NMR (500 MHz, DMSO-d_6) δ/ppm = 10.56 (s, 1H, CH, ^{a1}), 10.47 (d, ^3J = 10.7 Hz, 1H, CH, ^{b1}), 8.97 (d, ^3J = 10.7 Hz, 1H, NH, ^{b2}), 8.35 (d, ^3J = 1.7 Hz, 1H, NH, ^{a2}), 7.93 - 7.88 (m, 2H, aromatic, $^{a3, b3}$), 7.71 (d, ^3J = 8.8 Hz, 2H, aromatic, ^{a4}), 7.31 (d, ^3J = 8.6 Hz, 2H, aromatic, ^{b4}), 3.81 (s, 3H, CH_3, ^{5}).

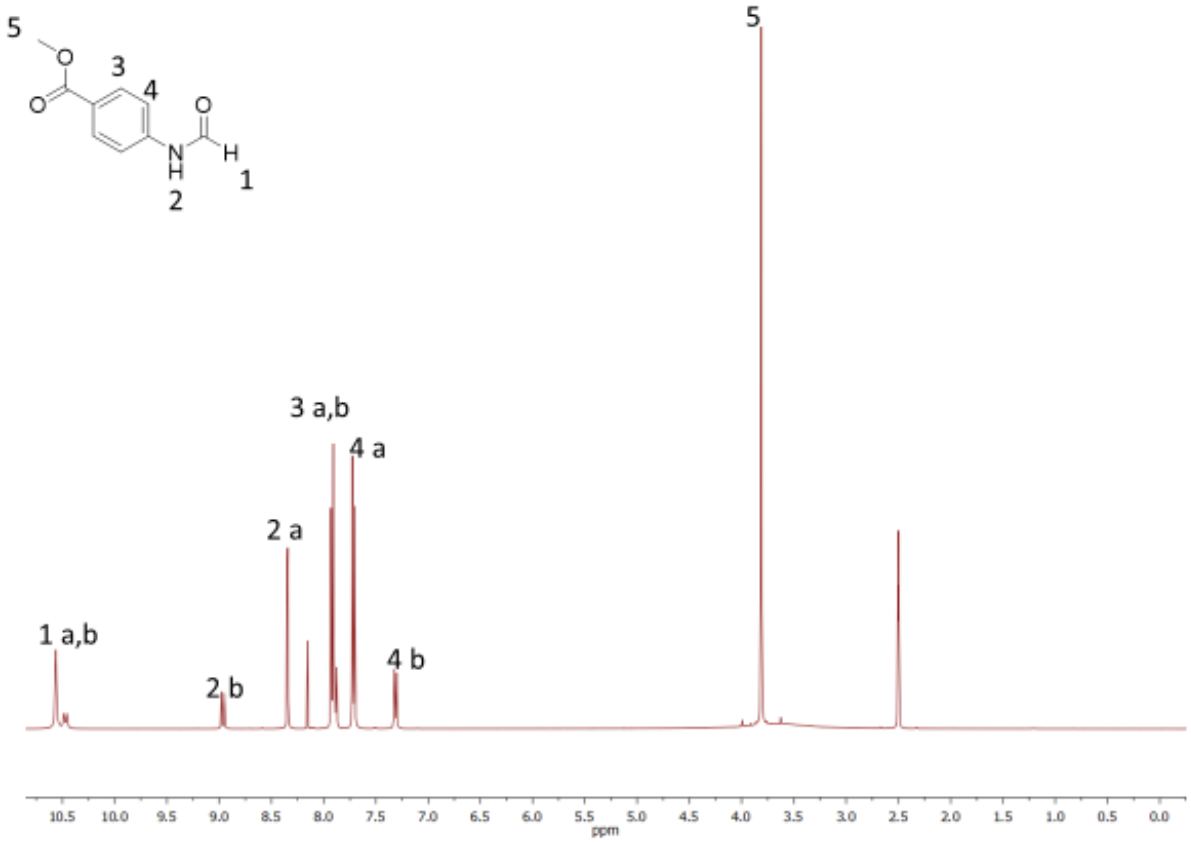

Figure 27: ^{1}H-NMR-spectrum of Methyl-4-formamidobenzoate.

^{13}C-NMR (126 MHz, $CDCl_3$) δ/ppm = 165.8, 163.2, 162.6, 160.2, 142.5, 130.8, 130.4, 124.4, 118.7, 116.5, 51.9.

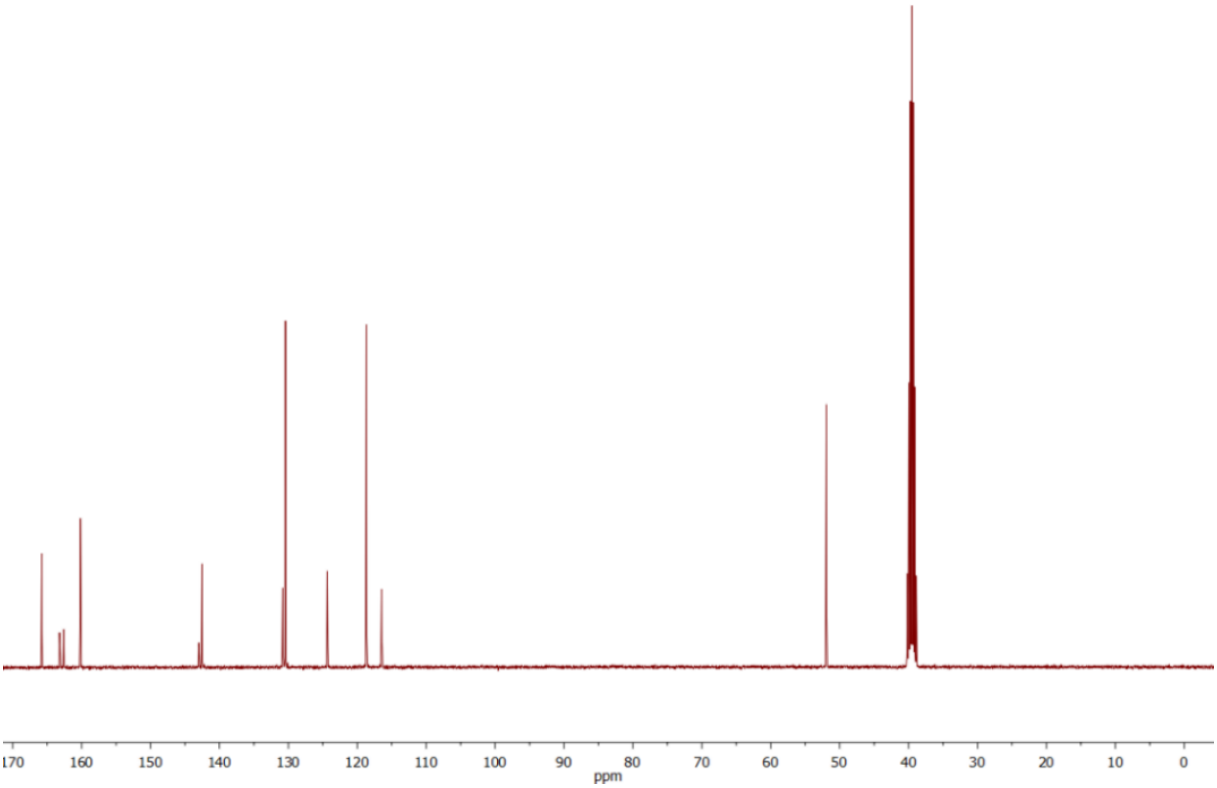

Figure 28: ^{13}C-NMR-spectrum of Methyl-4-formamidobenzoate.

EI-HRMS m/z: $[M]^+$ calculated for $[C_9H_9O_3N_1]^+$ = 179.0582, found: 179.0584, Δ = 0.1270 mmu.

IR (ATR platinum diamond): ν/cm^{-1} = 3182.0 (w), 3052.5 (w), 2961.9 (w), 2883.8 (w), 1715.5 (s), 1610.6 (s), 1522.1 (m), 1437.8 (m), 1419.3 (m), 1273.2 (s)1188.9 (s), 1038.7 (m), 1016.1 (m), 962. 6 (m), 884.5 (m), 847.4 (s), 816.6 (s), 763.1 (s), 687.0 (s), 635.6 (m), 522.5 (s), 506.0 (m), 479.3 (w), 456.6 (m).

6.3.2 Synthesis of other compounds

Methyl-4-aminobenzoate

4-Aminobenzoic acid (20.0 g, 146 mmol, 1.00 eq.) was dissolved in methanol (594 mL, 468 g, 14.6 mol, 100 eq.) and the mixture was cooled with an ice bath to 0°C. Subsequently, thionyl chloride (31.7 mL, 52.0 g, 438 mmol, 3.00 eq.) was added dropwise and the solution was stirred at room temperature overnight. The solution was neutralized with saturated $NaHCO_3$-solution and then K_2CO_3 was added till a pH-value of eight was acquired. Precipitating salts were dissolved by addition of water. Afterwards the organic phase was extracted with DCM (7 × 150 mL) and the combined organic layers were dried over sodium sulfate and filtered off. The product (22.0 g, 146 mmol) was obtained as slightly yellow crystals after removing the solvent under reduced pressure in quantitative yield.

R_f = 0.45 (cyclohexane/ethyl acetate, 2:1) visualized *via* UV quenching at 254 nm.

^{1}H-NMR (500 MHz, DMSO-d_6) δ/ppm = 7.65 (d, ^3J = 8.7 Hz, 2H, aromatic, ^{1}), 6.58 (d, ^3J = 8.7 Hz, 2H, aromatic, ^{2}), 5.97 (s, 2H, NH, ^{3}), 3.73 (s, 3H, CH_3, ^{4}).

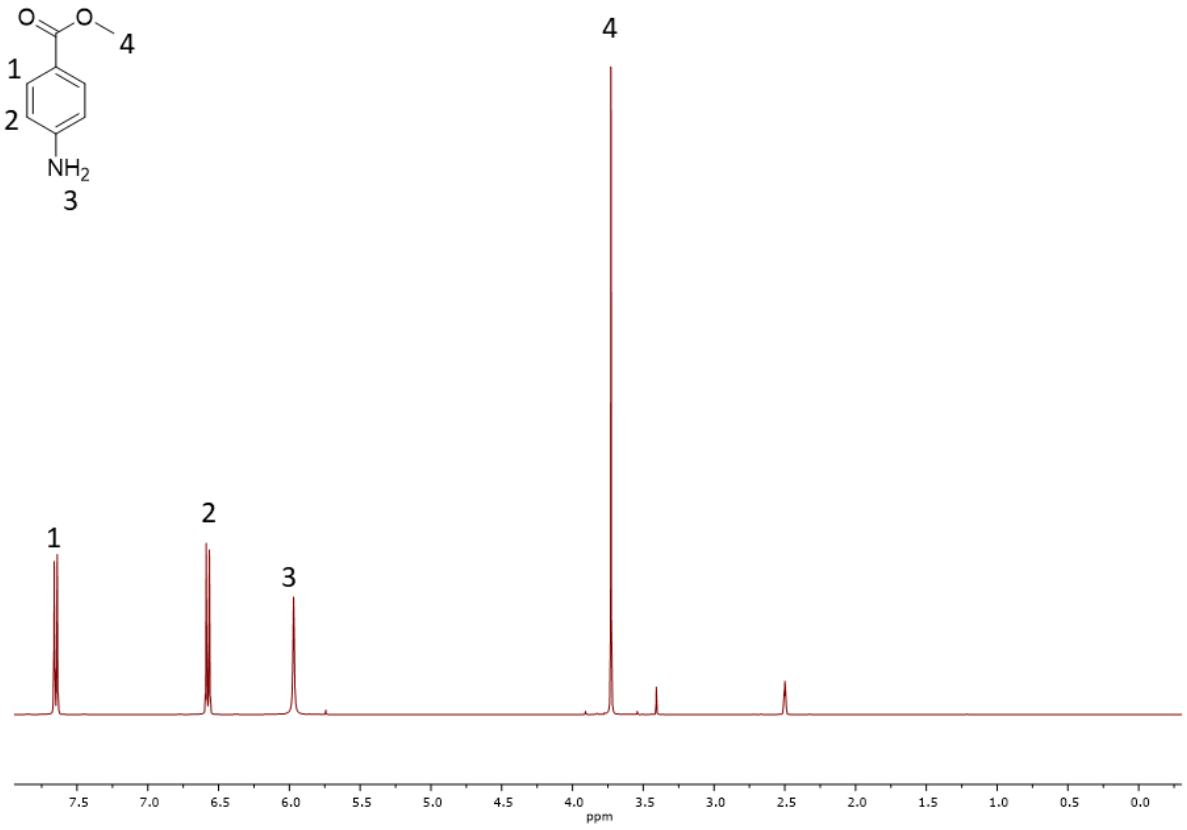

Figure 29: ^{1}H-NMR-spectrum of methyl-4-aminobenzoate.

^{13}C-NMR (126 MHz, $CDCl_3$) δ/ppm = 166.4, 153.5, 131.1, 115.8, 112.7, 51.2.

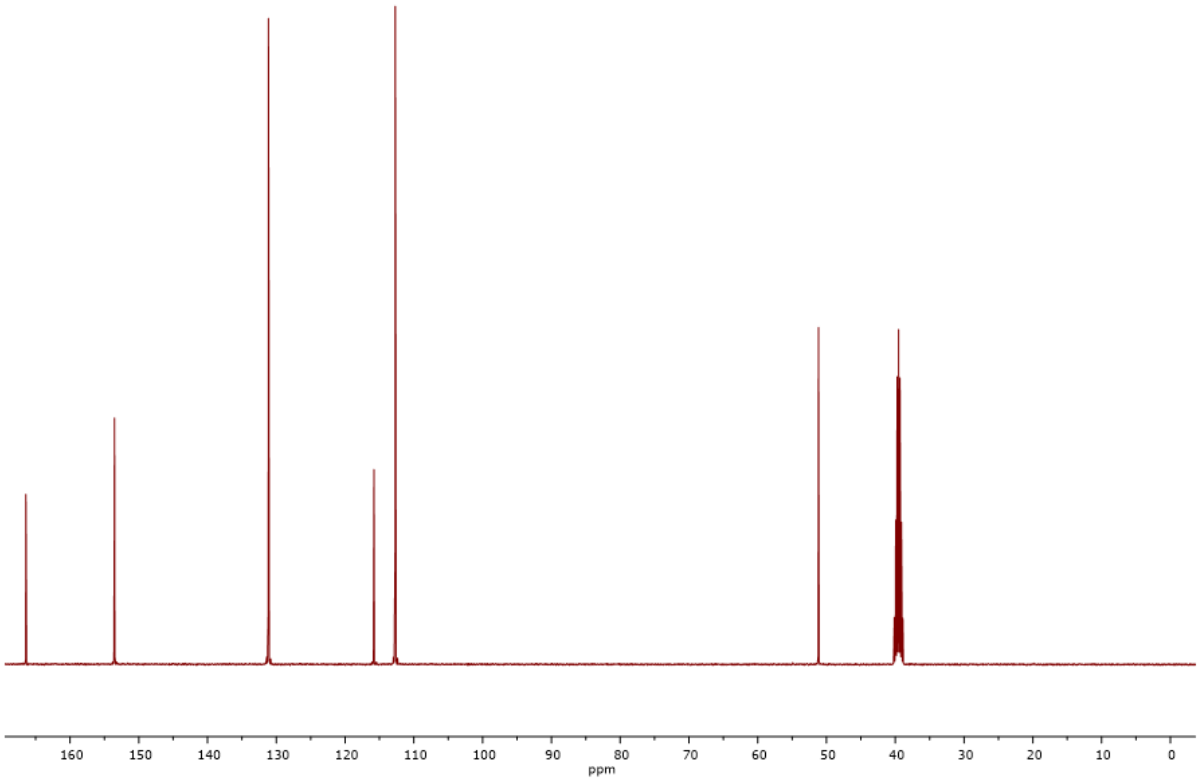

Figure 30: ^{13}C-NMR-spectrum of methyl-4-aminobenzoate.

EI-HRMS m/z: $[M]^+$ calculated for $[C_8H_9O_2N_1]^+$ = 151.0633, found: 151.0634, Δ = 0.0897 mmu.

IR (ATR platinum diamond): ν/cm^{-1} = 3406.2 (w), 3334.2 (m), 3229.3 (w), 2943.4 (w), 1680.5 (s), 1633.2 (m), 1594.1 (s), 1513.9 (m), 1433.7 (m), 1312.3 (3), 1281.5 (s), 1197.1 (w), 1174.5 (m), 1116.9 (s), 1077.8 (m), 849.5 (w), 767.2 (s), 697.3 (m), 586.2 (w), 506.0 (m).

Benzyl 11-formamidoundecanoate

11-Formamidoundecanoic acid (22.9 g, 100 mmol, 1.00 eq.) was suspended DCM (50 mL) and DIPEA (19.6 mL, 14.9 g, 115 mmol, 1.15 eq.) was added. Under stirring, benzyl bromide (17.8 mL, 25.7 g, 150 mmol, 1.50 eq.) in DCM (25 mL) was slowly added *via* a dropping funnel. The reaction mixture was stirred overnight at room temperature. After full conversion was indicated *via* TLC, triethylamine (7.62 mL, 5.57 g, 55.0 mmol, 0.550 eq.) was added and the reaction was stirred for another hour. Afterwards water (150 mL) was added, the phases were separated, and the aqueous phase was extracted with DCM (3 × 75 mL). The combined organic extracts were washed with water (3 × 150 mL). The combined organic extracts were dried over sodium sulfate, filtered and the solvent was removed under reduced pressure. The product was obtained as a slightly yellow solid (32.6 g, 102%) and was used without further purification. The analytical data is according to the literature.[193]

R_f = 0.25 (cyclohexane/ethyl acetate, 1:2) visualized *via* UV quenching at 254 nm and Seebach staining solution.

^{1}H-NMR (500 MHz, $CDCl_3$) δ/ppm = 8.15 (s, 1H, CH, ^{1a}), 8.03 (d, ^3J = Hz, 1H, CH, ^{1b}), 7.37 – 7.26 (m, 5H, aromatic, ^{2}), 5.65 (br, 1H, NH, ^{3}), 5.11 (s. 2H, CH_2, ^{4}), 3.28 (m, 2H, CH_2, ^{5a}), 3.19 (m, 2H, CH_2, ^{5b}), 2.34 (t, ^3J = 7.5 Hz, 2H, CH_2, ^{6}), 1.63 (p, ^3J = 7.5 Hz, 2H, CH_2, ^{7}), 1.63 (p, ^3J = 7.4 Hz, 2H, CH_2, ^{8}), 1.28 – 1.25 (m. 12H, CH_2, ^{9}).

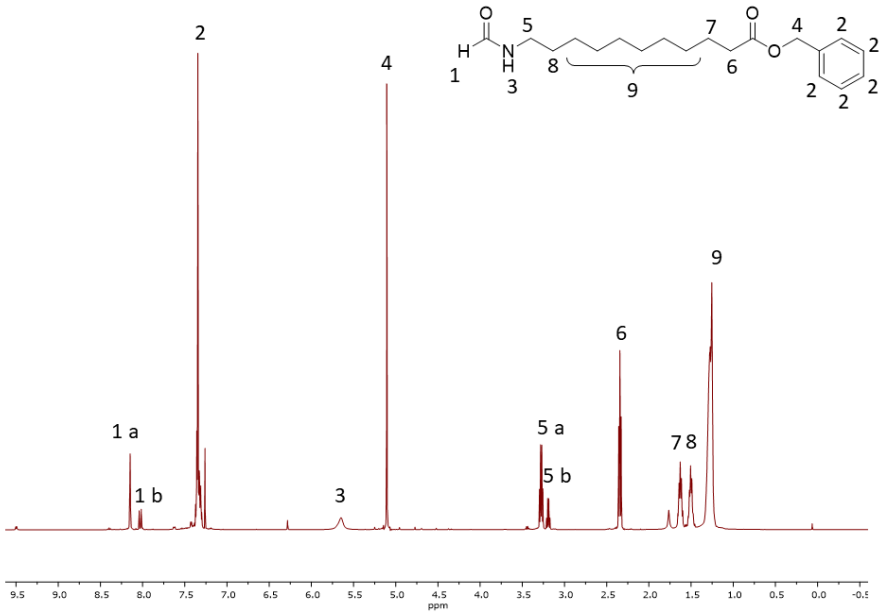

Figure 32: ^{1}H-NMR-spectrum of benzyl-11-formamidoundecanoate.

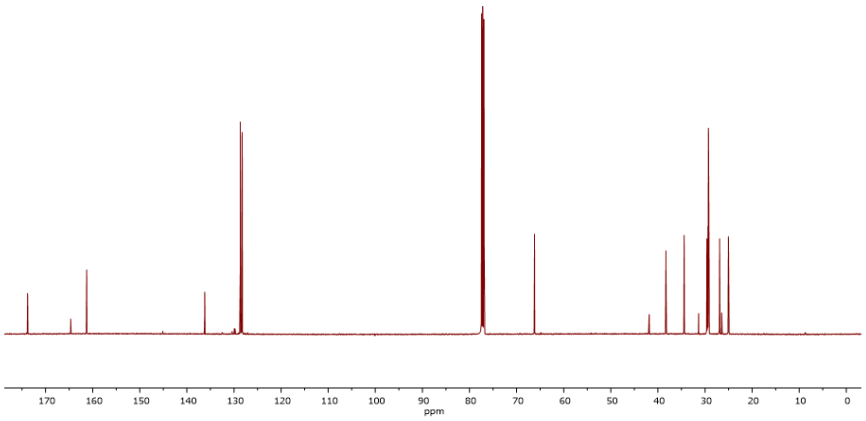

Figure 31: ^{13}C-NMR-spectrum of benzyl-11-formamidoundecanoate.

^{13}C-NMR (126 MHz, DMSO-d_6) δ/ppm = 173.8, 173.8, 164.7, 161.3, 145.13, 136.2, 128.7, 128.5, 128.3, 128.3, 66.2, 41.9, 38.3, 34.4, 31.4, 29.6, 29.5, 29.5, 29.4, 29.3, 29.2, 29.2, 27.0, 26.9, 26.5, 25.2, 25.0.

FAB-HRMS m/z: $[M+H]^+$ calculated for $[C_{19}H_{30}NO_3]^+$ = 320.2220, found: 320.2222, Δ = -0.20 mmu.

IR (ATR platinum diamond): ν/cm^{-1} = 3265.7 (w), 3069.9 (w), 2914.9 (m), 2877.4 (w), 2848.4 (w), 1731.9 (m), 1652.5 (s), 1556.6 (w), 1496.9 (w), 1470.8 (m), 1450.7 (w), 1417.4 (w), 1380.1 (m), 1351.6 (w), 1330.2 (w), 1300.0 (w), 1268.0 (w), 1246.6 (w), 1234.2 (w), 1213.3 (w), 1200.1 (w), 1160.5 (s), 1108.8 (w), 1083.2 (w), 1055.3 (w), 1029.2 (w), 997.2 (w), 938.8 (m), 923.5 (w), 903.9 (w), 866.6 (w), 825.6 (w), 806.7 (w), 753.5 (m), 718.8 (w), 695.9 (s), 609.4 (w), 520.1 (m), 487.6 (w), 451.7 (m).

6.3.3 Synthesis Procedure for P-3CR polymer 16

Using column purified diisocyanide 9

Decanedioic acid **14** (405 mg, 2.00 mmol, 1.00 eq.), heptanal **15** (1.69 mL, 1.37 mg, 0.12 mmol, 6.00 eq.) and 1,12-diisocyanododecane **9** (441 mg, 2.00 mmol, 1.00 eq.) were stirred under argon atmosphere at room temperature for 24 hours. The obtained solid was dissolved in DCM (3 mL) and was then precipitated into diethylether (75 mL). Polymer **16** (886 mg, M_n = 10517 Da, M_w = 16760 Da, PDI = 1.59) was obtained after filtration and removal of remaining solvent under reduced pressure as a brownish highly viscous oil in a yield of 67 % (in correspondence to the theoretical, maximal mass of the polymer).

Using diisocyanide 9 purified by washing

Decanedioic acid **14** (405 mg, 2.00 mmol, 1.00 eq.), heptanal **15** (1.69 mL, 1.37 mg, 0.12 mmol, 6.00 eq.) and 1,12-diisocyanododecane **9** (441 mg, 2.00 mmol, 1.00 eq.) were stirred under argon atmosphere at room temperature for 24 h. The obtained solid was dissolved in DCM (3 mL) and was then precipitated with diethylether (75 mL). Polymer **16** (886 mg, M_n = 10517 Da, M_w = 16760 Da, PDI = 1.59) was obtained after filtration and removal of remaining solvent under reduced pressure as a brownish highly viscous oil in a yield of 63 % (in correspondence to the theoretical, maximal mass of the polymer).

^{1}H-NMR (500 MHz, $CDCl_3$) δ/ppm = 6.06 (br, 2H, NH, ^{1}), 5.17-5.13 (m, 2H, CH, ^{2}), 3.27-3.21 (m, 4H, CH_2, ^{3}), 2.38 (t, ^3J = 7.5 Hz, 4H, CH_2, ^{4}), 1.88-1.75(m, 4H, CH_2, ^{5}), 1.68-1.59 (m, 4H, CH_2, ^{6}), 1.52-1.44 (m, 4H, CH_2, ^{7}), 1.35-1.24 (m, 40H, CH_2, ^{8}), 0.86 (t, ^3J = 7.0 Hz, CH_3, ^{9}).

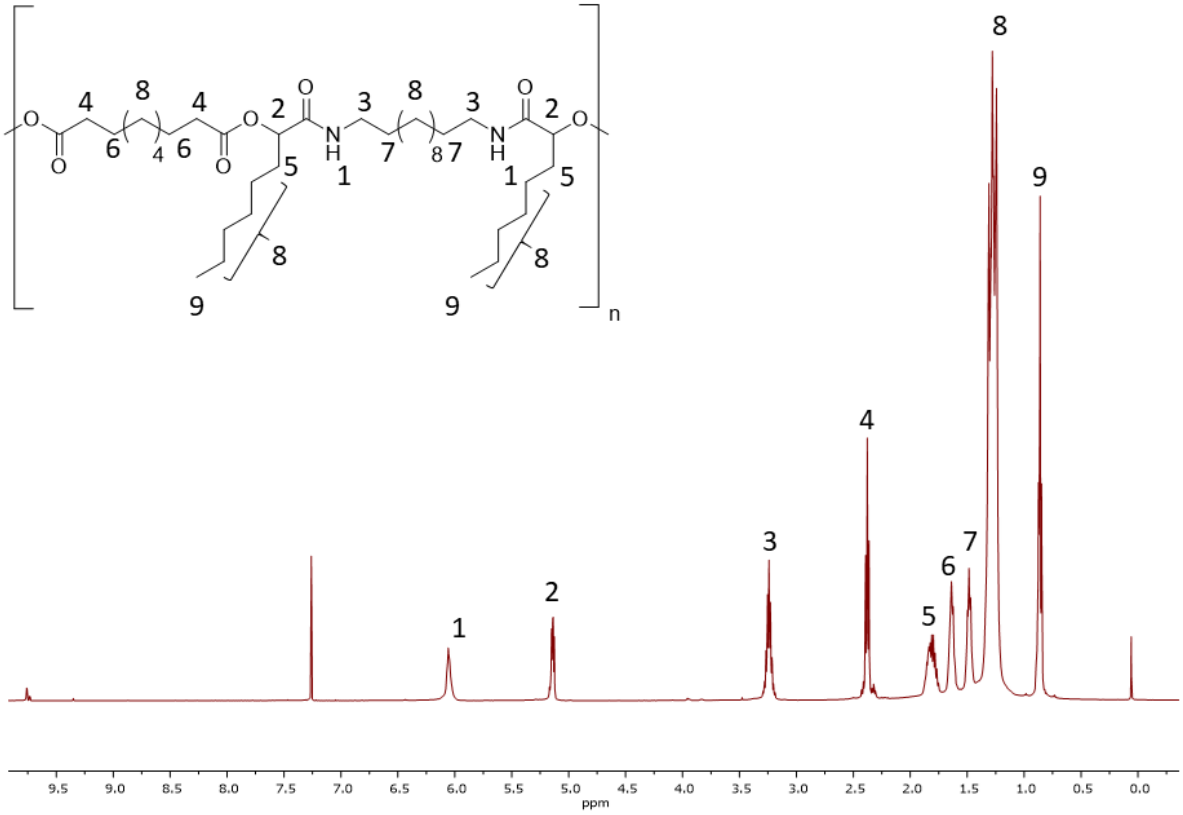

*Figure 33: ^{1}H-NMR-spectrum of passerine polymer **16**.*

^{13}C-NMR (126 MHz, DMSO-d_6) δ/ppm = 172.6, 170.0, 74.1, 39.4, 34.4, 32.1, 31.8, 29.7, 29.2, 29.0, 27.0, 25.0, 24.8, 22.7, 14.2.

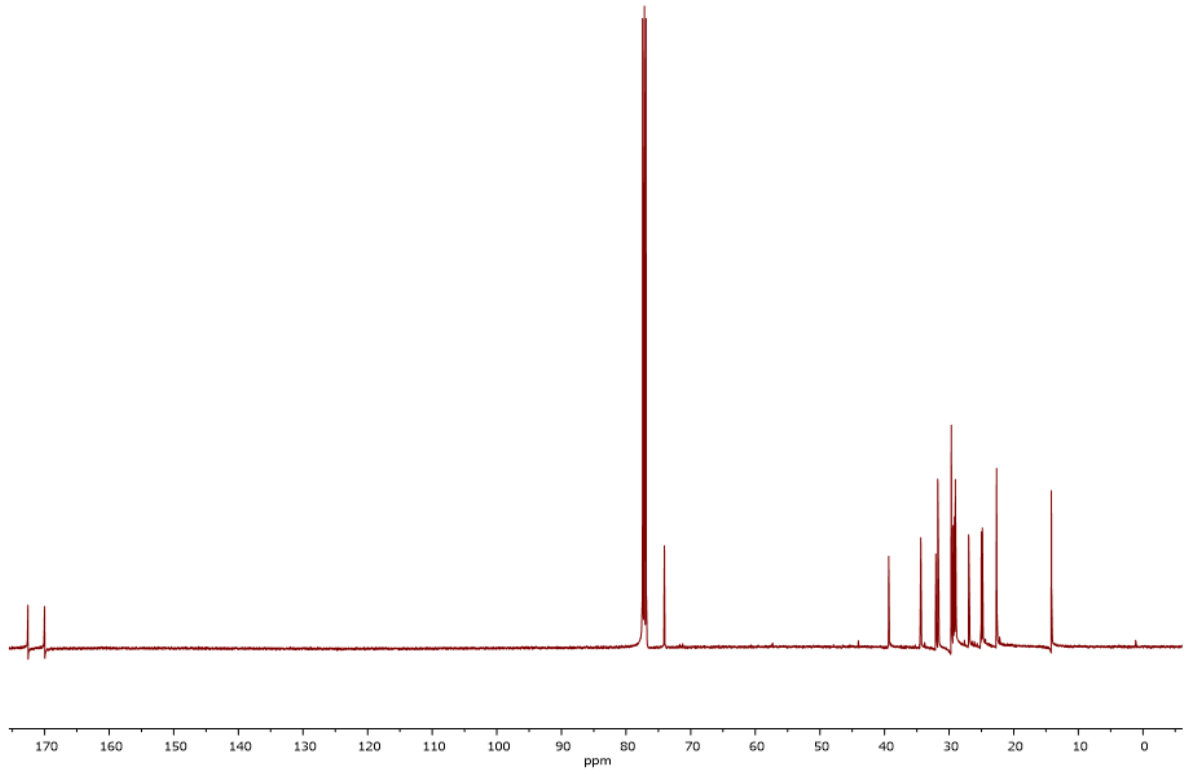

*Figure 34: ^{13}C-NMR-spectrum of passerine polymer **16**.*

IR (ATR platinum diamond): ν/cm^{-1} = 3291.3 (w), 2923 (s), 2853.7 (m), 1741.3 (m), 1653.3 (s), 1538.3 (m), 1464.0 (m), 1375.7 (w), 1236.9 (m), 1161.6 (m), 1095.5 (m), 723.0 (w).

GPC: Red curve: Passerini-polymer **16** when 1, 12-diisocyano dodecane **9** was used which was purified by flash column chromatography beforehand. M_n = 10517 Da, M_w = 16760, $Đ$ = 1.59.

Black curve: Passerini-polymer **16** when 1, 12-diisocyano dodecane **9** was used which was purified purified by washing beforehand. M_n = 8328 Da, M_w = 12615, $Đ$ = 1.51.

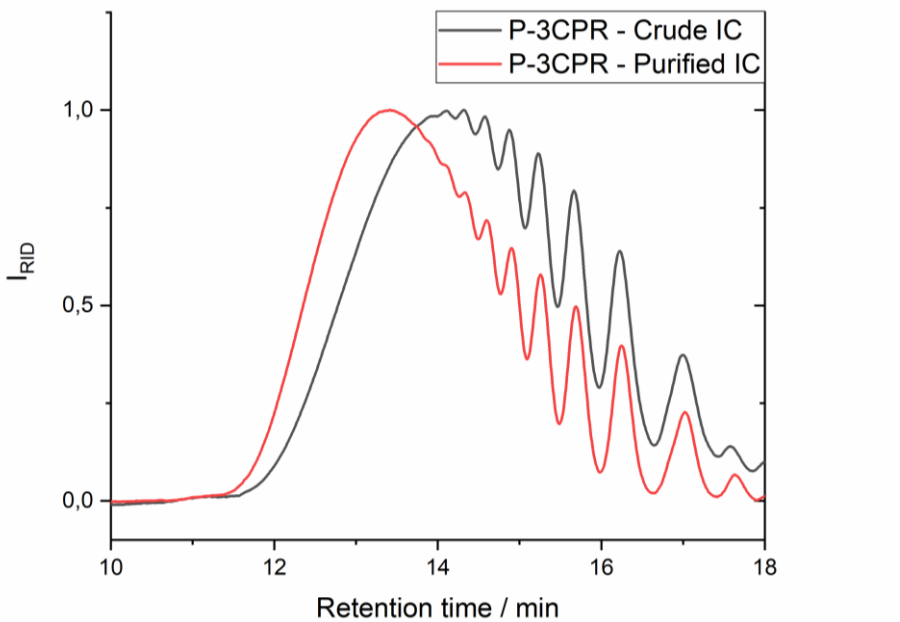

*Figure 35: SEC-curves of Passerini polymer **16**. The red curve shows the polymer obtained using the purified isocyanide (IC), the black one was obtained using isocyanide that was only purified by washing.*

6.3.4 GC-Screening, synthesis and characterization of isocyanides

General isocyanide screening with internal standard (3.00 mmol scale)

In order to determine the concentration of isocyanooctadecane in the GC screening experiments, a gas chromatography calibration curve with tetradecane as internal standard (IS) was compiled by measuring six samples

Table S1: Six sample of different concentrations of isocyanide **2** and the same concentration of IS were measured and the ratio of the area of the isocyanide **2** and the area of IS were calculated.[473]

*Table 33: GC-screening of compound **2**.*

Sample	A(**2**)	A(IS)	*c*(**2**) / mg/mL	*c*(IS) / mg/mL	*c*(**2**) / *c*(IS)	A(**2**) / A(IS)
1	2.76 E3	289	1.00	0.100	10.0	9.57
2	2.36 E3	289	0.800	0.100	8.00	8.16
3	1.81 E3	289	0.600	0.100	6.00	6.27
4	1.11 E3	289	0.400	0.100	4.00	3.83
5	492	289	0.200	0.100	2.00	1.70
6	1.69 E3	289	0.500	0.100	5.00	5.85

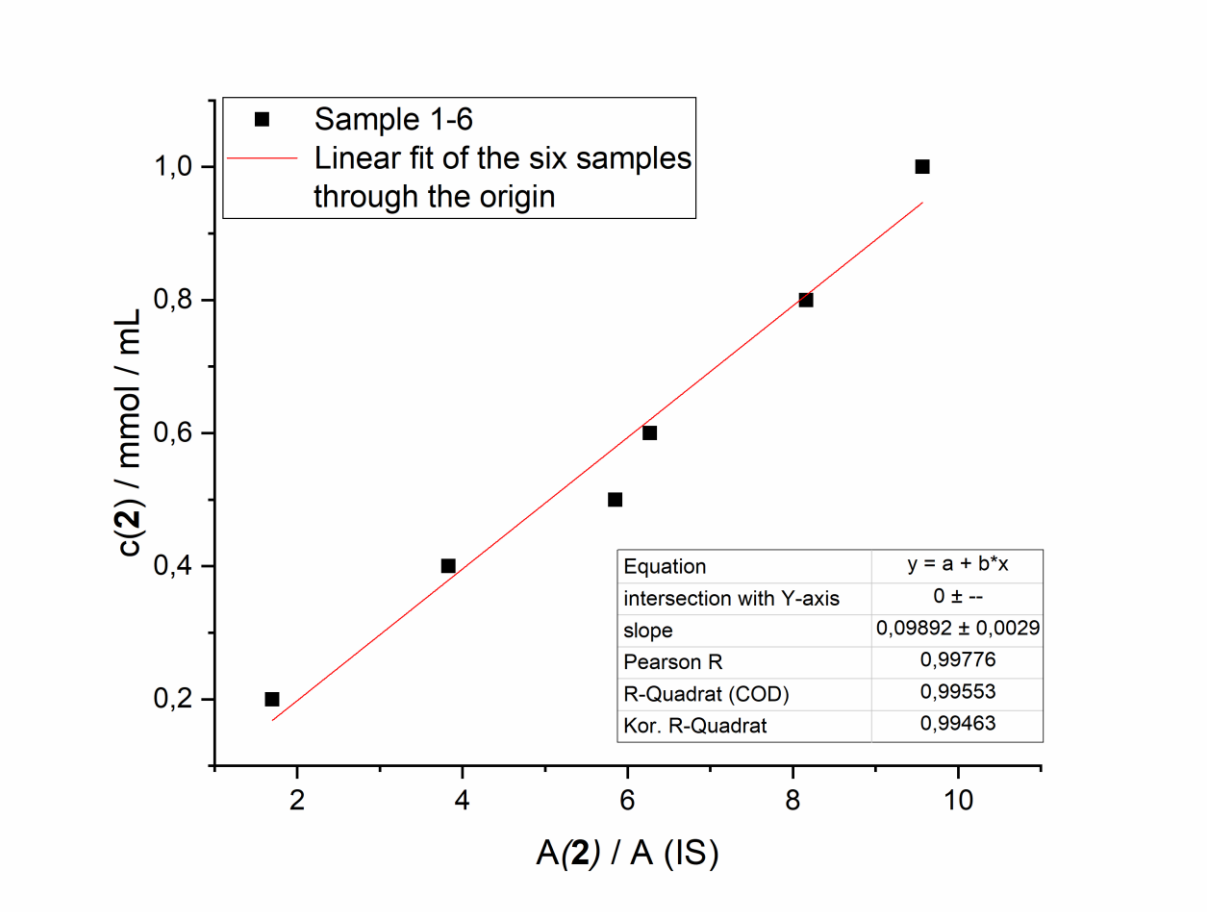

Figure 36: Calibration curve calculated using a linear fit (red line). The obtained slope was 0.0989 and the R^2-value was 0.996.[473]

In a typical GC screening experiment, 3.00 mmol of *N*-formamido octadecane **1** was dissolved in a solvent (various amount) and then, reacted with a dehydrating agent (various amounts) in presence of a base (various amounts) and a given amount of tetradecane (mostly 10 mol%). Samples were taken after different reactions times and the resulting areas of the signals of tetradecane and the product **2** were determined to calculate the yield of each specific reaction condition applying the following formulas:

$$R_{x/is} = \frac{A_x/A_{is}}{c_x/c_{is}} \quad (6)$$

$R_{x/is}$ is the slope of the calibration curve, whereas A_x, A_{is}, c_x and c_{is} correspond to the measured area and concentration of standard (is) and analyte (x).

$$c_x = \frac{c_x}{c_{is}} c_{is} \quad (7)$$

As the amount of internal standard and therefore its concentration is known, the unknown concentration of analyte (x) and the corresponding yield can be calculated, respectively.

General isocyanide synthesis in DCM (5.00 mmol scale)

The formamide (5.00 mmol, 1.00 eq.) was dissolved in DCM (5 mL) and pyridine (15.0 mmol, 3.00 eq.) was added. Subsequently, *p*-TsCl (7.50 mmol, 1.50 eq.) was added under cooling with a water bath. The cooling was removed, and the reaction mixture was stirred until full conversion (monitored *via* TLC, average reaction time of 2 hours) was observed. Afterwards, aqueous Na_2SO_4-solution (5 mL, 20 wt%) was added and the biphasic mixture was stirred for another 30 minutes. Water (10 mL) and DCM (10 mL) were added, and the organic phase was separated. The aqueous phase was extracted with DCM (3 × 5 mL), the organic extracts were combined and washed with water (3 × 5 mL) and saturated sodium chloride solution (2 × 5 mL). The organic extract was dried over sodium sulfate, filtered and the solvent was removed under reduced pressure. Further purification was not necessary in many cases. Nevertheless, purification by flash column chromatography (mixture of cyclohexane and ethyl acetate) could be applied to obtain the product in higher purity.

General isocyanide synthesis in DMC (5.00 mmol scale)

The formamide (5.00 mmol, 1.00 eq.) was dissolved in DMC (5 mL) and pyridine (15.0 mmol, 3.00 eq.) was added. Subsequently, *p*-TsCl (7.50 mmol, 1.50 eq.) was added under cooling with a water bath. The cooling was removed, and the reaction mixture was stirred until full conversion (monitored *via* TLC, average reaction time of 24 hours) was observed. Afterwards, aqueous Na_2SO_4-solution (5 mL, 20 wt%) were added and the biphasic mixture was stirred for another 30 minutes. Water (10 mL) and DMC (10 mL) were added, and the organic phase was separated. The aqueous phase was extracted with DMC (3 × 5 mL), the organic extracts were combined and washed with water (3 × 5 mL) and saturated sodium chloride solution (2 × 5 mL). The organic extract was dried over sodium sulfate, filtered and the solvent was removed under reduced pressure. Further purification was not necessary in many cases. Nevertheless, purification by flash column chromatography (mixture of cyclohexane and ethyl acetate) could be applied to obtain the product in higher purity).

1-Isocyano octadecane 2

Obtained as rose solid in a yield of 96 % (DCM) or 89 % (DMC).
R_f = 0.47 (cyclohexane/ethyl acetate, 15:1) visualized *via* UV quenching at 254 nm and vanillin staining solution.
^{1}H-NMR (500 MHz, $CDCl_3$) δ/ppm = 3.31 (tt, ^3J = 6.8 Hz, ^2J = 1.8 Hz, 2H, CH_2, ^{1}), 1.61 (m, 2H, CH_2, ^{2}), 1.36 (t, ^3J = 7.0 Hz, 2H, CH_2, ^{3}), 1.23-1.19 (m, 30H, CH_2, ^{4}), 0.81(t, ^3J = 7.0 Hz, 3H, CH_3, ^{5}).

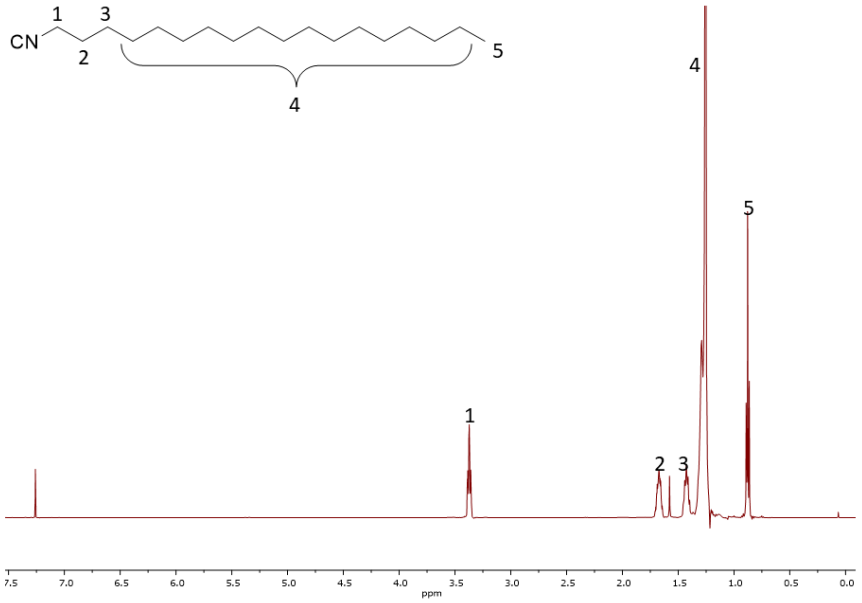

*Figure 37: ^{1}H-NMR-spectrum of isocyanide **2**.*

^{13}C-NMR (126 MHz, $CDCl_3$) δ/ppm = 155.7 (t), 41.7 (t), 32.1, 29.8, 29.7, 29.5, 29.3, 28.9, 26.5, 22.8, 14.3.

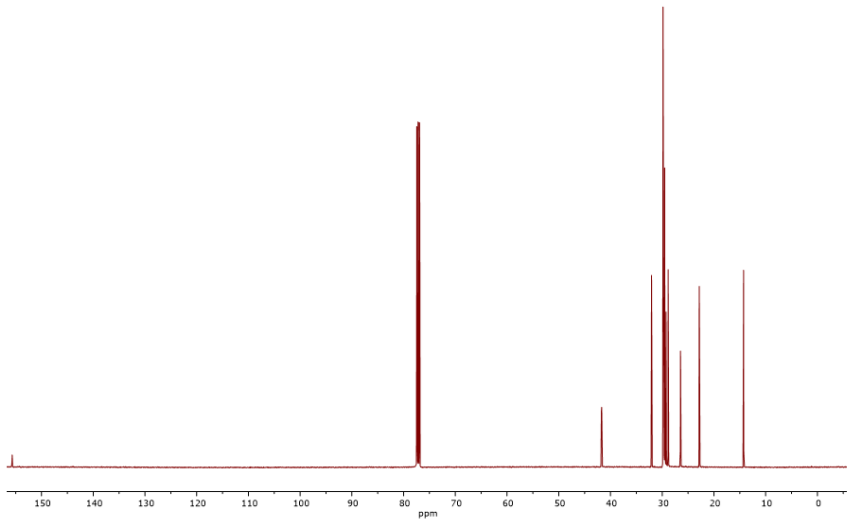

*Figure 38: ^{13}C-NMR-spectrum of isocyanide **2**.*

EI-HRMS m/z: $[M]^+$ calculated for $[C_{19}H_{37}N_1]^+$ = 279.2925, found: 279.2926, Δ = 0.1324 mmu.

IR (ATR platinum diamond): ν/cm^{-1} = 2912.6 (s), 2848.8 (s), 2151.5 (m), 1470.7 (m), 717.9 (m).

1-Isocyano dodecane 3

Obtained as yellow liquid in a yield of 90 % (DCM) and 94 % (DMC).
R_f = 0.58 (cyclohexane/ethyl acetate, 15:1) visualized *via* UV quenching at 254 nm and vanillin staining solution (orange).

^{1}H-NMR (500 MHz, $CDCl_3$) δ/ppm = 3.37 (tt, ^3J = 6.8 Hz, ^2J = 1.9 Hz, 2H, CH_2, ^{1}), 1.70-1.62 (m, 2H, CH_2, ^{2}), 1.42 (quint, ^3J = 7.3 Hz, 2H, CH_2, ^{3}), 1.30-1.26 (m, 16H, CH_2, ^{4}), 0.87 (t, ^3J = 7.0 Hz, CH_3, ^{5}).

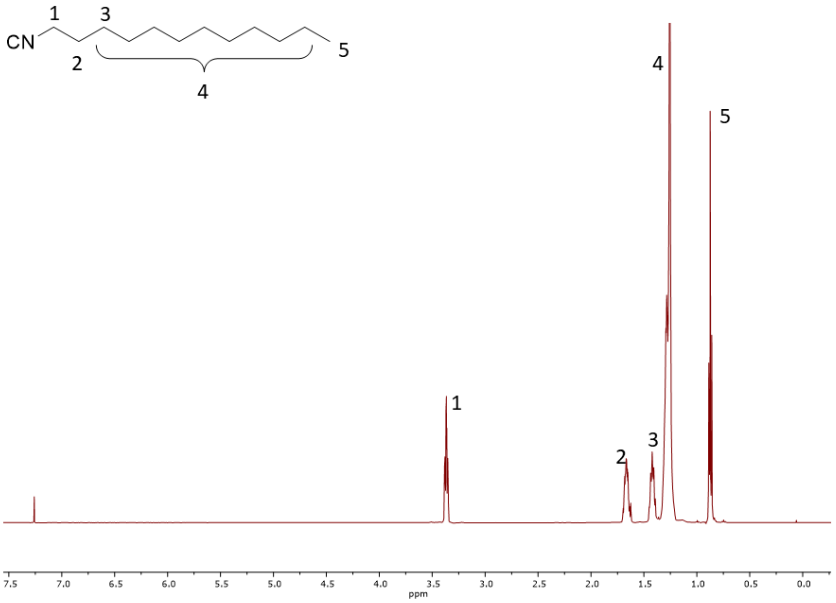

*Figure 39: ^{1}H-NMR-spectrum of isocyanide **3**.*

^{13}C-NMR (126 MHz, $CDCl_3$) δ/ppm = 155.7 (t), 41.7 (t), 32.0, 29.7, 29.6, 29.5, 29.4, 29.2, 28.8, 26.4, 22.8, 14.2.

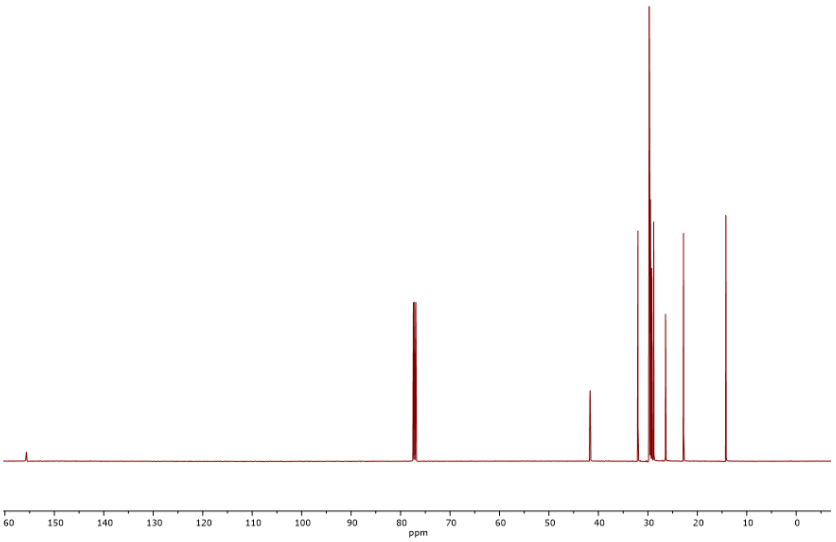

*Figure 40: ^{13}C-NMR-spectrum of isocyanide **3**.*

EI-HRMS m/z: $[M-H]^+$ calculated for $[C_{13}H_{24}N_1]^+$ = 194.1909, found: 194.1909, Δ = 0.0392 mmu.

IR (ATR platinum diamond): ν/cm^{-1} = 2922.9 (s), 2852.9 (s), 2145.4 (s), 1458.3 (m).

(*Z*)-1-Isocyanooctadec-9-ene 4

Was obtained as yellowish oil in a yield of 97 % (DCM) and 98 % (DMC)
R_f = 0.70 (cyclohexane/ethyl acetate, 9:1) visualized *via* vanillin staining solution (yellow/orange to brown).
^{1}H-NMR-spectra is in accordance with the literature.[503]

Benzyl 11-isocyanoundecanoate 5

Obtained as yellowish liquid in a yield of 97 % (DCM) and 87 % (DMC)
R_f = 0.63 (cyclohexane/ethyl acetate, 9:1) visualized *via* UV quenching at 254 nm and vanillin staining solution (brown).
^{1}H-NMR (500 MHz, $CDCl_3$) δ/ppm = 7.37-7.30 (m, 5H, aromatic, ^{1}), 5.11 (s, 2H, CH_2, ^{2}), 3.35 (tt, ^3J = 6.8 Hz, ^2J = 1.9 Hz, 2H, CH_2, ^{3}), 2.35 (t, ^3J = 7.5 Hz, 2H, CH_2, ^{4})1.69-1.61 (m, 4H, CH_2, ^{5}), 1.41 (quint, ^3J = 7.3 Hz, 4H, CH_2, ^{6}), 1,33-1.28 (m, 10H, CH_2, ^{7}).

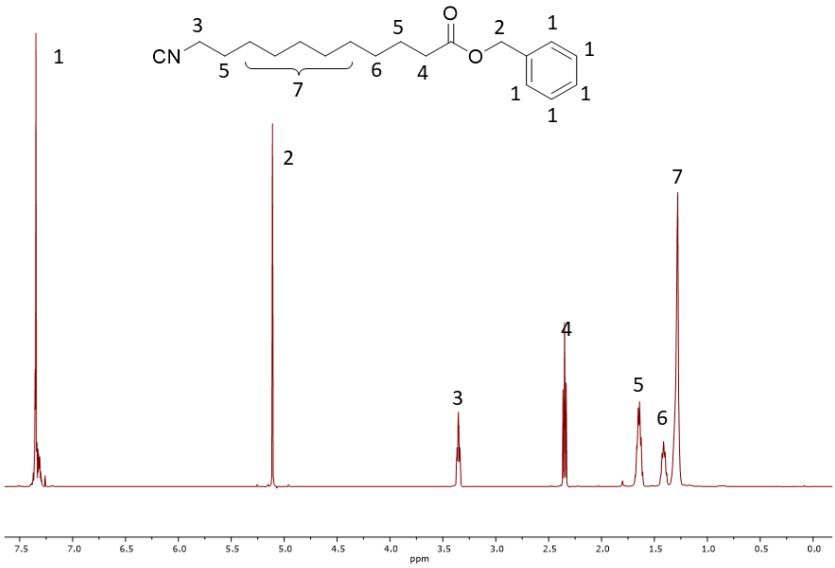

*Figure 41: ^{1}H-NMR-spectrum of isocyanide **5**.*

^{13}C-NMR (126 MHz, $CDCl_3$) δ/ppm = 173.6, 155.7 (br), 136.1, 128.5, 128.1, 66.0, 41.5 (t), 34.3, 29.3, 29.1, 29.0, 28.6, 26.3, 24.9.

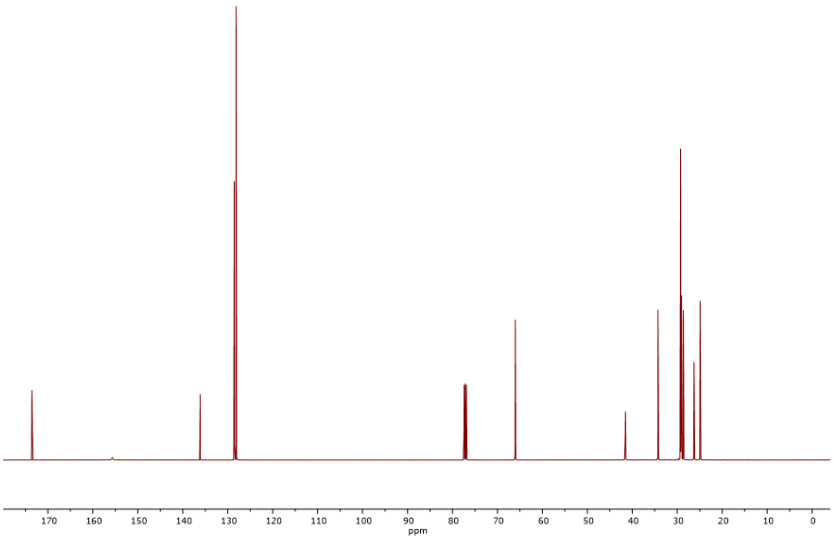

*Figure 42: ^{13}C-NMR-spectrum of isocyanide **5**.*

EI-HRMS m/z: $[M]^+$ calculated for $[C_{19}H_{27}O_2N_1]^+$ = 301.2042, found: 301.2043, Δ = 0.1494 mmu.
IR (ATR platinum diamond): ν/cm^{-1} = 2924.9 (s), 2855.0 (s), 2145.4 (m), 1734.0 (s), 1454.2 (m), 1162.2 (s), 736.4 (s), 697.3 (s).

6-Isocyanohexyl benzenesulfonate 6

Obtained as brown oil a yield of 53 % (DCM) and 68 % (DMC).
R_f = 0.69 (cyclohexane/ethyl acetate, 2:1) visualized *via* vanillin staining solution (orange).
^{1}H-NMR (500 MHz, $CDCl_3$) δ/ppm = 7.79 (d, ^3J = 8.4 Hz, 2H, aromatic, ^{1}), 7.35 (d, ^3J = 8.0 Hz, 2H, aromatic, ^{2}), 4.03 (t, ^3J = 6.3 Hz, 2H, CH_2, ^{3}), 3.35 (tt, ^3J = 6.6 Hz, ^2J = 1.9 Hz, 2H, CH_2, ^{4}), 2.45 (s, 3H, CH_3, ^{5}), 1.69-1.61 (m, 4H, CH_2, ^{6}), 1.44-1.33 (m, 4H, CH_3, ^{7}).

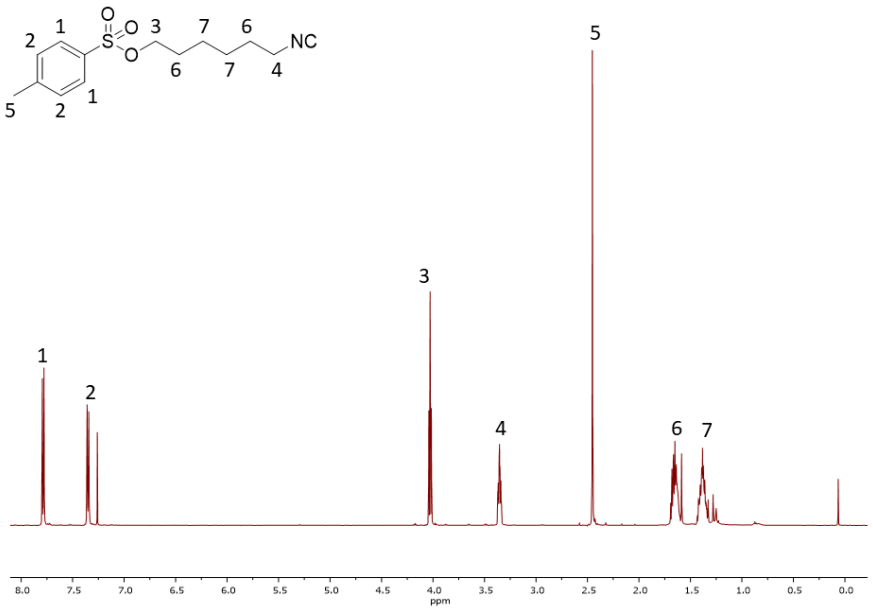

*Figure 44:^{13}C-NMR-spectrum of isocyanide **6**.*

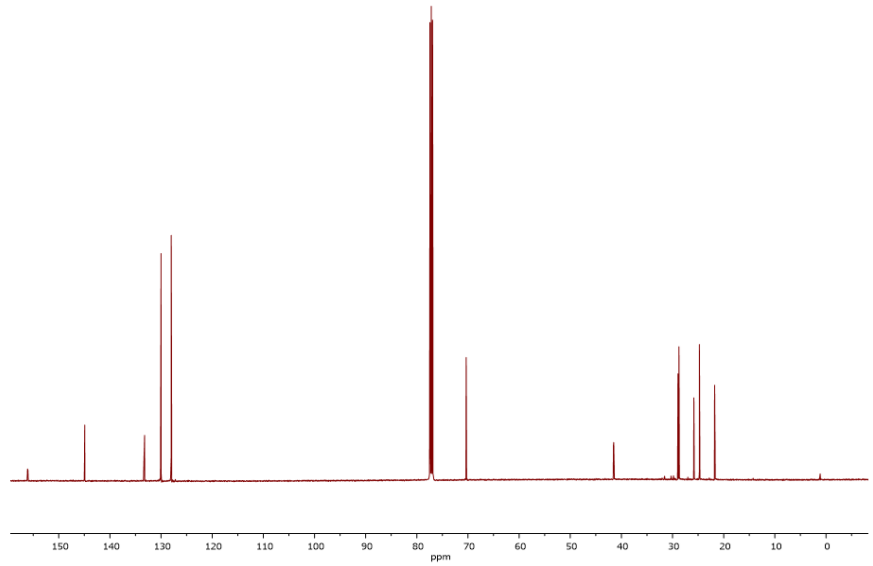

*Figure 43: ^{13}C-NMR-spectrum of isocyanide **6**.*

^{13}C-NMR (126 MHz, $CDCl_3$) δ/ppm = 156.1 (t), 144.9, 133.2, 130.0, 128.0, 70.3, 41.5 (t), 29.0, 28.8, 25.8, 24.8, 21.8.

EI-HRMS m/z: $[M]^+$ calculated for $[C_{14}H_{19}O_3N_1{}^{32}S_1]^+$ = 281.1086, found: 281.1086, Δ = 0.0435 mmu.

IR (ATR platinum diamond): ν/cm^{-1} = 2938.0 (w), 2862.9 (w), 2147.8 (w), 1597.7 (w), 1454.3 (w), 1353.4 (m), 1306.6 (w), 1187.9 (m), 1173.0 (s), 1096.5 (w), 1019.1 (w), 956.7 (m), 917.6 (m), 814.1 (m), 749.0 (w), 725.1 (w), 688.0 (w), 662.0 (s), 575.2 (m), 553.2 (s).

1,5-Diisocyano pentane 7

Obtained as brownish liquid in a yield of 48 % (DCM) and 82 % (DMC).
R_f = 0.48 (cyclohexane/ethyl acetate, 2:1) visualized *via* UV quenching at 254 nm and vanillin staining solution (orange).
^{1}H-NMR (500 MHz, $CDCl_3$) δ/ppm = 3.37 (tt, ^3J = 6.5 Hz, ^2J = 2.0 Hz, 4H, CH_2, ^{1}), 1.71-1.64 (m, 4H, CH_2, ^{2}), 1.58-1.52 (m, 2H, CH_2, ^{3}).

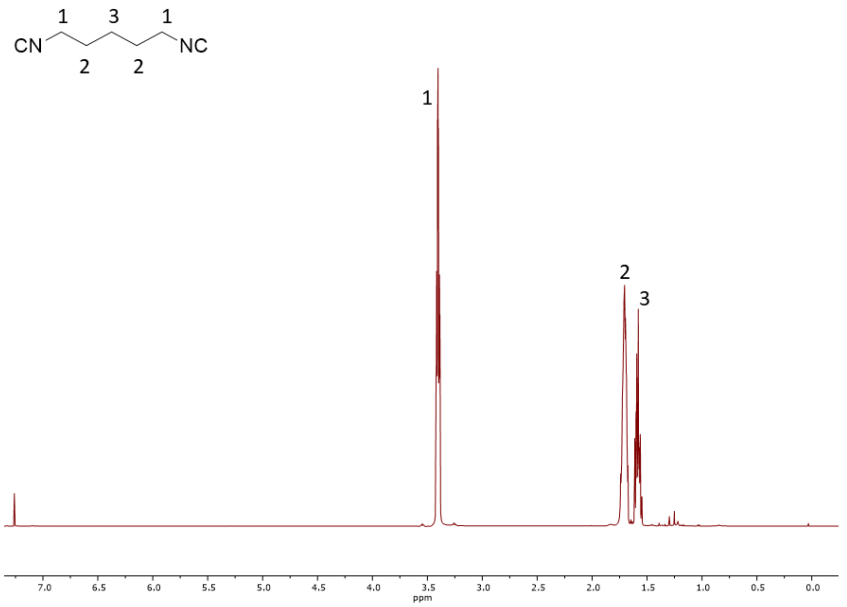

*Figure 45: ^{1}H-NMR-spectrum of isocyanide **7**.*

^{13}C-NMR (126 MHz, $CDCl_3$) δ/ppm = 156.3 (t), 41.3 (t), 28.2, 23.3.

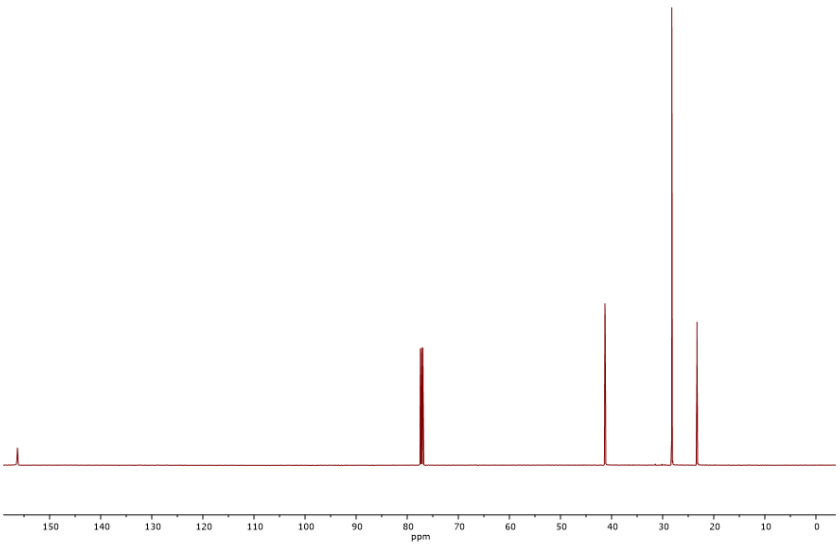

*Figure 46: ^{13}C-NMR-spectrum of isocyanide **7**.*

EI-HRMS m/z: $[M-H]^+$ calculated for $[C_7H_9N_2]^+$ = 121.0765, found: 121.0766, Δ = 0.0416 mmu.

IR (ATR platinum diamond): ν/cm^{-1} = 2922.7 (s), 2852.9 (s), 2145.4 (m), 1464.5 (m), 1352.4 (w), 722.0 (w).

1,10-Diisocyanido decane 8

Obtained as yellow liquid in a yield of 93 % (DCM) and 89 % (DMC).
R_f = 0.44 (cyclohexane/ethyl acetate, 4:1) visualized *via* UV quenching at 254 nm and vanillin staining solution (orange).
^{1}H-NMR (500 MHz, $CDCl_3$) δ/ppm = 3.37 (tt, ^3J = 6.8 Hz, ^2J = 1.8 Hz, 4H, CH_2, ^{1}), 1.69-1.62 (m, 4H, CH_2, ^{2}), 1.42 (quint, ^3J = 7.1 Hz, 4H, CH_2 ^{3}), 1.31-1.29 (m, 8H, CH_2, ^{4}).

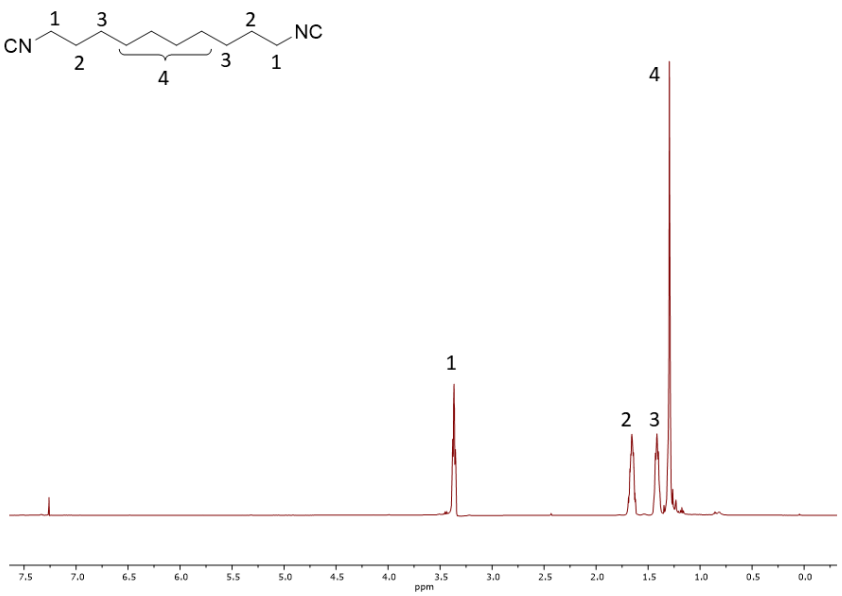

*Figure 47: ^{1}H-NMR-spectrum of isocyanide **8**.*

^{13}C-NMR (126 MHz, $CDCl_3$) δ/ppm = 155.8 (br), 41.6 (t), 29.2, 29.1, 28.7, 26.3.

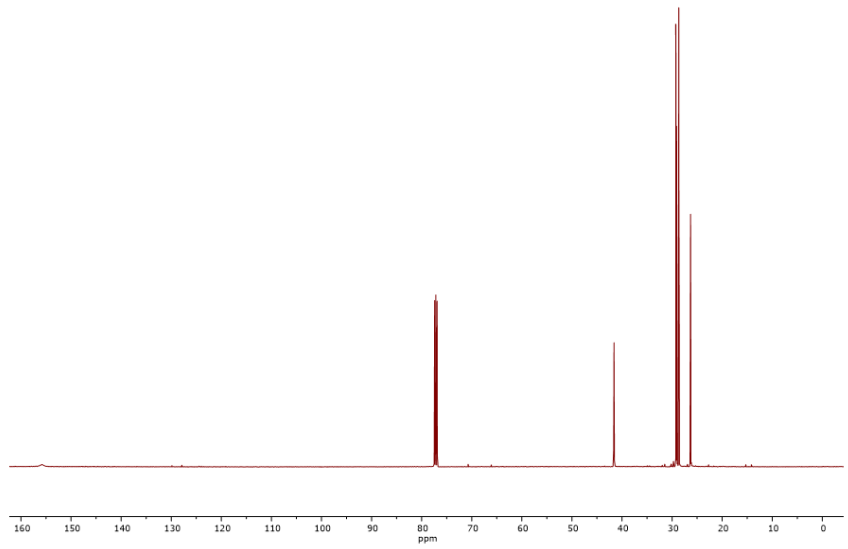

*Figure 48: ^{13}C-NMR-spectrum of isocyanide **8**.*

EI-HRMS m/z: $[M-H]^+$ calculated for $[C_{12}H_{19}N_2]^+$ = 191.1548, found: 191.1547, Δ = 0.1013 mmu.

IR (ATR platinum diamond): ν/cm^{-1} = 2927.0 (s), 2857.0 (s), 2145.4 (s), 1454.2 (m), 1351.4 (w).

1,12-Diisocyano dodecane 9

Obtained as yellow liquid in a yield of 87 % (DCM) and 97 % (DMC)
R_f = 0.44 (cyclohexane/ethyl acetate, 9:1) visualized *via* UV quenching at 254 nm and vanillin staining solution (orange).
^{1}H-NMR (500 MHz, $CDCl_3$) δ/ppm = 3.36 (tt, ^3J = 6.8 Hz, ^2J = 1.9 Hz, 4H, CH_2, ^{1}), 1.68-1.62 (m, 4H, CH_2, ^{2}), 1.41 (quint, ^3J = 7.3 Hz, 4H, CH_2, ^{3}), 1,3 -1.23 (m, 12H, CH_2, ^{4}).

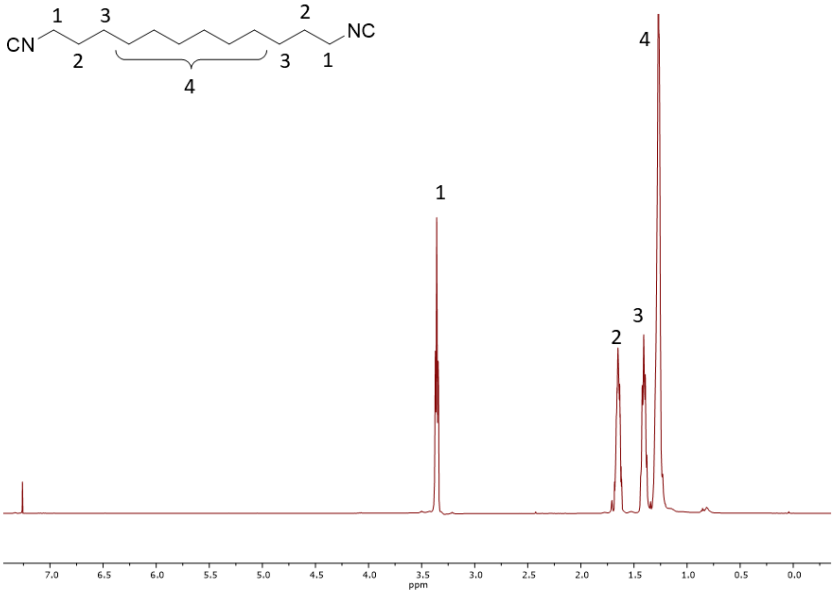

*Figure 49: ^{1}H-NMR-spectrum of isocyanide **9**.*

^{13}C-NMR (126 MHz, $CDCl_3$) δ/ppm = 155.6 (br), 41.6 (t), 29.4, 29.3, 29.1, 28.7, 26.3.

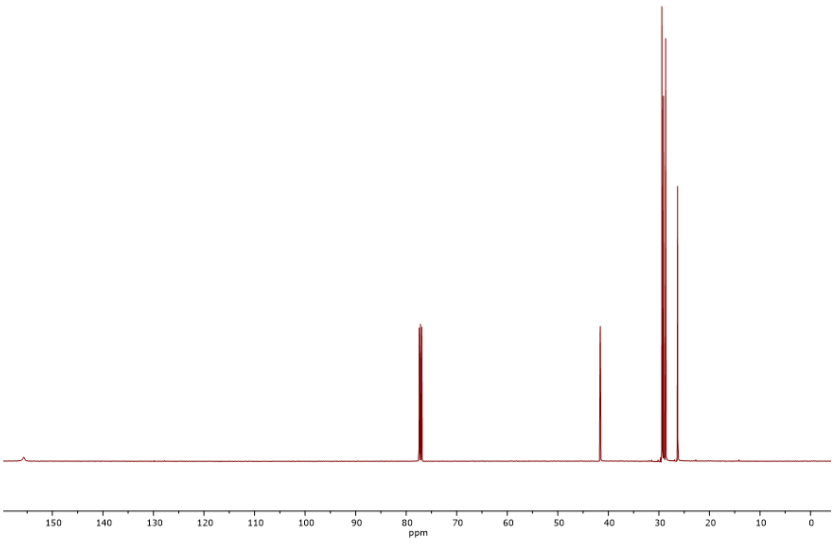

*Figure 50: ^{13}C-NMR-spectrum of isocyanide **9**.*

EI-HRMS m/z: $[M-H]^+$ calculated for $[C_{14}H_{23}N_2]^+$ = 219.1861, found: 219.1863, Δ = 0.2013 mmu.
IR (ATR platinum diamond): ν/cm^{-1} = 2924.9 (s), 2855.0 (s), 2145.4 (s), 1456.3 (m).

1-Isocyano cyclohexane 10

Was obtained as yellowish liquid in a yield of 67 % (DCM) and 68 % (DMC)
R_f = 0.57 (cyclohexane/ethyl acetate, 9:1) visualized *via* UV quenching at 254 nm, Seebach staining solution and vanillin staining solution (orange).
^{1}H-NMR-spectra was in accordance with the literature.[623]

1-Isocyano methylbenzene 11

Was obtained as dark brown liquid in a yield of 67 % (DCM) and 68 % (DMC)
R_f = 0.66 (cyclohexane/ethyl acetate, 10:1) visualized *via* Seebach staining solution and vanillin staining solution (orange).
^{1}H-NMR-spectra is in accordance with the literature.[503]

1-isocyano adamantane 12

Was obtained white solid in a yield of 79 % (DCM) and 78 % (DMC)
R_f = 0.83 (cyclohexane/ethyl acetate, 4:1) visualized *via* vanillin staining solution (orange).
^{1}H-NMR-spectra is in accordance with the literature.[503]

Methyl 4-isocyanobenzoate 13

The Methyl-4-formamidobenzoate (1.00 g, 5.58 mmol, 1.00 eq.) was dissolved in DCM (5.58 mL) and pyridine (1.53 mL, 1.50 g, 19.0 mmol, 3.40 eq.) was added. Subsequently, *p*-TsCl (1.81 g, 9.49 mmol, 1.70 eq.) was added under cooling with a water bath. The cooling was removed, and the reaction mixture was stirred for 165 minutes. Afterwards, aqueous, saturatedNa_2SO_4-solution (24 mL) were added and the biphasic mixture was stirred for another 30 minutes. Water (10 mL) and DCM (10 mL) were added, and the organic phase was separated. The aqueous phase was extracted with DCM (3 × 5 mL). The organic layers were dried over sodium sulfate, filtered and the solvent was removed under reduced pressure. The product was obtained as black solid (120 mg, 0.740 mmol) after purification by column chromatography (cyclohexane / ethyl acetate, 3 :1) in a yield of 13 %.

^{1}H-NMR (400 MHz, DMSO-d_6) δ/ppm = 8.02 (d, ^3J = 8.5 Hz, 2H, aromatic, ^{1}), 7.69 (d, ^3J = 8.5 Hz, 2H, aromatic, ^{2}), 3.86 (s, 3H, CH_3, ^{3}).

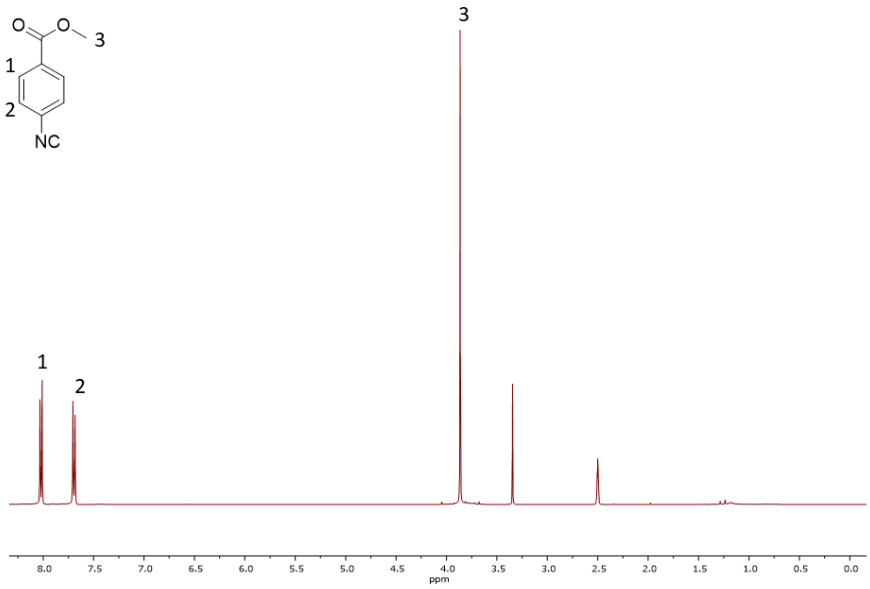

*Figure 51: ^{1}H-NMR-spectrum of isocyanide **13**.*

^{13}C-NMR (101 MHz, DMSO-d_6) δ/ppm = 166.6, 164.9, 130.6, 130.5, 129.2, 126.9.

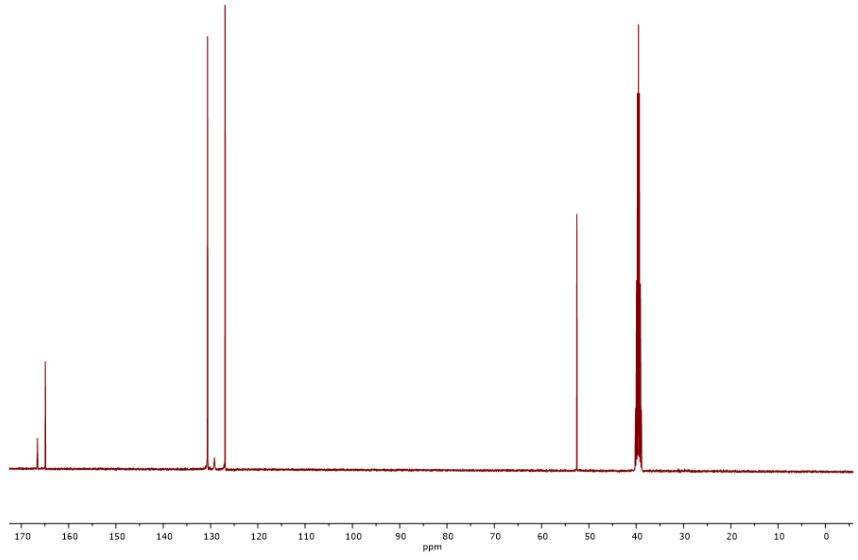

*Figure 52: ^{13}C-NMR-spectrum of isocyanide **13**.*

EI-HRMS m/z: $[M]^+$ calculated for $[C_9H_7O_2N_1]^+$ = 161.0477, found: 161.0475, Δ = -0.1514 mmu.

IR (ATR platinum diamond): ν/cm^{-1} = 3088.2 (w, br), 2952.8 (w), 2127.9 (s), 1715.5 (s), 1604.6 (m), 1504.1 (w), 1428.2 (m), 1272.2 (s), 1168.6 (m), 1102.9 (s), 1017.8 (m), 955.2 (m), 864.9 (s), 833.1 (m), 760.3 (s), 686.4 (m), 637.1 (w), 571.5 (m), 513.0 (m), 448.4 (w).

6.4 Synthesis of thioureas *via* AM-3CR and evaluation of their catalytic activities depending on their moieties

6.4.1 Quantification of hydrogen bonding strength *via* ^{31}P-NMR

The hydrogen bonding strength of thiourea compounds was determined adopting the protocol from Franz *et al*.[527] Here, less expensive $CDCl_3$ (dried over 4 Å molecular sieve) was used for the stock solution of $POEt_3$ (c = 0.18 M) instead of CD_2Cl_2. Dry CH_2Cl_2 was used to prepare a stock solution of the corresponding thiourea (c = 0.135 M) as suggested by Franz. For every compound, three samples were prepared from the same stock solution, which were measured three times each. Δ*δ*-values were calculated using the average chemical shift *δ* of three measurements of pure $POEt_3$ in $CDCl_3/CH_2Cl_2$ (1/4) solution, which was determined to be 51.40 ppm, and the average chemical shift δ of the respective thiourea complex. The ^{31}P-spectra (decoupled) were recorded on a 400 MHz-NMR instrument with 32 scans.

Table 34: Chemical shifts δ of $POEt_3$ after complexation by thiourea **17-27**. Each complexation was measured three times and an average is given as well as the *Δδ and the standard error of the mean (SEM).*

thiourea	chemical shift *δ* I/ppm	chemical shift *δ* II/ppm	chemical shift *δ* III/ppm	Ø(chemical shift δ)/ppm	Δ*δ*/ppm	Ø(SEM)/%
17[a)]	52.91	52.94	52.97	52.94	1.54	1.6
18[a)]	52.79	52.77	52.71	52.76	1.36	2.5
19	52.14	52.09	52.15	52.13	0.73	3.6
20	54.51	54.54	54.42	54.49	3.09	1.6
21	54.04	53.89	53.89	53.94	2.54	2.8
22	53.36	53.50	53.41	53.42	2.03	2.9
23[b)]	52.48	52.41	52.44	52.44	1.05	2.7
24[a), c)]	54.27	54.24	-	54.26	2.86	0.5
25[a)]	55.75	55.73	55.69	55.72	4.33	0.6
26	55.88	56.39	56.37	56.21	4.82	4.9
27[d)]	56.59	56.51	56.50	56.53	5.14	0.8

a) Compound is not entirely soluble in CH_2Cl_2. b) Compound was not entirely soluble in CH_2Cl_2, even in the doubled amount of solvent, but was measured nonetheless (c=0.0675 M instead of 0.135 M). c) The experiments were performed two times and the average is given. d) Compound showed poor solubility in CH_2Cl_2. Careful heating can facilitate the solubilizing process (*e.g.* water bath 50 °C).

The three ^{31}P-NMR measurements of all thioureas are depicted in the following. Please note that for weak hydrogen bonding, for instance in the case of thiourea **19**, a broadening of the signals was sometimes observed, resulting in a higher uncertainty of the obtained values, as also indicated in the table above (see Ø(SEM) values).

N, *N´*-dicyclohexyl thiourea 17

^{31}P-NMR (400 MHz, $CDCl_3$) δ/ppm = 52.97 (1)

52.94 (2)

52.91 (3)

Ø = 52.94 ppm

Δδ = 1.54 ppm

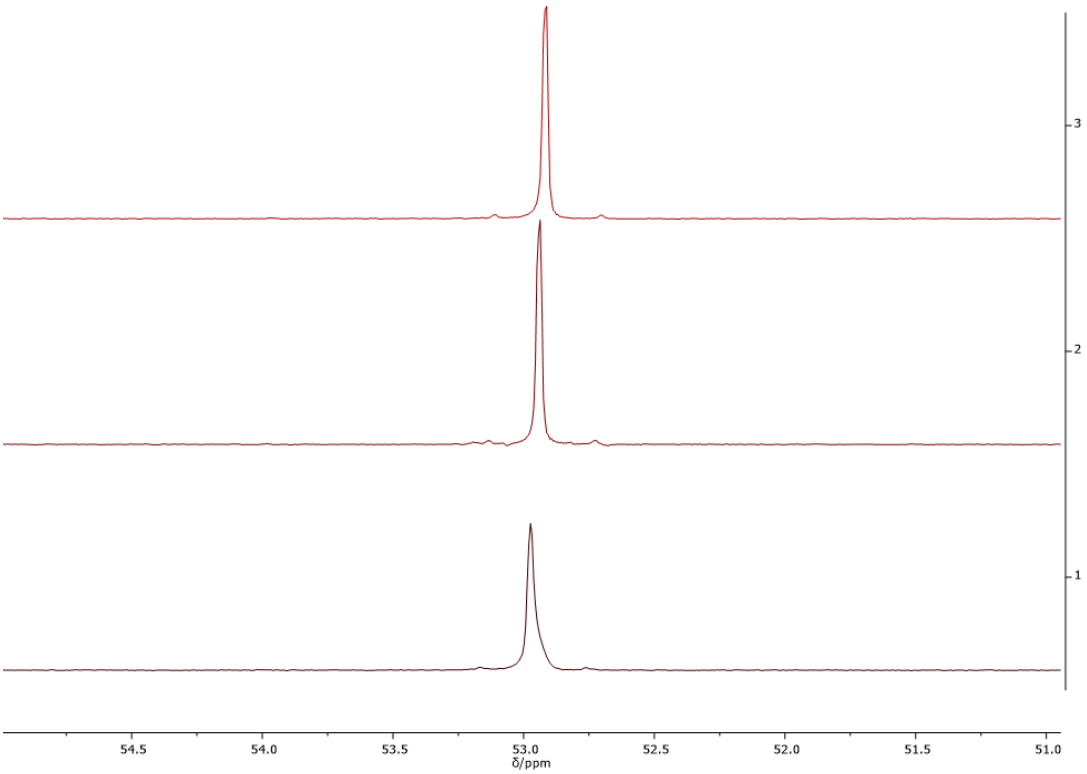

*Figure 53: ^{31}P-NMR-Spectrum of $POEt_3$ depicting the effect of the hydrogen bonding strength of thiourea **17**.*

Compound is not entirely soluble in CH_2Cl_2.

N-cyclohexyl thiourea 18

^{31}P-NMR (400 MHz, $CDCl_3$) δ/ppm = 52.79 (1)

52.71 (2)

52.77 (3)

Ø = 52.76 ppm

Δδ = 1.36 ppm

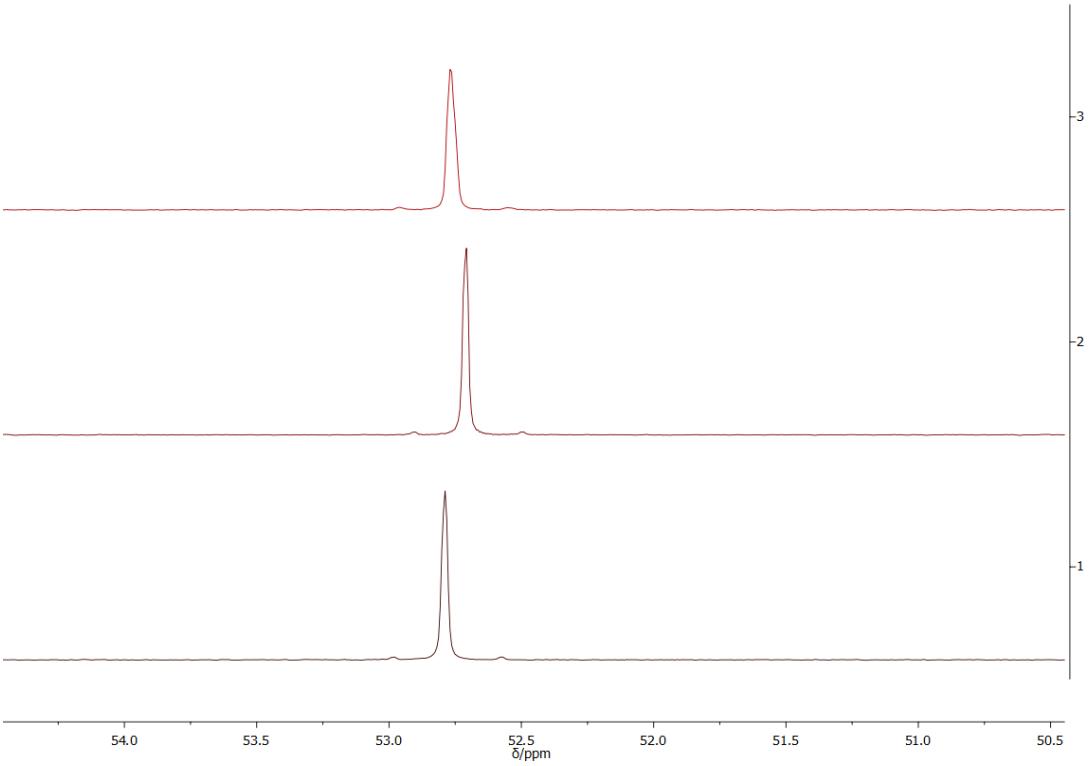

*Figure 54: ^{31}P-NMR-Spectrum of $POEt_3$ depicting the effect of the hydrogen bonding strength of thiourea **18**.*

Compound is not entirely soluble in CH_2Cl_2 but was measured anyway.

N-cyclohexylhydrazine carbothioamid 19

^{31}P-NMR (400 MHz, $CDCl_3$) δ/ppm = 52.14

52.06

52.28

Ø = 52.13 ppm

Δδ = 0.73 ppm

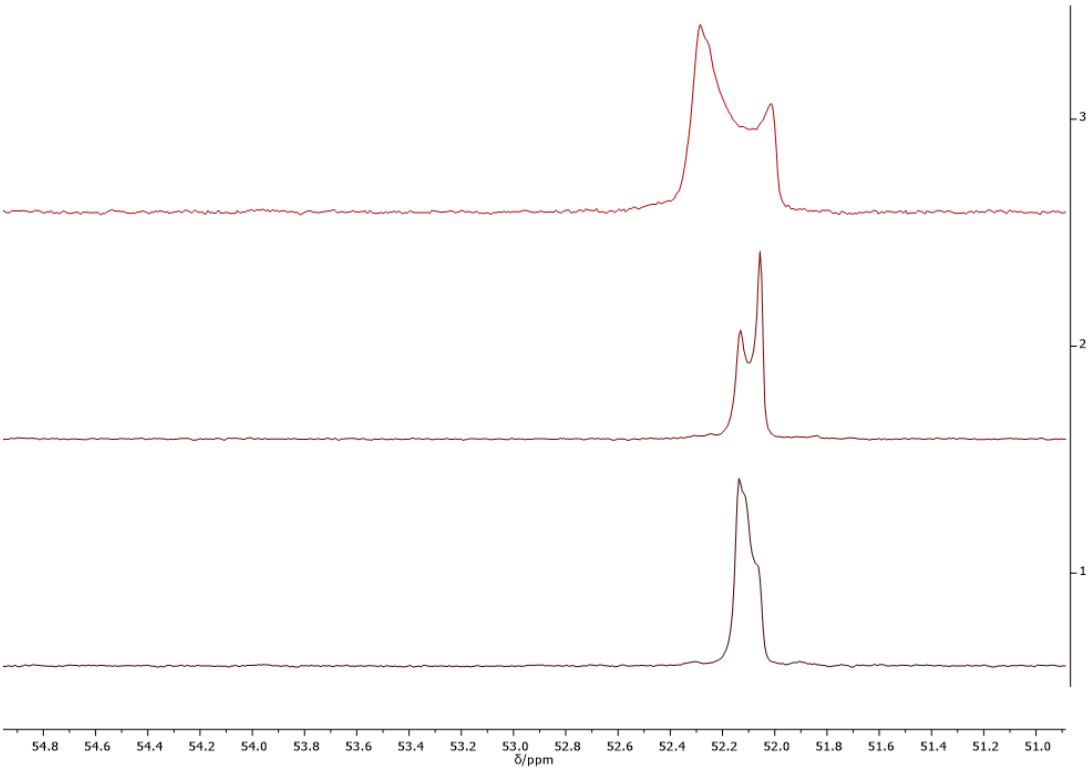

*Figure 55: ^{31}P-NMR-Spectrum of $POEt_3$ depicting the effect of the hydrogen bonding strength of thiourea **19**.*

N-furfuryl, *N´*-cyclohexyl thiourea 20

^{31}P-NMR (400 MHz, $CDCl_3$) δ/ppm = 54.51 (1)

54.54 (2)

54.42 (3)

Ø = 54.49 ppm

Δδ = 3.069ppm

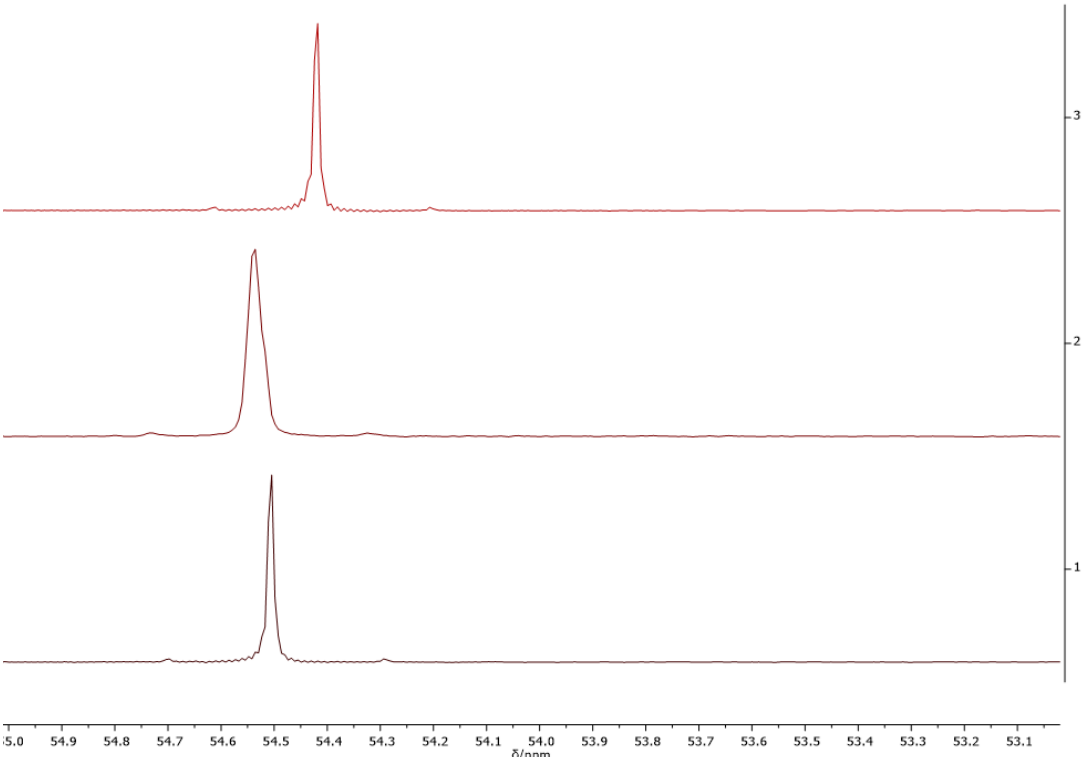

*Figure 56: ^{31}P-NMR-Spectrum of $POEt_3$ depicting the effect of the hydrogen bonding strength of thiourea **20**.*

N-benzyl, *N´*-cyclohexyl thiourea 21

^{31}P-NMR (400 MHz, $CDCl_3$) δ/ppm = 54.04 (1)

53.89 (2)

53.89 (3)

Ø = 53.94 ppm

Δδ = 2.54 ppm

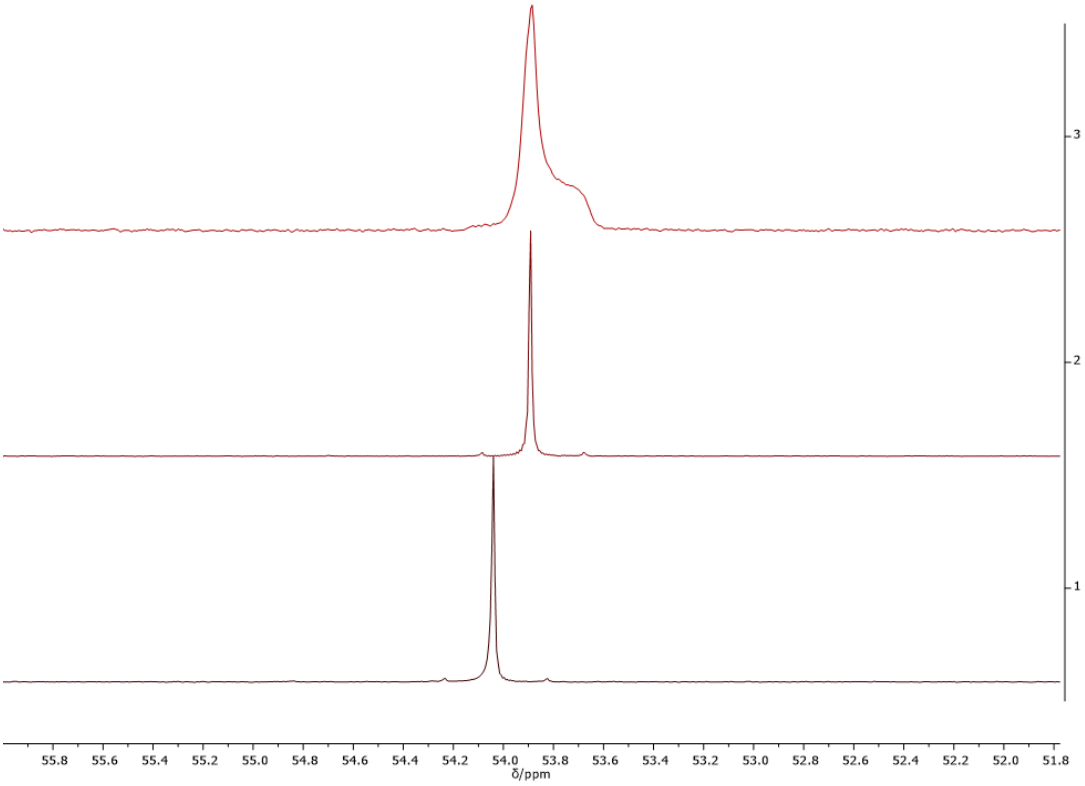

*Figure 57: ^{31}P-NMR-Spectrum of $POEt_3$ depicting the effect of the hydrogen bonding strength of thiourea **21**.*

N-phenyl, *N´*-cyclohexyl thiourea 22

^{31}P-NMR (400 MHz, $CDCl_3$) δ/ppm = 53.50 (1),

53.36 (2),

53.41 (3).

Ø = 53.42 ppm

Δδ = 2.02 ppm

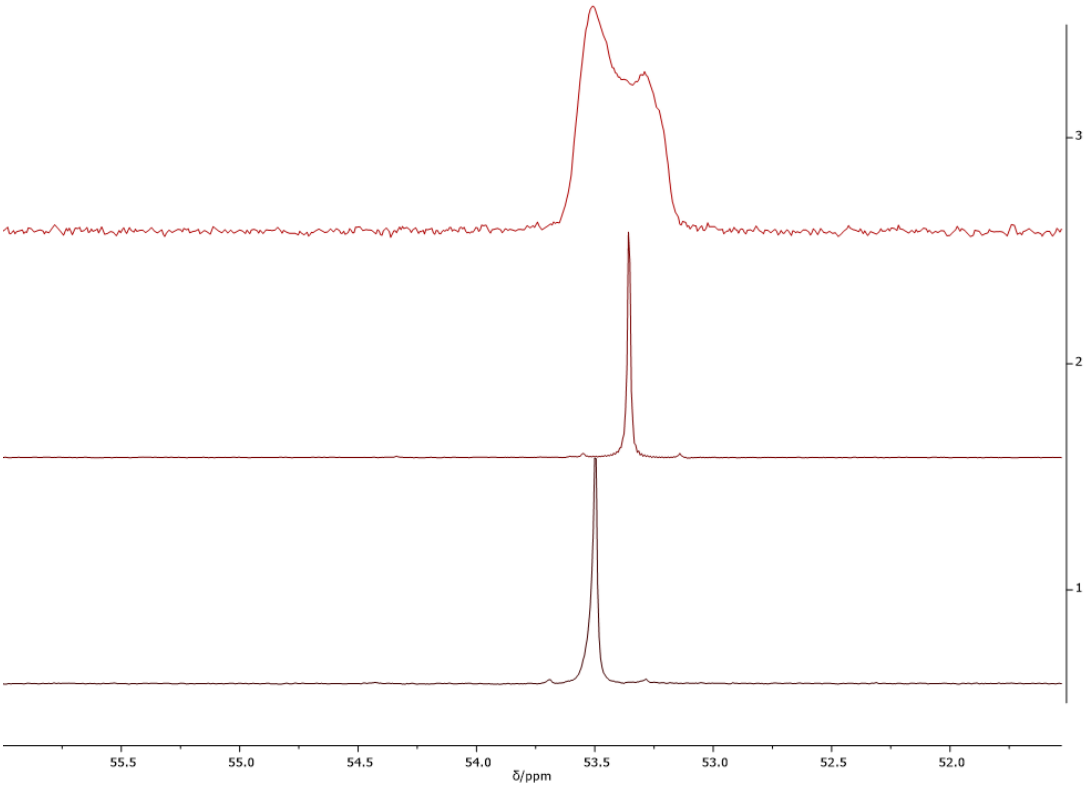

*Figure 58: ^{31}P-NMR-Spectrum of $POEt_3$ depicting the effect of the hydrogen bonding strength of thiourea **22**.*

1,4-bis(*N*-cyclohexylthioureido) benzene 23

^{31}P-NMR (400 MHz, $CDCl_3$) δ/ppm = 52.48 (1)

52.41 (2)

52.44 (3)

Ø = 52.44 ppm

Δδ = 1.05 ppm

Compound was not soluble in CH_2Cl_2, even in the doubled amount of solvent but was measured anyway (*c*=0.0675 M instead of 0.135 M).

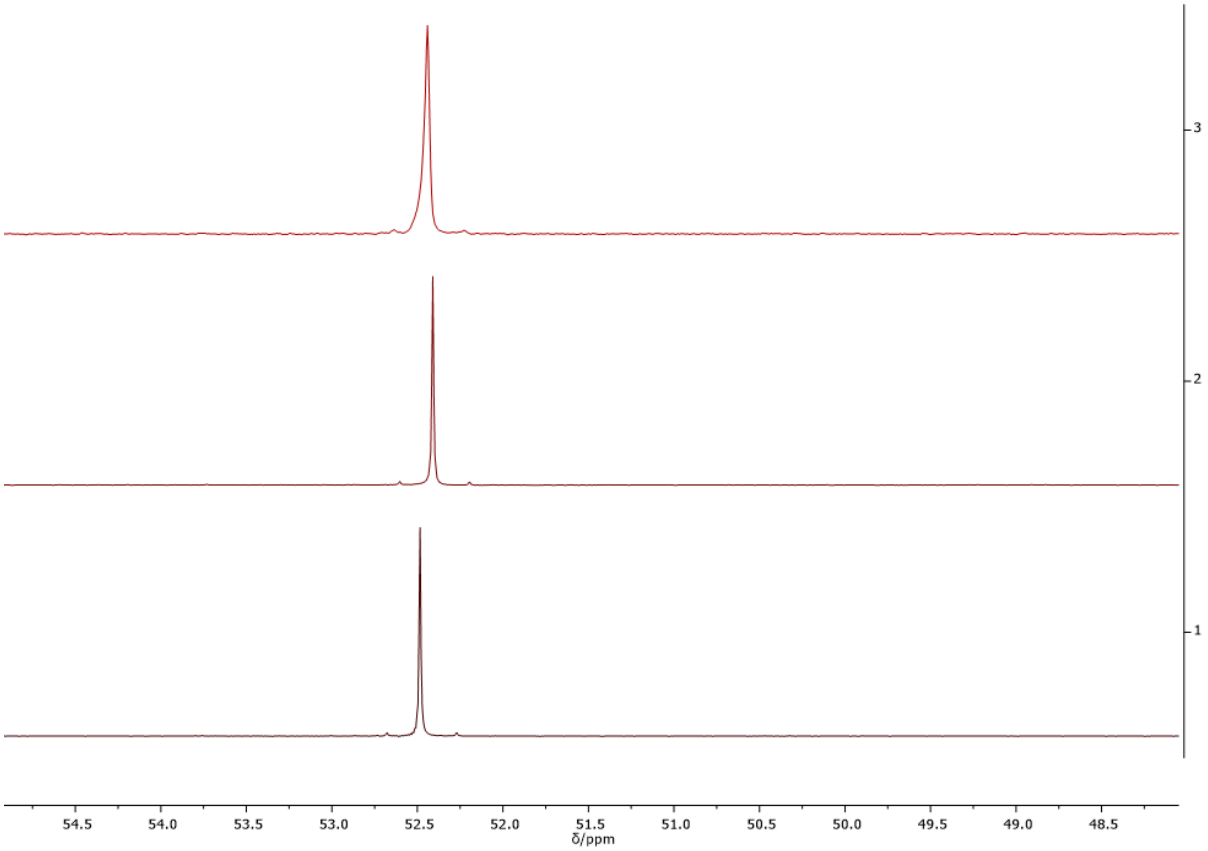

*Figure 59: ^{31}P-NMR-Spectrum of $POEt_3$ depicting the effect of the hydrogen bonding strength of thiourea **23**.*

N-(4-(methylbenzoate)), *N´*-cyclohexyl thiourea 24

^{31}P-NMR (400 MHz, $CDCl_3$) δ/ppm = 54.27 (1)

54.24 (2)

55.43 (3)

Ø = 54.65 ppm

Δδ = 3.25 ppm

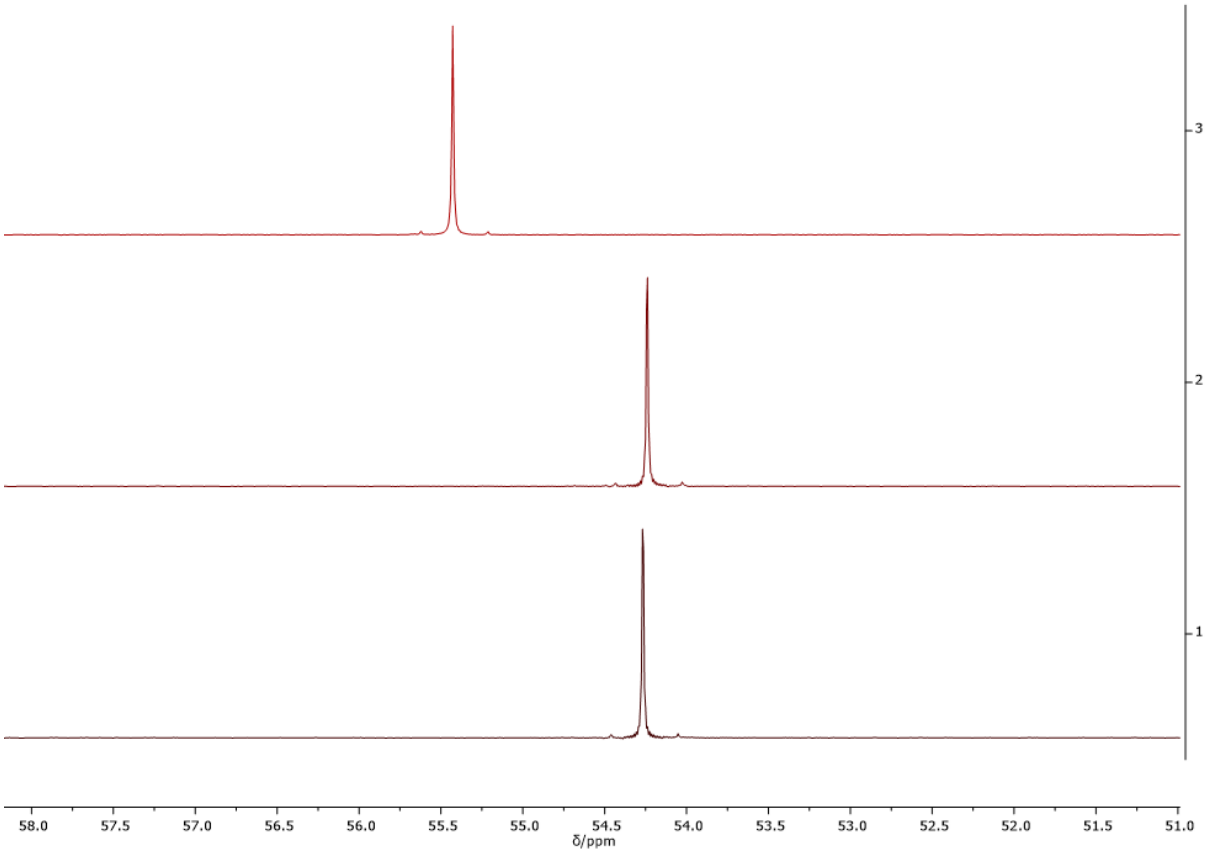

*Figure 60: ^{31}P-NMR-Spectrum of $POEt_3$ depicting the effect of the hydrogen bonding strength of thiourea **24**.*

Compound is not entirely soluble in CH_2Cl_2 but was measured anyway.

N-(5-(dimethylisophtalate)), *N´*-cyclohexyl thiourea 25

^{31}P-NMR (400 MHz, $CDCl_3$) δ/ppm = 55.75 (1)

55.73 (2)

55.69 (3)

Ø = 55.72 ppm

Δδ = 4.33 ppm

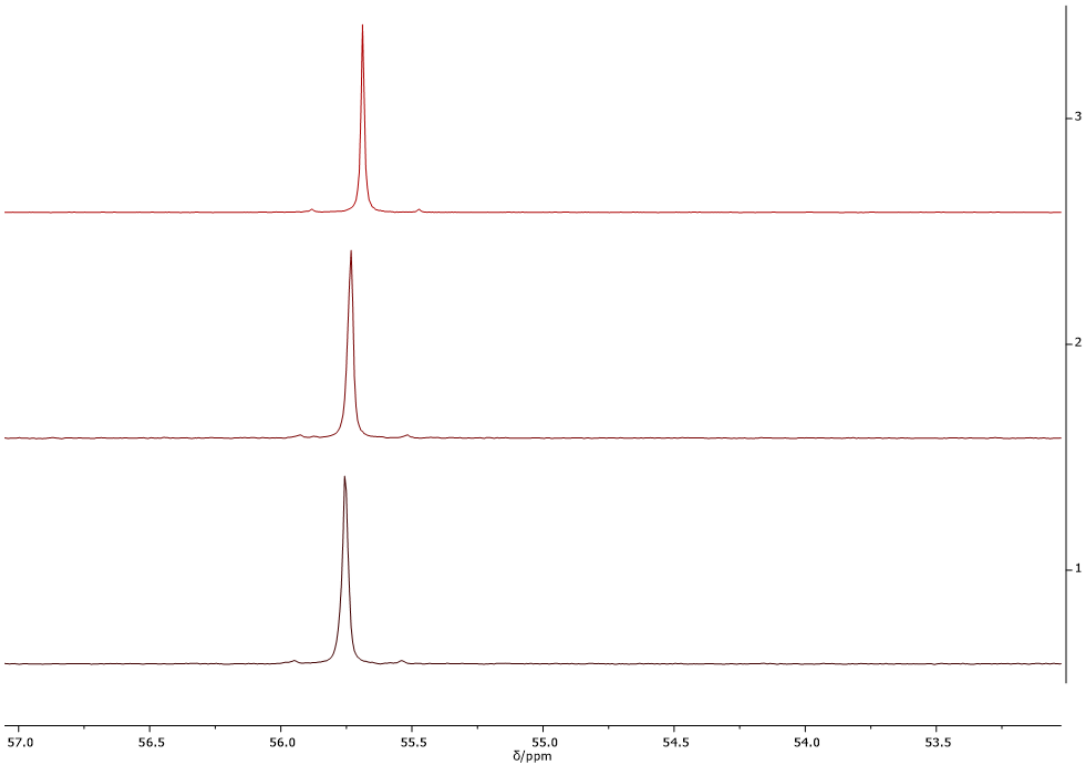

*Figure 61: ^{31}P-NMR-Spectrum of $POEt_3$ depicting the effect of the hydrogen bonding strength of thiourea **25**.*

Compound is not entirely soluble in CH_2Cl_2 but was measured anyway.

N-(4-(*n*-hexylsulfony)phenyl), *N´*-cyclohexyl thiourea 26

^{31}P-NMR (400 MHz, $CDCl_3$) δ/ppm = 55.88

56.39

56.37

Ø = 56.21 ppm

Δδ = 4.82 ppm

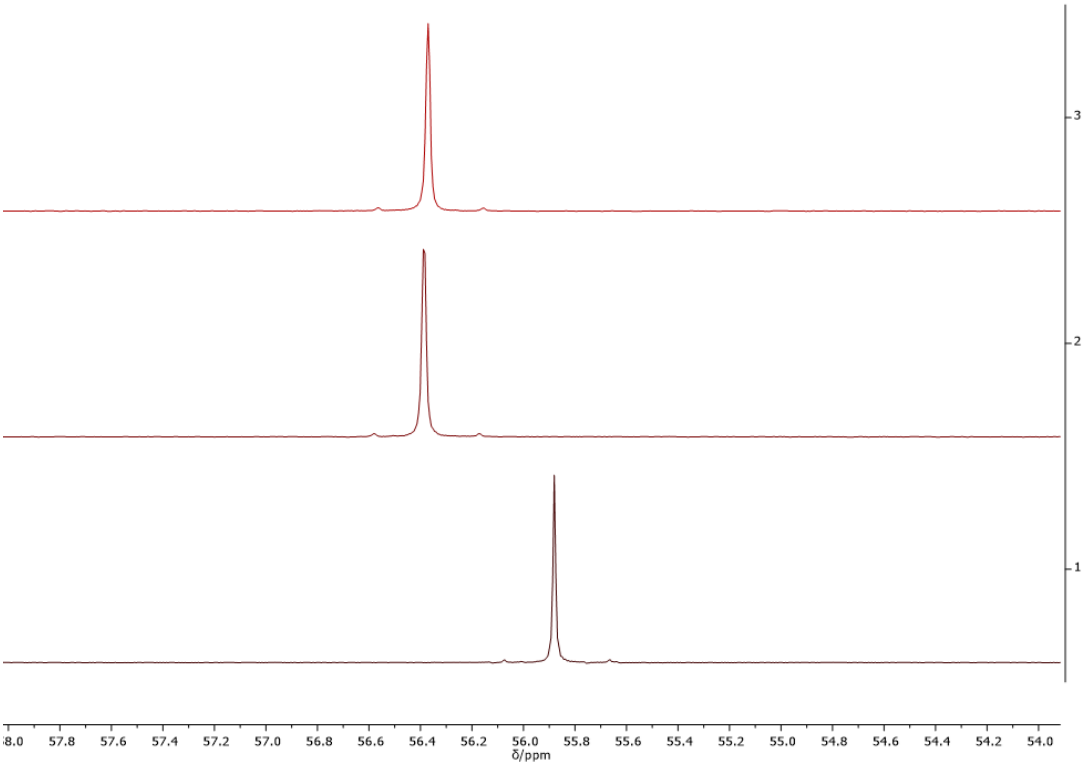

*Figure 62: ^{31}P-NMR-Spectrum of $POEt_3$ depicting the effect of the hydrogen bonding strength of thiourea **26**.*

N-3,5-bis(trifluormethyl)phenyl, *N´*-cyclohexyl thiourea 27

^{31}P-NMR (400 MHz, $CDCl_3$) δ/ppm = 56.59

56.51

56.50

Ø = 56.53ppm

Δδ = 5.14 ppm

Compound shows bad solubility in CH_2Cl_2. Careful, heating can facilitate the solubilizing process (e.g. water bath 50 °C).

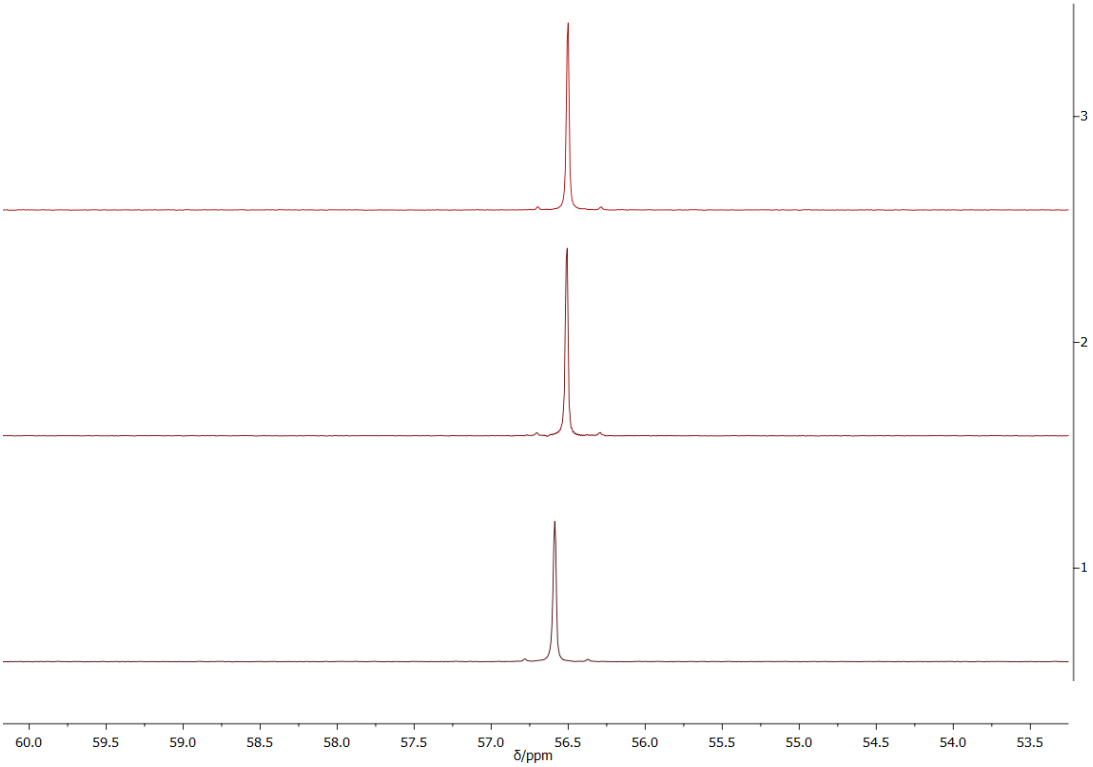

*Figure 63: ^{31}P-NMR-Spectrum of $POEt_3$ depicting the effect of the hydrogen bonding strength of thiourea **27**.*

6.4.2 Catalyst-screening for Ugi-four-component-reaction

The reaction was performed in commercially available NMR-tubes. Thus, stock solutions of the *tert*-butyl isocyanide (*c* = 1.05 M), acetic acid (*c* = 0.70 M), *p*-toluidine (*c* = 1.05 M) and the respective catalyst were prepared in $CDCl_3$ (dried over MS 3 Å). Since most of the catalysts showed low solubility in $CDCl_3$, *p*-methoxy benzaldehyde (*c* = 0.241 M) was added directly to the stock solution of each catalyst (*c* = 0.0175 M), resulting in a homogeneous solution. Then, 400 µL of the catalyst-aldehyde stock solution as well as 100 µL of each amine, carboxylic acid and isocyanide stock solution were added to the NMR-tube. Subsequently, it was closed and well shaken (*i.e.* turned around eight times) and left at room temperature for a given time. Thus, the stoichiometry for each reaction was: acetic acid **29** (4.00 µL, 4.20 mg, 70.0 µmol, 1.00 eq.), *p*-methoxy benzaldehyde **31** (11.7 µL, 13.2 mg, 96.6 µmol, 1.38 eq.), *p*-toluidine **30** (11.3 mg, 105 µmol, 1.50 eq.), *tert*-butyl isocyanide **32** (11.9 µL, 8.73 mg, 105 µL, 1.50 eq.) and the respective catalyst (7.0 µmol, 10.0 mol%) in 700 µL $CDCl_3$.

^{1}H-NMR measurements (500 MHz) were recorded after 66 hours, and after 6 days. Each catalyst was tested three times, while at least two different stock solutions of each compound were used (summary in Table 34). The conversion of the acetic acid was determined by integration of the C**H$_3$**-COOH-signal of the acid (singlet at 2.05 ppm, integral **A(X)**) and the C**H$_3$**-CONR-signal of the Ugi-product **28** (singlet at 1.83 ppm, integral **A(Y)**, for pure product analysis *vide infra*), since no overlapping of other signals was observed (including signals of every catalyst tested). Please note that the acetic acid signal was slightly shifted in the reaction mixture compared to the signal of pure acetic acid, probably due to the different solvent mixture. All remaining signals in the displayed spectra of the reaction mixture could be assigned to the starting materials and the formed products. No corresponding Passerini-product (see reference for corresponding Passerini signals[624]) or other side products involving the acetic acid were detected and thus, the conversion was calculated as followed:

$$conversion[\%] = \frac{A(Y)}{A(X) + A(Y)} \times 100 \tag{8}$$

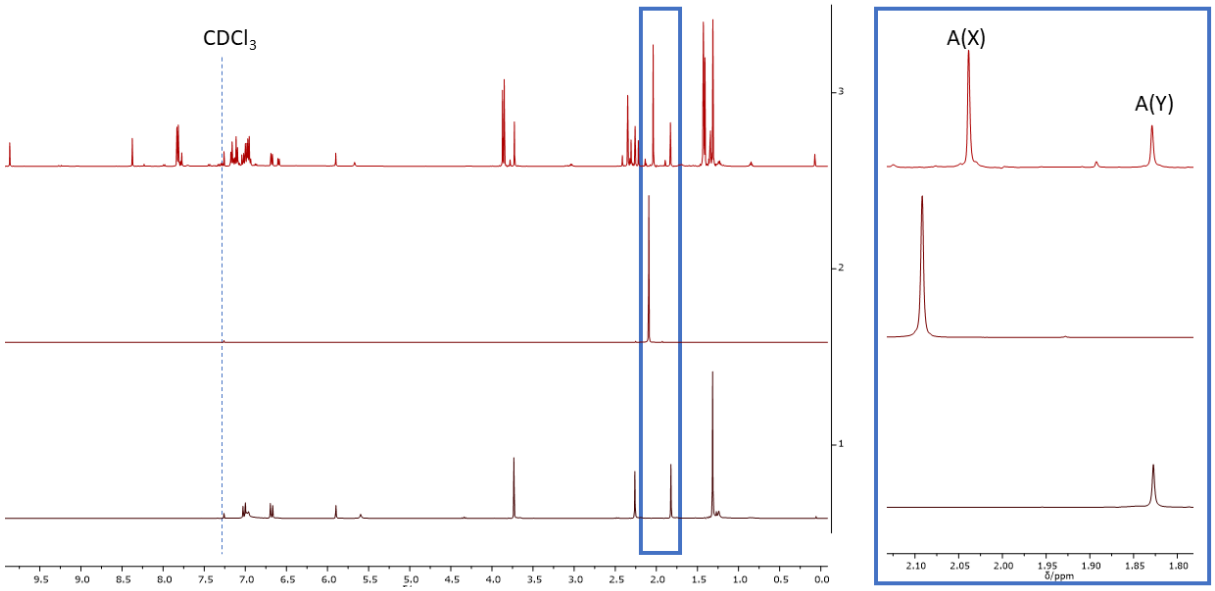

*Figure S2: On the left side, stacked ^{1}H-NMR spectra of the Ugi-4CR reaction mixture after 6 days using thiourea catalyst **26** (**3**) (top), the pure acetic acid **29** (**2**) (middle) and the corresponding isolated, pure Ugi-product **28** (**1**) (bottom) in $CDCl_3$ is shown exemplarily.*

*On the right side, a zoom-in to the C**H$_3$**-COOH-signal of the acetic acid as well as the C**H$_3$**-CONR-signal of the Ugi- product **28** clearly reveals that no other signals are overlapping.*

*Table 35: Summary of catalysis of an Ugi reaction forming product **28** by using thiourea compounds. Each 1H-NMR-experiment was performed three times and an average as well as standard error of the mean (SEM) is given.*

Catalyst [time]	Conversion I/%	Conversion II/%	Conversion III/%	Ø(Conversion)/%	Ø(SEM)/%
none [66 h]	14.5	13.8	13.8	14.0	2.5
none [6 days]	19.4	18.7	18.7	18.9	1.6
Schreiner catalyst [66 h]	24.8	27.0	27.0	26.3	3.9
Schreiner catalyst [6 d]	29.1	32.0	31.5	30.9	4.1
Schreiner catalyst 20 mol% [6 d]	32.4	32.9	32.9	32.7	0.7
17 [66 h]	11.5	12.3	11.5	11.8	3.1
17 [6 d]	16.7	16.7	16.7	16.7	0.0
18 [66 h]	14.5	15.3	12.3	14.0	9.0
18 [6 d]	20.6	20.6	17.4	19.5	7.9
19 [66 h]	13.0	13.0	9.9	12.0	12.3
19 [6 d]	18.0	17.4	13.8	16.4	11.3
20 [66 h]	14.5	14.5	11.5	13.5	10.5
20 [6 d]	20.0	20.0	16.7	18.9	8.3
21 [66 h]	10.7	12.3	11.5	11.5	5.6
21 [6 d]	17.4	16.7	17.4	17.1	1.9
22 [66 h]	19.4	13.0	14.5	15.6	17.2
22 [6 d]	18.0	18.7	19.4	18.7	2.9
23 [66 h]	15.3	15.3	13.8	14.8	4.7
23 [6 d]	20.6	20.0	18.7	19.8	4.1
24 [66 h]	14.5	14.5	13.8	14.3	2.4
24 [6 d]	20.0	20.6	20.6	20.4	1.7
25 [66 h]	16.7	16.7	16.0	16.4	2.0
25 [6 d]	21.9	21.3	23.1	22.1	3.4
26 [66 h]	22.5	18.7	22.5	21.2	8.4
26 [6 d]	29.6	27.0	28.6	28.4	3.7
26 20 mol% [6 d]	32.0	32.0	34.6	32.9	3.8
27 [66 h]	21.3	22.5	22.5	22.1	2.6
27 [6 d]	25.4	27.5	28.1	27.0	4.3
MeOH [40 mol%, 66 h]	13.0	13.0	14.5	13.5	5.2
MeOH [40 mol%, 6 d]	18.0	16.7	18.7	17.8	4.8

6.4.2.1 Synthesis of Ugi-product 28

In a 25 mL round bottom flask, acetic acid **29** (480 µL, 500 mg, 8.33 mmol, 1.00 eq.) was added to 17 mL of methanol. Subsequently, 4-methoxybenzaldehyde **31** (1.01 mL, 1.13 g, 8.33 mmol, 1.00 eq.), *p*-toluidine **30** (850 µL, 892 mg, 8.33 mmol, 1.00 eq.) and *tert*-butylisocyanide **32** (942 µL, 692 mg, 8.33 mmol, 1.00 eq.) were added and the resulting mixture was stirred for three days at room temperature. The crude reaction mixture was purified *via* column chromatography (ethyl acetate/cyclohexane (1:10→1:2)). The product was obtained as a colorless crystalline solid. (1.79 g, 4.86 µmol) in a yield of 58 %.

R_f = 0.43 in cyclohexane/ethyl acetate 5/1, visualized *via* vanillin staining solution.

^{1}H-NMR was according to literature.[625]

^{1}H-NMR (500 MHz, $CDCl_3$): δ/ppm = 7.03-6.66 (m, 8H, aromatic), 5.90 (s, 1H, NH), 5.60 (s, 1H, CH), 3.73 (s, 3H, CH_3), 2.26 (s, 3H, CH_3), 1.82 (s, 3H, CH_3), 1.31 (s, 9H, CH_3).

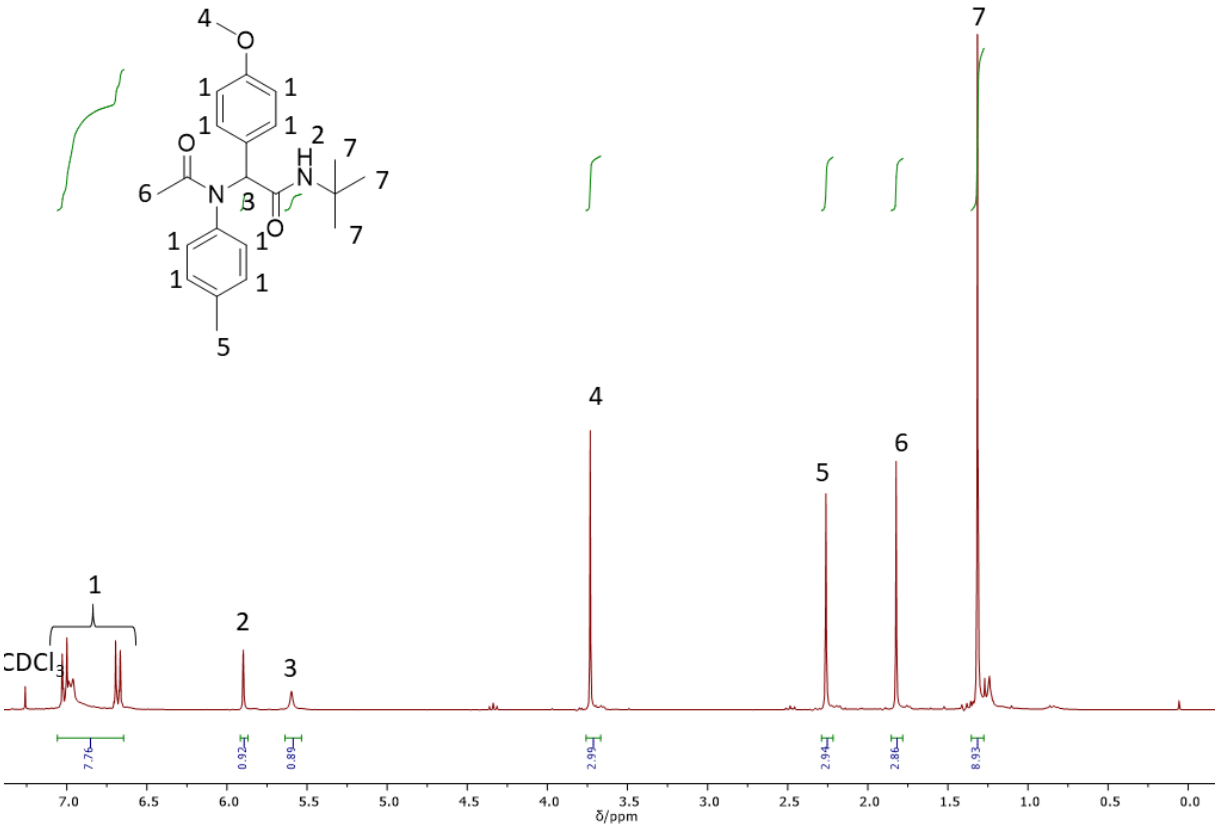

6.4.3 Catalyst-screening in for ring-opening of cyclic carbonate

The screening reactions were performed according to the synthesis protocol of Caillol and Andrioletti *et al.*[417] Propylene carbonate **33** (85.1 µL, 103 mg, 1.00 mmol, 1.00 eq.) and cyclohexylamine **34** (115 µL, 99.2 mg, 1.00 mmol, 1.00 eq.) were added to the respective thiourea catalyst (50.0 µmol, 5.00 mol%). In addition, biphenyl (18.5 mg, 0.120 eq.) was added as internal standard (reference used diphenylether) and the reaction mixture was stirred at room temperature for 30 or 60 minutes. Since the reaction mixture became more viscous with increasing conversion, preparing a homogenous GC-sample of the mixture was not possible (the conversion differed considerably if the experiment was repeated). Thus, two separate reactions for each reaction time (30 and 60 minutes) were performed and afterwards diluted with 1 mL of ethyl acetate each. The diluted reaction mixture was stirred for another 5 minutes resulting in a non-viscous, homogeneous solution appropriate for GC-analysis at the respective conditions (s. above for GC-program). Every reaction was performed three times, the average conversion of propylene carbonate **33** and the standard error of the mean (SEM) was calculated.

Retention time of the respective compound in the GC-chromatogram:

Propylen carbonate **33** 2.44 min

Product (both regioisomers **35a** and **35b**) 8.17 min

Biphenyl (internal standard) 6.08 min

*Table 36: GC-screening of the reaction of propylene carbonate **33** with cyclohexylamine **34** with or without catalyst. The conversion was determined after 30 and 60 minutes and the experiment was performed three times (conversion I-III) resulting in an average conversion and the respective standard error of the mean (SEM).*

Catalyst [time]	Conversion I/%	Conversion II/%	Conversion III/%	Ø(Conversion)/%	Ø(SEM)/%
none [30 min]	4.0	1.6	2.2	2.6	38.4
none [60 min]	7.5	8.5	4.0	4.0	28.7
Schreiner catalyst [30 min]	51.1	44.9	45.6	47.2	5.9
Schreiner catalyst [60 min]	55.1	61.1	57.0	57.8	4.3
27 [30 min]	67.8	63.8	60.5	64.1	4.7
27 [60 min]	67.6	71.6	72.0	70.4	2.8
26 [30 min]	62.1	59.1	56.6	59.2	3.8
26 [60 min]	68.6	68.4	67.4	68.1	0.7
25 [30 min]	54.5	54.6	56.1	55.1	1.3
25 [60 min]	66.4	63.9	65.6	65.3	1.6
23 [30 min]	20.5	20.4	23.3	21.4	6.3
23 [60 min]	36.8	29.5	31.3	32.5	9.5
22 [30 min]	27.3	26.8	26.9	27.0	0.8
22 [60 min]	43.4	34.2	36.0	37.9	10.4
20 [30 min]	15.9	17.1	15.2	16.1	4.8
20 [60 min]	34.5	26.6	27.7	29.6	11.9
17 [30 min]	10.7	13.8	11.8	12.11	10.6
17 [60 min]	29.5	21.6	24.2	25.1	13.2

6.4.4 Synthesis of thioureas

General synthesis of thiourea *via* MCR (GP1)

Elemental sulfur (0.140 eq., corresponds to 1.12 eq. of sulfur atoms) was suspended in methanol (1.0 M corresponding to n(isocyanide)), the respective amine (1.10 eq.) was added and a dark red to brownish reaction mixture was usually observed. Subsequently, the isocyanide component (1.00 eq.) was added and the reaction mixture was stirred at room temperature or up to 80°C (applying elevated temperature, a pressure tube was used) until full conversion was observed TLC. Subsequently, the solvent was removed under reduced pressure. The crude product was washed with methanol at 60°C for several minutes and then left to cool down to room temperature. After filtration and washing with minimal amount of methanol, the solvent was evaporated and the pure product was obtained. Deviations of this procedure are highlighted in the respective section.

N, *N´*-Dicyclohexyl thiourea 7

The synthesis was performed according to GP1. The reaction was conducted in bulk and cyclohexyl isocyanide **10** (228 µL, 200 mg, 1.83 mmol, 1.00 eq.), cyclohexylamine **34** (232 µL, 200 mg, 2.02 mmol, 1.10 eq.) and elemental sulfur (58.9 mg, 230 µmol, 0.126 eq.) were used. The reaction mixture was stirred at room temperature for 5 min. Then, 1.5 ml ethanol was added and the mixture was left overnight. The crude product was then filtered off using a frit and was washed with ethanol (1 × 0.5 mL). After removal of the remaining solvent, pure product was obtained as colorless solid (308 mg, 128 mmol) in a yield of 70%. Further product could be obtained by repeating the purification steps with the obtained mother liquor, but was not performed here.

R_f = 0.37 in cyclohexane/ethyl acetate 4/1 visualized *via* UV quenching at 254 nm.

^{1}H-NMR (500 MHz, DMSO-d_6) δ/ppm = 7.08 (d, ^3J = 8.1 Hz, 2H, NH, ^{1}), 3.96 (m, 2H, CH, ^{2}), 1.93-0.97 (m, 20H, CH_2).

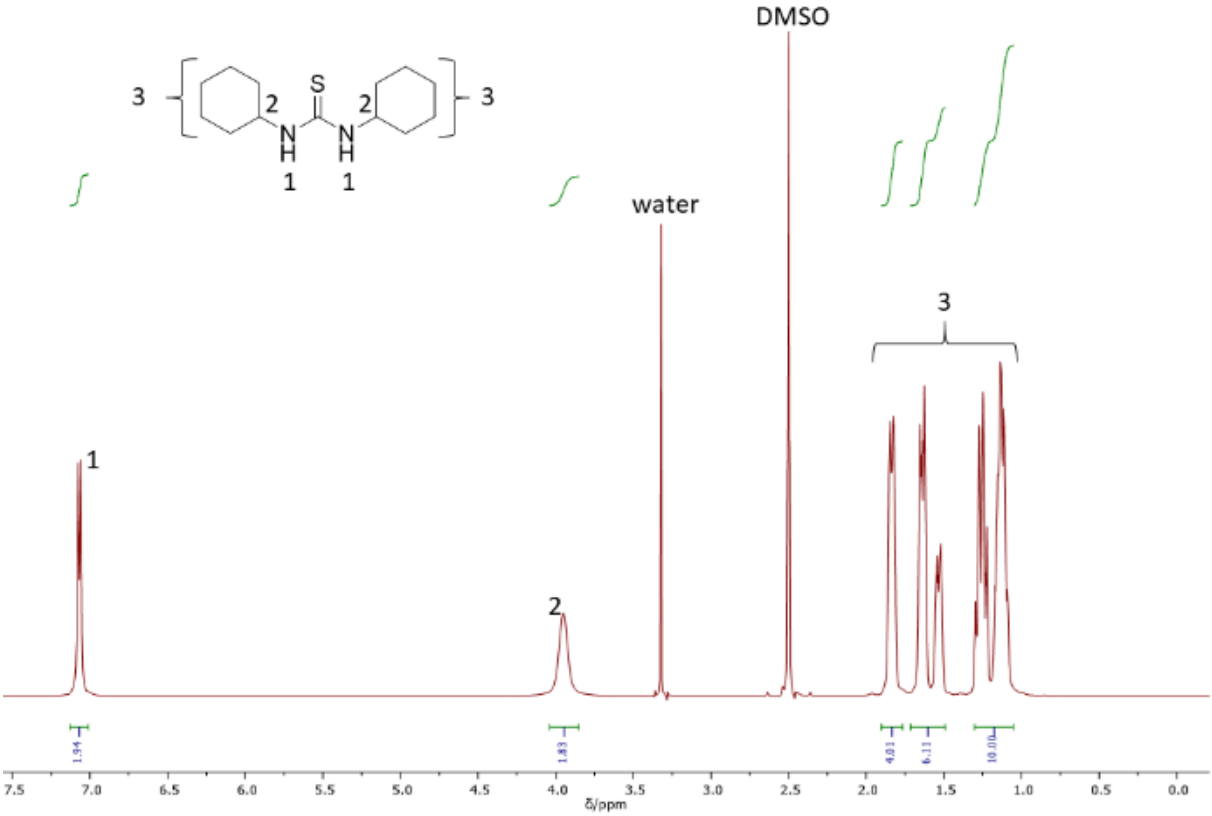

*Figure 64: ^{1}H-NMR-spectrum of thiourea **17**.*

^{13}C-NMR (126 MHz, DMSO-d_6) δ/ppm = 179.96 (C=S), 51.46 (CH), 32.35 (CH_2), 25.20 (CH_2), 24.49 (CH_2).

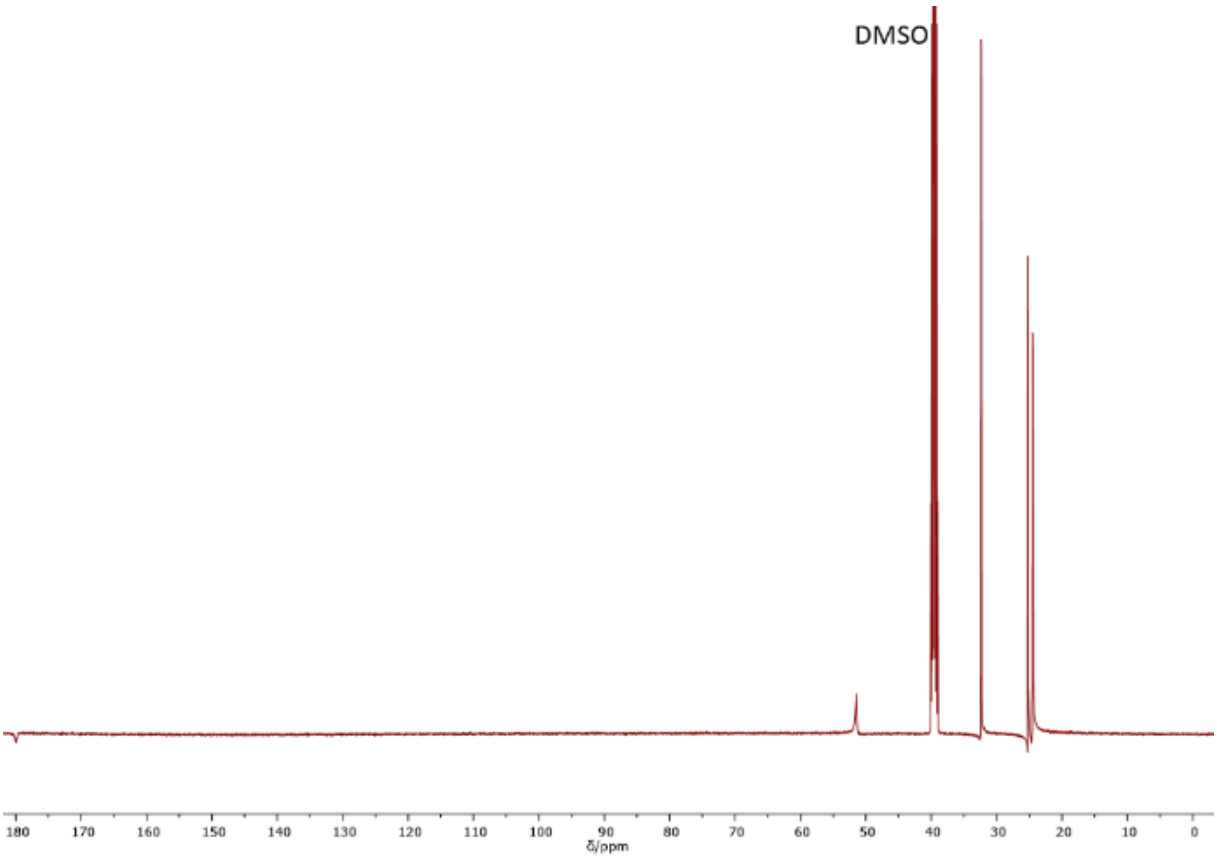

*Figure 65: ^{13}C-NMR-spectrum of thiourea **17**.*

EI-HRMS m/z: $[M]^+$ calculated for $[C_{13}H_{24}N_2S_1]$ = 240.1660, found: 240.1662, Δ = 0.1767 mmu.

IR (ATR platinum diamond): ν/cm^{-1} = 3289 (m), 2925 (vs), 2851 (s), 1549 (vs), 1504 (vs), 1450 (m), 1409 (m), 1378 (w), 1360 (w), 1341 (m), 1323 (w), 1296 (w), 1275 (m), 1255 (m), 1226 (vs), 1187 (m), 1154 (m), 1111 (w), 1074 (w), 983 (m), 887 (w), 771 (m), 588 (s), 551 (vs), 481 (w), 401 (w)

N-Cyclohexyl thiourea 18

The synthesis was performed according to an adapted procedure GP1. Isocyano cyclohexane **10** (342 µL, 300 mg, 2.75 mmol, 1.00 eq.) was reacted with 2.75 mL of 7 M methanolic ammonia solution (449µL, 328 mg, 19.3 mmol, 7.00 eq.) and elemental sulfur (98.7 mg, 385 µmol, 0.140 eq.). The reaction mixture was set under argon atmosphere and was stirred at 60 °C for 30 minutes. Afterwards, the reaction mixture was cooled to room temperature and was then stirred overnight. Washing with 2 mL methanol at 60°C as described in GP1 yielded the product after filtration. The mother liquor was collected, and the solvent was removed and washed again with 1 mL methanol to obtain a second fraction of product. Pure product was obtained as colorless crystals (345 mg, 2.18 mmol) in a yield of 79%.

R_f = 0.21 in cyclohexane/ethyl acetate 1/1 visualized *via* vanillin staining solution (cyan).

^{1}H-NMR (400 MHz, DMSO-d_6) δ/ppm = 7.45 (d, ^3J = 8.3 Hz, 1H, NH, ^{1}), 7.37-6.99 (m, 0.6H, NH_2, ^{2b}), 6.99-6.56 (m, 1.4H, NH_2, ^{2a}), 3.89 (m, 0.7H, CH, ^{3a}), 3.24 (m, 0.3H, CH, ^{3b}), 1.96-0.93 (m, 10H, CH_2, ^{4}).

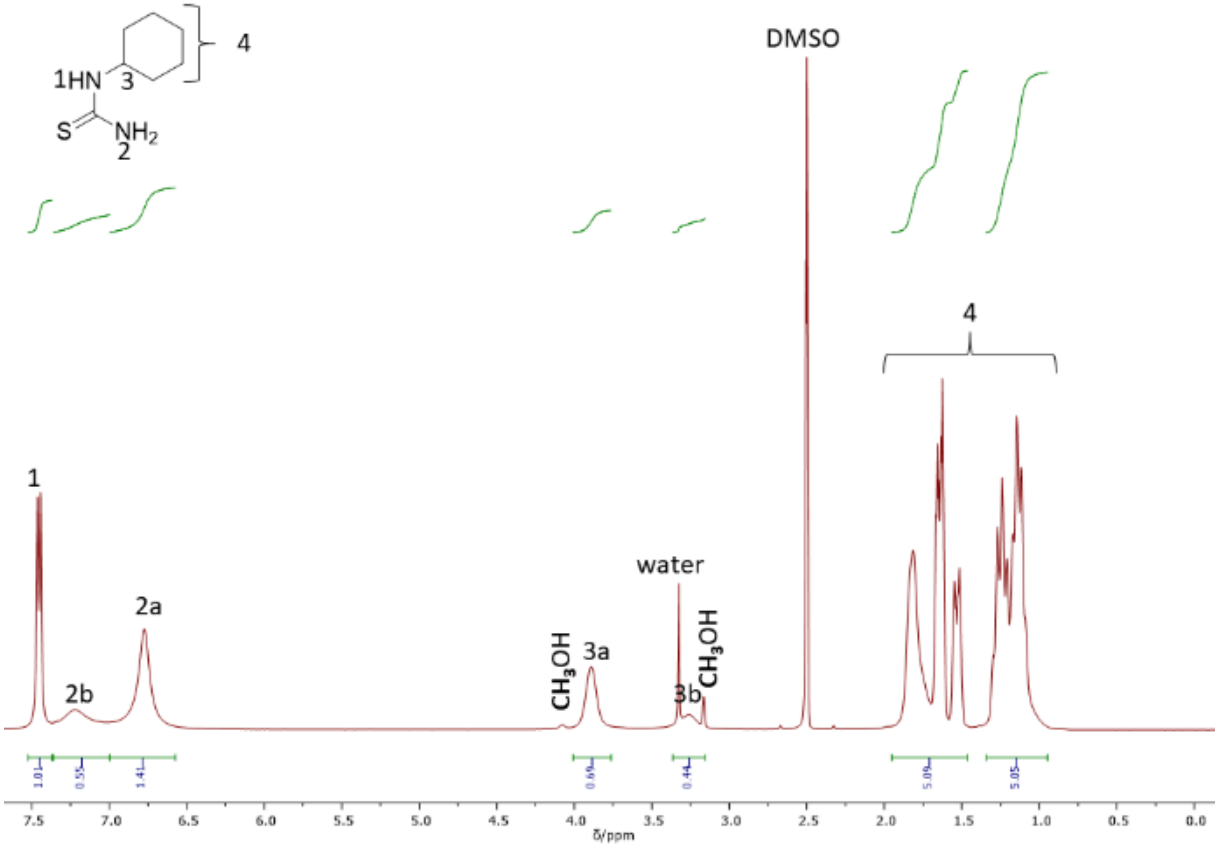

*Figure 66: ^{1}H-NMR-spectrum of thiourea **18**.*

^{13}C-NMR (126 MHz, DMSO-d_6) δ/ppm = 181.88 (C=S), 52.16 (CH) 32.24 (CH_2), 25.15 (CH_2), 24.46 (CH_2).

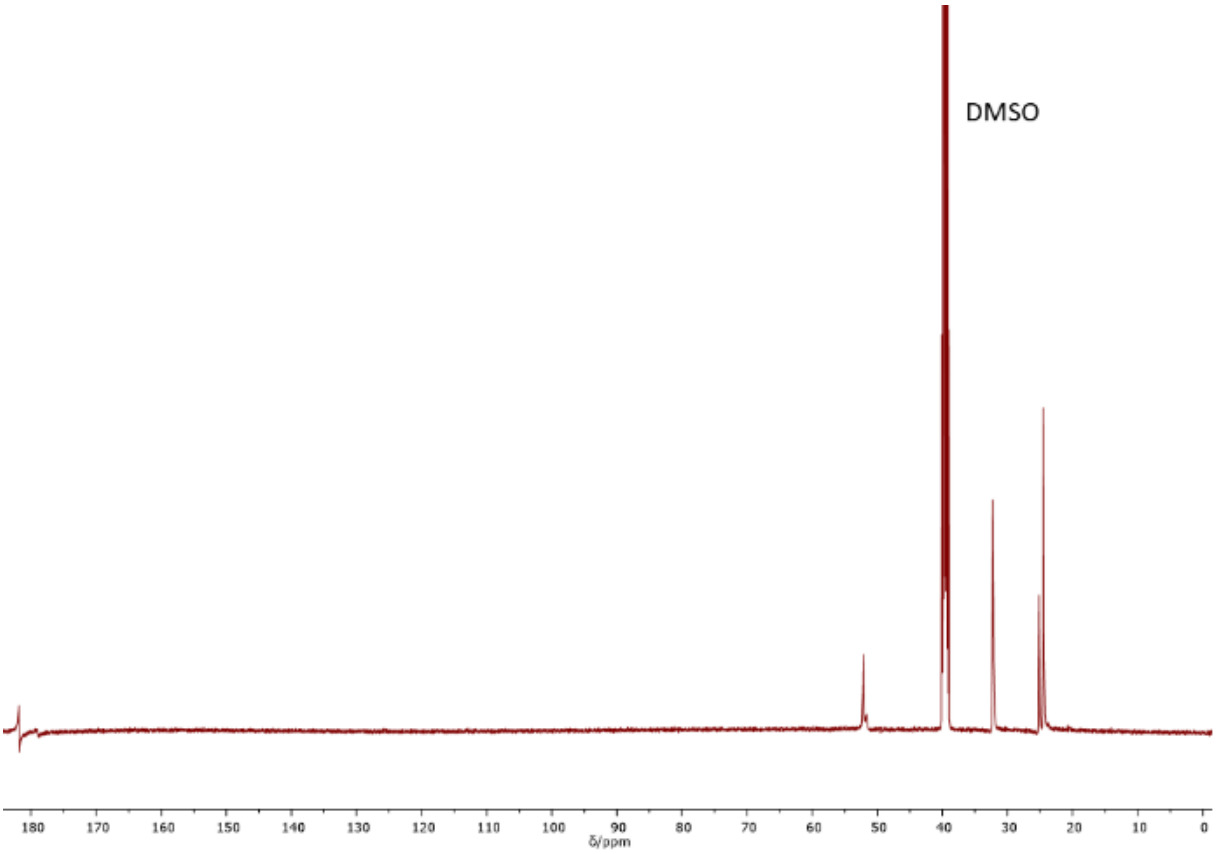

*Figure 67: ^{13}C-NMR-spectrum of thiourea **18**.*

EI-HRMS m/z: $[M]^+$ calculated for $[C_7H_{14}N_2S_1]$ = 158.0878, found: 158.0876, Δ = -0.1317 mmu.

IR (ATR platinum diamond): ν/cm^{-1} = 3332 (w), 3264 (w), 3153 (w), 3075 (w), 2919 (w), 2859 (w), 1615 (m), 1557 (s), 1504 (w), 1460 (w), 1452 (w), 1440 (m), 1415 (w), 1368 (m), 1341 (m), 1308 (w), 1286 (w), 1259 (w), 1230 (w), 1185 (w), 1156 (m), 1088 (w), 1072 (w), 1047 (w), 1026 (w), 9869 (m), 891 (w), 728 (m), 621 (w), 586 (s), 520 (s).

N-Cyclohexylhydrazine carbothioamid 19

The synthesis was performed according to GP1. Isocyano cyclohexane **10** (795 µL, 700 mg, 6.41 mmol, 1.00 eq.) was reacted with hydrazine monohydrate (343 µL, 353 mg, 7.05 mmol, 1.10 eq.) and elemental sulfur (230 mg, 898 µmol, 0.140 eq.) in 6.4 mL methanol. The reaction mixture was stirred at room temperature for 1 day. The precipitate was filtered off and the solvent of the mother liquor was evaporated. The residue was purified as described in GP 1 using 2 mL methanol for washing at 60°C. Both fractions were combined, and the product was obtained as a colorless solid (988 mg, 5.70 mmol) in a yield of 89%.

R_f = 0.22 in cyclohexane/ethyl acetate 1/2 visualized *via* UV quenching at 254 nm.

^{1}H-NMR (400 MHz, DMSO-d_6) δ/ppm = 8.54 (s, 1H, NH, ^{1}), 7.50 (d, ^3J = 8.3 Hz, 1H, NH, ^{2}), 4.44 (s, 2H, NH_2, ^{3}), 4.03 (m, 1H, CH, ^{4}), 1.91-1.03 (m, 10H, CH_2, ^{5}).

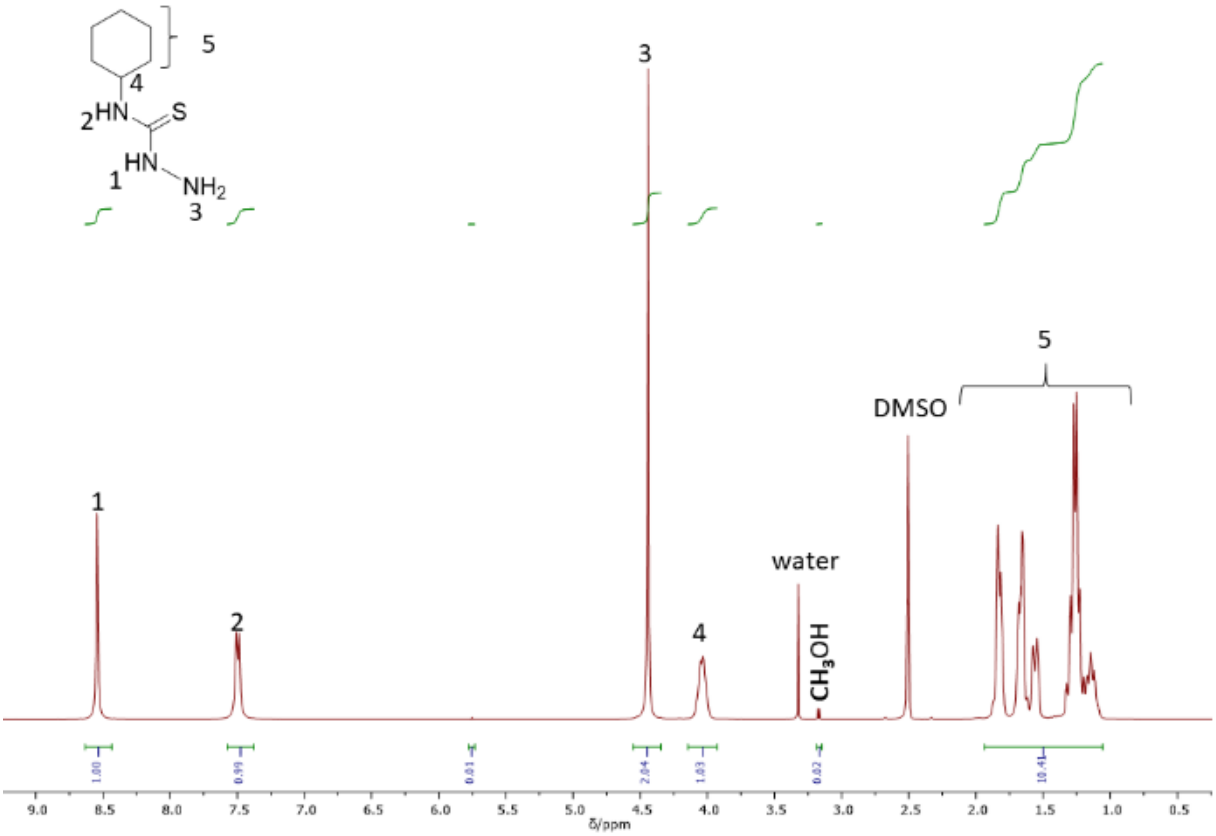

*Figure 68: ^{1}H-NMR-spectrum of thiourea **19**.*

^{13}C-NMR (101 MHz, DMSO-d_6) δ/ppm = 179.98 (C=S), 51.40 (CH), 32.33 (CH_2), 25.12 (CH_2), 24.70 (CH_2).

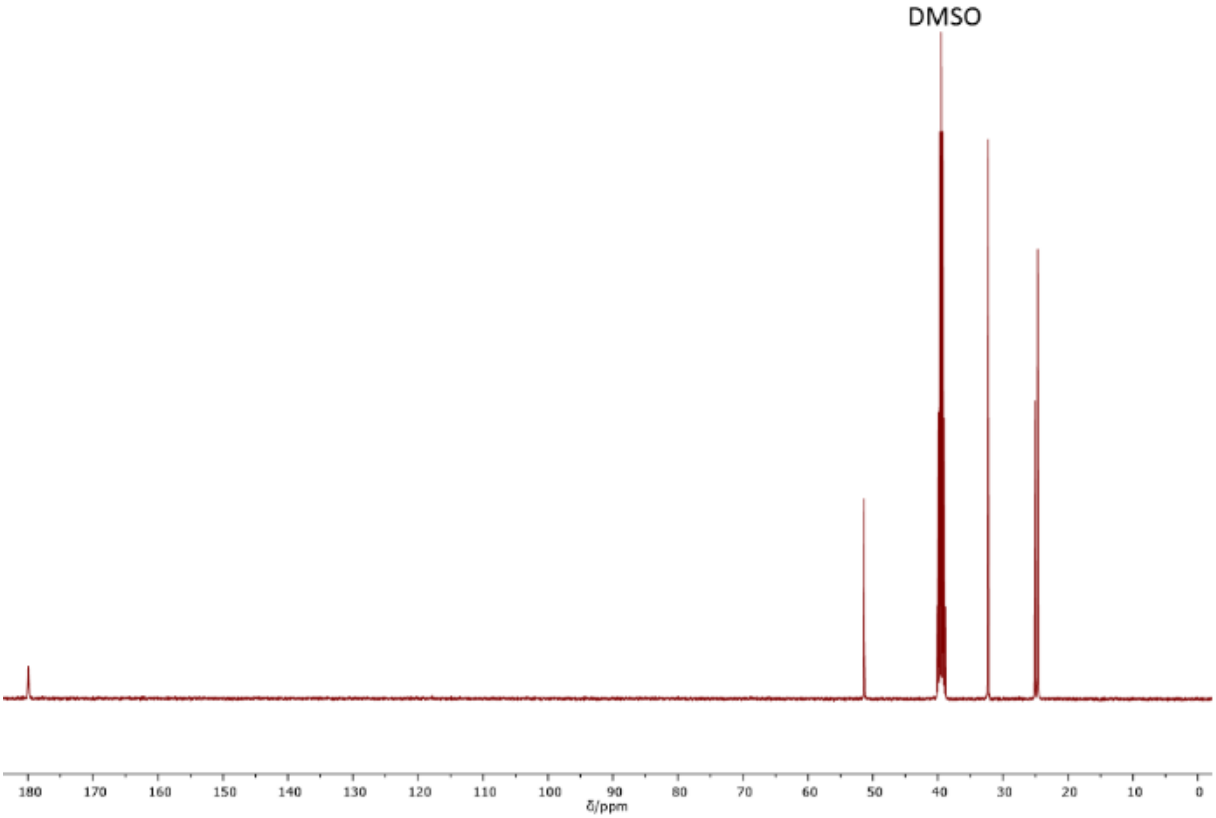

*Figure 69: ^{13}C-NMR-spectrum of thiourea **19**.*

EI-HRMS m/z: $[M]^+$ calculated for $[C_7H_{15}N_3S_1]$ = 173.0987, found: 173.0988, Δ = 0.1291 mmu.

IR (ATR platinum diamond): ν/cm^{-1} = 3334 (w), 3295 (w), 3139 (m), 2927 (vs), 2853 (m), 1625 (m), 1522 (vs), 1497 (s), 1448 (s), 1347 (w), 1310 (m), 1300 (m), 1269 (s), 1257 (s), 1232 (vs), 1193 (w), 1152 (m), 1111 (m), 1063 (w), 1053 (w), 1026 (w), 983 (w), 932 (s), 893 (s), 850 (m), 812 (s), 782 (vs), 730 (m), 664 (vs), 615 (vs), 586 (vs), 522 (m), 477 (w), 461 (m), 438 (w)

N-Furfuryl-*N*´-cyclohexyl thiourea 20

The synthesis was performed according to GP1. Isocyano cyclohexane **10** (341 µL, 300 mg, 2.75 mmol, 1.00 eq.) was reacted with furfurylamine (500 µL, 525 mg, 5,41 mmol, 1.97 eq.) and elemental sulfur (96.9 mg, 378 µmol, 0.140 eq.) in bulk. The reaction mixture was stirred at room temperature for 19 hours. Subsequently, 4 mL of 1.0 M aq. hydrochloric acid and 5 mL of ethyl acetate were added and the biphasic mixture was stirred overnight. Then, water (5 mL) and ethyl acetate (5 mL) were added and the phases were separated. The aqueous phase was extracted with ethyl acetate (1 × 10 mL) and the organic layers were combined, dried over sodium sulfate and filtered off. The pure product was obtained after flash column chromatography (cyclohexane/ethyl acetate 12/1 → 9/1; adding 5 V% of TEA to the eluent) as a brownish, slow crystallizing solid (508 mg, 2.13 mmol) in a yield of 78%.

R_f = 0.32 in cyclohexane/ethyl acetate 2/1 visualized *via* UV quenching at 254 nm and vanillin staining solution (blue to brown).

^{1}H-NMR (500 MHz, DMSO-d_6) δ/ppm = 7.60-7.47 (m, 1H, aromatic, NH, ^{1}), 7.34 (s, 1H, NH, ^{2}), 6.39 (dd, ^3J = 3.1 Hz, ^3J = 1.9 Hz, 1H, aromatic, ^{3}), 6.27 (d, ^3J = 2.7 Hz, 1H, aromatic, ^{4}), 4.69-4.55 (m, 2H, CH_2, ^{5}), 3.99 (m, 1H, CH, ^{6}), 1.89-1.06 (m, 10H, CH_2, ^{7}).

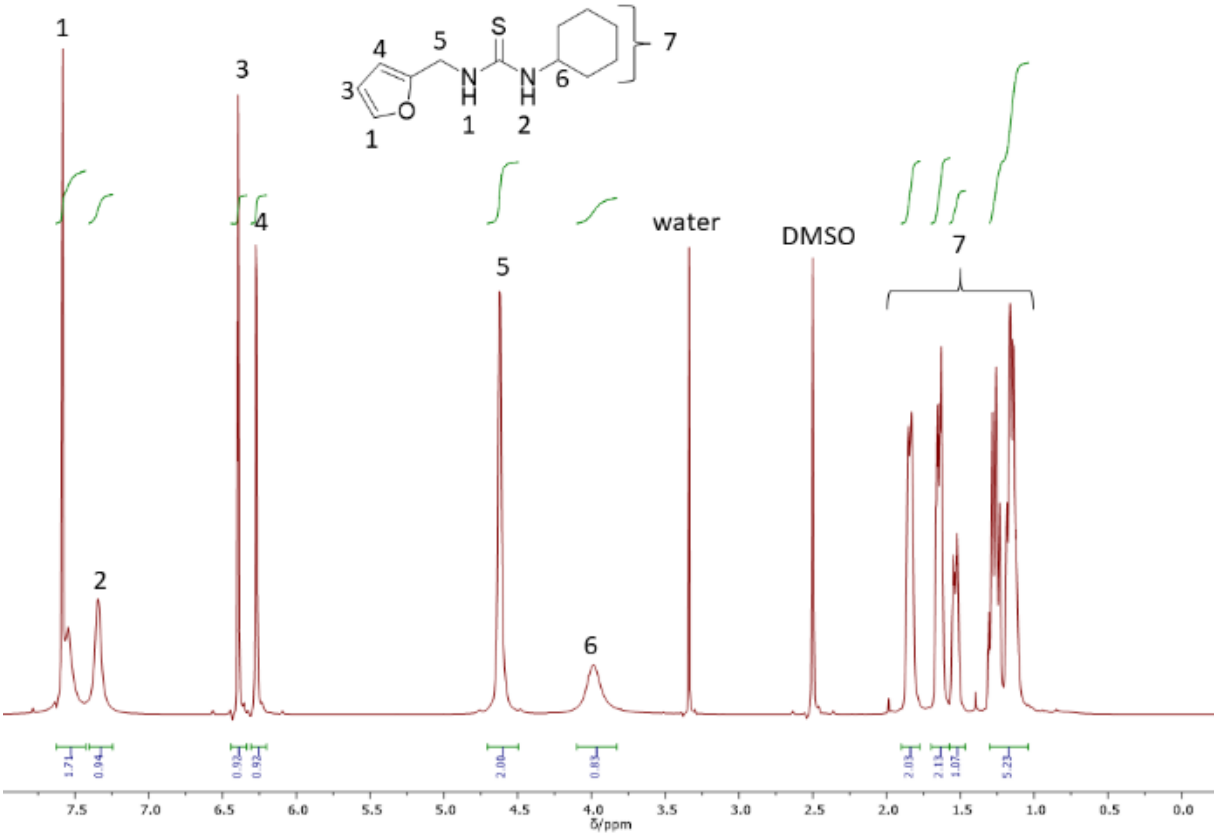

*Figure 70: ^{1}H-NMR-spectrum of thiourea **20**.*

^{13}C-NMR (126 MHz, DMSO-d_6) δ/ppm = 181.28 (C=S), 152.06 (aromatic), 142.11 (aromatic), 110.46 (aromatic), 107.17 (aromatic), 51.84 (CH), 40.26 (CH_2), 32.22 (CH_2), 25.17 (CH_2), 24.42 (CH_2).

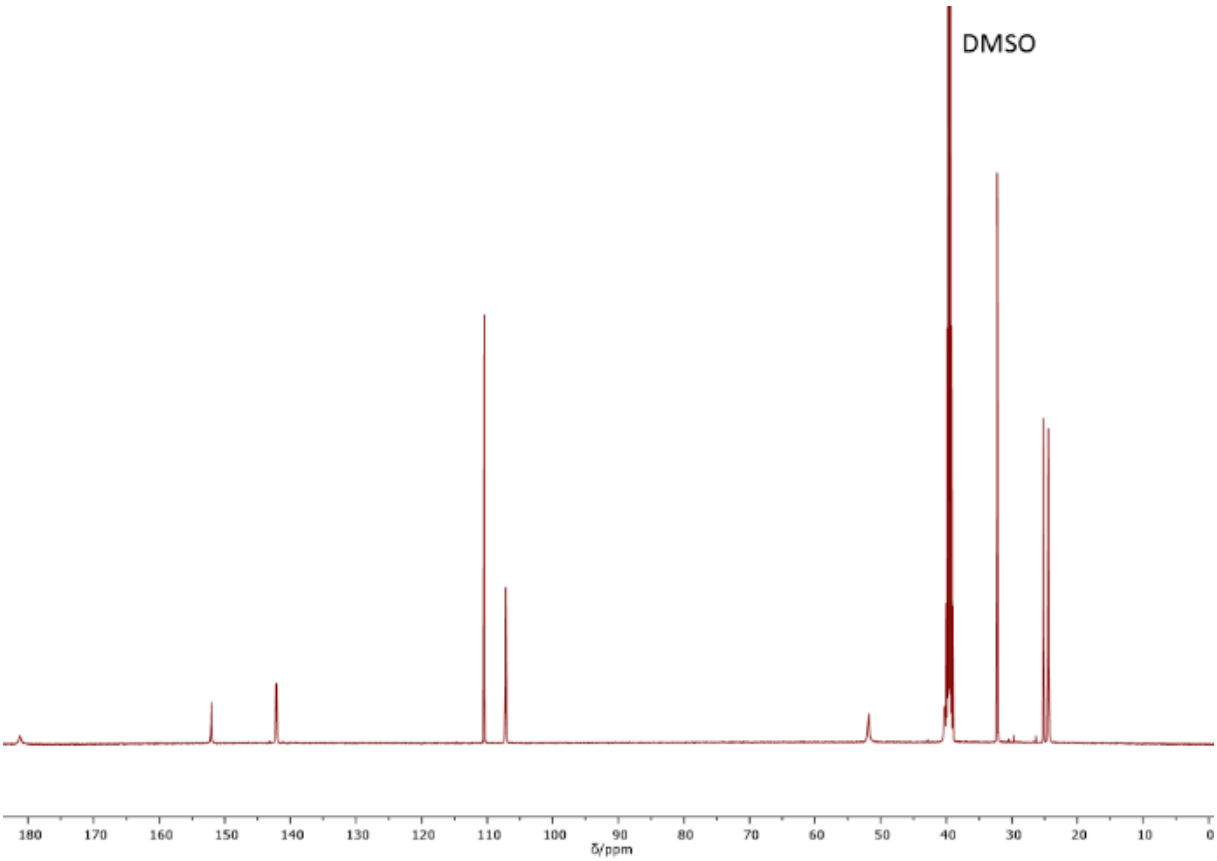

*Figure 71: ^{13}C-NMR-spectrum of thiourea **20**.*

EI-HRMS m/z: $[M]^+$ calculated for $[C_{12}H_{18}N_2S_1]$ = 238.1140, found: 238.1139, Δ = -0.0818 mmu.

IR (ATR platinum diamond): ν/cm^{-1} = 3295 (w), 3221 (s), 3017 (w), 2931 (s), 2855 (m), 1555 (vs), 1545 (vs), 1514 (vs), 1454 (m), 1446 (m), 1419 (m), 1335 (m), 1318 (m), 1306 (s), 1300 (s), 1249 (m), 1236 (s), 1197 (s), 1179 (vs), 1148 (s), 1090 (m), 1076 (s), 1063 (s), 1012 (s), 969 (w), 942 (s), 905 (w), 884 (m), 812 (m), 767 (s), 740 (vs), 642 (vs), 599 (s), 582 (s), 547 (vs), 481 (m), 465 (s), 407 (s)

N-Benzyl-*N´*-cyclohexyl thiourea 21

The synthesis was performed according to GP1. Isocyano cyclohexane **10** (342 µL, 300 mg, 2.75 mmol, 1.00 eq.) was reacted with benzylamine (330 µL mL, 324 mg, 3.02 mmol, 1.10 eq.) and elemental sulfur (97.5 mg, 379 µmol, 0.140 eq.) in bulk. The reaction mixture was stirred at room temperature for 20 minutes. Then, 2 mL of methanol were added to dissolve the formed precipitate and the mixture was stirred for another 40 minutes. The pure product was obtained after flash column chromatography (cyclohexane/ethyl acetate 9/1 → 7/3) as a brownish solid (603 mg, 2.43 mmol) in a yield of 88%.

R_f = 0.48 in cyclohexane/ethyl acetate 7/3 visualized *via* UV quenching at 254 nm.

^{1}H-NMR (400 MHz, DMSO-d_6) δ/ppm = 7.65 (s br, 1H, NH, ^{1}), 7.49-7.14 (m, 6H, aromatic, NH, ^{2}), 4.65 (m, 2H, CH_2, ^{3}), 3.98 (m, 1H, CH, ^{4}), 1.93-1.05 (m, 10H, CH_2, ^{5}).

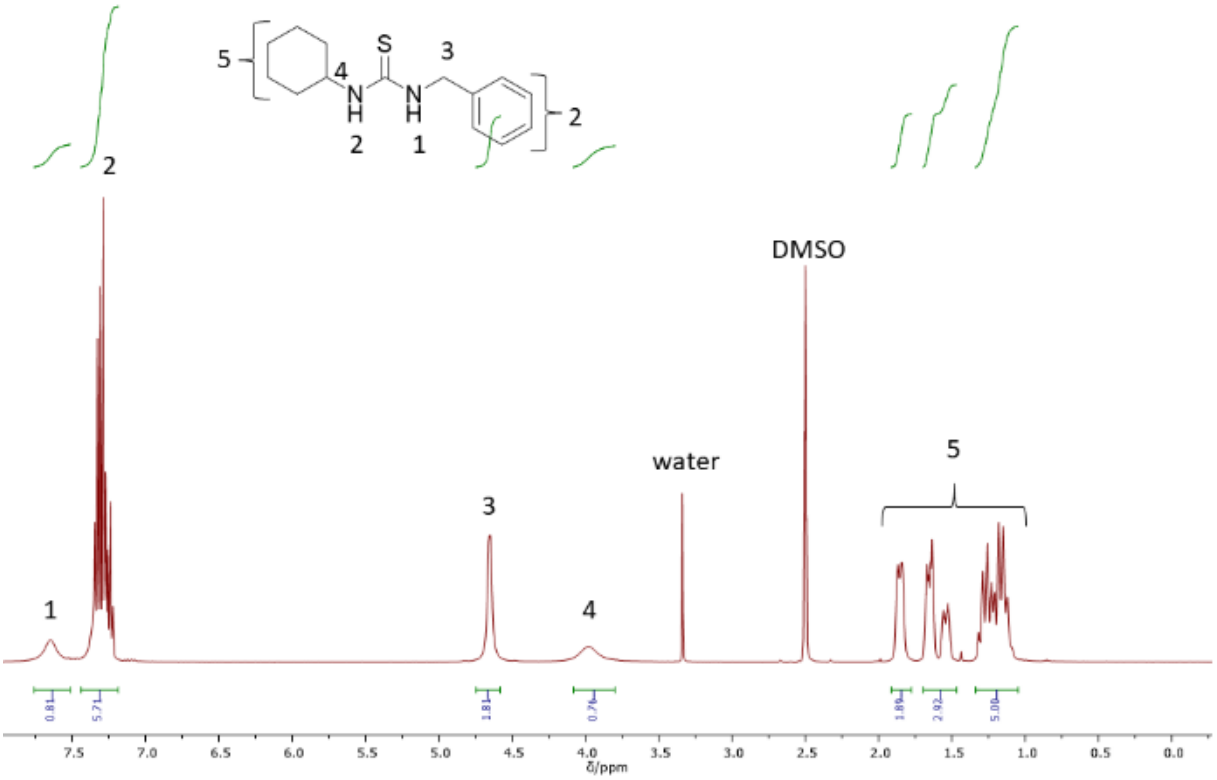

*Figure 72: ^{1}H-NMR-spectrum of thiourea **21**.*

^{13}C-NMR (101 MHz, DMSO-d_6) δ/ppm = 181.36 (C=S), 139.42 (aromatic), 128.25 (aromatic), 127.33 (aromatic), 126.81 (aromatic), 51.86 (CH), 46.86 (CH_2), 32.28 (CH_2), 25.17 (CH_2), 24.48 (CH_2).

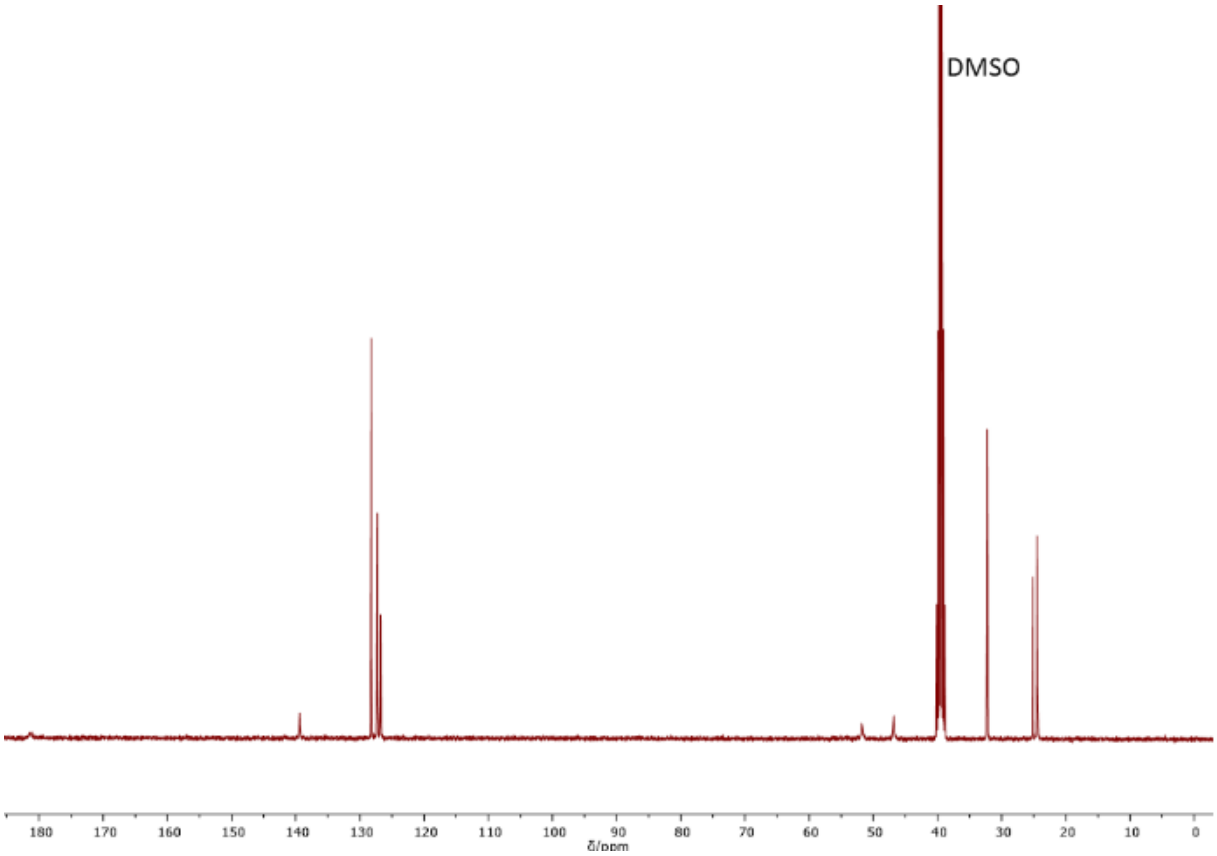

*Figure 73: ^{13}C-NMR-spectrum of thiourea **21**.*

EI-HRMS m/z: $[M]^+$ calculated for $[C_{14}H_{20}N_2S_1]$ = 248.1347, found: 248.1345, Δ = -0.1988 mmu.

IR (ATR platinum diamond): ν/cm^{-1} = 3308 (w), 3236 (s), 3020 (w), 2929 (s), 2855 (w), 1545 (vs), 1516 (vs), 1493 (s), 1454 (m), 1430 (m), 1405 (w), 1333 (m), 1321 (m), 1304 (m), 1290 (s), 1259 (w), 1214 (s), 1197 (s), 1185 (s), 1162 (w), 1148 (w), 1094 (m), 1068 (m), 1028 (w), 932 (m), 919 (w), 887 (w), 775 (m), 738 (vs), 703 (s), 697 (s), 642 (vs), 597 (s), 582 (s), 553 (vs), 483 (m)

N-Phenyl, *N´*-cyclohexyl thiourea 22

The synthesis was performed according to GP1. Phenyl isocyanide (350 mg, 3.39 mmol, 1.00 eq.) was used directly after its synthesis (s. phenyl isocyanide synthesis), reacting it with cyclohexylamine **34** (431 µL, 370 mg, 3.73 mmol, 1.10 eq.) and elemental sulfur (122 mg, 475 µmol, 0.140 eq.). The reaction mixture was stirred at 80 °C for 1 hour. Washing was performed with 2 mL methanol. After filtration, the product was obtained and the mother liquor was collected, and solvent was removed under reduced pressure. The remaining solid was washed again with methanol to yield a second fraction of product. The pure product was obtained as colorless solid (446 mg, 1.90 mmol) in a yield of 56%.

R_f = 0.64 in cyclohexane/ethyl acetate 1/1 visualized *via* UV quenching at 254 nm and vanillin staining solution (green).

^{1}H-NMR (400 MHz, DMSO-d_6) δ/ppm = 9.32 (s, 1H, NH, ^{1}), 7.60 (d, ^3J = 7.4 Hz, 1H, NH, ^{2}), 7.52-7.40 (m, 2H, aromatic, ^{3}), 7.36-7.23 (m, 2H, aromatic, ^{4}), 7.12-7.02 (m, 1H, aromatic, ^{5}), 4.09 (m, 1H, CH, ^{6}), 1.90-1.05 (m, 10H, CH_2, ^{7}).

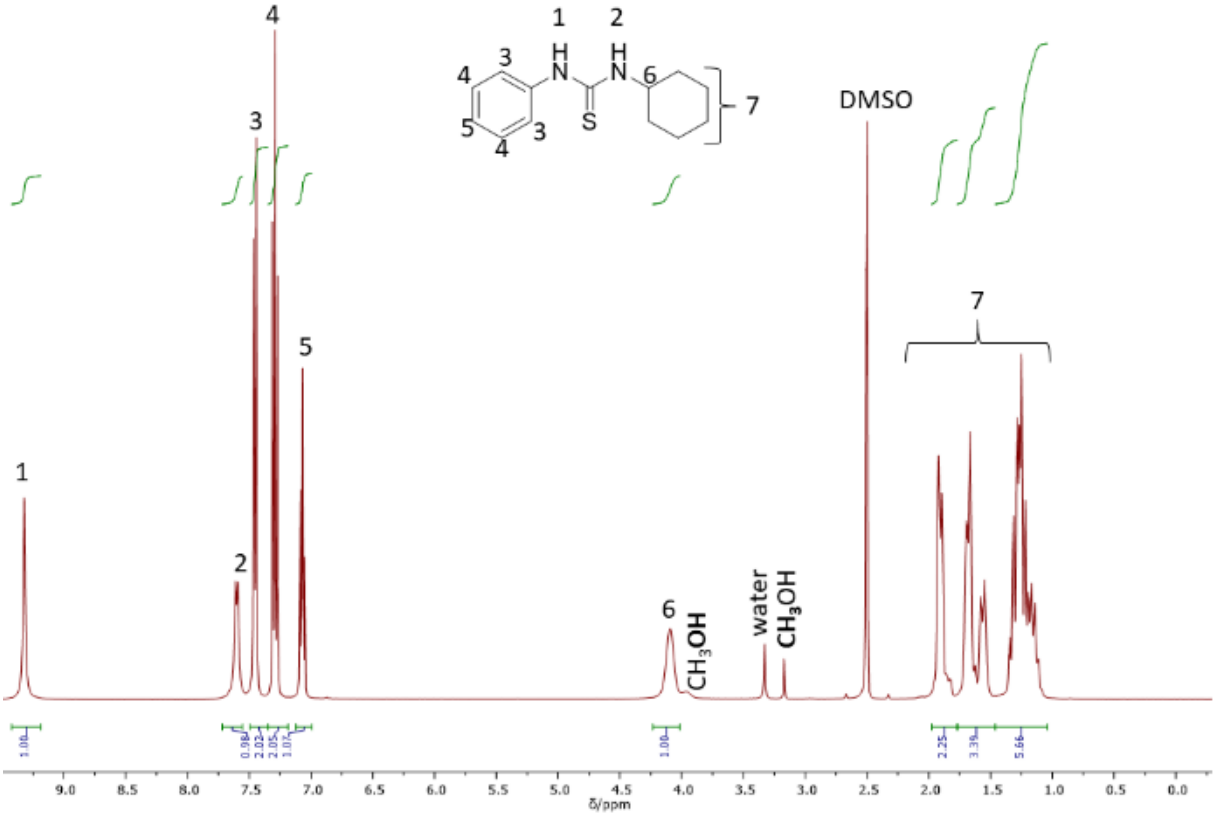

*Figure 74: ^{1}H-NMR-spectrum of thiourea **22**.*

^{13}C-NMR (101 MHz, DMSO-d_6) δ/ppm = 179.18 (C=S), 139.58 (aromatic), 128.42 (aromatic), 123.74 (aromatic), 122.65 (aromatic), 52.11 (CH), 31.87 (CH_2), 25.17 (CH_2), 24.54 (CH_2).

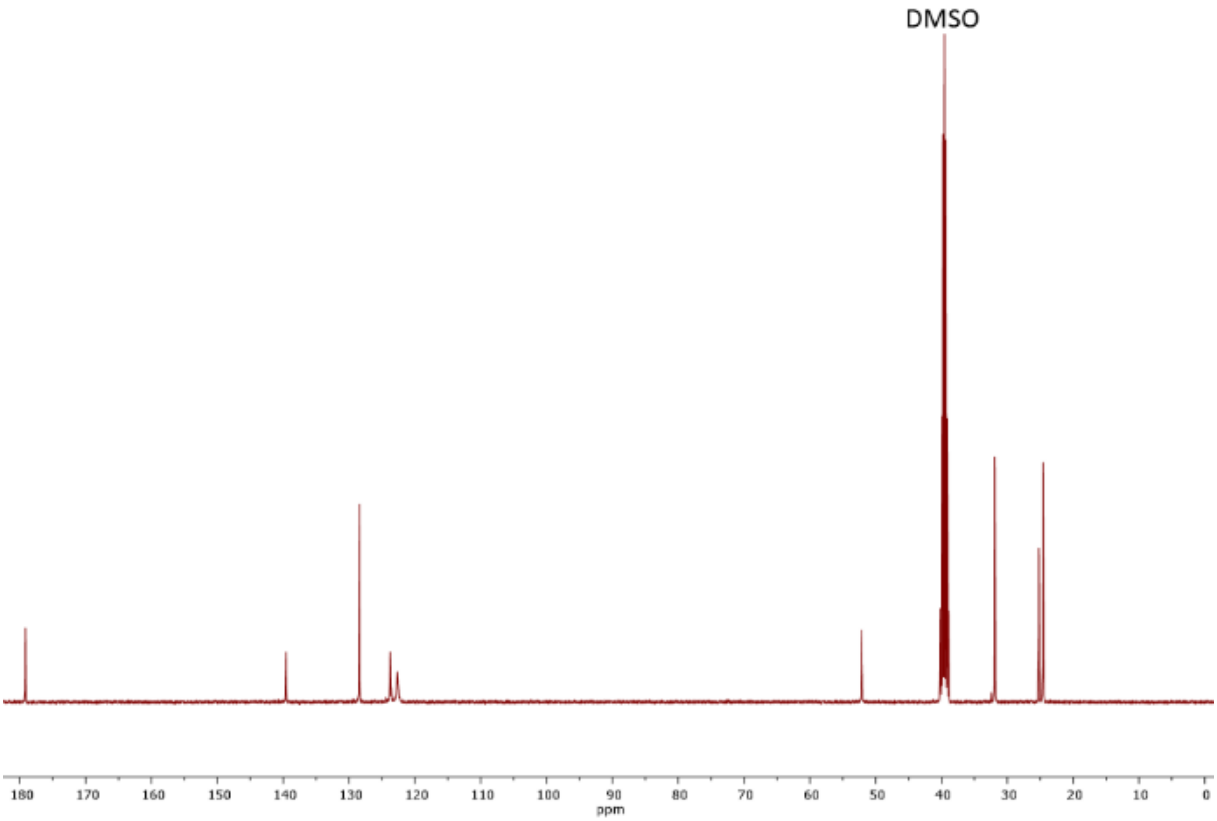

*Figure 75: ^{13}C-NMR-spectrum of thiourea **22**.*

EI-HRMS m/z: $[M]^+$ calculated for $[C_{13}H_{18}N_2S_1]$ = 234.1191, found: 234.1189, Δ = -0.1772 mmu.

IR (ATR platinum diamond): ν/cm^{-1} = 3236 (m), 2937 (m), 2921 (m), 2851 (m), 1590 (w), 1539 (vs), 1506 (vs), 1491 (vs), 1450 (s), 1395 (s), 1356 (m), 1345 (w), 1310 (m), 1290 (s), 1253 (s), 1236 (vs), 1199 (vs), 1183 (s), 1146 (vs), 1111 (s), 1074 (w), 1049 (w), 1024 (w), 983 (s), 893 (w), 854 (w), 823 (w), 790 (m), 740 (vs), 691 (vs), 652 (s), 621 (m), 599 (vs), 574 (vs), 535 (vs), 487 (vs), 436 (w), 420 (s).

1,4-Bis(*N*-cyclohexylthioureido) benzene 23

The synthesis was performed according to GP1. 1,4-Diisocyano benzene (168 mg, 1.31 mmol, 1.00 eq.) was reacted with cyclohexylamine **34** (333 µL, 286 mg, 2.89 mmol, 2.20 eq.) and elemental sulfur (94.2 mg, 367 µmol, 0.280 eq.). The reaction mixture was set under argon-atmosphere and was stirred at 80°C for 15 minutes. The crude product was washed with 5 mL methanol. To remove remaining methanol, an azeotrope was formed by adding 5 mL acetone and then removed under reduced pressure (3 ×). The pure product was obtained as yellow solid (375 mg, 960 µmol) in a yield of 73%.

R_f = 0.42 in cyclohexane/ethyl acetate 1/1 visualized *via* UV quenching at 254 nm.

^{1}H-NMR (400 MHz, DMSO-d_6) δ/ppm = 9.26 (s br, 2H, NH, ^{1}), 7.44 (m, 6H, NH, aromatic, ^{2}), 4.07 (s, 2H, CH, ^{3}), 2.06-0.99 (m, 20H, CH_2, ^{4}).

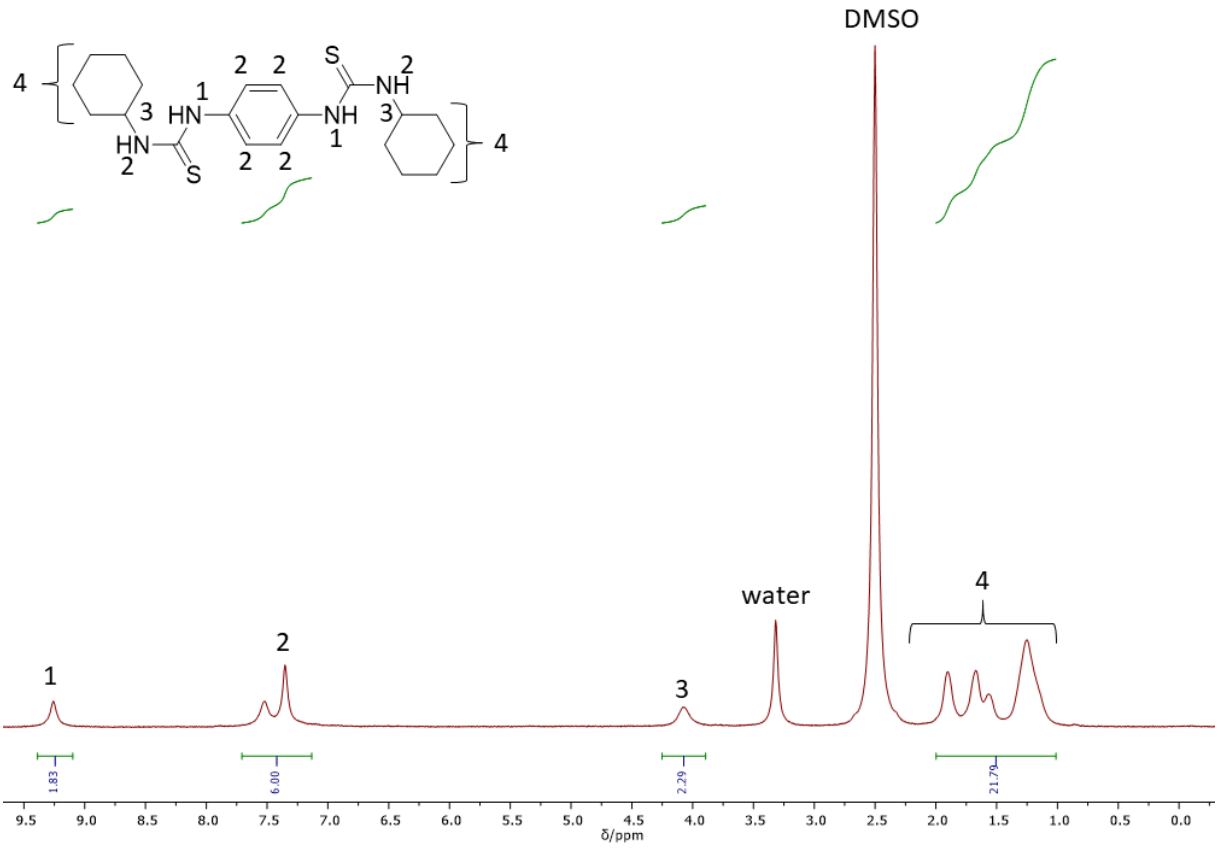

*Figure 76: ^{1}H-NMR-spectrum of thiourea **23**.*

^{13}C-NMR could not be recorded due to the poor solubility of the compound in typical deuterated solvents.

EI-HRMS m/z: $[M+H]^+$ calculated for $[C_{20}H_{30}N_4S_2]$ = 391.1990, found: 391.1988, Δ = -0.2511 mmu.

IR (ATR platinum diamond): ν/cm^{-1} = 3291 (w), 3246 (w), 3240 (w), 3233 (w), 2927 (m), 2851 (w), 1543 (vs), 1516 (vs), 1506 (vs), 1460 (w), 1448 (w), 1430 (m), 1382 (m), 1356 (m), 1302 (m), 1294 (m), 1265 (w), 1251 (m), 1226 (vs), 1199 (s), 1183 (m), 1152 (m), 1119 (m), 1107 (m), 1076 (w), 1047 (w), 1028 (w), 1014 (w), 981 (m), 965 (vw), 891 (w), 864 (w), 843 (w), 812 (w), 798 (w), 780 (w), 650 (m), 619 (w), 566 (s), 559 (s), 543 (vs), 516 (s), 502 (vs), 463 (w), 440 (w), 415 (s).

N-(4-(Methylbenzoate))-*N´*-cyclohexyl thiourea 24

The synthesis was performed according to GP1. Methyl 4-isocyanobenzoate **13** (344 mg, 2.13 mmol, 1.00 eq.) was reacted with cyclohexylamine **34** (269µmL, 233 mg, 2.35 mmol, 1.10 eq.), elemental sulfur (76.6 mg, 299 mmol, 0.140 eq.) and 2.1 mL of methanol. The reaction mixture was stirred at room temperature for 3 hours. DCM (2 mL) was added to dissolve the remaining isocyanide and the reaction was stirred at room temperature for another 24 hours. The solvent was removed under reduced pressure and a mixture of cyclohexane and ethyl acetate (10 mL, 7/3) were added to the crude product and the suspension was stored at -18 °C for 5 days. The product was obtained as an ochre solid in a yield of 38% (236 mg, 807 µmol) after filtration and washing with a minimal amount of methanol.

R_f = 0.38 in cyclohexane/ethyl acetate 2/1 visualized *via* UV quenching at 254 nm and vanillin staining solution (green).

^{1}H-NMR (400 MHz, DMSO-d_6) δ/ppm = 9.71 (s, 1H, NH, ^{1}), 7.98 (d, ^3J = 7.6 Hz, 1H, NH, ^{2}), 7.87 (d, ^3J = 8.7 Hz, 2H, aromatic, ^{3}), 7.71 (d, ^3J = 8.7 Hz, 2H, aromatic, ^{4}), 4.10 (m, 1H, CH, ^{5}), 3.81 (s, 3H, CH_3, ^{6}), 1.99-1.07 (m, 10H, CH_2, ^{7}).

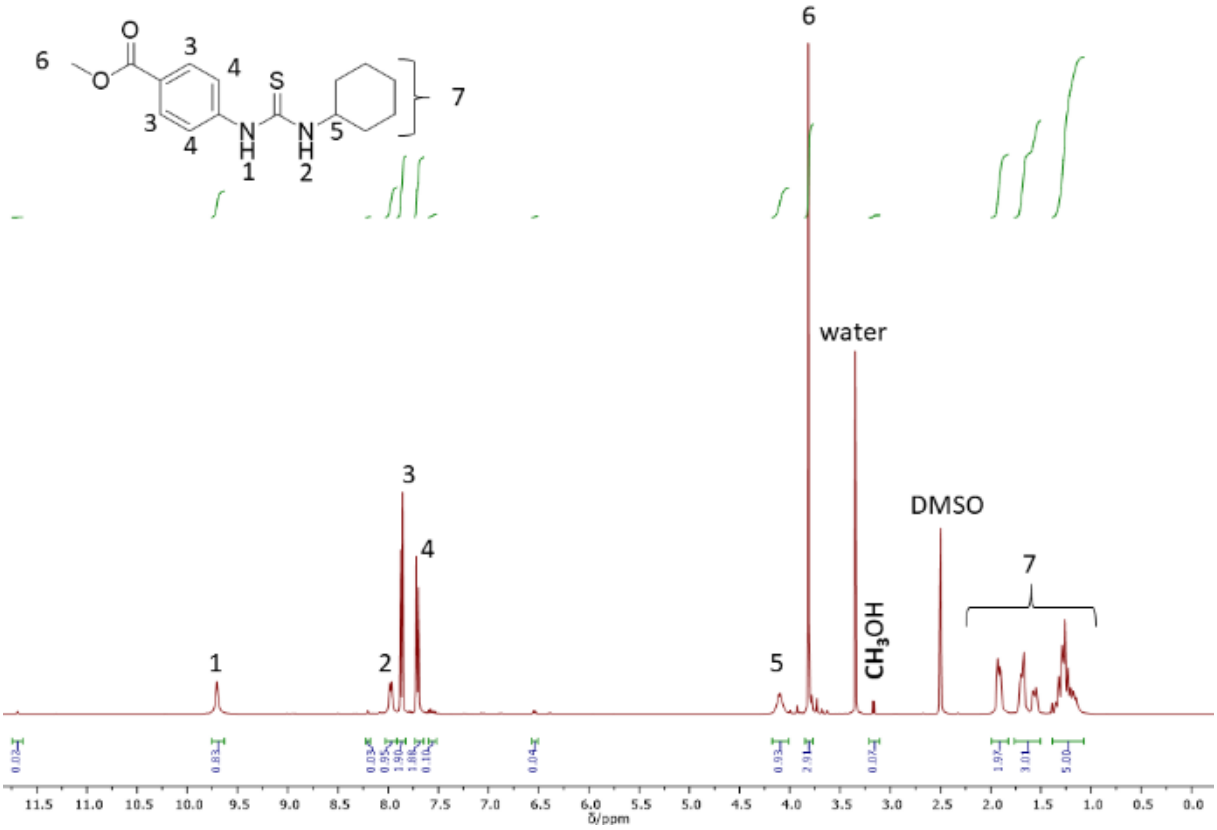

*Figure 77: ^{1}H-NMR-spectrum of thiourea **24**.*

^{13}C-NMR (101 MHz, DMSO-d_6) δ/ppm = 178.76 (C=S), 165.86 (C=O), 144.52 (aromatic), 129.77 (aromatic), 123.57 (aromatic), 120.47 (aromatic), 52.12 (CH), 51.87 (CH_3), 31.66 (CH_2), 25.14 (CH_2), 24.46 (CH_2).

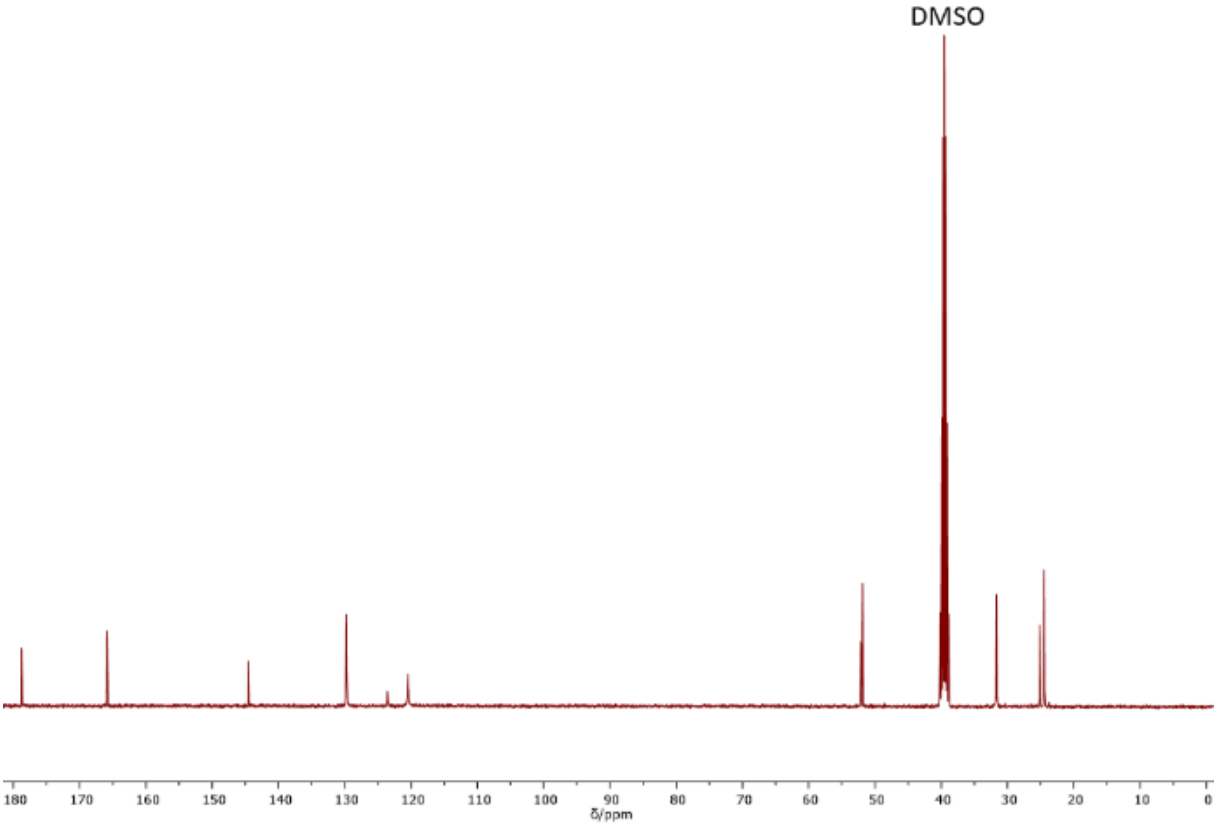

*Figure 78: ^{13}C-NMR-spectrum of thiourea **24**.*

EI-HRMS m/z: $[M]^+$ calculated for $[C_{15}H_{20}O_2N_2S_1]$ = 292.1245, found: 292.1246, Δ = 0.0803 mmu.

IR (ATR platinum diamond): ν/cm^{-1} = 3305 (w), 3186 (w), 3159 (w), 3089 (w), 3077 (w), 3020 (w), 2927 (w), 2853 (w), 1697 (vs), 1606 (m), 1541 (s), 1528 (vs), 1510 (s), 1436 (s), 1388 (w), 1358 (m), 1310 (s), 1284 (vs), 1242 (vs), 1199 (s), 1179 (vs), 1150 (s), 1113 (vs), 1014 (m), 983 (m), 963 (m), 891 (w), 864 (m), 847 (m), 833 (w), 812 (w), 790 (w), 765 (vs), 689 (s), 666 (vs), 594 (vs), 537 (m), 500 (s), 490 (s), 469 (m), 434 (m), 409 (m)

N-(5-(Dimethylisophtalate))-*N´*-cyclohexyl thiourea 25

The synthesis was performed according to GP1. 5-Isocyano dimethylisophtalate (1.00 g, 4.56 mmol, 1.00 eq.) was reacted with cyclohexylamine **34** (575 µL, 498 mg, 5.02 mmol, 1.10 eq.) and elemental sulfur (164 mg, 0.639 mmol, 0.140 eq.) in 5.06 ml methanol (0.90 M corresponding to n(isocyanide)). The reaction mixture was stirred at room temperature for 4 days. Afterwards, 13 ml methanol were added, and the mixture was left to crystallize for 3 days at room temperature. Filtration of the product and removal of the solvent yielded the pure product as colorless solid (1.31 g, 3.74 mmol) in a yield of 82%.

R_f = 0.38 in cyclohexane/ethyl acetate 2/1 visualized *via* UV quenching at 254 nm and vanillin staining solution (green).

^{1}H-NMR (400 MHz, DMSO-d_6) δ/ppm = 9.73 (s br, 1H, NH, ^{1}), 8.39 (d, ^4J =1.6 Hz, 2H, aromatic, ^{2}), 8.15 (m, 1H, aromatic, ^{3}), 7.92 (s br, 1H, NH, ^{4}), 4.09 (m, 1H, CH, ^{5}), 3.89 (s, 6H, CH_3, ^{6}), 2.00-1.09 (m, 10H, CH_2, ^{7}).

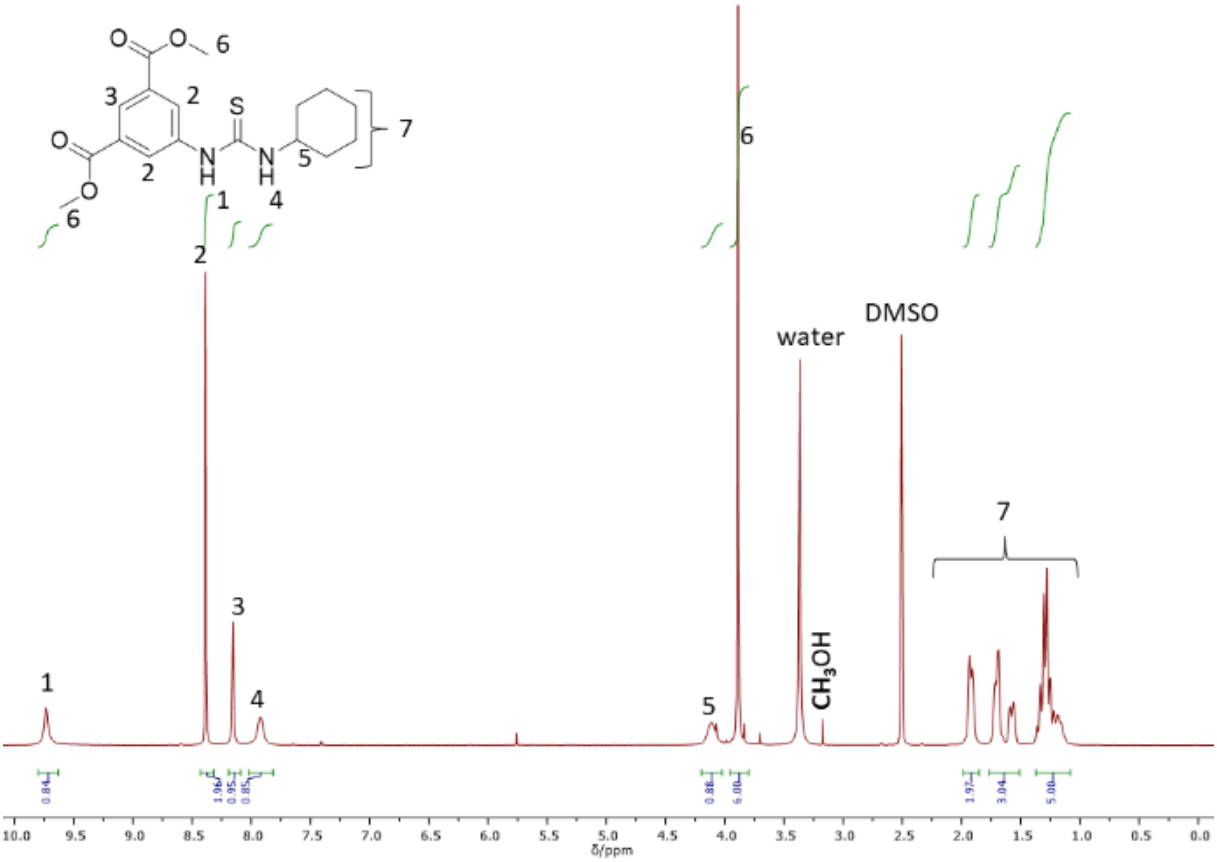

*Figure 79: ^{1}H-NMR-spectrum of thiourea **25**.*

^{13}C-NMR (101 MHz, DMSO-d_6) δ/ppm = 179.36 (C=S), 165.29 (C=O), 141.08 (aromatic), 130.15 (aromatic), 126.69 (aromatic), 124.08 (aromatic), 52.56 (CH_3), 52.19 (CH), 31.74 (CH_2), 25.15 (CH_2), 24.49 (CH_2).

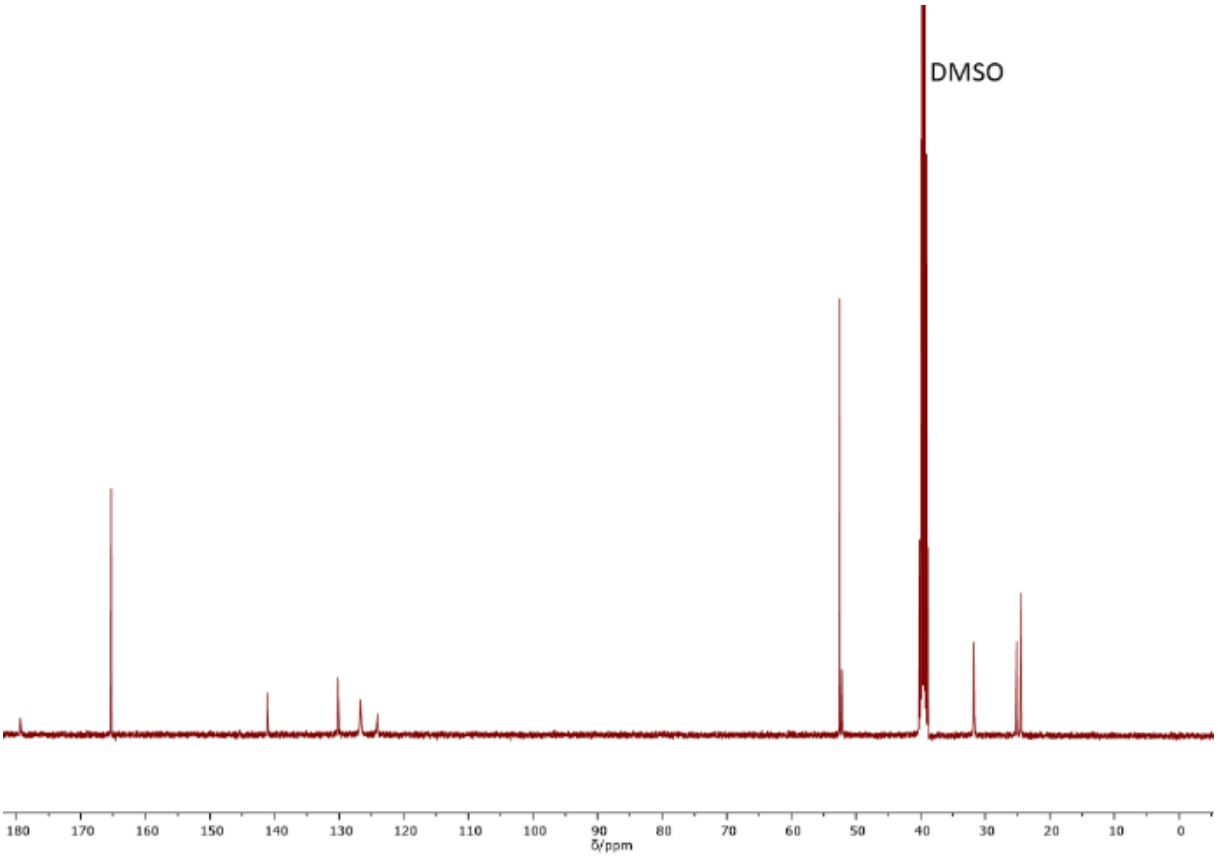

*Figure 80: ^{13}C-NMR-spectrum of thiourea **25**.*

EI-HRMS m/z: $[M]^+$ calculated for $[C_{17}H_{22}O_4N_2S_1]^+$ = 350.1300, found: 350.1300, Δ = -0.0708 mmu.

IR (ATR platinum diamond): ν/cm^{-1} = 3328 (w), 3020 (w), 2945 (w), 2927 (w), 2913 (w), 2847 (w), 1728 (vs), 1711 (vs), 1598 (w), 1530 (vs), 1448 (m), 1436 (s), 1382 (w), 1343 (vs), 1310 (w), 1300 (w), 1249 (vs), 1197 (vs), 1183 (vs), 1144 (vs), 1123 (m), 1109 (s), 996 (s), 981 (m), 907 (m), 893 (w), 880 (w), 852 (w), 821 (w), 792 (m), 757 (vs), 722 (w), 689 (w), 666 (m), 631 (vs), 605 (w), 592 (w), 547 (w), 510 (w), 483 (w), 455 (w), 434 (w).

N-(4-(*n*-Hexylsulfony)phenyl)-*N´*-cyclohexyl thiourea 26

The synthesis was performed according to GP1. 4-Isocyano hexylsulfoxybenzene (purity (w%=83%), 1.06 g 3.50 mmol, 1.00 eq.) was reacted with cyclohexylamine **34** (535 µL, 460 mg, 4.64 mmol, 1.33 eq.), elemental sulfur (151 mg, 590 µmol, 0.169 eq.) and 4 mL of methanol. The reaction mixture was stirred at room temperature for 17 hours. The pure product was obtained after column chromatography (cyclohexane/ethyl acetate 6/1→4/1) as a yellowish solid (693 mg, 1.81 mmol) in a yield of 52%.

R_f = 0.25 in cyclohexane/ethyl acetate 2/1 visualized *via* UV quenching at 254 nm and vanillin staining solution (green).

^{1}H-NMR (400 MHz, DMSO-d_6) δ/ppm = 9.77 (s, 1H, NH, ^{1}), 8.04 (d, ^3J = 7.9 Hz, 1H, NH, ^{2}), 7.84-7.78 (m, 2H, aromatic, ^{3}), 7.78-7.73 (m, 2H, aromatic, ^{4}), 4.10 (m, 1H, CH, ^{5}), 3.27-3.17 (m, 2H, CH_2, ^{6}), 2.00-1.10 (m, 18H, CH_2, ^{7}), 0.86-0.76 (t, ^3J = 6.9 Hz, 3H, CH_3, ^{8}).

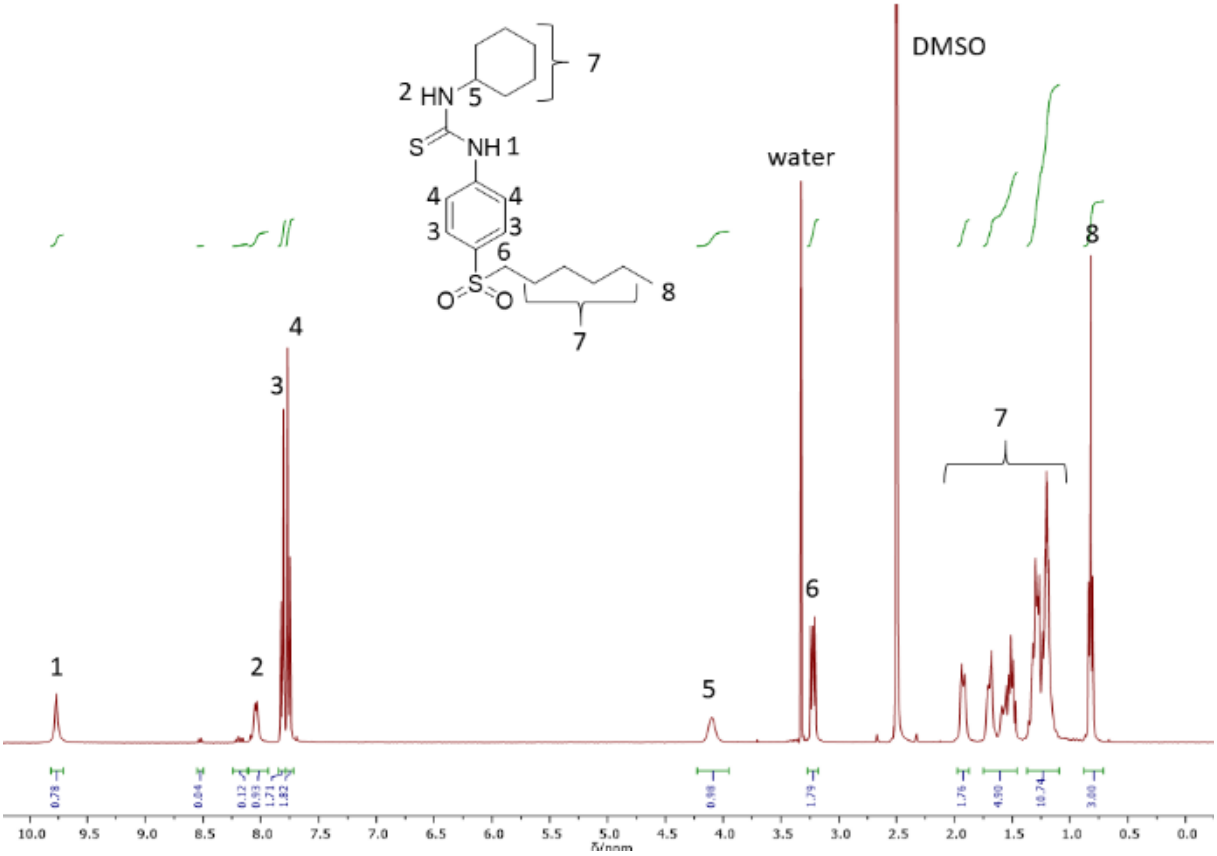

*Figure 81: ^{1}H-NMR-spectrum of thiourea **26**.*

^{13}C-NMR (101 MHz, DMSO-d_6) δ/ppm = 178.82 (C=S), 144.79 (aromatic), 132.34 (aromatic), 128.36 (aromatic), 120.74 (aromatic), 54.83 (CH_2), 52.17 (CH), 31.61 (CH_2), 30.64 (CH_2), 27.09 (CH_2), 25.13 (CH_2), 24.44 (CH_2), 22.37 (CH_2), 21.80 (CH_2), 13.80 (CH_3).

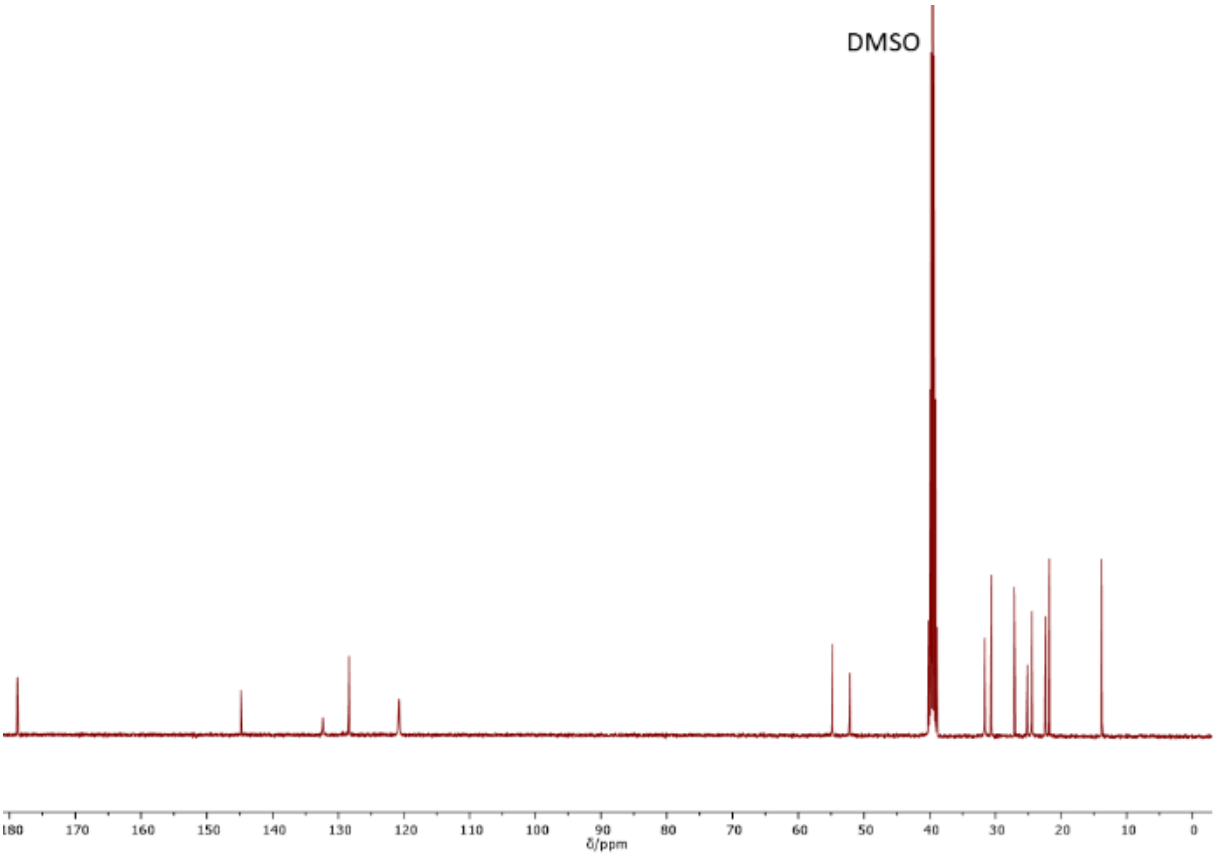

*Figure 82: ^{13}C-NMR-spectrum of thiourea **26**.*

EI-HRMS m/z: $[M]^+$ calculated for $[C_{19}H_{30}O_2N_1S_2]$ = 382.1743, found: 382.1741, Δ = -0.2105 mmu.

IR (ATR platinum diamond): ν/cm^{-1} = 3340 (w), 3223 (vw), 2929 (s), 2867 (w), 2853 (m), 1623 (w), 1596 (m), 1532 (vs), 1497 (s), 1465 (w), 1450 (m), 1419 (w), 1360 (w), 1333 (vs), 1312 (s), 1298 (s), 1273 (vs), 1251 (vs), 1212 (s), 1181 (m), 1135 (vs), 1111 (s), 1086 (vs), 1012 (w), 981 (w), 889 (w), 876 (w), 831 (s), 773 (m), 747 (m), 740 (m), 722 (m), 687 (m), 666 (s), 650 (s), 597 (vs), 572 (s), 549 (vs), 529 (vs), 490 (s), 442 (w).

N-(3,5-Bis(trifluormethyl)phenyl)-*N´*-cyclohexyl thiourea 27

Procedure A (MCR):

First, 3,5-bis(trifluormethyl) isocyanobenzene was synthesized using 3,5-bis(trifluoromethyl)phenyl formamide (1.00 g, 3.89 mmol, 1.00 eq.), which was dissolved in 11.8 mL DCM. The reaction mixture was cooled to 0 °C using an ice-water bath. Subsequently, DIPA (1.69 mL, 1.22 g, 12.1 mmol, 3.10 eq.) was added to the mixture and phosphorus oxychloride (473 µL, 775 mg, 5.06 mmol, 1.30 eq.) was added dropwise, while keeping the temperature at 0 °C. After addition, the cooling was removed and the mixture was stirred at room temperature for 3 hours. Afterwards, the reaction mixture was put directly on a filter column which was packed with cyclohexane and 5 V% of TEA and DCM was applied as eluent. After column chromatography the solvent and the majority of DIPA was removed under reduced pressure (please note that the isocyanide sublimes at 50 °C and around 50 mbar) yielding the crude product (673 mg, 2.81 mmol, corresponding to a yield of 72%), which was used immediately without further analysis since the isocyanide is sensitive to moisture.

The synthesis was performed according to GP1. The isocyanide was reacted with cyclohexylamine **34** (356 µL, 306 mg, 3.09 mmol, 1.10 eq.) and elemental sulfur (101 mg, 393 µmol, 0.140 eq.) without any solvent. The reaction mixture was stirred at room temperature for 1 hour. Then, 2.8 mL methanol was added and the reaction mixture was stirred for 5 days. The product was obtained after column chromatography (dryload, cyclohexane/ethyl acetate 20/1→13/1) as a slightly orange solid (376 mg, 1.02 mmol) in a yield of 26% (corresponding to the amount of formamide used).

Procedure B:

Cyclohexyl isothiocyanate (983 µL, 1.00 g, 7.08 mmol, 1.00 eq.) was dissolved in 7 mL DMSO. Subsequently, 3,5-bis(trifluormethyl) aniline (1.21 mL, 1.78 mg, 7.79 mmol, 1.10 eq.) and DABCO (874 mg, 7.79 mmol, 1.10 eq.) were added and the reaction mixture was stirred at 100 °C for 24 hours. Then, ethyl acetate (10 mL) and water (10 mL) were added, and the phases were separated. The aqueous phase was extracted with ethyl acetate (2 × 20 mL). The combined organic layers were washed with 1.0 M aqueous hydrochloric acid solution (2 × 25 mL) and water (2 × 25 mL), dried over sodium sulfate and filtered off. The crude product was purified by column chromatography (dryload, cyclohexane/ethyl acetate 30/1, adding 5 V% of acetic acid to the eluent) and the product was obtained as a colorless powder (1.28 g, 3.46 mmol) in a yield of 49%.

R_f = 0.55 in cyclohexane/ethyl acetate 3/1 visualized *via* UV quenching at 254 nm and vanillin staining solution (green).

^{1}H-NMR (500 MHz, DMSO-d_6) δ/ppm = 9.85 (s br, 1H, NH, [1]), 8.23 (s, 2H, aromatic, [2]), 8.15 (s br, 1H, NH, [2]), 7.70 (s, 1H, aromatic, [3]), 4.11 (m, 1H, CH, [4]), 1.96-1.10 (m, 10H, CH_2, [5]).

^{19}F-NMR (376 MHz, DMSO-d_6) δ/ppm = -61.63.

^{13}C-NMR (126 MHz, DMSO-d_6) δ/ppm = 179.22 (C=S), 142.01 (aromatic), 130.08 (q, ^2J = 32.0 Hz, aromatic), 123.27 (q, ^1J = 273.3 Hz, CF_3), 121.71 (aromatic), 115.81 (aromatic), 52.32 (CH), 31.58 (CH_2), 25.09 (CH_2), 24.43 (CH_2).

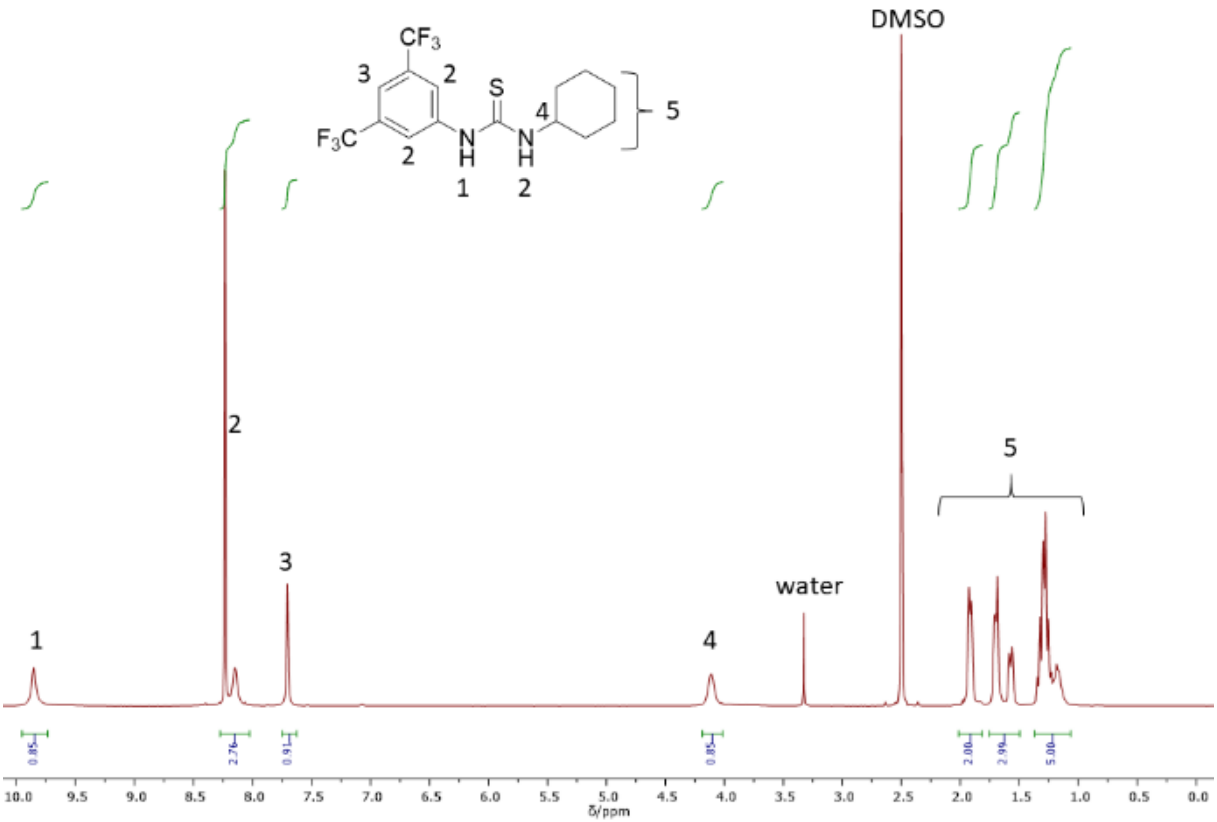

*Figure 84: [1]H-NMR-spectrum of thiourea **27**.*

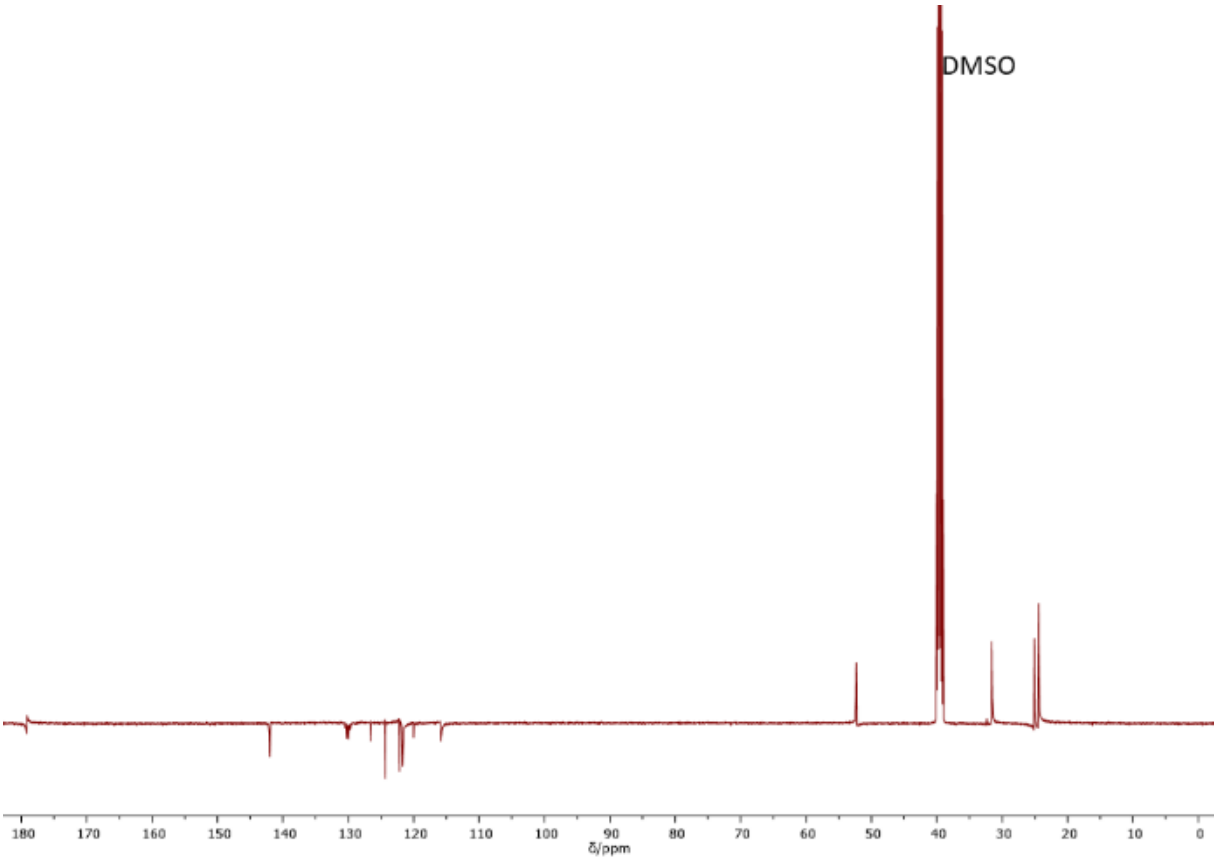

*Figure 83: [13]C-NMR-spectrum of thiourea **27**.*

EI-HRMS m/z: $[M+H]^+$ calculated for $[C_{15}H_{16}N_2F_6S_1]$ = 371.1011, found: 371.1011, Δ = 0.0181 mmu.

IR (ATR platinum diamond): ν/cm^{-1} = 3285 (vw), 3164 (vw), 3040 (w), 2933 (w), 2859 (w), 1553 (m), 1526 (s), 1467 (w), 1382 (s), 1364 (m), 1337 (m), 1267 (vs), 1177 (vs), 1127 (vs), 1105 (vs), 1039 (w), 1024 (w), 940 (m), 889 (vs), 862 (w), 847 (w), 753 (w), 706 (s), 679 (vs), 617 (w), 586 (w), 549 (w), 516 (w).

6.4.5 Synthesis of aromatic isocyanides

General synthesis of aromatic isocyanides (GP2)

The corresponding *N*-formamide (1.00 eq.) was dissolved in DCM (0.33 M corresponding to n(*N*-formamide)) and DIPA 3.10 eq.) was added. Subsequently, the reaction mixture was cooled to 0°C using an ice-water bath and phosphorus oxychloride (1.30 eq.) was added dropwise keeping the temperature at 0 °C. Afterwards, the cooling bath was removed, and the reaction was stirred at room temperature for 2 hours. After completion of the reaction, purification was performed *via* flash column chromatography (typically height of silica loading: 5 cm). Thereby, the reaction mixture was added dropwise directly onto the dry silica loaded column to quench the remaining phosphorus oxychloride. Then, the product was purified by eluting with DCM. Since some of the synthesized isocyanides were sensitive to moisture, purification was conducted as quickly as possible and the compounds were used directly for further synthesis. Deviations of GP2 are highlighted in the synthesis of the respective compound.

Methyl 4-isocyanobenzoate 13

The synthesis was performed according to GP2. Methyl 4-formamidobenzoate (10.0 g, 55.8 mmol, 1.00 eq.) was reacted with DIPA (24.3 mL, 17.5 g, 173 mmol, 3.10 eq.) and phosphorus oxychloride (6.78 mL, 11.1 g, 72.6 mmol, 1.30 eq.) in 169 mL DCM. First, remaining phosphorus oxychloride was quenched by adding 180 mL saturated sodium hydrogen carbonate solution to the reaction mixture and the biphasic mixture was stirred for another 30 minutes. The phases were separated and the aqueous phase was extracted with DCM (1 × 100 mL). The organic layers were combined, dried over sodium sulfate and filtered off. The crude product was purified *via* column chromatography (height 10 cm, cyclohexane/ethyl acetate 6/1) yielding the isocyanide as dark black solid with a GC purity of 95% (7.37 g, 45.8 mmol) in a yield of 82%. Please note that this compound sublimes at 50°C and 4 mbar, yielding needle shaped colorless crystals.

R_f = 0.55 in cyclohexane/ethyl acetate 2/1 visualized *via* UV quenching at 254 nm and vanillin staining solution (yellow).

^{1}H-NMR was according to the literature.[258]

^{1}H-NMR (300 MHz, DMSO-d_6) δ/ppm = 8.08-8.01 (m, 2H, aromatic, ^{1}), 7.76-7.69 (m, 2H, aromatic, ^{2}), 3.87 (s, 3H, CH_3, ^{3}).

Dimethyl 5-isocyanoisophtalate

The synthesis was performed according to GP2. Dimethyl 5-formamidoisophtalate (5.72 g, 24.1 mmol, 1.00 eq.) was reacted with DIPA (10.5 mL, 7.56 g, 74.8 mmol, 3.10 eq.) and phosphorus oxychloride (2.86 mL, 4.81 g, 31.4 mmol, 1.30 eq.) in 73 mL DCM. After completion of the reaction, remaining phosphorus oxychloride was quenched by adding 70 mL saturated sodium hydrogen carbonate solution to the reaction mixture and the biphasic mixture was stirred for another 30 minutes. The phases were separated and the aqueous phase was extracted with DCM (1 × 50 mL). The organic layers were combined, dried over sodium sulfate and filtered off. Purification of the crude product with flash column chromatography (cyclohexane/ethyl acetate 11/1) yielded the product as colorless needle-like crystals (3.91 g, 17.8 mmol) in a yield of 74%.

***R*$_f$** = 0.16 in cyclohexane/ethyl acetate 11/1 visualized *via* UV quenching at 254 nm and vanillin staining solution (orange).

^{1}H-NMR (500 MHz, DMSO-d_6) δ/ppm = 8.48 (s, 1H, aromatic, ^{1}), 8.31 (s, 2H, aromatic, ^{2}), 3.92 (s, 6H, CH_3, ^{3}).

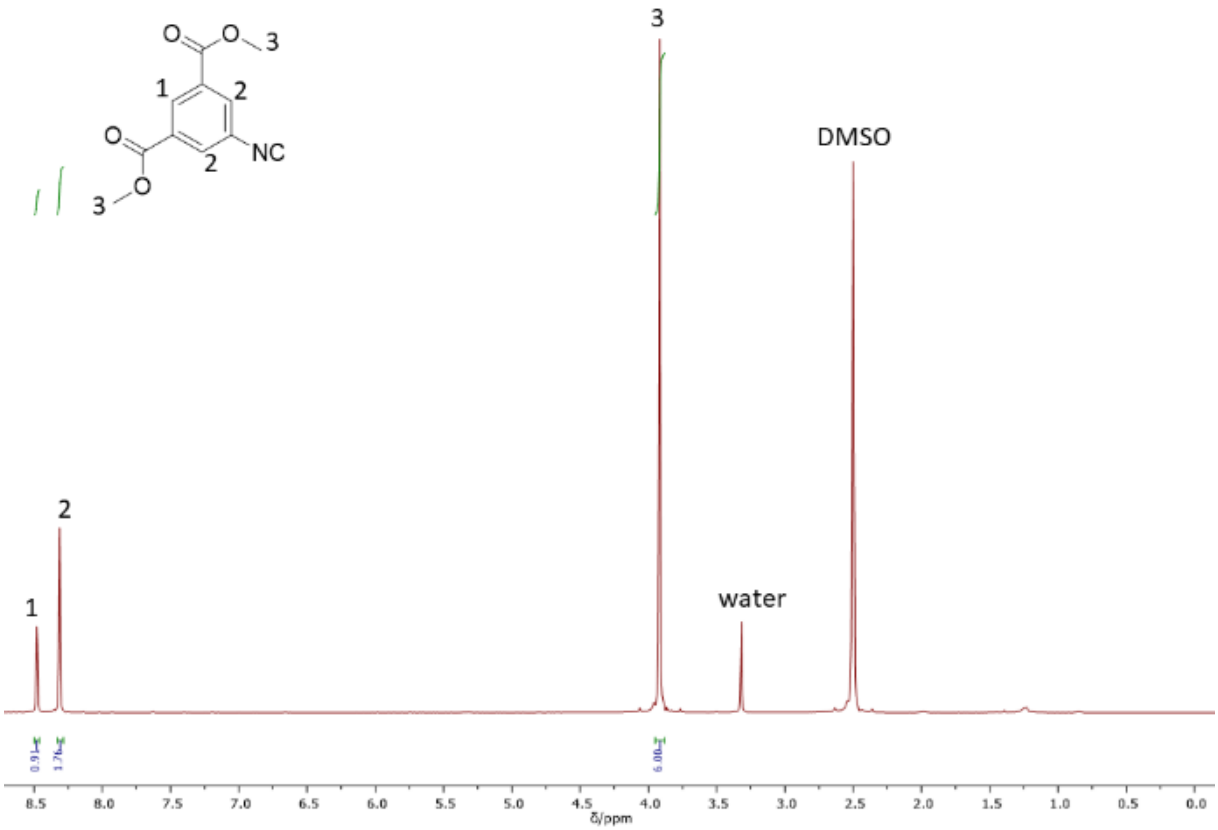

Figure 85: ^{1}H-NMR-spectrum of dimethyl 5-isocyanoisophthalate.

^{13}C-NMR (101 MHz, $CDCl_3$) δ/ppm = 166.56 (NC), 163.97 (**C**OOMe), 131.91 (aromatic), 131.05 (aromatic), 130.19 (aromatic), 52.94 (CH_3).

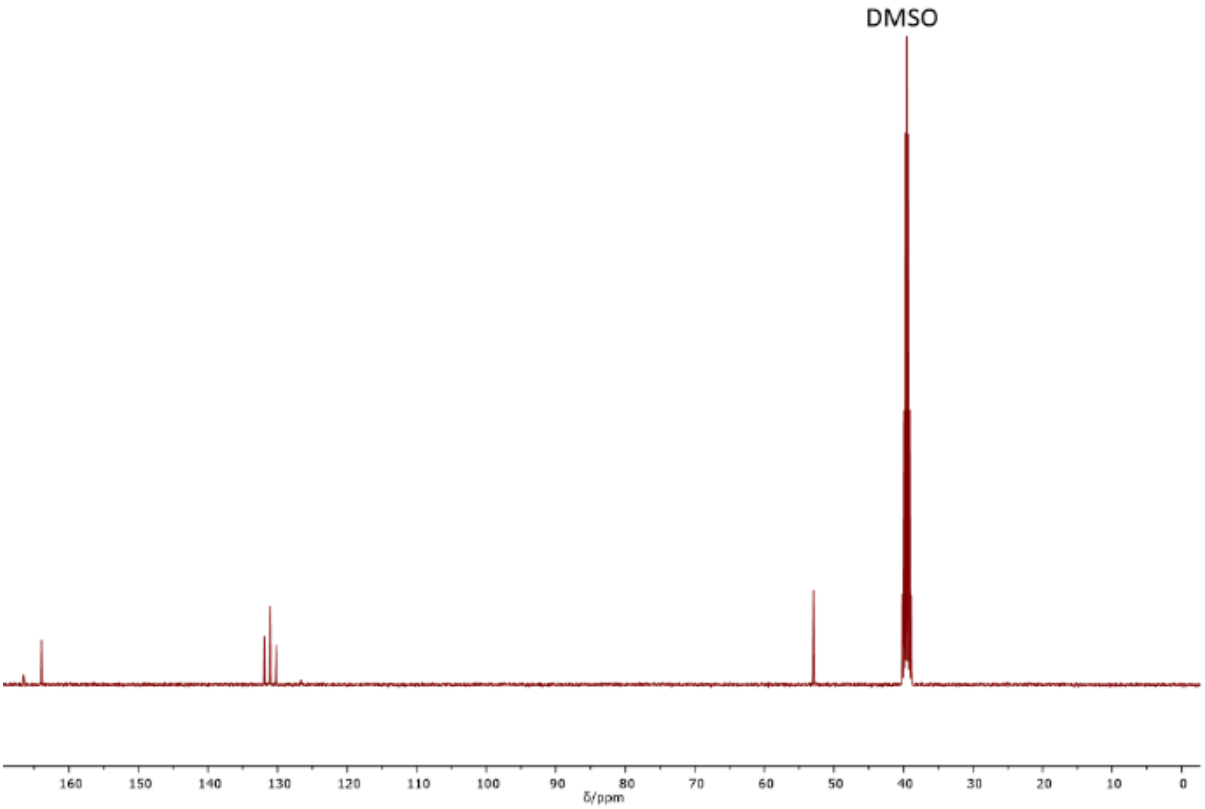

Figure 86: ^{13}C-NMR-spectrum of dimethyl 5-isocyanoisophthalate.

EI-HRMS m/z: $[M]^+$ calculated for $[C_{11}H_9N_1O_4]$ = 219.0532, found: 219.0532, Δ = 0.0674 mmu.

IR (ATR platinum diamond): ν/cm^{-1} = 3085 (m), 2958 (w), 2137 (m), 1728 (vs), 1454 (w), 1432 (s), 1349 (w), 1316 (s), 1259 (m), 1238 (vs), 1201 (vs), 1172 (vs), 1121 (s), 1105 (s), 983 (vs), 932 (s), 917 (s), 880 (vs), 784 (w), 749 (vs), 726 (s), 664 (m), 588 (w), 551 (w), 463 (vs), 411 (m).

4-(*n*-Hexylsulfonyl) isocyanobenzene

The synthesis was performed according to GP2. 4-(*n*-Hexylsulfonyl) formamidobenzene (500 mg, 1.86 mmol, 1.00 eq.) was reacted with DIPA (802 µL, 582 mg, 5.75 mmol, 3.10 eq.) and phosphorus oxychloride (226 µL, 370 mg, 2.41 mmol, 1.30 eq.) in 5.6 mL DCM. After completion of the reaction, purification was performed *via* flash column chromatography (height of silica loading: 5 cm). Thereby, the reaction mixture was added dropwise directly onto the dry silica loaded column to quench the remaining phosphorus oxychloride. Then, the product was purified by eluting with DCM. The product was obtained as red-brown solid (295 mg, 1.17 mmol) in a yield of 63%. Please note that the compound is moisture sensitive and starts decomposing to the starting material while purifying. The purity was determined by ^{1}H-NMR and was 83 wt% (s. below, 9% starting material and 14% DIPA). The crude isocyanide was used directly for synthesis of thiourea **10**.

R_f = 0.83 in cyclohexane/ethyl acetate 1/1 visualized *via* UV quenching at 254 nm and vanillin staining solution (orange).

^{1}H-NMR (400 MHz, DMSO-d_6) δ/ppm = 8.03(d, ^{3}J = 8.5 Hz, 2H, aromatic, ^{1}), 7.87 (d, ^{3}J = 8.5 Hz, 2H, aromatic, ^{2}), 3.40-3.33 (m, 2H, CH_2, ^{3}), 1.60-1.45 (m, 2H, CH_2, ^{4}), 1.37-1.08 (m, 6H, CH_2, ^{5}), 0.82 (t, ^{3}J = 6.7 Hz, 3H, CH_3, ^{6}).
Please note that signals highlighted with the appendix "*" are signals from the starting material.

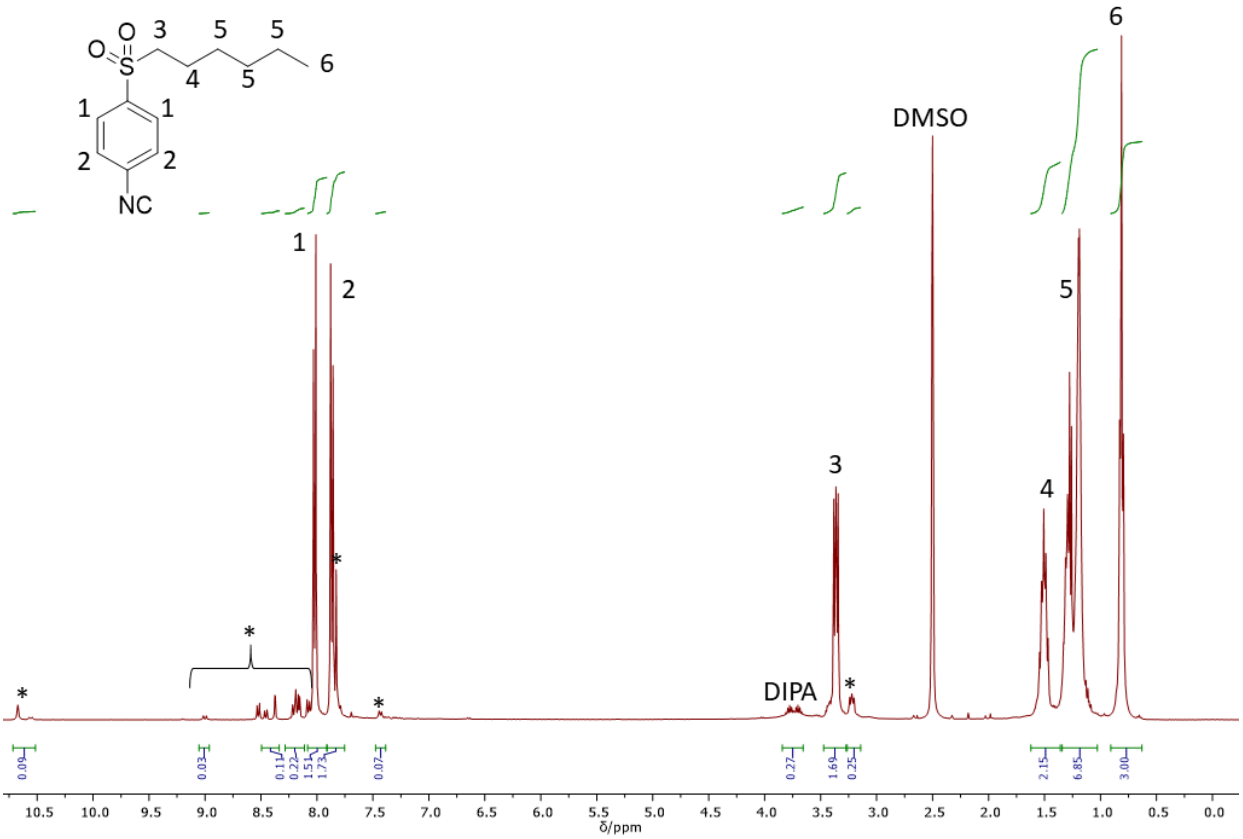

Figure 87: ^{1}H-NMR-spectrum of 4-(n-hexylsulfonyl) isocyanobenzene.

Further analysis was not performed due to the sensitivity of the compound.

1,4-Diisocyanobenzene

The synthesis was performed according to GP2. 1,4-Diformamidobenzene (3.00 g, 18.3 mmol, 1.00 eq.) was reacted with DIPA (15.8mL, 11.5 mg, 113 mmol, 6.20 eq.) and phosphorus oxychloride (4.44 mL, 7.28 g, 47.5 mmol, 2.60 eq.) in 55.5 mL DCM. After completion of the reaction, purification was performed *via* flash column chromatography (height of silica loading: 5 cm). Thereby, the reaction mixture was added dropwise directly onto the dry silica loaded column to quench the remaining phosphorus oxychloride. Then, the product was purified by eluting with DCM. The product was obtained as brown crystalline solid (1.66 g, 13.0 mmol) in a yield of 71%.

***R*$_f$** = 0.68 in cyclohexane/ethyl acetate 2/1 visualized *via* UV quenching at 254 nm and vanillin staining solution (yellow).

^{1}H-NMR (400 MHz, DMSO-d$_6$) δ/ppm = 7.73 (s, 4H, aromatic, ^{1}).

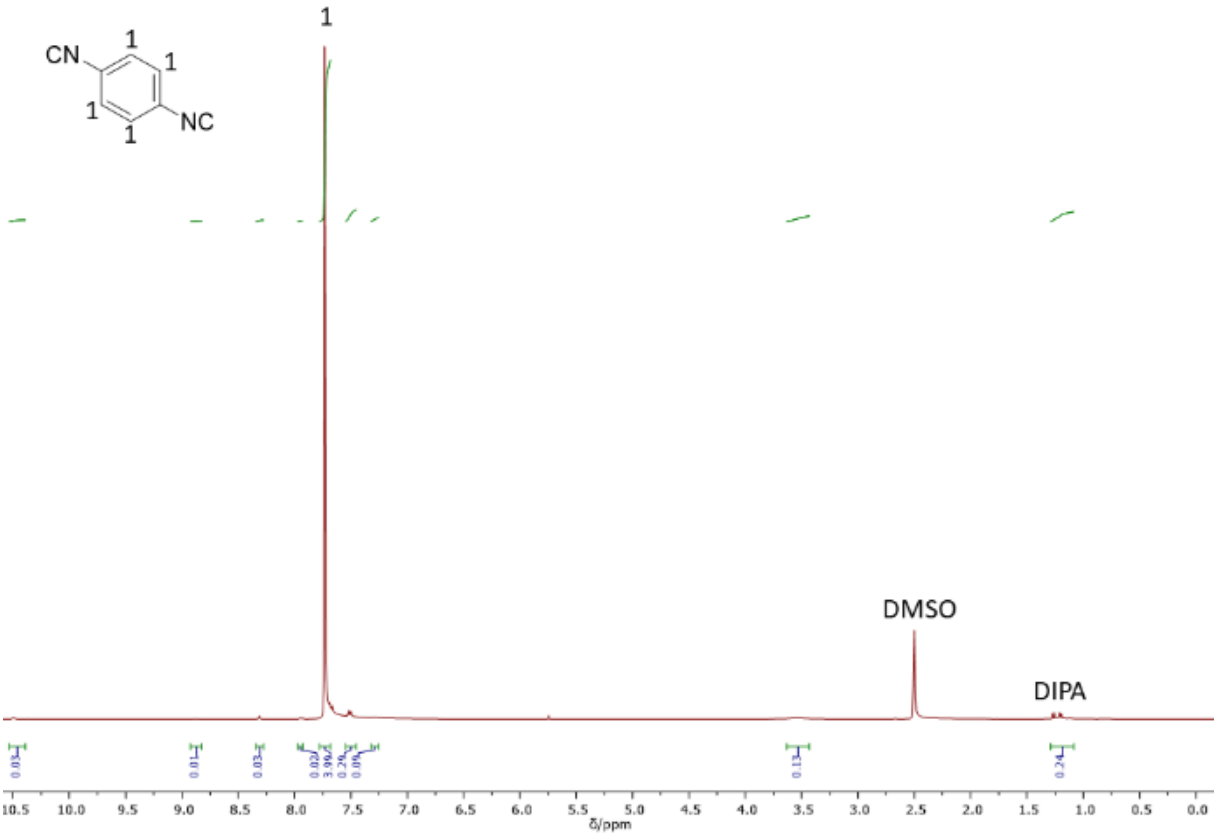

Figure 88: ^{1}H-NMR-spectrum of 1,4-diisocyanobenzene.

^{13}C-NMR (126 MHz, DMSO-d$_6$) δ/ppm = 166.41 (NC), 128.09 (aromatic).

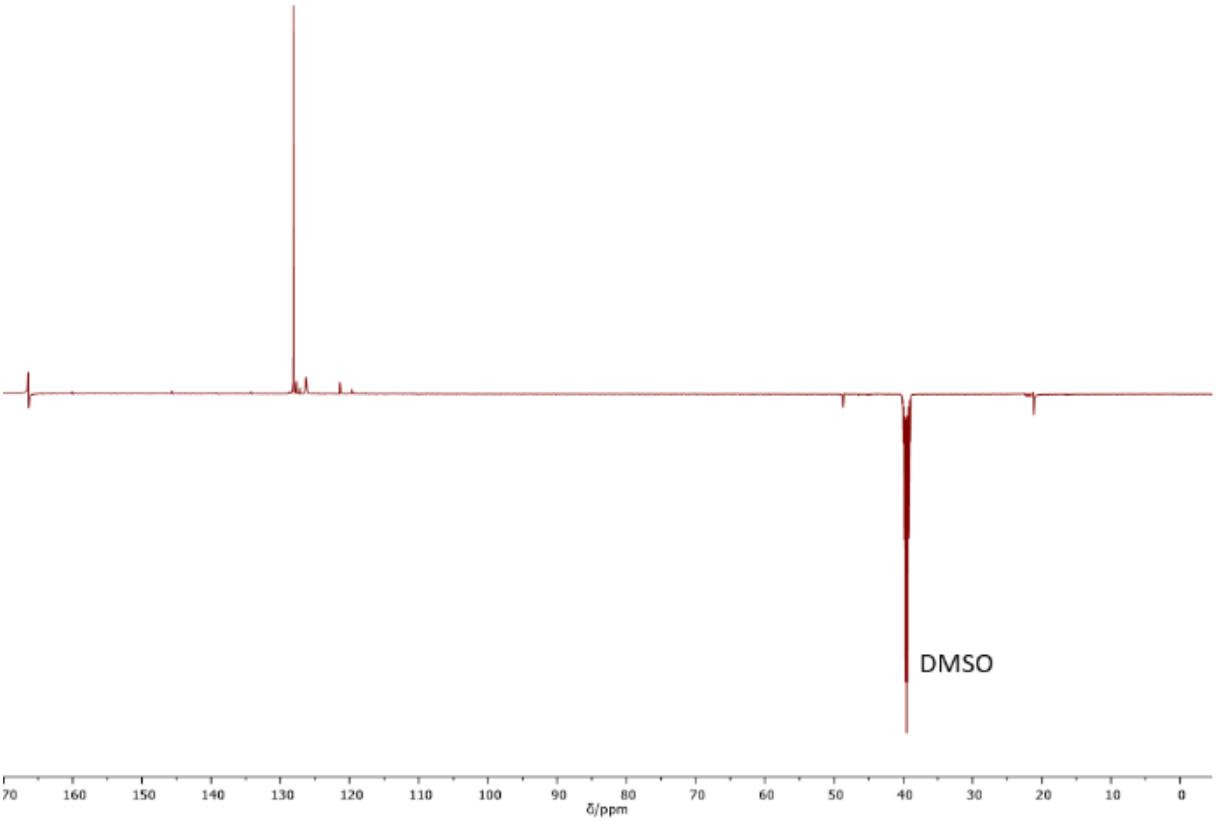

Figure 89: ^{13}C-NMR-spectrum of 1,4-diisocyanobenzene.

EI-HRMS m/z: $[M]^+$ calculated for $[C_8H_4N_2]$ = 128.0374, found: 128.0374, Δ = -0.0395 mmu.

IR (ATR platinum diamond): ν/cm^{-1} = 3092 (w), 2976 (w), 2129 (m), 1732 (w), 1724 (w), 1680 (w), 1502 (m), 1485 (m), 1411 (m), 1284 (s), 1273 (s), 1240 (m), 1203 (m), 1183 (m), 1174 (m), 1154 (m), 1140 (m), 1119 (m), 1024 (m), 996 (m), 843 (vs), 662 (s), 555 (s), 527 (vs), 496 (s), 481 (s), 473 (s), 448 (s).

6.4.6 Synthesis of aromatic *N*-formamides

General synthesis of aromatic *N*-formamides (GP3)

Formic acid (4.00 eq.) was added to the corresponding amine (1.00 eq.) in a flask equipped with a Dimroth-condenser and the mixture was stirred at 60°C for 24 hours. Subsequently, the remaining formic acid and water were removed under reduced pressure. The obtained *N*-formamides were used without further purification.

3,5-Bis(trifluoromethyl)phenyl formamide

The synthesis was performed according to GP3. 3,5-Bis(trifluoromethyl) aniline (1.00 g, 4.36 mmol, 1.00 eq.) was reacted with formic acid (1.65 mL, 2.01 g, 43.6 mmol, 10.0 eq.). Subsequently, the remaining formic acid and water were removed under reduced pressure. The product was obtained as colorless needles (1.12 g, 4.36 mmol) in quantitative yield. Please note that the product exhibits static properties.

R_f = 0.39 in cyclohexane/ethyl acetate 2/1 visualized *via* UV quenching at 254 nm and vanillin staining solution (yellow).

^{1}H-NMR (400 MHz, DMSO-d_6) δ/ppm = 10.82 (s, 0.8H, CHO, ^{1a}), 10.56 (d, ^3J = 10.5 Hz, 0.2H, CHO, ^{1b}), 9.04 (d, ^3J = 10.6 Hz, 0.2H, NH, ^{2b}), 8.43 (d, ^3J = 1.5 Hz, 0.8H, NH, ^{2a}), 8.22 (s, 1.6H, aromatic, ^{3a}), 7.87 (s, 0.4H, aromatic, ^{3b}), 7.72 (s, 0.8H, aromatic, ^{4a}), 7.67 (s, 0.2H, aromatic, ^{4b}).

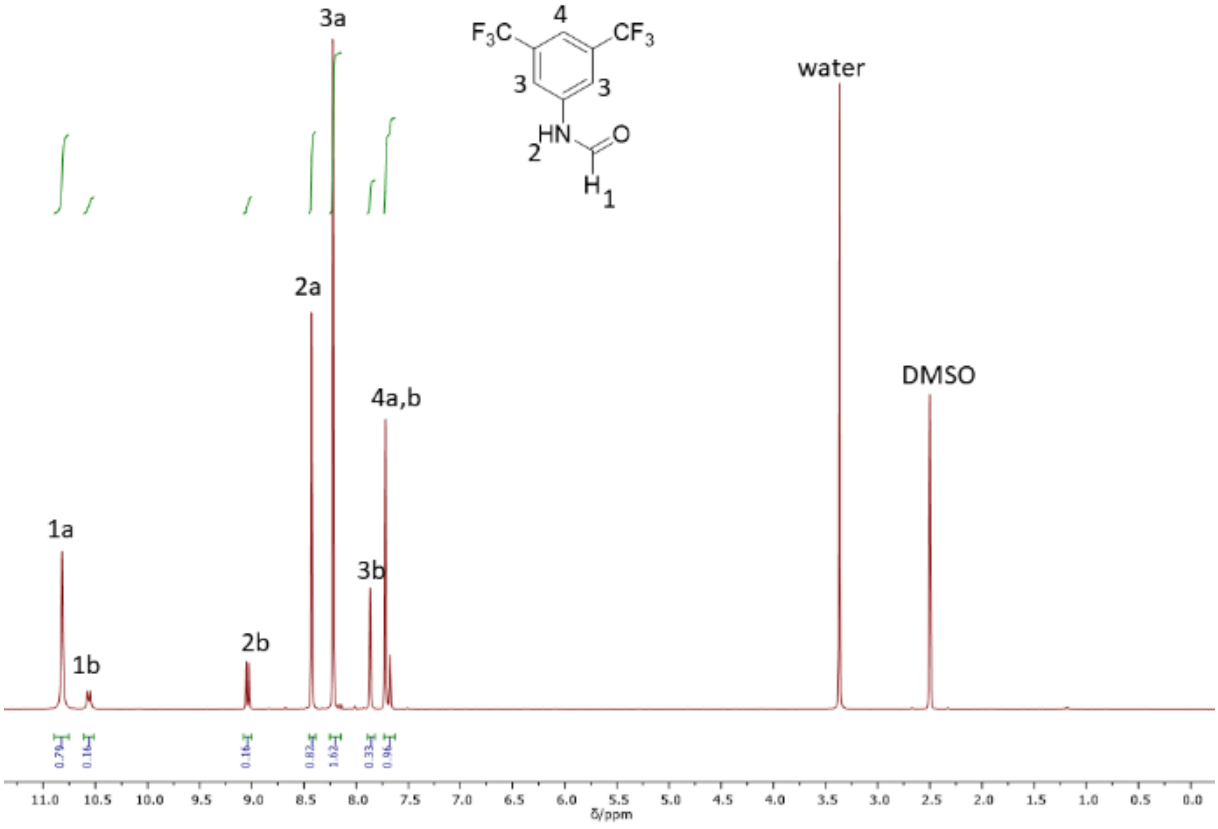

Figure 90: ^{1}H-NMR-spectrum of 3,5-bis(trifluoromethyl)phenyl formamide..

19F-NMR (376 MHz, DMSO-d_6) δ/ppm = -66.33.

^{13}C-NMR (101 MHz, DMSO-d_6) δ/ppm = 162.98 (C=O, ^{b}), 160.80 (C=O, ^{a}), 140.88 (aromatic, ^{1b}), 140.05 (aromatic, ^{1a}), 131.34 (q,^2J = 32.9 Hz, aromatic, ^{2b}) 130.91 (q,^2J = 32.9 Hz, aromatic, ^{2a}), 123.13 (q,^1J = 273.7 Hz, CF_3), 118.90 (q, ^3J = 4.1 Hz, aromatic, ^{3a}), 117.24-117.04 (m, aromatic, ^{3b}), 116.40 (sept., ^3J = 4.0 Hz, aromatic, ^{4a}), 116.07-115.81 (m, aromatic, ^{4b}).

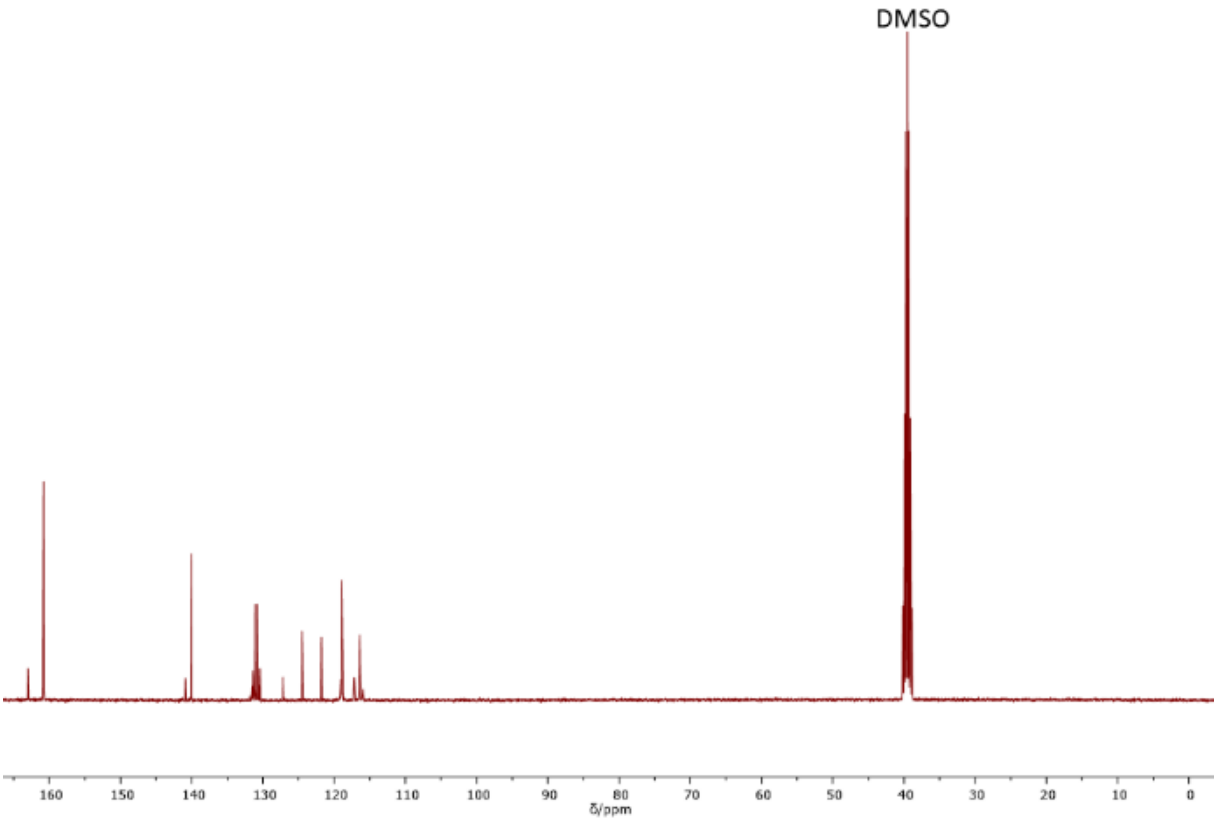

Figure 91: ^{13}C-NMR-spectrum of 3,5-bis(trifluoromethyl)phenyl formamide..

EI-HRMS m/z: $[M]^+$ calculated for $[C_9H_5O_1N_1F_6]$ = 257.0275, found: 257.0274, Δ = -0.1638.

IR (ATR platinum diamond): ν/cm^{-1} = 3285 (w), 3244 (w), 3106 (vw), 2921 (vw), 1705 (w), 1680 (m), 1623 (w), 1561 (m), 1551 (m), 1471 (m), 1440 (w), 1407 (m), 1372 (m), 1269 (vs), 1168 (s), 1131 (vs), 1107 (vs), 1000 (w), 915 (m), 899 (m), 882 (s), 827 (m), 751 (m), 724 (m), 699 (s), 679 (vs), 510 (m), 405 (m).

Methyl 4-formamidobenzoate

The synthesis was performed according to GP3. Methyl 4-aminobenzoate (6.50 g, 43.0 mmol, 1.00 eq.) was reacted with formic acid (6.49 mL, 7.92 g, 172 mmol, 4.00 eq.). Subsequently, the remaining formic acid and water were removed under reduced pressure. The product was obtained as colorless solid (7.40 g, 41.2 mmol) in a yield of 96%.

R_f =0.13 in cyclohexane/ethyl acetate 2/1 visualized *via* UV quenching at 254 nm and vanillin staining solution (yellow).

^{1}H-NMR (400 MHz, DMSO-d_6) δ/ppm = 10.56 (s, 0.7H, CHO, ^{1a}), 10.47 (d, ^3J = 10.7 Hz, 0.3H, CHO, ^{1b}), 8.96 (d, ^3J = 10.7 Hz, 0.3H, NH, ^{2b}), 8.35 (d, ^3J = 1.7 Hz, 0.7H, NH, ^{2a}), 7.98-7.83 (m, 2H, aromatic, ^{3a,b}), 7.71 (d,^{3} J = 8.7 Hz, 1.4H, aromatic, ^{4a}), 7.31 (d, ^3J = 8.6 Hz, 0.6H, ^{4b}), 3.81 (s, 3H, CH_3, ^{5}).

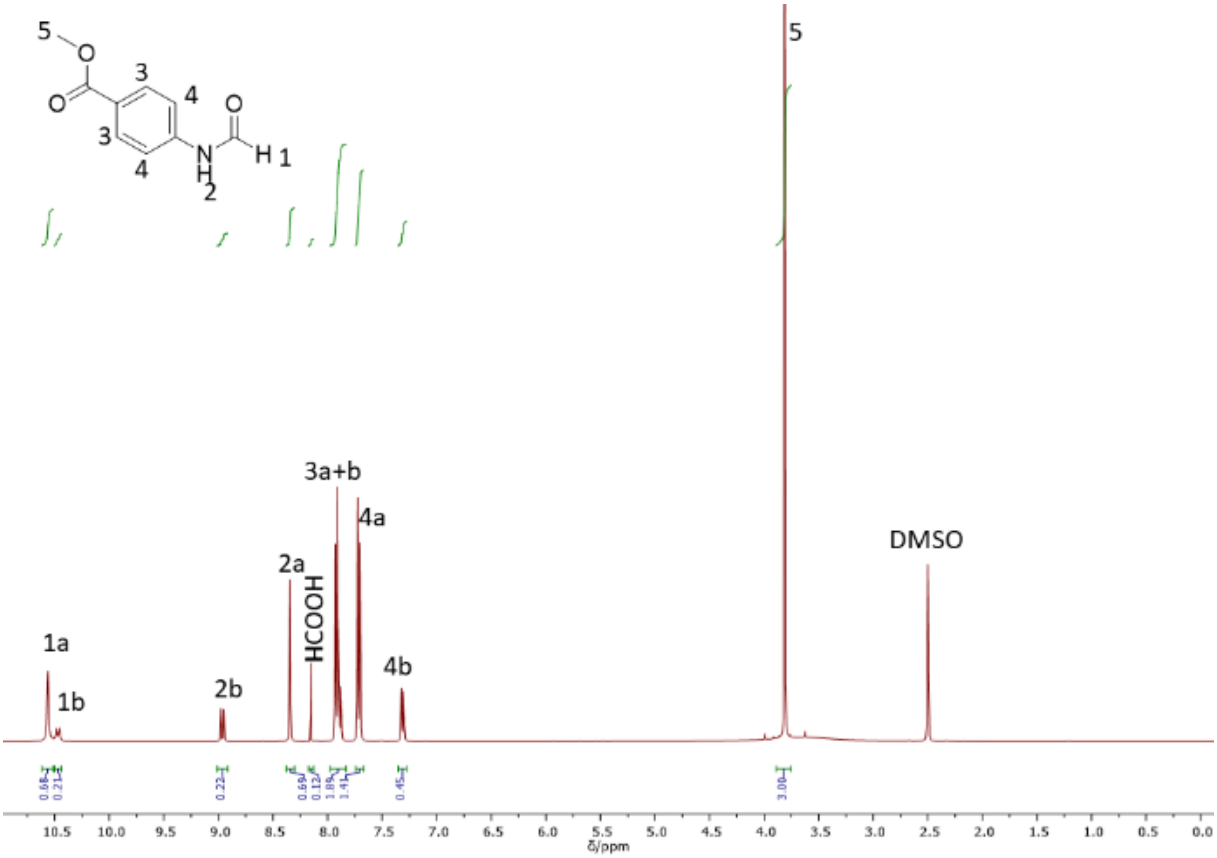

Figure 92: ^{1}H-NMR-spectrum of methyl-4-formaidobenzoate.

^{13}C-NMR (101 MHz, DMSO-d_6) δ/ppm = 165.76 (**C**$OOCH_3$, ^{a}), 163.21 (**C**$OOCH_3$, ^{b}), 162.59 (C=O, ^{b}), 160.18 (C=O, ^{a}), 143.0 (aromatic, ^{1b}), 142.53 (aromatic, ^{1a}), 130.82 (aromatic, ^{2b}), 130.42 (aromatic, ^{2a}), 124.38 (aromatic, ^{3a}), 124.28 (aromatic, ^{3a}), 118.67 (aromatic, ^{3a}), 116.46 (aromatic, ^{3b}), 51.93 (CH_3).

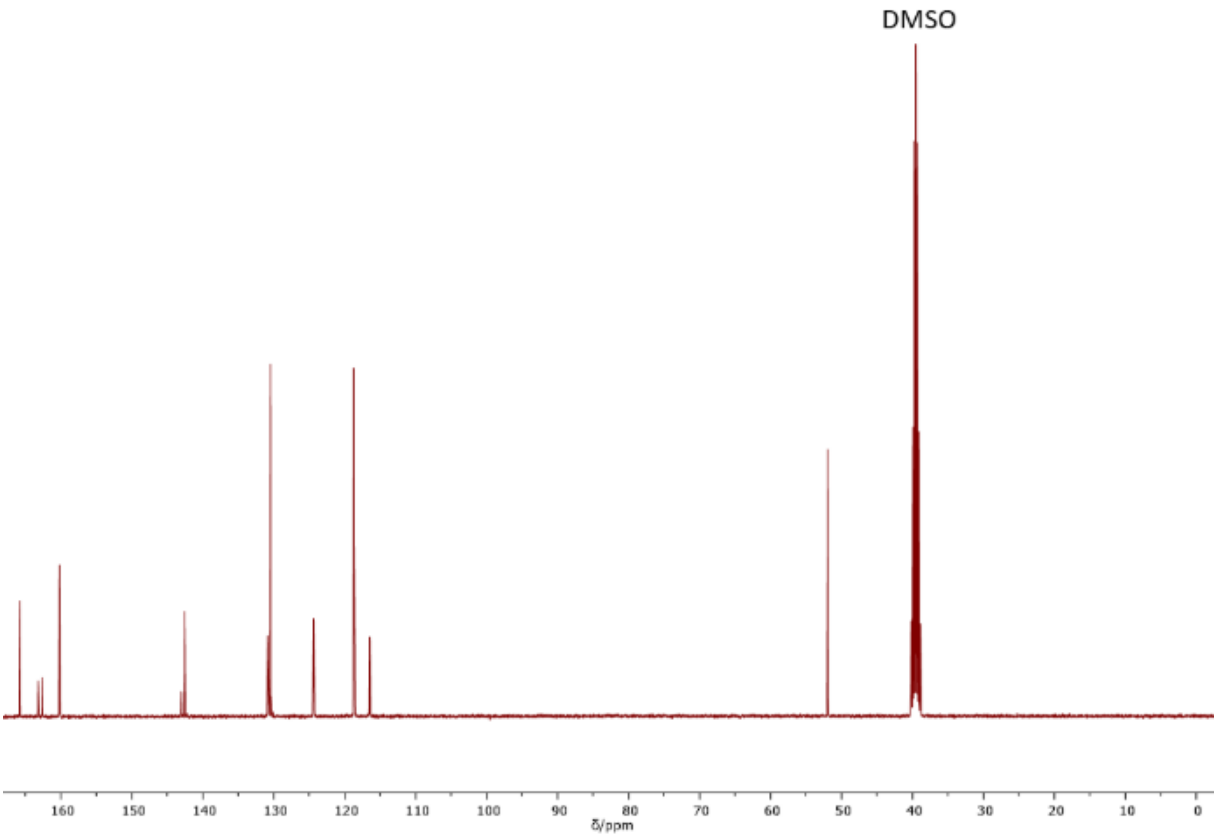

Figure 93: ^{13}C-NMR-spectrum of methyl-4-formaidobenzoate.

EI-HRMS m/z: $[M]^+$ calculated for $[C_9H_9O_3N_1]$ = 179.0582, found: 179.2584, Δ = 0.1270 mmu.

IR (ATR platinum diamond): ν/cm^{-1} = 3462 (w), 3367 (w), 3240 (w, br), 3048 (w, br), 1705 (s), 1691 (s), 1680 (s), 1594 (vs), 1567 (s), 1520 (m), 1436 (s), 1310 (s), 1275 (vs), 1181 (vs), 1168 (vs), 1113 (vs), 1014 (m), 963 (s), 884 (m), 850 (s), 833 (s), 817 (s), 808 (s), 763 (vs), 695 (vs), 636 (m), 619 (m), 570 (w), 506 (vs), 498 (vs), 457 (s), 403 (s).

Dimethyl 5-formamidoisophtalate

The synthesis was performed according to GP3. Dimethyl 5-aminoisophtalate **40** (1.00 g, 4.78 mmol, 1.00 eq.) was reacted with formic acid (1.44 ml, 1.76 g, 38.2 mmol, 8.00 eq.). Subsequently, the remaining formic acid and water were removed under reduced pressure. The product was obtained as colourless powder (1.08 g, 4.54 mmol) in a yield of 95 %.

R_f = 0.81 ethyl acetate visualized *via* UV quenching at 254 nm and vanillin staining solution (deep blue).

^{1}H-NMR (400 MHz, DMSO-d_6) δ/ppm = 10.58 (s, 0.8H, CHO, ^{1a}), 10.41 (d, ^3J = 10.7 Hz, 0.2H, CHO,^{1b}), 8.91 (d, ^3J = 10.7 Hz, 0.2H, NH, ^{2b}), 8.40 (d, ^4J = 1.5 Hz, 1.6H, aromatic, ^{3a}), 8.35 (d, ^3J = 1.6 Hz, 0.8H, NH, ^{2a}), 8.10 (t, ^4J = 1.5 Hz, 0.8H, aromatic, ^{4a}), 8.07-8.05 (m, 0.2H, aromatic, ^{4b}), 7.94 (d, ^4J = 1.1 Hz, 0.4H, ^{3b}), 3.87 (s, 6H, CH_3, ^{5}).

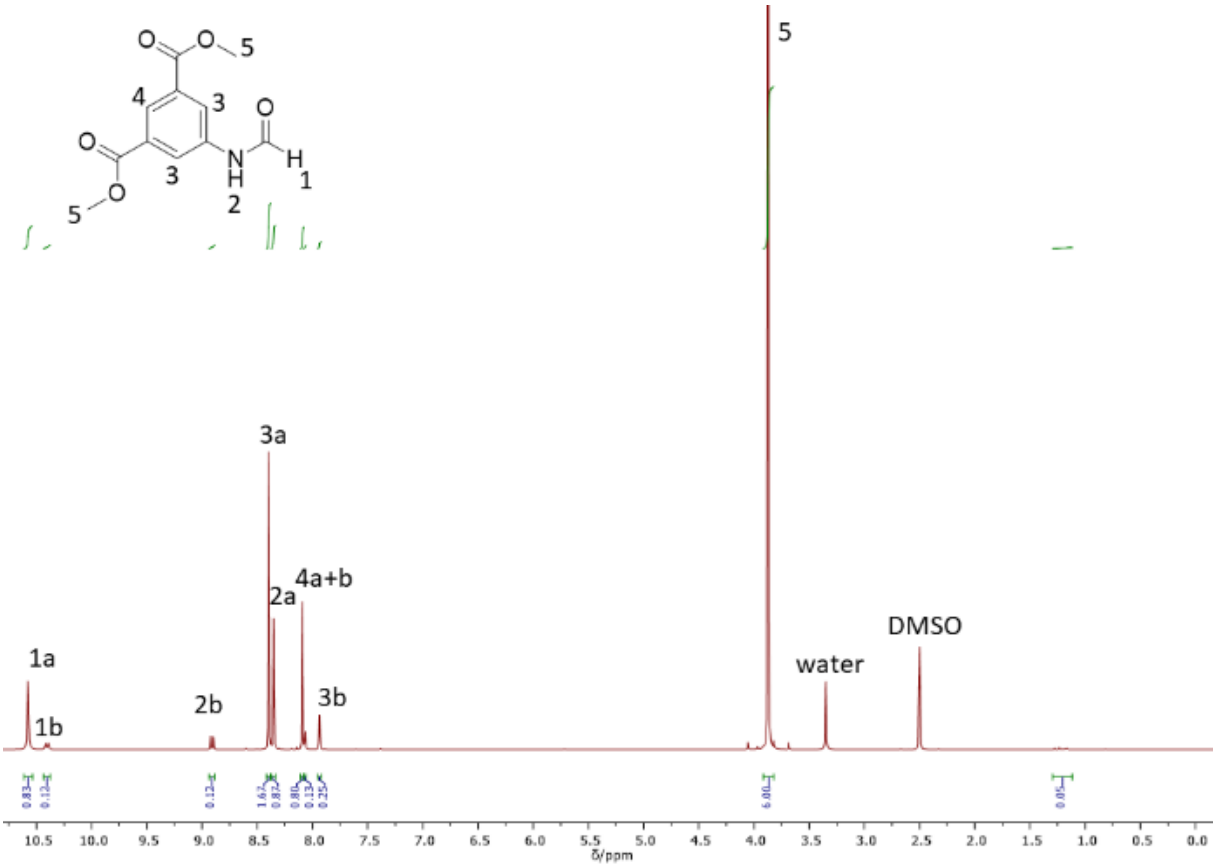

Figure 94: ^{1}H-NMR-spectrum of dimethyl-5-formaidoisophthalate.

^{13}C-NMR (101 MHz, DMSO-d_6) δ/ppm = 165.12 (**C**OOCH$_3$), 162.56 (C=O, ^{b}), 160.18 (C=O, ^{a}), 139.60 (aromatic, ^{1b}), 139.08 (aromatic, ^{1a}), 131.70 (aromatic, ^{2b}), 130.70 (aromatic, ^{2a}), 124.35 (aromatic, ^{3a}), 124.14 (aromatic, ^{3b}), 123.46 (aromatic, ^{4a}), 121.50 (aromatic, ^{4b}), 52.52 (CH_3).

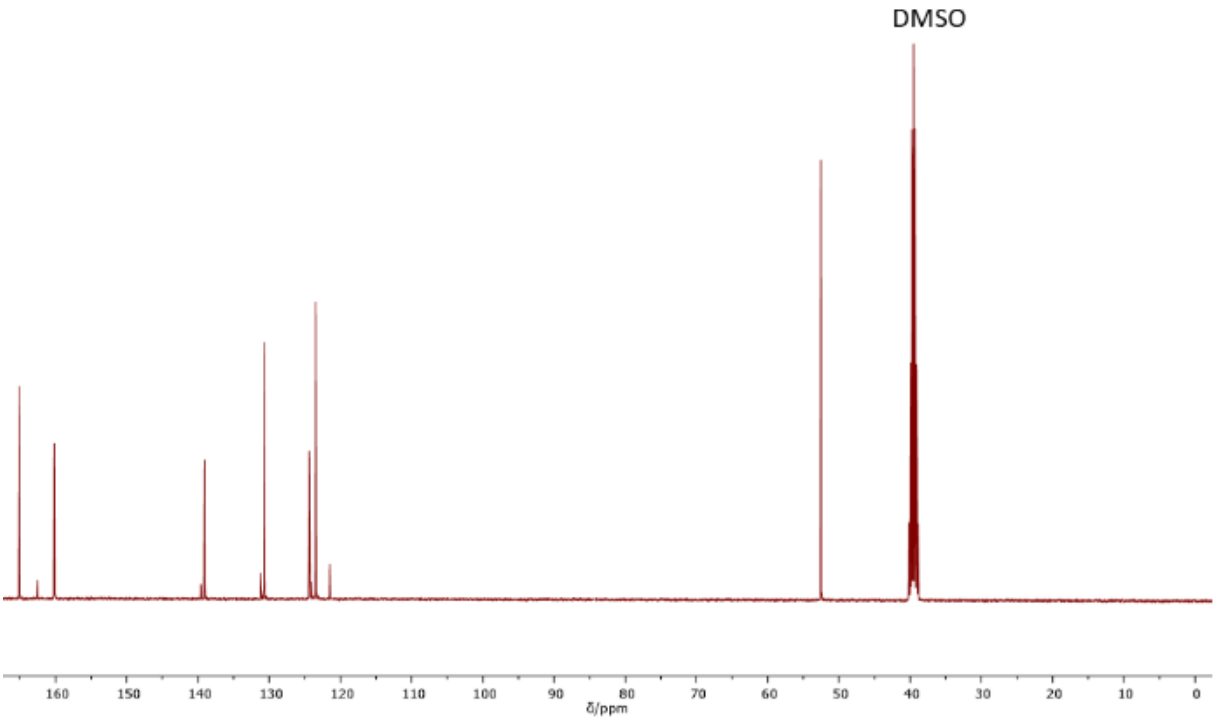

Figure 95: ^{13}C-NMR-spectrum of dimethyl-5-formaidoisophthalate.

EI-HRMS m/z: $[M]^+$ calculated for $[C_{11}H_{11}NO_5]$ = 237.0637, found: 237.0636, Δ = -0.1045 mmu.
IR (ATR platinum diamond): $\tilde{\nu}$/cm^{-1} = 3315 (m), 3067 (w), 2957 (w), 1688 (s), 1603 (m), 1521 (w), 1441 (m), 1403 (m), 1341 (m), 1314 (m), 1248 (s), 1206 (s), 1133 (m), 1012 (m), 980 (m), 895 (m), 750 (s), 721 (m), 692 (m), 586 (m), 460 (w).

4-(*n*-Hexylsulfonyl) formamidobenzene

The synthesis was performed according to GP3. 4-(*n*-Hexylsulfonyl) aniline (397 mg, 1.64 mmol, 1.00 eq.) was reacted with formic acid (621 µL, 757 mg, 16.5 mmol, 10.0 eq.). Subsequently, the remaining formic acid and water were removed under reduced pressure. The product was obtained as brown solid (420 mg, 1.56 mmol) in a yield of 95 %.

R_f = 0.06 cyclohexane/ethyl acetate 2/1 visualized *via* UV quenching at 254 nm.

^{1}H-NMR (400 MHz, DMSO-d_6) δ/ppm = 10.66 (s, 0.8H, CHO, ^{1a}), 10.56 (d, ^3J = 10.6 Hz, 0.2H, CHO, ^{1b}), 9.00 (d, ^3J = 10.6 Hz, 0.2H, NH, ^{2b}), 8.38 (d, ^3J = 1.6 Hz, 0.8H, NH, ^{2a}), 7.83 (m, 3.6H, aromatic, $^{3a, 3b, 4a}$), 7.43 (d, ^3J = 8.6 Hz, 0.4H, aromatic, ^{4b}), 3.30-3.13 (m, 2H, CH_2, ^{5}), 1.61-1.42 (quint., ^3J = 7.6 Hz, 2H, CH_2, ^{6}), 1.38-1.06 (m, 6H, CH_2, ^{7}), 0.80 (t, ^3J = 6.8 Hz, 3H, CH_3, ^{8}).

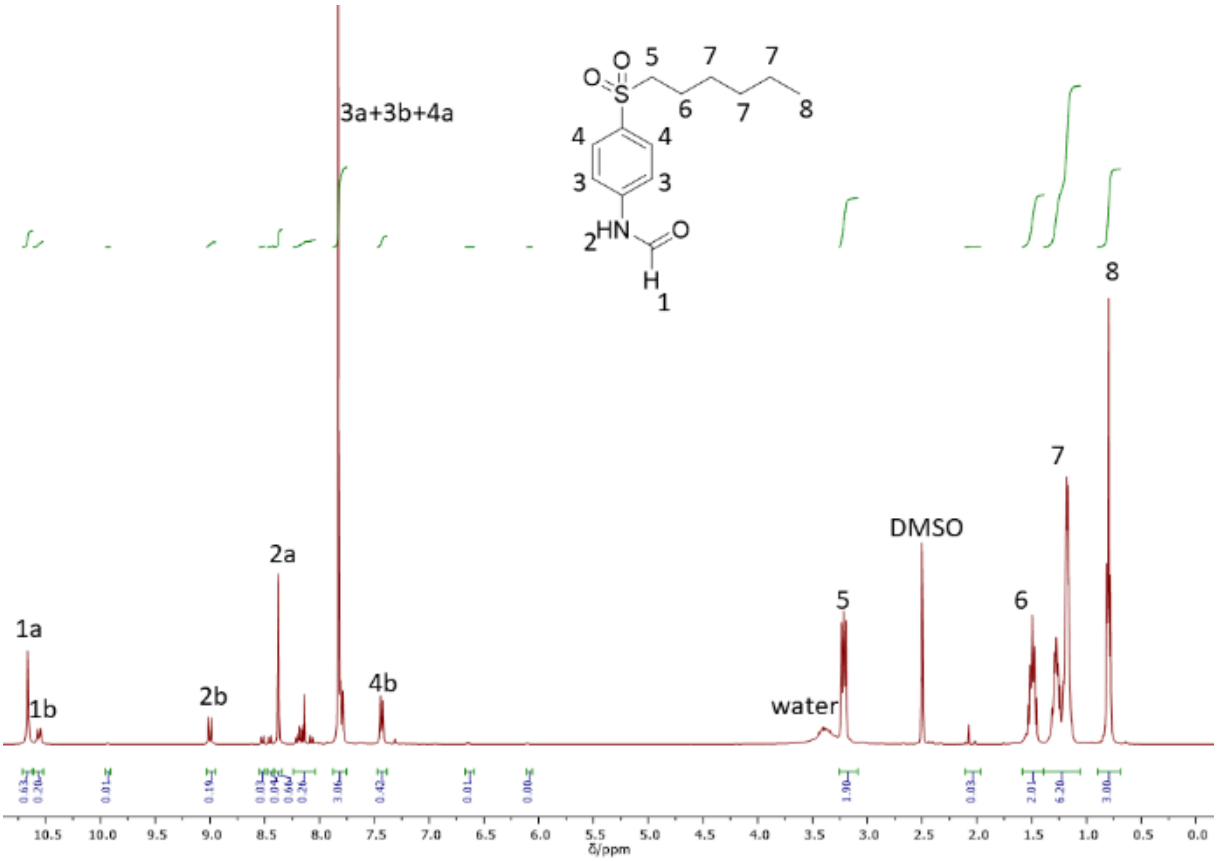

Figure 96: ^{1}H-NMR-spectrum of 4-(n-hexylsulfonyl) formamidobenzene.

^{13}C-NMR (101 MHz, DMSO-d_6) δ/ppm = 162.70 (C=O, ^{b}), 160.38 (C=O, ^{a}), 143.34 (aromatic, ^{1b}), 142.73 (aromatic, ^{1a}), 133.25 (aromatic, ^{2a}), 133.16 (aromatic, ^{2b}), 129.47 (aromatic, ^{3b}), 129.09 (aromatic, ^{3a}), 119.07 (aromatic, ^{4a}), 116.81 (aromatic, ^{4b}), 54.85 (CH_2), 30.63 (CH_2), 27.09 (CH_2), 22.37 (CH_2), 21.79 (CH_2), 13.78 (CH_3).

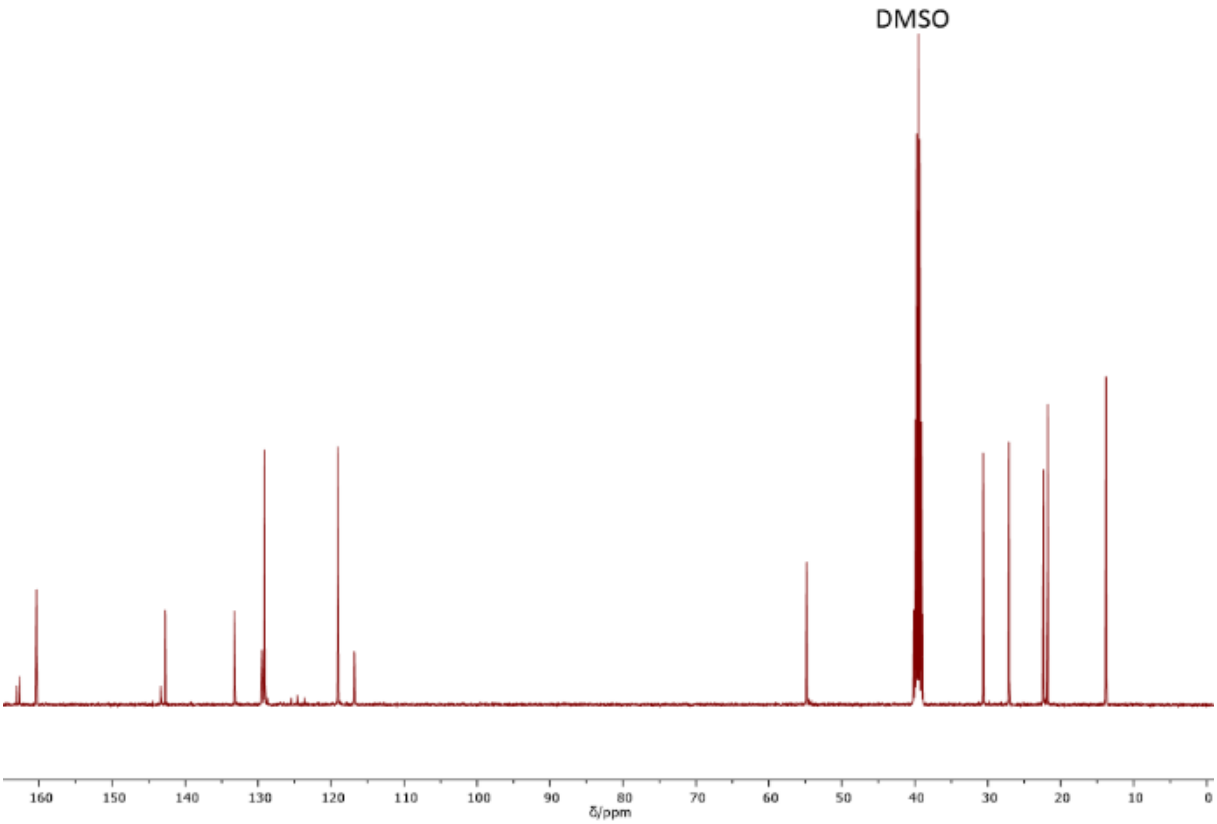

Figure 97: ^{13}C-NMR-spectrum of 4-(n-hexylsulfonyl) formamidobenzene.

EI-HRMS m/z: $[M]^+$ calculated for $[C_{13}H_{19}O_3N_1S_1]^+$ = 269.1086, found: 269.1087, Δ = 0.1205 mmu.

IR (ATR platinum diamond): ν/cm^{-1} = 3070 (vw), 2963 (w), 2934 (w), 2857 (vw), 1682 (m), 1589 (m), 1490 (vw), 1468 (w), 1416 (w), 1273 (s), 127 (m), 1134 (s), 1083 (m), 1033 (w), 1012 (w), 833 (w), 767 (m), 723 (w), 707 (w), 618 (m), 536 (m), 496 (m), 462 (w), 423 (vw).

1,4-Diformamidobenzene

The synthesis was performed according to GP3. *p*-Phenylendiamin (20.0 g, 185 mmol, 1.00 eq.) was converted using formic acid (55.8 mL, 68.1 g, 1.48 mol, 8.00 eq.). Subsequently, the remaining formic acid and water were removed under reduced pressure. The product was obtained as pale-violet powder (30.4 g, 185 mmol) in quantitative yield.

R_f = 0.28 ethyl acetate, visualized *via* UV quenching at 254 nm.

^{1}H-NMR (400 MHz, DMSO-d_6) δ/ppm = 10.17-10.03 (m, 2H, CHO, $^{1a, 1b}$), 8.71-8.66 (m, 0.4H, NH, ^{2b}), 8.25-8.21 (m, 1.6H, NH, ^{2a}), 7.567-51 (m, 3.2H,aromatic, ^{3a}), 7.16-7.12 (m, 0.8H, aromatic, ^{3b}).

Third rotamer is present, but could not be assigned (see below).

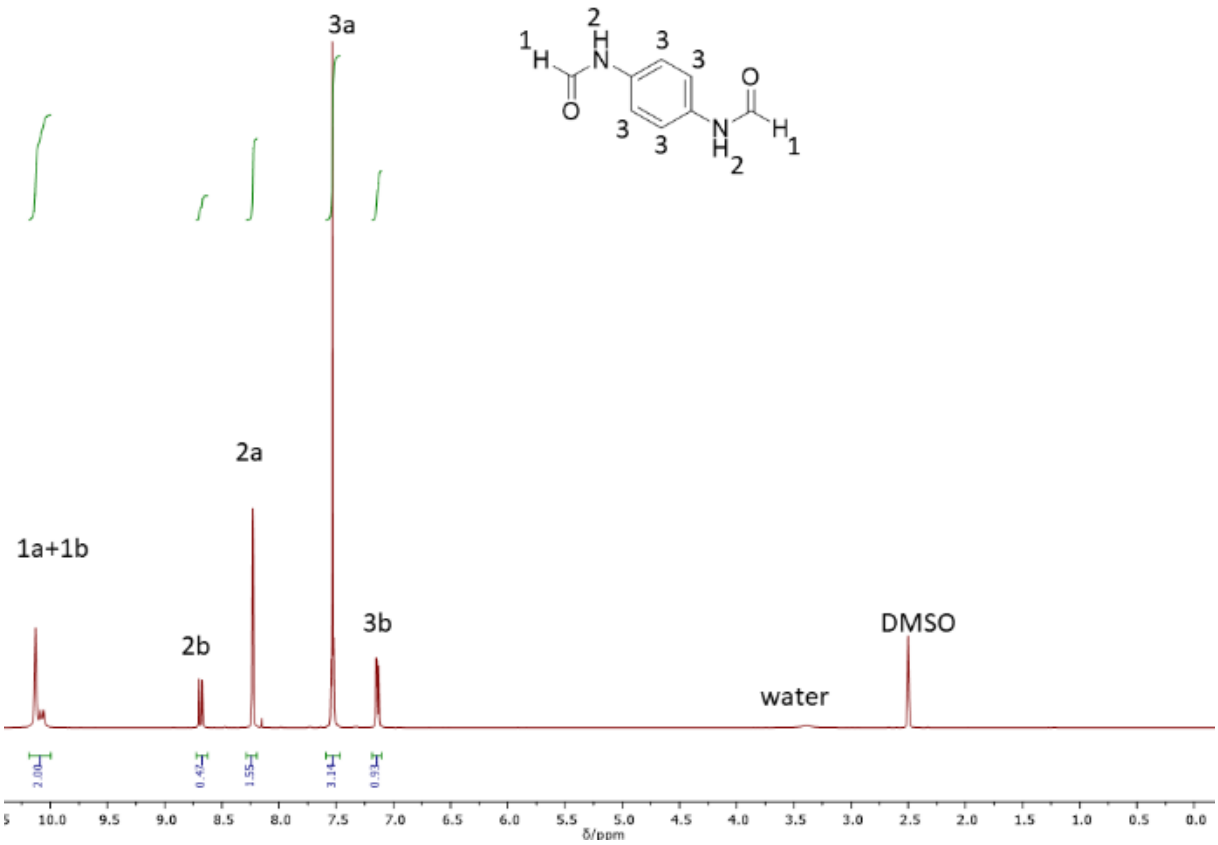

Figure 98: ^{1}H-NMR-spectrum of 1,4-difrmaidobenzene.

^{13}C-NMR (101 MHz, DMSO-d_6) δ/ppm = 163.19 (C=O), 162.59 (C=O), 159.45 (C=O), 159.41 (C=O, [a]), 134.46 (aromatic), 134.43 (aromatic), 134.09 (aromatic, [a]), 134.04 (aromatic), 120.32 (aromatic), 119.74 (aromatic, [a]), 119.00 (aromatic), 118.39 (aromatic).

In the ^{1}H-NMR, further rotamer signals are present, but could not be assigned due to peak overlapping. However, ^{13}C-NMR clearly shows four signals of each carbon species (C=O, and each aromatic-carbon), resulting from three rotamers: (*Z*, *Z*; one signal), (*Z*, *E*; two signals) and (*E*, *E*; one signal) of the *N*, *N´*-diformamides.

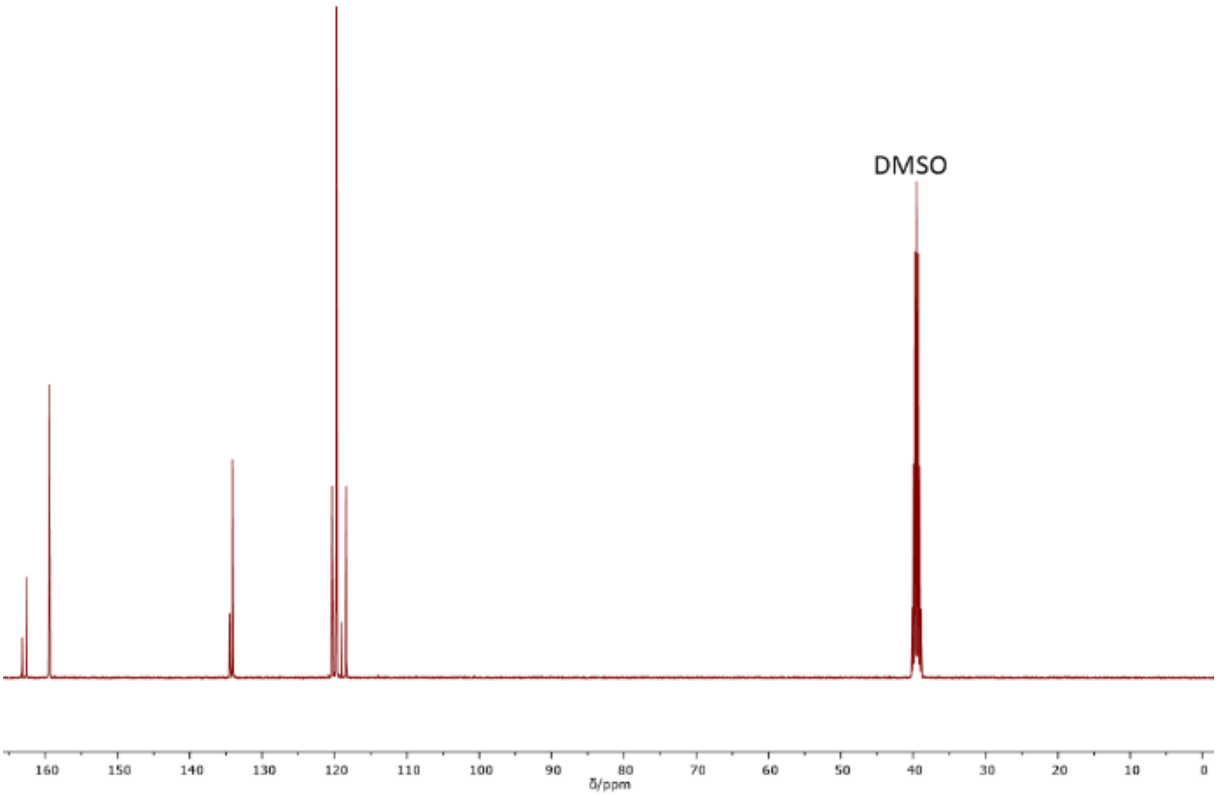

Figure 99: ^{13}C-NMR-spectrum of 1,4-difrmaidobenzene.

EI-HRMS m/z: $[M]^+$ calculated for $[C_8H_8N_2O_2]$ = 164.0586, found: 164.0587, Δ = 0.0814 mmu.

IR (ATR platinum diamond): ν/cm^{-1} = 3153 (w), 3036 (w), 2987 (w), 2939 (w), 2861 (w), 2781 (w), 1699 (s), 1650 (s), 1530 (m), 1489 (s), 1411 (m), 1399 (m), 1296 (vs), 1222 (m), 1111 (w), 1037 (m), 878 (s), 827 (vs), 757 (vs), 537 (vs), 518 (vs), 506 (vs), 424 (s), 411 (vs)

6.4.7 Synthesis of miscellaneous compounds

Methyl 4-aminobenzoate

4-aminobenzoic acid (20.0 g, 146 mmol, 1.00 eq.) was dissolved in methanol (290 mL, 229 g, 7.15 mol, 49.0 eq.) and 87 mL of 6 M aqueous hydrochloric acid solution was added. The mixture was stirred under reflux for 2 hours. Water (400 mL) was added, and the mixture was neutralized using sodium hydrogen carbonate and potassium carbonate. After 12 hours at room temperature, a precipitate formed, which was filtered off and dried under reduced pressure. The product was obtained as yellow needle-like crystals (14.9 g, 98.7 mmol) in a yield of 68%.

***R*$_f$** = 0.45 in cyclohexane/ethyl acetate 2/1 visualized *via* UV quenching at 254 nm and vanillin staining solution (yellow).

^{1}H-NMR (400 MHz, DMSO-d_6) δ/ppm = 7.68-7.63 (m, 2H, aromatic, ^{1}), 6.61-6.54 (m, 2H, aromatic, ^{2}), 5.97 (s, 2H, NH_2, ^{3}), 3.73 (s, 3H, CH_3, ^{4}).

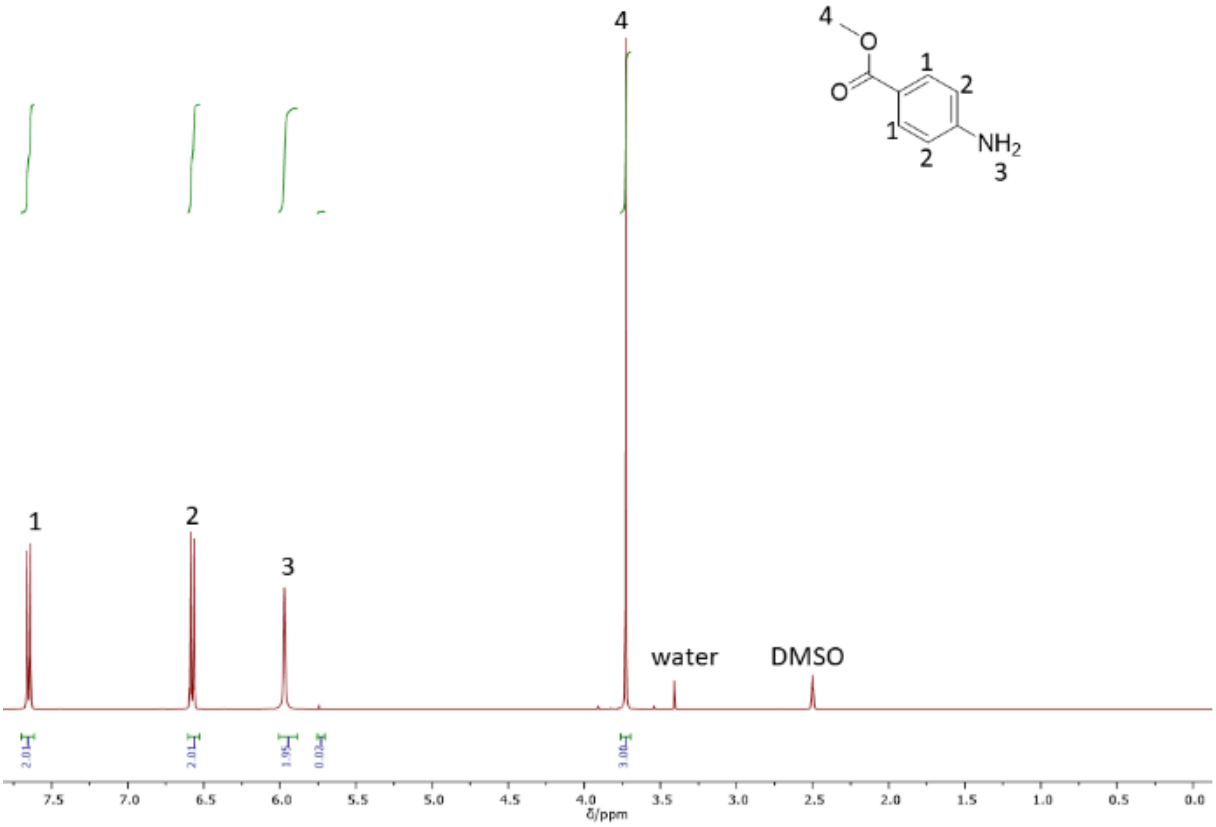

Figure 100: ^{1}H-NMR-spectrum of methyl 4-aminobenzoate.

^{13}C-NMR (101 MHz, DMSO-d_6) δ/ppm = 166.41 (**C**$OOCH_3$), 153.52 (quaternary-aromatic), 131.13 (aromatic), 115.80 (quaternary-aromatic), 112.70 (aromatic), 51.17 (CH_3).

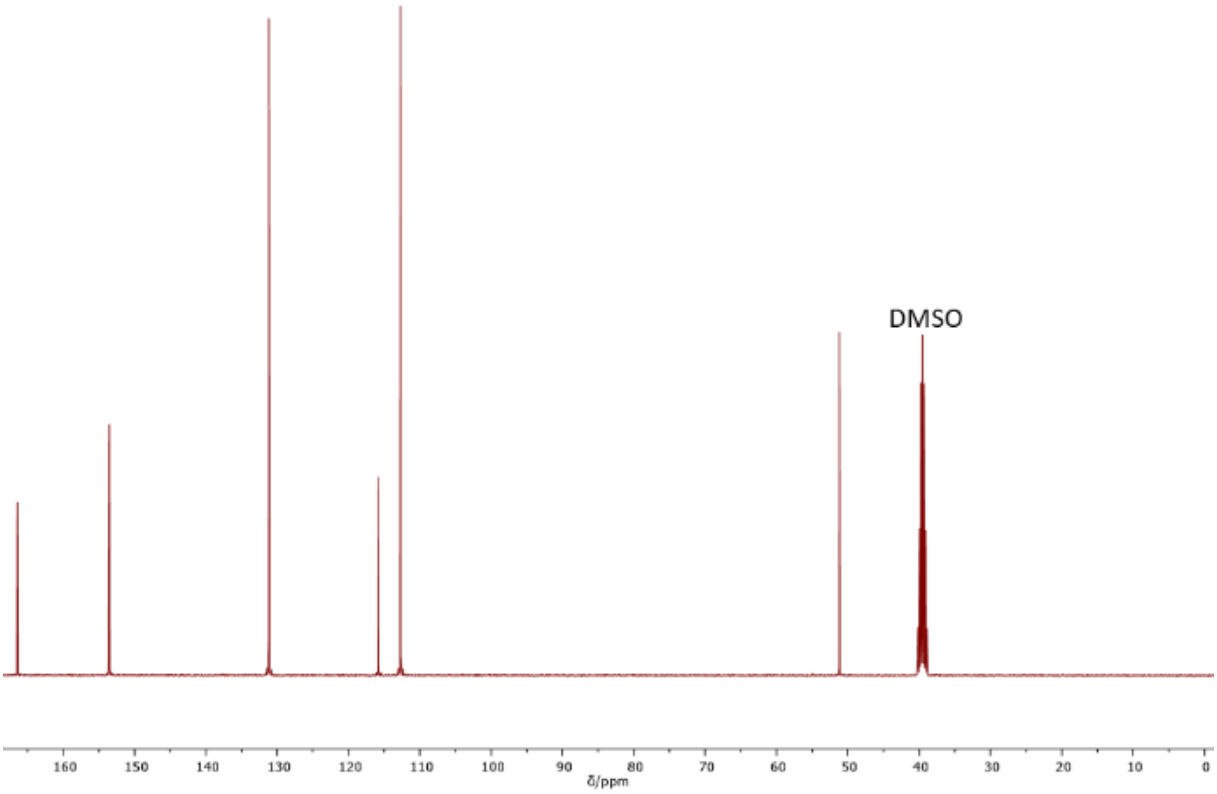

Figure 101: ^{13}C-NMR-spectrum of methyl 4-aminobenzoate.

EI-HRMS m/z: $[M]^+$ calculated for $[C_8H_9O_2N_1]$ = 151.0633, found: 151.0634, Δ = 0.0897 mmu.

IR (ATR platinum diamond): ν/cm^{-1} = 3464 (m), 3369 (s), 3246 (w), 2950 (w), 1678 (s), 1656 (m), 1625 (s), 1592 (vs), 1567 (vs), 1520 (s), 1460 (w), 1434 (vs), 1314 (vs), 1284 (vs), 1181 (vs), 1166 (vs), 1121 (vs), 1074 (s), 1014 (m), 963 (s), 835 (vs), 769 (vs), 697 (vs), 638 (m), 619 (vs), 559 (m), 506 (vs), 494 (vs), 459 (vs), 401 (vs)

Dimethyl 5-aminoisophtalate 40

5-Aminoisophtalic acid (5.00 g, 27.6 mmol, 1.00 eq.) was dissolved in methanol (112 mL, 88.4 g, 2.76 mol, 100 eq.) and cooled to 0°C applying an ice-water bath. Subsequently, thionyl chloride (12.0 mL, 19.7 g, 166 mmol, 6.00eq.) was added dropwise (one drop per five seconds) keeping the temperature below 5 °C. After the addition, the cooling was removed and the reaction mixture was stirred at room temperature for 16 hours. Subsequently, the remaining thionyl chloride was quenched and a pH-value of eight was adjusted using saturated aqueous sodium hydrogen carbonate solution and solid potassium carbonate. Water (300 mL) was added to dissolve precipitated salts and the organic layer was separated. The aqueous phase was extracted with DCM (2 × 50 mL) and the organic phases were combined, dried over sodium sulfate and filtered off. The product (5.16 g, 24.7 mmol) was obtained as a slightly yellow crystalline solid in a yield of 89% after removal of the solvent under reduced pressure.

R_f = 0.83 ethyl acetate, visualized *via* UV quenching at 254 nm and vanillin staining solution (yellow).

^{1}H-NMR (400 MHz, DMSO-d_6) δ/ppm = 7.64 (t, ^4J = 1.6 Hz, 1H, aromatic, ^{1}), 7.41 (d, ^4J = 1.6 Hz, 2H, ^{2}), 5.73 (s, 2H, NH_2, ^{3}), 3.83 (s, 6H, CH_3, ^{4}).

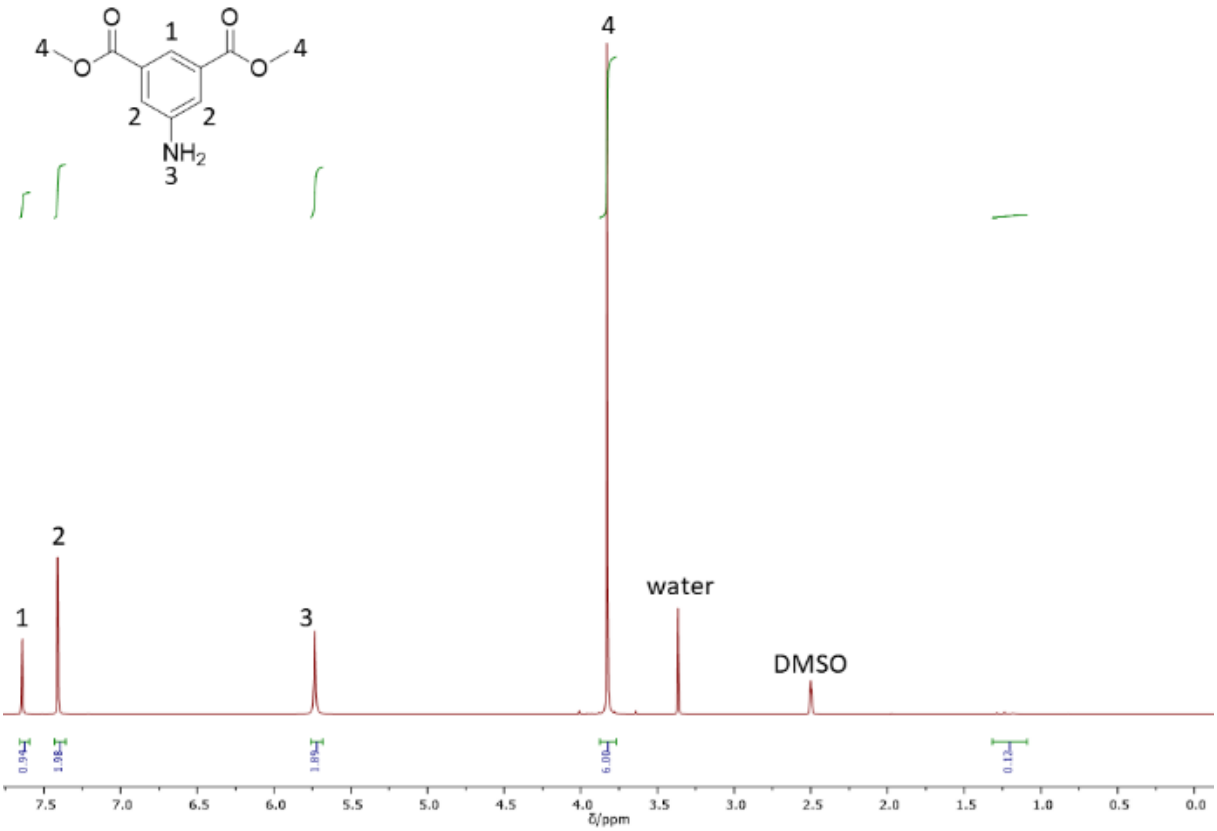

Figure 102: ^{1}H-NMR-spectrum of dimethyl-5-aminoisophthalate.

^{13}C-NMR (101 MHz, DMSO-d_6) δ/ppm = 166.01 (**C**$OOCH_3$), 149.56 (quaternary-aromatic), 130.66 (aromatic), 118.13 (aromatic), 116.71 (quaternary-aromatic), 52.15 (CH_3).

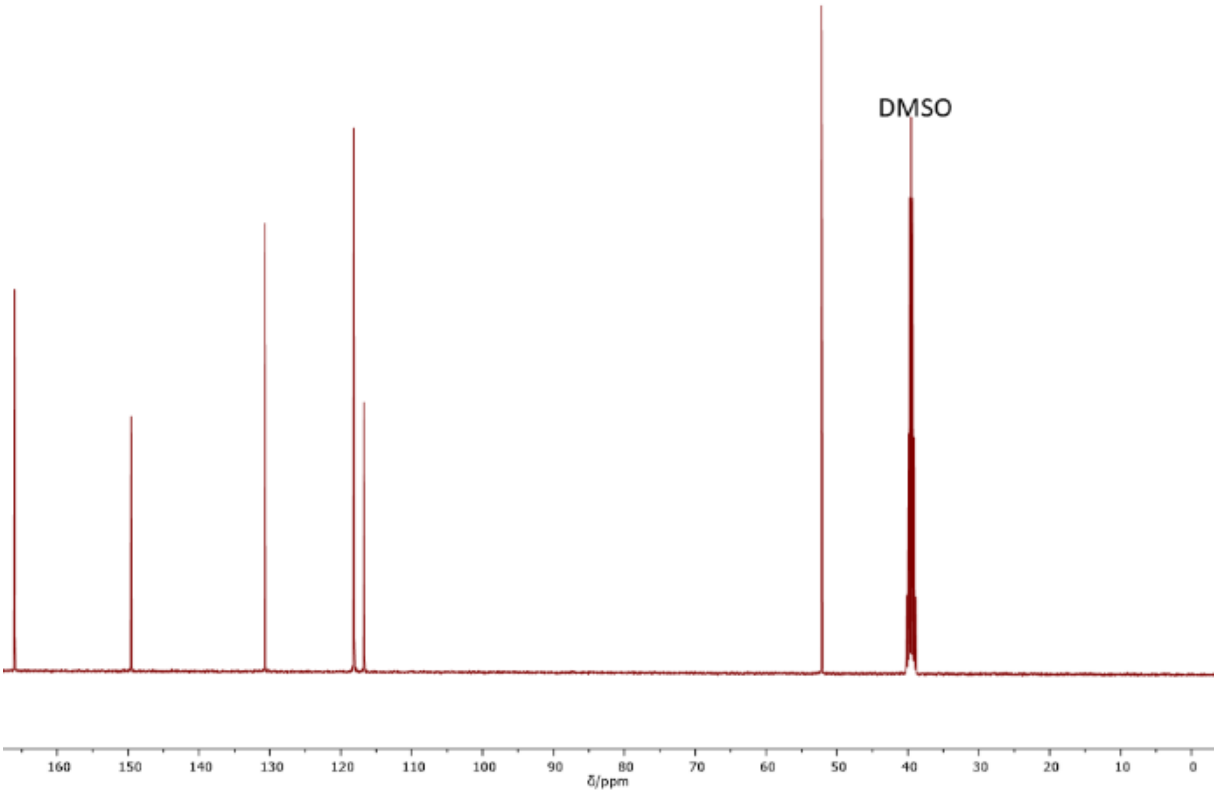

Figure 103: ^{13}C-NMR-spectrum of dimethyl-5-aminoisophthalate.

EI-HRMS m/z: $[M]^+$ calculated for $[C_{10}H_{11}NO_4]$ = 209.0688, found: 209.0687, Δ = -0.1554 mmu.

IR (ATR platinum diamond): ν/cm^{-1} = 3454 (m), 3369 (m), 3251 (w), 2961 (w), 1709 (s), 1645 (m), 1600 (s), 1437 (s), 1250 (s), 1003 (s), 943 (m), 870 (m), 758 (s), 725 (m), 667 (w), 539 (w), 410 (w).

4-(*n*-Hexylsulfonyl) aniline

4-(*n*-Hexylthio) aniline (2.32 g, 11.1 mmol, 1.00 eq.) was dissolved in 22 mL acetonitrile and 9.7 mL of aqueous hydrogen peroxide solution (35w% in water, 3.43 mL, 3.77 g, 111 mmol, 10.0eq.) was added. The reaction mixture was stirred at 60°C for 23 hours. Then, the reaction mixture was cooled down to room temperature, same amount of hydrogen peroxide was added, and the mixture was again stirred at 60°C for another 17 hours. Subsequently, ~25 mL of saturated sodium sulfite solution was added slowly while cooling the biphasic mixture with a water bath. The organic phase was separated and the aqueous phase was extracted with ethyl acetate (2 × 30 mL). The organic layers were combined, dried over sodium sulfate, filtered off and solvent was removed under reduced pressure. The product (2.67 g, 11.8 mmol) was obtained as orange solid in a quantitative yield.

$\mathbf{R_f}$ = 0.19 in cyclohexane/ethyl acetate 2/1 visualized *via* UV quenching at 254 nm.

^{1}H-NMR (400 MHz, DMSO-d_6) δ/ppm = 7.48-7.42 (m, 2H, aromatic, [1]), 6.67-6.62 (m, 2H, aromatic, [2]), 6.11 (s, 2H, NH_2, [3]), 3.13-2.94 (m, 2H, CH_2, [4]), 1.52-1.43 (m, 2H, CH_2, [5]), 1.34-1.11 (m, 6H, CH_2, [6]), 0.82 (t, ^3J = 6.8 Hz, 3H, CH_3, [7]).

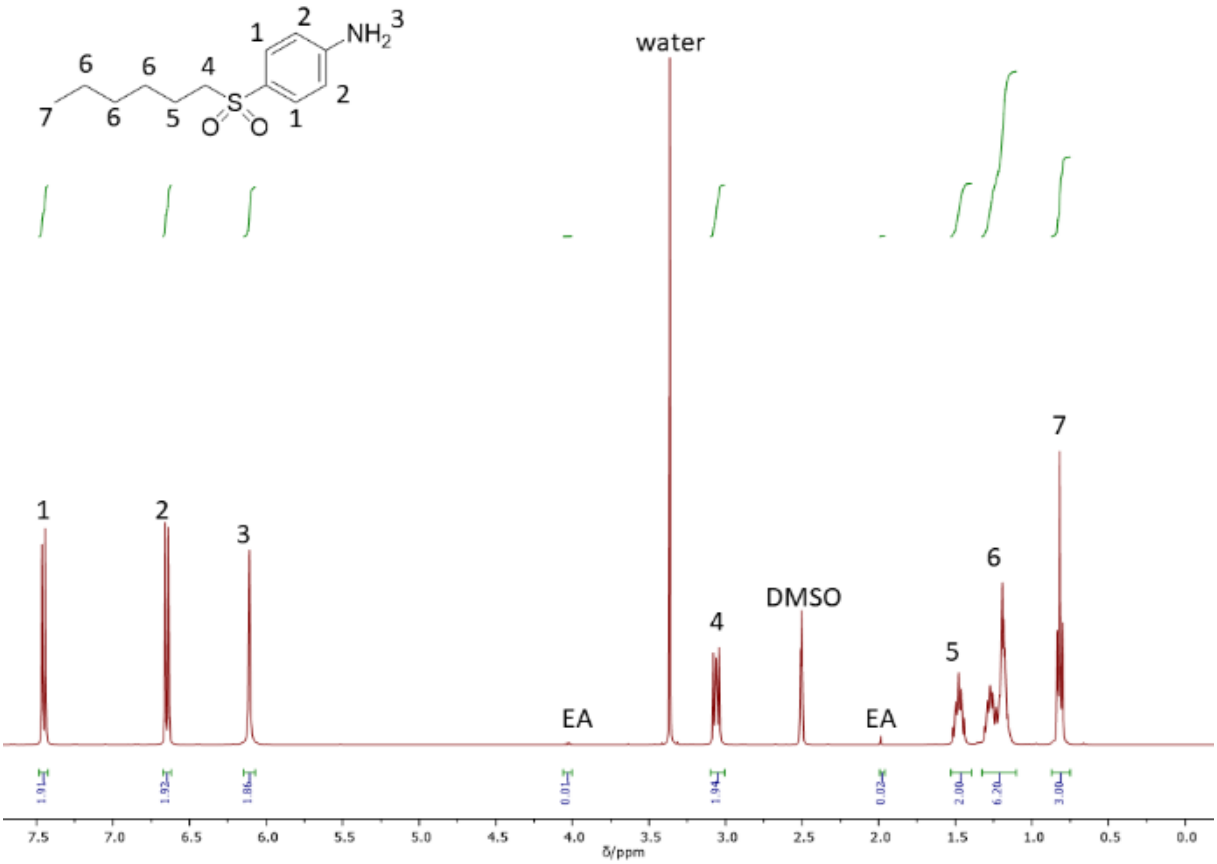

Figure 104: ^{1}H-NMR-spectrum of 4-(n-hexylsulfony) aniline.

^{13}C-NMR (101 MHz, DMSO-d_6) δ/ppm = 153.54 (quaternary-aromatic), 129.53 (aromatic), 123.72 (quaternary-aromatic) , 112.74 (aromatic), 55.45 (CH_2), 30.70 (CH_2), 27.12 (CH_2), 22.64 (CH_2), 21.81 (CH_2), 13.81 (CH_3).

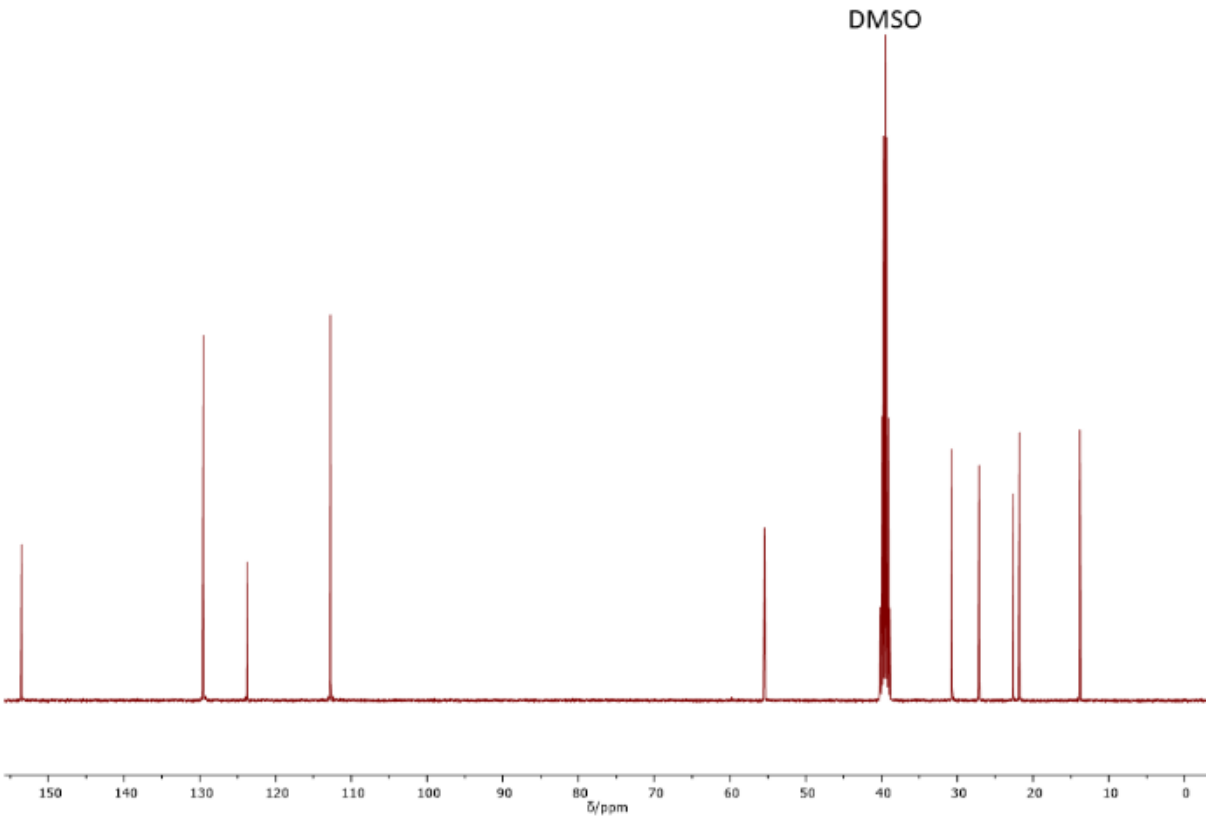

Figure 105: ^{13}C-NMR-spectrum of 4-(n-hexylsulfony) aniline.

EI-HRMS m/z: $[M]^+$ calculated for $[C_{12}H_{19}O_2N_1S_1]$ = 241.1137, found: 241.1135, Δ = -0.1221 mmu.

IR (ATR platinum diamond): ν/cm^{-1} = 3466 (w), 3377 (m), 2950 (w), 2935 (w), 2917 (w), 2853 (w), 1625 (s), 1594 (vs), 1504 (w), 1465 (w), 1316 (w), 1273 (vs), 1265 (s), 1242 (w), 1216 (w), 1127 (vs), 1078 (vs), 1047 (w), 977 (w), 841 (m), 823 (m), 794 (m), 780 (vs), 726 (w), 650 (m), 564 (vs), 522 (vs), 496 (vs), 475 (vs), 424 (vs).

4-(*n*-Hexylthio) aniline

The product was synthesized using synthesis protocol of Wang *et al.*[626] using 4-amino thiophenol (3.33 g, 26.6 mmol, 1.00 eq.), hexyl bromide (3.72 mL, 4.39 g, 26.6 mmol, 1.00 eq.), sodium hydroxide (1.06 g, 26.6 mmol, 1.00 eq.) and 81 mL ethanol. The product was obtained as brown oil (2.51 g, 12.0 mmol) in a yield of 45%.

R_f = 0.55 in cyclohexane/ethyl acetate 2/1 visualized *via* UV quenching at 254 nm and vanillin staining solution (yellow).

^{1}H-and ^{13}C-NMR-measurements were consistent with the measurements in $CDCl_3$ of the literature.[626]

^{1}H-NMR (400 MHz, DMSO-d_6) δ/ppm = 7.09-7.03 (m, 2H, aromatic, ^{1}), 6.54-6.47 (m, 2H, aromatic, ^{2}), 5.20 (s, 2H, NH_2, ^{3}), 2.67 (t, ^3J = 7.1 Hz, 2H, CH_2, ^{4}), 1.44 (quint. ^3J = 7.2 Hz, 2H, CH_2, ^{5}), 1.37-1.14 (m, 6H, CH_2, ^{6}), 0.84 (t, ^3J = 6.9 Hz, 3H, CH_3, ^{7}).

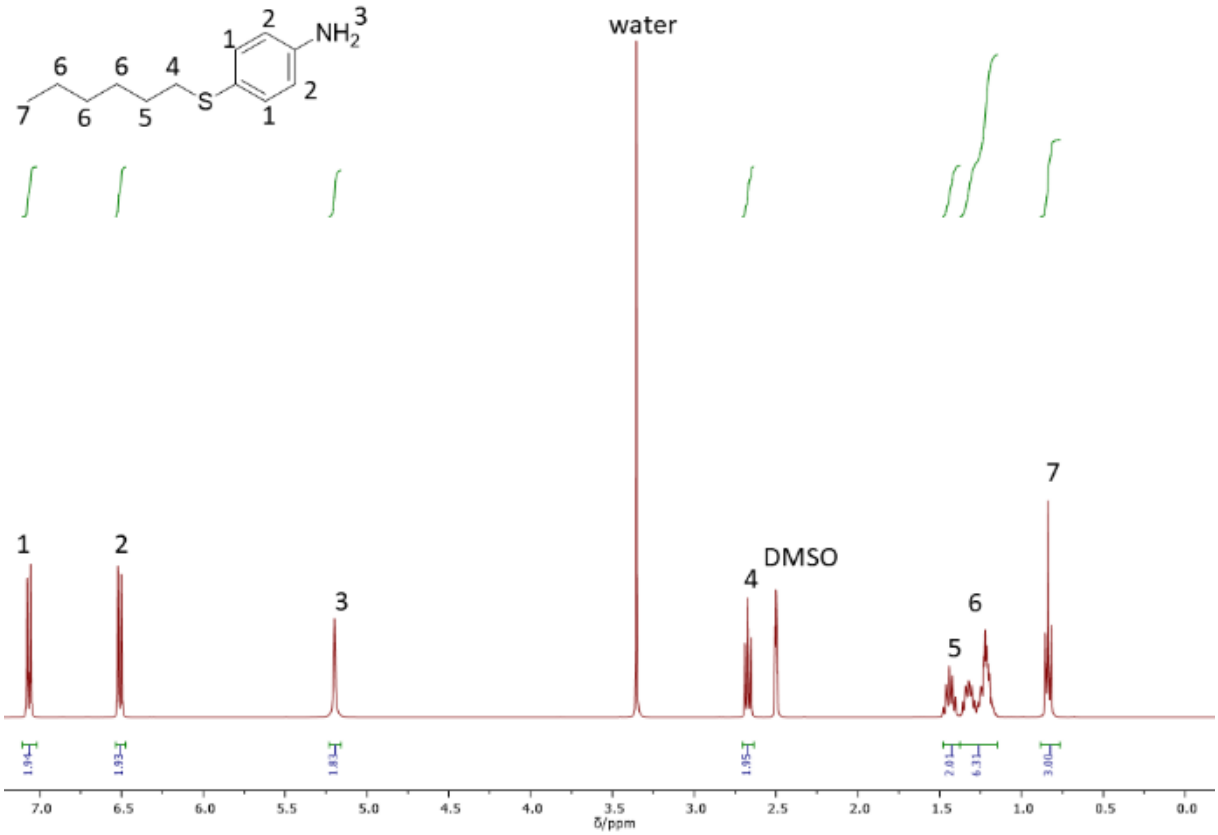

Figure 106: ^{1}H-NMR-spectrum of 4-(n-hexylthio) aniline.

^{13}C-NMR (101 MHz, DMSO-d_6) δ/ppm = 148.27 (quaternary-aromatic), 133.55 (aromatic), 119.12 (quaternary-aromatic), 114.41 (aromatic), 35.70 (CH_2), 30.84 (CH_2), 28.79 (CH_2), 27.62 (CH_2), 22.02 (CH_2), 13.90 (CH_3).

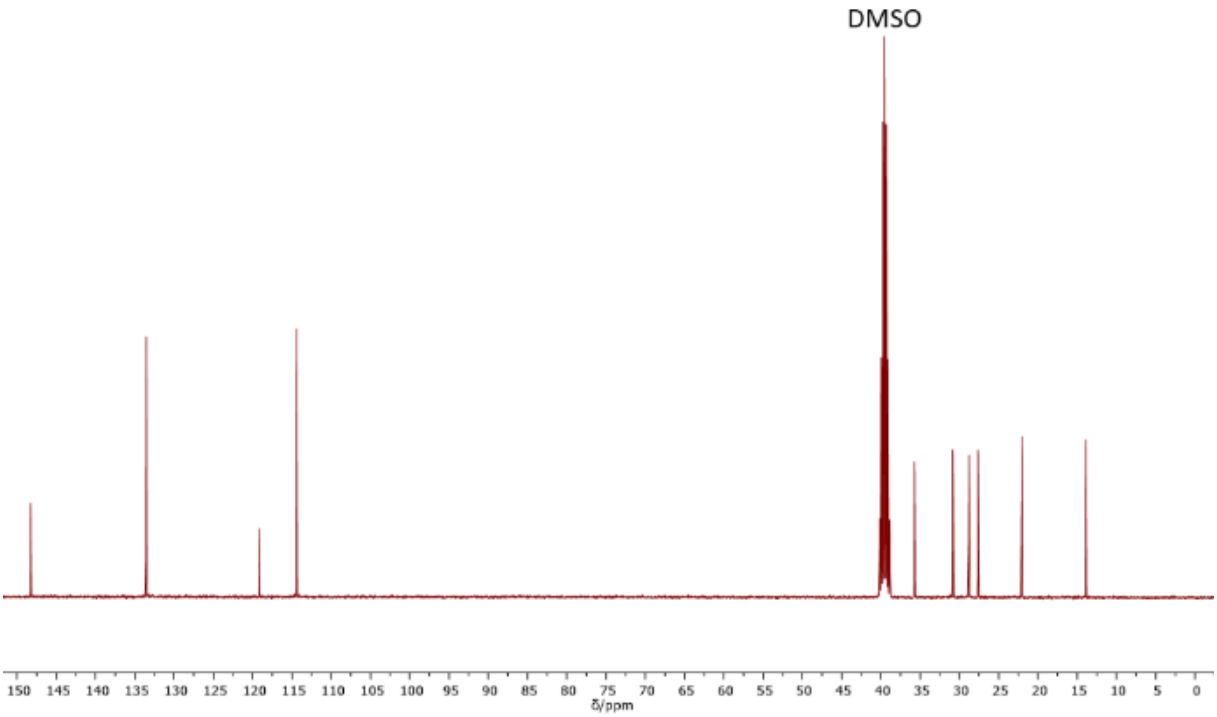

Figure 107: ^{13}H-NMR-spectrum of 4-(n-hexylthio) aniline.

6.5 Transferring catalytical active thiourea motifs into polymers

6.5.1 Poly(thiourea)s *via* step-growth AM-3CPR

6.5.1.1 Decomposition of thiourea 36 to the respective amine 40

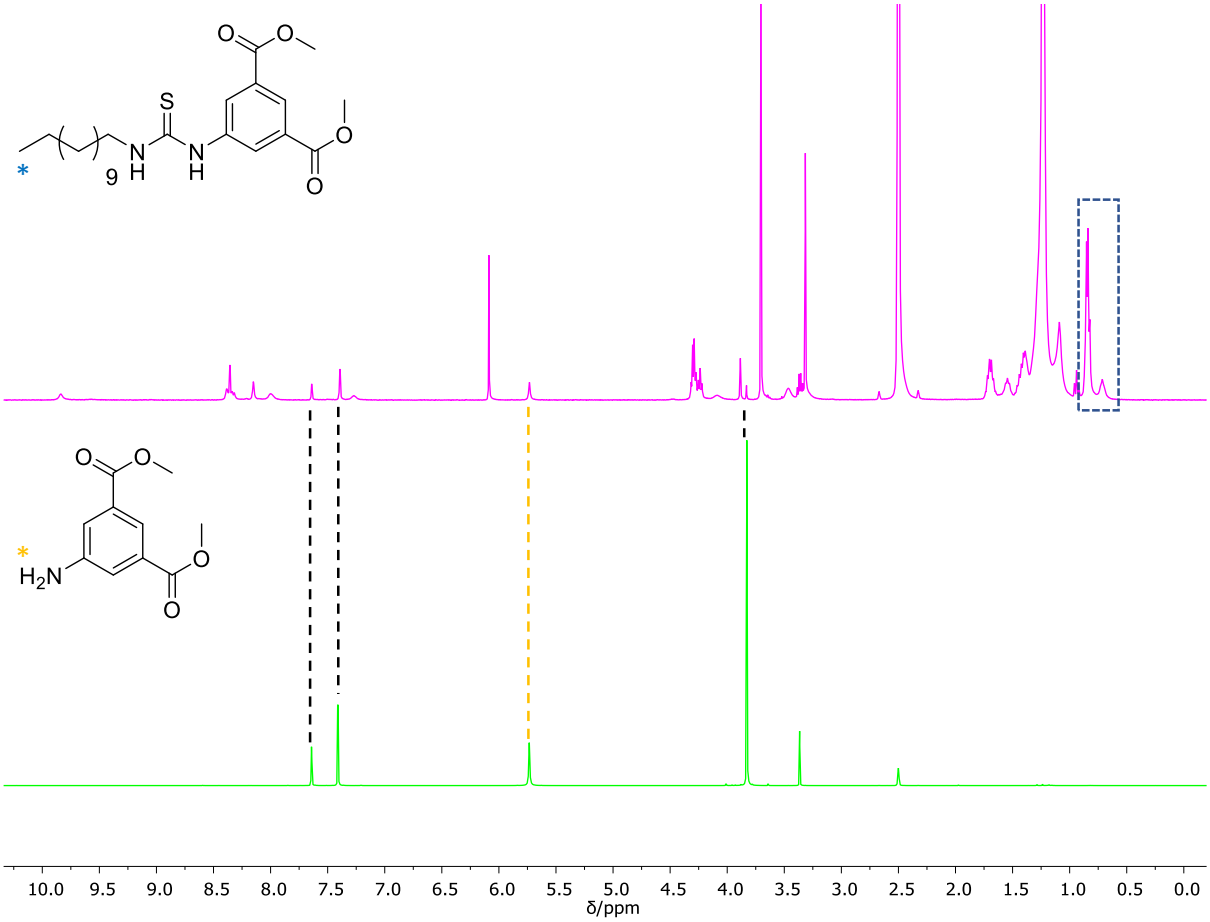

*Figure 108: Comparison of ^{1}H-NMR-spectra. Top: the reaction of thiourea **36** with dodecanol **37** (2.00 eq.) and Ti(O^{i}Bu)$_4$ at 90 °C after one day depicting a certain degree of decomposition of the thiourea to the respective amine **40**. Bottom: the respective amine **40**. Signals of the amine in the reaction mixture (top) are highlighted by dashed lines. Integration of the amine signal (dashed orange line) and referencing on the CH_3 groups of the thiourea **36** as well as dodecanol **37** (blue dashed box) allowed the determination of the degree of decomposition. Full decomposition would result in a ratio of NH_2 to CH_3 signals 2:9. In this example the ratio was 0.42:9 corresponding to a degree of decomposition of the thiourea group of 21%.*

6.5.1.2 SEC-curves of polycondensation between TU 36 and decanol 46

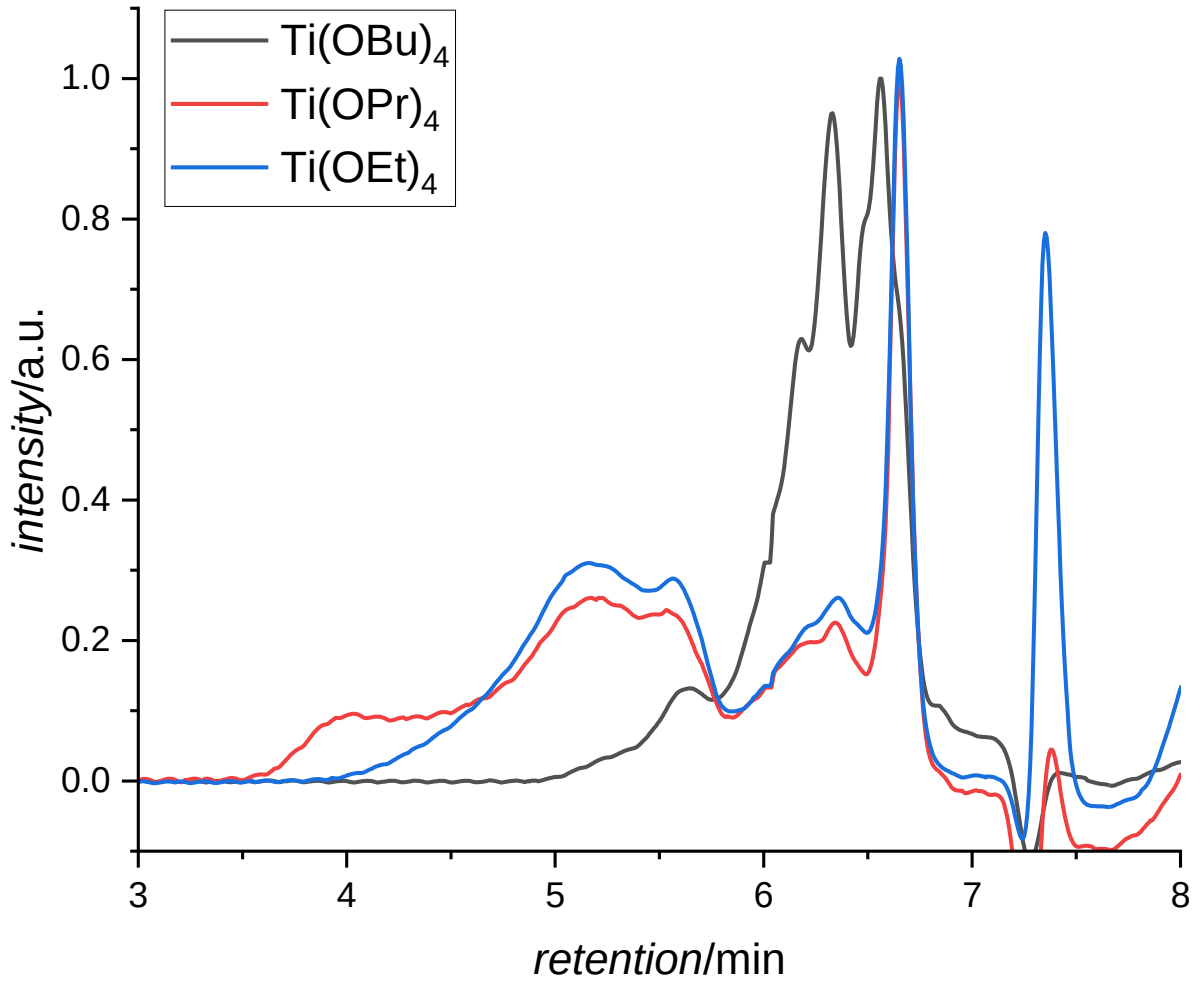

*Figure 109: SEC-curves of the polymers **45** obtained using different titaniumalkoxides after one day depicted in Table16*

6.5.1.3 Synthesis of compounds

5-trifluoromehtylphenyl-1,3-di-*N*-formamide

The diamine (2.00 g, 11.4 mmol, 1.00 eq.) was put together with formic acid (3.43 mL, 4.18 g, 8.00 eq.) and was stirred under heating at 65 °C for 24 hours. Afterwards, the remaining formic acid and water were removed under reduced pressure and the product was obtained as lightly brown powder (1.32 g, 5.66 mmol) in quantitative yield.

Three rotamers were present and assigned as far as possible.

^{1}H-NMR (400 MHz, DMSO-d_6) δ/ppm = 10.55 (d, ^{3}J = 10.9 Hz, 2H, CHO, ^{1a}), 10.46-10.36 (m, 2H, CHO, ^{1b,c}), 8.92 (d, ^{3}J = 10.7 Hz, 2H, NH, ^{2c}), 8.86 (d, ^{3}J = 10.7 Hz, 2H, NH, ^{2b}), 8.33 (d, ^{3}J = 1.8 Hz, 2H, NH, ^{2a}), 8.05 (d, ^{4}J = 1.9 Hz, 1H, aromatic, ^{3a}), 7.76 (d, ^{4}J = 1.9 Hz, 2H, ^{4a}), 7.72 (s, 2H, aromatic, ^{4b}), 7.59 (d, ^{4}J = 2.1 Hz, 1H, aromatic, ^{3b}), 7.34 (s, 2H, aromatic, ^{4c}).

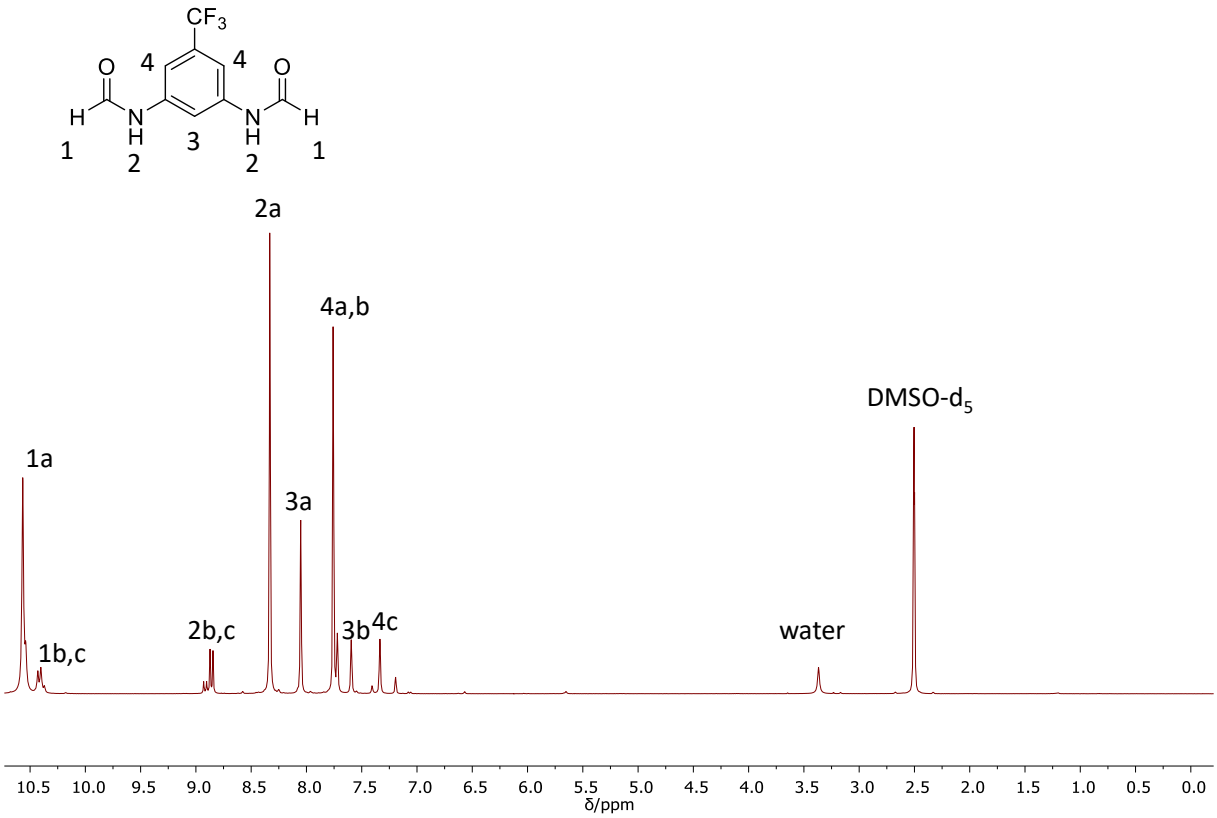

Figure 110: ^{1}H-NMR-spectrum of 5-trifluoromethyl phenyl-1,3-N-diformamide.

^{13}C-NMR (101 MHz, DMSO-d_6) δ/ppm = 162.81 (C=O), 162.58 (C=O), 160.29 (C=O), 160.22 (C=O ^{a}), 140.10 (quarternary-aromatic), 139.90 (quarternary-aromatic), 139.56 (quarternary-aromatic, ^{a}), 130.82-129.54 (quarternary-aromatic, ^{a}), 123.82 (^{1}J = 821 Hz, CF_3), 112.65 (aromatic, ^{a}), 111.27 (aromatic), 110.82 – 109.67 (aromatic, ^{a}), 108.92 – 107.41 (aromatic).

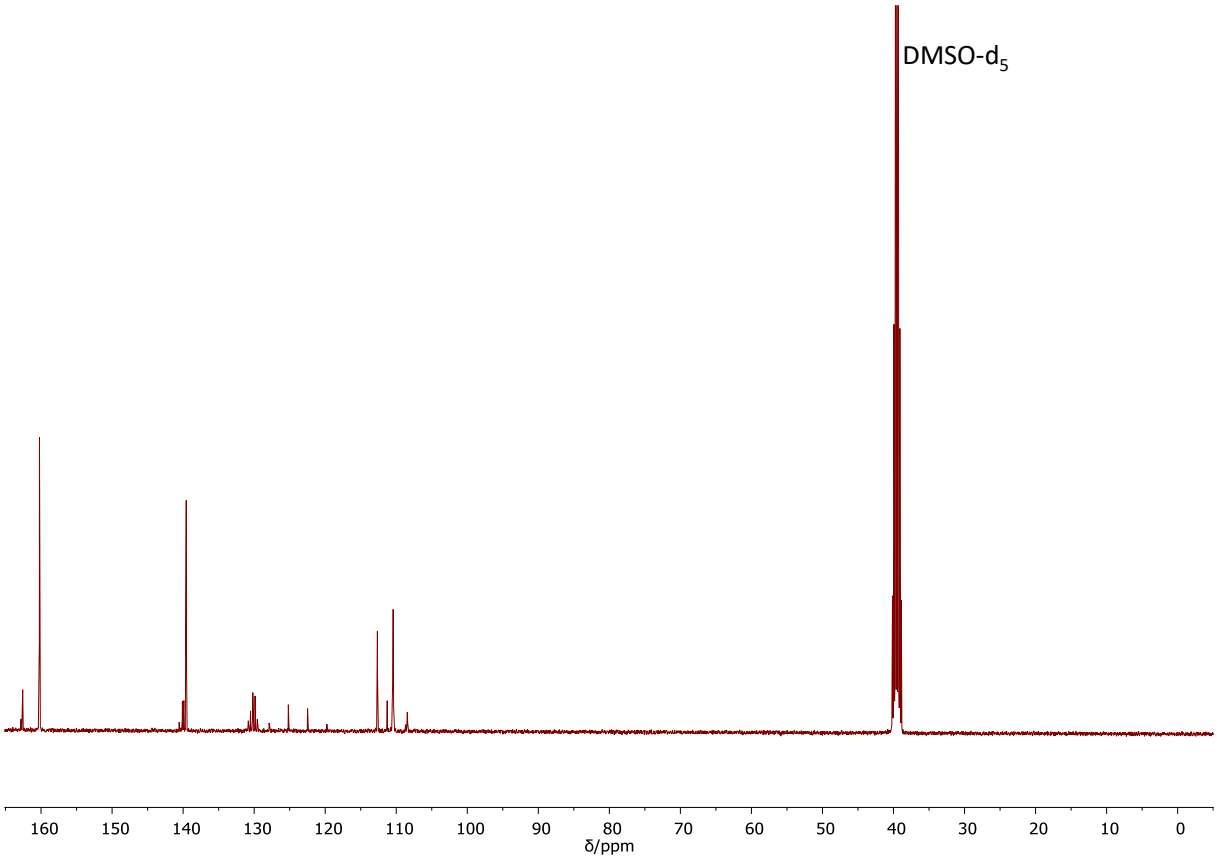

Figure 111: ^{13}C- NMR-spectrum of 5-trifluoromethyl phenyl-1,3-N-diformamide.

EI-HRMS m/z: $[M]^+$ calculated for $[C_9H_7O_2N_2F_3]$ = 232.0454, found: 232.0453, Δ = -0.0884 mmu.

IR (ATR platinum diamond): ν/cm^{-1} = 3464 (m), 3369 (s), 3303 (w), 3246 (w), 3180 (w), 3044 (w), 3034 (w), 2995 (w), 2950 (w), 2847 (w), 1678 (s), 1656 (m), 1625 (s), 1592 (vs), 1567 (vs), 1520 (s), 1473 (w), 1460 (w), 1434 (vs), 1314 (vs), 1284 (vs), 1181 (vs), 1166 (vs), 1121 (vs), 1074 (s), 1014 (m), 963 (s), 835 (vs), 769 (vs), 697 (vs), 638 (m), 619 (vs), 594 (m), 566 (m), 506 (vs), 494 (vs), 459 (vs), 401 (vs).

Dimethyl 5-(3-dodecylthioureido)isophthalate 36

Elemental sulfur (339 mg, 1.32 mmol, 0.14 eq., corresponds to 1.12 eq. of sulfur atoms) was suspended in 9.4 mL DMF (*c*(isocyanide) = 1.0 M), dodecylamine (2.40 mL, 1.92 mg, 10.4 mmol, 1.10 eq.) was added and a dark brown reaction mixture was observed. Subsequently, dimethyl-5-isocyanidoisophtalate (2.07 g, 9.43 mmol, 1.00 eq.) was added and the reaction mixture was stirred at room temperature for 13 hours. Subsequently, the solvent was removed under reduced pressure. The crude product was washed with 120 mL methanol at 60°C for several minutes and then left to cool down to room temperature. After filtration and washing with minimal amount of methanol (30 mL), the solvent was evaporated and the pure product was obtained as colorless, voluminous and static solid (2.85 g, 6.53 µmol) in a yield of 69%.

^{1}H-NMR (400 MHz, DMSO-d_6) δ/ppm = 9.84 (s, 1H, NH, ^{1}), 8.36 (s, 2H, aromatic, ^{2}), 8.16 (s, 1H, aromatic, ^{3}), 8.00 (s, 1H, NH, ^{4}), 3.89 (s, 6H, CH_3, ^{5}), 3.47 (s, 2H, CH_2, ^{6}), 1.66 – 1.43 (m, 2H, CH_2, ^{7}), 1.37-1.14 (m, 18H, CH_2, ^{8}), 0.85 (t, ^3J = 6.3 Hz, 3H, CH_3, ^{9}).

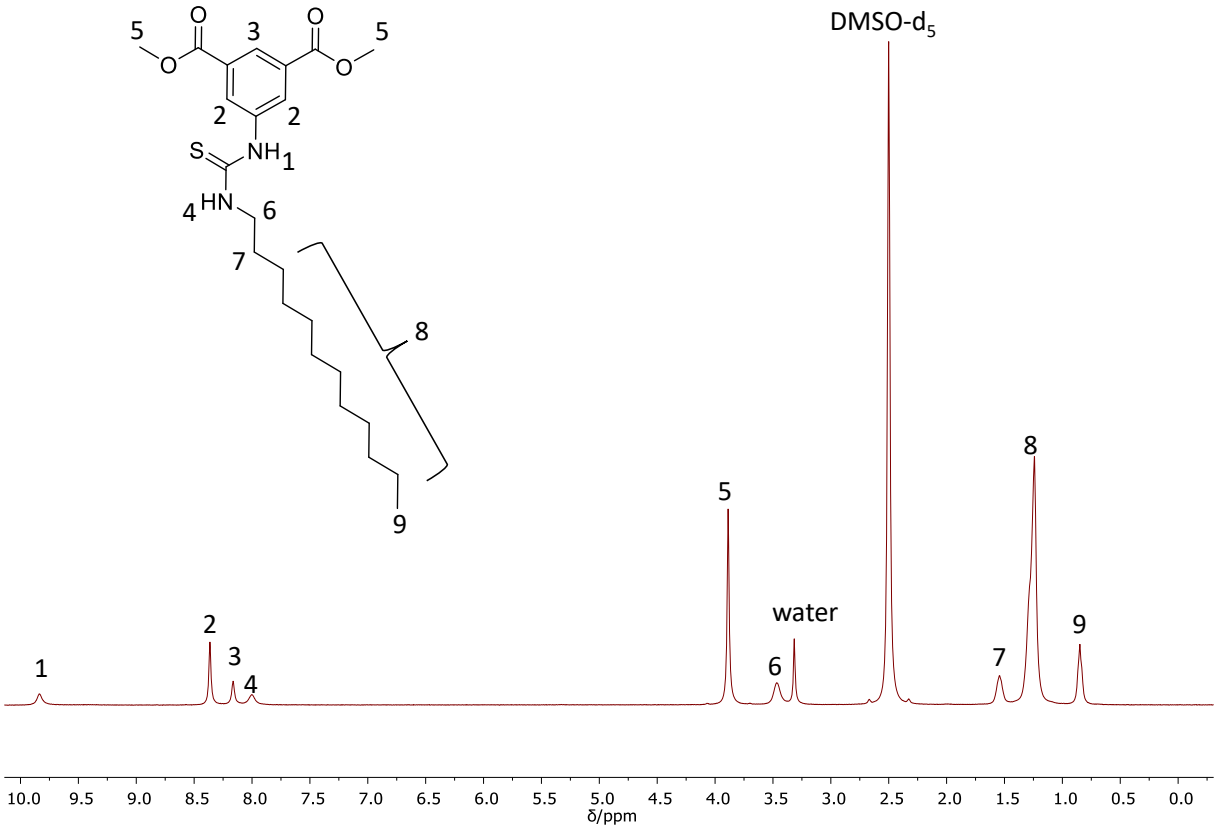

*Figure 112: ^{1}H-NMR-spectrum of dimethyl 5-(5-dodecylthioureido)isophthalate **36**.*

Synthesis of *O*-hexyl, *N*-dodecyl thionocarbamate

The synthesis protocol was a modification of the protocol of Gais and Böhme.[627]

A solution of hexyl alcohol (301 µL, 247 mg, 2.42 mmol, 1.1 eq.) in THF (*c*(alcohol)=2.25 M, V(THF)=1.08 mL) was slowly added at 0 °C to a suspension of sodium hydride (60w% in mineral oil, 63.3 mg, 2.64 mmol, 1.20 eq.) in THF (*c*(NaH)=2.25 M, V(THF)=1.17 mL). After the suspension was stirred at 0 °C for 1 h, a solution of dodecyl isothiocyanate **41** (500 mg, 2.20 mmol, 1.00 eq.) in THF (*c*(isothiocyanate)=4.5 M, V(THF)=489 µL) was added *via* a syringe. The mixture was then stirred for 80 minutes and then, quenched by the addition of 1.08 mL of saturated aqueous $NaHCO_3$. The aqueous phase was then extracted with ethyl acetate (3×), and the combined organic phases were dried over sodium sulfate and filtered off. Concentration of the organic phases in vacuo and purification of the residue by column chromatography (CH:EA, 60:1) gave the product (499 mg, 1.51 mmol) in a yield of 69%.

R_f = 0.48 in cyclohexane/ethyl acetate 50:1 visualized *via* vanillin staining solution (blue).

Two rotamers were present in a ratio of 0.67:0.33 determined by NH signal[1]. The respective rotamers were assigned if possible.

^{1}H-NMR (400 MHz, DMSO-d_6) δ/ppm = 9.13 – 9.09 (t, ^3J = 5.6 Hz, 1H, NH, ^{1b}), 9.06 (t, ^3J = 5.6 Hz, 1H, NH, ^{1a}), 4.34 (t, ^3J = 6.4 Hz, 2H, CH_2, ^{2b}), 4.30 (t, ^3J = 6.7 Hz, 2H, CH_2, ^{2a}), 3.32 (m, 2H, CH_2, ^{3a}), 3.10 (q, ^3J = 6.1 Hz, 2H, CH_2, ^{3b}) 1.69-1.55 (m, 2H, CH_2, ^{4}), 1.52-1.40 (m, 2H, CH_2, ^{5}), 1.39 – 1.07 (m, 24H, CH_2, ^{6}), 0.90-0.82 (m, 6H, CH_3, ^{7}).

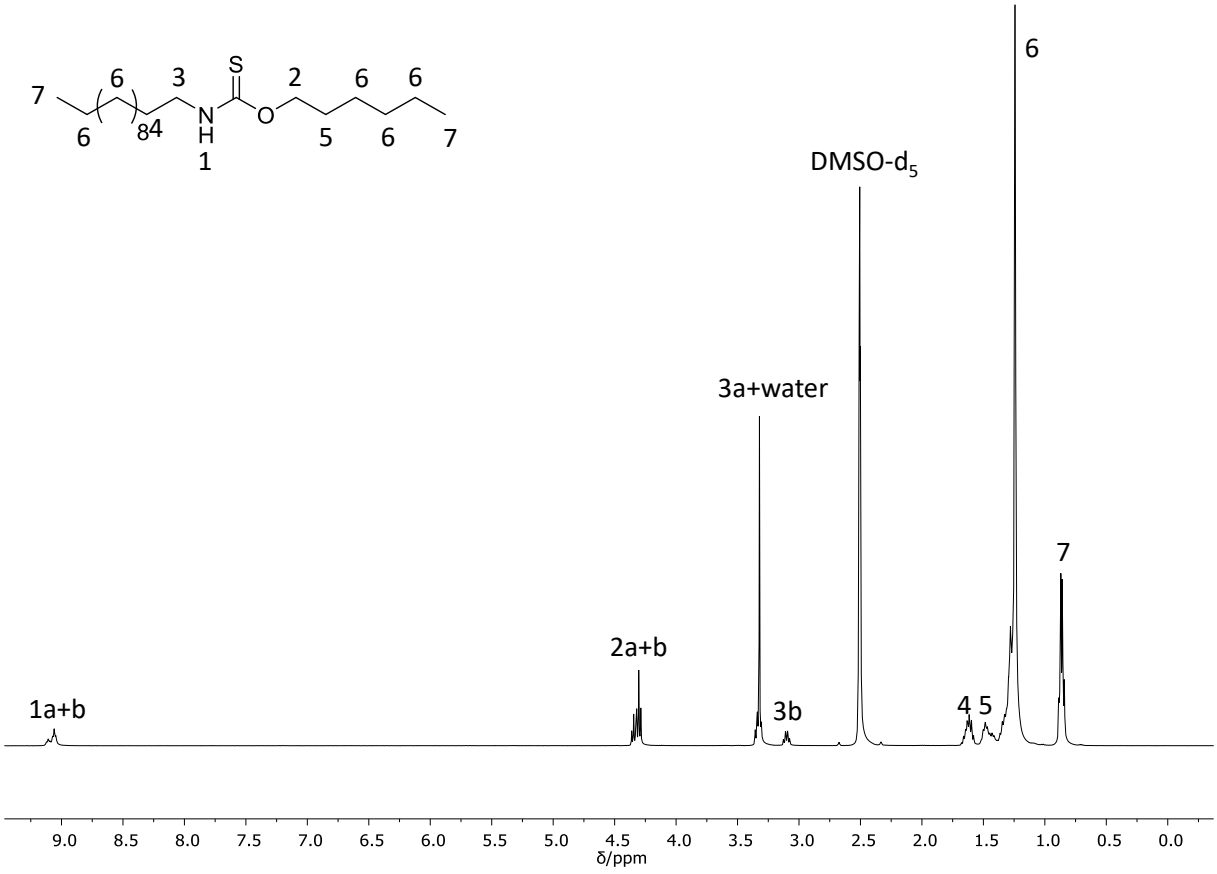

Figure 113: ^{1}H-NMR-spectra of O-hexyl, N-dodecyl thionocarbamate.

^{13}C-NMR (101 MHz, DMSO-d_6) δ/ppm = 189.95 (C=S, ^{a}), 188.45 (C=S, ^{b}), 70.46 (CH_2-O, ^{b}), 69.45 (CH_2-O, ^{a}), 44.97 (CH_2-NH, ^{a}), 42.59 (CH_2-NH, ^{b}), 31.77 (CH_2), 31.40 (CH_2), 31.34 (CH_2), 29.50 (CH_2), 29.47 (CH_2), 29.43 (CH_2), 29.40 (CH_2), 29.17 (CH_2), 29.13 (CH_2), 29.11 (CH_2), 29.00 (CH_2), 28.76 (CH_2), 28.63 (CH_2), 28.21 (CH_2), 26.74 (CH_2), 26.66 (CH_2), 25.60 (CH_2), 25.44 (CH_2), 22.56 (CH_2), 22.50 (CH_2), 14.42 (CH_3), 14.34 (CH_3), 14.29 (CH_3).

6.5.2 Poly(thioether-ester)s bearing thiourea functions in side chains by poly-Thiol-Ene reaction

Diallyl-5-aminoisophthalate

5-Aminoisophtalic acid (4.00 g, 22.1 mmol, 1.00 eq.) was dissolved in allylalcohol (45.1 mL, 38.5 g, 662 mol, 30.0 eq.) and cooled to 0°C applying an ice-water bath. Subsequently, thionyl chloride (9.6 mL, 15.8 g, 132 mmol, 6.00eq.) was added dropwise (one drop per five seconds) keeping the temperature below 5 °C. After the addition, the cooling was removed and the reaction mixture was stirred at room temperature overnight. Subsequently, the remaining thionyl chloride was quenched and a pH-value of eight was adjusted using saturated aqueous sodium hydrogen carbonate solution and solid potassium carbonate. Water was added to dissolve precipitated salts and the organic layer was separated. The aqueous phase was extracted with DCM (2 times) and the organic phases were combined, dried over sodium sulfate and filtered off. The product (4.56 g, 17.4 mmol) was obtained as a red to brown crystal solid in a yield of 79% after removal of the solvent under reduced pressure.

^{1}H-NMR (400 MHz, DMSO-d_6) δ/ppm = 7.68 (t, ^4J = 1.5 Hz, 1H, aromatic, ^{1}), 7.44 (d, ^4J = 1.5 Hz, 2H, aromatic, ^{2}), 6.09–5,99 (m, 2H, C**H**=CH_2, ^{3}), 5.78 (s, 2H, NH_2, ^{4}), 5.42–5.26 (m, 4H, CH=C**H$_2$** , ^{5}), 4.79 (dt, ^3J = 5.4 Hz, ^4J = 1.5 Hz, 4H, CH_2, ^{6}).

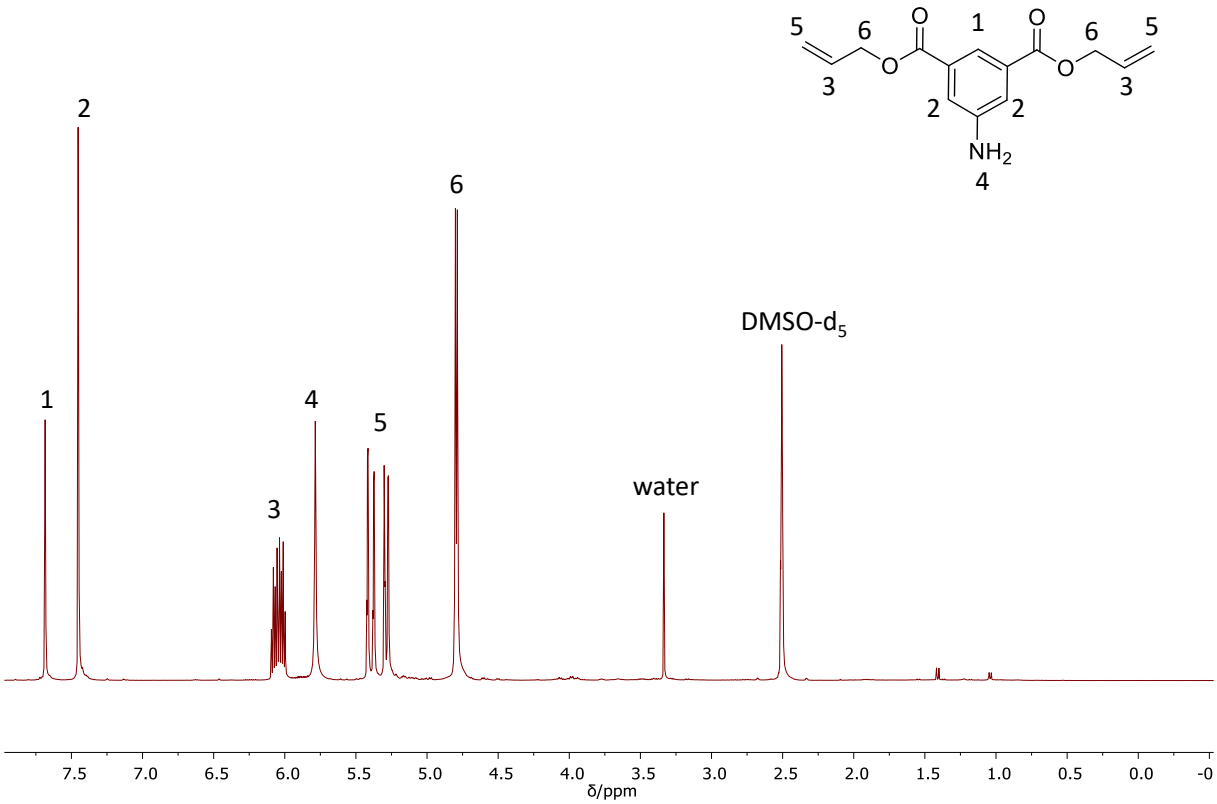

Figure 114: ^{1}H-NMR-spectrum of diallyl-5-aminoisophthalate.

IR (ATR platinum diamond): ν/cm^{-1} = 3474 (w), 3380 (w), 3219 (vw), 3087 (vw), 2941 (vw), 2880 (vw), 1701 (vs), 1625 (m), 1602 (m), 1442 (m), 1372 (s), 1333 (vs), 1271 (m), 1226 (vs), 1162 (w), 1123 (vs), 1094 (m), 985 (vs), 934 (vs), 921 (vs), 897 (vs), 887 (s), 850 (m), 786 (w), 755 (vs), 726 (m), 675 (m), 646 (m), 621 (m), 555 (s), 514 (m), 487 (m), 457 (m), 401 (m).

Diallyl-5-formamidoisophthalate

5-amino diallylisophthalacid ester (4.04 g, 17.3 mmol, 1.00 eq.) and formic acid (5.2 mL, 6.38 g, 139 mmol, 8.00 eq.) were put in a flask and stirred at 60 °C for 19 hours. Afterwards, the remaining formic acid and water were removed under reduced pressure. The product was obtained as brown solid (4.75 g, 16.4 mmol) in a yield of 95%.

^{1}H-NMR (400 MHz, DMSO-d_6) δ/ppm = 10.66 (s, 1H, CHO, ^{1a}), 10.44 (d, ^{3}J = 10.9 Hz, 1H, CHO, ^{1b}), 8.95 (d, ^{3}J = 10.7 Hz, 1H, NH, ^{2b}), 8.51 (d, ^{4}J = 1.6 Hz, 2H, aromatic ^{3a}), 8.38 (d, ^{3}J = 1.7 Hz, 1H, NH, ^{3}), 8.23-8.18 (m, 1H, ^{4a,b}), 8.06 (d, ^{4}J = 1.6 Hz, 2H, aromatic, ^{3b}), 6.11 – 6.01 (m, 2H, ^{5}), 5.47 – 5.22 (m, 4H, ^{6}), 4.85 (dt, ^{3}J = 5.5, ^{4}J = 1.5 Hz, 4H, ^{7}).

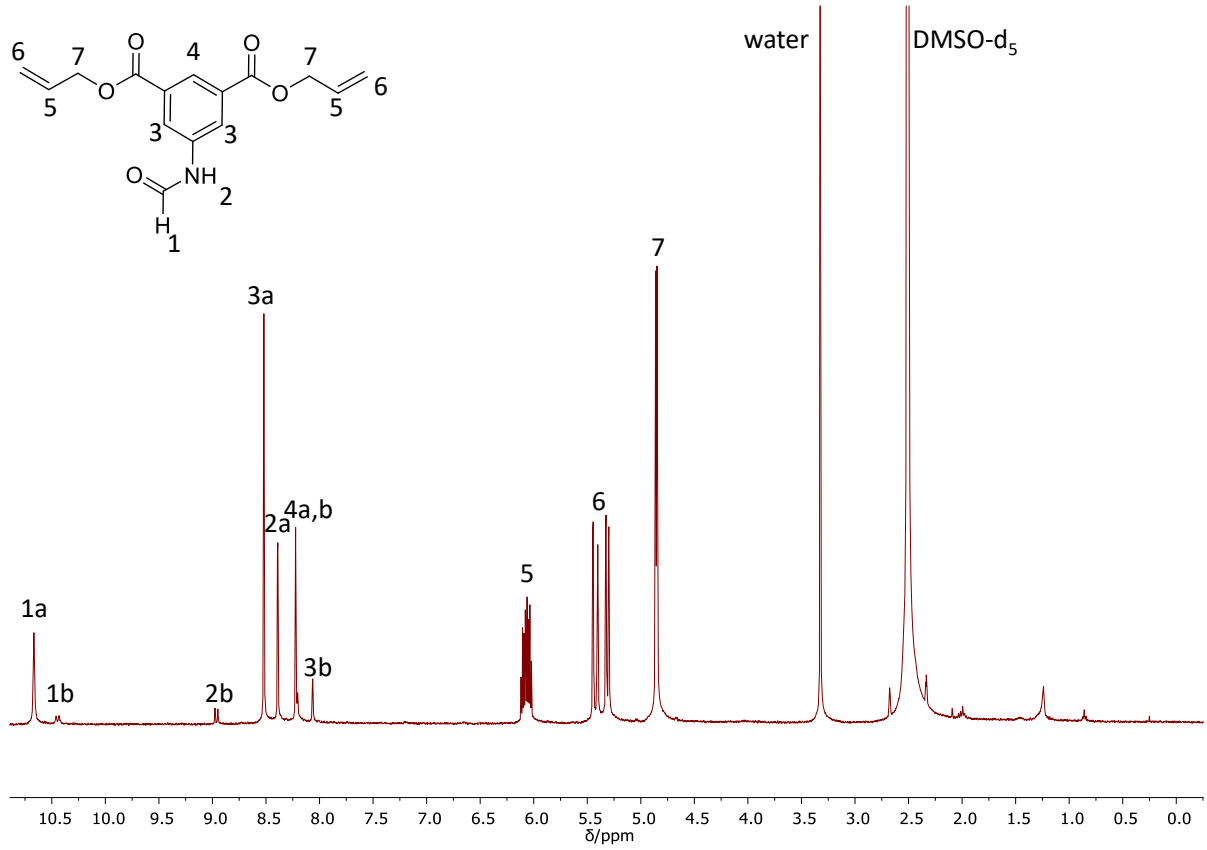

Figure 115: ^{1}H-NMR-spectrum of diallyl-5-fromaidoisophthalate

^{13}C-NMR (101 MHz, DCM-d_2) δ/ppm = 164.78 (C=O, ^{b}) 164.37 (C=O), 160.40 (C=O, ^{a}), 139.31 (quarternay-aromatic), 132.43 (**C**H=CH_2), 130.86 (quarternay-aromatic), 124.43 (aromatic, ^{a}), 124.21 (aromatic, ^{b}), 123.75 (aromatic, ^{a}), 121.86 (aromatic, ^{b}), 118.35 (CH=**C**H_2), 65.65 (CH_2).

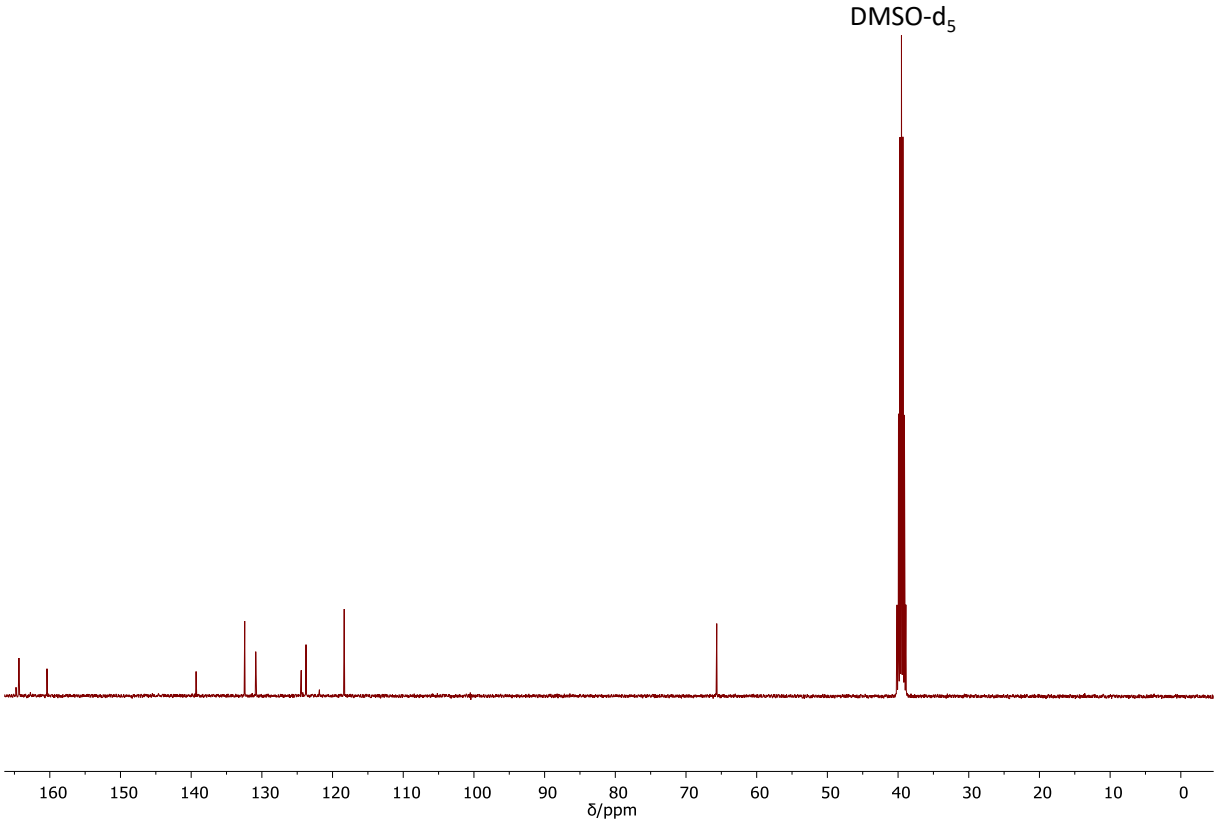

Figure 116: ^{13}C-NMR-spectrum of diallyl-5-formamidoisophthalate.

IR (ATR platinum diamond): ν/cm^{-1} = IR = 3431 (vw), 3353 (vw), 3308 (w), 3198 (vw), 3087 (vw), 3069 (vw), 3022 (vw), 2989 (vw), 1699 (vs), 1685 (vs), 1650 (m), 1611 (s), 1600 (s), 1520 (w), 1454 (w), 1425 (w), 1399 (w), 1376 (m), 1331 (s), 1312 (vs), 1267 (s), 1234 (vs), 1201 (vs), 1140 (s), 1113 (m), 1010 (m), 983 (s), 950 (w), 926 (s), 899 (m), 753 (vs), 724 (m), 693 (s), 671 (w), 650 (w), 617 (w), 580 (w), 555 (w), 461 (vw), 422 (vw).

Diallyl-5-isocyanidoisophthalate

Diallyl-5-formamidoisophtalate (1.50 g, 5.19 mmol, 1.00 eq.) was reacted with DIPA (2.27 mL, 1.63 g, 16.1 mmol, 3.10 eq.) and phosphorus oxychloride (630 µL, 1.03 g, 6.74 mmol, 1.30 eq.) in 16 mL DCM. After completion of the reaction, remaining phosphorus oxychloride was quenched by adding 16 mL saturated sodium hydrogen carbonate solution to the reaction mixture and the biphasic mixture was stirred for another 30 minutes. The phases were separated and the aqueous phase was extracted with DCM (1 ×). The organic layers were combined, dried over sodium sulfate and filtered off. Purification of the crude product with flash column chromatography (cyclohexane/ethyl acetate 7/1+3V% TEA) yielded the product as brown liquid (436 mg, 1.61 mmol) in a yield of 31%. The product was immediately converted in an AM-3CR.

^{1}H-NMR (400 MHz, DMSO-d_6) δ/ppm = 8.52 (t, ^4J = 1.6 Hz, 1H, aromatic, ^{1}), 8.36 (d, ^4J = 1.6 Hz, 2H, aromatic, ^{2}), 6.11 – 6.02 (m, 2H, C**H**=CH_2, ^{3}), 5.48 – 5.26 (m, 4H, CH=C**H_2**, ^{4}), 4.87 (dt, ^3J = 5.5 Hz, ^4J = 1.5 Hz, 4H, CH_2, ^{5}).

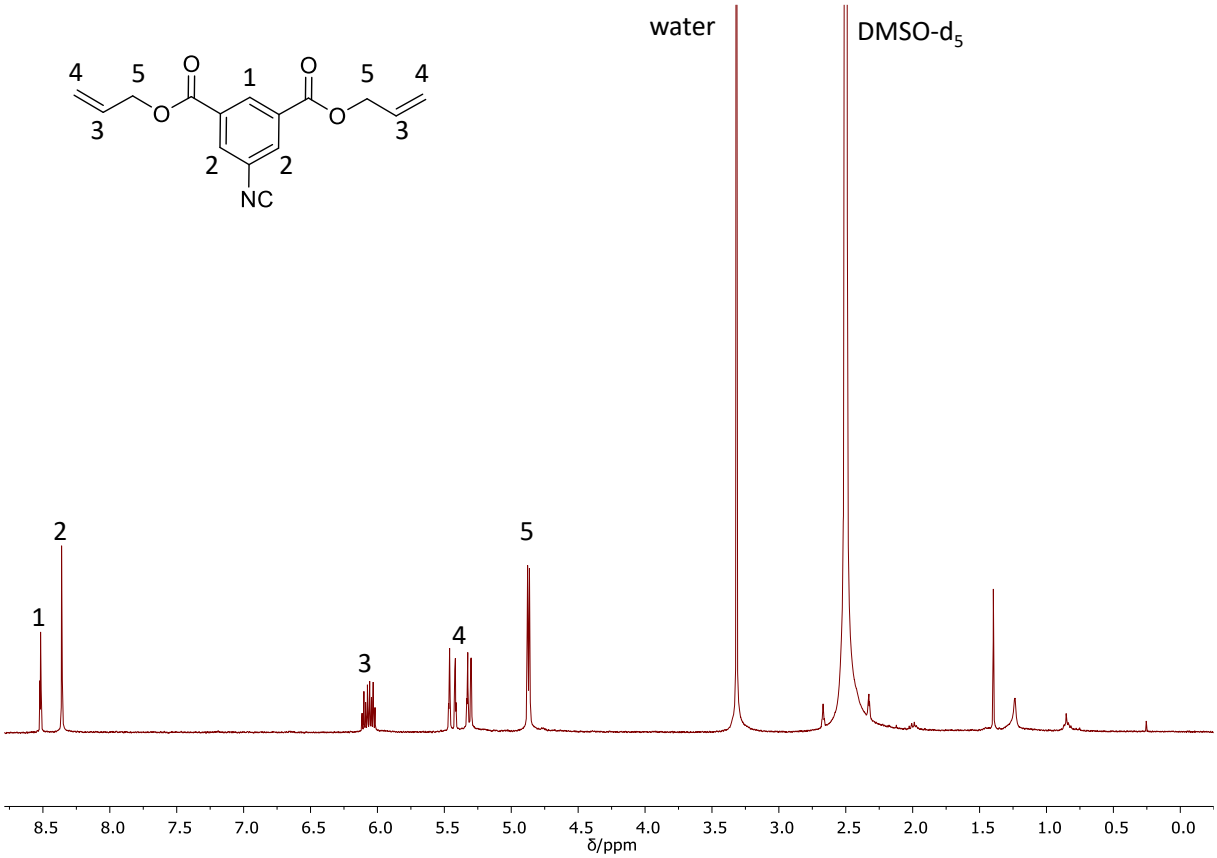

Figure 117: ^{1}H-NMR-spectrum of diallyl-5-isocyanidoisophthalate.

Diallyl 5-(3-dodecylthioureido)isophthalate 47

Elemental sulfur (26.5 mg, 103 µmol, 0.14 eq., corresponds to 1.12 eq. of sulfur atoms) was suspended in 1.5 mL methanol (*c*(isocyanide) = 0.5 M), dodecylamine (188 µL, 150 mg, 811 µmol, 1.10 eq.) was added and a dark red to brownish reaction mixture was observed. Subsequently, diallyl-5-ioscyanidoisophtalate (200 mg, 737 µmol, 1.00 eq.) was added and the reaction mixture was stirred at room temperature overnight. Subsequently, the solvent was removed under reduced pressure. The crude product was washed with methanol at 60°C for several minutes and then left to cool down to room temperature. After filtration and washing with minimal amount of methanol, the solvent was evaporated and the pure product was obtained (277 mg, 568 µmol) in a yield of 77%.

^{1}H-NMR (400 MHz, DMSO-d_6) δ/ppm = 9.87 (s br, 1H, NH, ^{1}), 8.42 (d, ^4J = 1.6 Hz, 2H, aromatic, ^{2}), 8.19 (m, 1H, aromatic, ^{3}), 8.01 (s br, 1H, NH, ^{4}), 6.11 – 6.01 (m, 2H, C**H**=CH_2, ^{5}), 5.45 – 5.28 (m, 4H, CH=C**H$_2$**, ^{6}), 4.84 (dt, ^3J = 5.4 Hz, ^4J = 1.5 Hz, 4H, C**H$_2$**, ^{7}), 3.47 (m, 2H, CH_2, ^{8}), 1.59 – 1.50 (m, 2H, CH_2, ^{9}), 1.32 – 1.20 (m, 18H, CH_2, ^{10}), 0.89 – 0.80 (m, 3H, CH_3, ^{11}).

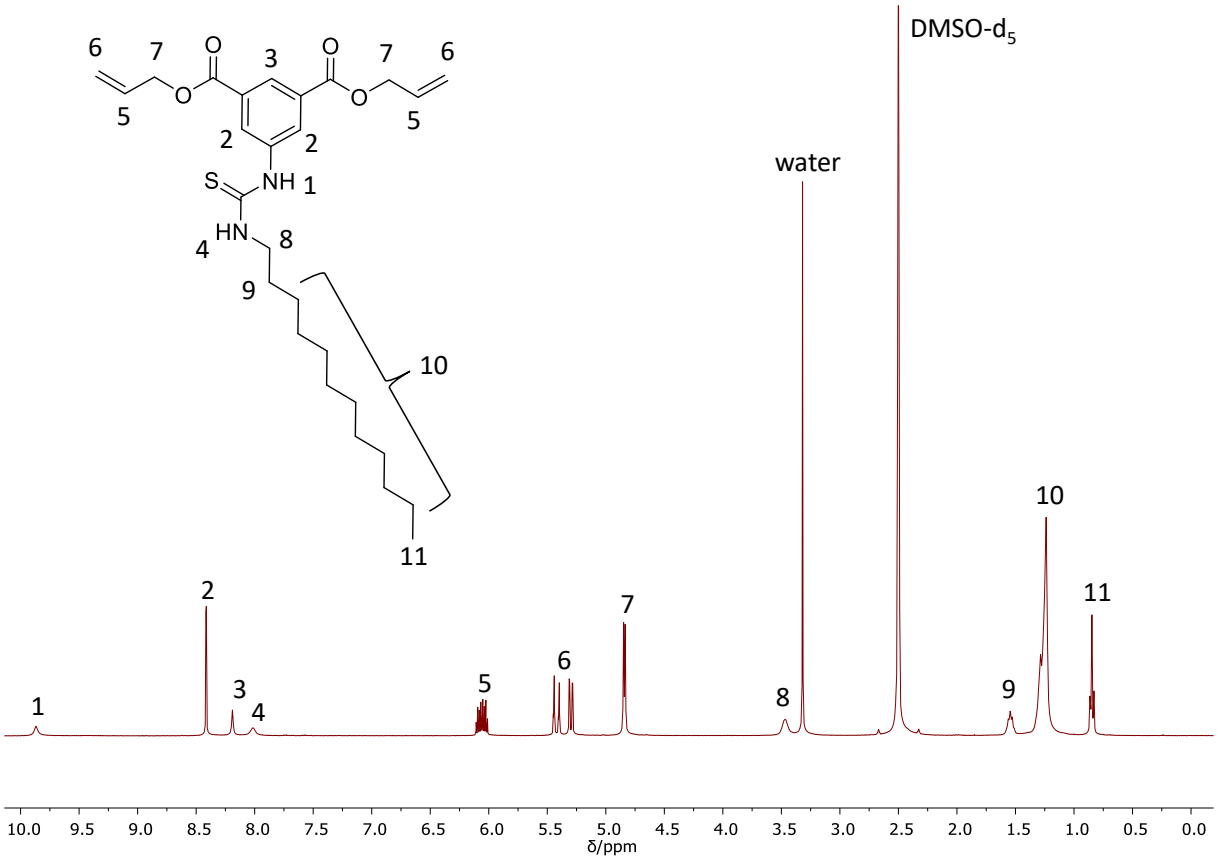

*Figure 118: ^{1}H-NMR-spectrum of Diallyl 5-(3-dodecylthioureido)isophthalate **47**.*

6.5.3 Poly(norbornene)s bearing thiourea functions in their side chains by ring-opening metathesis polymerization (ROMP)

6.5.3.1 Screening of ROMP of thiourea-norbornene 50

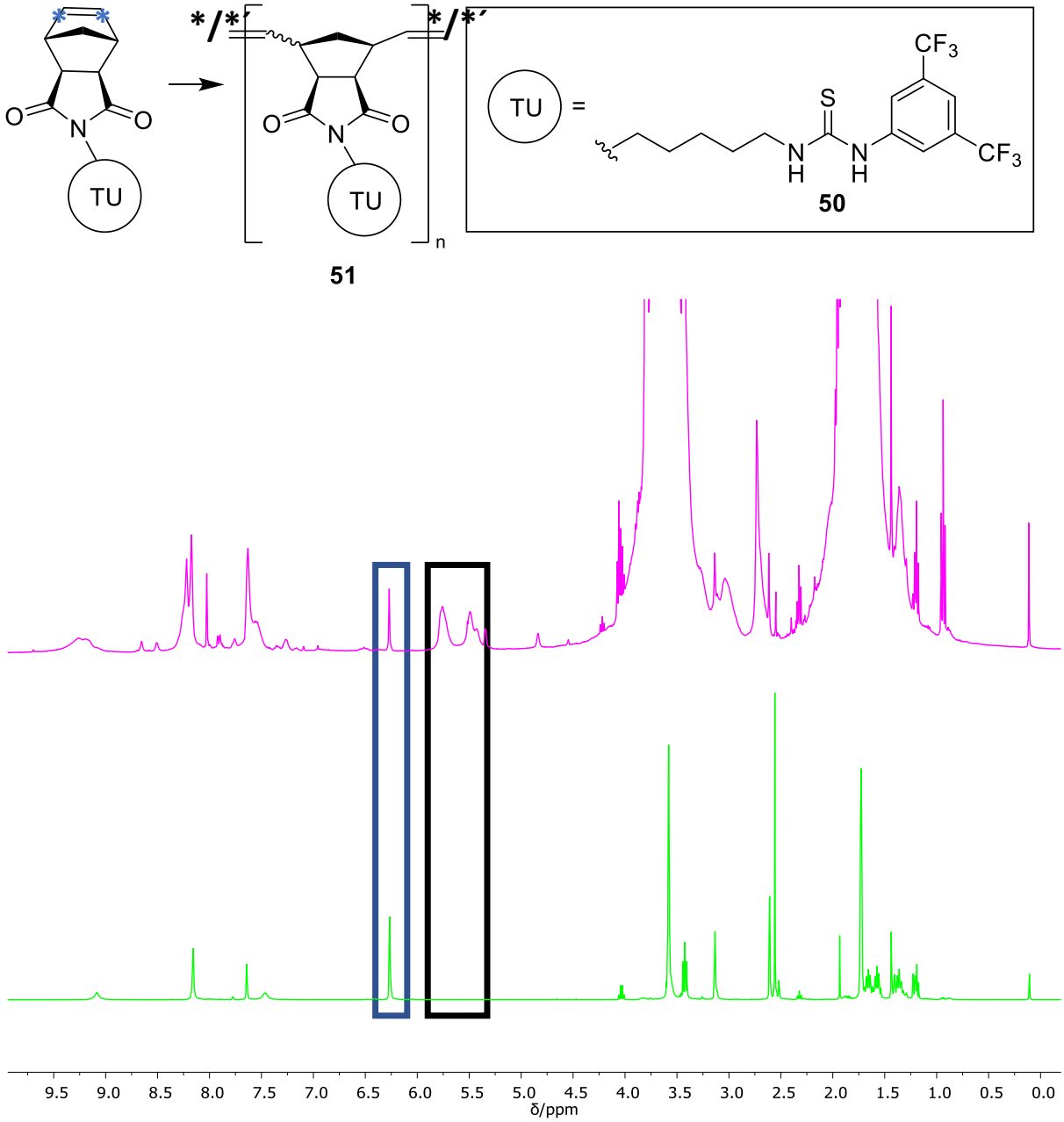

*Figure 119: Reaction scheme of a ROMP of thiourea norbornene **50** and stacked ^{1}H-NMR-spectra in THF-d$_7$. Bottom: isolated thiourea norbornene **50** (green). Top: its reaction in a ROMP using 5 mol% Grubbs catalyst 3rd generation after 1 hour. Note that the reaction was performed in non-deuterated THF and thus, the THF-signals are significantly larger while additional signal in the aromatic region can be assigned to the catalyst. Since polymer will form cis and trans double bonds two signals are obtained (thus * and *´, see black box).*

*Conversion can be calculated by using the integral of the double bond of the starting material (blue * and blue box) comparing to the formed double bonds signal of the polymer (black * and *´as well as black box) following the calculation:*

$$conversion(\%) = \left(1 - \frac{I_{SM}}{I_{SM} + I_P}\right) * 100 \quad (9)$$

Whereas I_{SM} and I_P are the integral of the double bond signals of the starting material and the polymer, respectively.

6.5.3.2 Screening of *co*-ROMP of thiourea norbornene 50 and norbornene 52

*Table 37: Qualitative screening of solubility of a series of poly(thiourea norbornene **50**-co-norbornene **52**)s **54** in DCM and THF obtained by ROMP in dependance of the amount of catalyst used and the ratio between monomer **50** and **52**.*

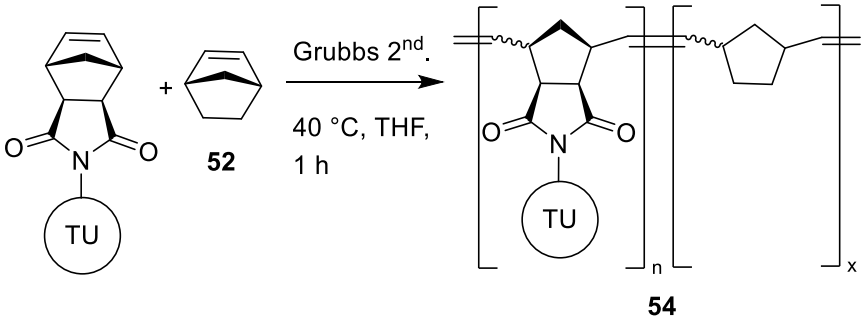

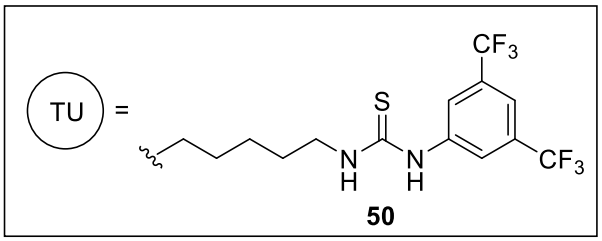

entry	cat.-loading/mol%	$M_{n,\,theo.}$/kDa[a)]	ratio 50:52	solubility in DCM[b)]	solubility in THF[b)]
1	10	3.1	1:1	-	-
2	10	2.0	1:3	✓	✓
3	10	1.4	1:9	✓	✓
4	3	6.7	1:3	-	✓
5	3	4.6	1:9	✓	✓
6	2	6.8	1:9	-	-

The respective ratio of the monomers was applied while monomer **50** was first dissolved in THF (dry, *c*(thiourea **50**)=0.1 M) and the respective amount of Grubbs 2nd generation catalyst was added. Subsequently, a stock solution of norbornene **52**, using the same amount of THF as applied in the reaction mixture, was added dropwise over the whole reaction time of one hour *via* syringe pump theoretical. a) Molecular weight of the respective *co*-polymers **54** were calculated according to their ratio dependent and averaged monomer molecular weight. b) Qualitative determination by naked eye after quenching with ethyl vinyl ether.

The M_n was calculated as depicted for entry 4 of Table 36:

Using 3 mol% of Grubbs 2nd generation catalyst and a ratio of monomers **50**:**52**, 1:3 the theoretical M_n was calculated as followed:

$$M_n = DP \times M_{av.} \quad (I); \qquad DP = \frac{[M]}{[I]} \quad (10); \qquad M_{av.} = xM(\mathbf{50}) + yM(\mathbf{52}) \quad (III)$$

Whereas $M_{av.}$ is the average molecular weight of the monomer unit considering the applied ratio of monomers x and y, [M] and [I] are the concentrations of the overall amount of double bonds in both monomers and catalyst, respectively. Transferring (II) and (III) into (I) yield:

$$M_n = \frac{[M]}{[I]} \times (xM(\mathbf{50}) + yM(\mathbf{52}))$$

With M(**50**)=519.51 g mol^{-1} and M(**52**)=94.16 g mol^{-1} the M_n is obtained:

$$M_n = \frac{1}{0.03} \times (0.25 \times 519.51\ \frac{g}{mol} + 0.75 \times 94.16\ \frac{g}{mol}) = 6.68\ \frac{g}{mol}$$

6.5.3.3 Synthesis of thiourea norbornene 50

(3aR,4R,7S,7aS)-2-(5-aminopentyl)-3a,4,7,7a-tetrahydro-1H-4,7-methanoisoindole-1,3(2H)-dione

The procedure was provided by Dr. D. Barther. 1,5-Diaminopentane (6.4 mL, 5.61 g, 54.9 mmol, 3.00 eq.) was dissolved in 68 mL DMSO and added in a two-necked flask equipped with a rubber septum and an air condenser. The solution was heated to 130 °C. Subsequently, exo-norbornene-2,3-dicarboxanhydride (3.00 g, 18.3 mmol, 1.00 eq.) was dissolved in 23 mL DMSO and added to the amine solution over a period of five hours *via* syringe pump. The reaction was stirred at 130 °C overnight. After cooling to ambient temperature, 150 mL DCM were added and the mixture was washed with water (3 x 150 mL) and brine (100 mL) and dried over $MgSO_4$. The solvent was removed under reduced pressure. The compound was obtained after column chromatography (12:1→9:1) as a viscous brown liquid (3.23 g, 13.0 mmol) in a yield of 71%.

R_f = 0.55 in cyclohexane/ethyl acetate 2/1 visualized *via* UV quenching at 254 nm and vanillin staining solution (yellow).

^{1}H-NMR (400 MHz, DMSO-d_6): δ/ppm = 6.30 (m, 2H, ^{1}), 3.36 – 3.26 (m, 4H, ^{2,3}), 3.09 (t, ^3J = 1.8 Hz, 2H, ^{4}), 2.68 (d, ^3J = 1.4 Hz, 2H, ^{5}), 2.54 (m, 2H, ^{6}), 1.49 – 1.16 (m, 6H, ^{7,8,9}), 1.29 – 1. (m, 1H, ^{10a}), 1.15 – 1.08 (m, 1H, ^{10b}).

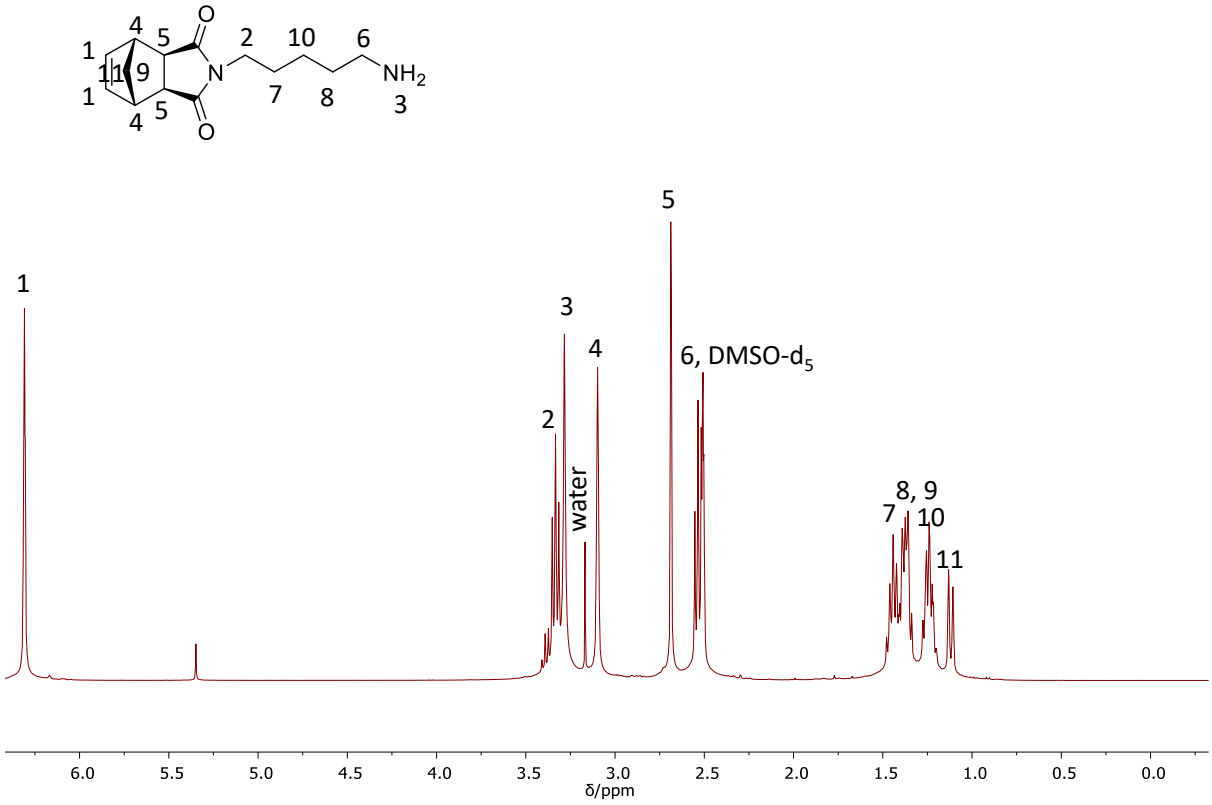

Figure 120: ^{1}H-NMR-spectrum of the amino-norbornene.

^{13}C-NMR (101 MHz, DMSO-d_6) δ/ppm = 177.62 (C=O), 137.60 (CH=CH), 47.21 (CH), 44.43 (CH), 40.46 (CH_2), 37.83 (CH_2), 31.46 (CH_2), 27.01 (CH_2), 23.63 (CH_2).

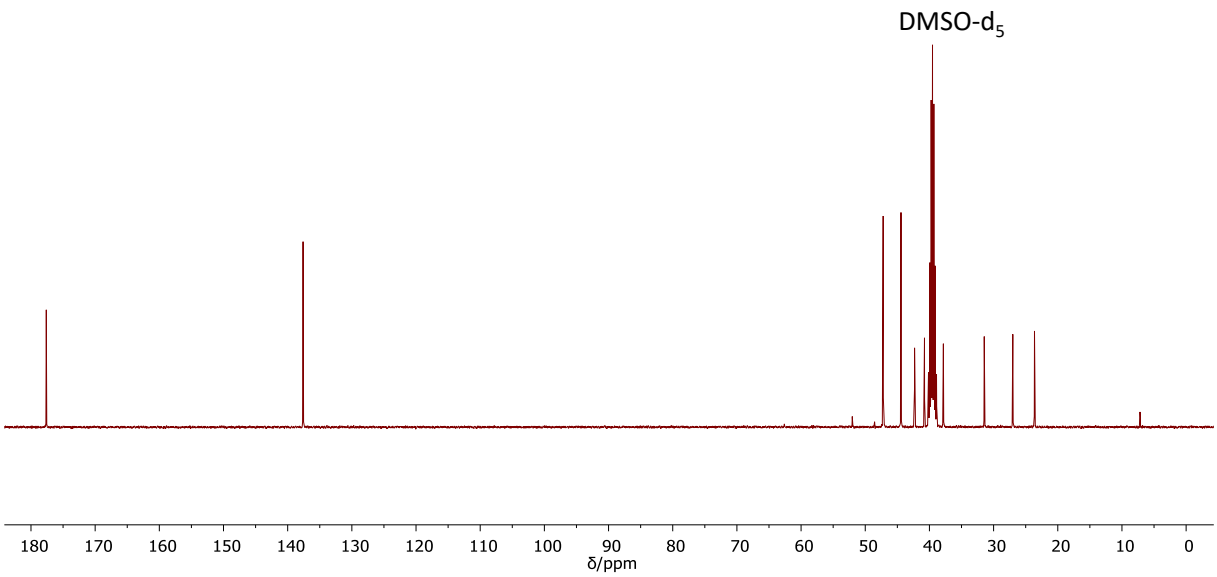

Figure 121: ^{13}C-NMR-spectrum of the amino-norbornene.

1-(3,5-bis(trifluoromethyl)phenyl)-3-(5-((3aR,4R,7S,7aS)-1,3-dioxo-1,3,3a,4,7,7a-hexahydro-2H-4,7-methanoisoindol-2-yl)pentyl)thiourea 50

(3aR,4R,7S,7aS)-2-(5-aminopentyl)-3a,4,7,7a-tetrahydro-1H-4,7-methanoisoindole-1,3(2H)-dione (1.81, 7.30 mmol, 1.00 eq.) was put in a Schlenk-flask that was purged three times with argon and set under an argon atmosphere. Then dry DCM (V=14.5 mL) was added dissolving the amine. An ice-water bath was used to cool the solution to 0 °C. Then, 3,5-bis(trifluoromethyl)phenyl isothiocyanate (1.33 mL, 1.98, 7.30 mmol, 1.00 eq.) was added dropwise and the resulting mixture was stirred at room temperature overnight. Subsequently, the solvent was removed under reduced pressure. The pure products was obtained by column chromatography (dry load, CH:EA, 3:1→1:1) as a yellowish slow crystallizing solid (2.78 g, 5.35 mmol) in a yield of 73%.

^{1}H-NMR (400 MHz, DCM-d_2) δ/ppm = 8.18 (s, 1H, NH, ^{1}), 8.04 (s, 2H, aromatic, ^{2}), 7.68 (s, 1H, aromatic, ^{3}), 6.65 (s, 1H, NH, ^{4}), 6.29 (s, 2H, CH, ^{5}), 3.57 (br, 2H, CH_2, ^{6}), 3.49 (t, ^{3}J = 6.9 Hz, 2H, CH_2, ^{7}), 3.21 (s, 2H, CH, ^{8}), 2.68 (s, 2H, CH, ^{9}), 1.71 (quin., ^{3}J = 7.1 Hz, 2H, CH_2, ^{10}), 1.61 (quin. ^{3}J = 6.9 Hz, 2H, CH_2, ^{11}), 1.50 (d, ^{2}J = 9.9 Hz, 1H, CH_2, ^{12}), 1.37 (quin., ^{3}J = 7.1 Hz, 2H, CH_2, ^{13}), 1.20 (d, ^{2}J = 9.9 Hz, 1H, CH_2, ^{14}).

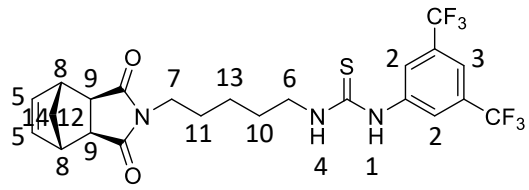

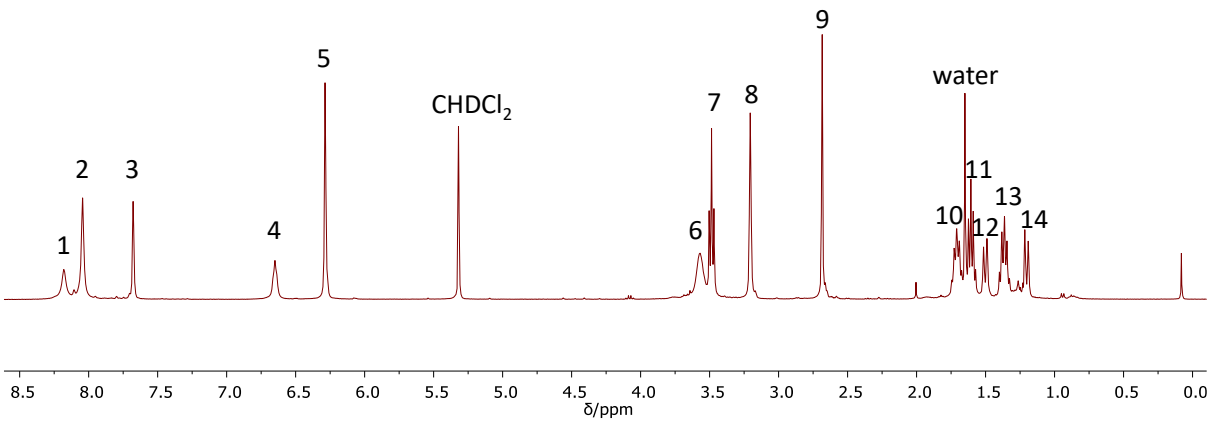

*Figure 122: ^{1}H-NMR-spectrum of TU-norbornene **50**.*

^{13}C-NMR (101 MHz, DCM-d_2) δ/ppm = 181.57 (C=S), 179.23 (C=O), 140.86 (quartenary-aromatic), 138.30 (C=C), 132.51 (q, ^{2}J = 34.3 Hz, quarternary-aroamtic), 124.09 (aromatic), 123.74 (q, ^{1}J = 273.8 Hz, CF_3), 118.90 (aromatic), 48.49 (CH), 45.78 (CH), 45.35 (CH_2), 43.24 (CH_2), 38.11 (CH_2), 27.72 (CH_2), 27.49 (CH_2), 24.28 (CH_2).

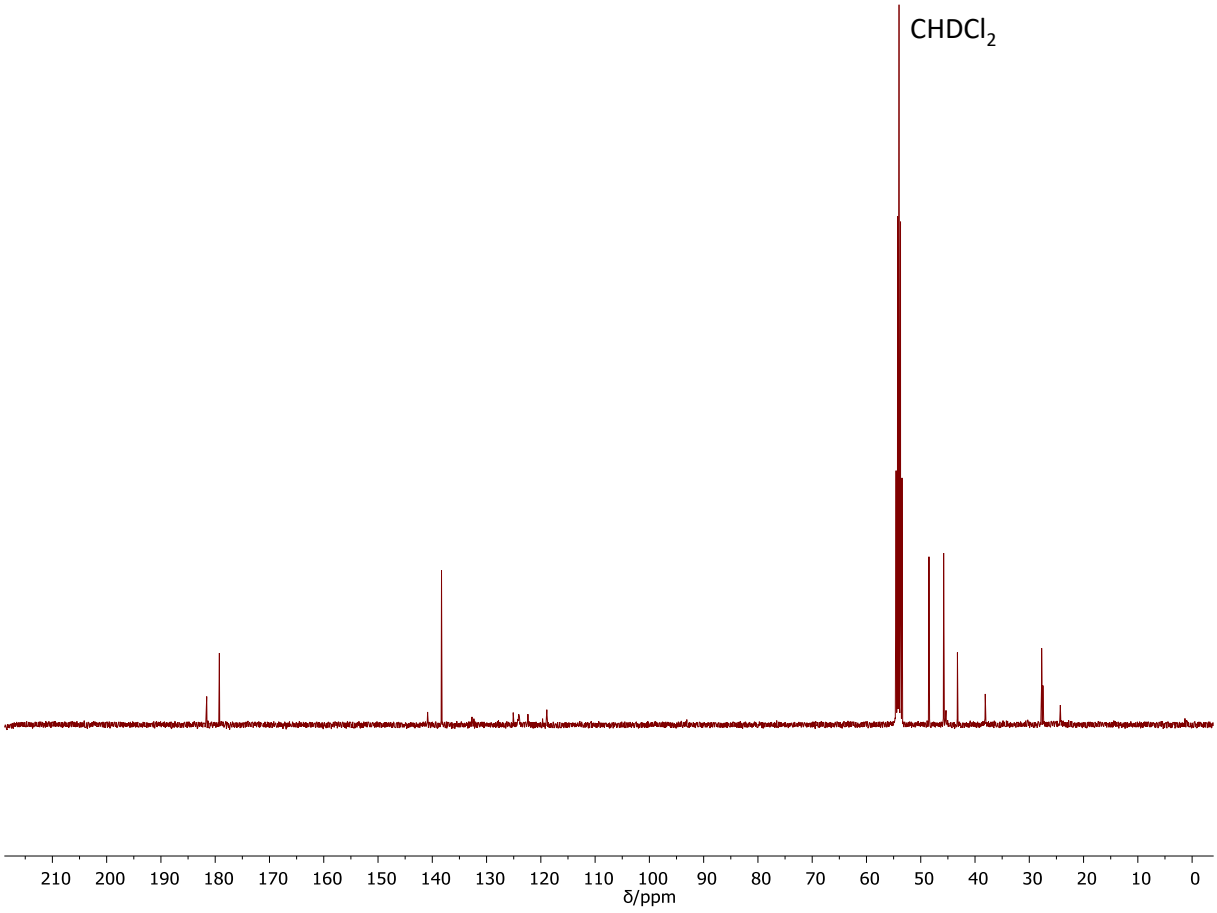

*Figure 123: ^{13}C-NMR-spectrum of TU-norbornene **50**.*

^{19}F-NMR (376 MHz, DMSO-d_6) δ/ppm = -63.32.

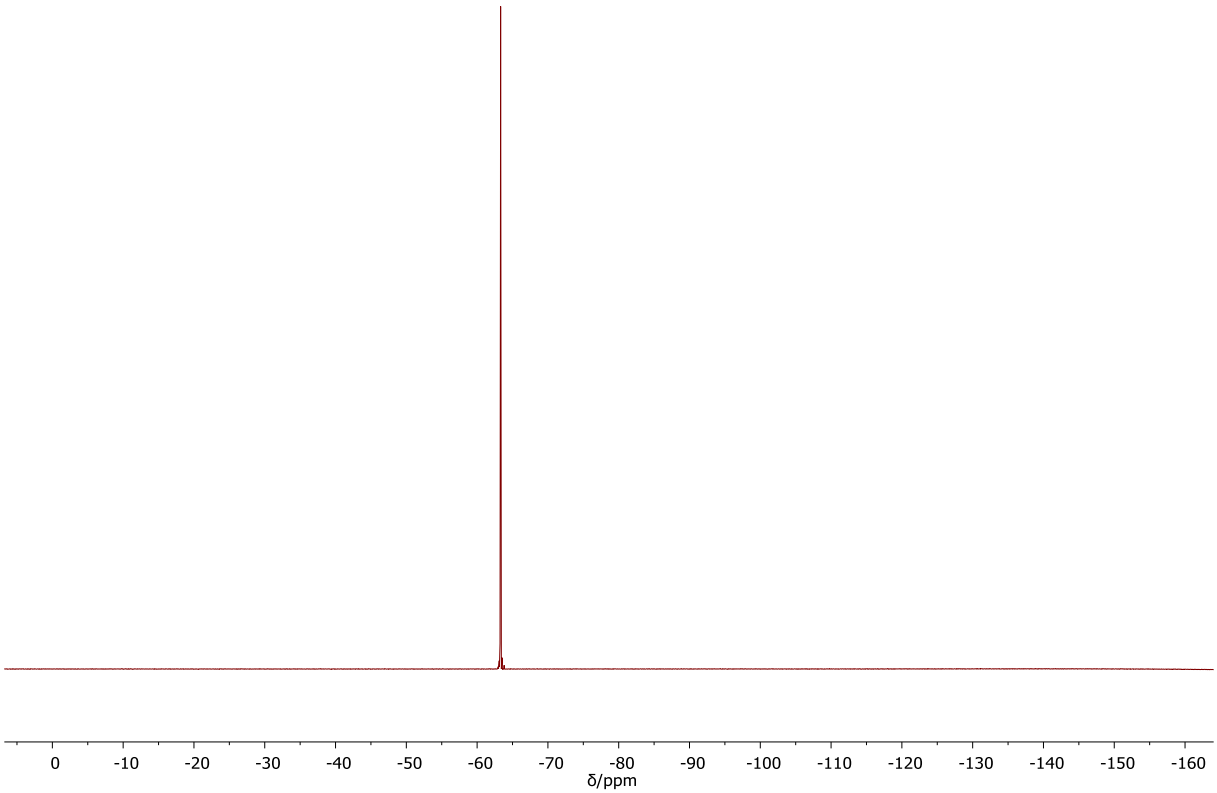

*Figure 124: 19F-NMR-spectrum of TU-norbornene **50***

***HRMS (FAB)**: calculated m/z for $C_{23}H_{24}O_2N_3F_6{}^{32}S_1$ [M+H]⁺ = 520.1488, found: 520.1489, Δ = 0.0618 mmu*

IR (ATR platinum diamond): ν/cm^{-1} = 3316 (w), 3067 (vw), 2983 (vw), 2941 (w), 2865 (vw), 1769 (w), 1683 (vs), 1623 (w), 1539 (m), 1471 (w), 1438 (w), 1382 (s), 1376 (s), 1343 (m), 1273 (vs), 1218 (w), 1168 (vs), 1123 (vs), 1109 (vs), 1028 (w), 1016 (w), 1000 (w), 946 (w), 882 (m), 847 (w), 782 (w), 720 (m), 701 (m), 681 (s), 664 (w), 642 (m), 615 (w), 599 (w), 522 (w), 428 (w) cm-1

6.6 A more sustainable isothiocyanate synthesis by amine catalyzed sulfurization of isocyanides with elemental sulfur

6.6.1 Optimization of the reaction conditions *via* GC-screening

Every synthesis set up for subsequent GC screening was prepared with the same general procedure. In a 10 mL screw-cap vial, n-dodecyl isocyanide **41** (195 mg, 1.00 mmol, 1.00 eq.) along with biphenyl (internal standard (IS) 38.6 mg, 250 µmol, 0.25 eq.) were dissolved in the respective amount of solvent. After complete dissolution of the isocyanide and biphenyl, a t0 sample was taken for GC analysis. Subsequently, the appropriate amounts of catalyst and elemental sulfur were added along with a stirring bar and the mixture was stirred for the duration of the given reaction time and temperature. Unless there were no specific reaction conditions (runs 18, 39-41), a metal block with twelve slots was used to allow simultaneous stirring and heating of the reactions. After a certain reaction time, a GC-sample (1.5 mg/mL of substance dissolved in ethyl acetate and prefiltered) was taken immediately.

The isocyanide conversion was calculated by evaluating the ratio of integrals for the isocyanide and IS using the following equation:

$$Conversion(Isocyanide)[\%] = 100\% \times (1 - \frac{A(IC, tx) \times A(IS, t0)}{A(IC, t0) \times A(IS, tx)})$$

A(IC, t0) = Integral of the isocyanide peak (t0 = 0 min)

A(IC, tx) = Integral of the isocyanide peak (tx = x min)

A(IS, t0) = Integral of IS peak (t0 = 0 min)

A(IS, tx) = Integral of IS peak (tx = x min)

*Table 38: Complete screening of several reaction conditions for the conversion of isocyanides (IC) **3** to isothiocyanates **41**.*

entry	Base{eq.}	solvent{V}	eq. of S_8	*T*/°C	*t*	conversion/%
1	DMAP{1.00}	DMSO {1 mL}	2.00	r.t.	2 h	38
2	NMI{1.00}	DMSO {1 mL}	2.00	r.t.	2 h	38
3	DBU{1.00}	DMSO {1 mL}	2.00	r.t.	2 h	99
4	DABCO{1.00}	DMSO {1 mL}	2.00	r.t.	2 h	84
5	TEA{1.00}	DMSO {1 mL}	2.00	r.t.	2 h	76
6	TBD{1.00}	DMSO {1 mL}	2.00	r.t.	2 h	100
7a	TBD{0.50}	DMSO {1 mL}	2.00	r.t.	2 h	96
7b	TBD{0.50}	DMSO {1 mL}	2.00	r.t.	22 h	100
8a	TBD{0.20}	DMSO {1 mL}	2.00	r.t.	2 h	75
8b	TBD{0.20}	DMSO {1 mL}	2.00	r.t.	22 h	94
9a	TBD{0.10}	DMSO {1 mL}	2.00	r.t.	2 h	36
9b	TBD{0.10}	DMSO {1 mL}	2.00	r.t.	22h	69
10a	DBU{0.10}	DMSO {1 mL}	2.00	r.t.	2 h	57
10b	DBU{0.10}	DMSO {1 mL}	2.00	r.t.	24 h	67
11	TBD{0.10}	DMSO {1 mL}	2.00	40	2 h	85
12	TBD{0.10}	DMSO {1 mL}	2.00	60	2 h	100
13	TBD{0.10}	DMSO {1 mL}	2.00	80	2 h	100
14	TBD{0.10}	ACN {1 mL}	2.00	40	2 h	22
15	TBD{0.10}	EA {1 mL}	2.00	40	2 h	0.76
16[1.)]	TBD{0.10}	Acetone {1 mL}	2.00	40	2 h	69
17	TBD{0.10}	Me-THF {1 mL}	2.00	40	2 h	3.8
18	TBD{0.10}	DMC {1 mL}	2.00	40	2 h	4.2
19	TBD{0.10}	Cyclohexane {1 mL}	2.00	40	2 h	6.4
20	TBD{0.10}	GBL {1 mL}	2.00	40	2 h	92
21	TBD{0.10}	Cyrene™ {1 mL}	2.00	40	2 h	100
22	TBD{0.10}	MEK {1 mL}	2.00	40	2 h	8.2
23	TBD{0.10}	Cyrene™ {1 mL}	2.00	40	30 min	85
24	TBD{0.10}	Cyrene™ {500 µL}	2.00	40	30 min	99
25	TBD{0.10}	Cyrene™ {250 µL}	2.00	40	30 min	100
26	TBD{0.10}	Cyrene™ {167 µL}	2.00	40	30 min	100

27	TBD{0.10}	-	2.00	40	30 min	6.7
28	TBD{0.05}	Cyrene™ {167 µL}	2.00	40	30 min	98
29	TBD{0.02}	Cyrene™ {167 µL}	2.00	40	30 min	82
30	TBD{0.01}	Cyrene™ {167 µL}	2.00	40	30 min	40
31	TBD{0.10}	Cyrene™ {167 µL}	1.50	40	30 min	100
32	TBD{0.10}	Cyrene™ {167 µL}	1.12	40	30 min	98
33a	DBU{0.05}	Cyrene™ {500 µL}	1.12	40	30 min	59
33b	DBU{0.05}	Cyrene™ {500 µL}	1.12	40	4 h	100
34a	DBU{0.02}	Cyrene™ {500 µL}	1.12	40	30 min	29
34b	DBU{0.02}	Cyrene™ {500 µL}	1.12	40	20 h	99
35	DBU{0.02}	Cyrene™ {167 µL}	1.12	40	4 h	100
36a	DBU{0.01}	Cyrene™ {167 µL}	1.12	40	4 h	78
36b	DBU{0.01}	Cyrene™ {167 µL}	1.12	40	20 h	96
37[2.)]	TBD{0.10}	Cyrene™ {1 mL}	2.00	40	30 min	24
38[3.)]	TBD{0.10}	Cyrene™ {1 mL}	2.00	40	10 min	53
39a[4.)]	TBD{0.10}	Cyrene™ {1 mL}	2.00	40	10 min	63
39b[4.)]	TBD{0.10}	Cyrene™ {1 mL}	2.00	40	20 min	91
39c[4.]	TBD{0.10}	Cyrene™ {1 mL}	2.00	40	30 min	98

1.) The experiment was performed in a pressure vial.

2.) The experiment was performed in a microwave

3.) The experiment was performed in an ultrasonic bath at a frequency of 37 kHz

4.) The experiment was performed in an ultrasonic bath at a frequency of 80 kHz

6.6.2 Synthesis of Isothiocyanates

General synthesis of isothiocyanates (GP1-A)

The corresponding solid isocyanide (1.00 eq., mp. >40 °C) was dissolved in dihydrolevoglucosenone (Cyrene™; c(isocyanide) = 2 M) and elemental sulfur (1.12 eq. of sulfur atoms) was added. After addition of 5 mol% of 1,8-diazabicyclo[5.4.0] undec-7-ene (DBU) the reaction mixture was stirred for 4 hours at 40°C. After completion of the reaction the pure product was obtained by optimized flash column chromatography applying a dry loaded small column (typically height of silica loading around 5-8 cm, see Figure 125) and a mixture of cyclohexane and ethyl acetate. Deviations of this procedure are given in the section of the respective substrate.

General synthesis of isothiocyanates (GP1-B)

The corresponding liquid isocyanide (1.00 eq., mp. ≤40 °C) was dissolved in dihydrolevoglucosenone (Cyrene™; c(isocyanide) = 6 M) and elemental sulfur 1.12 eq. of sulfur atoms) was added. After addition of 2 mol% of 1,8-diazabicyclo[5.4.0] undec-7-ene (DBU) the reaction mixture was stirred for 4 hours at 40°C. After completion of the reaction pure product was obtained by optimized flash column chromatography applying a dry loaded small column (typically height of silica loading around 5-8 cm, see Figure 125) and a mixture of cyclohexane and ethyl acetate yielded the pure product. Deviations of this procedure are given in the section of the respective substrate.

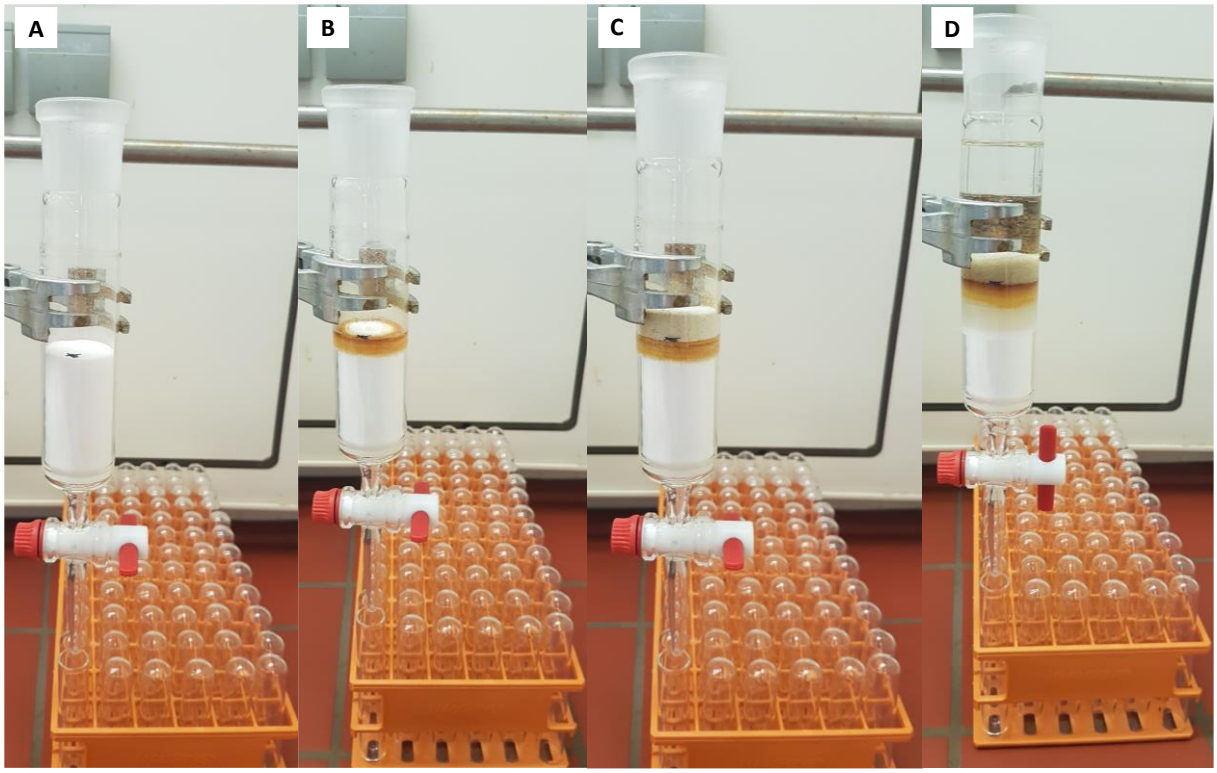

*Figure 125: Pictures of the purification of the obtained ITCs by a dry loaded column (height: 5 cm, width: 3 cm). The silica gel is put in the column (**A**) and then the crude product is applied directly after full conversion was observed via TLC (**B**). After adding sand, the eluent can be applied (**C**). The solvent frontier of the wetted silica gel can also be easily determined (compare **C** and **D**).*

n-Dodecyl isothiocyanate 41

n-Dodecyl isocyanide **3** (488 mg, 2.50 mmol, 1.00 eq.) was converted as described in GP1-B using elemental sulfur (89.8 mg, 350 µmol, 1.120 eq.), DBU (7.46 µL, 7.61 mg, 50.0 µmol, 2 mol%) and 417 µL Cyrene™. Flash column chromatography was performed using a mixture of cyclohexane yielding the product (499 mg, 2.19 mmol) as colorless liquid in a yield of 88% (15.5 mmol scale, 87%).

E-factor (2.5mmol): 1.26, E-factor (15.5mmol): 1.31

Purity was 97% according to GC-analysis.

EA: Found: C, 68.85; H, 11.3; N, 6.3; S, 14.75%. Calc. for $C_{13}H_{25}NS$: C, 68.7; H, 11.1; N, 6.2; S, 14.1%

R_f = 0.56 in cyclohexane visualized *via* UV quenching at 254 nm and vanillin staining solution (deep blue).

^{1}H-NMR (500 MHz, $CDCl_3$) δ / ppm = 3.50 (t, ^3J = 6.7 Hz, 2H,^{1}), 1.69 (m, 2H,^{2}), 1.40 (quint., ^3J = 6.7 Hz, 2H,^{3}), 1.28 (m, 16H,^{4}), 0.88 (t, ^3J = 6.9 Hz, 3H,^{5}).

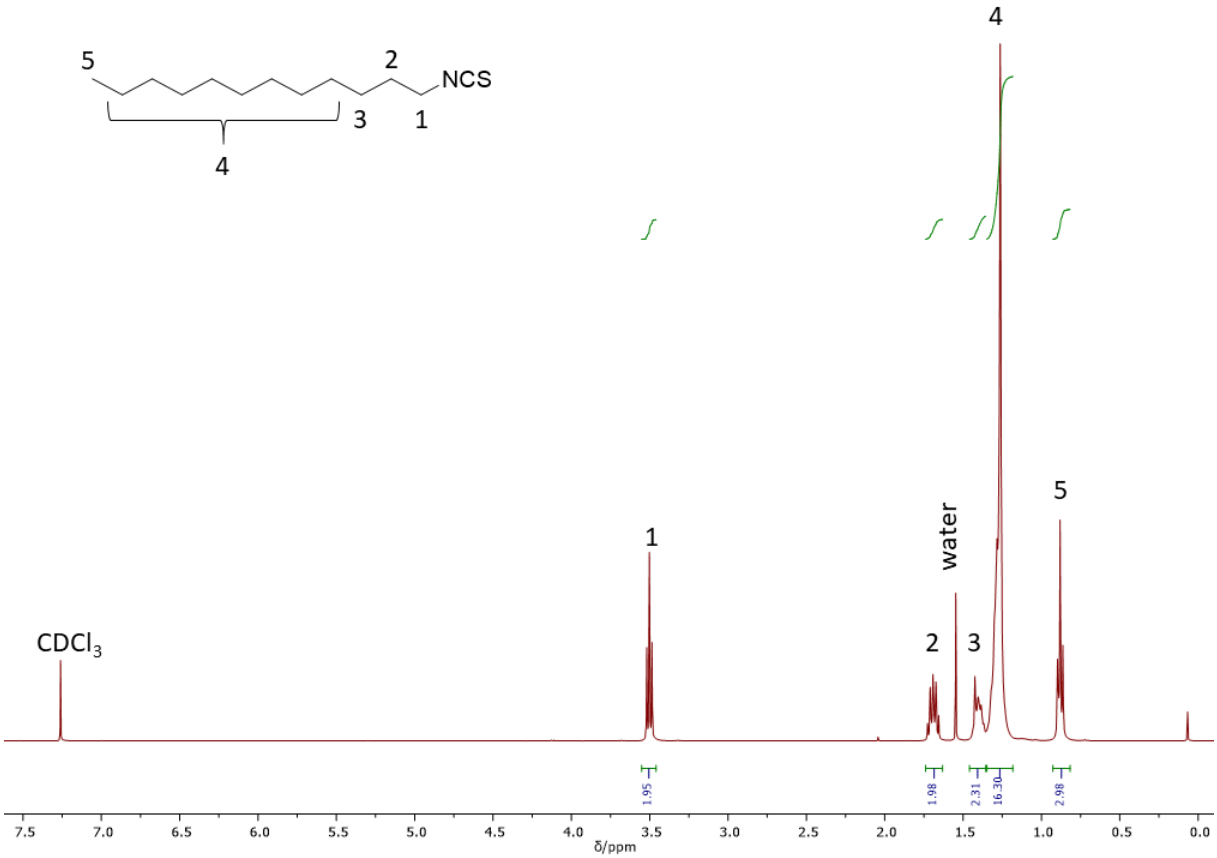

*Figure 126: ^{1}H-NMR-spectrum of ITC **41**.*

^{13}C NMR (126 MHz, $CDCl_3$) δ / ppm = 129.54 (NCS), 45.08 (**C**H_2-NCS), 30.19 (CH_2), 29.98 (CH_2), 29.62 (CH_2), 29.52 (CH_2), 29.41 (CH_2), 29.35 (CH_2), 28.83 (CH_2), 26.58 (CH_2), 22.70 (CH_2), 14.14 (CH_3).

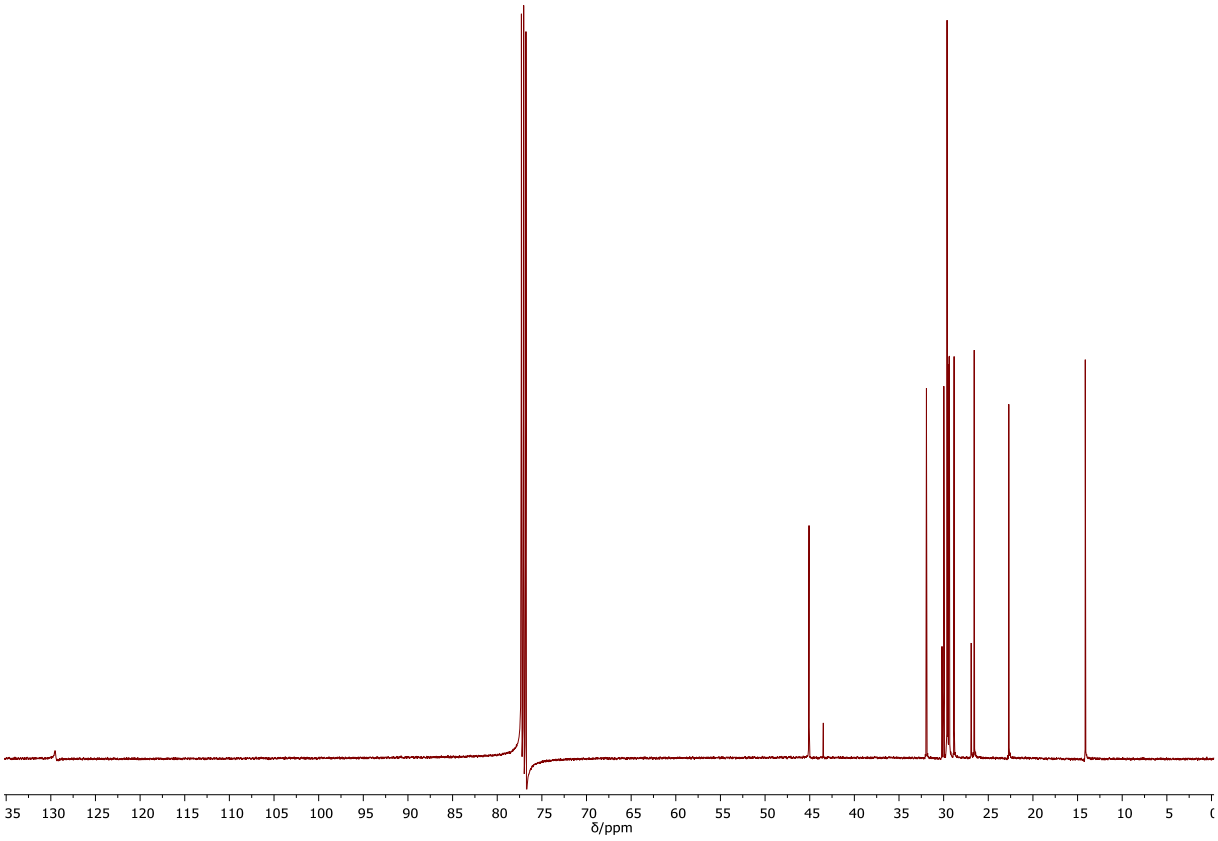

*Figure 127: ^{13}C-NMR-spectrum of ITC **41**.*

HRMS (EI): calculated m/z for $C_{13}H_{25}N_1S_1$ [M^+] = 227.1708, found: 227.1706, Δ = - 0.1871 mmu.

IR: *v*/cm^{-1} = 2921.3 (vs), 2852.2 (s), 2082.2 (s), 1455.0 (m), 1345.4 (m), 721.5 (w), 446.1 (w).

n-Pentyl isothiocyanate 56

n-Pentyl isocyanide (243 mg, 2.50 mmol, 1.00 eq.) was converted as described in GP1-B using elemental sulfur (89.2 mg, 350 µmol, 1.12 eq.), DBU (7.46 µL, 7.61 mg, 50.0 µmol, 2 mol%) and 417 µL Cyrene™. The reaction mixture was stirred for 5 hours. Flash column chromatography was performed using cyclohexane yielding the product (177 mg, 1.37 mmol) as a colorless liquid in a yield of 55%.

E-factor: 3.86

Purity was 98% according to GC-analysis.

$\mathbf{R_f}$ = 0.77 in cyclohexane/ethyl acetate = 3:1 visualized *via* UV quenching at 254 nm and vanillin staining solution (deep blue).

^{1}H-NMR (400 MHz, $CDCl_3$) δ / ppm = 3.50 (t, ^3J = 6.6 Hz, 2H, CH_2, ^{1}), 1.70 (quint., ^3J = 7.0 Hz, 2H, CH_2, ^{2}), 1.47 – 1.25 (m, 4H, CH_2, ^{3}), 0.92 (t, ^3J = 7.1 Hz, 3H, CH_3, ^{4}).

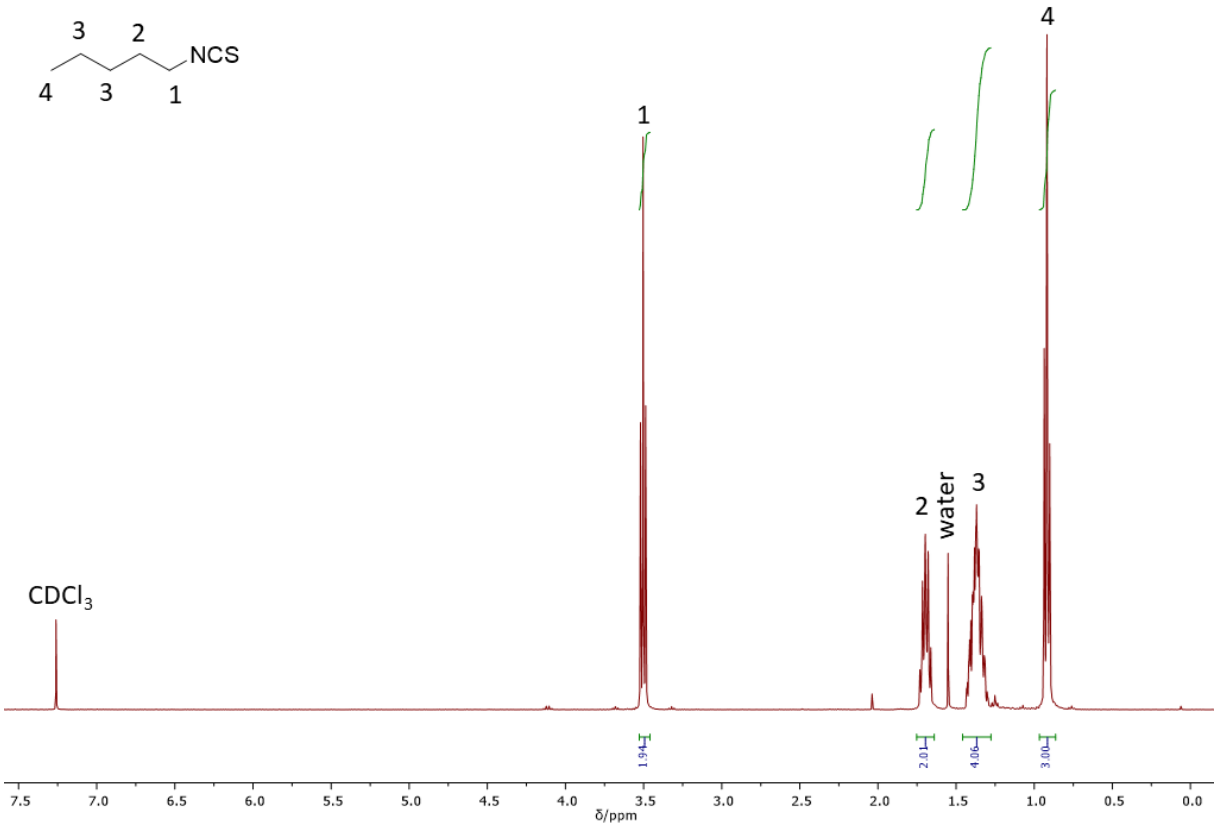

*Figure 128: ^{1}H-NMR-spectrum of ITC **56**.*

^{13}C NMR (101 MHz, $CDCl_3$) δ / ppm = 129.56 (NCS), 45.16 (**C**H_2-NCS), 29.78 (CH_2), 28.81 (CH_2), 22.05 (CH_2), 13.99 (CH_3).

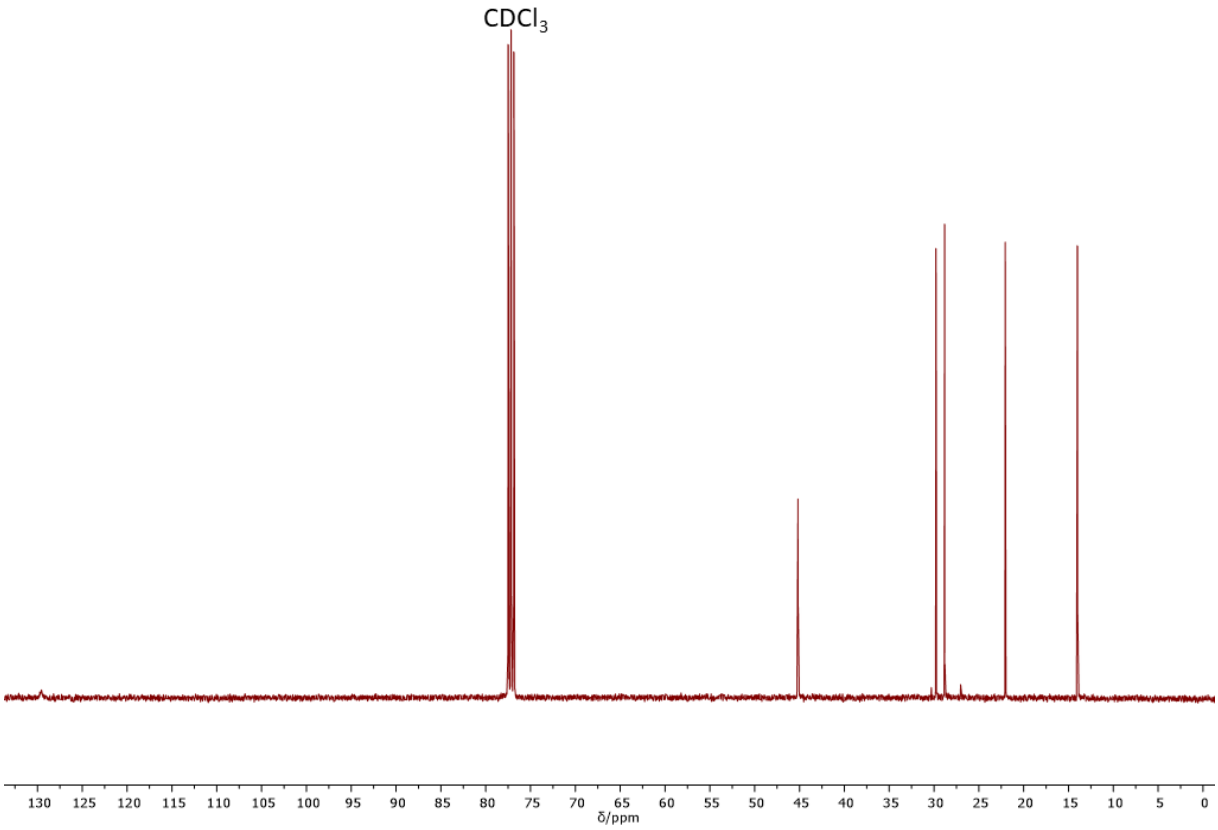

*Figure 129: ^{13}C-NMR-spectrum of ITC **56**.*

HRMS (ESI): calculated m/z for $C_6H_{12}N_1S_1$ [M+H$^+$] = 130.0685, found: 130.0685, Δ = 0.04 mmu.

IR: *ν* / cm^{-1} = 2956 (m), 2929 (m), 2871 (w), 2860 (w), 2176 (s), 2149 (s), 2081 (vs), 1452 (w), 1344 (s), 921 (w), 731 (w), 684 (w), 640 (w), 524 (w), 450 (w).

1,10-Diisothiocyanato decane 57

1,10-Diisocyanido decane **8** (481 mg, 2.50 mmol, 1.00 eq.) was converted as described in GP1-B using elemental sulfur (180 mg, 700 µmol, 2.24 eq.), DBU (7.46 µL, 7.61 mg, 50.0 µmol, 2 mol%) and 417 µL Cyrene™. Flash column chromatography was performed using cyclohexane yielding the product (531 mg, 2.07 mmol) as a yellowish liquid in a yield of 83%.

E-factor: 1.27

Purity was 97% according to GC-analysis.

EA: Found: C, 56.95; H, 8.0; N, 10.8; S, 24.3 Calc. for $C_{12}H_{20}N_2S_2$: C, 56.2; H, 7.9; N, 10.9; S, 25.0%.

R_f = 0.72 in cyclohexane/ethyl acetate = 3:1 visualized *via* UV quenching at 254 nm and vanillin staining solution (deep blue).

^{1}H-NMR (400 MHz, $CDCl_3$) δ / ppm = 3.50 (t, ^3J = 6.6 Hz, 4H, CH_2, ^{1}), 1.69 (quint., ^3J = 7.0 Hz, 4H, CH_2, ^{2}), 1.46-1.25 (m, 12H, CH_2, ^{3,4}).

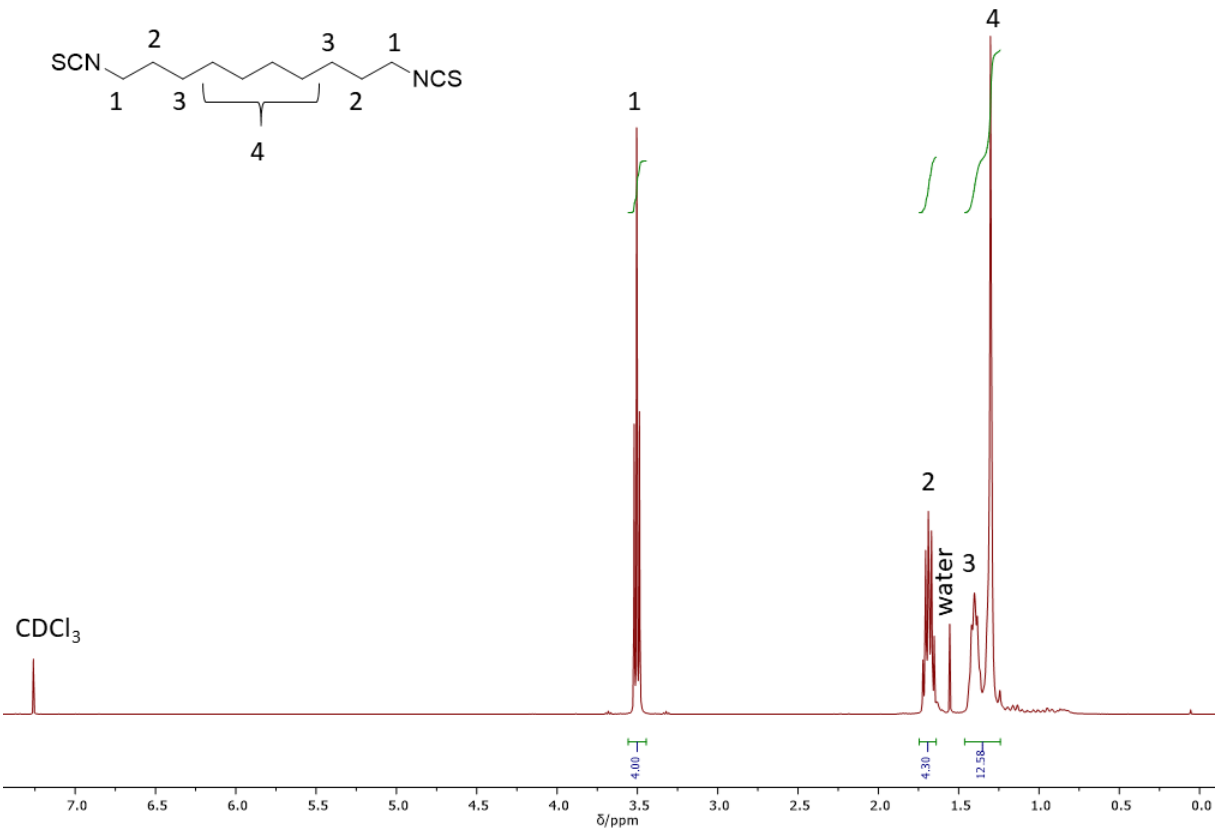

*Figure 130: ^{1}H-NMR-spectrum of ITC **57**.*

^{13}C NMR (101 MHz, $CDCl_3$) δ / ppm = 129.59 (NCS), 45.16 (**C**H_2-NCS), 30.03 (CH_2), 29.31 (CH_2), 28.82 (CH_2), 26.62 (CH_2).

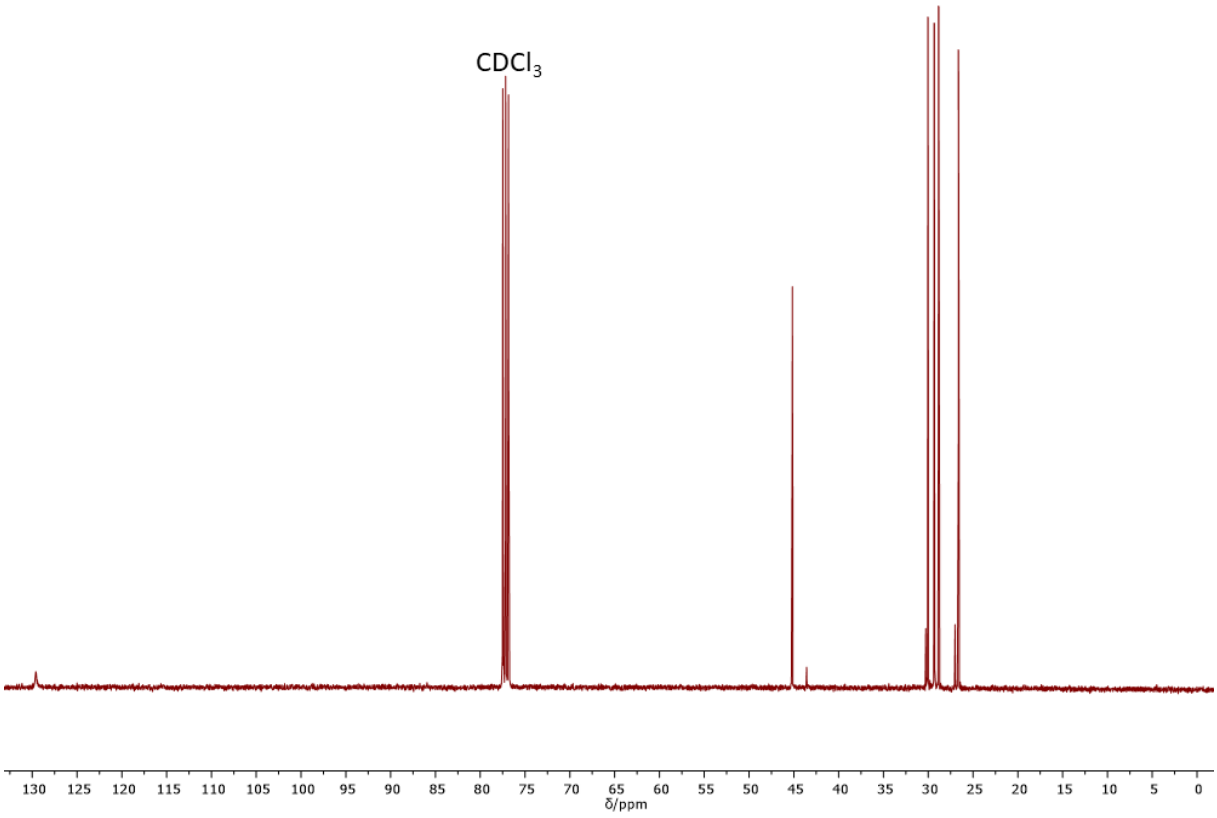

*Figure 131: ^{13}C-NMR-spectrum of ITC **57**.*

HRMS (EI): calculated m/z for $C_{12}H_{20}N_2S_2$ [M^+] = 256.1062, found: 256.1064, Δ = 0.1719 mmu.

IR: *v* / cm^{-1} = 2924 (s), 2853 (m), 2176 (s), 2075 (vs), 1449 (m), 1344 (s), 722 (w), 684 (w), 639 (w), 518 (w), 450 (w).

1,12-Diisothiocyanato dodecane 58

1,12-Diisocyanido dodecane **9** (551 mg, 2.50 mmol, 1.00 eq.) was converted as described in GP1-B using elemental sulfur (180 mg, 700 µmol, 2.24 eq.), DBU (7.46 µL, 7.61 mg, 50.0 µmol, 2 mol%) and 417 µL Cyrene™. The reaction was stirred for 3 hours. Flash column chromatography was performed using a mixture of cyclohexane/ethyl acetate = 50:1 yielding the product (569 mg, 2.00 mmol) as a yellowish liquid in a yield of 80%.

E-factor: 1.21

Purity was 98% according to GC-analysis.

EA: Found: C,59.55; H, 8.5; N, 10.1; S, 22.5 Calc. for $C_{14}H_{24}N_2S_2$: C, 59.1; H, 8.5; N, 9.85; S, 22.5%.

$\mathbf{R_f}$ = 0.85 in cyclohexane/ethyl acetate = 3:1 visualized *via* UV quenching at 254 nm and vanillin staining solution (deep blue).

^{1}H-NMR was according to literature.[628]

^{1}H-NMR (400 MHz, $CDCl_3$) δ / ppm = 3.50 (t, ^3J = 6.6 Hz, 4H, CH_2, ^{1}), 1.78-1.60 (m, 4H, CH_2, ^{2}), 1.49-1.15 (m, 16H, CH_2, ^{3,4}).

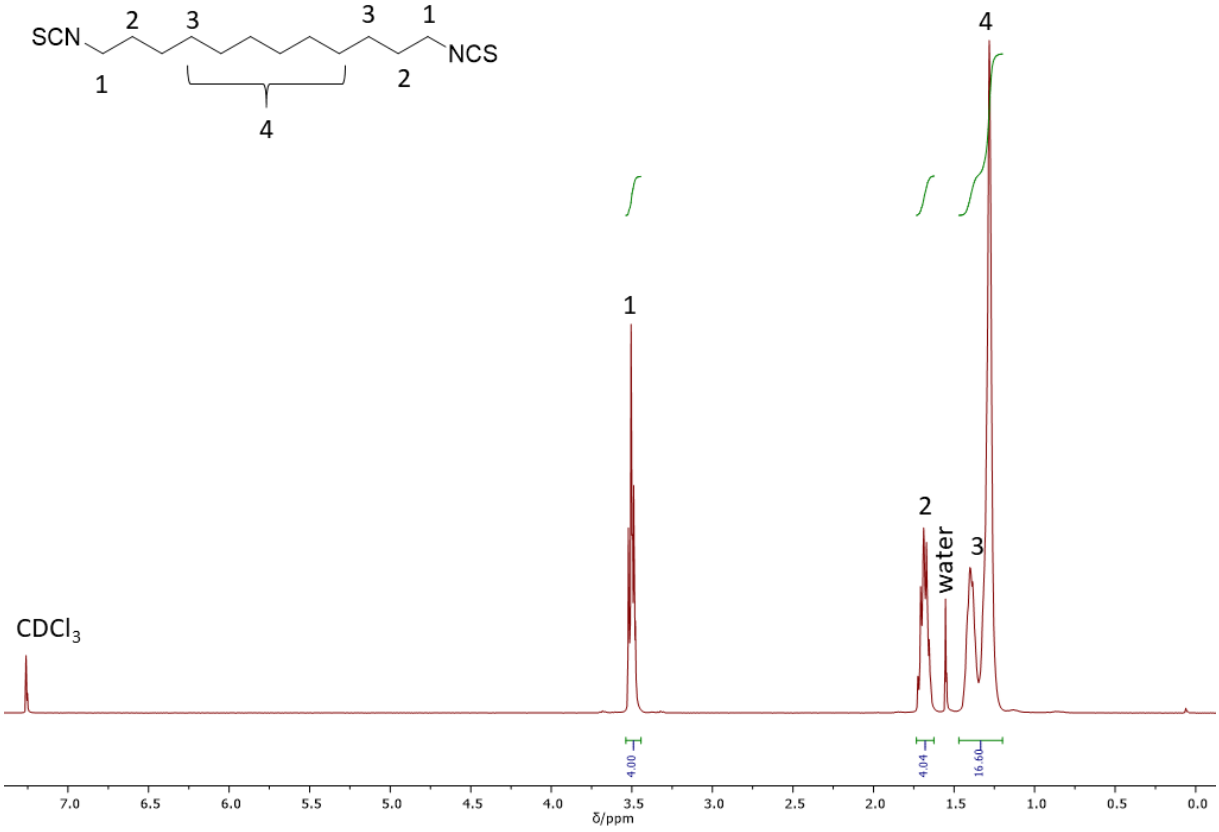

*Figure 132: ^{1}H-NMR-spectrum of ITC **58**.*

tert-Butyl isothiocyanate 59

tert-Butyl isocyanide **32** (1.75 mL, 1.29 mg, 15.5 mmol, 1.00 eq.) was converted as described in GP1-B using elemental sulfur (557 mg, 2.17 µmol, 1.12 eq.), DBU (46.3 µL, 47.2 mg, 310 µmol, 2 mol%) and 2.6 mL Cyrene™. The reaction was stirred for 5 hours. The product (854 mg, 7.41 mmol) was obtained after distillation (50 °C, 10 mbar) as a colorless liquid in a yield of 48%.

E-factor: 4.71

Purity was 97% according to GC-analysis.

$\mathbf{R_f}$ = 0.82 in cyclohexane/ethyl acetate = 9:1 visualized *via* UV quenching at 254 nm.

^{1}H-NMR was according to literature.[629]

^{1}H-NMR (400 MHz, $CDCl_3$) δ / ppm = 1.43 (s, CH_3, ^{1}).

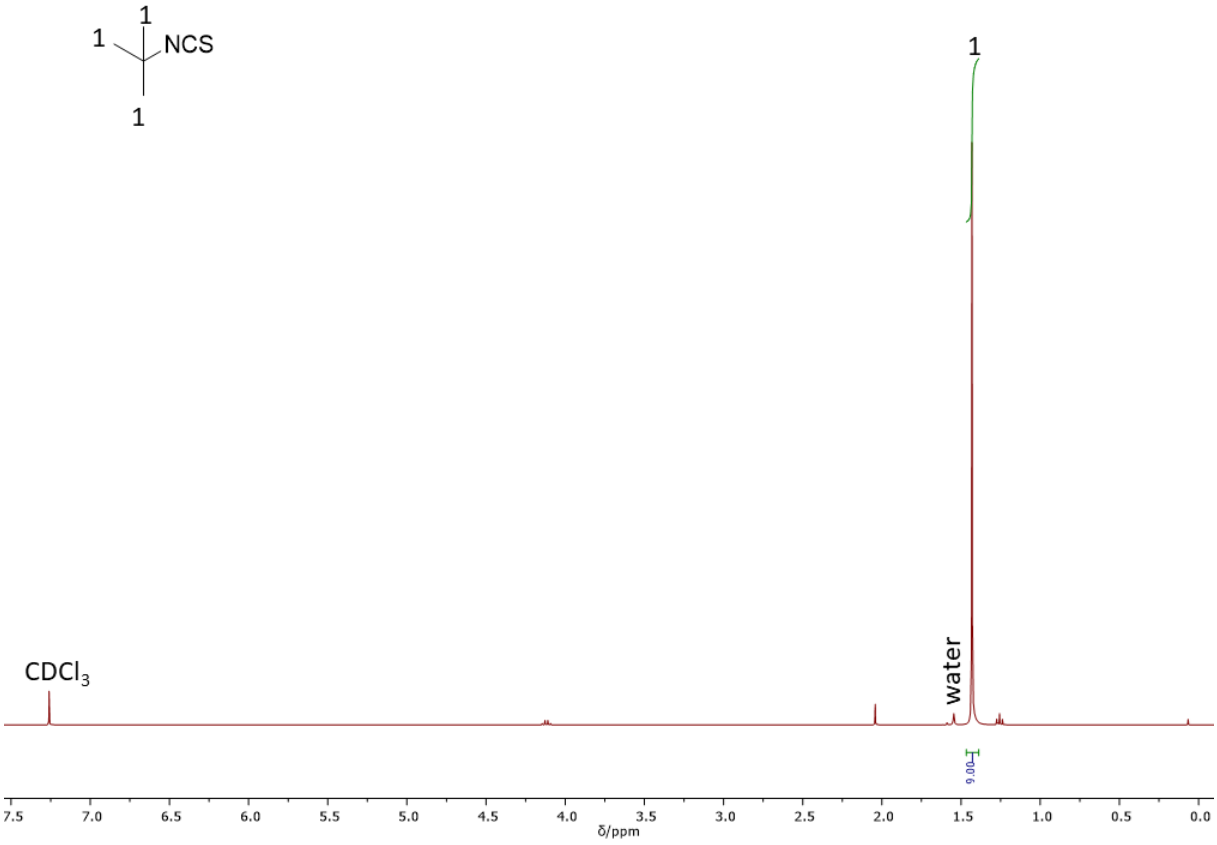

*Figure 133: ^{1}H-NMR-spectrum of ITC **59**.*

HRMS (ESI): calculated m/z for $C_5H_{10}N_1S_1$ [M+H$^+$] = 116.05306, found: 116.05285, Δ = - 0.15 mmu.

Adamantyl isothiocyanate 60

Adamantyl isocyanide **12** (403 mg, 2.50 mmol, 1.00 eq.) was converted as described in GP1-A using elemental sulfur (89.8 mg, 350 µmol, 1.12 eq.), DBU (18.7 mL, 19.0 mg, 125 µmol, 5 mol%) and 1.25 mL Cyrene™. The reaction was stirred for 5 hours. Flash column chromatography was performed using cyclohexane yielding the product (407 mg, 2.10 mmol) as colorless crystals in a yield of 84%.

E-factor: 4.10

Purity was 99% according to GC-analysis.

EA: Found: C, 68.3; H, 7.8; N, 7.3; S, 16.4 Calc. for $C_{11}H_{15}NS$: C, 68.35; H, 7.8; N, 7.25; S, 16.6 %.

$\mathbf{R_f}$ = 0.79 in cyclohexane/ethyl acetate = 9:1 visualized *via* UV quenching at 254 nm and vanillin staining solution (deep blue).

^{1}H-NMR was according to literature.[630]

^{1}H-NMR (400 MHz, $CDCl_3$) δ / ppm = 2.10 (s, br, 3H, CH, ^{1}), 1.97 (d, ^3J = 2.9 Hz, 6H, CH_2, ^{2}), 1.69-1.60 (m, 6H, CH_2, ^{3}).

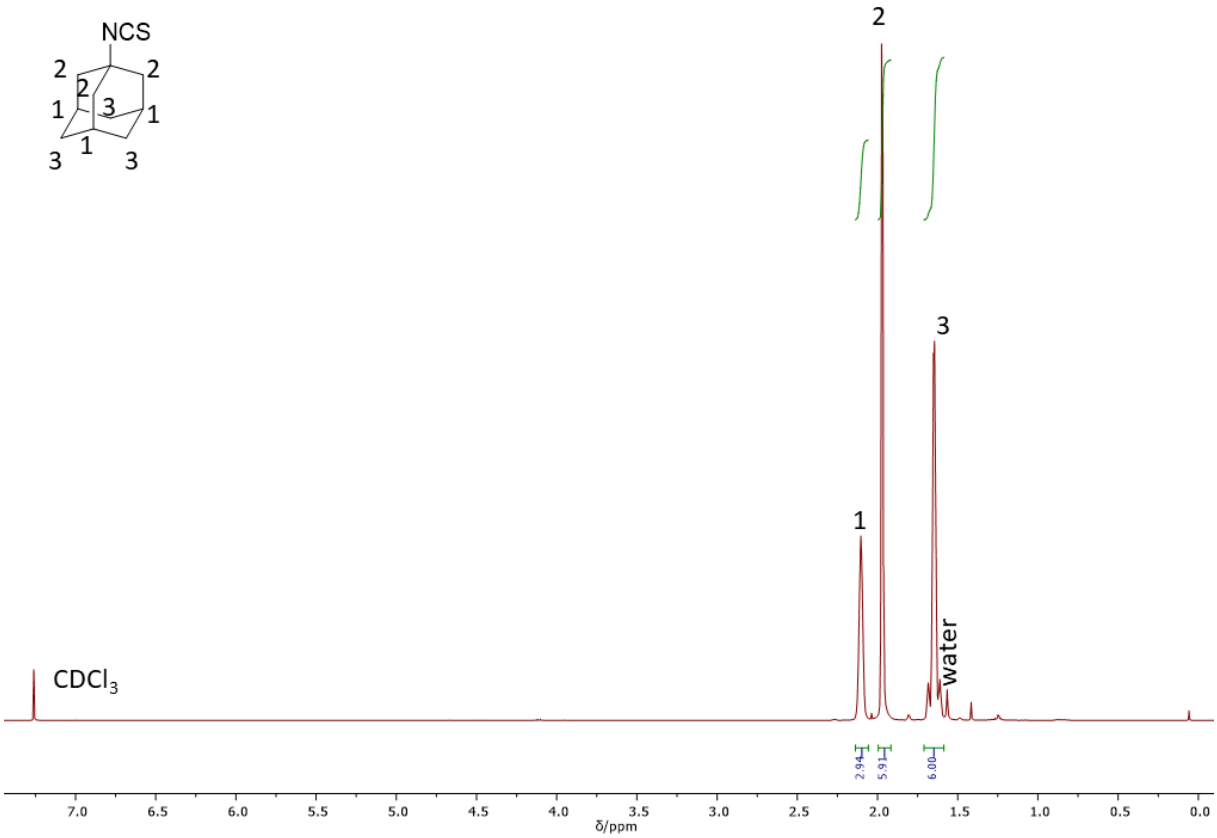

*Figure 134: ^{1}H-NMR-spectrum of ITC **60**.*

Cyclohexyl isothiocyanate 61

Cyclohexyl isocyanide **10** (273 mg, 2.50 mmol, 1.00 eq.) was converted as described in GP1-B using elemental sulfur (89.8 mg, 350 µmol, 1.12 eq.), DBU (7.46 µL, 7.61 mg, 50.0 µmol, 2 mol%) and 417 µL Cyrene™ or GBL. The reaction mixture was stirred for 4 hours in Cyrene™ and 23 hours in GBL. Flash column chromatography was performed using cyclohexane yielding the product (290 mg, 2.06 mmol in Cyrene™ or 238 mg, 1.68 mmol in GBL)) as a colorless liquid in a yield of 82% (Cyrene™) or 67% (GBL), (15.5 mmol scale in Cyrene™, 5h, 85%).

E-factor (2.50 mmol, Cyrene™): 2.08, E-factor (2.50 mmol, GBL): 2.81, E-factor (15.5 mmol): 1.99

Purity was 97% (Cyrene™), 98% (GBL), 99% (15.5 mmol scale) according to GC-analysis.

$\mathbf{R_f}$ = 0.77 in cyclohexane/ethyl acetate = 9:1 visualized *via* UV quenching at 254 nm and vanillin staining solution (deep blue).

^{1}H-NMR was according to literature.[631]

^{1}H-NMR (400 MHz, $CDCl_3$) δ / ppm = 3.68 (tt, ^3J = 7.8, 3.7 Hz, 1H, CH, ^{1}), 1.98-1.29 (m, 10H, CH_2, ^{2}).

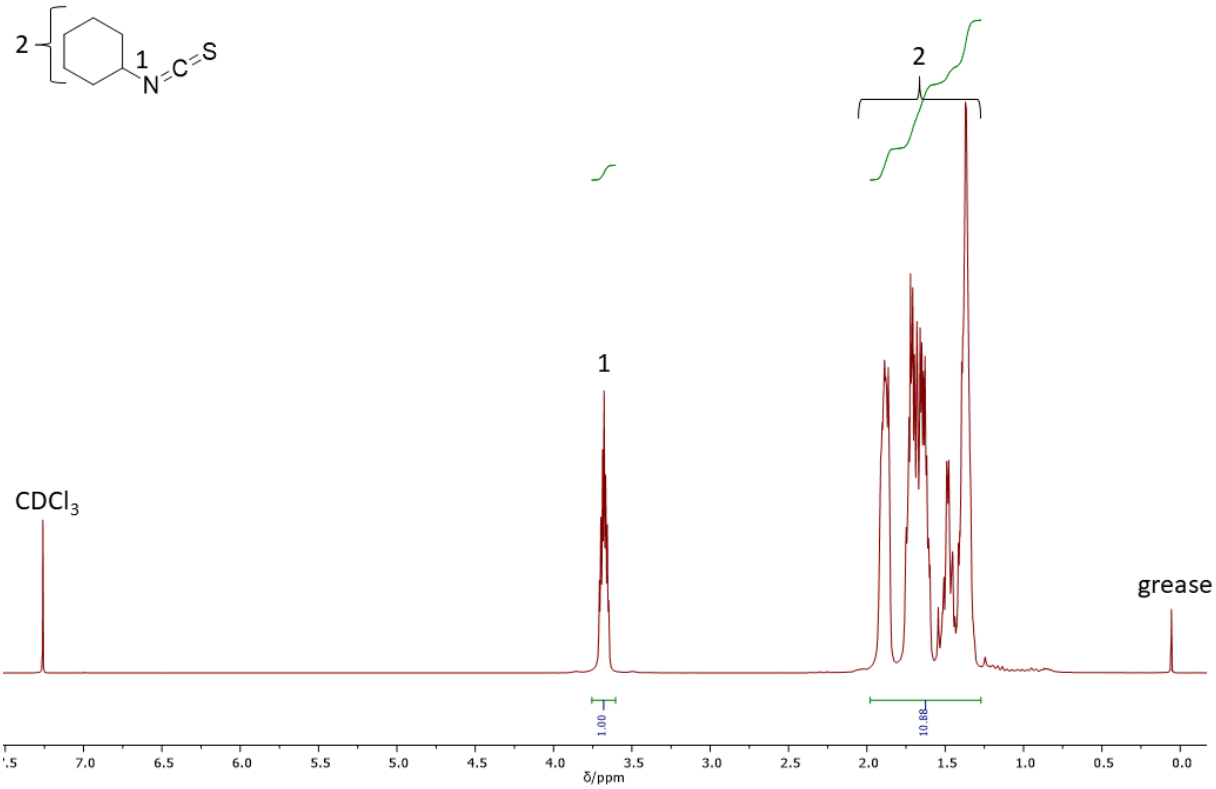

*Figure 135: ^{1}H-NMR-spectrum of ITC **61**.*

IR: ν / cm^{-1} = 2932 (vs), 2857 (m), 2174 (m), 2091 (vs), 2054 (vs), 1448 (m), 1361 (s), 1347 (w), 1319 (m), 1310 (m), 1262 (w), 1244 (w), 1145 (vw), 1133 (vw), 1088 (vw), 1010 (w), 986 (w), 891 (w), 861 (w), 854 (w), 800 (w), 720 (m), 701 (m), 537 (w), 497 (m), 473 (w), 441 (w).

5-Isothiocyanato-1-(isothiocyanatomethyl)-1,3,3-trimethyl cyclohexane 62

5-Isocyanido-1-(isocyanidomethyl)-1,3,3-trimethyl cyclohexane (421 mg, 2.21 mmol, 1.00 eq.) was converted as described in GP1-B using elemental sulfur (159 mg, 619 µmol, 2.24 eq.), DBU (6.60 µL, 6.73 mg, 44.2 µmol, 2 mol%) and 368 µL Cyrene™. Flash column chromatography was performed using cyclohexane yielding the product (511 mg, 2.01 mmol) as a colorless solid in a yield of 91% (d.r. = 3.95:0 determined *via* GC).

E-factor: 1.06

Purity was 99% according to GC-analysis.

$\mathbf{R_f}$ = 0.82 and 0.89 in cyclohexane/ethyl acetate = 3:1 visualized *via* UV quenching at 254 nm and vanillin staining solution (deep blue).

^{1}H-NMR (400 MHz, $CDCl_3$) δ / ppm = 3.87 (tt, ^3J = 11.9 Hz, 3.7 Hz, 0.77H, CH, ^{1a}), 3.74 (tt, ^3J = 11.8 Hz, 3.8 Hz, 0.21H, CH, ^{1b}), 3.52 (d, ^2J = 14.3 Hz, 0.22H, SCN-CH_2, ^{2b}), 3.41 (d, ^2J = 14.3 Hz, 0.22H, SCN-CH_2, ^{2b}), 3.26 (s, 1.55H, SCN-CH_2, ^{2a}), 2.02-1.86 (m, 2H, CH_2, $^{3a+b}$), 1.52 (m, 0.21H CH_2, ^{4b}), 1.44-1.23 (m, 3H, CH_2, $^{3a+b, 4a+b}$), 1.18-1.06 (m, 4H, CH_2, CH_3, $^{4a, 5a+b}$), 1.06-0.96 (m, 6H, CH_3, $^{6a+b}$).

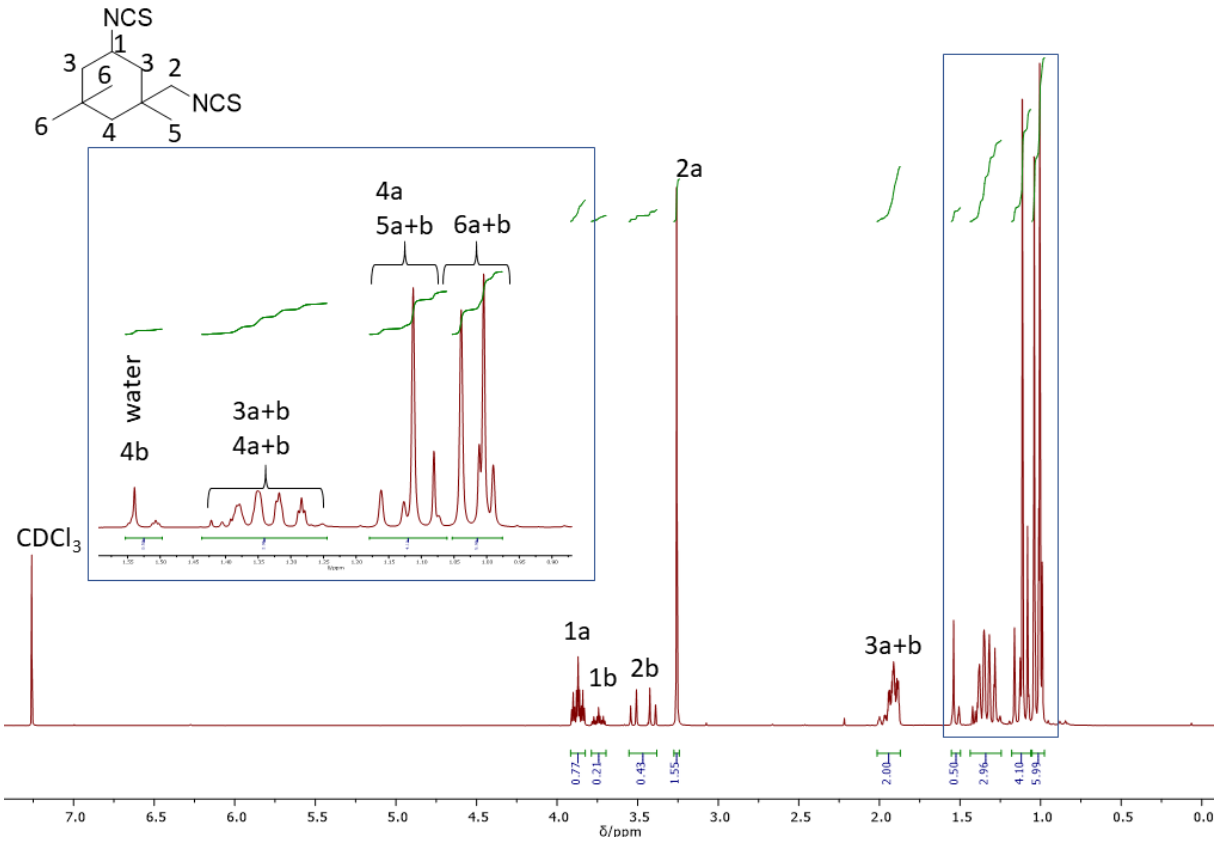

*Figure 136: ^{1}H-NMR-spectrum of ITC **62**.*

^{13}C-NMR (101 MHz, $CDCl_3$) δ / ppm = 131.65 (NCS), 58.78 (NCS-**C**H_2, [a]), 53.16 (NCS-**C**H_2, [b]), 51.08 (CH, [a]), 50.93 (CH, [b]), 46.38 (CH_2, [a]), 46.10 (CH_2, [b]), 42.14 (CH_2, [b]), 41.97 (CH_2, [a]), 37.16 ($C_{quart.}$, [b]), 37.13 ($C_{quart.}$, [a]), 34.61 (CH_3, [a]), 34.32 (CH_3, [b]), 31.91 ($C_{quart.}$, [a]), 31.70 ($C_{quart.}$, [b]), 29.90 (CH_3, [b]), 27.56 (CH_3, [a]), 27.30(CH_3, [b]), 23.53 (CH_3, [a]).

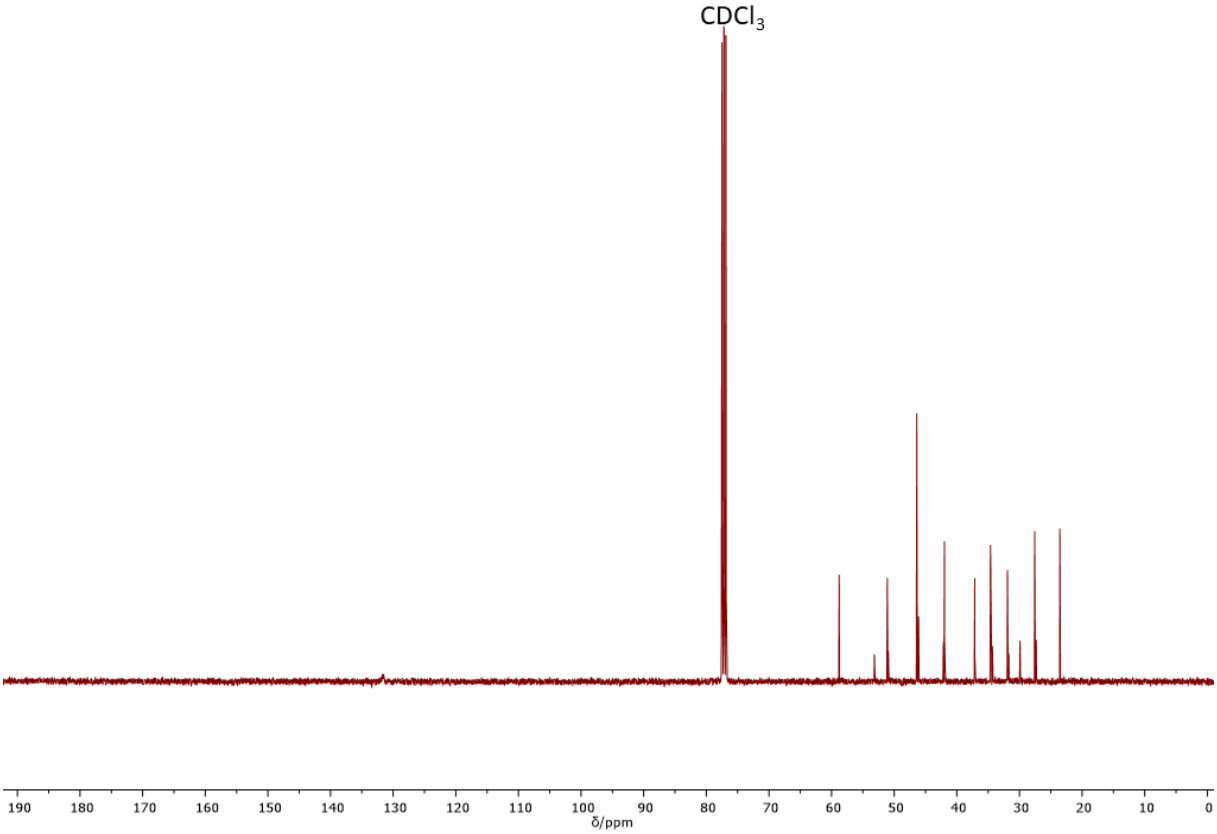

*Figure 137: ^{13}C-NMR-spectrum of ITC **62**.*

HRMS (EI): calculated m/z for $C_{12}H_{18}N_2S_2$ [M^+] = 254.0906, found: 254.0905, Δ = - 0.1426 mmu.

IR: *ν*/cm^{-1} = 2953 (w), 2932 (w), 2870 (w), 2174 (vs), 2067 (vs), 1460 (m), 1446 (w), 1388 (w), 1368 (m), 1360 (s), 1333 (m), 1300 (w), 1249 (w), 1213 (w), 1198 (w), 1142 (w), 1078 (vw), 1064 (vw), 1033 (vw), 1000 (vw), 959 (w), 922 (w), 904 (w), 892 (w), 870 (w), 793 (m), 713 (m), 694 (s), 594 (w), 518 (w), 492 (w), 466 (m), 445 (m), 402 (w).

Oleyl isothiocyanate 63

Oleyl isocyanide **4** (694 mg, 81 w%, 2.02 mmol, 1.00 eq.) was converted as described in GP1-B using elemental sulfur (89.8 mg, 350 µmol, 1.38 eq.), DBU (7.46 µL, 7.61 mg, 50.0 µmol, 3 mol%) and 417 µL Cyrene™. Flash column chromatography was performed using cyclohexane yielding the product (704 mg, 1.90 mmol) as a colorless liquid in a yield of 94%.

E-factor (2.50 mmol, Cyrene™): 1.22

Purity was 83% according to GC-analysis.

EA: Found: C, 73.3; H, 11.6; N, 5.1; S, 10.5 Calc. for $C_{19}H_{35}NS$: C, 73.7; H, 11.4; N, 4.5; S, 10.4%.

R_f = 0.54 in cyclohexane visualized *via* UV quenching at 254 nm and vanillin staining solution (deep blue).

^{1}H-NMR (400 MHz, $CDCl_3$) δ / ppm = 5.43 – 5.26 (m, 2H, CH, ^{1}), 3.50 (t, ^3J = 6.6 Hz, 2H, CH_2, ^{2}), 1.99 (m, 4H, CH_2, ^{3}), 1.68 (p, ^3J = 6.8 Hz, 2H, CH_2, ^{4}), 1.46 – 1.17 (m, 22H, CH_2, ^{5}), 0.87 (t, ^3J = 6.7 Hz, 3H, CH_3, ^{6}).

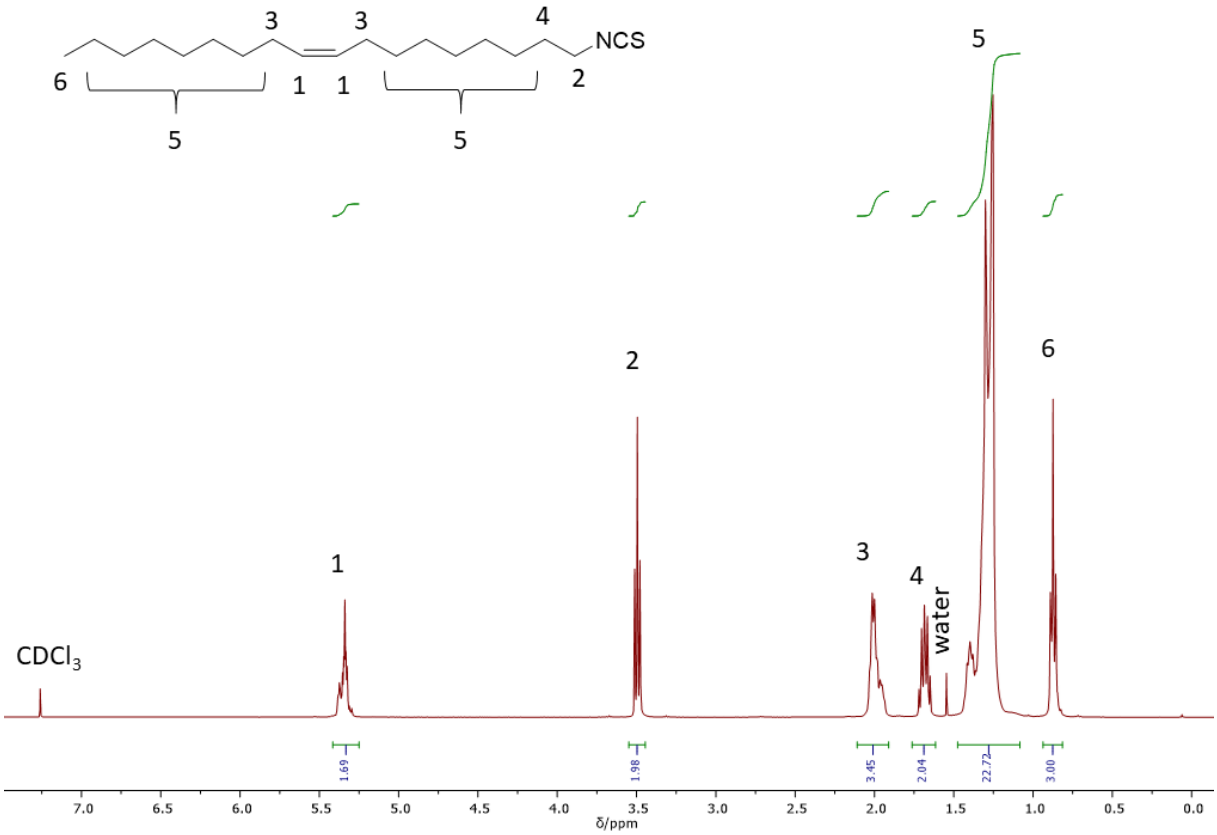

*Figure 138: ^{1}H-NMR-spectrum of ITC **63**.*

^{13}C-NMR (101 MHz, $CDCl_3$) δ / ppm = 130.13 (C=C), 129.81 (C=C), 129.69 (NCS), 45.17 (**C**H_2-NCS), 32.03 (CH_2), 30.09 (CH_2), 29.88 (CH_2), 29.80 (CH_2), 29.65 (CH_2), 29.44 (CH_2), 29.40 (CH_2), 29.25 (CH_2), 28.90 (CH_2), 27.33 (CH_2), 27.27 (CH_2), 26.66 (CH_2), 22.81 (CH_2), 14.23 (CH_3).

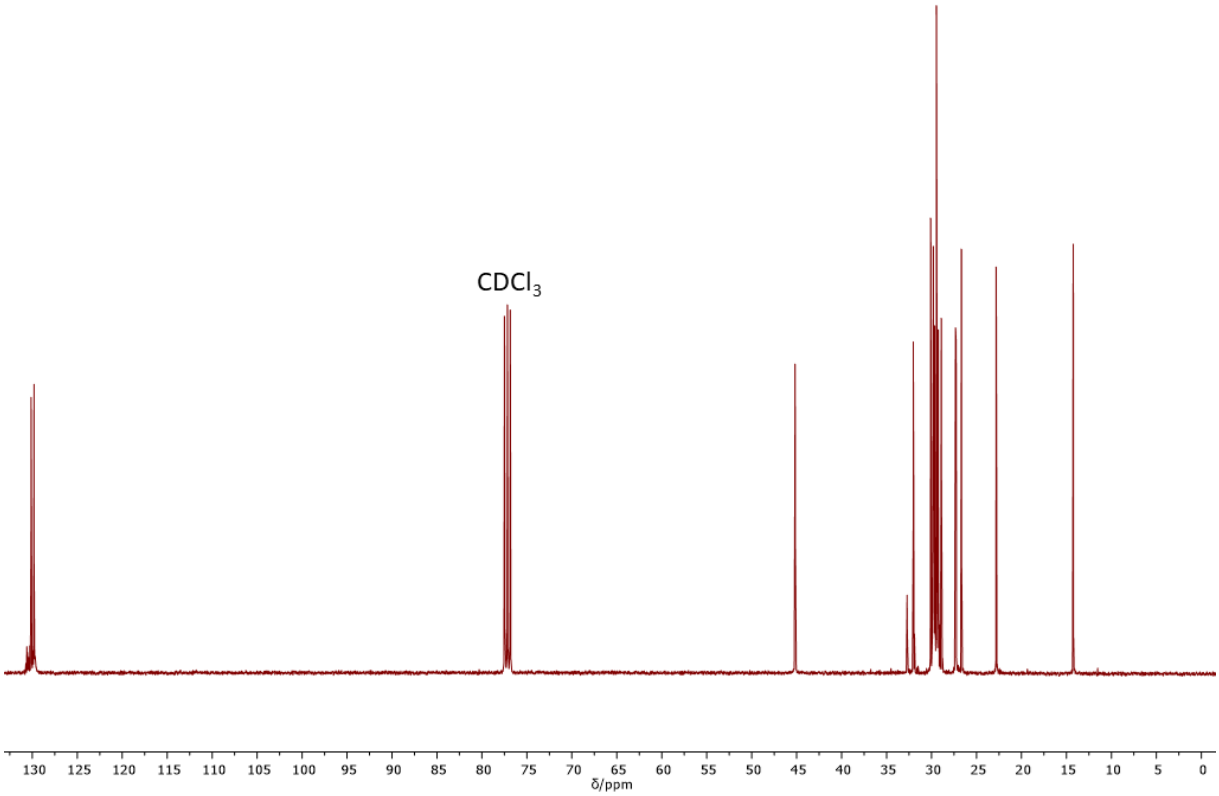

*Figure 139: ^{13}C-NMR-spectrum of ITC **63**.*

HRMS (EI): calculated m/z for $C_{19}H_{35}N_1S_1$ [M^+] = 309.2485, found: 309.2486, Δ = 0.1316 mmu.

IR: $\tilde{\nu}$/cm^{-1} = 3006 (vw), 2921 (vs), 2853 (vs), 2184 (w), 2082 (vs), 1456 (m), 1346 (m), 967 (w), 722 (w), 690 (w), 465 (w), 455 (w).

2-Morpholinoethyl isothiocyanate 64

2-Morpholinoethyl isocyanide (351 mg, 2.50 mmol, 1.00 eq.) was converted as described in GP1-B using elemental sulfur (89.8 mg, 350 µmol, 1.12 eq.), DBU (7.46 µL, 7.61 mg, 50.0 µmol, 2 mol%) and 417 µL Cyrene™. Flash column chromatography was performed using cyclohexane → cyclohexane/ethyl acetate = 2:1 yielding the product (307 g, 1.78 mmol) as a yellow liquid in a yield of 71%.

E-factor: 2.16

Purity was 97% according to GC-analysis.

EA: Found: C, 48.4; H, 7.0; N, 15.65; S, 17.5 Calc. for $C_7H_{12}N_2O_1S_1$: C, 48.8; H, 7.0; N, 16.3; S, 18.6%.

R_f = 0.28 in cyclohexane/ethyl acetate = 1:3 visualized *via* UV quenching at 254 nm and vanillin staining solution (deep blue).

^{1}H-NMR was according to literature. [632]

^{1}H-NMR (400 MHz, $CDCl_3$) δ / ppm = 3.72-3.68 (m, 4H, CH_2, ^{1}), 3.60-3.55 (m, 2H, CH_2, ^{2}), 2.67-2.62 (m, 2H, CH_2, ^{3}), 2.52-2.48 (m, 4H, CH_2, ^{4}).

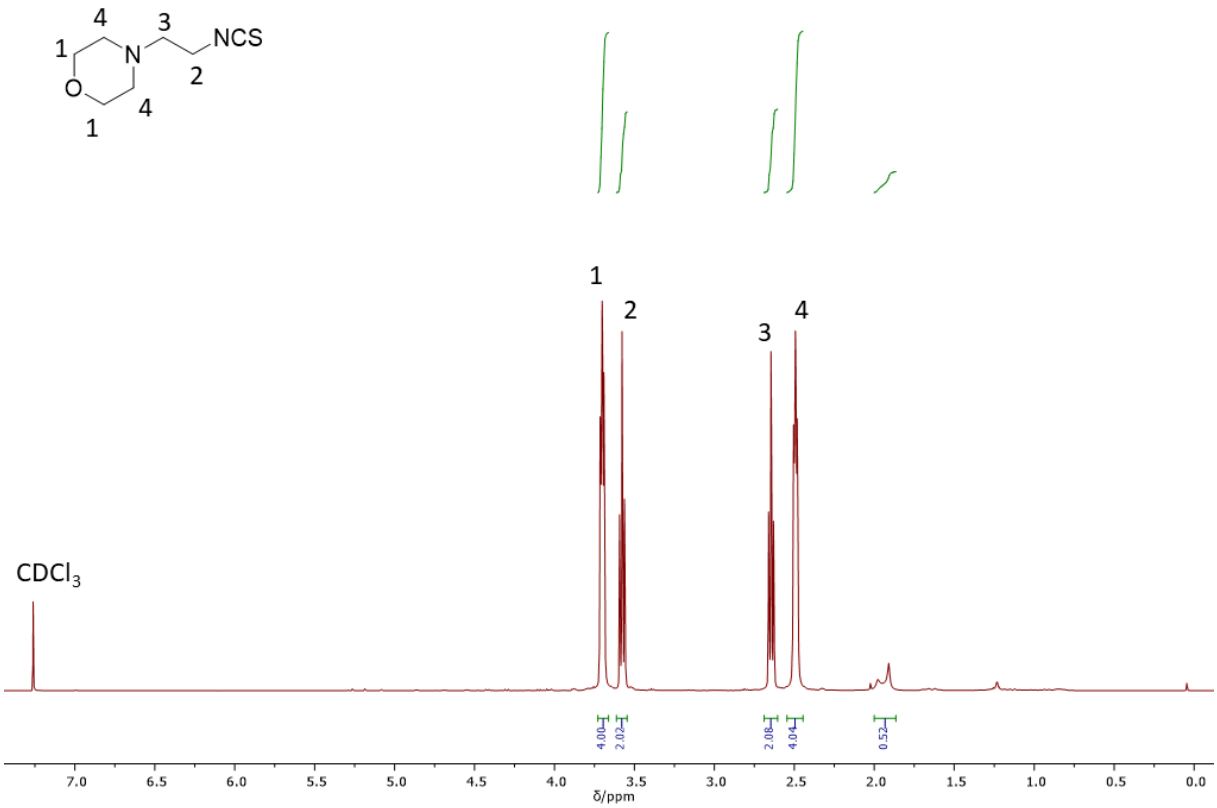

*Figure 140: ^{1}H-NMR-spectrum of ITC **64**.*

Methyl-2-isothiocyanato-3-phenyl propionate 65

Methyl-2-isocyanido-3-phenyl propionate (438 mg, 2.31 mmol, 1.00 eq.) was as like described in GP1-B using elemental sulfur (89.8 mg, 350 µmol, 1.21 eq.), DBU (7.46 µL, 7.61 mg, 50.0 µmol, 2 mol%) and 417 µL Cyrene™. The reaction was stirred for 23 hours. Flash column chromatography was performed using cyclohexane/ethyl acetate = 50:1 yielding the product (267 mg, 1.21 mmol) as a yellow liquid in a yield of 52%.

E-factor: 2.97

Purity was 98% according to GC-analysis.

$\mathbf{R_f}$ = 0.52 in cyclohexane/ethyl acetate = 3:1 visualized *via* UV quenching at 254 nm and vanillin staining solution (deep blue).

EA: Found: C,59.15; H, 4.95; N, 7.2; S, 14.1 Calc. for $C_{11}H_{11}N_1O_2S_1$: C, 59.7; H, 5.0; N, 6.3; S, 14.5%.

^{1}H-NMR was according to literature.[630]

^{1}H-NMR (400 MHz, $CDCl_3$) δ / ppm = 7.40-7.19 (m, 5H, aromatic, ^{1}), 4.48 (dd, ^3J = 8.4, 4.8 Hz, 1H, CH, ^{2}), 3.80 (s, 3H, CH_3, ^{3}), 3.25 (dd, ^2J = 13.8, ^3J = 4.7 Hz, 1H, CH_2, ^{4}), 3.13 (dd, ^2J = 13.8, ^3J = 8.4 Hz, 1H, CH_2, ^{4}).

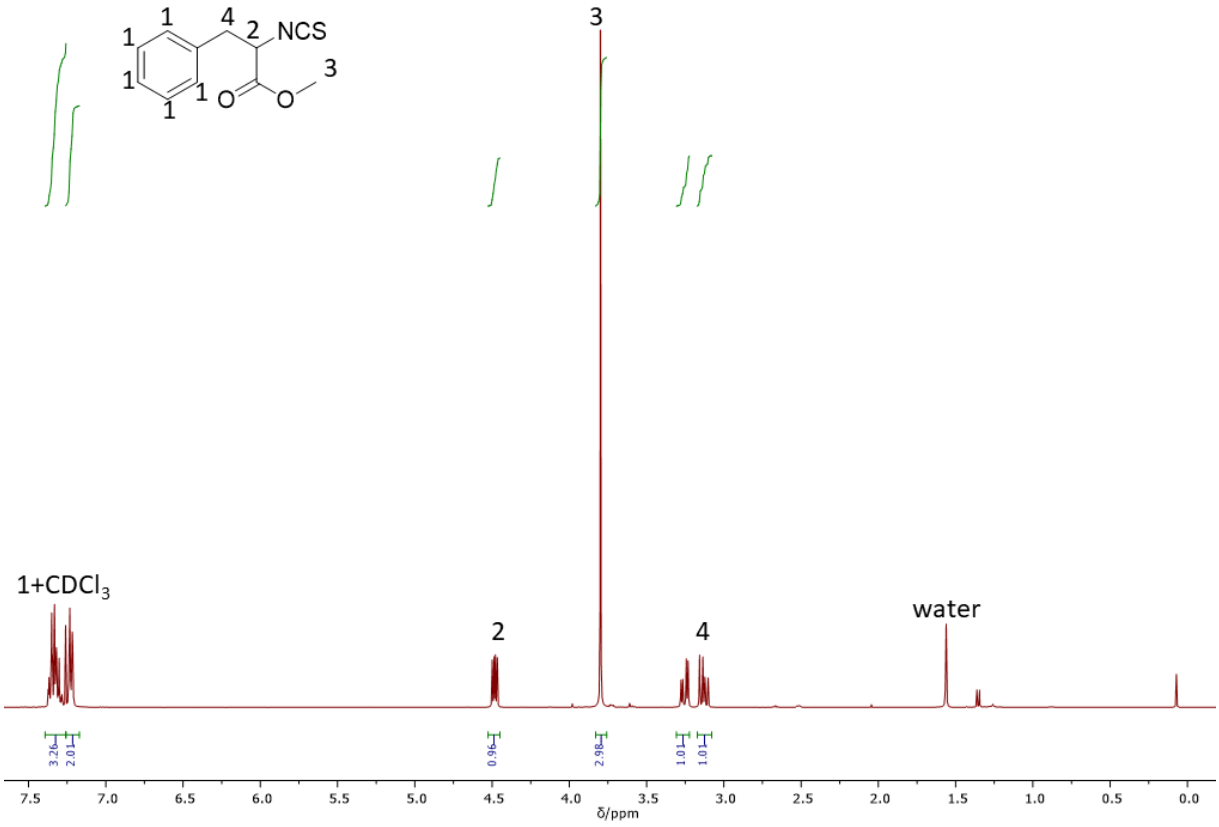

*Figure 141: ^{1}H-NMR-spectrum of ITC **65**.*

Methyl-2-isothiocyanato-4-(methylthio) butanoate 66

Methyl-2-isocyanido-4-(methylthio) butanoate (433 mg, 2.50 mmol, 1.00 eq.) was converted as described in GP1-B using elemental sulfur (89.8 mg, 350 µmol, 1.12 eq.), DBU (7.46 µL, 7.61 mg, 50.0 µmol, 2 mol%) and 417 µL Cyrene™. The reaction was stirred for 6 hours. Flash column chromatography was performed using cyclohexane/ethyl acetate = 20:1 yielding the product (296 mg, 1.44 mmol) as a yellow liquid in a yield of 58%.

Purity was >99% according to GC-analysis.

E-factor: 2.55

R_f = 0.51 in cyclohexane/ethyl acetate = 5:1 visualized *via* UV quenching at 254 nm and vanillin staining solution (deep blue).

EA: Found: C,40.9; H, 5.3; N, 7.0; S, 31.4 Calc. for $C_7H_{11}N_1O_2S_2$: C, 41.0; H, 5.4; N, 6.8; S, 31.2%.

^{1}H-NMR was according to literature.[630]

^{1}H-NMR (400 MHz, $CDCl_3$) δ / ppm = 4.55 (dd, ^3J = 8.3 Hz, 4.8 Hz, 1H, CH, ^{1}), 3.81 (s, 3H, CH_3, ^{2}), 2.71-2.55 (m, 2H, CH_2, ^{3}), 2.23-2.11 (m, 2H, CH_2, ^{4}), 2.10 (s, 3H, CH_3, ^{5}).

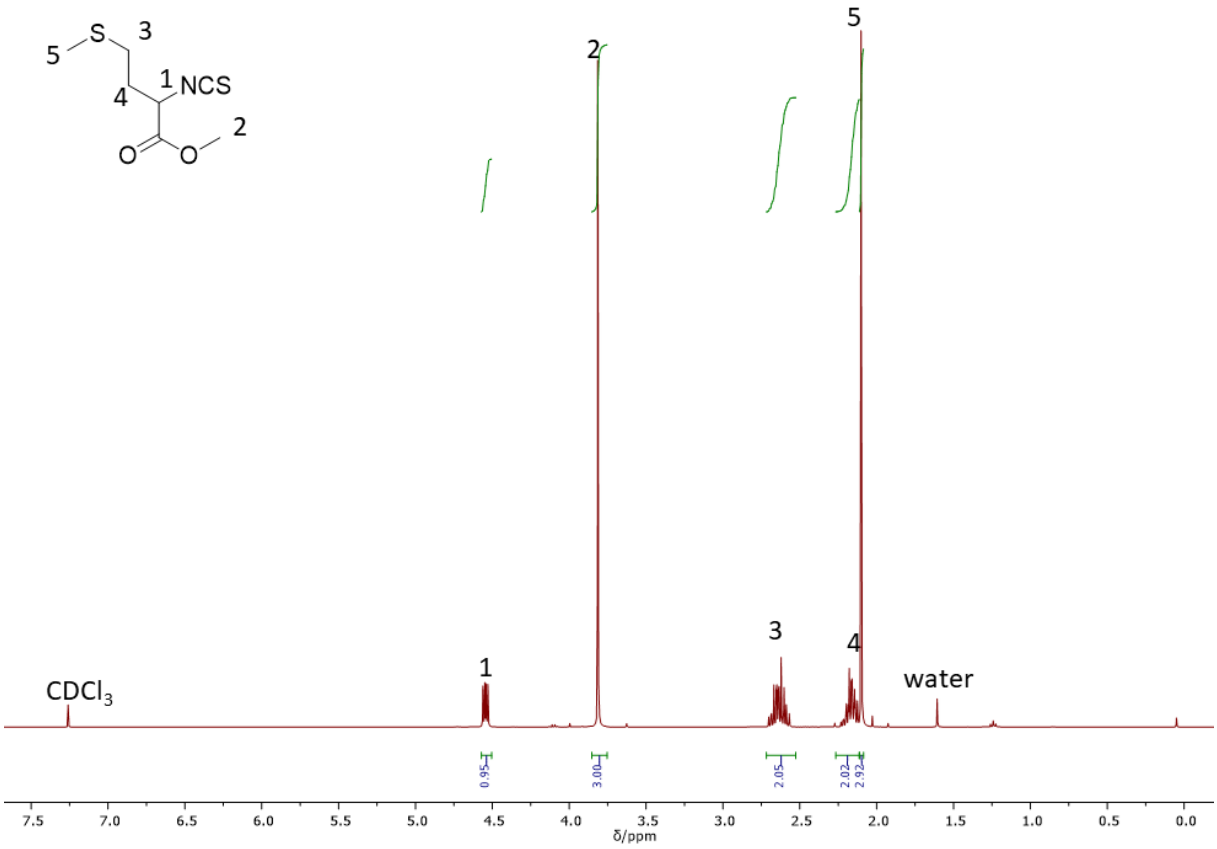

*Figure 142: ^{1}H-NMR-spectrum of ITC **66**.*

Benzyl-11-isothiocyanato undecanoate 67

Benzyl-11-isocyanido undecanoate **5** (754 mg, 2.50 mmol, 1.00 eq.) was as like described in GP1-B using elemental sulfur (89.8 mg, 350 µmol, 1.12 eq.), DBU (7.46 µL, 7.61 mg, 50.0 µmol, 5 mol%) and 417 µL Cyrene™. The reaction was stirred for 22 hours. Please note that for the 15.5 mmol scale 2 mol% of DBU were used. Flash column chromatography was performed using cyclohexane/ethyl acetate = 50:1 yielding the product (267 g, 1.21 mmol) as a colorless liquid in a yield of 77% (15.5 mmol scale, 24 h, 83%).

E-factor (2.50 mmol): 1.18, E-factor (15.5 mmol): 0.989

Purity was >99% according to GC-analysis.

EA: Found: C, 68.6; H, 8.5, N, 4.6; S, 9.4 Calc. for $C_{19}H_{27}N_1O_2S_1$: C, 68.4; H, 8.2; N, 4.2; S, 9.6 %.

R_f = 0.50 in cyclohexane/ethyl acetate = 9:1 visualized *via* UV quenching at 254 nm and vanillin staining solution (deep blue).

^{1}H-NMR (400 MHz, $CDCl_3$) δ / ppm = 7.40-7.29 (m, 5H, aromatic, ^{1}), 5.11 (s, 2H, CH_2, ^{2}), 3.50 (t, ^3J = 6.6 Hz, 2H, CH_2, ^{3}), 2.35 (t, ^3J = 7.5 Hz, 2H, ^{4}), 1.74-1.58 (m, 4H, CH_2, ^{5}), 1.45-1.21 (m, 12H, CH_2, ^{6}).

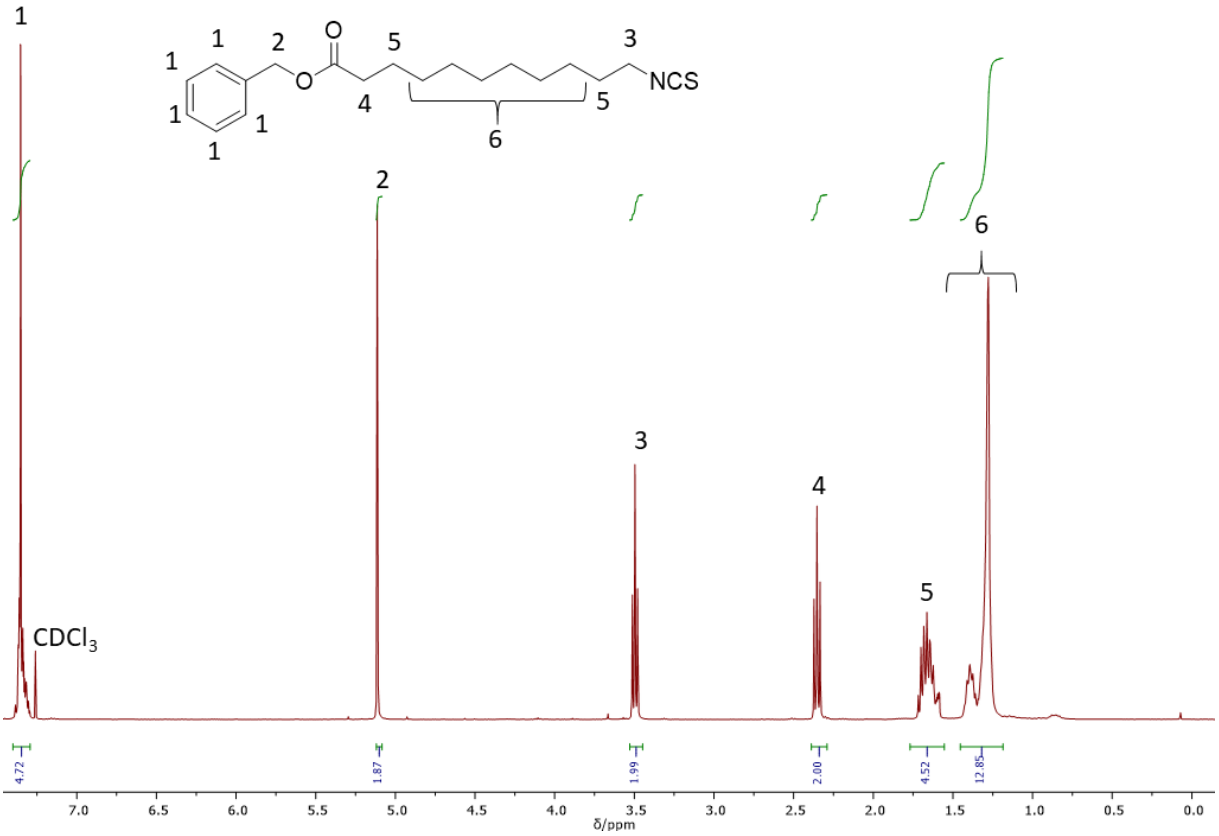

*Figure 143: ^{1}H-NMR-spectrum of ITC **67**.*

^{13}C-NMR (101 MHz, $CDCl_3$) δ / ppm = 173.79 (C=O), 136.26 (aromatic), 129.58 (NCS), 128.66 (aromatic), 128.28 (aromatic), 66.19 (**C**H_2-Ph), 45.17 (**C**H_2-NCS), 34.43 (**C**H_2-COOBn), 30.06 (CH_2), 29.40 (CH_2), 29.38 (CH_2), 29.27 (CH_2), 29.19 (CH_2), 28.88 (CH_2), 26.65 (CH_2), 25.04 (CH_2).

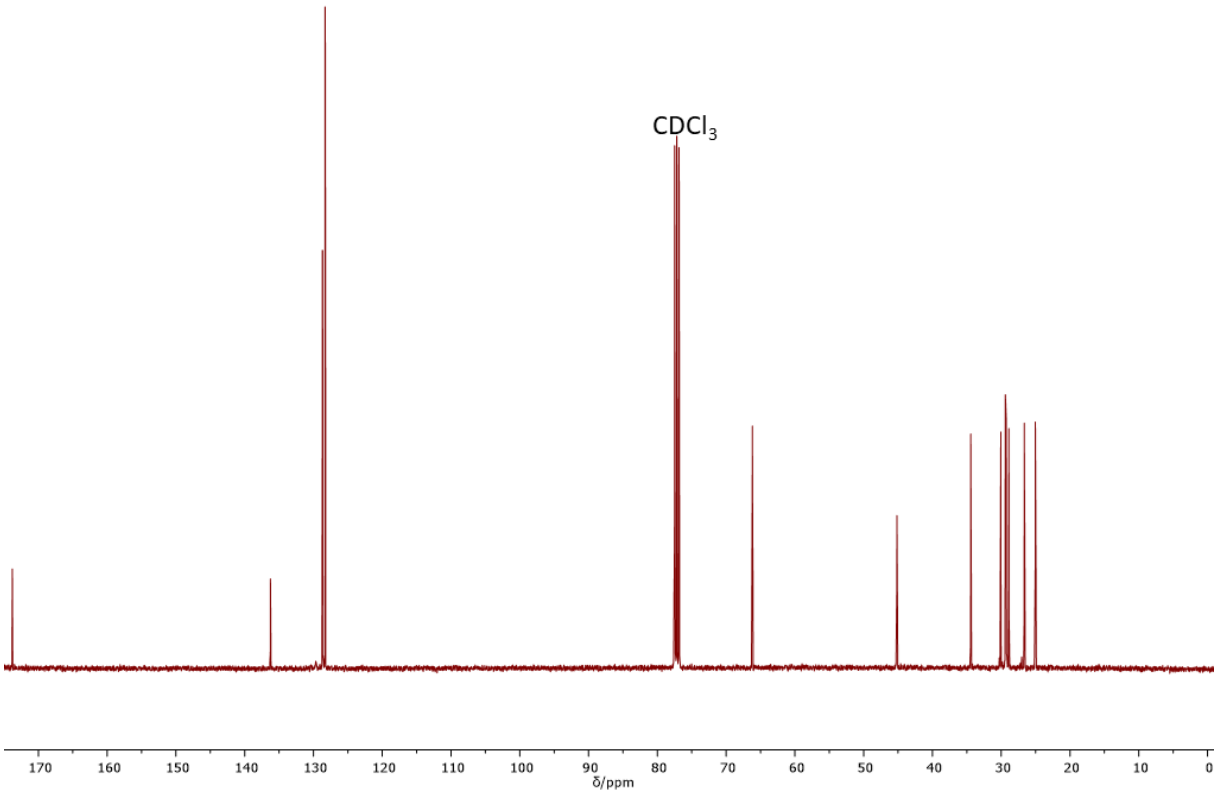

*Figure 144: ^{13}C-NMR-spectrum of ITC **67**.*

HRMS (EI): calculated m/z for $C_{19}H_{27}O_2N_1S_1$ [M^+] = 333.1757, found: 333.1758, Δ = 0.0781 mmu.

IR: $\tilde{\nu}$/cm^{-1} = 2925 (s), 2853 (m), 2179 (m), 2092 (vs), 1732 (vs), 1455 (m), 1346 (m), 1256 (m), 1228 (m), 1213 (m), 1160 (vs), 1102 (m), 1027 (w), 1001 (w), 980 (w), 735 (s), 696 (vs), 500 (w), 455 (w).

Benzyl isothiocyanate 68

Benzyl isocyanide **11** (304 µL, 298 mg, 2.50 mmol, 1.00 eq.) was as like described in GP1-B using elemental sulfur (89.8 mg, 350 µmol, 1.12 eq.), DBU (7.46 µL, 7.61 mg, 50.0 µmol, 2 mol%) and 417 µL Cyrene™. The reaction was stirred for 5 hours. Flash column chromatography was performed using cyclohexane yielding the product (281 g, 1.88 mmol) as a colorless liquid in a yield of 75%.

E-factor: 2.25

Purity was 97% according to GC-analysis.

$\mathbf{R_f}$ = 0.69 in cyclohexane/ethyl acetate = 9:1 visualized *via* UV quenching at 254 nm and vanillin staining solution (deep blue).

^{1}H-NMR was according to literature.[631]

^{1}H-NMR (400 MHz, $CDCl_3$) δ / ppm = 7.42-7.30 (m, 5 H, aromatic, ^{1}), 4.72 (s, 2H, CH_2, ^{2}).

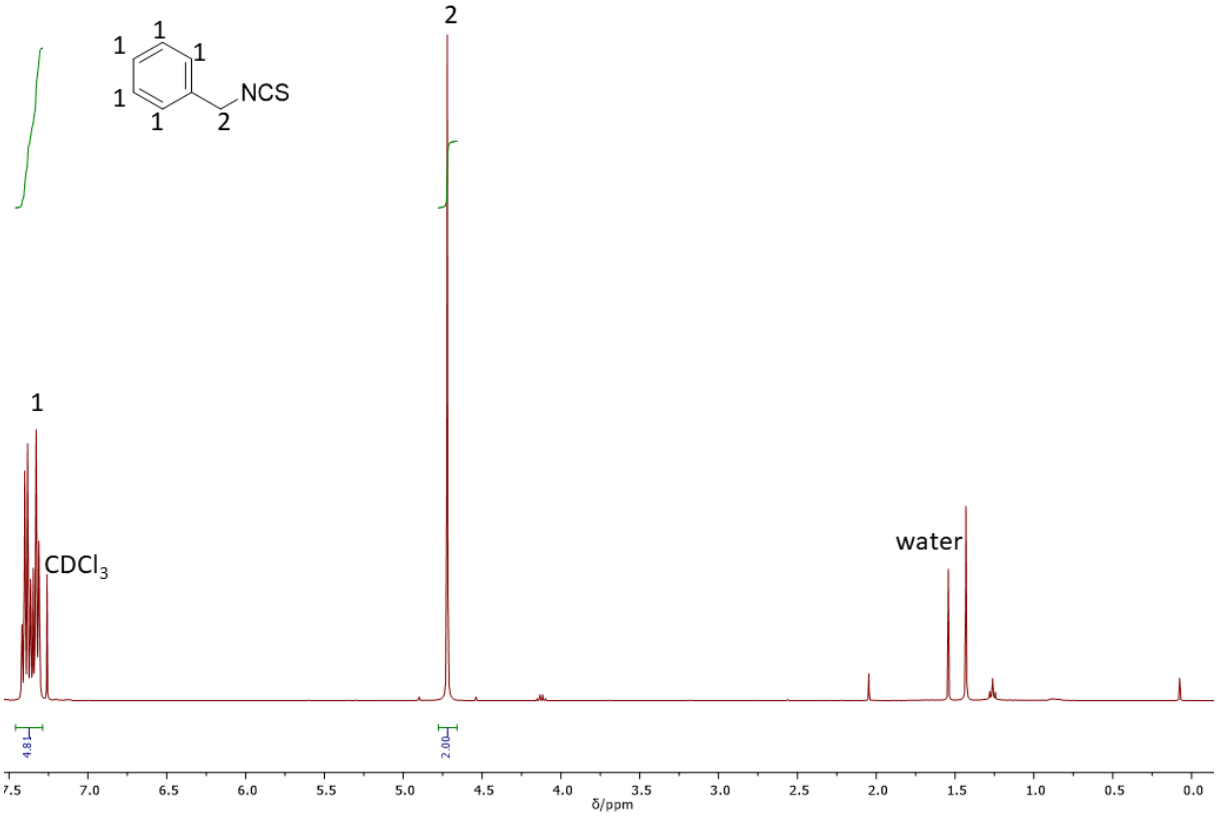

*Figure 145: ^{1}H-NMR-spectrum of ITC **68**.*

IR: *v* / cm^{-1} = 3061 (vw), 3030 (vw), 2925 (vw), 2849 (vw), 2166 (m), 2073 (vs), 1495 (w), 1454 (m), 1438 (m), 1345 (s), 1302 (w), 1199 (w), 1072 (w), 1028 (w), 812 (w), 730 (m), 695 (vs), 574 (m), 453 (m).

Tosylmethyl isothiocyanate 69

Tosylmethyl isocyanide (488 mg, 2.50 mmol, 1.00 eq.) was converted as described in GP1-A using elemental sulfur (89.8 mg, 350 µmol, 1.12 eq.), DBU (18.7 µL, 19.0 mg, 125 µmol, 5 mol%) and 1.25 mL GBL. The reaction was stirred for 24 hours. Flash column chromatography was performed using cyclohexane/ethyl acetate (10:1→8:1) yielding the product (193 mg, 850 µmol) as an orange solid in a yield of 34%.

E-factor: 11.1

Purity was >99% according to GC-analysis.

$\mathbf{R_f}$ = 0.45 in cyclohexane/ethyl acetate = 3:1 visualized *via* UV quenching at 254 nm and vanillin staining solution (deep blue).

^{1}H-NMR (400 MHz, $CDCl_3$) δ / ppm = 7.86-7.79 (m, 2H, aromatic, ^{1}), 7.55 (d, ^3J = 8.0 Hz, 2H, aromatic, ^{2}), 5.41 (s, 2H, CH_2, ^{3}), 2.45 (s, 3H, CH_3, ^{4}).

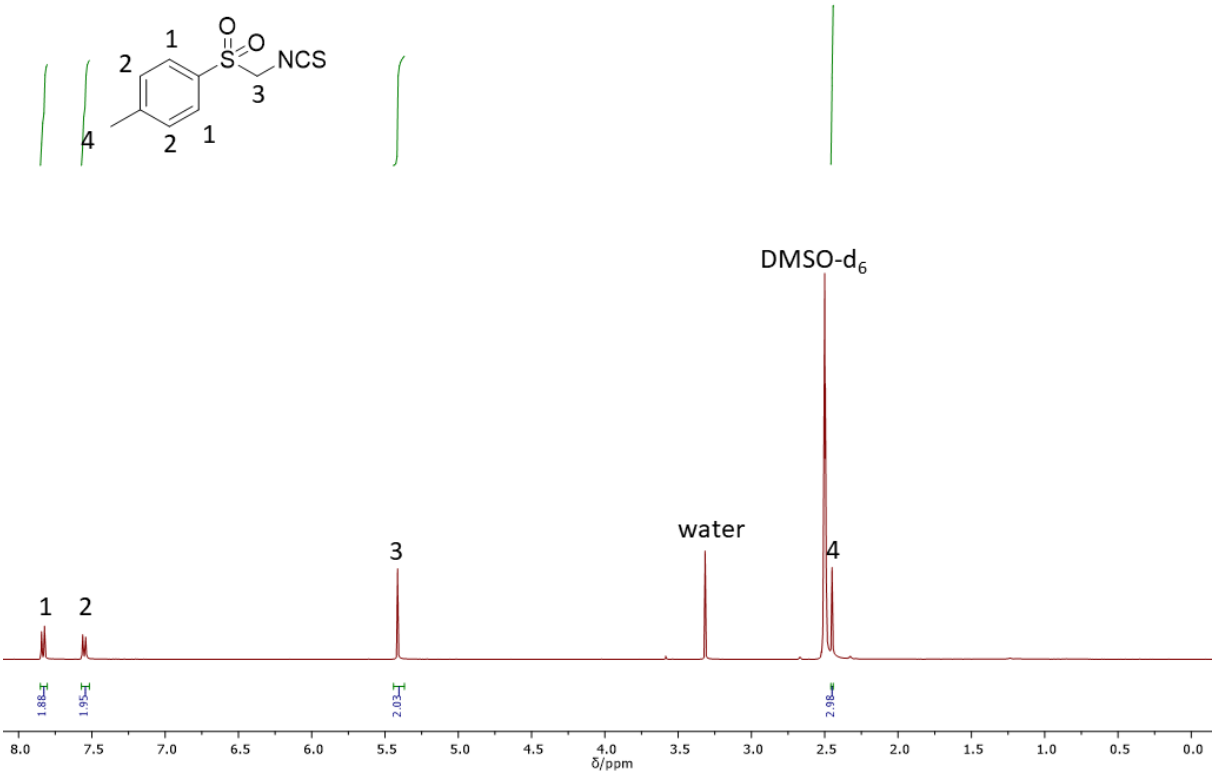

*Figure 146: ^{1}H-NMR-spectrum of ITC **69**.*

^{13}C-NMR (101 MHz, $CDCl_3$) δ / ppm = 145.98 (aromatic), 133.20 (aromatic), 130.28 (aromatic), 128.59 (aromatic), 63.32 (CH_2), 21.17 (CH_3). Signal of the SCN-carbon was not observed.

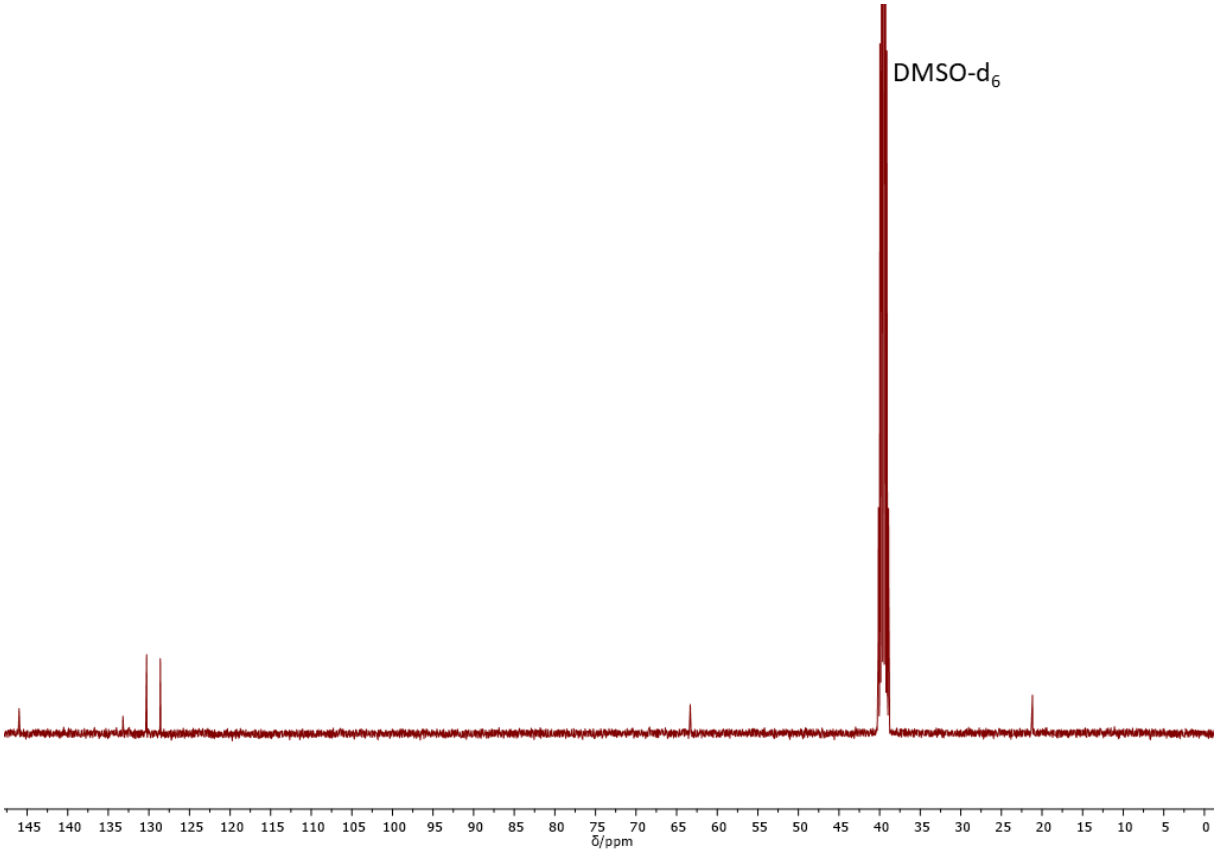

*Figure 147: ^{13}C-NMR-spectrum of ITC **69**.*

HRMS (EI): calculated m/z for $C_9H_9O_2N_1S_2$ [M^+] = 227.0069, found: 227.0069, Δ = -0.0411 mmu.

IR: *v* / cm^{-1} = 2985 (w), 2927 (w), 2853 (vw), 2289 (w), 2057 (vs), 2045 (vs), 1594 (w), 1491 (w), 1417 (w), 1378 (w), 1323 (vs), 1302 (w), 1269 (vs), 1218 (w), 1142 (vs), 1082 (vs), 1041 (w), 1016 (w), 901 (s), 815 (s), 738 (vs), 703 (s), 625 (s), 553 (vs), 508 (vs), 457 (vs), 426 (s).

2,6-Dimethyl phenyl isothiocyanate 70

2,6-Dimethylphenyl isocyanide (328 mg, 2.50 mmol, 1.00 eq.) was converted as described in GP1-A using elemental sulfur (89.8 mg, 350 µmol, 1.12 eq.), DBU (18.7 µL, 19.0 mg, 125 µmol, 5 mol%) and 1.25 mL Cyrene™ or GBL, respectively. The reaction was stirred for 5 (Cyrene™) or 4 (GBL) hours. Flash column chromatography was performed using cyclohexane yielding the product (322 g, 1.98 mmol Cyrene™ or 388 mg, 2.37 mmol in GBL) as a colorless liquid in a yield of 80% (Cyrene™) or 95% (GBL, 15.5 mmol scale, 90% in Cyrene™).

E-factor (2.50 mmol in Cyrene™): 5.30, E-factor (2.50 mmol in GBL): 3.84, E-factor (15.5 mmol in Cyrene™): 4.53

Purity was 98% (Cyrene™ and GBL), >99% (15.5 mmol in Cyrene™) according to GC-analysis.

$\mathbf{R_f}$ = 0.73 in cyclohexane/ethyl acetate = 9:1 visualized *via* UV quenching at 254 nm and vanillin staining solution (deep blue).

^{1}H-NMR was according to literature.[633]

^{1}H-NMR (400 MHz, $CDCl_3$) δ / ppm = 7.09-7.02 (m, 3H, aromatic, ^{1}), 2.38 (s, 6H, CH_3, ^{2}).

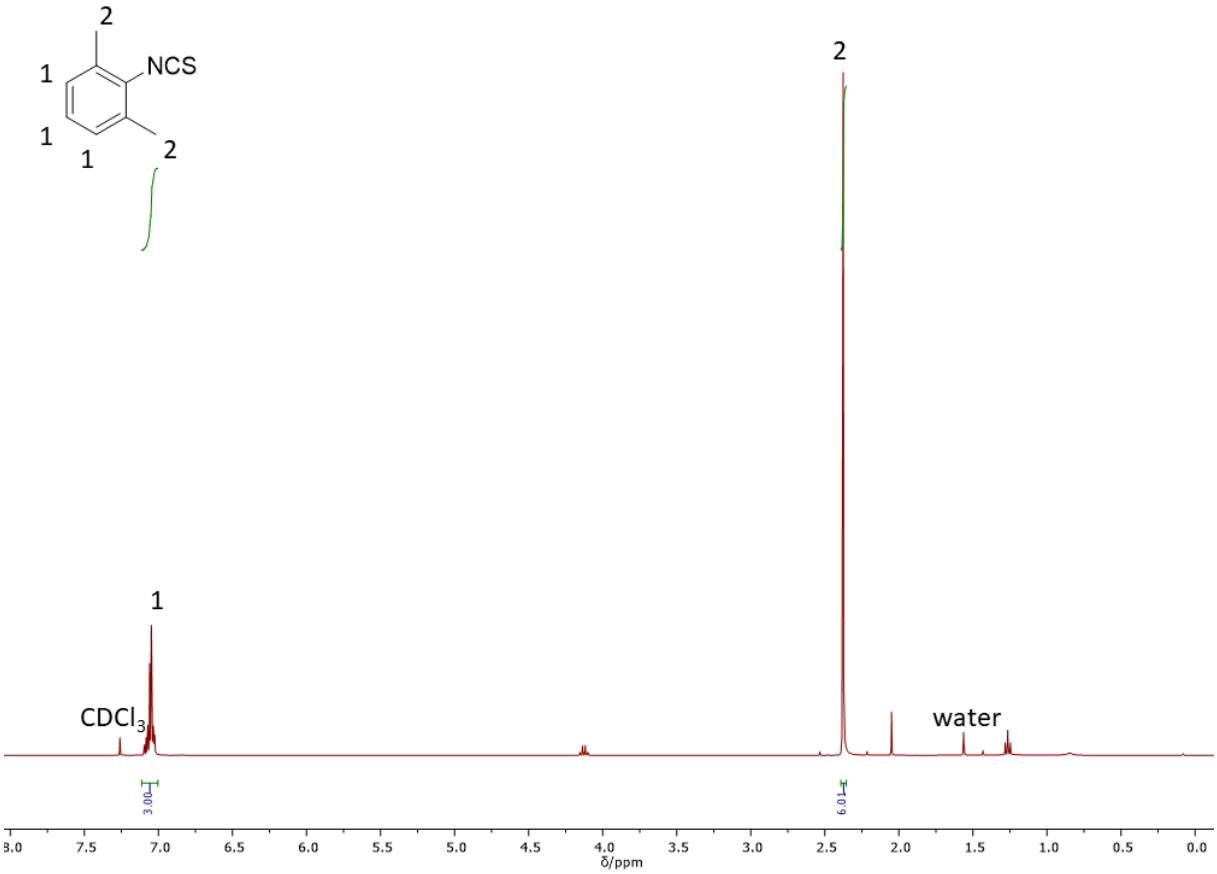

*Figure 148: ^{1}H-NMR-spectrum of ITC **70**.*

2-Isothiocyanato naphthalene 71

2-Isocyanido naphthalene (383 mg, 2.50 mmol, 1.00 eq.) was converted as described in GP1-A using elemental sulfur (89.8 mg, 350 µmol, 1.12 eq.), DBU (18.7 µL, 19.0 mg, 125 µmol, 5 mol%) and 1.25 mL Cyrene™. Flash column chromatography was performed using cyclohexane yielding the product (322 g, 1.39 mmol) as a colorless solid in a yield of 56%.

E-factor (2.50 mmol): 8.45

Purity was >99% according to GC-analysis.

EA: Found: C, 71.35; H, 3.7; N, 7.6; S, 17.1 Calc. for $C_{11}H_7N_1S_1$: C, 71.3; H, 3.8; N, 7.5; S, 17.3 %.

R_f = 0.60 in cyclohexane visualized *via* UV quenching at 254 nm and vanillin staining solution (deep blue).

^{1}H-NMR was according to literature. [631]

^{1}H-NMR (400 MHz, $CDCl_3$) δ / ppm = 7.86-7.75 (m, 3H, aromatic, ^{1}), 7.68 (d, ^4J = 2.1 Hz, 1H, aromatic, ^{2}), 7.56-7.47 (m, 2H, aromatic, ^{3}), 7.31 (dd, ^3J = 8.7 Hz, ^4J = 2.1 Hz, 1H, aromatic, ^{4}).

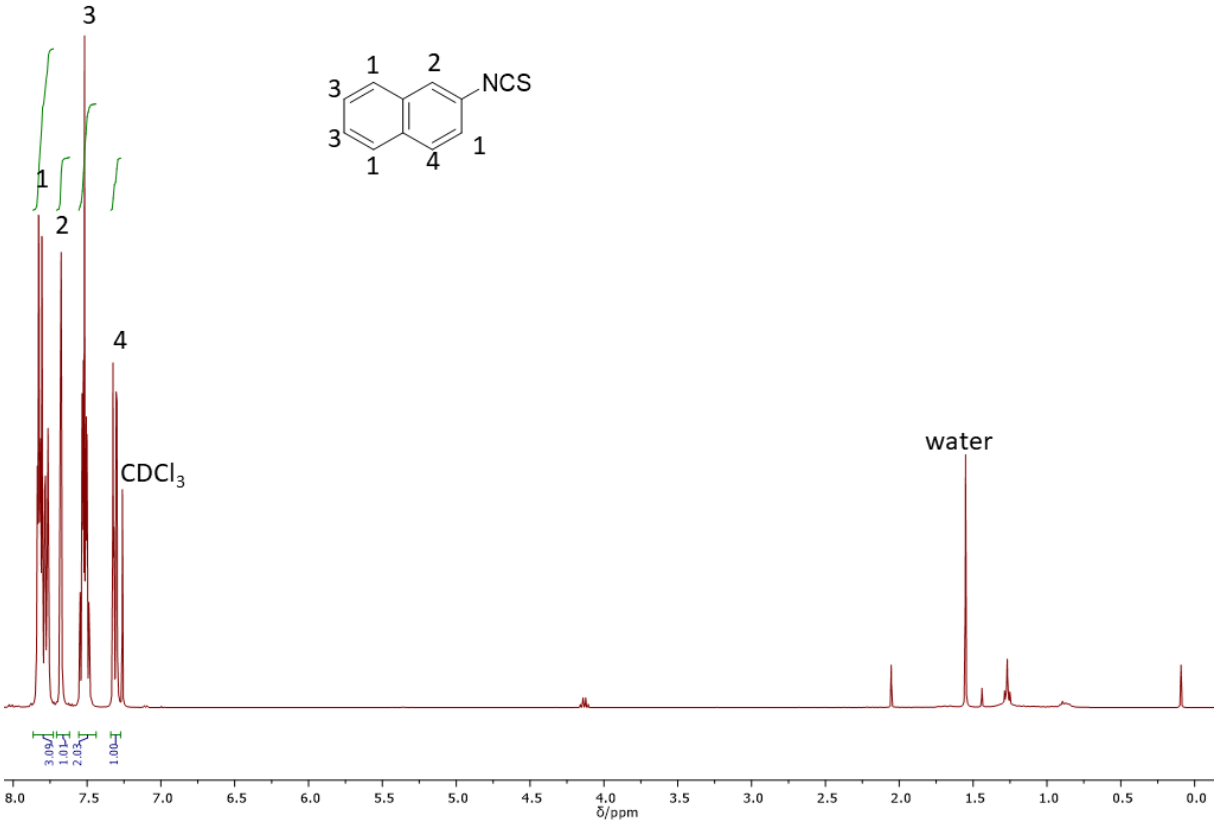

*Figure 149: ^{1}H-NMR-spectrum of ITC **71**.*

4-Methoxyphenyl isothiocyanate 72

4-Methoxyphenyl isocyanide (333 mg, 2.50 mmol, 1.00 eq.) was converted as described in GP1-B using elemental sulfur (89.8 mg, 350 µmol, 1.12 eq.), DBU (7.46 µL, 7.61 mg, 50 µmol, 2 mol%) and 417 µL Cyrene™ or GBL. The reaction was stirred for 5 hours for Cyrene™ and GBL. Flash column chromatography was performed using cyclohexane yielding the product (346 mg, 2.09 mmol in Cyrene™, 388, 2.35 mmol GBL) as a colorless liquid in a yield of 85% (Cyrene™) or 94% (GBL).

E-factor (2.50 mmol in Cyrene™): 1.74, E-factor (2.50 mmol in GBL): 1.32

Purity was 99 (Cyrene™) and 95% (GBL)% according to GC-analysis.

$\mathbf{R_f}$ = 0.67 in cyclohexane/ethyl acetate = 3:1 visualized *via* UV quenching at 254 nm and vanillin staining solution (deep blue).

EA (Cyrene™): Found: C, 57.2; H, 4.3; N, 8.5; S, 18.9 Calc. for C_8H_7NS: C, 58.2; H, 4.3; N, 8.5; S, 19.4%.

EA (GBL): Found: C, 57.9; H, 4.5; N, 8.2; S, 18.1 Calc. for C_8H_7NS: C, 58.2; H, 4.3; N, 8.5; S, 19.4%.

^{1}H-NMR was according to literature.[631]

^{1}H-NMR (400 MHz, $CDCl_3$) δ / ppm = 7.16 (d, ^3J = 8.9 Hz, 2H, aromatic, ^{1}), 6.85 (d, ^3J = 9.0 Hz, 2H, aromatic, ^{2}), 3.80 (s, 3H, CH_3, ^{3}).

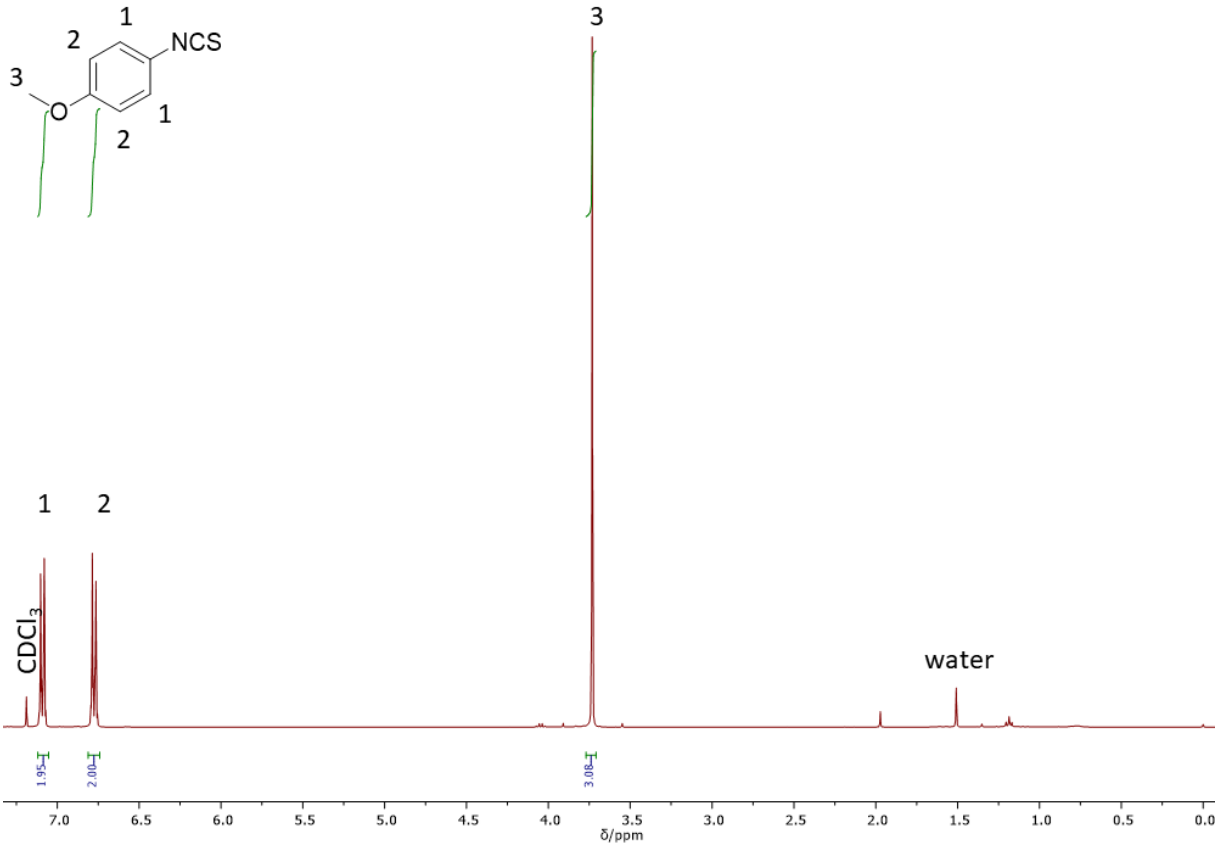

*Figure 150: ^{1}H-NMR-spectrum of ITC **72**.*

3,4,5-Trimethoxyphenyl isothiocyanate 73

3,4,5-Trimethoxyphenyl isocyanide (483 mg, 2.50 mmol, 1.00 eq.) was converted as described in GP1-B using elemental sulfur (89.8 mg, 350 µmol, 1.12 eq.), DBU (7.46 µL, 7.61 mg, 50.0 µmol, 2 mol%) and 417 µL Cyrene™. Flash column chromatography was performed using cyclohexane yielding the product (390 mg, 1.73 mmol) as a colorless solid in a yield of 69%.

E-factor (2.50 mmol): 1.85

Purity was >99% according to GC-analysis.

R_f = 0.62 in cyclohexane/ethyl acetate = 3:1 visualized *via* UV quenching at 254 nm and vanillin staining solution (deep blue).

EA: Found: C, 53.5; H, 5.0; N, 6.1; S, 13.6 Calc. for $C_{10}H_{11}N_1O_3S_1$: C, 53.3; H, 4.9; N, 6.2, S, 14.2%.

^{1}H-NMR (400 MHz, $CDCl_3$) δ / ppm = 6.59 (s, 2H, aromatic, ^{1}), 3.84 (s, 6H, CH_3, ^{2}), 3.83 (s, 3H, CH_3, ^{3}).

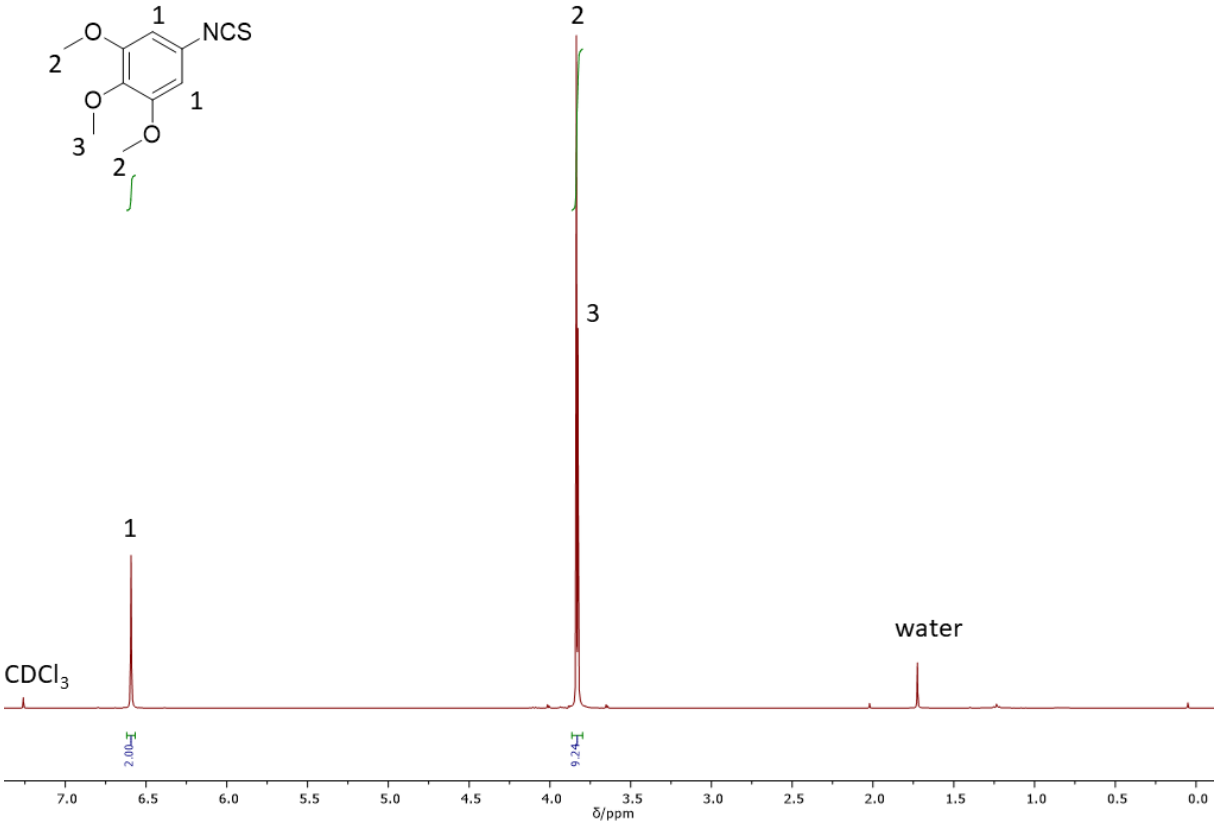

*Figure 151: ^{1}H-NMR-spectrum of ITC **73**.*

^{13}C-NMR (101 MHz, $CDCl_3$) δ / ppm = 163.18 (aromatic), 153.52 (aromatic), 139.24 (aromatic), 122.00 (NCS), 104.13 (aromatic), 61.09 (CH_3), 56.41 (CH_3).

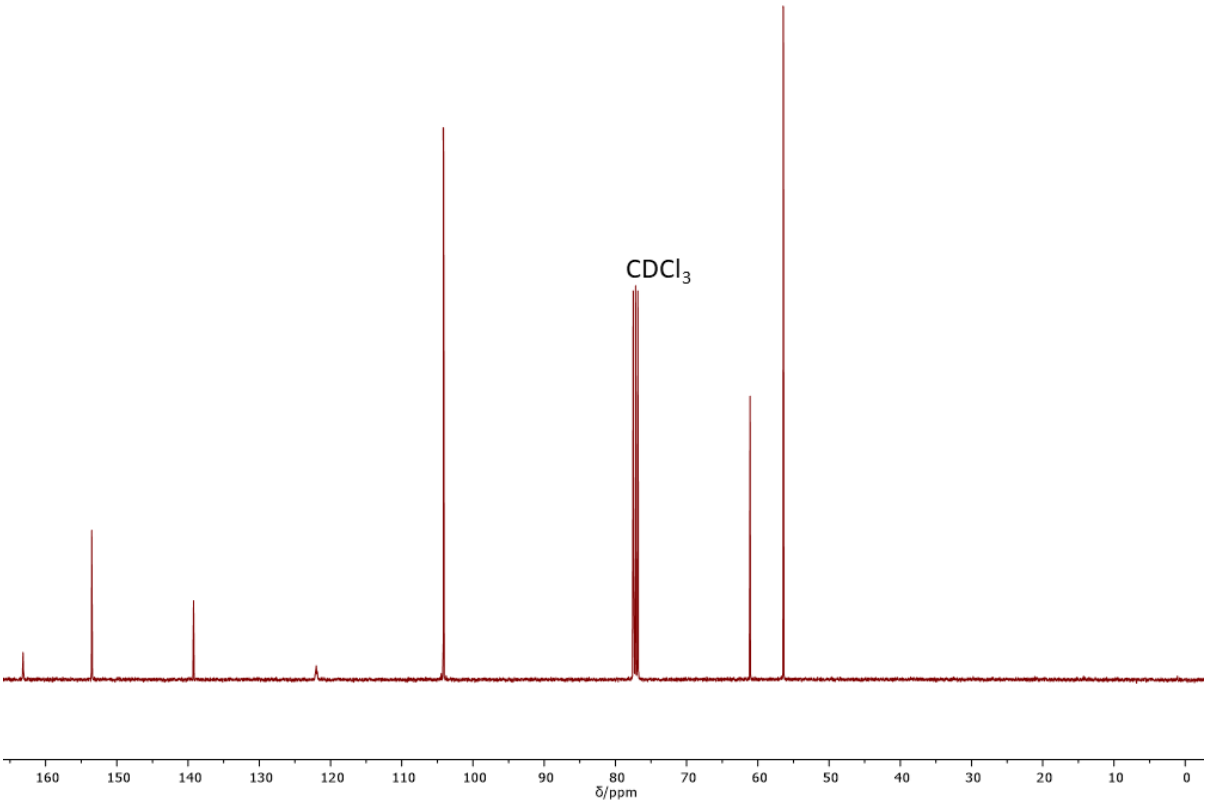

*Figure 152: ^{13}C-NMR-spectrum of ITC **73**.*

HRMS (EI): calculated m/z for $C_{10}H_{11}O_3N_1S_1$ [M^+] = 225.0454, found: 225.0453, Δ = -0.1382 mmu.

IR: *v* / cm^{-1} = 2972 (w), 2943 (w), 2921 (w), 2836 (w), 2114 (vs), 2096 (s), 1582 (vs), 1499 (s), 1465 (s), 1456 (s), 1430 (s), 1415 (vs), 1339 (s), 1304 (w), 1230 (vs), 1185 (m), 1164 (m), 1119 (vs), 1014 (m), 991 (vs), 870 (w), 827 (vs), 808 (vs), 761 (s), 728 (vs), 671 (m), 605 (m), 525 (s), 483 (m), 430 (m).

5-Isothiocyanatodimethyl isophthalate 74

5-isocyanidodimethyl isophtlate (438 mg, 2.00 mmol, 1.00 eq.) was converted as described in GP1-A using elemental sulfur (71.8 mg, 280 µmol, 1.12 eq.), DBU (14.9 µL, 15.2 mg, 100 µmol, 5 mol%) and 1.0 mL GBL. Conventional flash column chromatography was performed using cyclohexane/ethyl acetate = 10:1 yielding the product (224 mg, 89.2 mmol) as a colorless solid in a yield of 45%.

E-factor: 7.37

R_f = 0.37 in cyclohexane/ethyl acetate = 10:1 visualized *via* UV quenching at 254 nm and vanillin staining solution (blue to greenish).

^{1}H-NMR (400 MHz, DMSO-d_6) δ / ppm = 8.32 (t, ^4J = 1.6 Hz, 1H, aromatic, ^{1}), 8.11 (d, ^4J = 1.5 Hz, 2H, aromatic, ^{2}), 3.86 (s, 6H, CH_3, ^{3}). Please note that, the compound is decomposing in DMSO-d_6 over time probably depending on the amount of water.

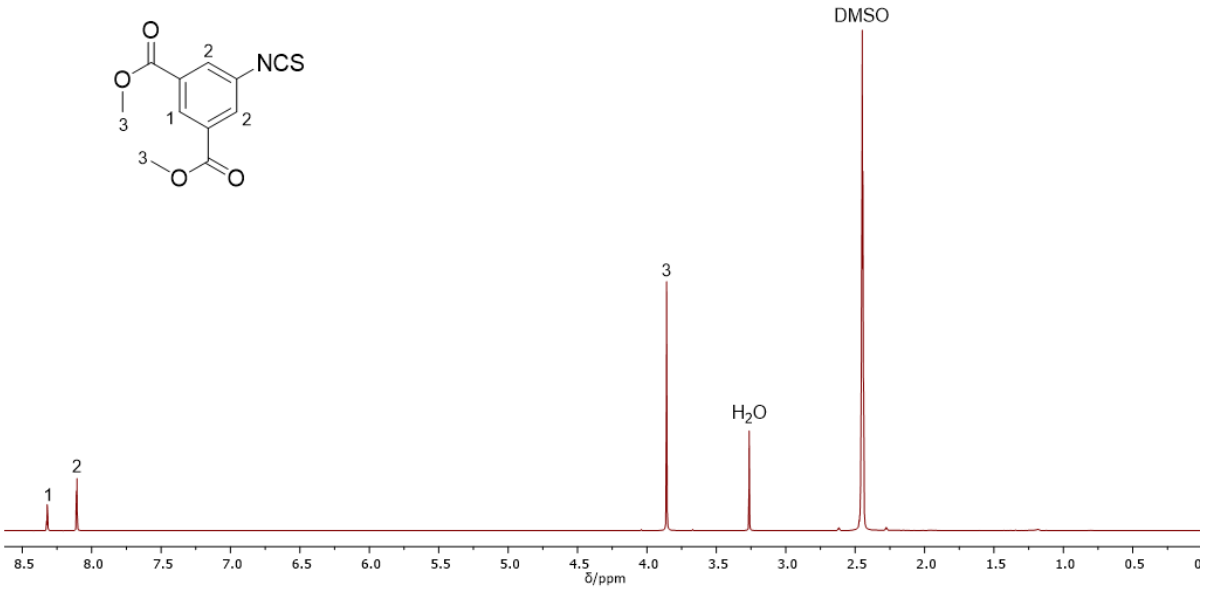

*Figure 153: ^{1}H-NMR-spectrum of ITC **74**.*

^{13}C-NMR (126 MHz, $CDCl_3$) δ / ppm = 164.23 (**C**OOMe), 136.44 (SCN), 131.81 (aromatic), 131.75 (aromatic), 130.49 (aromatic), 128.05(aromatic), 52.84 (CH_3).

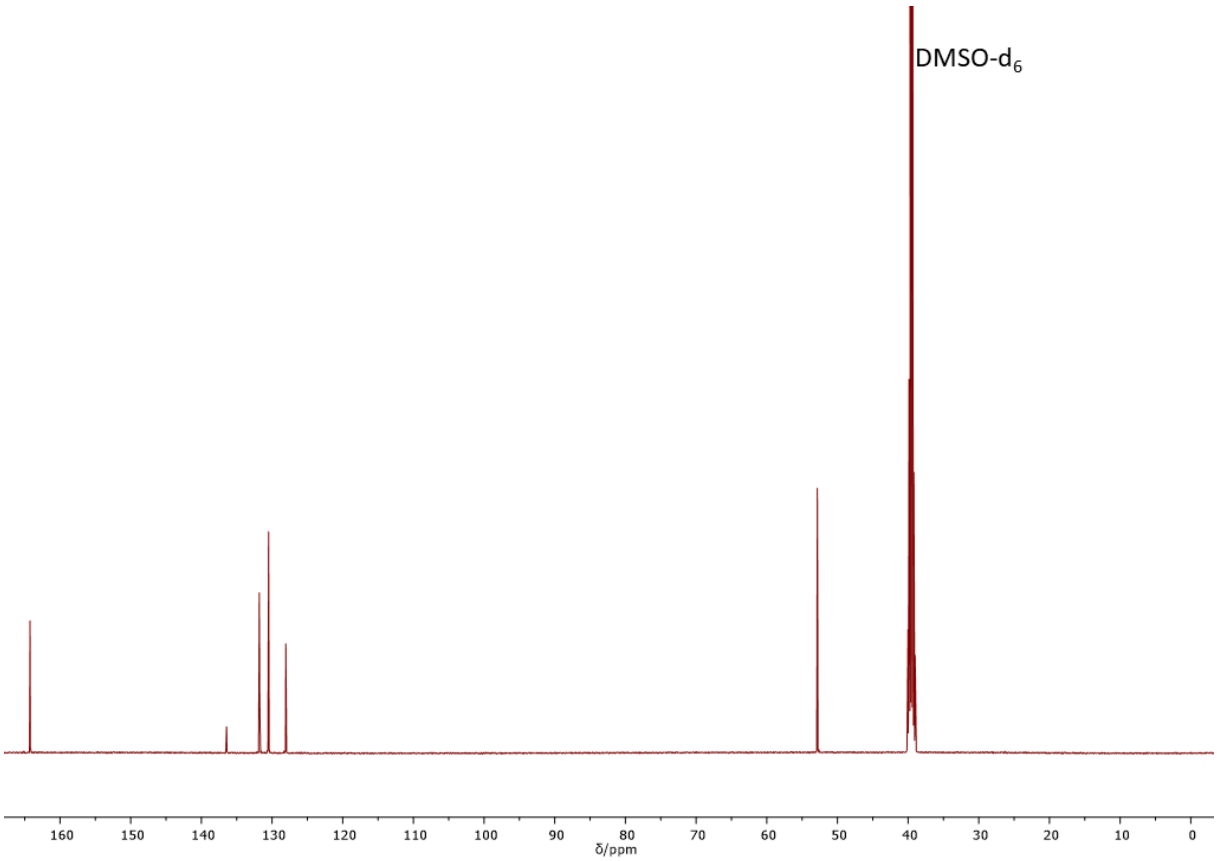

*Figure 154: ^{13}C-NMR-spectrum of ITC **74**.*

HRMS (EI): calculated m/z for $C_{11}H_{10}O_4N_1S_1$ $[M+H]^+$ = 252.0331, found: 252.0331, Δ = - 0.1892 mmu

IR: *v* / cm^{-1} = 3085.1 (w), 2953.1 (w), 2129.0 (s,), 1722.9 (vs), 1600.1 (m), 1431.5 (s), 1336.5 (s), 1228.5 (vs), 1120.9 (s), 1102.3 (m), 994.3 (s), 945.8 (m), 911.1 (m), 872.7 (m), 814.0 (w), 751.3 (s), 721.0 (s), 664.7 (m), 480.1 (m), 439.7 (w), 412.3 (m).

6.6.3 Synthesis of isocyanides

5-Isocyanido-1-(isocyanidomethyl)-1,3,3-trimethyl cyclohexane

5-Formamido-1-(formamidomethyl)-1,3,3-trimethyl cyclohexane (5.30 g, 23.4 mmol, 1.00 eq.) and diisopropylamine (20.4 mL, 14.7 g, 145 mmol, 6.20 eq.) was dissolved in DCM (71 mL) and cooled to 0 °C with an ice-water bath. Then, phosphoryl chloride (5.7 mL, 9.34 g, 60.9 mmol, 2.60 eq.) were added dropwise keeping the tempearute at 0 °C. Afterwards, the ice-water bath was removed and the colorless reaction solution was stirred at room temperature for 4 hours. The yellow reaction mixture was quenched by adding 71 mL saturated, aqueous sodium hydrogen carbonate solution and stirred for further 15 minutes until CO_2 formation had ceased. The organic layer was separated and the aqueous phase was extracted with DCM (1 × 30 mL). The combined organic layers were removed from solvent under reduced pressure and purification by flash column chromatography using cyclohexane/ethyl acetate (10:1) yielded the product (2.88 mg, 15.1 mmol, mixture of isomers) as a yellow viscous liquid in a yield of 65% (d.r. = 2.96:1 determined *via* NMR).

R_f = 0.68 in cyclohexane/ethyl acetate = 3:1 visualized *via* UV quenching at 254 nm and vanillin staining solution (orange).

^{1}H-NMR (400 MHz, $CDCl_3$) δ / ppm = 3.80 – 3.71 (m, 0.73H, CN-CH, ^{1a}), 3.66 – 3.54 (m, 0.24H, CN-CH, ^{1b}), 3.44 – 3.23 (q, ^2J = 14.3 Hz, 0.48H, CN-CH_2, ^{2b}), 3.12 (s, 1.42H, CN-CH_2, ^{2a}), 2.09 – 1.89 (m, 2H, CH_2, $^{3a+b}$), 1.68 – 1.07 (m, 7H, CH_2, CH_3, $^{3a+3b+4a+4b}$), 1.05 – 0.96 (m, 6H, CH_3, $^{5a+b}$).

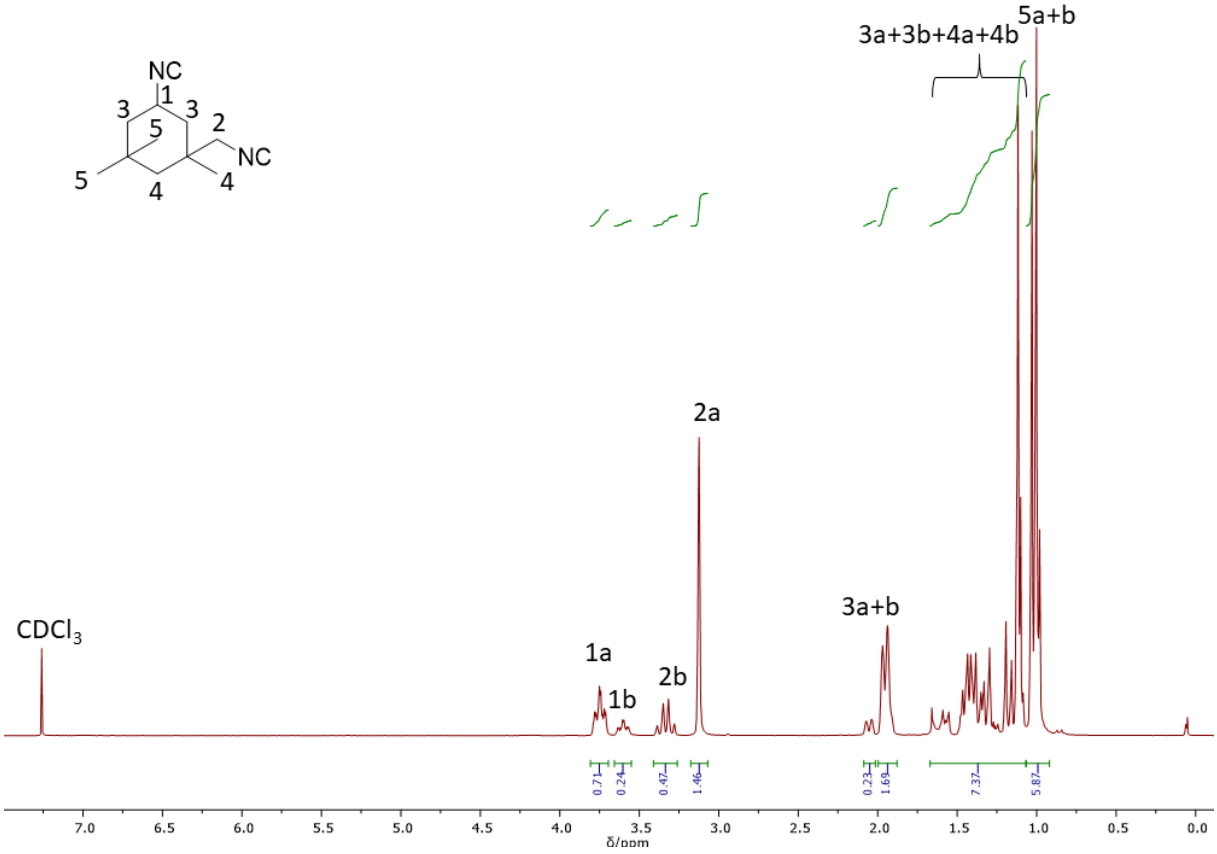

Figure 155: ^{1}H-NMR-spectrum of 5-isocyanido-1-(isocyanidoomethyl)-1,3,3-trimethyl cyclohexane.

^{13}C-NMR (101 MHz, $CDCl_3$) δ / ppm = 158.24-158.01 (m, **C**N-CH_2, a+b), 155.51 (t, **C**N-CH, b), 155.33 (t, **C**N-CH, a), 55.58 (t, CN-**C**H_2, a), 49.92 (t, CN-**C**H_2, b),47.20-46.89 (m, CN-**C**H, a+b), 45.92 (CH_2), 45.88 (CH_2, a), 45.69 (CH_2, b), 41.49 (CH_2, b), 41.38 (CH_2, a), 35.25 ($C_{quart.}$, a), 35.11 ($C_{quart.}$, b), 34.42 (CH_3, a), 34.23 (CH_3, b), 31.48 ($C_{quart.}$, a), 31.34 ($C_{quart.}$, b), 29.52 (CH_3, b), 27.36 (CH_3, a), 26.79 (CH_3, b), 23.18 (CH_3, a).

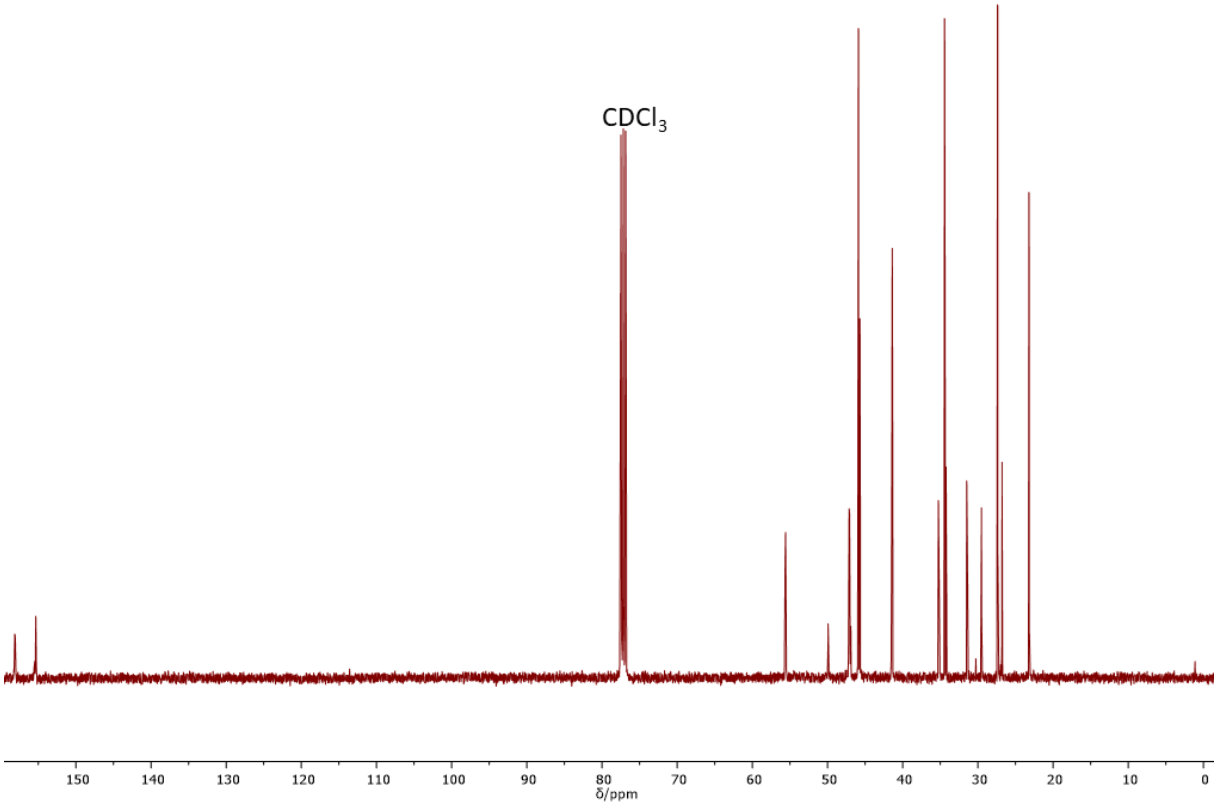

Figure 156: ^{13}C-NMR-spectrum of 5-isocyanido-1-(isocyanidoomethyl)-1,3,3-trimethyl cyclohexane.

HRMS (ESI): calculated m/z for $C_{12}H_{19}N_2$ [M+H$^+$] = 191.1543, found: 191.1541, Δ = - 0.18 mmu.

IR: *v* / cm^{-1} = 2956 (w), 2936 (w), 2874 (w), 2142 (vs), 1463 (m), 1391 (w), 1368 (w), 1251 (vw), 1201 (vw), 1145 (vw), 1017 (vw), 967 (w), 943 (m), 921 (w), 897 (vw), 864 (w), 769 (vw), 620 (vw), 503 (w), 442 (vw), 390 (vw).

Methyl-2-isocyano-3-phenyl propionate

Methyl-2-formamido-3-phenyl propionate (21.5 g, 104 mmol, 1.00 eq.) was dissolved in 343 mL dichloromethane and diisopropylamine (347.5 mL, 4.10 g, 321 mmol, 3.10 eq.) were added and the reaction mixture was cooled to 0 °C using an ice-water bath. Subsequently, phosphorous oxy chloride (12.6 mL, 20.6 g, 134 mmol, 1.30 eq.) was added dropwise keeping the temperature at 0 °C. Afterwards, the ice-water bath was removed and the reaction solution was stirred at room temperature for two hours. Subsequently, the reaction was quenched by addition of sodium carbonate solution (20 %, 126 mL) at 0 °C using an ice-water bath. After stirring this mixture for 30 minutes, 60 mL water and 60 mL dichloromethane were added. The aqueous phase was separated and the organic layer was washed with water (3 x 50 mL) and brine (50 mL). The combined organic layers were dried over sodium sulfate and the solvent was evaporated under reduced pressure. The crude product was then purified by column chromatography (cyclohexane / ethyl acetate 6:1). The product was obtained as slightly yellow oil (16.4 g, 86.7 mmol) in a yield of 84%.

R_f = 0.42 in cyclohexane/ethyl acetate = 4:1 visualized *via* UV quenching at 254 nm and vanillin staining solution (orange).

^{1}H-NMR was according to literature.[634]

^{1}H-NMR (400 MHz, $CDCl_3$) δ / ppm = 7.26-7.11 (m, 5H, aromatic, ^{1}), 4.35 (dd, ^3J = 8.3, 4.9 Hz, 1H, CH, ^{2}), 3.68 (s, 3H, CH_3, ^{3}), 3.14 (dd, ^2J = 13.8 Hz, ^3J = 4.9 Hz, 1H, CH_2, ^{4}), 3.03 (dd, ^2J = 13.8 Hz, ^3J = 8.3 Hz, 1H, CH_2, ^{4}).

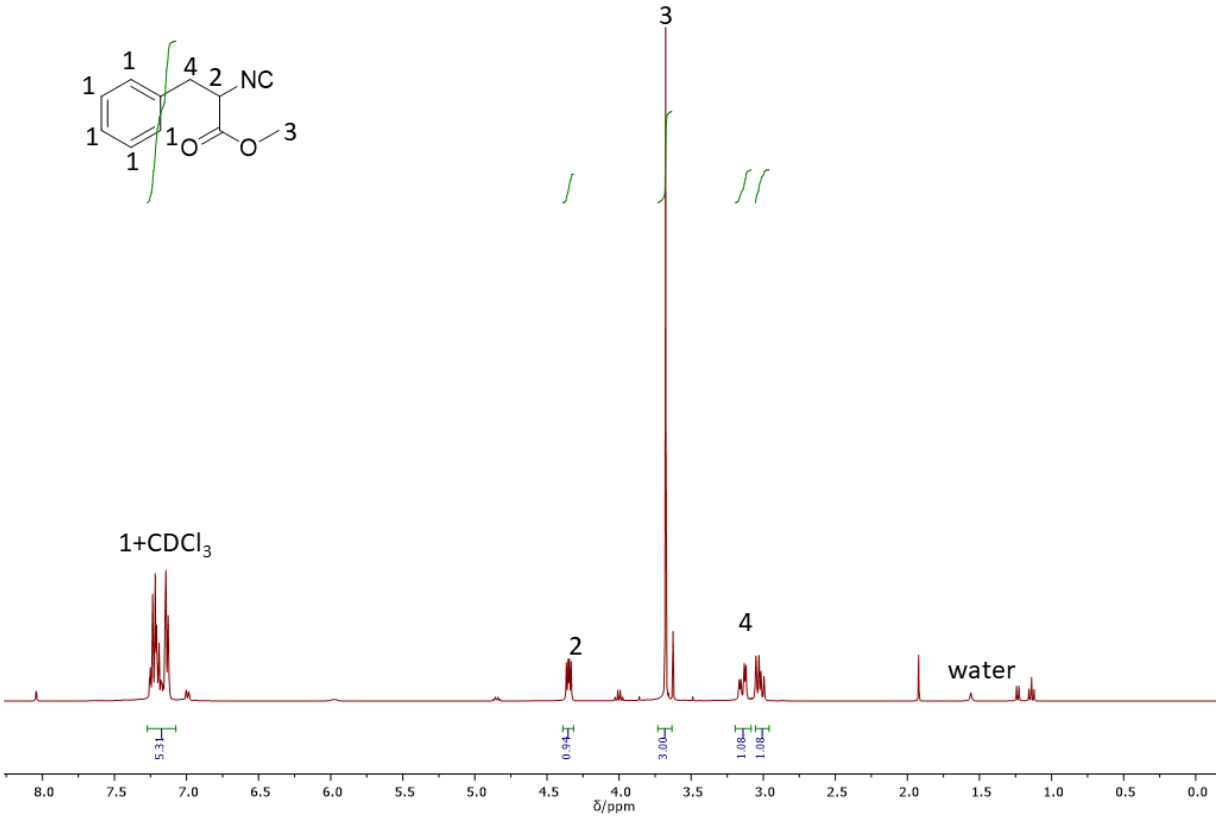

Figure 157: ^{1}H-NMR-spectrum of methyl-2-isocyanido-3-phenyl propionate.

Methyl-2-isothiocyanato-4-(methylthio) butanoate

Methyl-2-formamido-4-(methylthio) butanoate (4.00 g, 20.9 mmol, 1.00 eq.) was dissolved in 69 mL dichloromethane and diisopropylamine (9.15 mL, 6.56 g, 64.8 mmol, 3.10 eq.) was added and the reaction mixture was cooled to 0 °C using an ice-water bath. Subsequently, phosphorous oxy chloride (2.54 mL, 4.17 g, 27.2 mmol, 1.30 eq.) was added dropwise keeping the temperature at 0 °C. Afterwards, the ice-water bath was removed and the reaction solution was stirred at room temperature for two hours. The reaction was quenched by addition of sodium carbonate solution (20 %, 20 mL) at 0 °C using an ice-water bath. After stirring this mixture for 30 minutes, 15 mL water and 15 mL dichloromethane were added. The aqueous phase was separated and the organic layer was washed with water (3 x 25 mL) and brine (25 mL). The combined organic layers were dried over sodium sulfate and the solvent was evaporated under reduced pressure. The crude product was then purified by column chromatography (cyclohexane/ethyl acetate 9:1→8:1). The product was obtained as slightly yellow oil (2.86 g, 16.5mmol) in a yield of 79%.

R_f = 0.32 in cyclohexane/ethyl acetate = 5:1 visualized *via* UV quenching at 254 nm and vanillin staining solution (orange).

^{1}H-NMR was according to literature.[634]

^{1}H-NMR (400 MHz, $CDCl_3$) δ / ppm = 4.54 (dd, ^3J = 8.0 Hz, 5.3 Hz, 1H, CH, ^{1}), 3.82 (s, 3H, CH_3, ^{2}), 2.75-2.60 (m, 2H, CH_2, ^{3}), 2.24-2.13 (m, 2H, CH_2, ^{4}), 2.10 (s, 3H, CH_3, ^{5}).

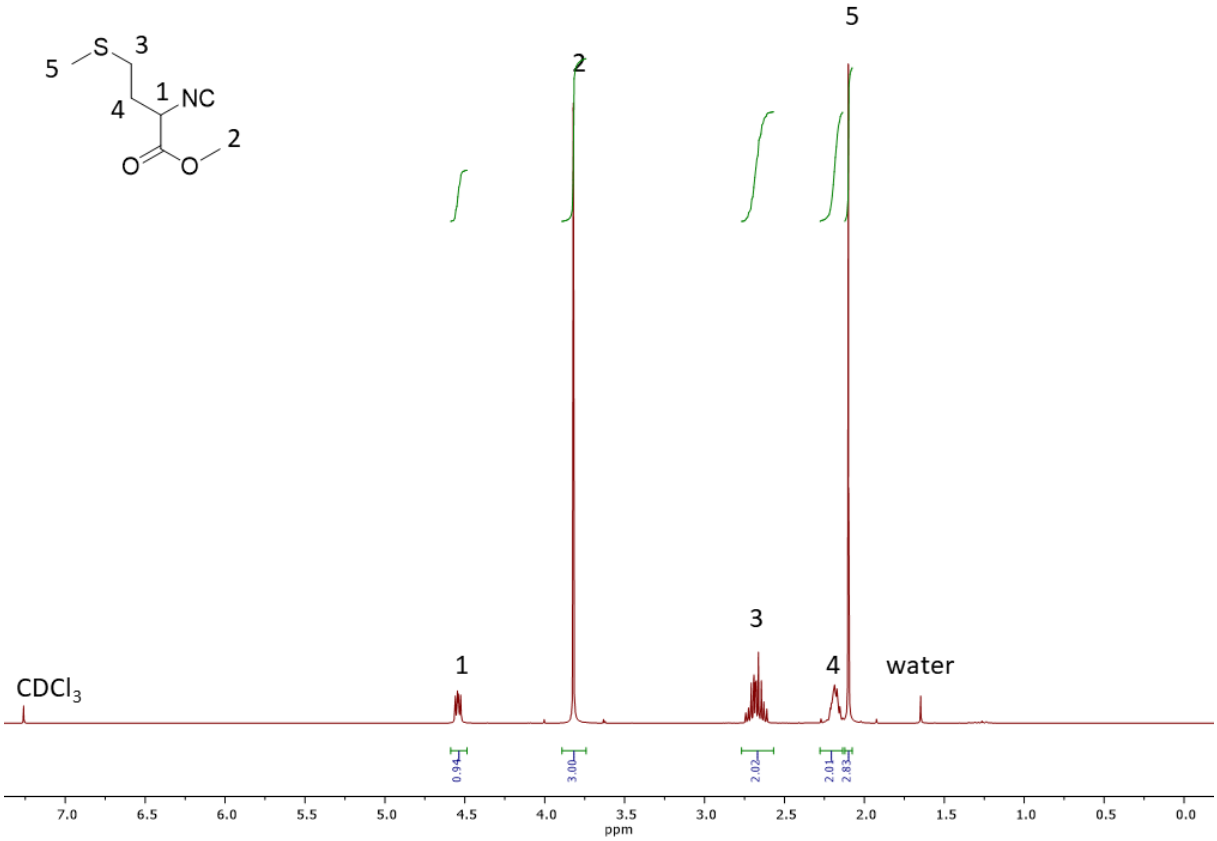

Figure 158: ^{1}H-NMR-spectrum of methyl-2-isocyanido-4-(methylthio) butanoate.

3,4,5-trimethoxypehnyl isocyanide

3,4,5-Trimethoxyphenyl formamide (1.04 g, 4.95 mmol, 1.00 eq.) was dissolved in 15 mL dichloromethane and diisopropylamine (2.16 mL, 1.55 g, 15.34 mmol, 3.10 eq.) was added and the reaction mixture was cooled to 0 °C using an ice-water bath. Subsequently, phosphorous oxy chloride (587 µL, 986 mg, 6.43 mmol, 1.30 eq.) was added dropwise keeping the temperature at 0 °C. Afterwards, the ice-water bath was removed and the colorless reaction solution was stirred at room temperature for two hours. The reaction mixture was quenched by adding 15 mL saturated, aqueous sodium hydrogen carbonate solution and stirred for further 15 minutes until CO_2 formation had ceased. The organic layer was separated and the aqueous phase was extracted with DCM (1 × 10 mL). The combined organic layers were removed from solvent under reduced pressure and purification by flash column chromatography using cyclohexane/ethyl acetate (14:1→10:1) yielded the product (819 mg, 4.24 mmol) as a yellowish liquid in a yield of 86%.

R_f = 0.46 in cyclohexane/ethyl acetate = 3:1 visualized *via* UV quenching at 254 nm and vanillin staining solution (orange).

^{1}H-NMR (400 MHz, DMSO-d_6) δ / ppm = 6.94 (s, 2H, aromatic, ^{1}), 3.80 (s, 6H, CH_3, ^{2}), 3.67 (s, 3H, CH_3, ^{3}).

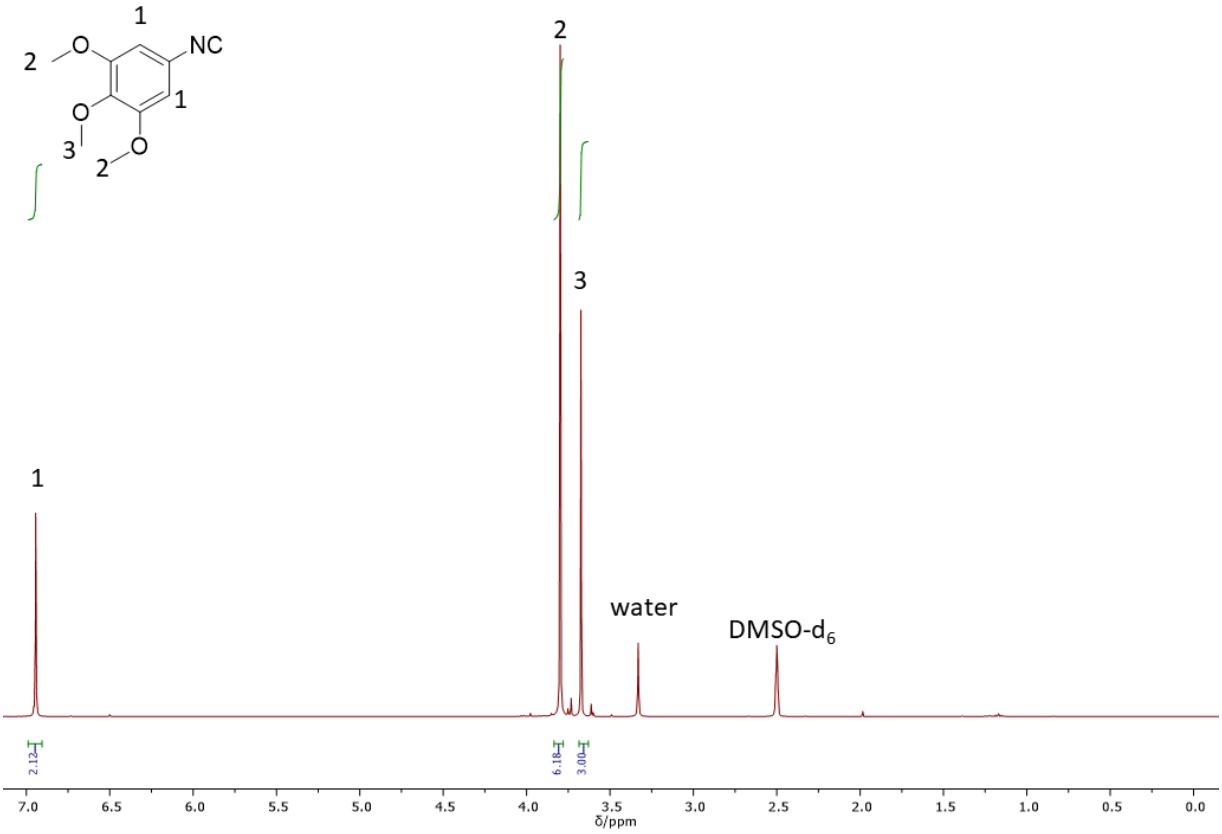

Figure 159: ^{1}H-NMR-spectrum of 3,4,5-trimethoxyphenyl isocyanide.

^{13}C-NMR (101 MHz, DMSO-d_6) δ / ppm = 162.92 (aromatic-quaternary), 153.21 (aromatic-quaternary), 138.67 (aromatic-quaternary), 121.16 (CN), 104.35 (aromatic), 60.18 (CH_3), 56.33. (CH_3).

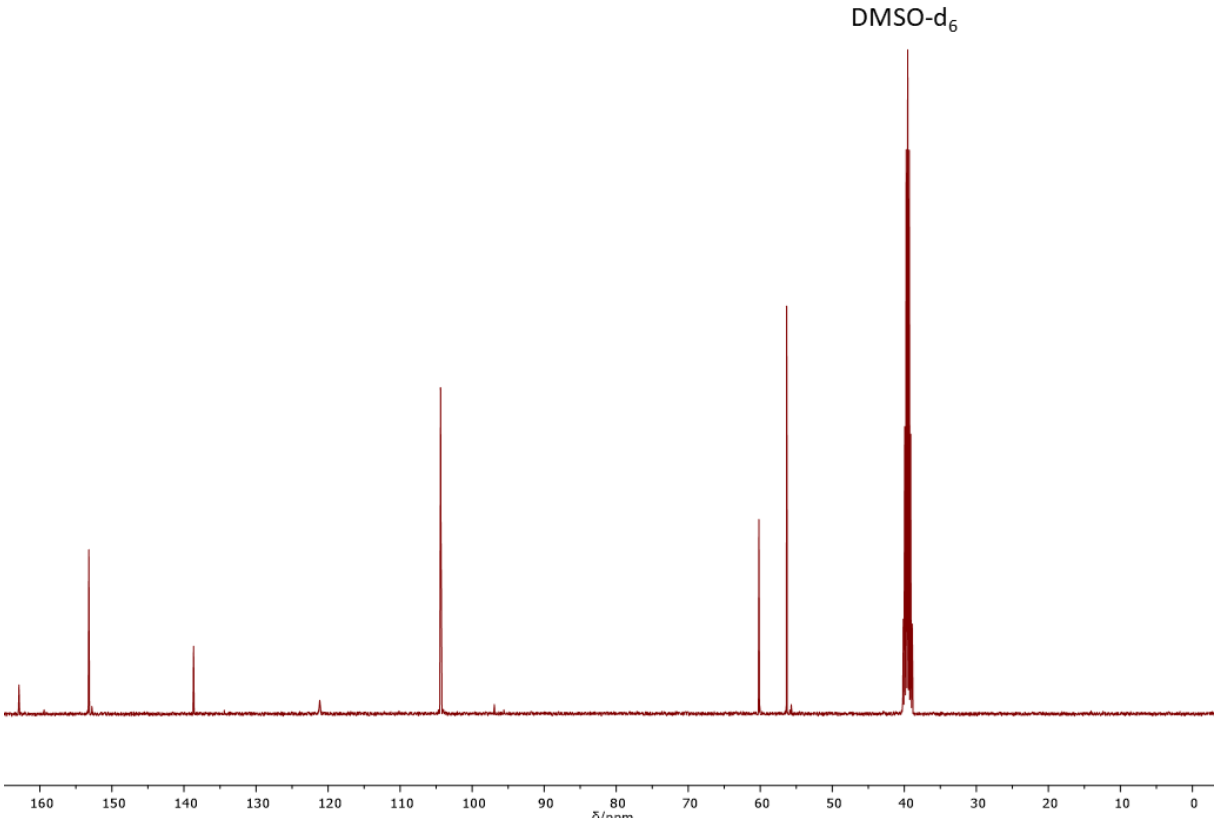

Figure 160: ^{13}C-NMR-spectrum of 3,4,5-trimethoxyphenyl isocyanide.

HRMS (EI): calculated m/z for $C_{10}H_{11}N_1O_3$ [M^+] = 193.0733, found: 193.0734, Δ = 0.0446 mmu.

IR: *v* / cm^{-1} = 3009 (vw), 2972 (w), 2939 (w), 2832 (w), 2131 (m), 1590 (s), 1502 (s), 1456 (s), 1444 (s), 1430 (m), 1417 (s), 1331 (m), 1230 (vs), 1177 (w), 1125 (vs), 1000 (vs), 961 (s), 839 (vs), 817 (m), 810 (m), 778 (s), 747 (w), 679 (w), 617 (m), 522 (w), 500 (w).

6.6.4 Synthesis of *N*-formamides

5-Formamido-1-(formamidomethyl)-1,3,3-trimethyl cyclohexane

Isophorendiamine (5.43 mL, 5.00 g, 29.4 mmol, 1.00 eq.) was dissolved in ethyl formiate (23.6 mL, 21.7 g, 294 mmol, 10.0 eq.) and was stirred under reflux for 24 hours. Afterwards, the remaining ethylformiate as well as the ethanol were removed under reduced pressure and the crude formamide (5.30 g) was used without further purification.

3,4,5-Trimethoxyphenyl formamide

3,4,5-trimethoxyphenyl amine (1.50 g, 8.19 mmol, 1.00 eq.) was dissolved in formic acid (1.24 mL, 1.51 g, 32.8 mmol, 4.00 eq.) and was stirred under reflux for 18 hours. Afterwards, the remaining formic acid as well as water were removed under reduced pressure and the crude formamide (1.83 g) was used without further purification.

6.6.5 Synthesis of PolyTUs

General synthesis of polyTUs (GP2)

The diisothiocyanate (1.00 eq.) was dissolved in DMF (*c*(diisothiocyaante) = 1.0 M) and diamino pentane **76** (1.00 eq.) was added. The reaction was stirred at room temperature until full conversion of the diisothiocyanate was indicated by TLC. Subsequently, methanol (5 times the amount of used DMF) was added to precipitate the polythiourea. After filtration, the product was washed with minimal amounts of methanol and dried under reduced pressure to remove the remaining solvent. Deviations of this procedure are given in the section of the respective substrate.

PolyTU 77

The polymer was synthesized according to procedure GP2. Diisothiocyante **57** (256 mg, 1.00 mmol, 1.00 eq.) and diamino pentane **76** (117µL, 102 mg, 1.00 mmol, 1.00 eq.) were dissolved in 1 mL DMF and the reaction mixture was stirred for 2 h. The product was obtained as a colourless solid (314 mg) in a yield of 88%.

^{1}H-NMR (400 MHz, $CDCl_3$) δ / ppm = 7.30 (br, 4H, NH, ^{1}), 3.34 (br, 8H, CH_2, ^{2}), 1.47 (p, ^3J = 7.2 Hz, 8H, CH_2, ^{3}), 1.25 (br, 14H, CH_2, ^{4}).

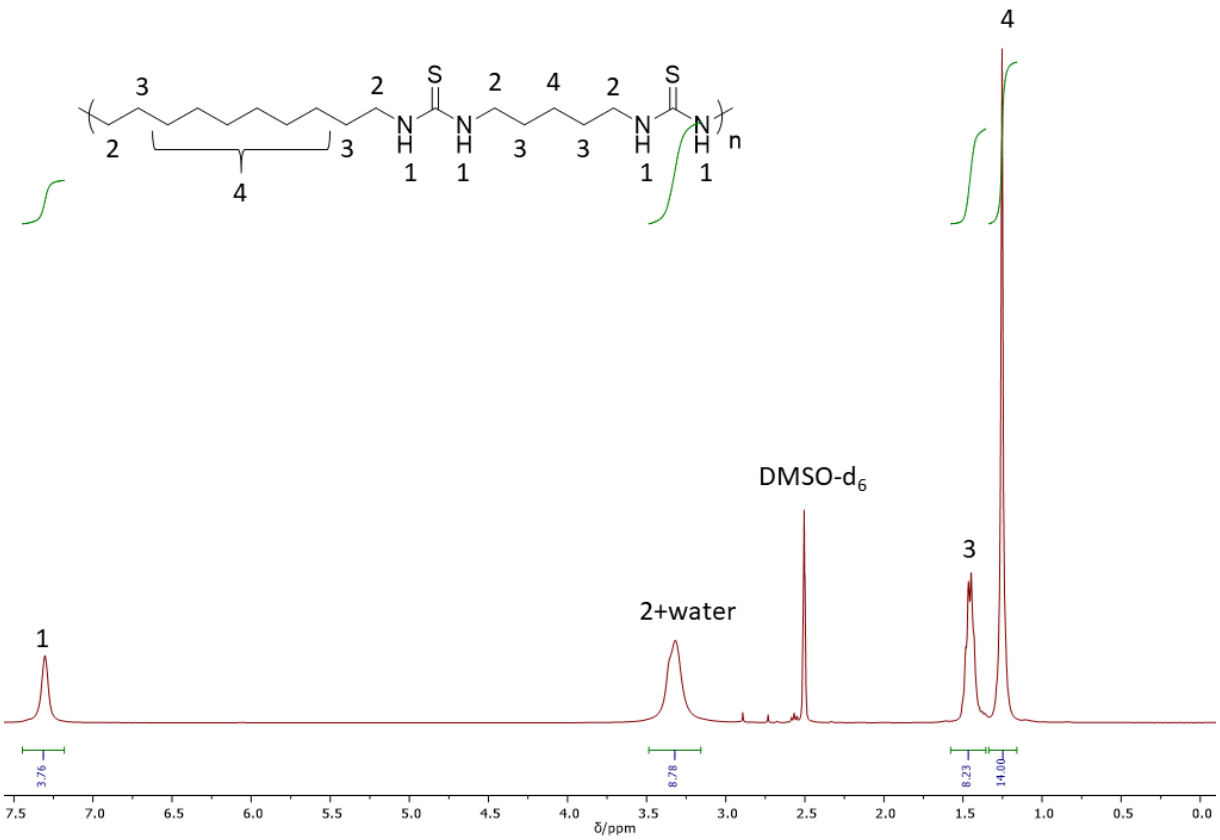

*Figure 161: ^{1}H-NMR-spectrum of polyTU **77**.*

^{13}C-NMR (101 MHz, $CDCl_3$) δ / ppm = 181.55 (br, HNC=SNH), 43.41 (NHC=SNH-**C**H_2), 29.01 (CH_2), 28.82 (CH_2), 28.59 (CH_2), 26.43 (CH_2), 23.82 (CH_2).

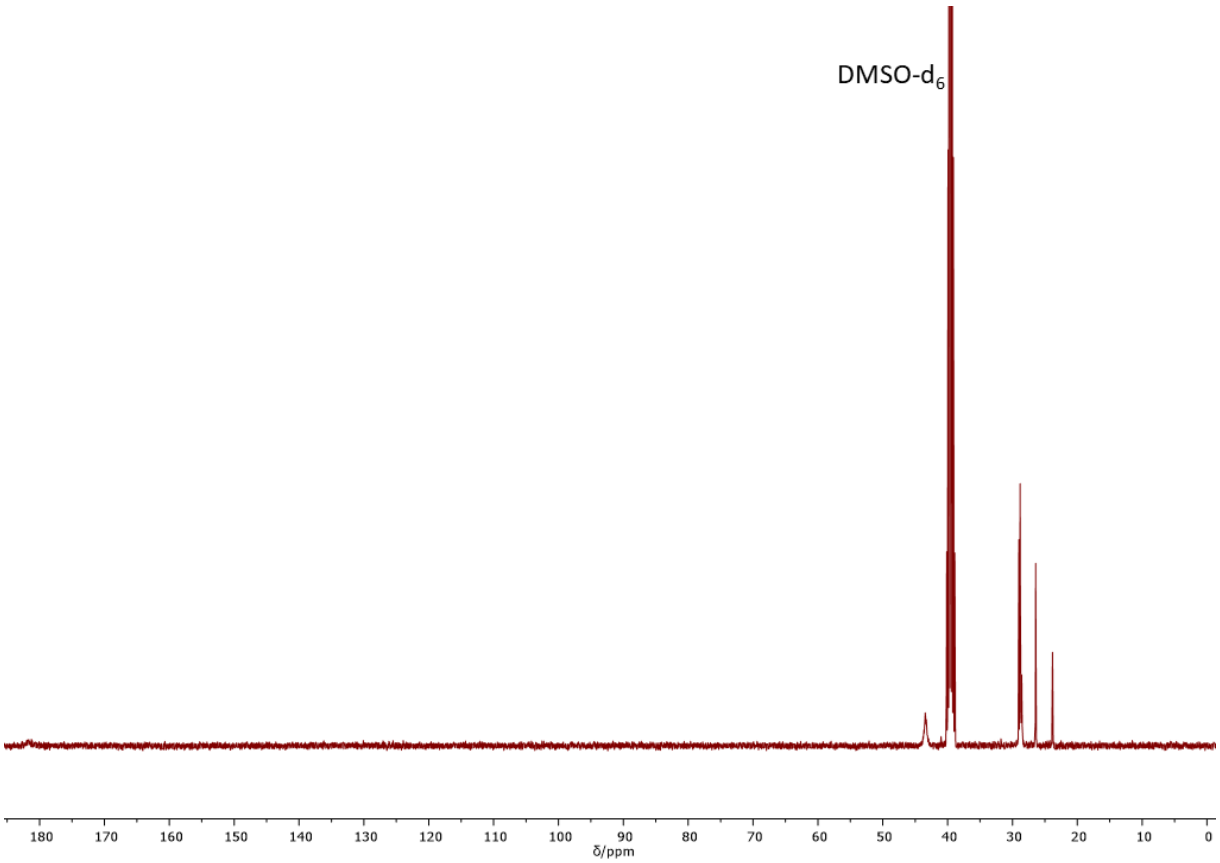

*Figure 162: ^{13}C-NMR-spectrum of polyTU **77**.*

IR: *v* / cm^{-1} = 3237 (br, m), 3065 (br, w), 2917 (s), 2849 (s), 1544 (vs), 1460 (m), 1349 (vs), 1290 (vs), 1237 (s), 1054 (m), 728 (s), 674 (vs), 579 (s), 540 (vs)

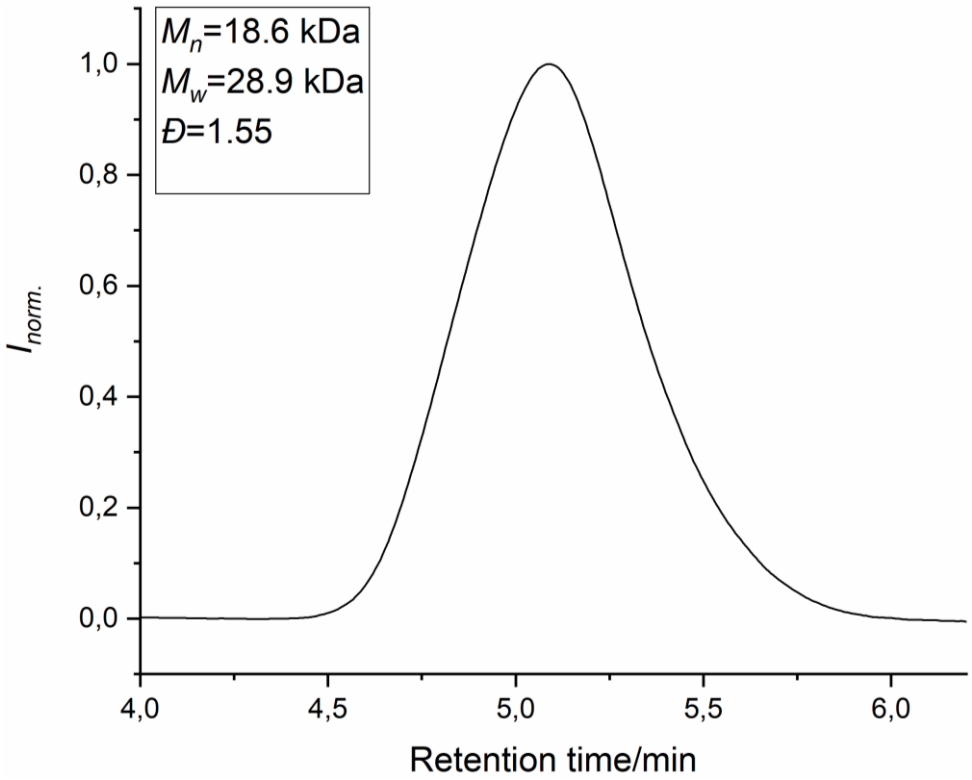

*Figure 163: SEC-trace of polyTU **77**.*

PolyTU 78

The polymer was synthesized according to the procedure GP2. Diisothiocyante 58 (284 mg, 1.00 mmol, 1.00 eq.) and diamino pentane **76** (117µL, 102 mg, 1.00 mmol, 1.00 eq.) were dissolved in 1 mL DMF and the reaction mixture was stirred for 2 h. Remaining solvent was removed in a vacuum oven (80 °C, 10 mbar, 16 hours). The product was obtained as a colourless solid (387 mg) in a quantitative yield.

^{1}H-NMR (400 MHz, $CDCl_3$) δ / ppm = 7.29 (br, 4H, NH, ^{1}), 3.35 (br, 8H, CH_2, ^{2}), 1.46 (p, ^3J = 7.2 Hz, 8H, CH_2, ^{3}), 1.25 (br, 18H, CH_2, ^{4}).

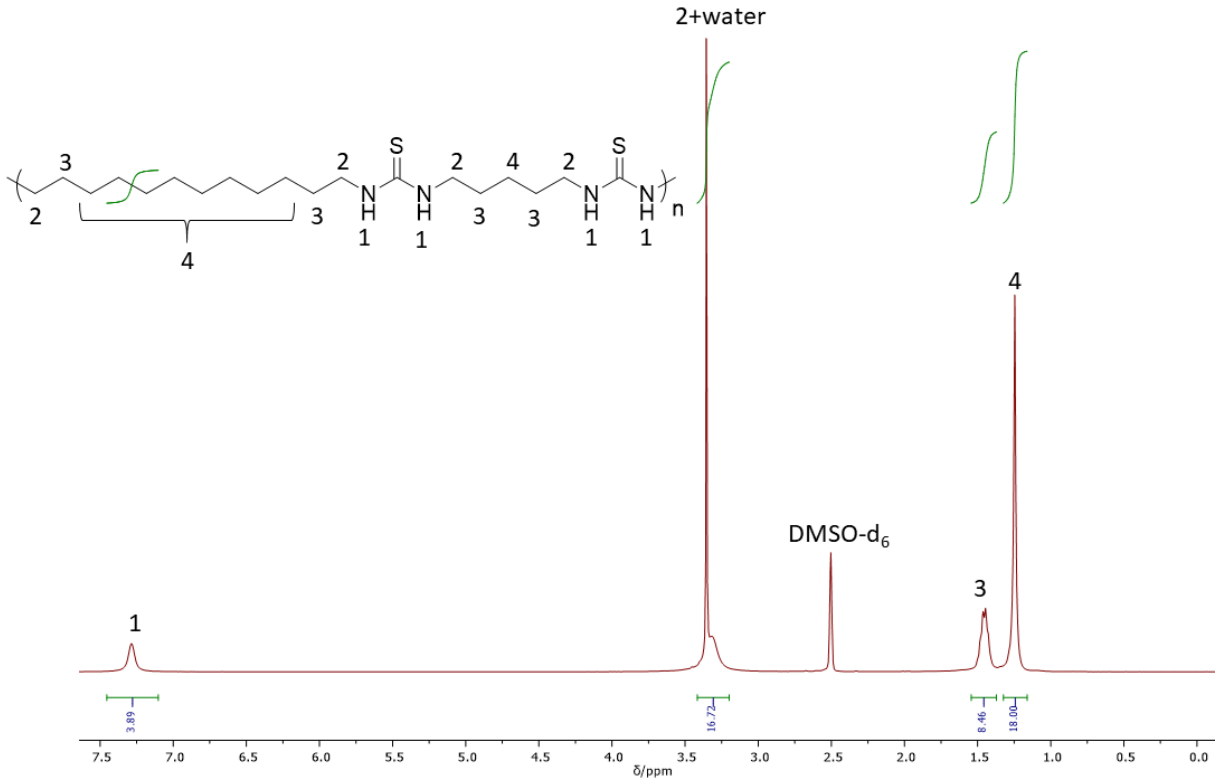

*Figure 164: ^{1}H-NMR-Spectrum of polyTU **78**.*

^{13}C-NMR (101 MHz, $CDCl_3$) δ / ppm = 181.89 (br, HNC=SNH), 43.45 (HNC=SNH-**C**H_2), 29.08 (CH_2), 28.85 (CH_2), 28.61 (CH_2), 26.45 (CH_2), 23.84 (CH_2).

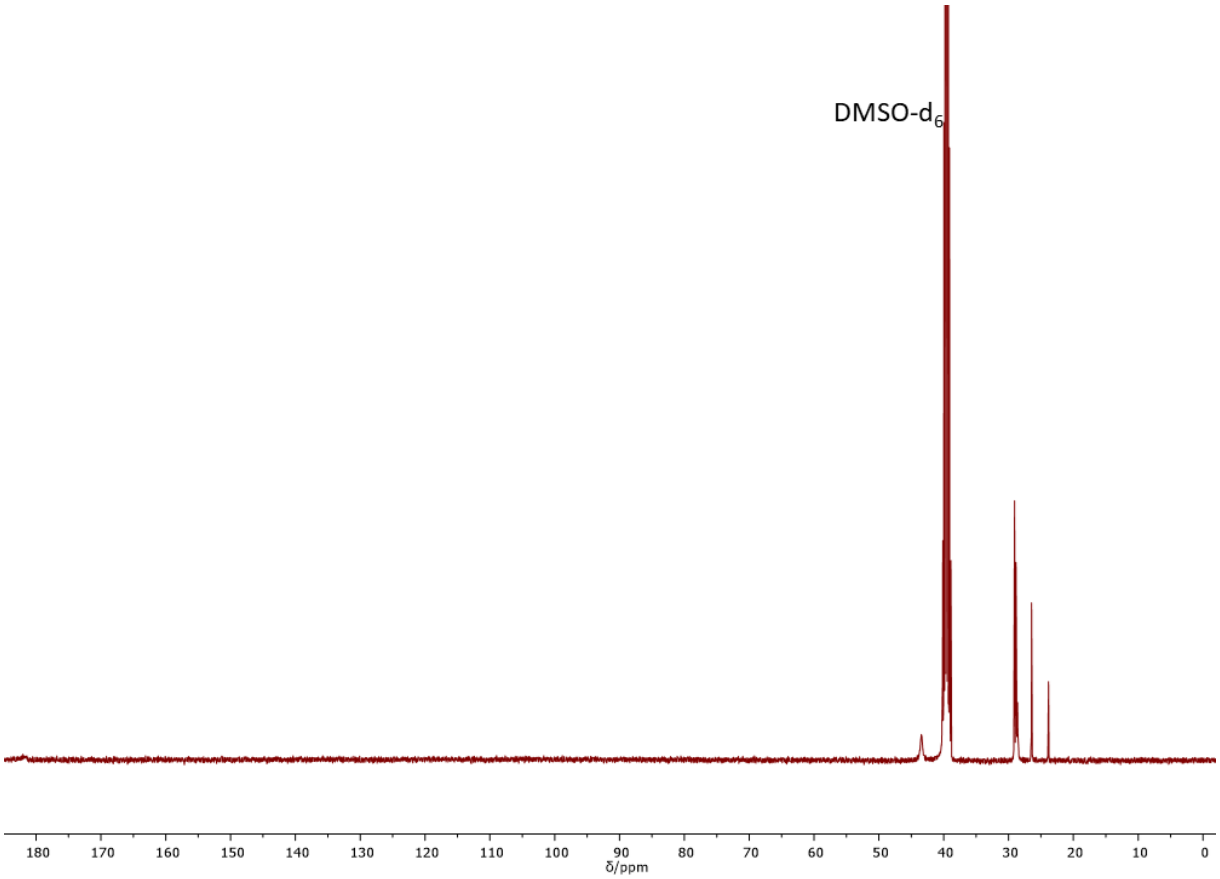

*Figure 165: ^{13}C-NMR-Spectrum of polyTU **78**.*

IR: *v* / cm^{-1} = 3237 (br, w), 3071 (br, w), 2919 (vs), 2850 (s), 1551 (vs), 1466 (w), 1353 (s), 1319 (m), 1285 (s), 1242 (m), 1064 (w), 728 (w), 669 (m), 577 (m), 544 (m), 509 (w), 475 (w).

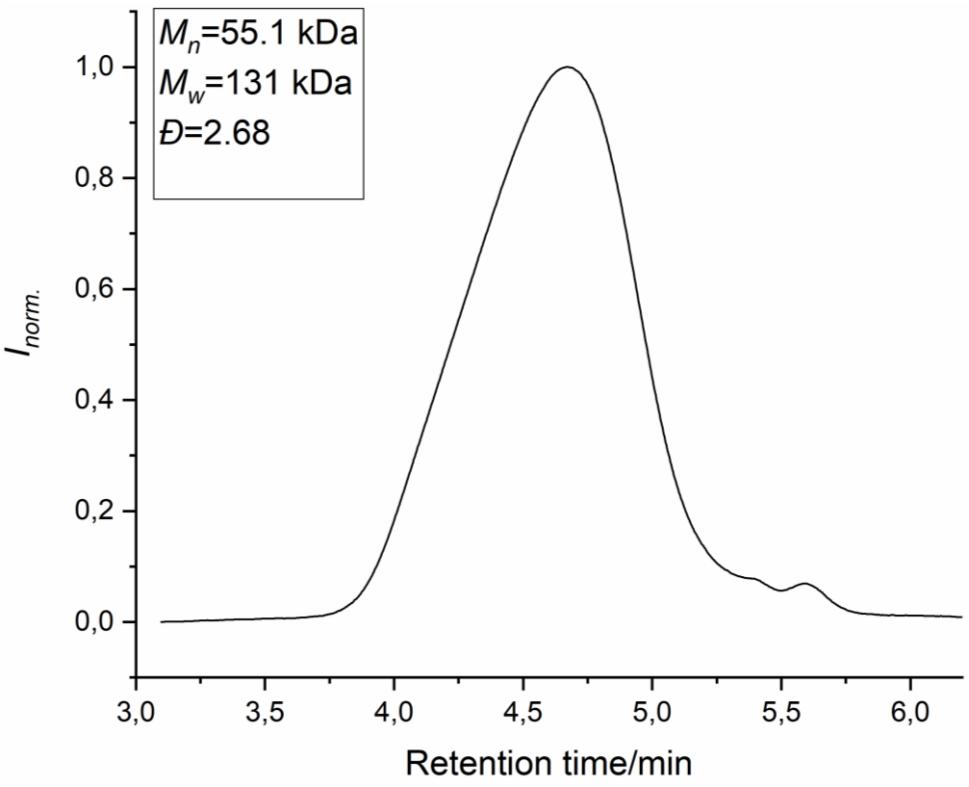

*Figure 166: SEC-trace of polyTU **78**.*

PolyTU 79

The polymer was synthesized according to the procedure GP2. Diisothiocyante **62** (254 mg, 1.00 mmol, 1.00 eq.) and diamino pentane **76** (117µL, 102 mg, 1.00 mmol, 1.00 eq.) were dissolved in 1 mL DMF and the reaction mixture was stirred for 2 h. The crude product was obtained as a hollow polymer orb and thus, was crushed with a mortar. Remaining DMF was removed by vacuum oven (80 °C, 10 mbar, overnight) followed by washing in minimal amount of methanol under reflux to remove remaining DMF. The product was obtained as a colourless solid (376 mg) in a quantitative yield.

^{1}H-NMR (400 MHz, $CDCl_3$) δ / ppm = 7.58-6.89 (m, 4H, NH, ^{1}), 4.41 (br, 0.76H, CH, ^{2}), 4.09 (br, 0.61H, CH_2, ^{2}), 3.57-3.07 (m, 5.63H, CH_2, CH, ^{2}), 1.81-0.76 (m, 21H, CH_3, CH_2, ^{3}).

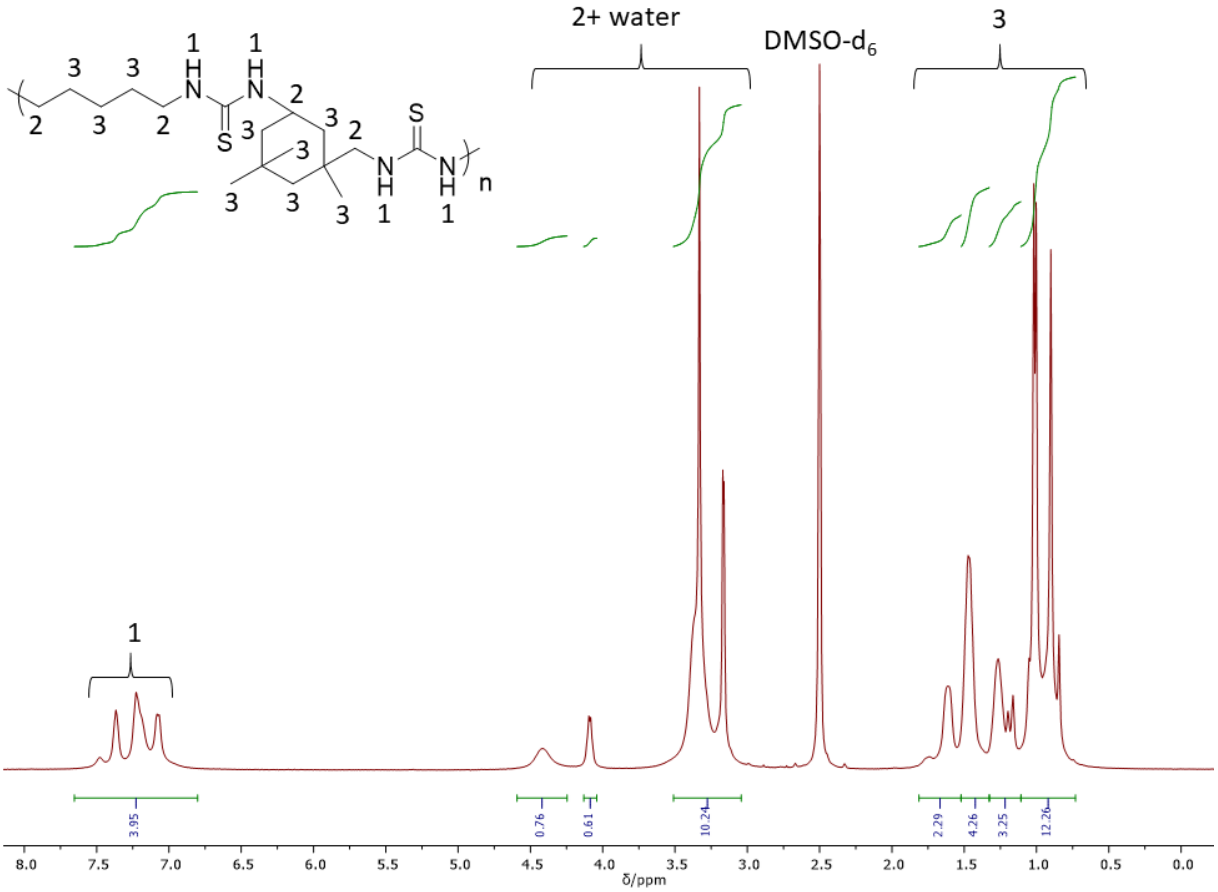

*Figure 167: ^{1}H-NMR-Spectrum of polyTU **79**.*

^{13}C-NMR (101 MHz, $CDCl_3$) δ / ppm = 183.53 (br, HNC=SNH), 181.34 (br, HNC=SNH), 57.48, 48.60, 47.24, 46.78, 45.32, 43.59, 43.35, 41.24, 36.33, 35.81, 34.93, 31.66, 31.50, 29.86, 28.62, 27.52, 23.89, 23.22.

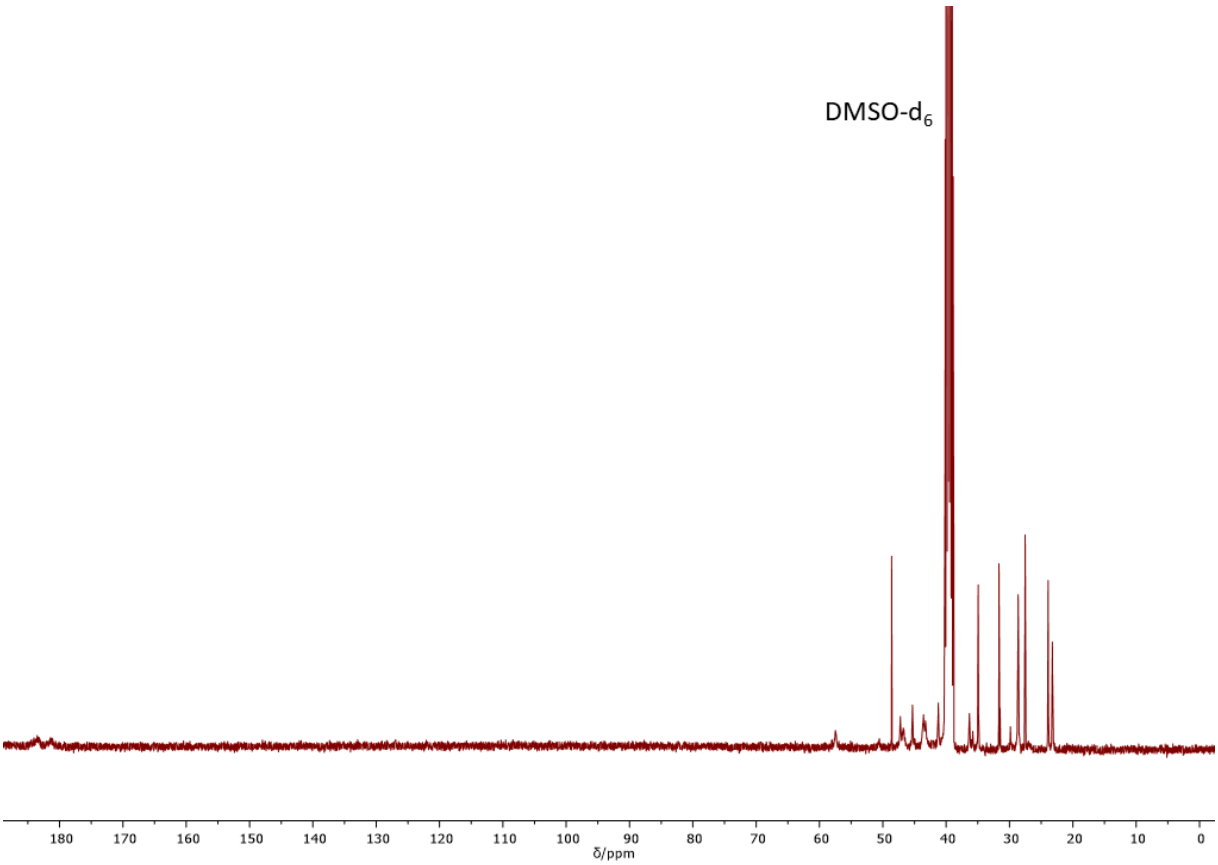

*Figure 168: [13]C-NMR-Spectrum of polyTU **79**.*

IR: *v* / cm^{-1} = 3248 (br, s), 3060 (br, w), 2924 (br, s), 2850 (br, m), 1734 (w), 1534 (vs), 1460 (m), 1305 (s), 1235 (vs), 1210 (vs), 1196 (vs), 1068 (s), 1014 (vs), 696 (w), 660 (w), 507 (m), 456 (s)

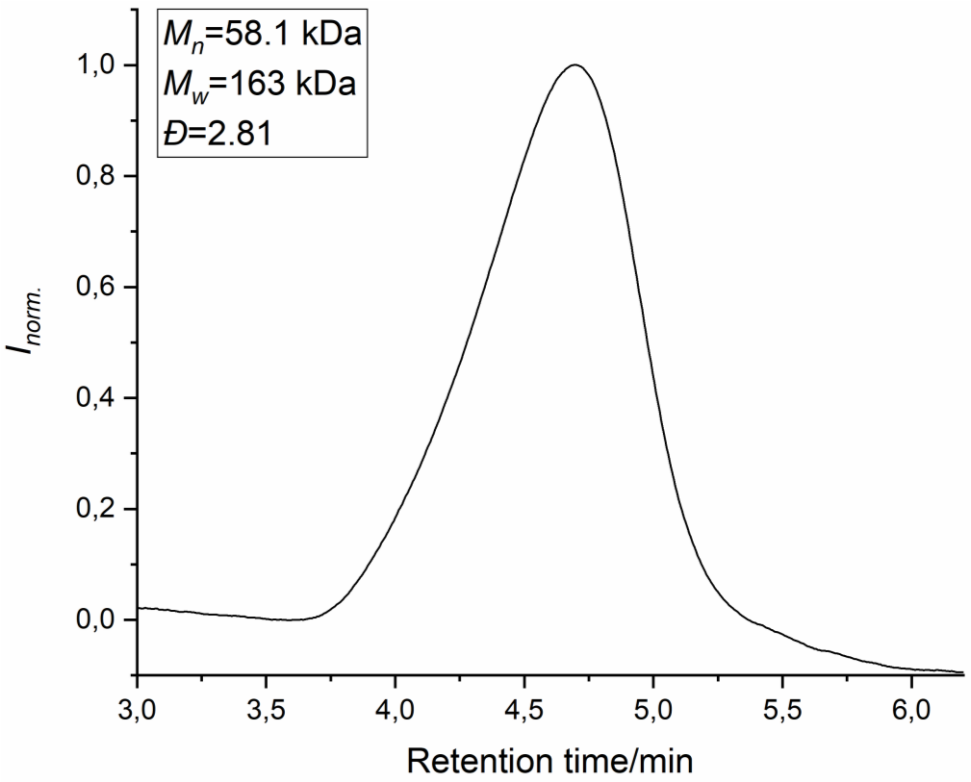

*Figure 169: SEC-trace of polyTU **79**.*

6.6.6 E-factor calculation

E-factors were calculated with the following equation:

$$E = \frac{m_{waste}}{m_{product}} = \frac{\sum_{i=1}^{n}((n_i - \nu_i * n_{product}) * M_i) + m_{cat} + m_{solvent}}{m_{product}} \quad (10)$$

$m_{product}$ = isolated mass of product considering the GC-purity
$n_{product}$ = isolated molar amount of product
n_i = originally used molar amount of reactant i
ν_i = stoichiometric coefficient of reactant i (1 for IC, 0.125 for S_8)
m_{cat} = mass of used DBU
$m_{solvent}$ = mass of reaction solvent

m(product): was calculated considering the purity obtained by GC.

6.7 Reaction of activated sulfur with benzhydryl carbenes-unexpected alkene formation

6.7.1 Pictures of the work-up of 83

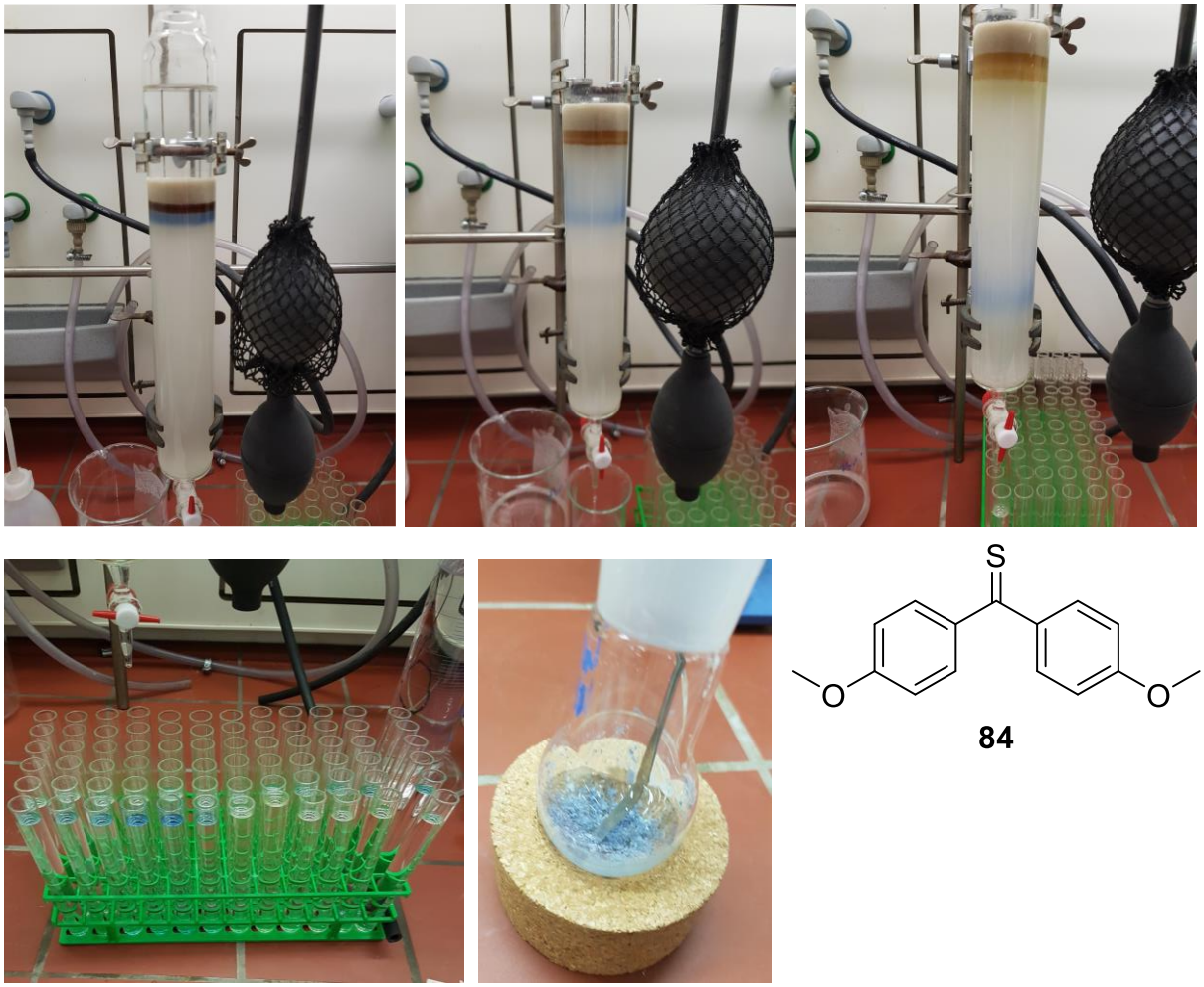

Figure 170: Pictures of the work-up of tetra(4-methoxyphenyl)ethylene ***83*** *obtained after the reaction of the respective tosylhydrazone* ***82*** *with elemental sulfur and sodium hydride. The top part depicts the column chromatography in which the product fraction can be seen by visual observation due to a blue coloration, which arises not from product* ***83*** *but probably from the respective thioketone* ***84*** *that is formed as an intermediate in this reaction exhibiting a very similar R_f-valuer. In addition, the obtained fractions from the column chromatography and product* ***83*** *in high purity (pure according to ^{1}H-NMR) are depicted (bottom) exhibiting also the characteristic blue coloration, which can probably be assigned to the presence of thioketone* ***84****.*

6.7.2 Synthesis of tetraarylethylenes

Tetraphenylethylene 85

Benzophenone tosylhydrazone (600 mg, 1.71 mmol, 1.00 eq.) was dissolved in 1.7 mL DMSO. Then, elemental sulfur (87.8 mg, 342 µmol, 0.20 eq. corresponding to 1.60 eq. of sulfur atoms) and potassium carbonate (284 mg, 2.05 mmol), 1.20 eq.) were added and the dark brown suspension was heated to 100 °C for 30 minutes. After cooling to ambient temperature, 3 mL of methanol was added. Subsequently, DCM and water were added and the organic layer was separated. The aqueous layer was extracted (3x) and the combined organic extracts were washed with water (2x), dried over sodium sulfate and filtered off. The crude product was purified by column chromatography (CH:EA, 99:1) yielding the pure product (275 mg, 827 µmol) as colorless solid in a yield of 97%.

R_f = 0.67 in cyclohexane/ethyl acetate = 49:1 visualized *via* UV quenching at 254 nm and fluorescence at 365 nm.

^{1}H-NMR (400 MHz, $CDCl_3$) δ / ppm = 7.12-7.07 (m, 12H, aromatic, [1]), 7.04-7.01 (m, 8, aromatic, [2])

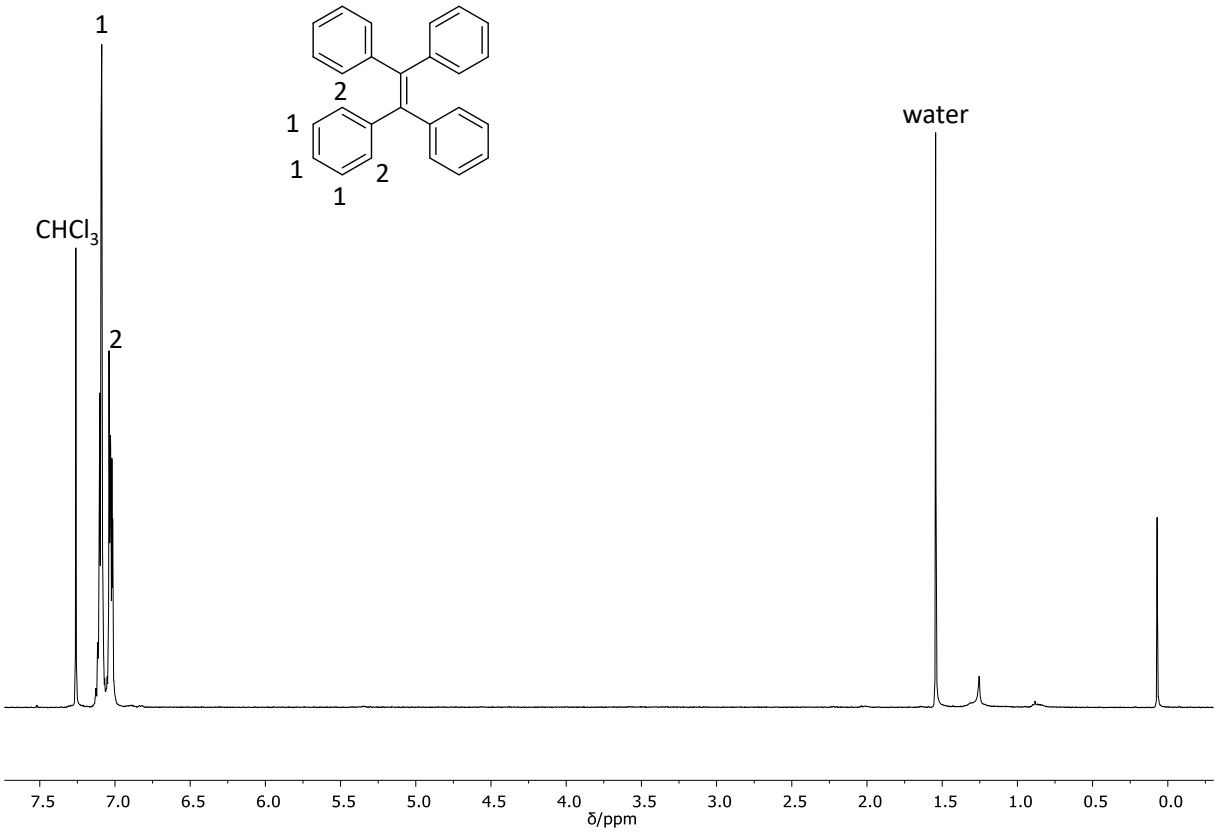

*Figure 171: ^{1}H-NMR-spectrum of tetraphenylethylene **85**.*

^{13}C-NMR (101 MHz, $CDCl_3$) δ / ppm = 143.72 (quarternary-aromatic), 140.95 (C=C), 131.32 (aromatic), 127.63 (aromatic), 126.40 (aromatic).

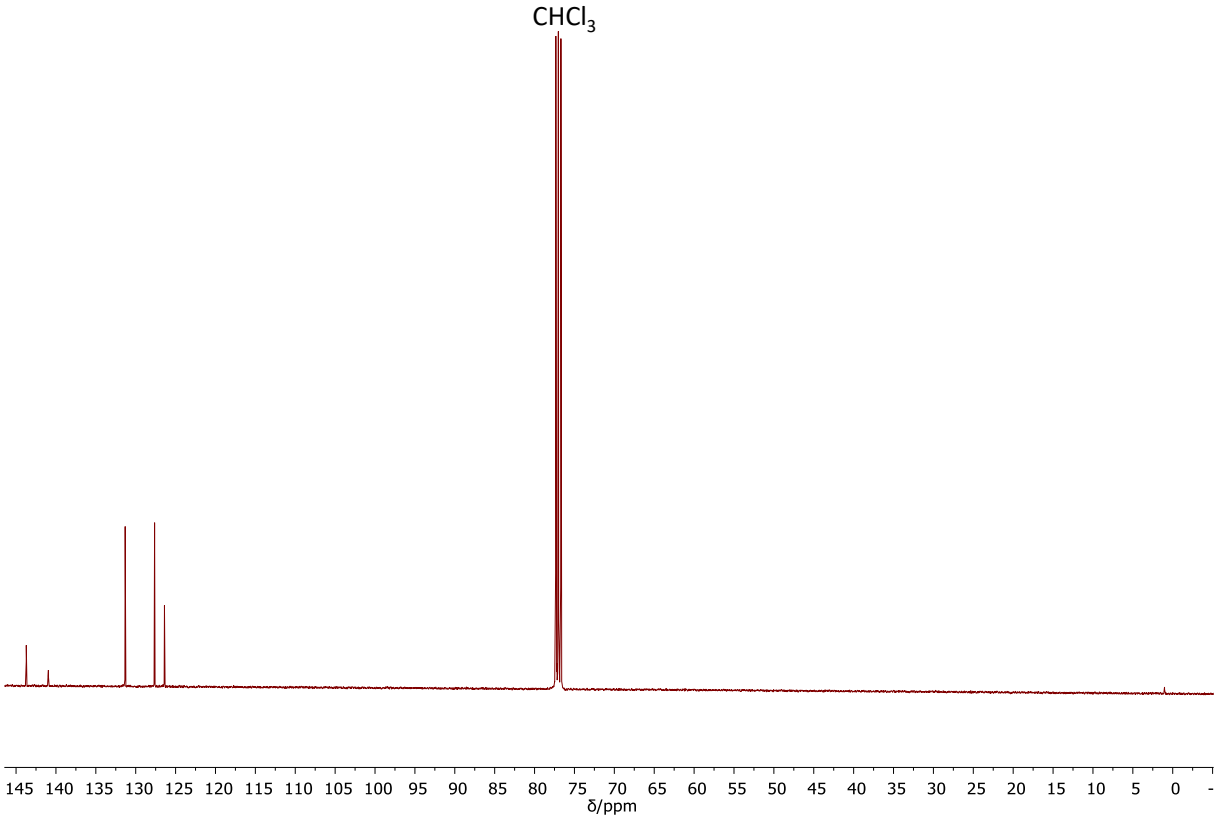

*Figure 172: ^{13}C-NMR-spectrum of tetraphenylethylene **85**.*

HRMS (EI): calculated m/z for $C_{26}H_{20}$ [M^+] = 332.1560, found:3321.1557, Δ = -0.2189 mmu.

IR: *v* / cm^{-1} = 3077 (vw), 3050 (vw), 3015 (vw), 2923 (w), 2853 (vw), 1954 (vw), 1886 (vw), 1814 (vw), 1746 (vw), 1594 (w), 1574 (vw), 1489 (w), 1442 (m), 1154 (vw), 1074 (w), 1026 (w), 1002 (vw), 981 (w), 913 (vw), 907 (vw), 778 (w), 759 (m), 745 (s), 695 (vs), 625 (s), 615 (m), 568 (m), 471 (w), 465 (w), 442 (vw)

Tetra(4-methoxyphenyl)ethylene 83

4,4-´dimethoxybenzophenone tosylhydrazone **82** (600 mg, 1.46 mmol, 1.00 eq.) was dissolved in 1.5 mL DMSO. Then, elemental sulfur (75.0 mg, 292 µmol, 0.20 eq. corresponding to 1.60 eq. of sulfur atoms) and potassium carbonate (242 mg, 1.75 mmol, 1.20 eq.) were added and the dark brown suspension was heated to 100 °C for 30 minutes. After cooling to ambient temperature, the crude product was directly applied for column chromatography (CH:EA, 8:1) yielding the pure product (331 mg, 730 µmol) as colorless solid in quantitative yield.

R_f = 0.41 in cyclohexane/ethyl acetate = 5:1 visualized *via* UV quenching at 254 nm and fluorescence at 365 nm.

^{1}H-NMR (400 MHz, DMSO-d_6) δ / ppm = 6.85 (d, ^3J = 8.8 Hz, 8H, aromatic, ^{1}), 6.70 (d, ^3J = 8.9 Hz, 8H, aromatic, ^{2}), 3.68 (s, 12H, CH_3, ^{3}).

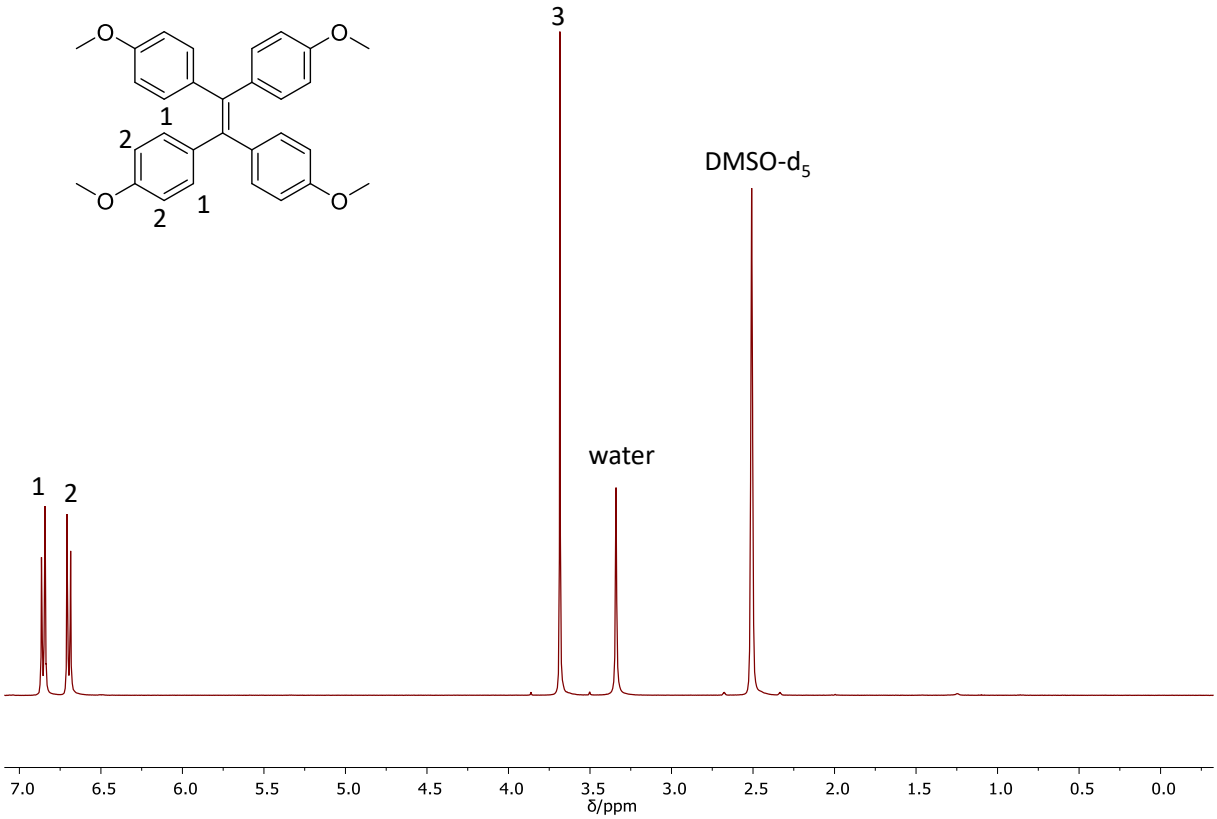

*Figure 173: ^{1}H-NMR-spectrum of tetra(4-methoxyphenyl)ethylene **83**.*

^{13}C-NMR (101 MHz, DMSO-d_6) δ / ppm = 157.43 (quarternary-aromatic), 137.98 (C=C), 136.24 (quarternary-aromatic), 131.97 (aromatic), 113.19 (aromatic), 54.88 (CH_3).

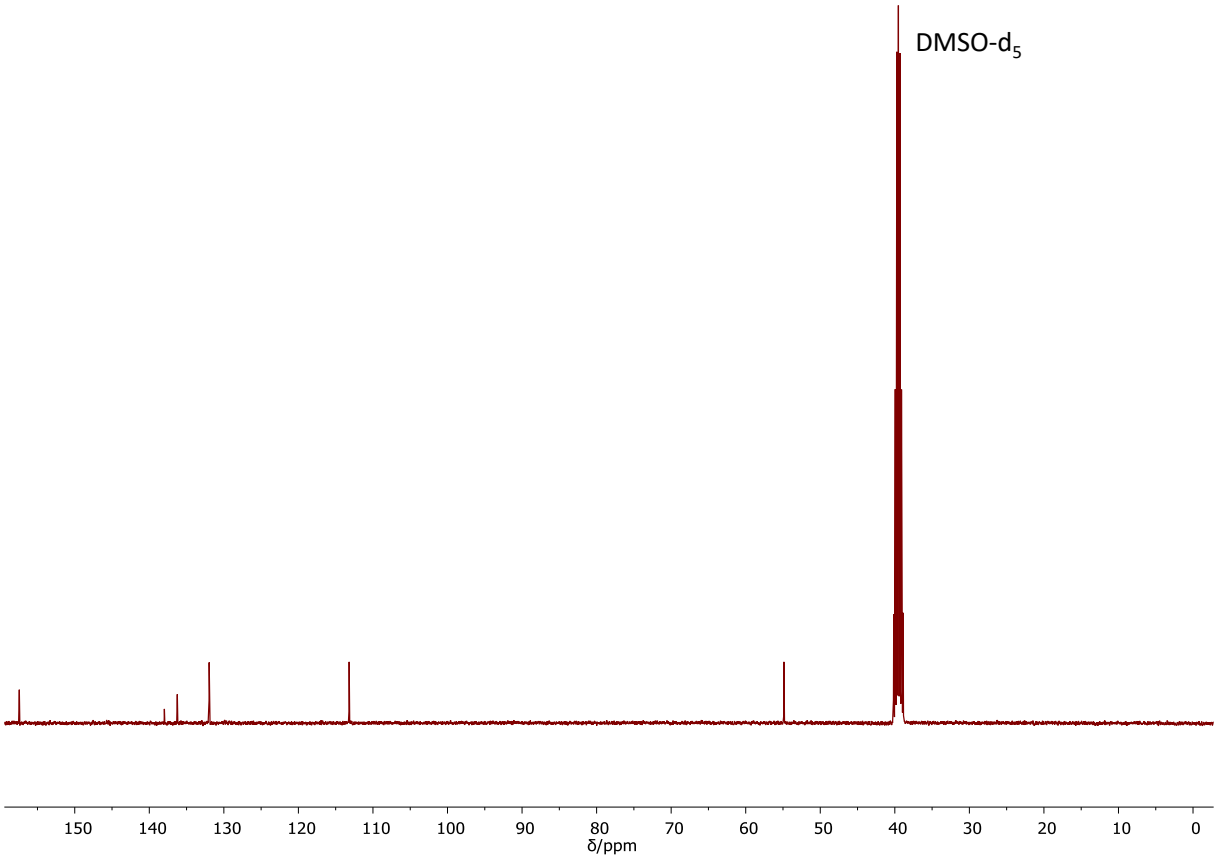

*Figure 174: ^{13}C-NMR-spectrum of tetra(4-methoxyphenyl)ethylene **83**.*

HRMS (EI): calculated m/z for $C_{30}H_{28}$ [M^+] = 452.1982, found: 452,1981, Δ = -0.0641 mmu.

IR: *v* / cm^{-1} = IR = 3050 (vw), 3026 (vw), 3001 (vw), 2948 (vw), 2890 (vw), 2828 (w), 1896 (vw), 1882 (vw), 1862 (vw), 1604 (m), 1571 (w), 1506 (vs), 1454 (m), 1440 (w), 1409 (w), 1294 (s), 1271 (w), 1238 (vs), 1183 (w), 1168 (vs), 1105 (m), 1031 (vs), 1012 (m), 977 (w), 954 (vw), 862 (w), 829 (vs), 808 (vs), 765 (m), 745 (w), 708 (vw), 588 (vs), 568 (w), 525 (m), 510 (w) cm-1

6.7.3 Synthesis of benzhydryltosylhydrazones

Benzophenonetosylhydrazone

This protocol followed the procedure of Wang *et al.*[635] Benzophenone (2.50 g, 13.7 mmol, 1.00 eq.) was dissolved in 10 mL ethanol. Then, tosylhydrazine (2.55 g, 13.72 mmol, 1.00 eq.) and *p*-toluenesulfonic acid monohydrate (26.1 mg, 137 µmol, 0.01 eq.) were added and the mixture was stirred at reflux overnight. After cooling to ambient temperature the precipitate was filtered off, recrystallized from ethanol yielding the product as colorless solid (4.01 g, 11.4 mmol) in a yield of 83%.

^{1}H-NMR (400 MHz, DMSO-d_6) δ / ppm = 10.45 (s, 1H, NH, ^{1}), 7.91 – 7.77 (d, ^3J = 8.2 Hz, 2H, aromatic, ^{2}), 7.56 – 7.48 (m, 3H, aromatic, ^{3}), 7.44 (d, ^3J = 8.1 Hz, 2H, aromatic, ^{4}), 7.41 – 7.30 (m, 3H, aromatic, ^{5}), 7.28 – 7.18 (m, 4H, aromatic, ^{6,7}), 2.40 (s, 3H, CH_3, ^{7}).

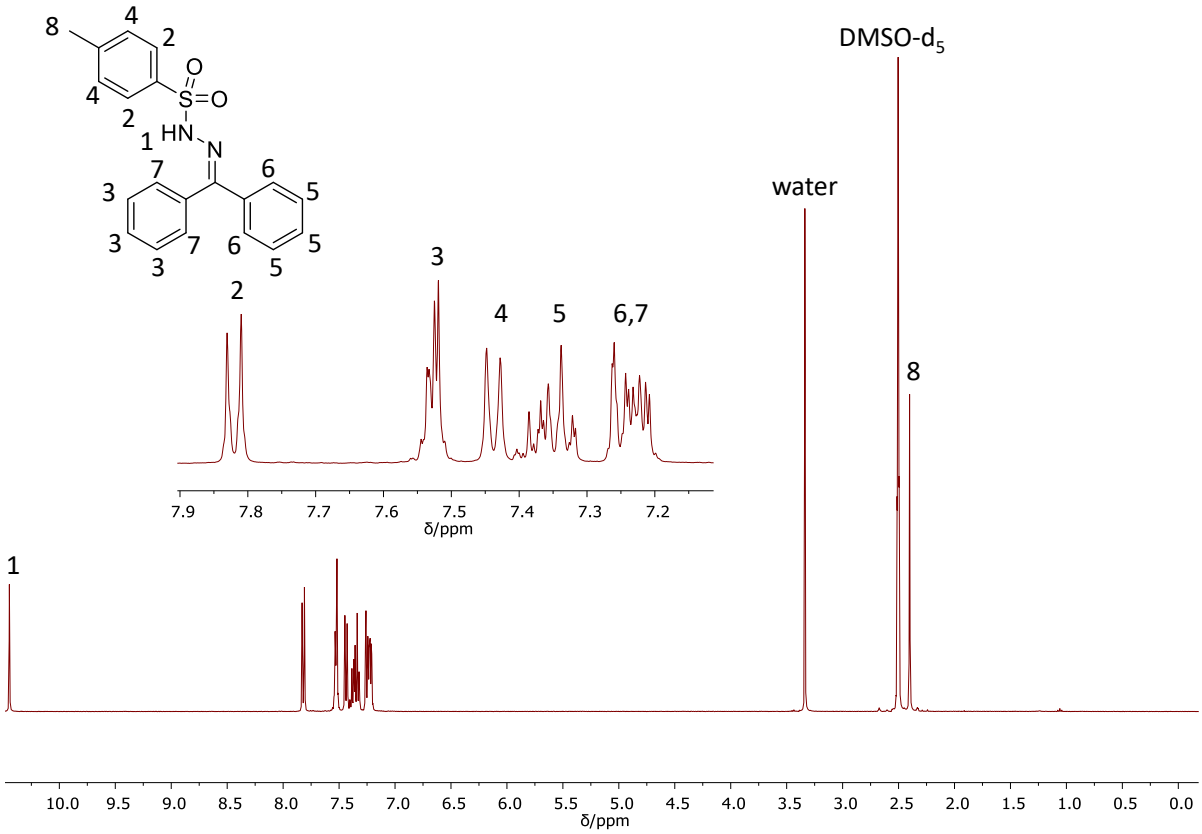

Figure 175: ^{1}NMR-spectrum of benzophenonetosylhydrazone. **^{13}C-NMR** (101 MHz, DMSO-d_6) δ / ppm = 154.55 (C=N), 143.35 (quarternary-aromatic), 137.16 (quarternary-aromatic), 136.06 (quarternary-aromatic), 132.56 (quarternary-aromatic), 129.70 (quarternary-aromatic), 129.44 (aromatic), 129.38 (quarternary-aromatic), 128.82 (aromatic), 128.35 (aromatic), 127.75 (aromatic), 127.22 (aromatic), 21.06 (CH_3).

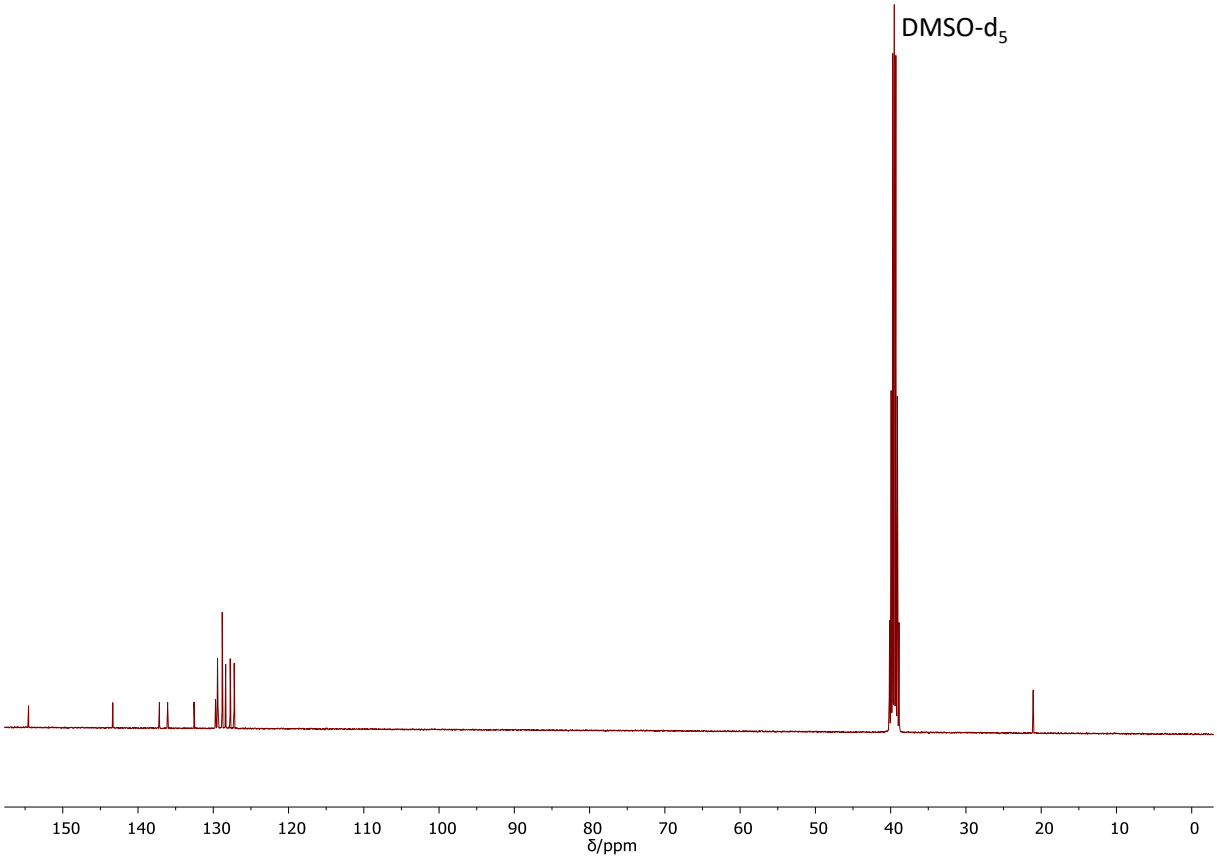

Figure 176: ^{13}C-NMR-spectrum of benzophenonetosylhydrazone.

HRMS (EI): calculated m/z for $C_{20}H_{18}N_2O_2{}^{32}S_1$ [M^+] = 350.1084, found: 350.1082, Δ = -0.1130 mmu.

IR: ν / cm^{-1} = IR = 3213 (w), 3063 (vw), 3030 (vw), 1954 (vw), 1896 (vw), 1818 (vw), 1771 (vw), 1446 (w), 1376 (s), 1349 (s), 1318 (m), 1302 (w), 1168 (vs), 1055 (m), 1026 (w), 977 (m), 874 (m), 812 (m), 771 (vs), 697 (vs), 666 (vs), 640 (m), 609 (w), 553 (vs), 543 (vs), 508 (s), 477 (w), 453 (m).

4,4-´Dimethoxy benzophenonetosylhydrazone 82

This protocol followed the procedure of Wang *et al.*[635] Benzophenone (5.00 g, 20.6 mmol, 1.00 eq.) was dissolved in 10 mL ethanol. Then, tosylhydrazine (3.84 g, 20.6 mmol, 1.00 eq.) and *p*-toluenesulfonic acid monohydrate (39.2 mg, 206 µmol, 0.01 eq.) were added and the mixture was stirred at reflux overnight. After cooling to ambient temperature the precipitate was filtered off, recrystallized from ethanol yielding the product as colorless needles (5.64 g, 13.7 mmol) in a yield of 67%.

^{1}H-NMR (400 MHz, DMSO-d_6) δ / ppm = 10.20 (s, 1H, NH, ^{1}), 7.80 (d, ^3J = 8.2 Hz, 2H, aromatic, ^{2}), 7.42 (d, ^3J = 8.0 Hz, 2H, aromatic, ^{3}), 7.19 (d, ^3J = 8.8 Hz, 2H,aromatic, ^{4}), 7.16 (d, ^3J = 8.8 Hz, 2H, aromatic, ^{5}), 7.07 (d, ^3J = 8.8 Hz, 2H, aromatic, ^{6}), 6.89 (d, ^3J = 8.8 Hz, 2H, ^{7}), 3.83 (s, 3H, CH_3, ^{8}), 3.75 (s, 3H, CH_3, ^{9}), 2.40 (s, 3H, CH_3, ^{10}).

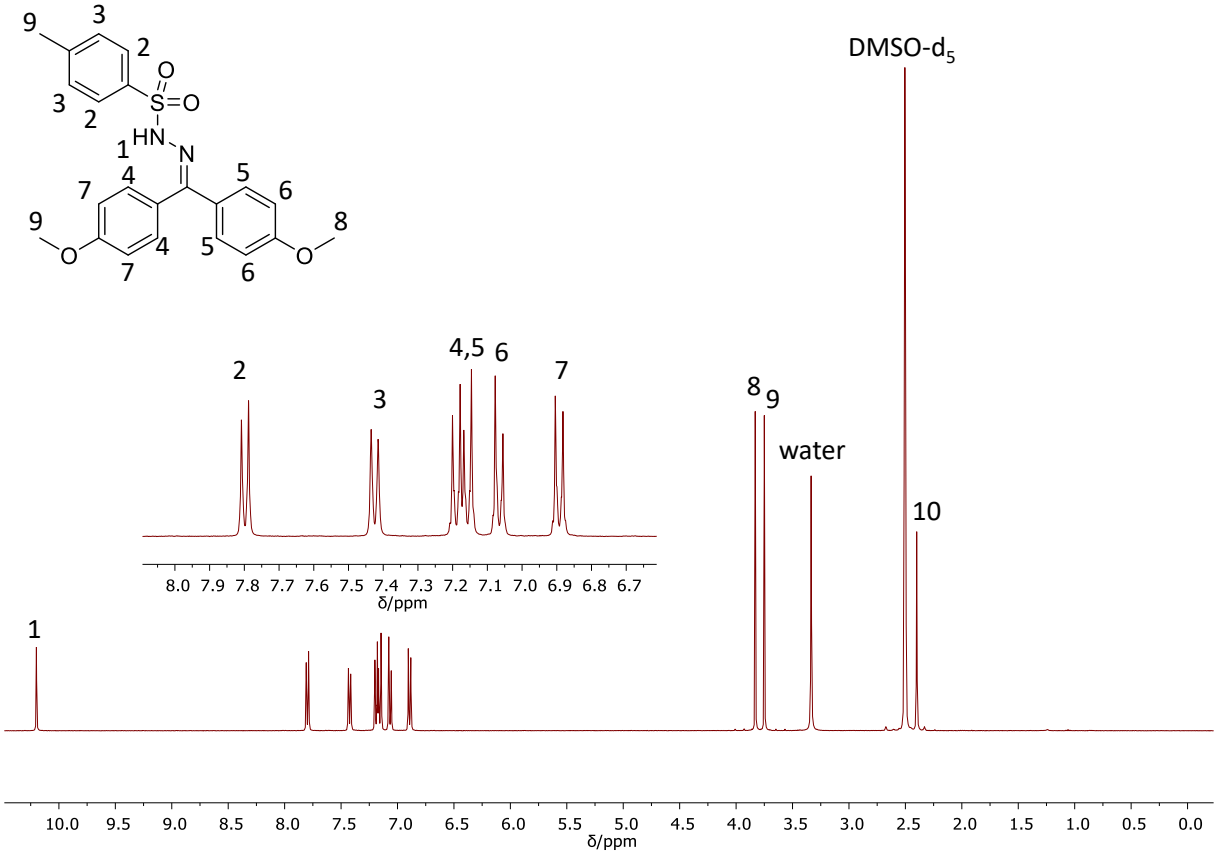

*Figure 177: ^{1}H-NMR-spectrum of 4,4´-dimethoxybenzophenonetosylhydrazone **82**.*

^{13}C-NMR (101 MHz, DMSO-d_6) δ / ppm = 160-46 (quarternary-aromatic), 159.84 (quarternary-aromatic), 154.47 (C=N), 143.19 (quarternary-aromatic), 136.12(quarternary-aromatic), 130.48(aromatic), 129.99 (quarternary-aromatic), 129.35 (aromatic), 128.91 (aromatic), 127.76 (aromatic), 124.76 (quarternary-aromatic),.114.10 (aromatic), 113.70 (aromatic), 55.23 (CH_3), 21.05 (CH_3).

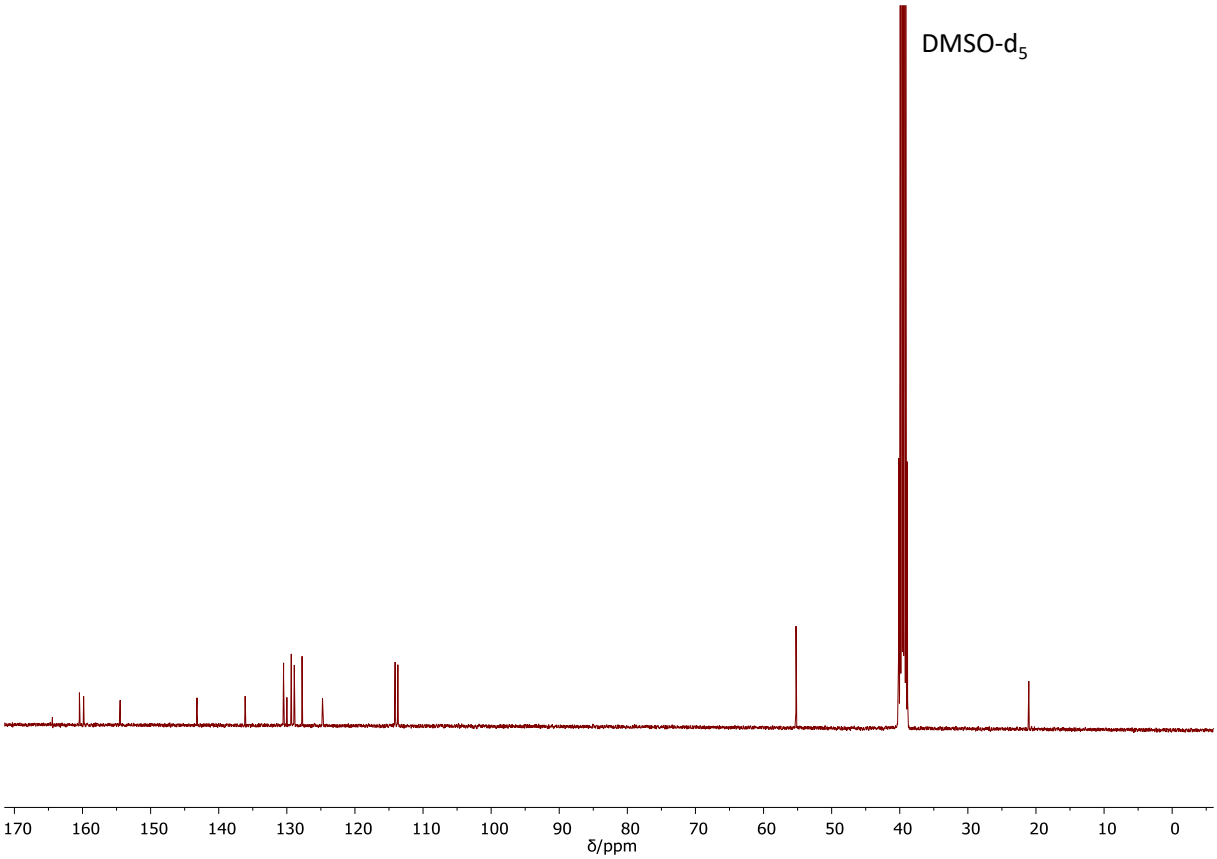

*Figure 178: ^{13}C-NMR-spectrum of 4,4´dimethoxy benzophenonetosylhydrazone **82**.*

HRMS (EI): calculated m/z for $C_{22}H_{23}N_2O_4{}^{32}S_1$ $[M+H]^+$ = 411.1373, found: 411.1375, Δ = 0.1535 mmu.

IR: *v* / cm^{-1} = 3201 (w), 3063 (vw), 3030 (vw), 3005 (vw), 2954 (vw), 2925 (vw), 2832 (vw), 2032 (vw), 1909 (vw), 1808 (vw), 1609 (m), 1578 (w), 1510 (s), 1495 (w), 1440 (w), 1419 (w), 1388 (m), 1341 (m), 1310 (s), 1298 (m), 1251 (vs), 1187 (w), 1174 (m), 1158 (vs), 1113 (w), 1092 (w), 1053 (m), 1031 (s), 1012 (m), 985 (s), 954 (w), 887 (m), 831 (vs), 812 (s), 784 (w), 734 (w), 706 (m), 689 (m), 662 (vs), 631 (w), 617 (w), 597 (m), 580 (m), 545 (vs), 518 (s), 498 (m), 481 (m), 444 (w), 413 (w), 405 (w).

6.8 Polythiosemicarbazones by Condensation of Dithiosemicarbazides and Dialdehydes

6.8.1 Dialdehyde synthesis

4,4'-(Ethyne-1,2-diyl) dibenzaldehyde 93

4-Bromo benzaldehyde (685 mg, 3.70 mmol, 1.00 eq.), 4-ethynyl benzaldehyde (482 mg, 3.70 mmol, 1.00 eq.), $Pd(PPh_3)_2Cl_2$,(130 mg, 185. µmol, 0.05 eq.) and CuI (35.3 mg, 185 µmol, 0.05 eq.) was added to a pressure tube with 20 mL dry THF (c(4-bromo benzaldehyde) = 0.133 M)). The mixture was purged for 5 minutes with an argon balloon and then was set under an argon funnel. Subsequently, TEA (9.3 mL, 6.74 g, 66.6 mmol, 18.0 eq.) was added with a syringe and the tube was closed. The black mixture was heated to 85 °C and stirred for two hours until TLC showed full conversion of the alkyne. After cooling to room temperature, all volatiles were removed under reduced pressure. Purification *via* column chromatography using DCM as eluent yielded the product as white crystals (527 mg, 2.25 mmol) in a yield of 61%. Proton NMR-analysis showed that the purity of the obtained compound was >96%, while the impurity was the respective Glaser product.

R_f (cyclohexane/ethyl acetate[5:1] = 0.41 visualizable *via* fluorescence quenching at 254 nm.

^{1}H-NMR was in accordance with literature. [636]

^{1}H-NMR (400 MHz, $CDCl_3$) δ/ppm = 10.04 (s, 2H, CH, ^{1}), 7.90 (d, ^3J = 8.4 Hz, 4H, aromatic, ^{2}), 7.71 (d,^{3} J = 8.2 Hz, 4H, aromatic, ^{3}).

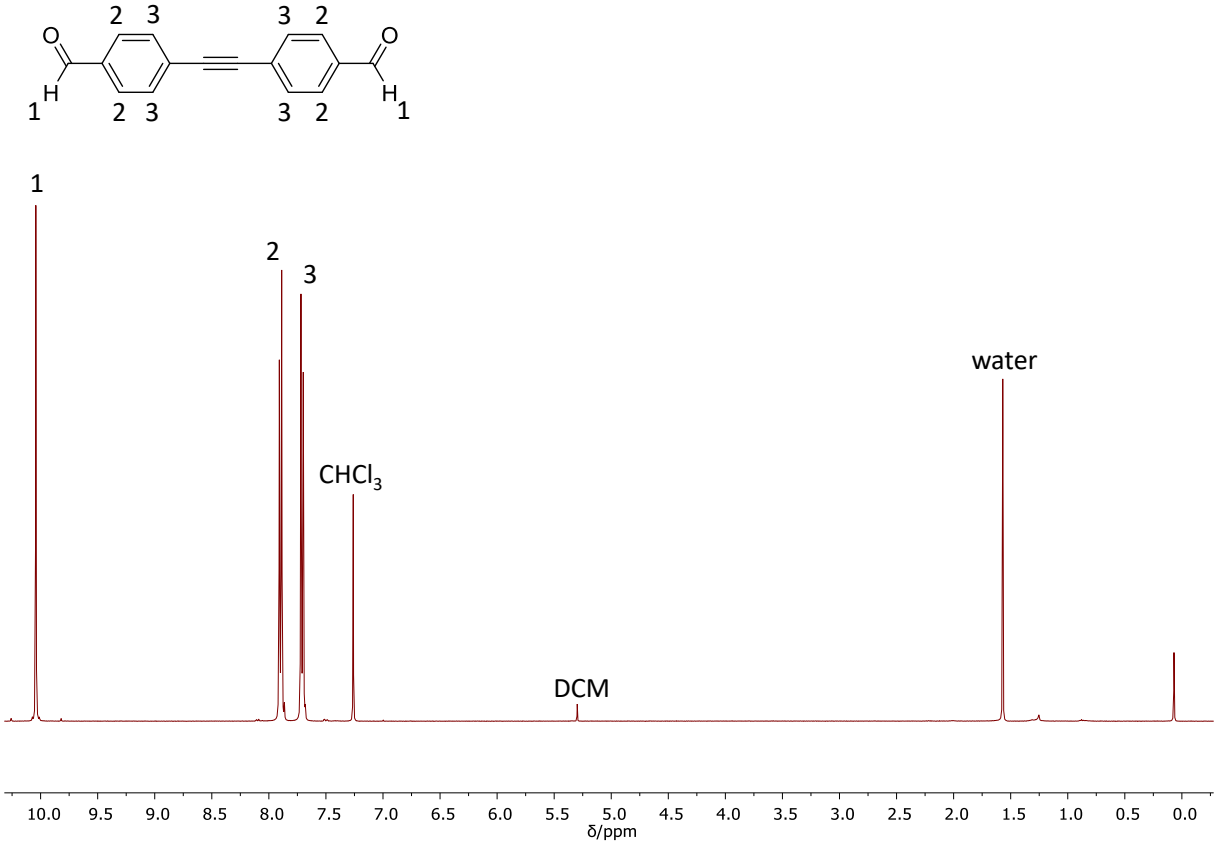

*Figure 179: Proton NMR-spectrum of **93**.*

6.8.2 Di-*N*-formamide syntehsis

1,6-Diisocyano hexane

A modified synthesis protocol of Meier *et al.* was used:[592]

1,6-*N*-formamido hexane (3.31 g, 19.22 mmol, 1.00 eq.) was dissolved in 58.2 mL DCM (c(di-*N*-formamide) = 0.33 M) and TEA (16.6 mL, 12.1 g, 119 mmol, 6.20 eq.) was added. Subsequently, the reaction mixture was cooled to 0°C using an ice-water bath and phosphorus oxychloride (4.67 mL, 7.66 g, 50.0 mmol, 2.60 eq.) was added dropwise, keeping the temperature at 0 °C. Afterwards, the cooling bath was removed, and the reaction was stirred at room temperature for 2 hours. After completion of the reaction, the reaction mixture was quenched with 60 mL of aqueous saturated $NaHCO_3$ solution. Subsequently, the organic layer was separated, the aqueous phase was extracted with DCM (1×30 mL) and the combined organic layers were washed with water (1×40 mL). The organic mixture was concentrated to a volume of ca. 5 mL. Purification was performed via flash column chromatography (typical height of silica loading: 6 cm). The reaction mixture was added dropwise directly onto the dry silica loaded column. Then, the product was purified by eluting with cyclohexane/ethyl acetate (2:1). The product was obtained as yellowish liquid (1.35 g, 9.91 mmol) in a yield of 52 %

R_f (cyclohexane/ethyl acetate[2:1] = 0.45 visualizable *via* vanillin staining (orange).

^{1}H-NMR was in accordance with spectra provided by Sigma-Aldrich.

^{1}H-NMR (400 MHz, $CDCl_3$) δ/ppm =3.41 (tt, ^3J = 6.5 Hz, $^2J_{NH}$ = 1.9 Hz, 4H, CH_2, ^{1}), 1.77-1.64 (m, 4H. CH_2, ^{2}), 1.53-1.48 (q, J = 7.4, 3.5 Hz, 4H, CH_2, ^{3}).

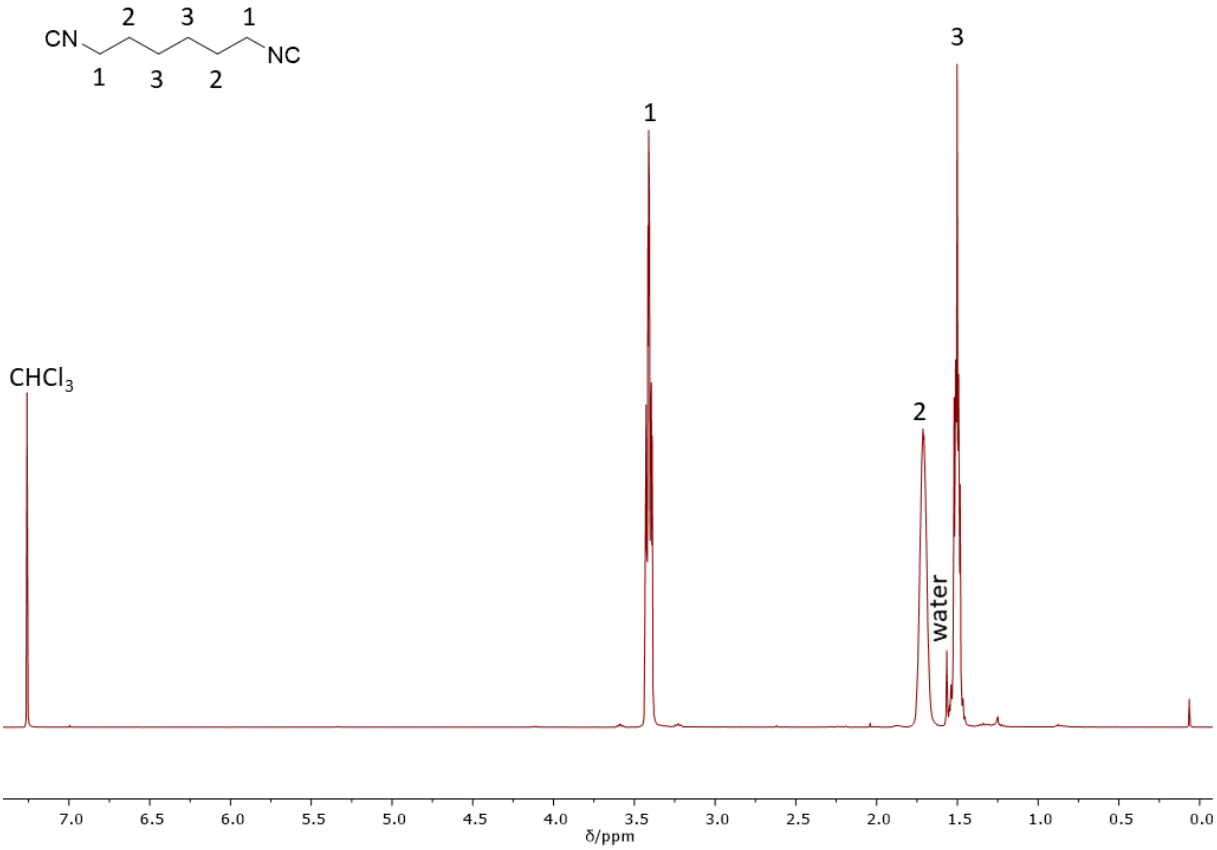

Figure 180: Proton NMR-spectrum of 1,6-diisocyano hexane.

***Trans*-1,4-diisocyano cyclohexane**

A modified synthesis protocol of Meier *et al.* was used:[592]

Trans-1,4-di-*N*-formamido cyclohexane (2.02 g, 11.9 mmol, 1.00 eq.) was dissolved in 36 mL DCM (c(di-*N*-formamide) = 0.33 M) and TEA (10.3 mL, 7.46 g, 73.7 mmol, 6.20 eq.) was added. Subsequently, the reaction mixture was cooled to 0°C using an ice-water bath and phosphorus oxychloride (2.89 mL, 4.74 g, 30.9 mmol, 2.60 eq.) was added dropwise keeping the temperature at 0 °C. After completion of the reaction, the reaction mixture was quenched with 35 mL of aqueous saturated $NaHCO_3$ solution, and the precipitated salt was filtered off. Subsequently, the organic layer was separated, the aqueous phase was extracted with DCM (3×30 mL) and the combined organic layers were washed with water (1×60 mL). The organic mixture was concentrated to a volume of ca. 5 mL. Purification was performed via flash column chromatography (typically height of silica loading: 9 cm) eluting with cyclohexane/ethyl acetate (8:1 → 6:1). The product was obtained as colorless solid (1.19 g, 8.80 mmol) in a yield of 74%.

R_f (cyclohexane/ethyl acetate[8:1] = 0.26 visualizable *via* vanillin staining (orange).

^{1}H-NMR (400 MHz, DMSO-d_6) δ/ppm = 3.88 (s, 2H, CH, ^{1}), 1.99-1.89 (m, 4H, CH_2, ^{2}), 1.67-1.58 (m, 4H, CH_2, ^{2}).

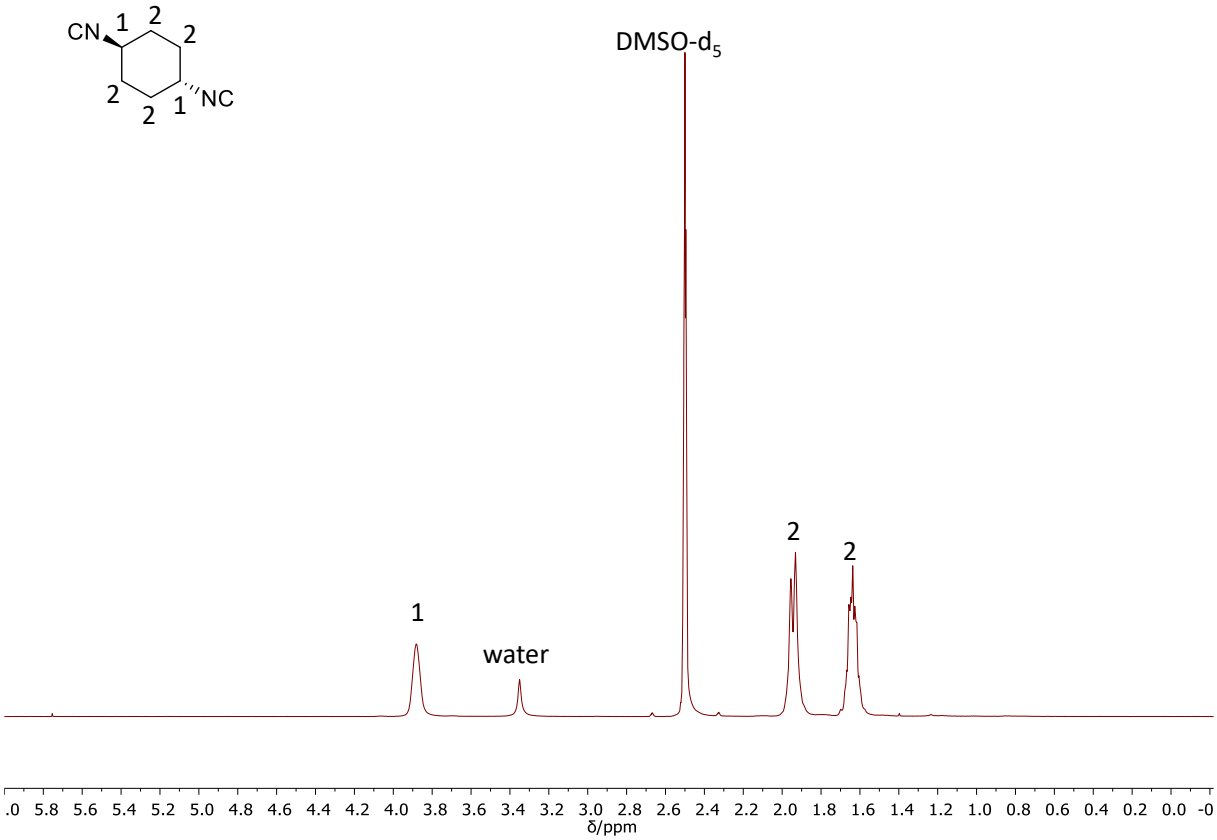

Figure 181: Proton NMR-spectrum of trans-1,4-diisocyano cyclohexane.

^{13}C-NMR (126 MHz, DMSO-d_6) δ/ppm = 156.24 (t, CN), 49.63 (t, CH), 26.75 (CH_2).

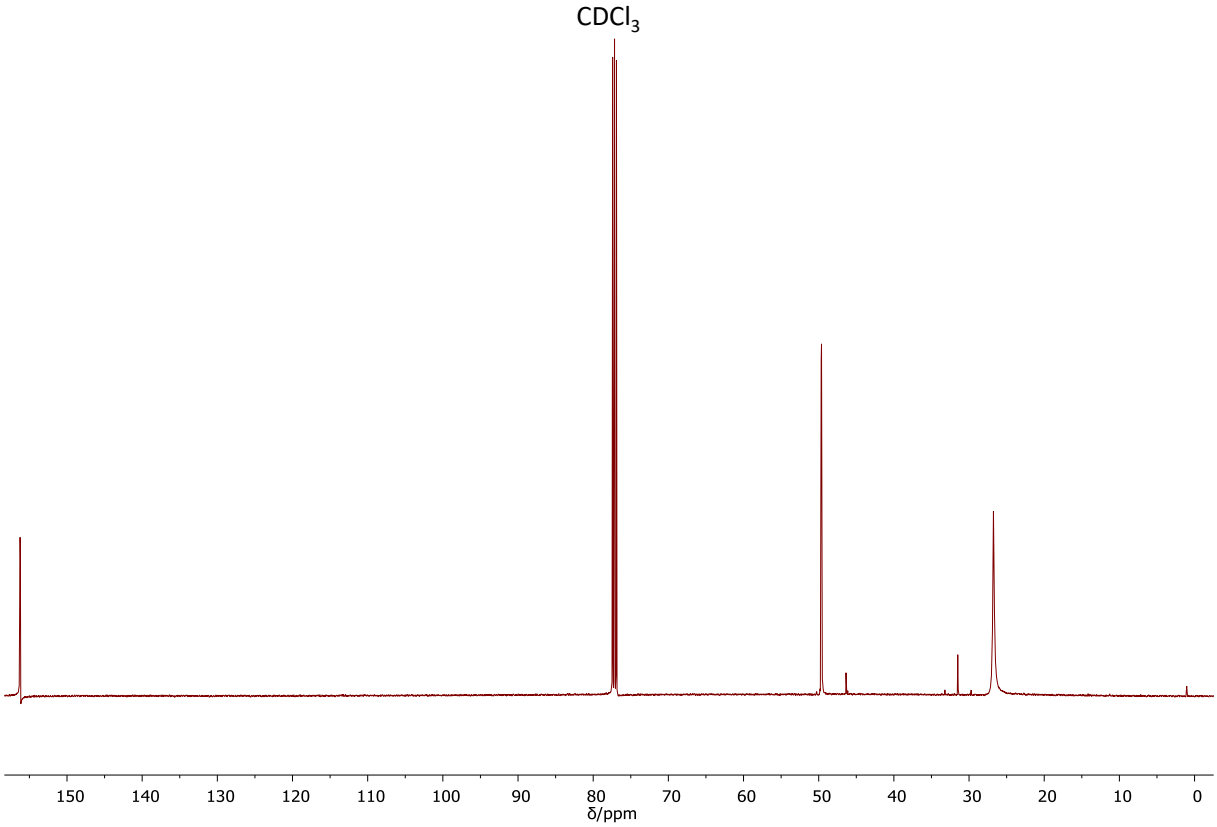

Figure 182: Carbon NMR-spectrum of trans-1,4-diisocyano cyclohexane.

HRMS (EI): calculated m/z for $C_8H_{18}N_6S_2$ [M+] = 262.1029, found: 262.1030, Δ = 0.0945 mmu.

IR: ν / cm^{-1} = 3270 (m), 3075 (w), 2956 (w), 2935 (w), 2859 (w), 2137 (s), 1652 (vs), 1551 (m), 1446 (s), 1393 (s), 1331 (m), 1257 (m), 1220 (s), 1006 (w), 971 (w), 921 (s), 761 (w), 730 (w), 673 (w), 500 (m), 420 (m) cm^{-1}.

1,4-Bisisocyanomethyl benzene

A modified synthesis protocol of Meier *et al.* was used:[592]

N,N-´(1,4-Phenylenebis(methylene)) diformamide (3.22 g, 16.8 mmol, 1.00 eq.) was dissolved in 50.8 mL DCM (c(di-*N*-formamide) = 0.33 M) and TEA (14.5 mL, 10.5 g, 104 mmol, 6.20 eq.) was added. Subsequently, the reaction mixture was cooled to 0°C using an ice-water bath and phosphorus oxychloride (4.07 mL, 6.68 g, 43.6 mmol, 2.60 eq.) was added dropwise keeping the temperature at 0 °C. After completion of the reaction, the reaction mixture was quenched with 60 mL of aqueous saturated $NaHCO_3$ solution and 20 mL of DCM was added. Subsequently, the organic layer was separated, the aqueous phase was extracted with DCM (2×20 mL) and the combined organic layers were washed with water (1×40 mL). The organic mixture was dried over sodium sulfate and concentrated to a volume of ca. 5 mL. Purification was performed via flash column chromatography (typically height of silica loading: 6 cm). Thereby, the reaction mixture was added dropwise directly onto the dry silica loaded column. Then, the product was purified by column chromatography eluting with cyclohexane/ethyl acetate (4:1) + 3V% of TEA. The product was obtained as brown solid (1.87 g, 12.0 mmol) in a yield of 71%.

R_f (cyclohexane/ethyl acetate[2:1] = 0.66 visualizable *via* vanillin staining (orange).

^{1}H-NMR was in accordance with literature.[637]

^{1}H-NMR (400 MHz, $CDCl_3$) δ/ppm = 7.43 (s, 4H, aromatic, ^{1}), 4.88 (t, $^2J_{NH}$ = 2.1 Hz, 4H, ^{2}).

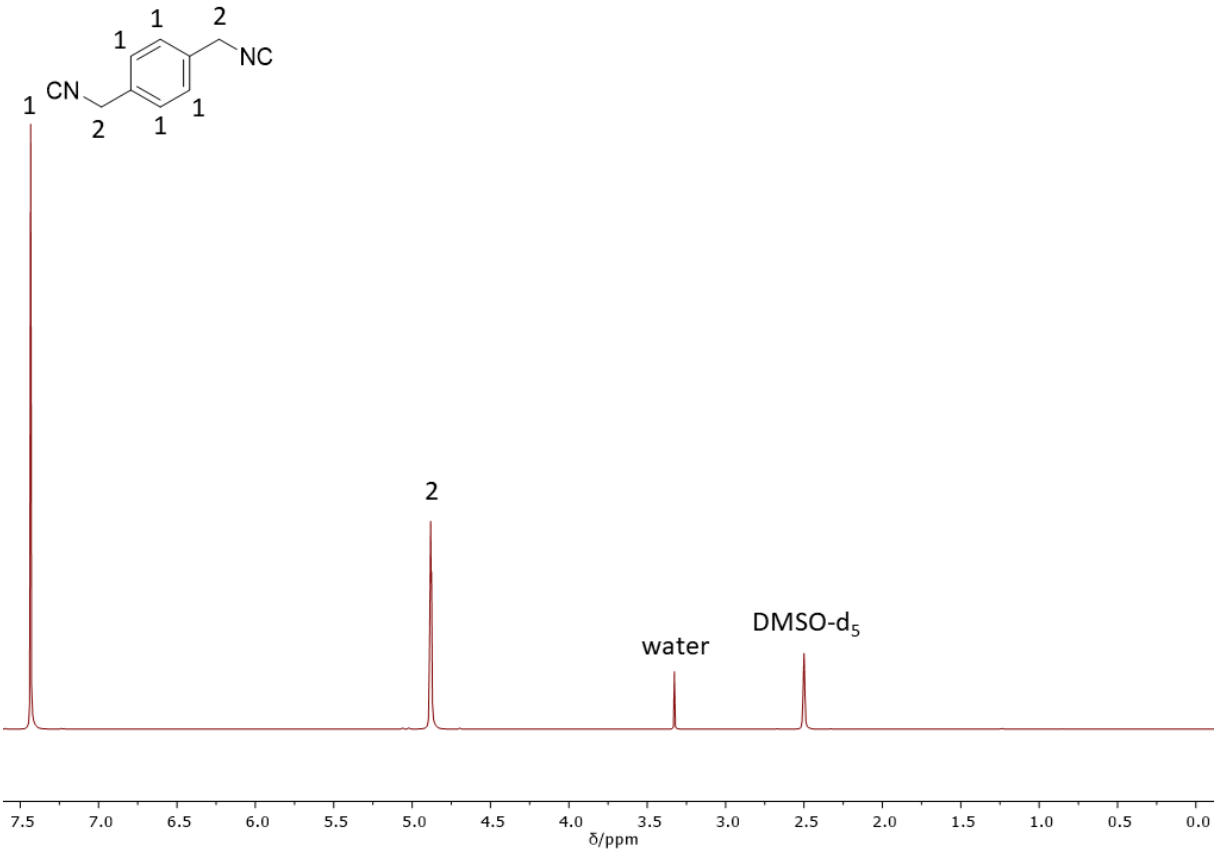

Figure 183: Proton NMR-spectrum of 1,4-bisisocyanomethyl benzene.

6.8.3 Dithiosemicarbazide syntehsis

General procedure for dithiosemicarbazide synthesis

The respective diisocyanide (1.00 eq.) was dissolved in methanol (c(diioscyanide) = 1 M) and elemental sulfur was added (0.28 eq., corresponding to 2.24 eq. of S atoms). Subsequently, hydrazine monohydrate (2.00 eq.) and DBU (10 mol%) were added, whereas a dark brown colored mixture was formed. The reaction was stirred at room temperature for the respective amount of time. The formed precipitate was filtered and washed with a minimal amount of methanol. After removing the remaining amount of solvent under reduced pressure, the pure product was obtained.

***N*,*N*'-(Dodecane-1,12-diyl) bis(hydrazinecarbothioamide) 86**

1,12-Diisocyano dodecane (1.91 g, 8.66 mmol, 1.00 eq.), elemental sulfur (622 mg, 2.42 mmol, 0.28 eq.), hydrazine monohydrate (842 µL, 867 mg, 17.3 mmol, 2.00 eq.) and DBU (129 µL, 132 mg, 866 µmol, 0.10 eq.) were used in 8.7 mL methanol following the general procedure. The reaction was complete after two hours. After work-up, the product was obtained as colorless powder (2.50 g, 7.17 mmol) in a yield of 83%.

^{1}H-NMR (400 MHz, DMSO-d_6) δ/ppm = 8.53 (s, 2H, NH, ^{1}), 7.78 (br, 2H, NH, ^{2}), 4.43 (br, 4H, NH_2, ^{3}), 3.42 (q, ^3J = 6.7 Hz, 4H, CH_2, ^{4}), 1.49 (quint., ^3J = 7.1 Hz,4H, CH_2, ^{5}), 1.25 (m, 16H, CH_2, ^{6}).

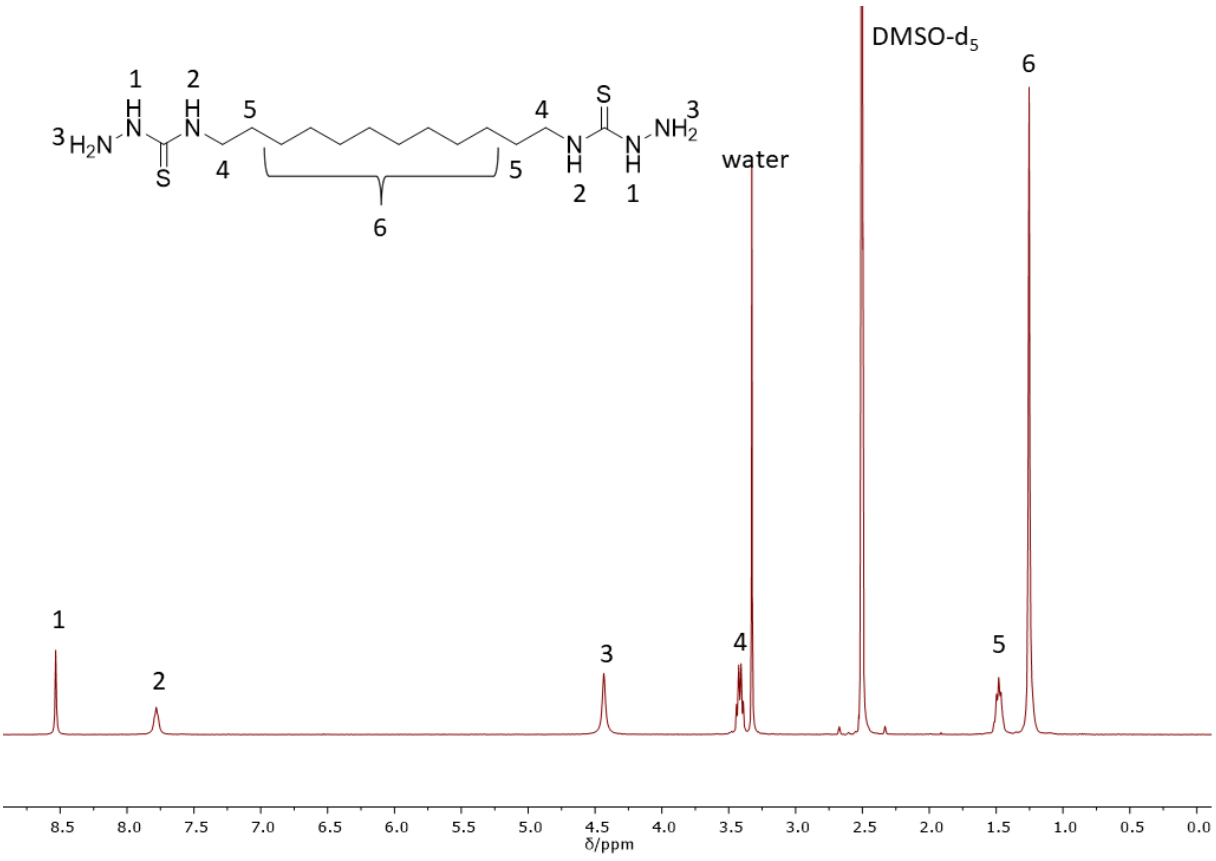

*Figure 184: Proton NMR-spectrum of **86**.*

^{13}C-NMR (101 MHz, DMSO-d_6) δ/ppm = 181.10 (C=S), 42.84 (CH_2-NH), 29.10 (CH_2), 29.03 (CH_2), 28.84 (CH_2), 26.34 (CH_2).

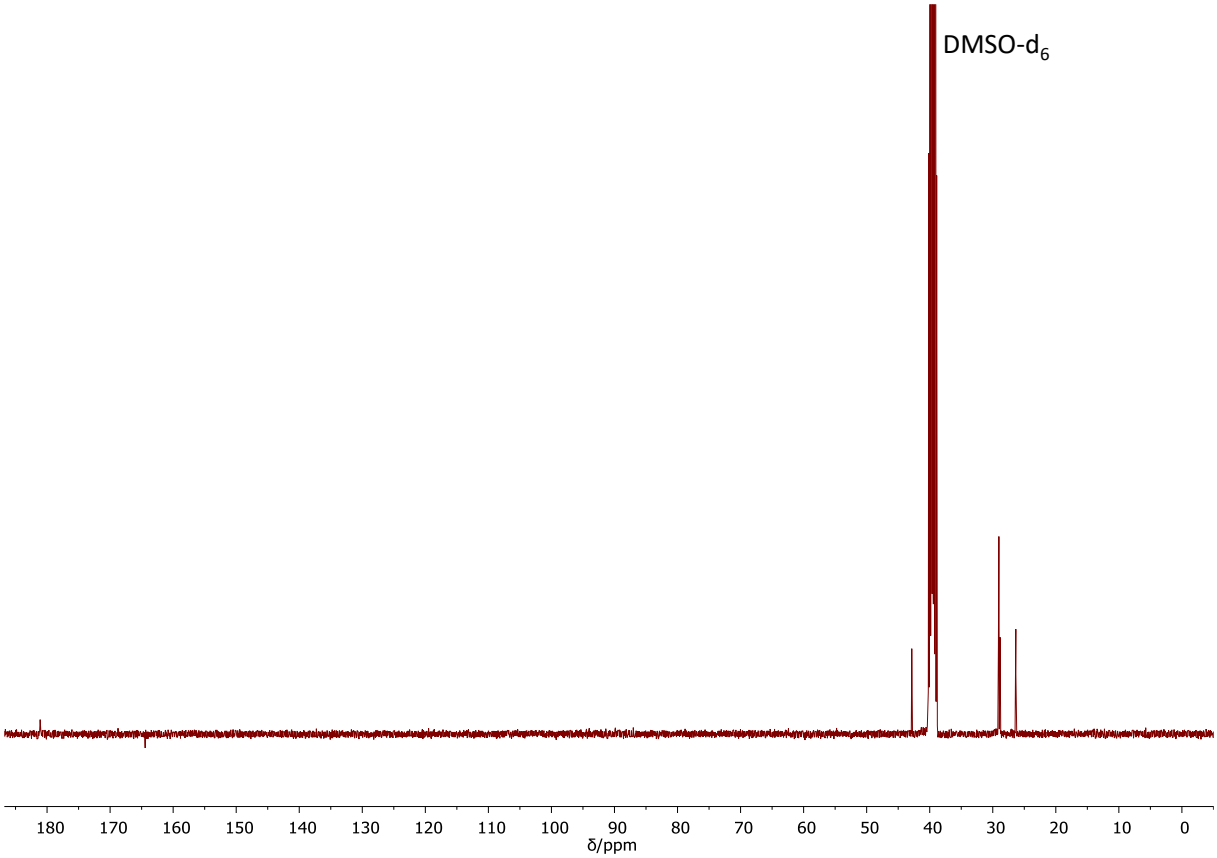

*Figure 185: Carbon NMR-spectrum of **86**.*

HRMS (EI): calculated m/z for $C_{14}H_{32}N_6S_2$ [M+] = 348.2126, found: 348.2124 Δ = 0.1713 mmu.

IR: ν / cm^{-1} = 3355 (w), 3312 (m), 3293 (m), 3227 (w), 3219 (w), 3192 (m), 3161 (m), 3151 (m), 3096 (w), 2964 (w), 2931 (m), 2913 (vs), 2847 (vs), 1623 (w), 1604 (s), 1530 (vs), 1495 (vs), 1469 (vs), 1438 (m), 1388 (w), 1321 (m), 1304 (m), 1279 (s), 1261 (vs), 1242 (vs), 1222 (s), 1195 (m), 1162 (w), 1156 (w), 1133 (w), 1096 (w), 1078 (w), 1051 (s), 1031 (w), 1016 (w), 930 (s), 882 (w), 833 (w), 798 (m), 773 (s), 718 (m), 636 (vs), 603 (s), 584 (s), 562 (s), 543 (s), 537 (s), 483 (w), 469 (w) cm^{-1}

***N*,*N*'-(Hexane-1,5-diyl)bis(hydrazinecarbothioamide) 87**

1,5-Diisocyano hexane (1.31 g, 9.62 mmol, 1.00 eq.), elemental sulfur (691 mg, 2.69 mmol, 0.28 eq.), hydrazine monohydrate (935 µL, 963 mg, 19.2 mmol, 2.00 eq.) and DBU (144 µL, 146 mg, 962 µmol, 0.10) were used in 9.6 mL methanol following the general procedure. The reaction was complete after three hours. After work-up, the product was obtained as colorless fine powder (2.21 g, 8.36 mmol) in a yield of 87%.

^{1}H-NMR (400 MHz, DMSO-d_6) δ/ppm = 8.52 (s, 2H, NH, ^{1}), 7.78 (t, ^3J = 6.0 Hz, 2H, NH, ^{2}), 4.43 (br, 4H, NH_2, ^{3}), 3.42 (q, ^3J = 6.7 Hz, 4H, CH_2, ^{4}), 1.48 (quint., ^3J = 6.8 Hz, 4H, CH_2, ^{5}), 1.31-1.16 (m, 4H, CH_2, ^{6}).

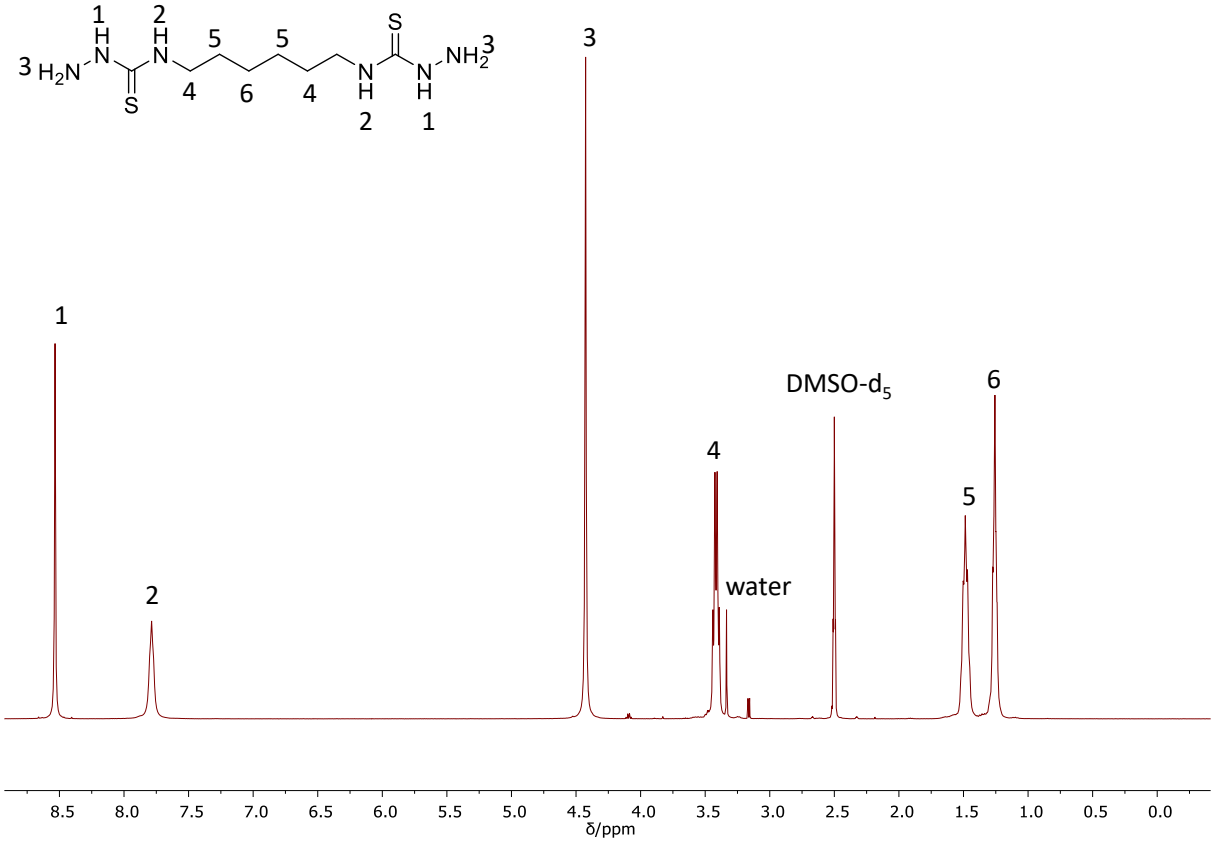

Figure 186: Proton NMR-spectrum of 87.

^{13}C-NMR (101 MHz, DMSO-d_6) δ/ppm = 181.08 (C=S), 42.84 (CH_2), 29.12 (CH_2), 26.19 (CH_2).

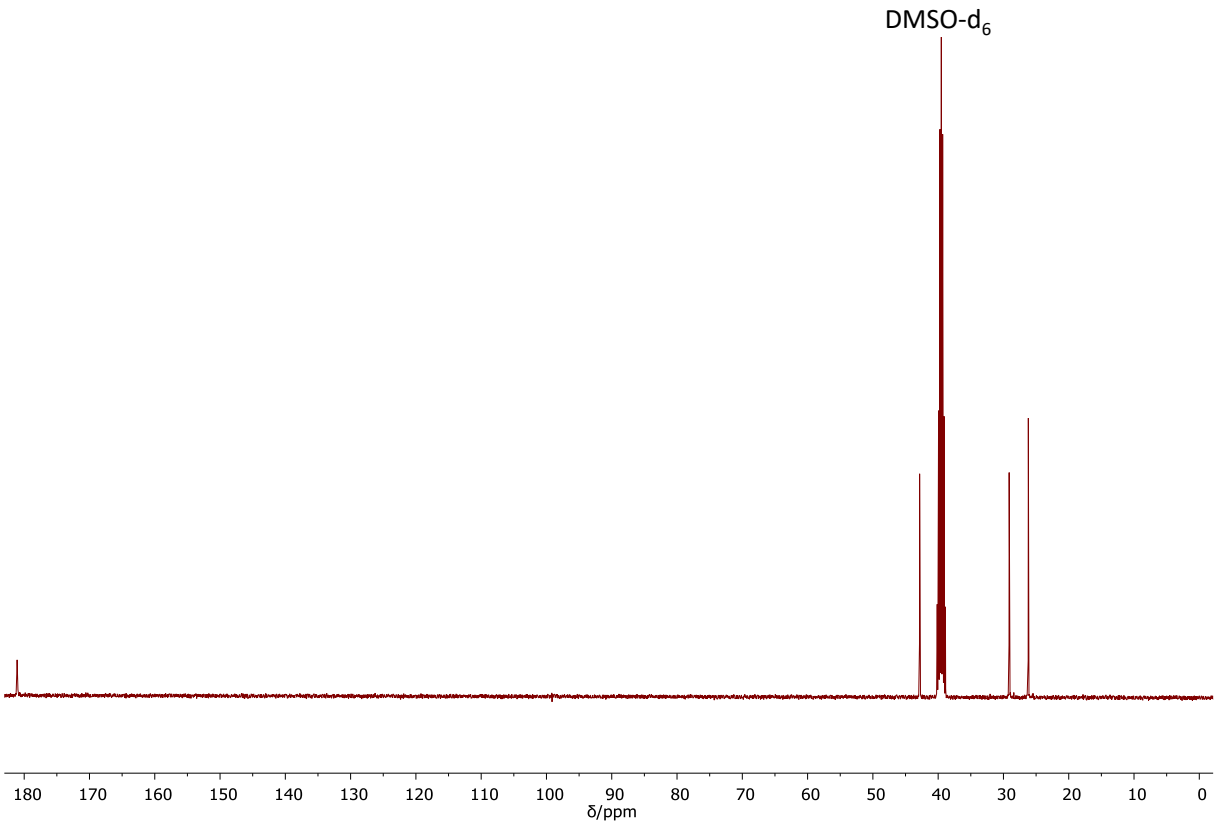

*Figure 187: Carbon NMR-spectrum of **87**.*

HRMS (EI): calculated m/z for $C_8H_{20}N_6S_2$ [M+] = 264.1185, found: 264.1184, Δ = -0.1726 mmu.

IR: ν / cm^{-1} = 3338 (w), 3316 (w), 3252 (w), 3176 (m), 3110 (w), 2987 (w), 2954 (w), 2925 (w), 2847 (w), 1621 (m), 1537 (s), 1510 (s), 1469 (m), 1444 (w), 1425 (w), 1390 (w), 1362 (w), 1323 (w), 1296 (w), 1257 (s), 1222 (m), 1179 (s), 1096 (w), 1061 (m), 1010 (w), 950 (s), 794 (w), 771 (w), 732 (w), 708 (w), 586 (vs), 572 (vs), 481 (w), 428 (w) cm^{-1}.

***N,N'*-(*Trans*-cyclohexane-1,4-diyl) bis(hydrazinecarbothioamide) 88**

Trans-1,4-diisocyano cyclohexane (825 mg, 6.15 mmol, 1.00 eq.), elemental sulfur (442 mg, 1.72 mmol, 0.28 eq.), hydrazine monohydrate (598 µL, 616 mg, 12.3 mmol, 2.00 eq.) and DBU (91.8 µL, 93.6 mg,615 µmol, 0.10) were used in 6.2mL methanol following the general procedure. The reaction was complete after one hours. After work-up, the product was obtained as colorless solid (1.40 g, 5.32 mmol) in a yield of 87%.

^{1}H-NMR (400 MHz, DMSO-d_6) δ/ppm = 8.56 (s, 2H, NH, ^{1}), 7.53 (d, ^3J = 8.7 Hz, 2H, NH, ^{2}), 4.44 (s, 4H, NH_2, ^{3}), 4.04 (br, 2H, CH), 1.86 (m, 4H, CH_2, ^{4}), 1.36 (m, 4H, CH_2, ^{4}).

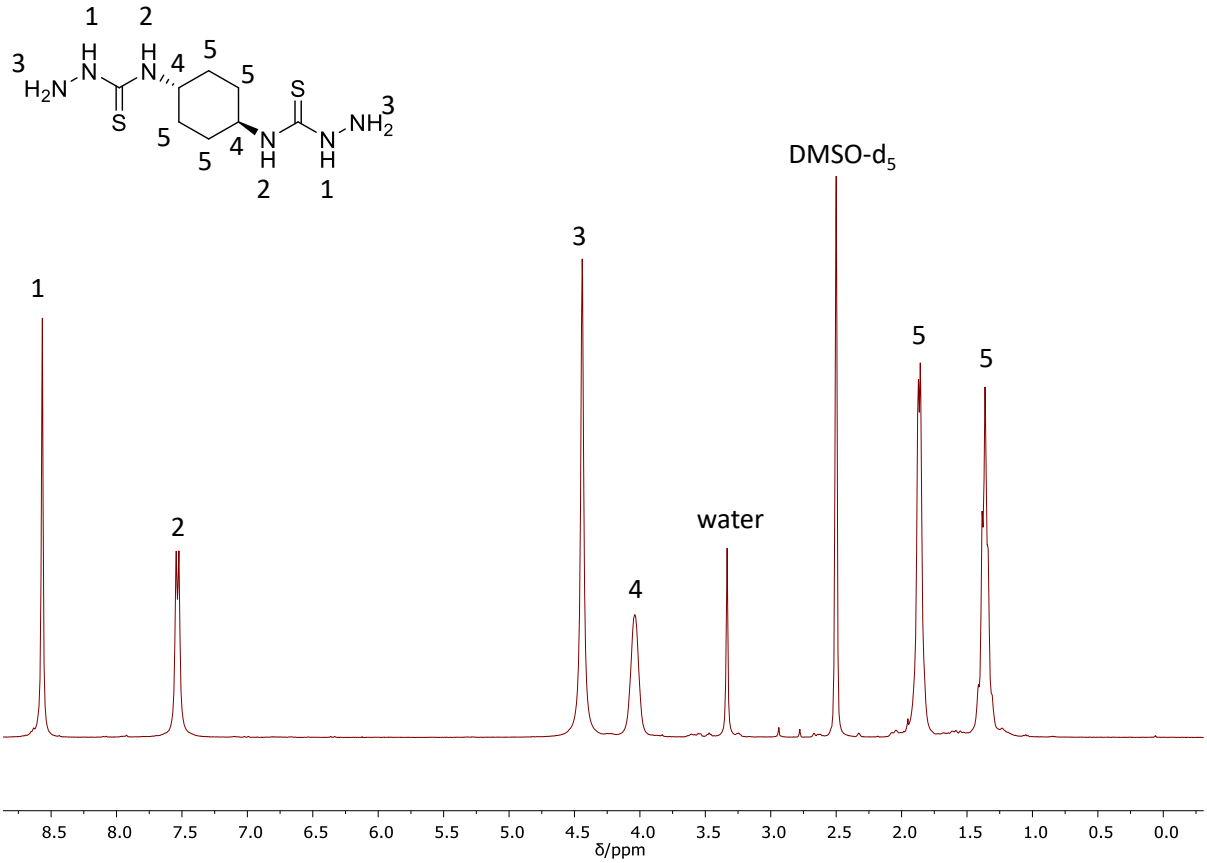

*Figure 188: Proton NMR-spectrum of **88**.*

^{13}C-NMR (101 MHz, DMSO-d_6) δ/ppm = 180.08 (C=S), 51.14 (CH), 31.00 (CH_2).

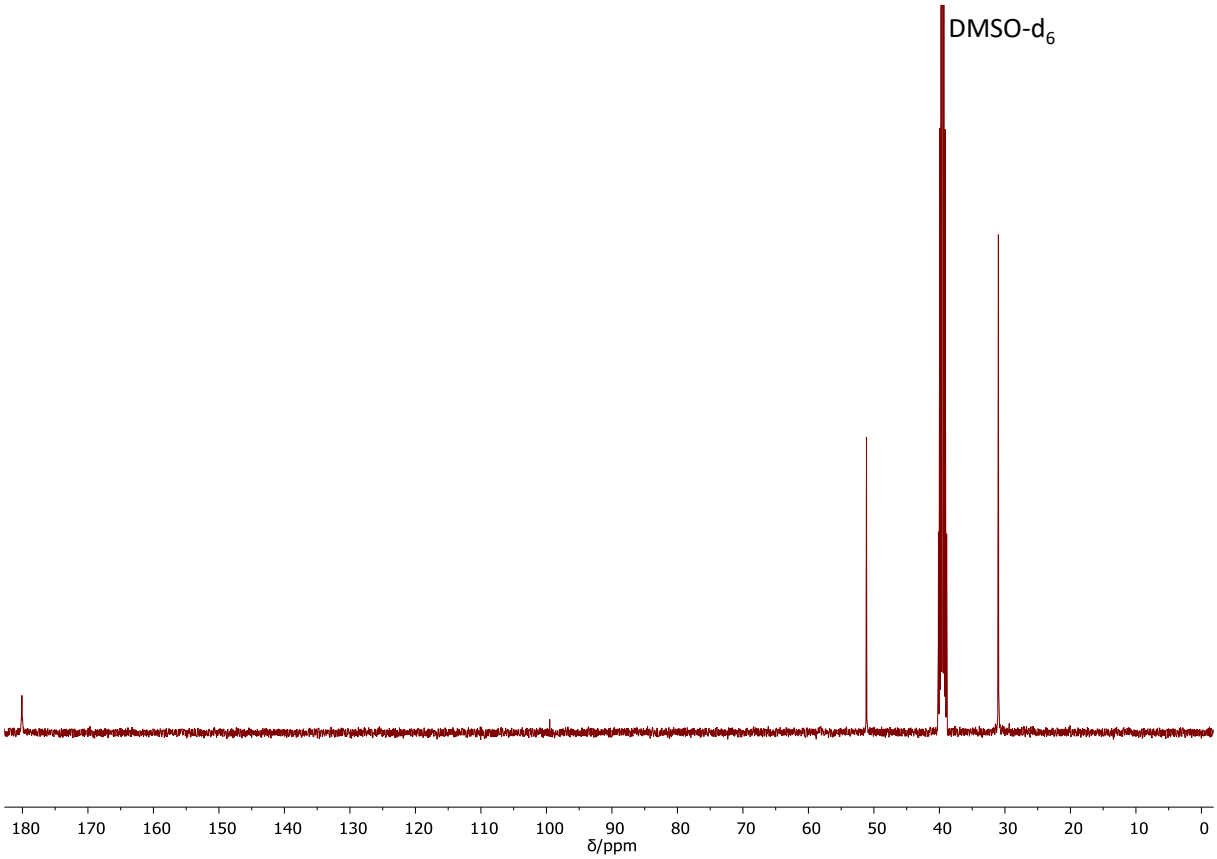

*Figure 189: Carbon NMR-spectrum of **88**.*

HRMS (EI): calculated m/z for $C_8H_{18}N_6S_2$ [M+] = 262.1029, found: 262.1030, Δ = 0.0945 mmu.

IR: ν / cm^{-1} = 3330 (w), 3301 (w), 3190 (m), 3122 (w), 2989 (w), 2943 (w), 2904 (vw), 2851 (vw), 1637 (m), 1534 (vs), 1506 (vs), 1456 (w), 1360 (vw), 1312 (w), 1302 (w), 1277 (m), 1234 (vs), 1133 (w), 1061 (w), 987 (vw), 950 (vs), 903 (w), 889 (w), 817 (vs), 607 (vs), 564 (vs), 525 (w), 471 (vw) cm^{-1}.

***N,N'*-(1,4-Phenylene-bis(methylene))-bis(hydrazinecarbothioamide) 89**

1,4-bisisocyanomethyl Benzene (1,70 g, 10.9 mmol, 1.00 eq.), elemental sulfur (166 mg, 1.09 mmol, 0.28 eq.), hydrazine monohydrate (1.06 mL, 1.09 mg, 21.77 mmol, 2.00 eq.) and DBU (162 µL, 166 mg, 1.09 mmol, 0.10) were used in 10.9 mL methanol following the general procedure. The reaction was complete after 2.5 hours. After work-up, the product had to be recrystallized from 112 mL of a mixture of MeOH/DMSO (53/47) for three days. By adding 60 mL DMSO and seven days in the freezer, additional product could be precipitated. After filtration and washing with a minimal amount of methanol, the remaining solvents were removed at 10 mbar at 120 °C. The product was obtained as colorless solid (2.07 g, 7.29 mmol) in a yield of 67%.

^{1}H-NMR (400 MHz, DMSO-d_6) δ/ppm = 8.72 (s, 2H, NH, ^{1}), 8.24 (br, 2H, NH, ^{2}), 4.67 (d, ^3J = 6.0 Hz, 4H, CH_2, ^{3}), 4.49 (s, 4H, NH_2, ^{4}).

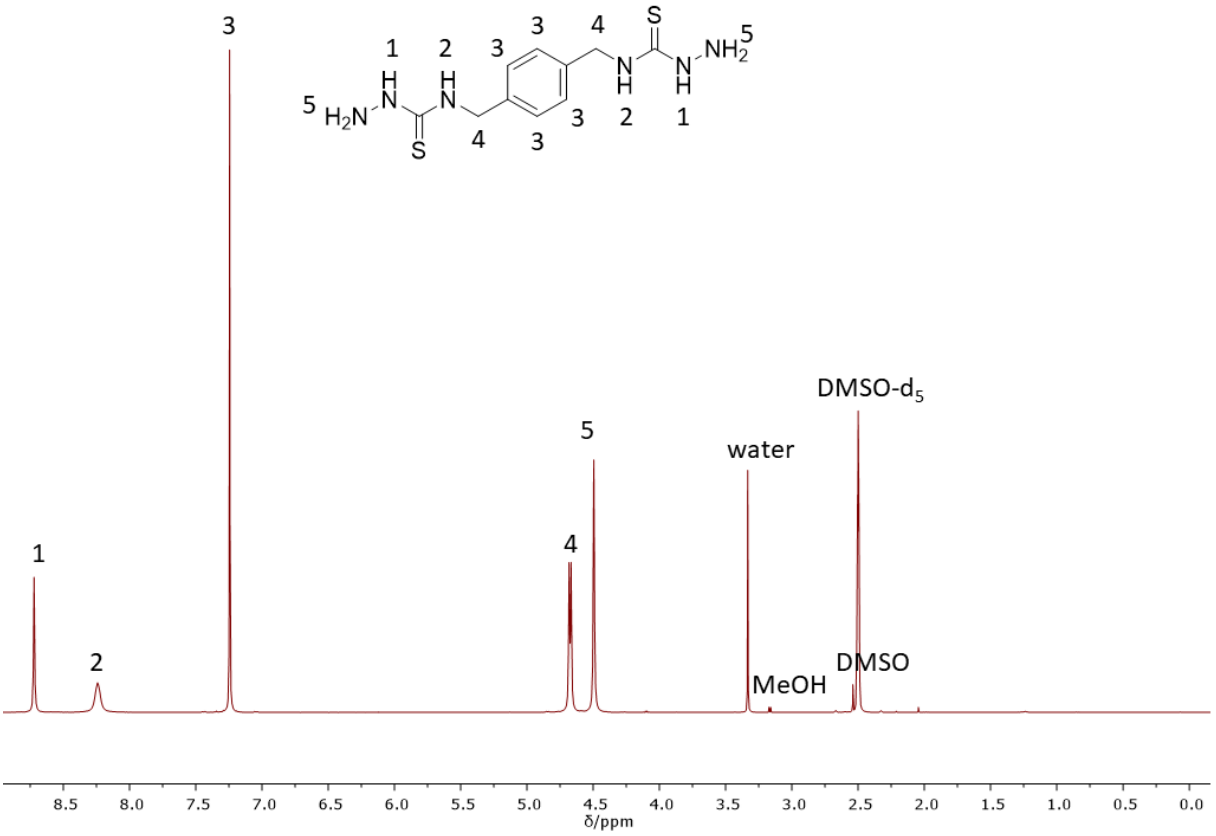

*Figure 190: Proton NMR-spectrum of **89**.*

^{13}C-NMR (101 MHz, DMSO-d_6) δ/ppm = 181.46 (C=S), 138.21 (quaternary-aromatic), 127.22 (aromatic), 45.93 (CH_2).

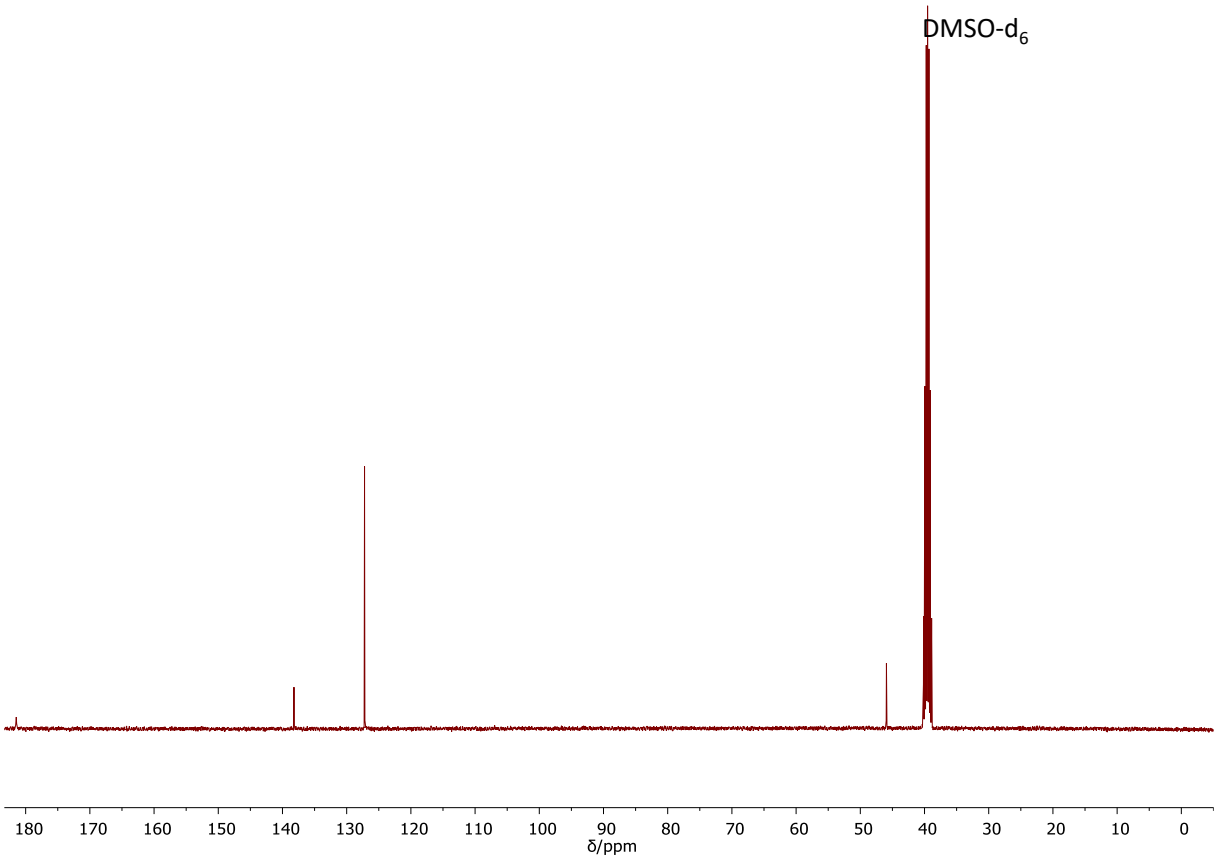

*Figure 191: Carbon NMR-spectrum of **89**.*

HRMS (EI): calculated m/z for $C_{10}H_{16}N_6S_2$ [M+] = 284.08779, but not found. However, several fragments were assigned:

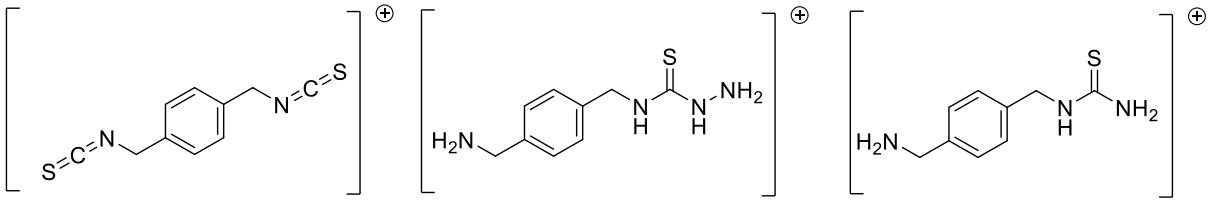

IR: ν / cm^{-1} = 3308 (s), 3250 (m), 3194 (m), 2919 (w), 1615 (m), 1532 (vs), 1514 (s), 1481 (vs), 1427 (m), 1306 (m), 1267 (s), 1224 (s), 1199 (vs), 1105 (m), 1051 (m), 940 (s), 884 (m), 852 (s), 763 (s), 745 (s), 671 (s), 609 (vs), 582 (vs), 520 (vs), 461 (m) cm^{-1}.

***N*,*N*'-(1,4-Phenylene) bis(hydrazinecarbothioamide) 90**

1,4-bisisocyano Benzene (743 g, 5.80 mmol, 1.00 eq.), elemental sulfur (417 mg, 1.62 mmol, 0.28 eq.), hydrazine monohydrate (564 µL, 581 mg, 11.6 mmol, 2.00 eq.) and DBU (86.6 µL, 88.3 mg, 580 µmol, 0.10) were used in 5.8 mL methanol following the general procedure. After work-up, the product was obtained as beige solid (820 g, 3.20 mmol) in a yield of 55%.

However, the substance underwent rapid decomposition in solution and no carbon NMR spectra was taken.

HRMS (EI): calculated m/z for $C_8H_{12}N_6S_2$ [M+] = 256.05649, found: 255.9, HRMS was not possible. Additionally, several fragments were assigned:

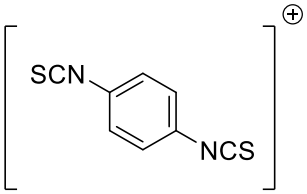

Exact Mass: 191,98104
found: 191.9

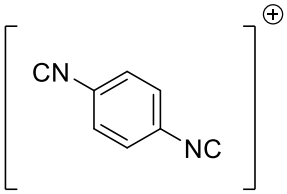

Exact Mass: 128,03690
found: 127.9

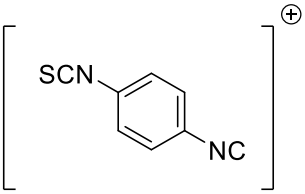

Exact Mass: 160,00897
found: 159.9

IR: ν / cm^{-1} = 3322 (w), 3293 (w), 3233 (w), 3188 (m), 3168 (m), 3032 (w), 3003 (w), 2997 (w), 2958 (w), 2902 (w), 2133 (vw), 1619 (m), 1592 (w), 1545 (vs), 1508 (vs), 1493 (vs), 1415 (w), 1358 (w), 1302 (m), 1271 (vs), 1207 (vs), 1100 (w), 1065 (m), 1016 (w), 971 (w), 905 (s), 829 (vs), 788 (m), 765 (m), 730 (s), 689 (s), 664 (s), 638 (s), 594 (s), 586 (s), 512 (vs), 477 (m), 407 (m) cm^{-1}.

In solid state, the compound is bench stable to at least 8 months, although the isothiocyanate group had formed due to decomposition in minor extent, as seen by the vibration at 2133 cm^{-1}.

6.8.4 Poly(Thiosemicarbazone) ((*co*-)poly(TSC)) synthesis

General procedure of polyTSC synthesis

The respective dithiosemicarbazide (100 mg, 1.00 eq.) and dialdehyde (1.00 eq.) were added to DMSO (c(dithiosemicarbazide) = 1.5 M) and the reaction was stirred at r.t. for 2-4 hours. In some cases, due to bulkier moieties introduced by either dithiosemicarbazide or aldehyde, additional reaction time at 100 °C and 500 mbar for 17 hours was required. Subsequently, the formed polymer was first completely solubilized by addition of DMSO, in some cases under sonification (50 °C and 37 kHz), and then precipitated by dropwise addition of the polymer solution to 30 mL of cold water. The polymer was filtered, suspended in 30 mL water, and refluxed for one hour and subsequently cooled and filtered to remove DMSO. This process was repeated three times. The polymer was obtained after drying at 100 °C and 12 mbar for at least 20 hours. Any deviations from this general procedure are described for the respective polymer.

General procedure of co-polyTSC synthesis

The respective dithiosemicarbazides (varying in ratios of 70:30, 50:50 and 90:10, 1.00 eq. of thiosemicarbazide group) and terephthaldeyhde **6** (1.00 eq. of aldehyde group) were added to DMSO (c(total amount of dithiosemicarbazide) = 1.5 or 1.0 M) and the reaction was stirred at r.t. for 3 hours. Subsequently, the formed polymer was first completely solubilized by addition of DMSO, in some cases under sonification (50 °C and 37 kHz), and then precipitated by dropwise addition of the polymer solution to 30 mL of cold water. The polymer was filtered, suspended in 30 mL water, and refluxed for one hour and subsequently cooled and filtered to remove DMSO. This process was repeated three times. The polymer was obtained after drying at 100 °C and 12 mbar for at least 20 hours. Any deviations from this general procedure are described for the respective polymer.

The ratio of dithiosemicarbazide monomers incorporated into the polymer backbone was determined by comparison of integrals of respective signals of each monomer moiety clearly distinct from other signals, see respective co-polymer analysis.

PolyTSC P1

N,*N*'-(Dodecane-1,12-diyl) bis(hydrazinecarbothioamide) **86** (100 mg, 287 mmol, 1.00 eq.) and therephthaldehyde **91** (38.5 mg, 287 mmol, 1.00 eq.) were used in 191 µL DMSO following the general procedure. The reaction was finished after 2 hours at room temperature. No additional DMSO was added to the reaction mixture for solubilizing the polymer for precipitation. After work-up, the product was obtained as yellow polymer ball (108 mg) in a yield of 84%.

N,*N*'-(Dodecane-1,12-diyl) bis(hydrazinecarbothioamide) **86** (1.00 g, 2.87 mol, 1.00 eq.) and therephthaldehyde **91** (385 mg, 2.87 mmol, 1.00 eq.) were used in 1.9 mL DMSO following the general procedure. The reaction was finished after 2 hours at room temperature. 2 mL NMP were added to the reaction mixture for solubilizing the polymer using a sonification bath (50 °C, 80 kHz) for precipitation out of 400 mL of water. After work-up, the product was obtained as yellow polymer balls (1.25 g) in a yield of 98% containing less than 1 w% DMSO.

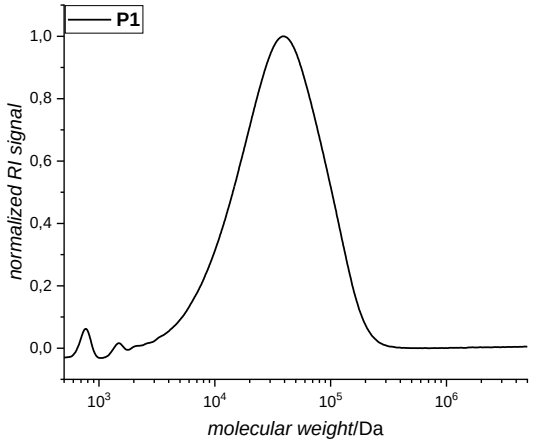

*Figure 192: SEC-trace of **P1**.*

^{1}H-NMR (400 MHz, DMSO-d_6) δ/ppm = 11.50 (s, 2H, NH, ^{1}), 8.54 (t, ^3J = 6.0 Hz, 2H, NH, ^{2}), 8.05 (s, 2H, CH, ^{3}), 7.82 (s, 4H, aromatic, ^{4}), 3.54 (q, ^3J = 6.7 Hz, 4H, CH_2, ^{5}), 1.62-1.52 (m, 4H, CH_2, ^{6}), 1.32-1.17 (m, 16H, CH_2, ^{7}).

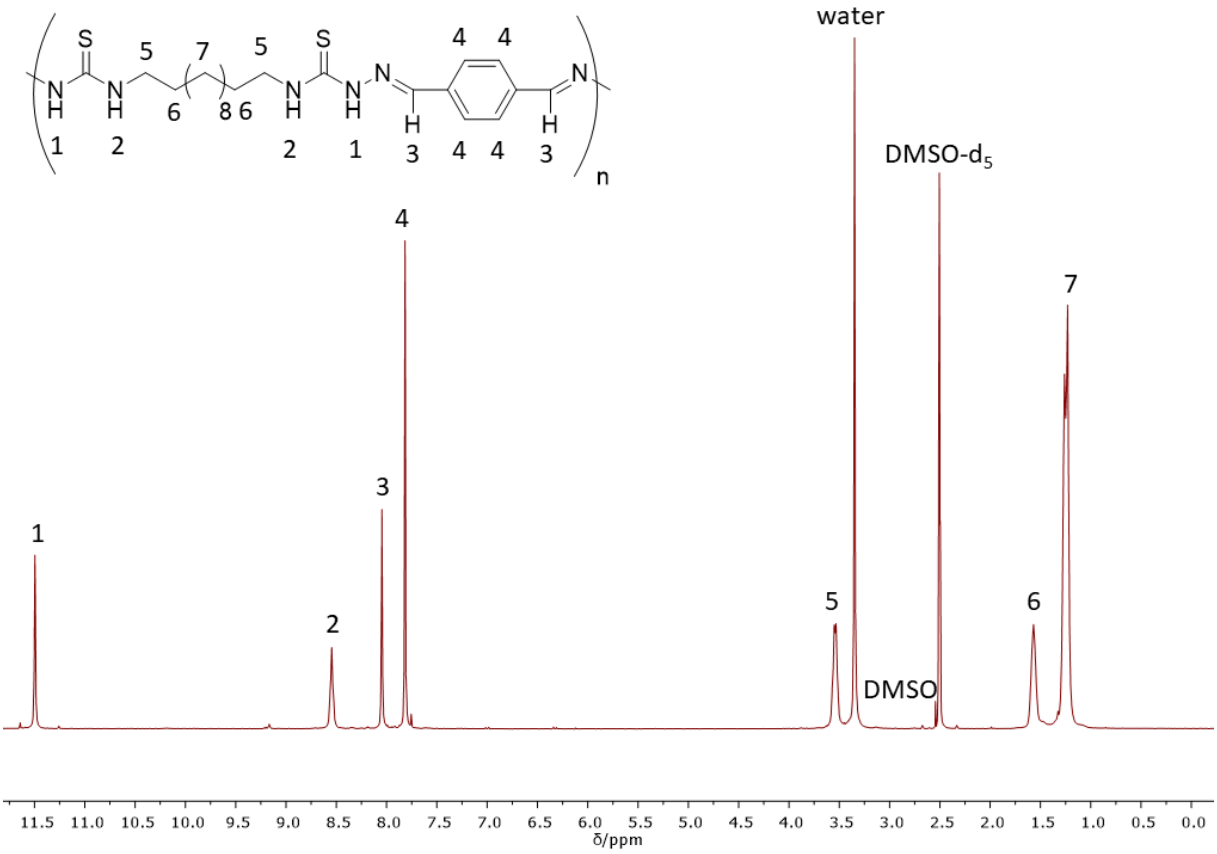

*Figure 193: Proton NMR-spectrum of **P1**.*

^{13}C-NMR (101 MHz, DMSO-d_6) δ/ppm = 176.82 (C=S), 141.09 (C=N), 135.37 (quaternary-aromatic), 127.41 (aromatic), 43.55 (CH_2), 30.53-28.32 (m, CH_2), 26.39 (CH_2).

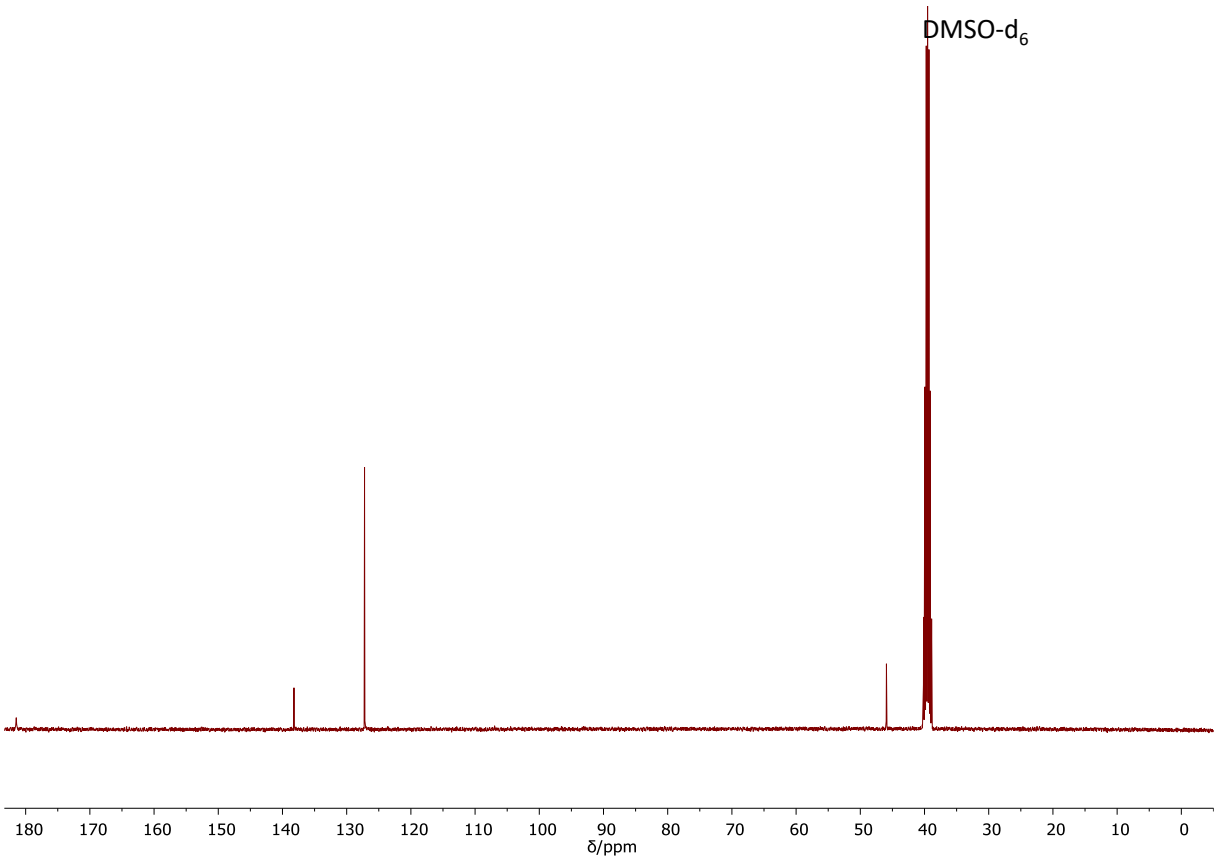

*Figure 194: Carbon NMR-spectrum of **P1**.*

IR: ν / cm^{-1} = 3270 (vw, br), 3147 (vw, br), 2921 (m), 2851 (w), 1530 (vs), 1485 (vs), 1415 (w), 1318 (w), 1290 (w), 1226 (s), 1201 (s), 1117 (w), 1096 (m), 940 (w), 829 (vw), 784 (vw), 720 (vw), 582 (w), 535 (m), 496 (w) cm^{-1}.

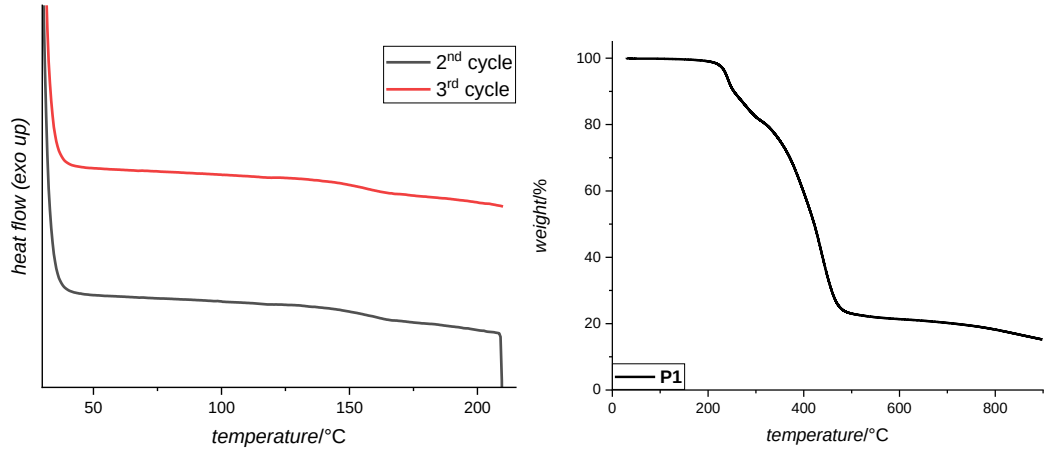

*Figure 195: Left: DSC-curve of **P1** from 25-210 °C at 30 K/min. Right: TGA-curve from 25-900 °C.*

PolyTSC P2

N,*N*'-(Hexane-1,6-diyl) bis(hydrazinecarbothioamide) **87** (100 mg, 378 mmol, 1.00 eq.) and therephthaldehyde **91** (38.5 mg, 378 mmol, 1.00 eq.) were used in 252 µL DMSO following the general procedure. The reaction was finished after 2 hours at room temperature. 1.1 mL of DMSO were added to the reaction mixture for solubilizing the polymer for precipitation. After work-up, the product was obtained as yellow flakes (124 mg) in a yield of 90%.

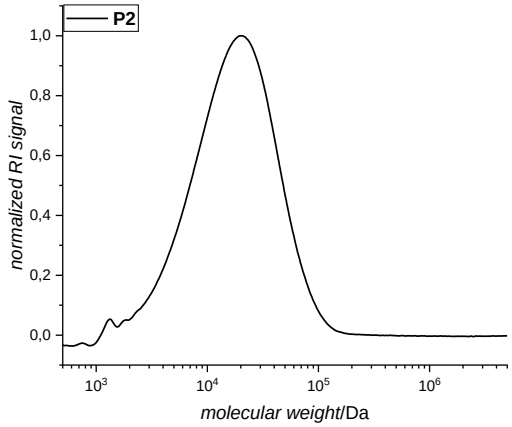

*Figure 196: SEC-trace of **P2**. M_n=13.2 kDa, M_w=24.1 kDa, Đ=1.83 (crude SEC displayed: M_n=14.9 kDa, M_w=20.0 kDa, Đ=1.34).*

^{1}H-NMR (400 MHz, DMSO-d_6) δ/ppm = 11.49 (s, 2H, NH, ^{1}), 8.57 (t, ^3J = 6.1 Hz, 2H, NH, ^{2}), 8.04 (s, 2H, CH, ^{3}), 7.82 (s, 4H, aromatic, ^{4}), 3.65-3.49 (m, 4H, CH_2, ^{5}), 1.69-1.53 (m, 4H, CH_2, ^{6}), 1.41-1.24 (m, 4H, CH_2, ^{7}).

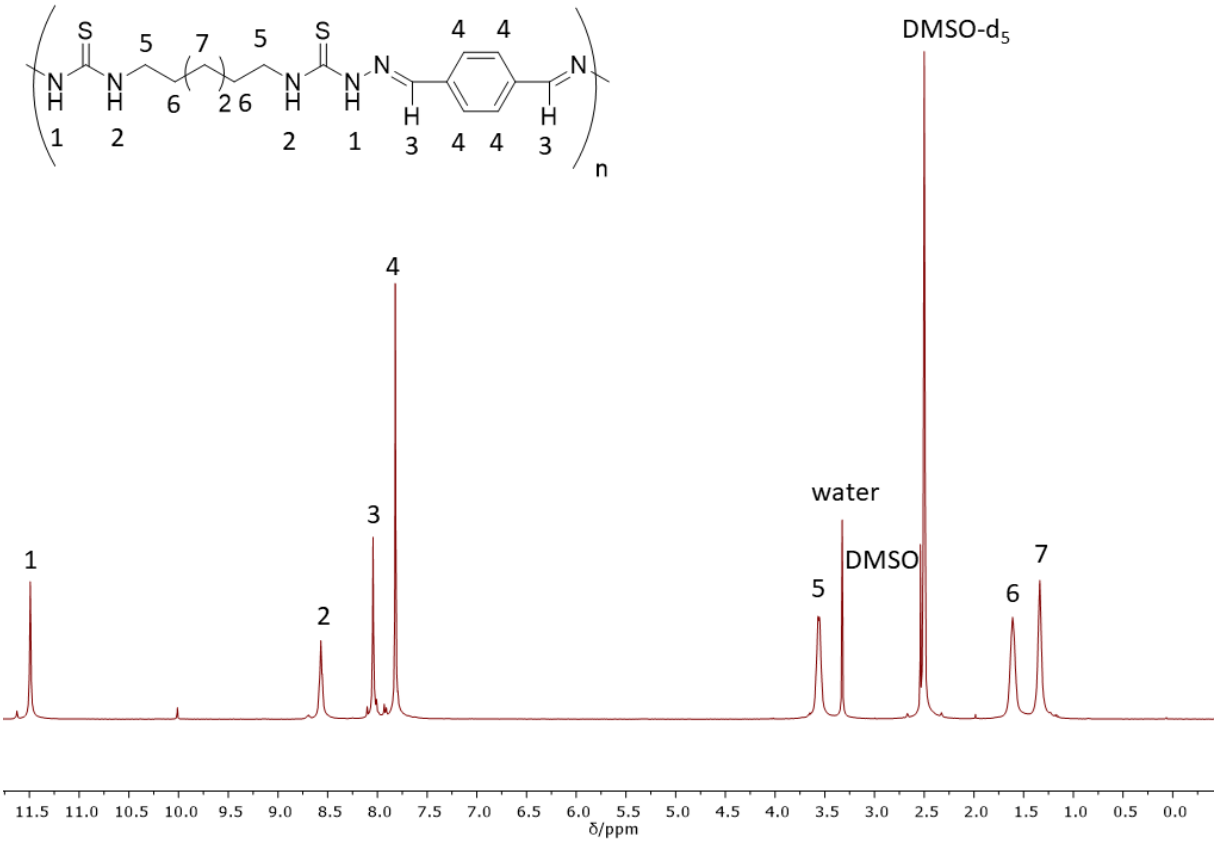

*Figure 197: Proton NMR-spectrum of **P2**.*

^{13}C-NMR (101 MHz, DMSO-d_6) δ/ppm = 176.85 (C=S), 141.14 (C=N), 135.34 (quaternary-aromatic), 127.41 (aromatic), 43.49 (CH_2), 28.88 (CH_2), 26.19 (CH_2).

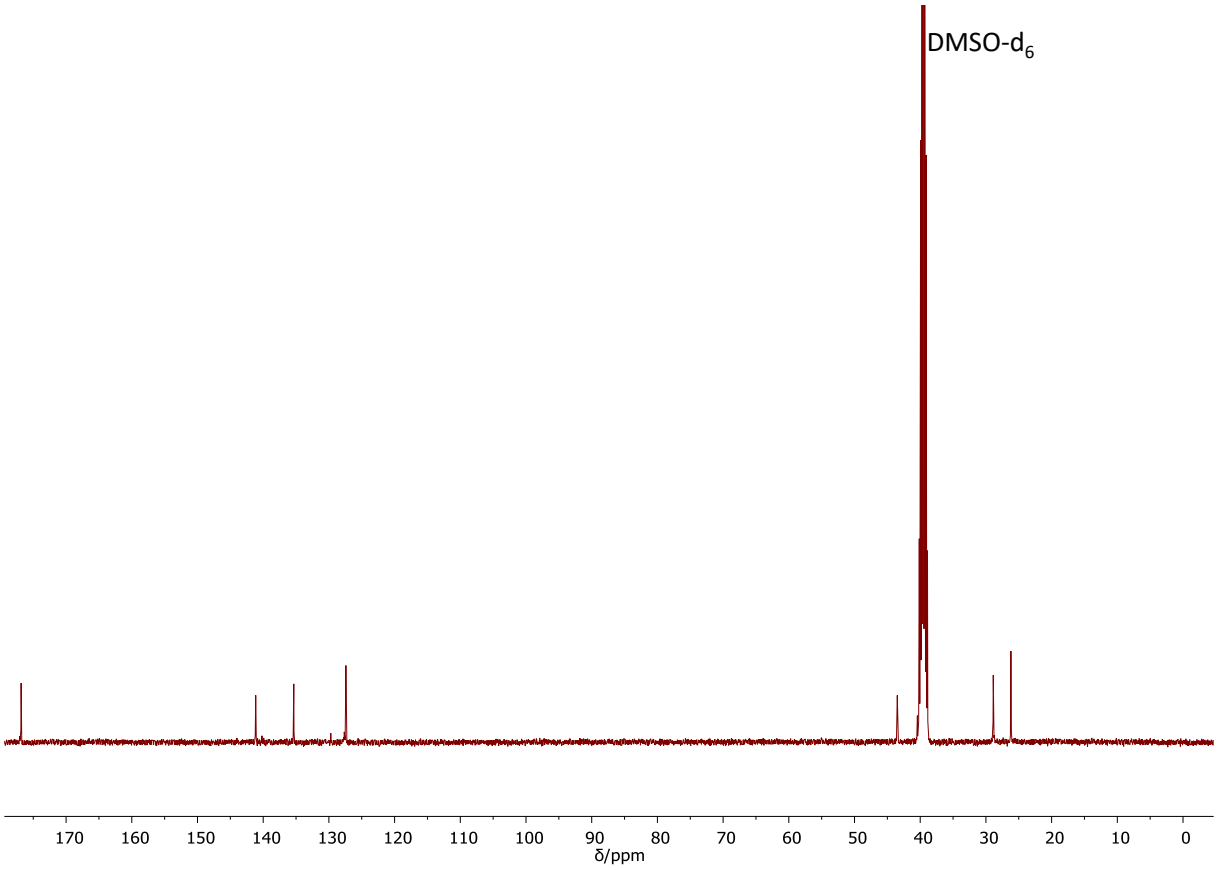

*Figure 198: Carbon NMR-spectra of **P2**.*

IR: ν / cm^{-1} = 3324 (vw, br), 3155 (w, br), 2927 (w), 2855 (w), 1697 (vw), 1627 (vw), 1530 (vs), 1485 (vs), 1415 (w), 1318 (w), 1290 (w), 1230 (s), 1195 (s), 1172 (m), 1117 (m), 1092 (s), 1014 (w), 938 (w), 827 (w), 780 (vw), 730 (vw), 642 (vw), 584 (w), 535 (w), 516 (w), 492 (w), 477 (w) cm^{-1}.

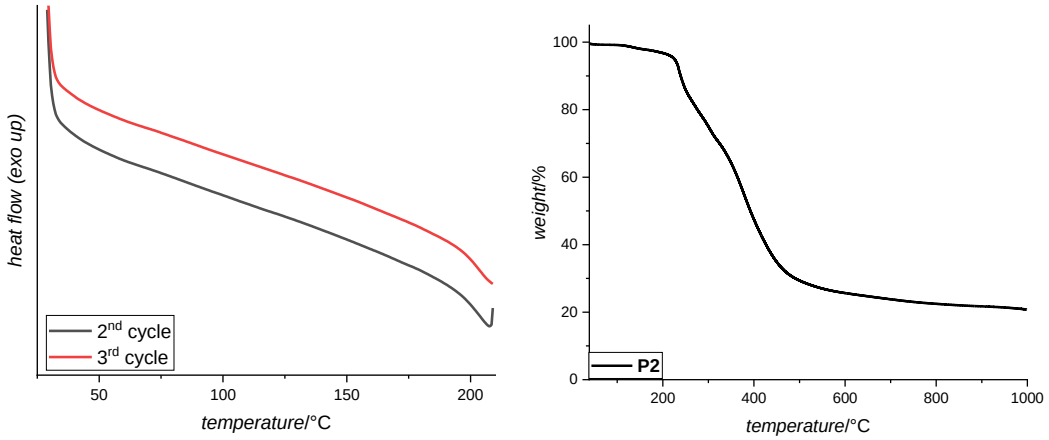

*Figure 199: Left: DSC-curve of **P2** from 25-210 °C at 30 K/min. Right: TGA-curve from 25-1000 °C.*

PolyTSC P3

N,*N'*-(*Trans*-cyclohexane-1,4-diyl) bis(hydrazinecarbothioamide) **88** (100 mg, 381 mmol, 1.00 eq.) and therephthaldehyde **91** (51.1 mg, 381 mmol, 1.00 eq.) were used following the general procedure. As the monomer exhibited low solubility, the concentration was set to 1.0 M, leading to addition of in 381 µL DMSO. The reaction mixture was stirred at room temperature for 4 hours and then for 17 hours at 100 °C ad 500 mbar. Since the polymer was not soluble in DMSO anymore, it was suspended in 10 mL water and was stirred for one hour at 1400 rpm. The polymer was filtered, suspended in 30 ml water, and washed under reflux for one hour. This process was repeated three times. The polymer (137 mg) was obtained after drying at 100 °C and 12 mbar for at least 24 hours as orange powder in quantitative yields.

IR: ν / cm^{-1} = 3291 (w, br), 3153 (w, br), 2929 (w), 2853 (w), 1691 (w), 1602 (vw), 1514 (vs), 1477 (vs), 1415 (m), 1372 (w), 1329 (w), 1290 (m), 1261 (m), 1224 (m), 1187 (vs), 1125 (s), 1086 (s), 1022 (w), 1012 (w), 975 (w), 965 (w), 936 (w), 907 (w), 868 (w), 825 (w), 808 (m), 656 (vw), 594 (w), 533 (w), 477 (w) cm^{-1}.

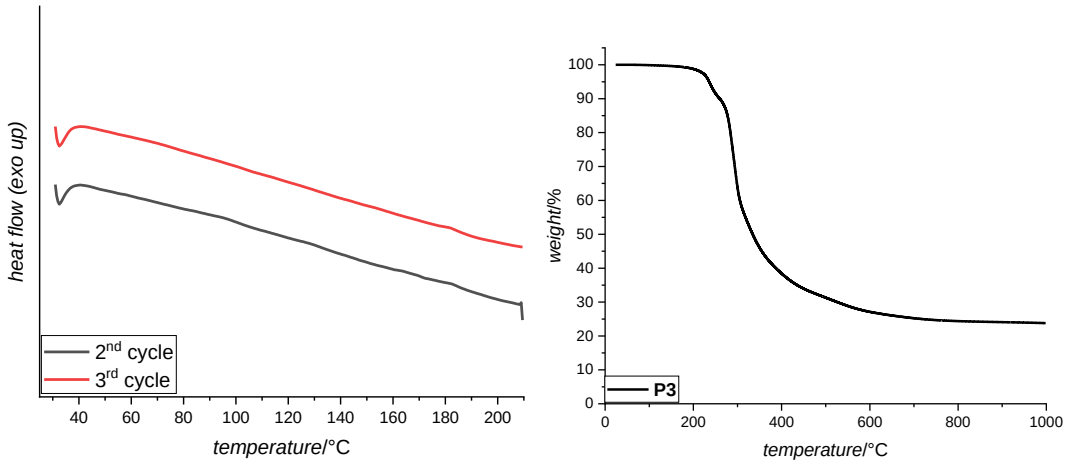

*Figure 200: Left: DSC-curve of **P3** from 25-210 °C at 30 K/min. Right: TGA-curve from 25-1000 °C.*

PolyTSC P4

N,*N*'-(1,4-Phenylenebis(methylene)) bis(hydrazinecarbothioamide) **89** (100 mg, 352 mmol, 1.00 eq.) and therephthaldehyde **91** (47.2 mg, 352 mmol, 1.00 eq.) were used in 234 µL DMSO following the general procedure. The reaction mixture was stirred at room temperature for 4 hours and then for 17 hours at 100 °C ad 500 mbar. Since the polymer was not soluble in DMSO anymore, it was suspended in 10 mL water and was stirred for one hour at 1400 rpm. The polymer was filtered, suspended in 30 ml water, and washed under reflux for one hour. This process was repeated three times. The polymer (134 mg) was obtained after drying at 100 °C and 12 mbar for at least 24 hours as yellow solid in quantitative yields.

IR: ν / cm^{-1} = 3342 (vw, br), 3151 (w, br), 2991 (w), 2921 (vw), 1693 (vw), 1602 (vw), 1520 (vs), 1485 (vs), 1415 (w), 1321 (w), 1284 (m), 1273 (m), 1224 (s), 1187 (vs), 1115 (m), 1098 (m), 1074 (m), 1018 (w), 965 (w), 934 (m), 825 (w), 782 (w), 638 (w), 619 (w), 580 (w), 564 (w), 531 (s) cm^{-1}

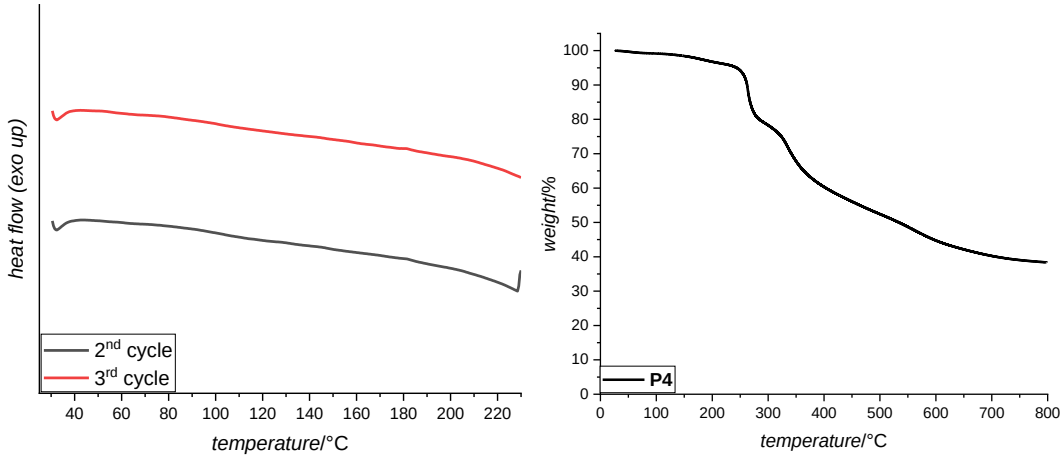

*Figure 201: Left: DSC-curve of **P4** from 25-230 °C at 30 K/min. Right: TGA-curve from 25-800 °C.*

Co-PolyTSC P5

N,*N*'-(1,4-Phenylenebis(methylene)) bis(hydrazinecarbothioamide) **89** (50.0 mg, 176 µmol, 1.00 eq.), *N*,*N*'-(dodecyl-1,12-diyl) bis(hydrazinecarbothioamide) **86** (26.3 mg, 75.4 µmol, 0.43 eq.), terephthaldehye **91** (33.7 mg, 251 µmol, 1.43 eq.) were used in 168 µL DMSO following the general procedure. 1.25 mL of DMSO were added to the reaction mixture for solubilizing the polymer for precipitation. After work-up, the product was obtained as yellow brittle solid (74.6 mg) in a yield of 74%.

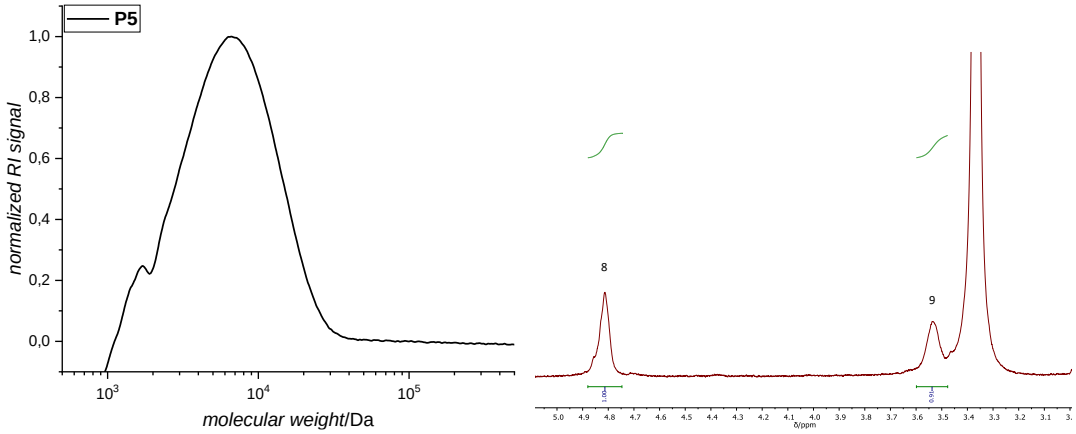

*Figure 202: Left: SEC-trace of **P5**. Right: Zoom-in of proton NMR-spectrum of **P5** for ratio determination of dithiosemicarbazide moieties. Ratio A:A´(see also Figure S25 below) = 52:48.*

^{1}H-NMR (500 MHz, DMSO-d_6) δ/ppm = 11.66 (s, 2H. NH, ^{1}), 11.49 (s, 2H, NH, ^{2}), 9.09 (s br, 2H, NH, ^{3}), 8.55 (s br, 2H, NH, ^{4}), 8.10-8.00 (m, 4H, CH, ^{5}), 7.82 (s, 8H, aromatic, ^{6}), 7.30 (s, 4H. aromatic, ^{7}), 4.81 (s, 4H, CH_2, ^{8}), 3.54 (s, 4H, CH_2, ^{9}), 1.57 (s, 4H, CH_2, ^{10}), 1.33-1.17 (m, 16H, CH_2, ^{11}).

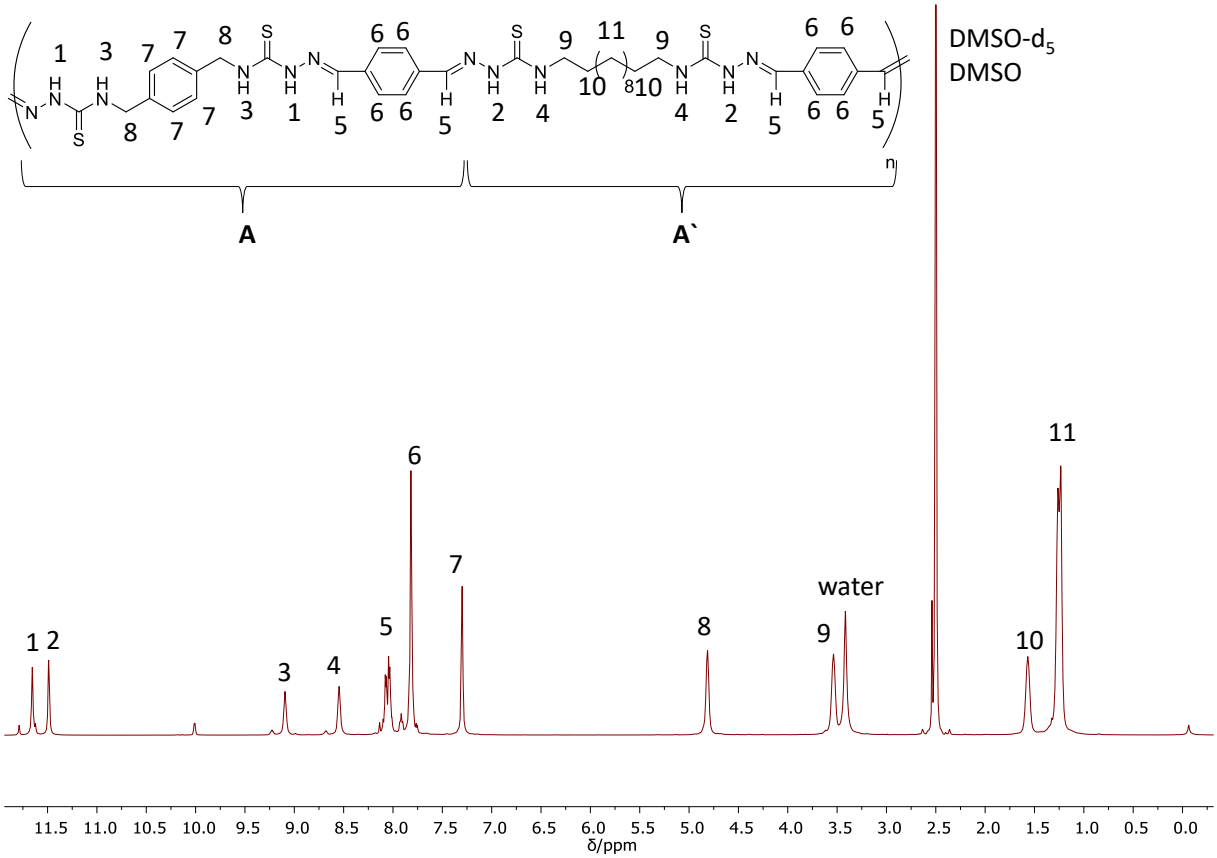

*Figure 203: Proton NMR-spectrum of **P5**.*

^{13}C-NMR (126 MHz, DMSO-d_6) δ/ppm = 177.49 (C=S), 176.80 (C=S), 141.53 (C=N), 141.10 (C=N), 137.80 (quaternary-aromatic), 135.37 (quaternary-aromatic), 127.41 (aromatic), 127.09 (aromatic), 46.41 (CH_2), 43.54 (CH_2), 29.05 (CH_2), 28.84 (CH_2), 26.37 (CH_2).

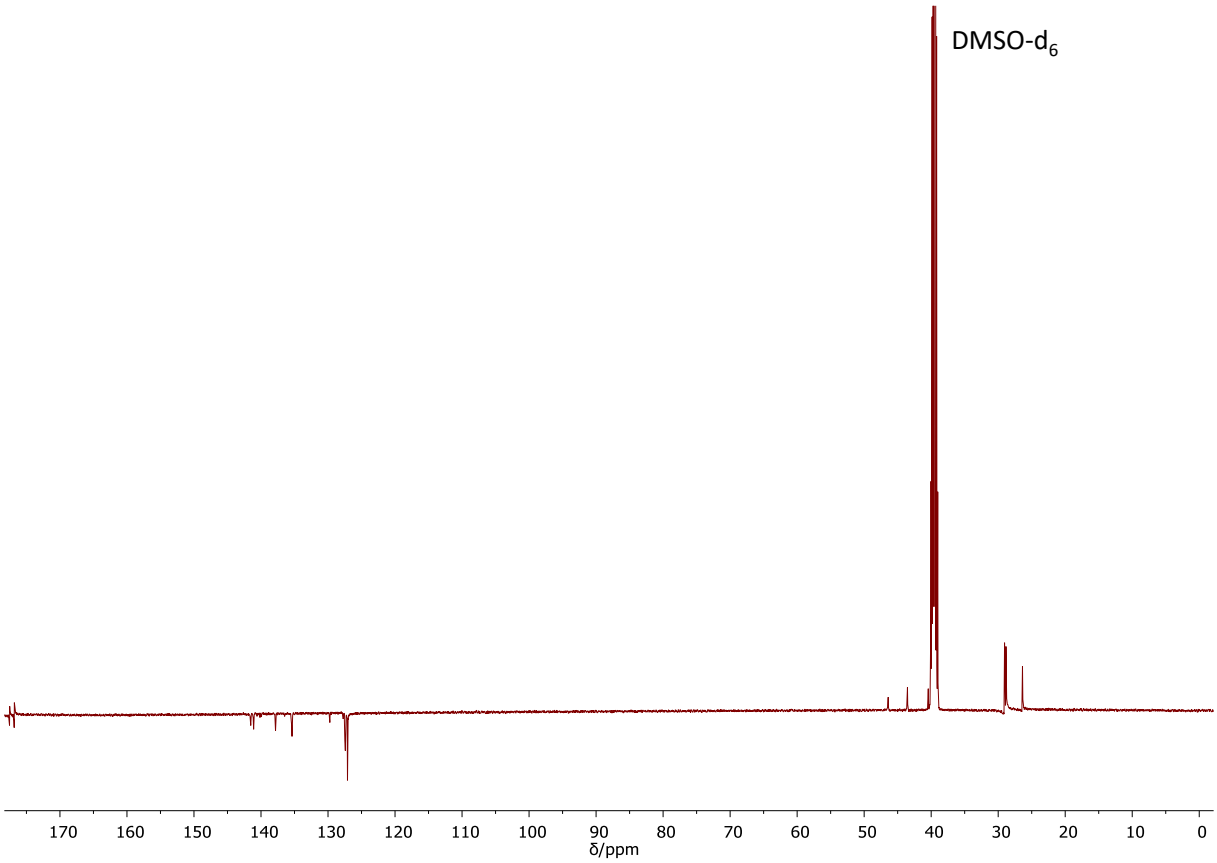

*Figure 204: Carbon NMR-spectrum of **P5**.*

IR: ν / cm^{-1} = 3338 (vw, br), 3145 (w, br), 2991 (w), 2921 (w), 2849 (w), 1693 (w), 1598 (vw), 1520 (vs), 1483 (vs), 1415 (w), 1321 (w), 1286 (m), 1271 (m), 1224 (s), 1187 (vs), 1115 (s), 1096 (s), 1018 (w), 963 (w), 934 (m), 825 (w), 782 (w), 576 (w), 533 (m), 479 (w), 457 (w) cm^{-1}

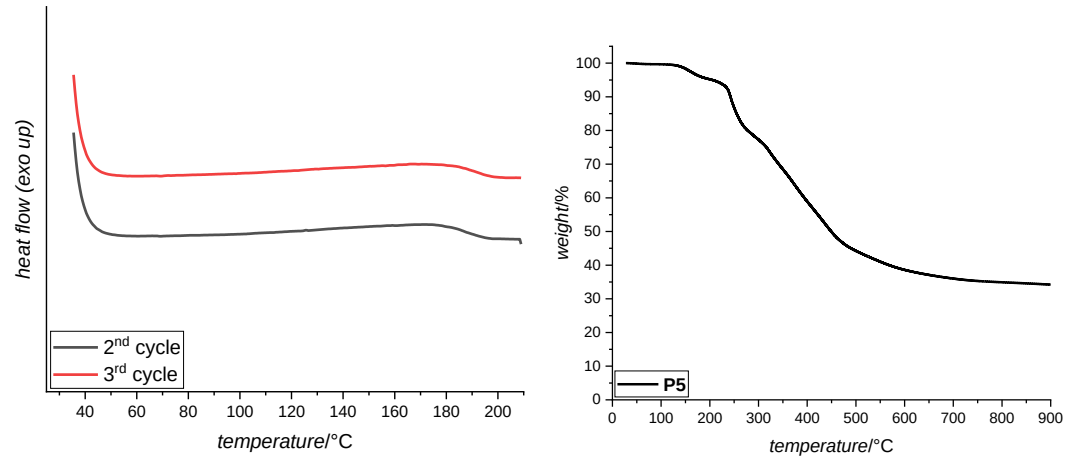

*Figure 205: Left: DSC-curve of **P5** from 25-200 °C at 30 K/min. Right: TGA-curve from 25-900 °C.*

Co-PolyTSC P6

N,*N*'-(1,4-Phenylenebis(methylene)) bis(hydrazinecarbothioamide) **89** (50.0 mg, 176 µmol, 1.00 eq.), *N*,*N*'-(dodecyl-1,12-diyl) bis(hydrazinecarbothioamide) **86** (61.3 mg, 176 µmol, 1.00 eq.), terephthaldehye **91** (47.2mg, 352 µmol, 2.00 eq.) were used in 234 µL DMSO following the general procedure. 1.25 mL of DMSO were added to the reaction mixture for solubilizing the polymer for precipitation. After work-up, the product was obtained as yellow brittle solid (85.8 mg) in a yield of 59%.

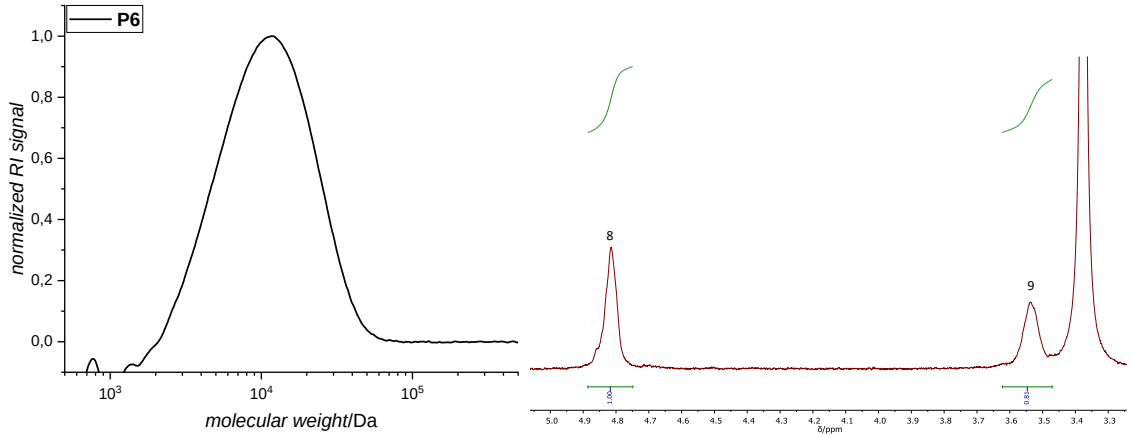

*Figure 206: Left: SEC-traces of **P6**. Right: Zoom-in of proton NMR-spectra of **P6** for ratio determination of dithiosemicarbazide moieties. Ratio A:A´ (see also Figure S29 below) = 56:44.*

^{1}H-NMR (400 MHz, DMSO-d_6) δ/ppm = 11.66 (s, 2H. NH, [1]), 11.49 (s, 2H, NH, [2]), 9.10 (t, ^3J = 6.5 Hz, 2H, NH, [3]), 8.56 (s br, 2H, NH, [4]), 8.10-8.00 (m, 4H, CH, [5]), 7.82 (s, 8H, aromatic, [6]), 7.32-7.28 (m, 4H. aromatic, [7]), 4.81 (s, 4H, CH_2, [8]), 3.53 (s, 4H, CH_2, [9]), 1.57 (s, 4H, CH_2, [10]), 1.33-1.17 (m, 16H, CH_2, [11]).

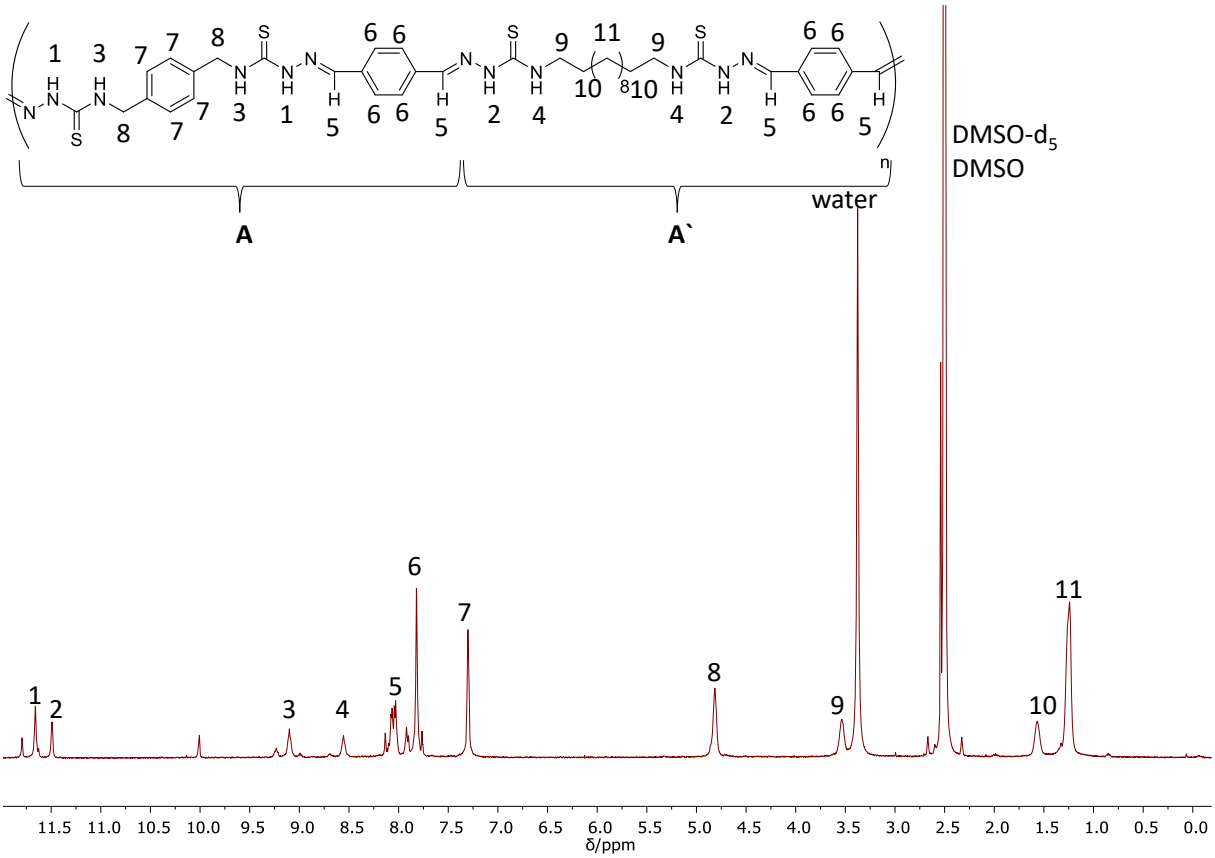

*Figure 207: Proton NMR-spectrum of **P6**.*

^{13}C-NMR (101 MHz, DMSO-d_6) δ/ppm = 177.51 (C=S), 176.81 (C=S), 141.51 (C=N), 141.10 (C=N), 138.82 (quaternary-aromatic), 135.37 (quaternary-aromatic), 127.41 (aromatic), 127.10 (aromatic), 46.42 (CH_2), 43.53 (CH_2), 29.04 (CH_2), 28.83 (CH_2), 26.36 (CH_2).

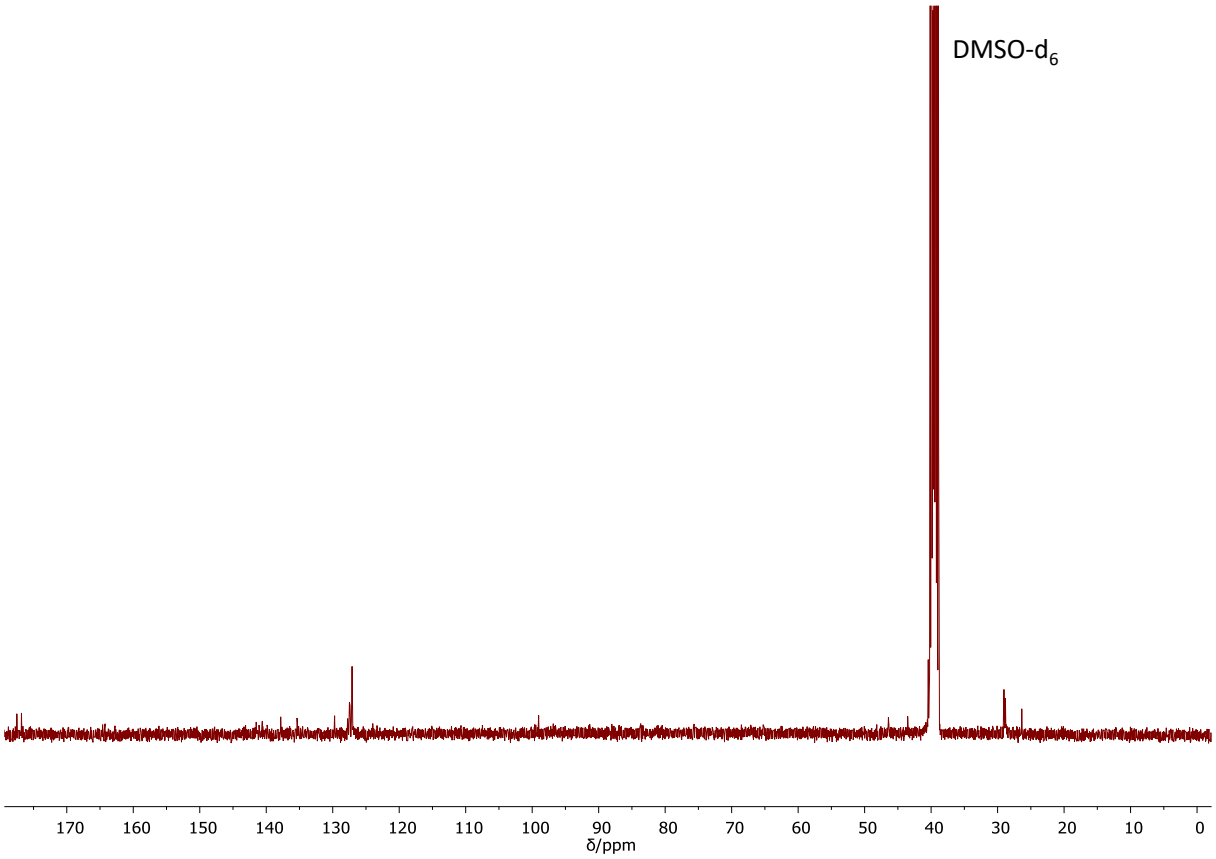

*Figure 208: Carbon NMR-spectrum of **P6**.*

IR: ν / cm^{-1} = 3310 (vw, br), 3147 (w, br), 2987 (w), 2921 (w), 2849 (w), 1693 (vw), 1604 (vw), 1522 (vs), 1483 (vs), 1415 (w), 1318 (w), 1286 (m), 1271 (m), 1224 (s), 1187 (vs), 1115 (m), 1096 (s), 1016 (w), 963 (w), 934 (w), 825 (w), 782 (w), 722 (vw), 642 (vw), 572 (w), 533 (m), 479 (w) cm^{-1}.

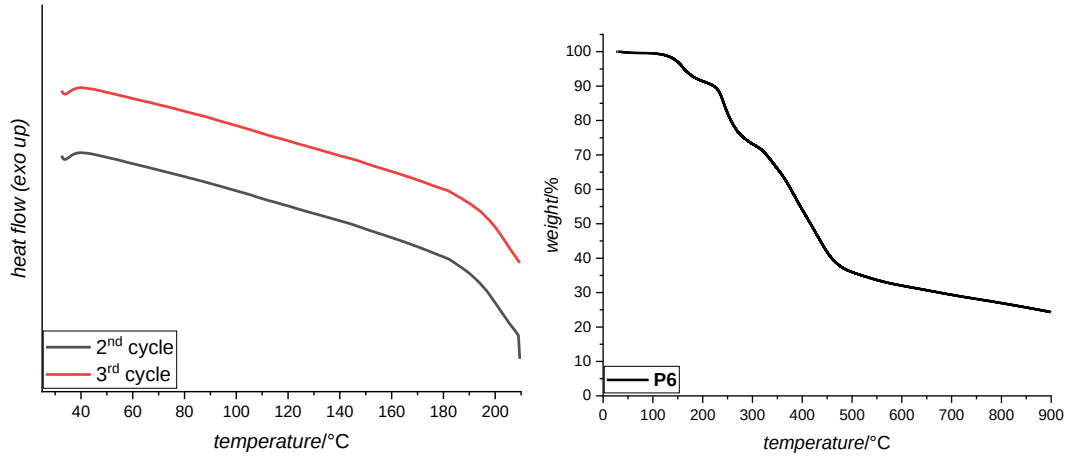

*Figure 209: Left: DSC-curve of **P6** from 25-200 °C at 30 K/min. Right: TGA-curve from 25-900 °C.*

Co-PolyTSC P7

N,*N*'-(1,4-Phenylenebis(methylene)) bis(hydrazinecarbothioamide) **89** (25.0 mg, 87.9 µmol, 1.00 eq.), *N*,*N*'-(dodecyl-1,12-diyl) bis(hydrazinecarbothioamide) **86** (71.4mg, 205 µmol, 2.33 eq.), terephthaldehye **91** (39.3 mg, 293 µmol, 3.33 eq.) were used in 195 µL DMSO following the general procedure. 850 µL of DMSO were added to the reaction mixture for solubilizing the polymer for precipitation. After work-up, the product was obtained as yellow powder (76.9 mg) in a yield of 62%.

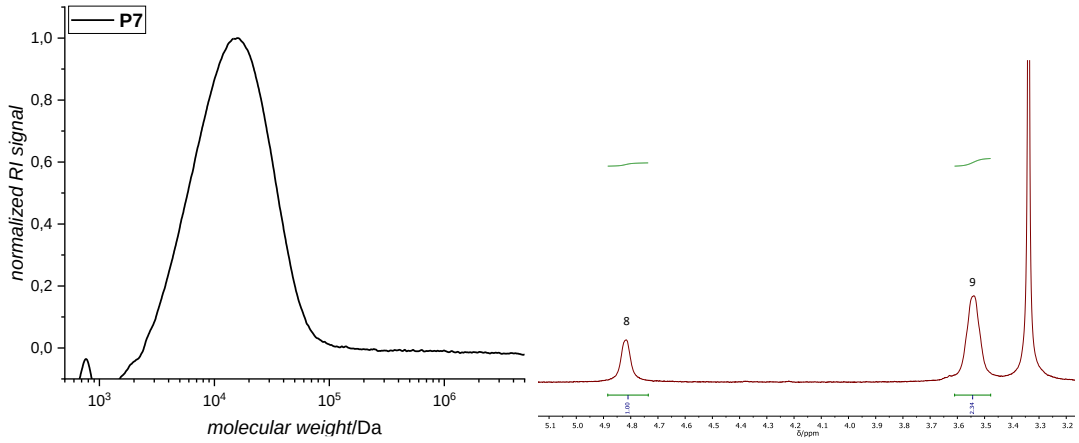

*Figure 210: Left: SEC-traces of **P7**. Right: Zoom-in of proton NMR-spectra of **P7** for ratio determination of dithiosemicarbazide moieties. Ratio A:A´ (see also Figure S33 below) = 30:70.*

^{1}H-NMR (400 MHz, DMSO-d_6) δ/ppm = 11.66 (s, 2H. NH, ^{1}), 11.49 (s, 2H, NH, ^{2}), 9.10 (t, ^{3}J = 5.6 Hz, 2H, NH, ^{3}), 8.56 (s br, 2H, NH, ^{4}), 8.10-8.00 (m, 4H, CH, ^{5}), 7.82 (s, 8H, aromatic, ^{6}), 7.32-7.28 (m, 4H. aromatic, ^{7}), 4.81 (s, 4H, CH_2, ^{8}), 3.54 (s, 4H, CH_2, ^{9}), 1.57 (s, 4H, CH_2, ^{10}), 1.33-1.15 (m, 16H, CH_2, ^{11}).

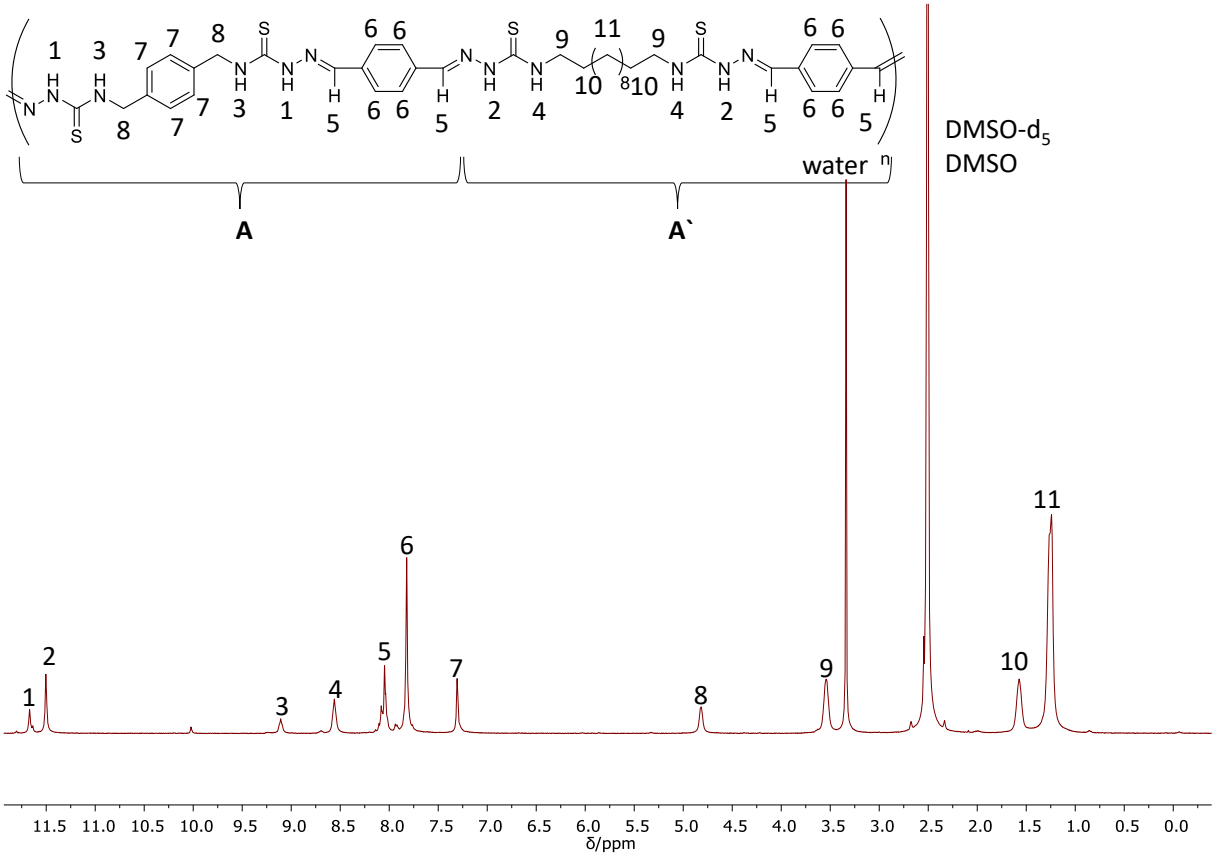

*Figure 211: Proton NMR-spectrum of **P7**.*

^{13}C-NMR (101 MHz, DMSO-d_6) δ/ppm = 177.51 (C=S), 176.81 (C=S), 141.53 (C=N), 141.10 (C=N), 138.82 (quaternary-aromatic), 135.37 (quaternary-aromatic), 127.41 (aromatic), 127.10 (aromatic), 46.42 (CH_2), 43.53 (CH_2), 29.04 (CH_2), 28.83 (CH_2), 26.36 (CH_2).

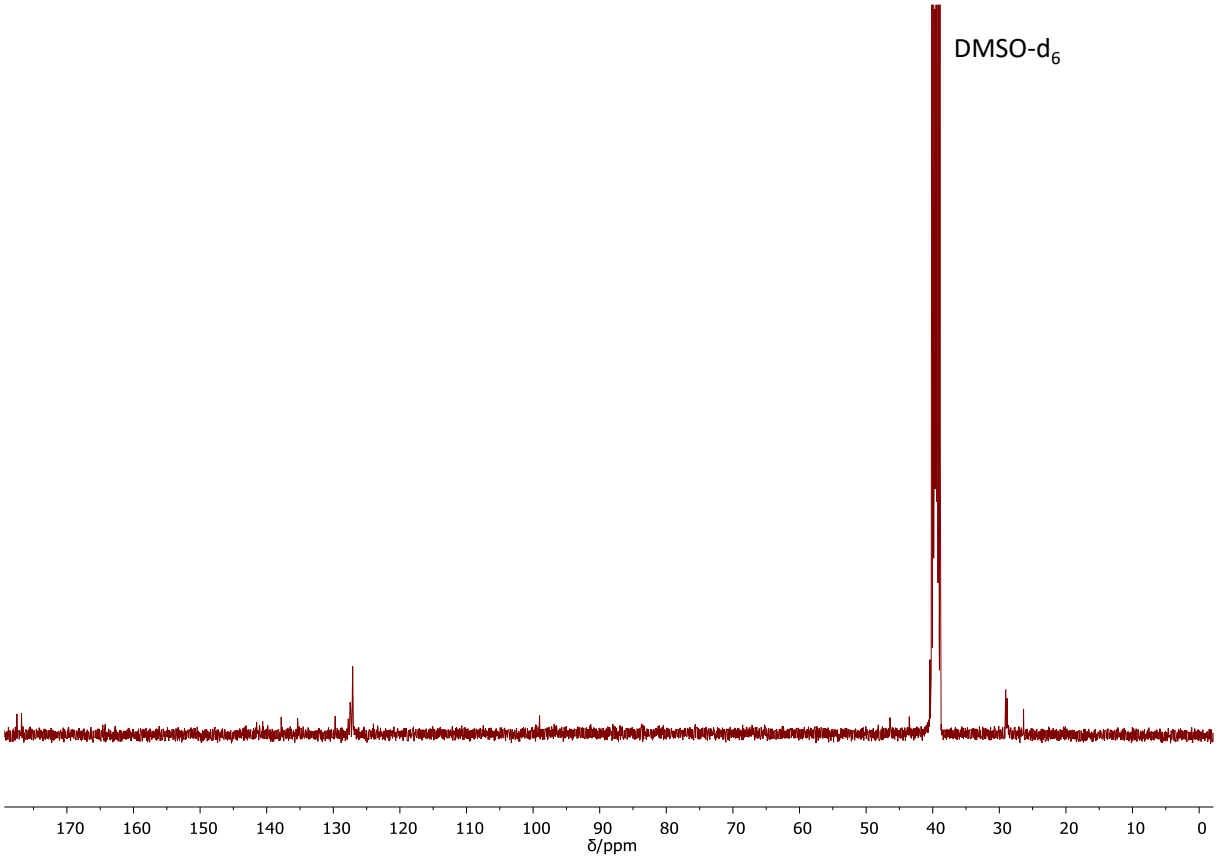

*Figure 212: Carbon NMR-spectrum of **P7**.*

IR: ν / cm^{-1} = 3320 (vw, br), 3147 (w, br), 2923 (m), 2851 (w), 1693 (vw), 1602 (vw), 1526 (vs), 1485 (vs), 1415 (w), 1316 (w), 1288 (m), 1224 (s), 1189 (s), 1096 (s), 1014 (w), 936 (w), 827 (w), 780 (w), 722 (vw), 640 (w), 576 (w), 564 (w), 533 (m), 500 (w), 483 (w) cm^{-1}.

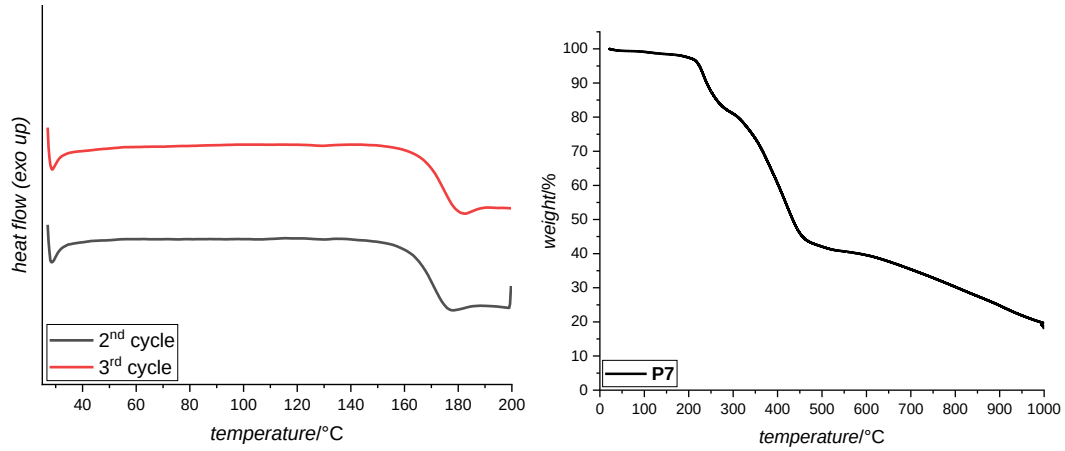

*Figure 213: Left: DSC-curve of **P7** from 25-200 °C at 30 K/min. Right: TGA-curve from 25-1000 °C.*

Co-PolyTSC P10

N,*N*'-(*Trans*-cyclohexane-1,4-diyl) bis(hydrazinecarbothioamide) **88** (25.0 mg, 98.3 µmol, 1.00 eq.), *N*,*N*'-(dodecyl-1,12-diyl) bis(hydrazinecarbothioamide) **86** (77.4mg, 222 µmol, 2.33 eq.), terephthaldehye **91** (42.6 mg, 317 µmol, 3.33 eq.) were used in 408 µL DMSO (c(TSC)=0.75 M) following the general procedure. 5 mL of DMSO were added to the reaction mixture for solubilizing the polymer, however, it was only partially dissolved. Thus, the insoluble part was filtered and the soluble part was precipitated in 30 ml cold water. Both fractions were combined and the usual work-up was applied. The product was obtained as yellow flakes (76.7 mg) in a yield of 58%.

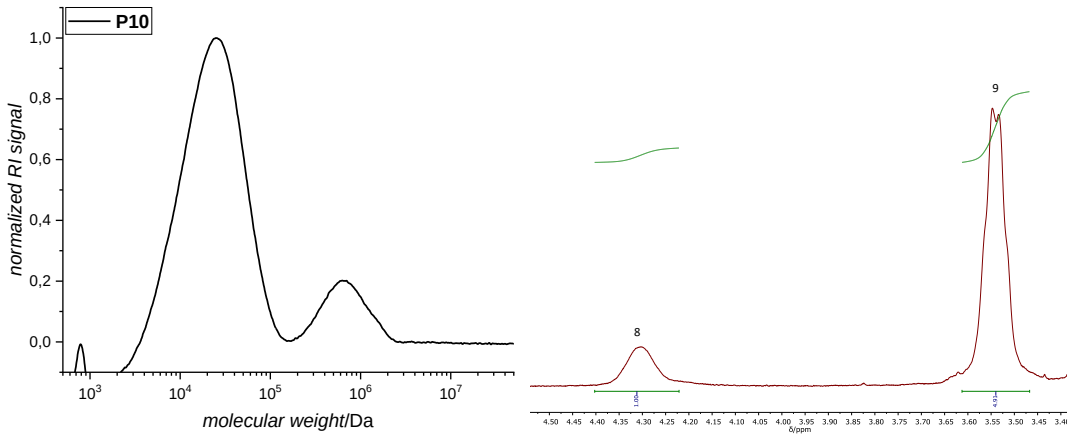

*Figure 214: Left: SEC-traces of **P10**. Right: Zoom-in of roton NMR-spectra of **P10** for ratio determination of dithiosemicarbazide moieties. Ratio A:A´ (see also Figure S37 below) = 29:71.*

^{1}H-NMR (400 MHz, DMSO-d_6) δ/ppm = 11.54 (s, 2H, NH, ^{1}), 11.50 (s, 2H, NH, ^{2}), 8.55 (t, ^3J = 6.3 Hz, 2H, NH, ^{3}), 8.16 (d, ^3J = 7.8 Hz, 2H, NH, ^{4}), 8.08-8.02 (m, 4H, CH, ^{5}), 7.83 (s, 4H, aromatic, ^{6}), 7.82 (s, 4H, aromatic, ^{7}), 4.30 (s br, 2H, CH, ^{8}), 3.54 (q, ^3J = 6.9 Hz, 4H, CH_2, ^{9}), 1.96 (s br, 4H, CH_2, ^{10}), 1.69-1.50 (m, 8H, CH_2, ^{10}), 1.34-1.17 (m, 16H, CH_2, ^{11}).

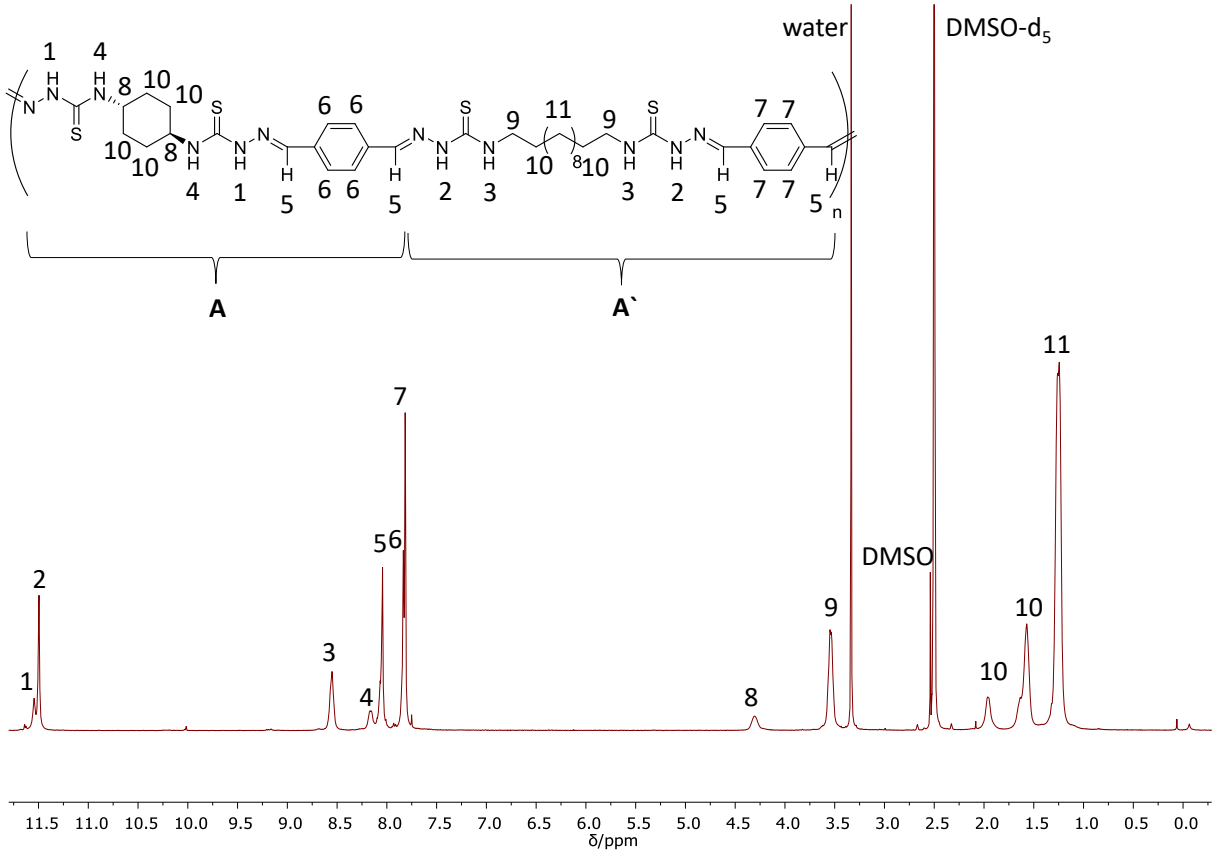

*Figure 215: Proton NMR-spectrum of **P10**.*

^{13}C-NMR (101 MHz, DMSO-d_6) δ/ppm = 176.82 (C=S), 175.90 (C=S), 141.58 (C=N), 141.09 (C=N), 135.48 (quaternary-aromatic), 135.36 (quaternary-aromatic), 135.21 (quaternary-aromatic), 127.56 (aromatic), 127.41 (aromatic), 52.17 (CH), 43.54 (CH_2), 30.43 (CH_2), 29.05(CH_2), 28.85 (CH_2), 26.38 (CH_2).

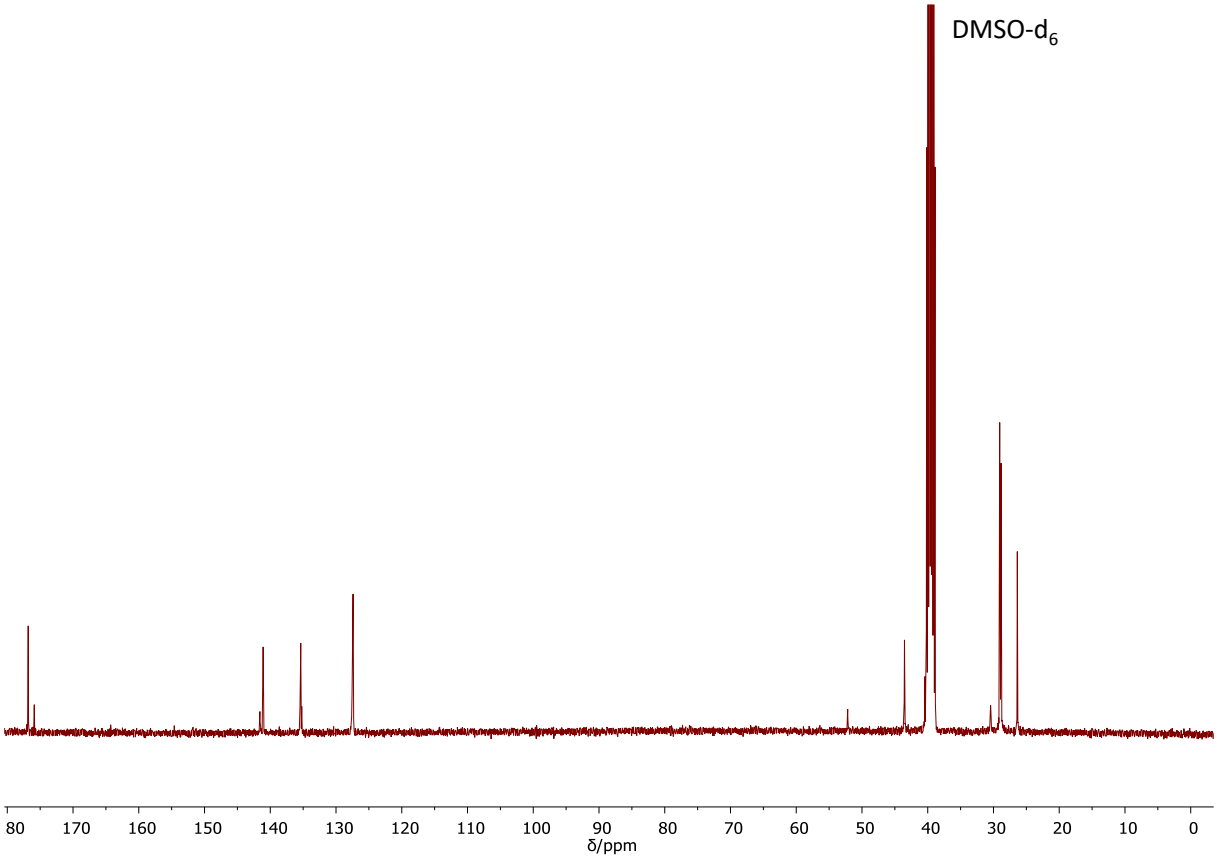

*Figure 216: Carbon NMR-spectrum of **P10**.*

IR: ν / cm^{-1} = 3349 (vw, br), 3143 (vw, br), 2923 (w), 2851 (w), 1691 (vw), 1594 (vw), 1524 (vs), 1485 (vs), 1415 (w), 1370 (vw), 1321 (w), 1290 (m), 1226 (s), 1191 (vs), 1119 (m), 1096 (s), 1014 (w), 975 (w), 938 (w), 872 (vw), 827 (w), 786 (w), 726 (w), 638 (w), 564 (m), 535 (s), 490 (m) cm^{-1}.

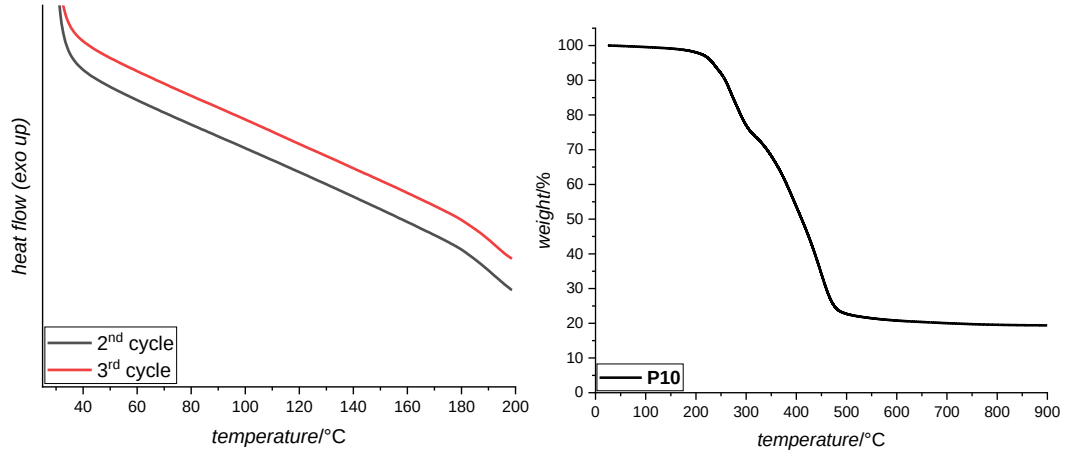

*Figure 217: Left: DSC-curve of **P10** from 25-210 °C at 30 K/min. Right: TGA-curve from 25-900 °C.*

Co-PolyTSC P11

N,*N*'-(*Trans*-cyclohexane-1,4-diyl) bis(hydrazinecarbothioamide) **88** (7.00 mg, 26.7 µmol, 1.00 eq.), *N*,*N*'-(dodecyl-1,12-diyl) bis(hydrazinecarbothioamide) **86** (83.7 mg, 240 µmol, 9.00 eq.), terephthaldehye **91** (35.8 mg, 267 µmol, 10.0 eq.) were used in 267 µL DMSO following the general procedure. 950 µL of DMSO were added to the reaction mixture for solubilizing the polymer for precipitation. After work-up, the product was obtained as yellow porous solid (98.0 mg) in a yield of 84%.

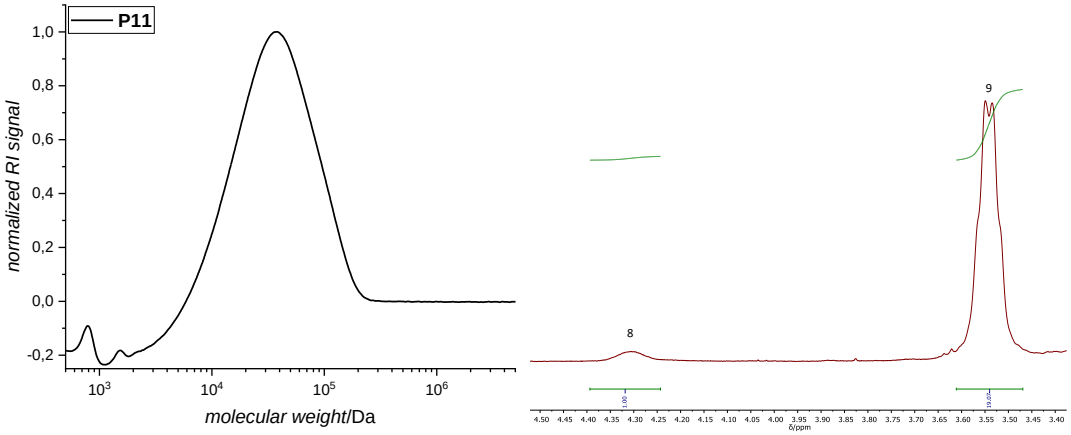

*Figure 218: Left: SEC-traces of **P11**. Right: Zoom-in of proton NMR-spectra of **P11** for ratio determination of dithiosemicarbazide moieties. Ratio A:A´ (see also Figure S41 below) = 9:91.*

^{1}H-NMR (400 MHz, DMSO-d_6) δ/ppm = 11.54 (s, 2H, NH, ^{1}), 11.50 (s, 2H, NH, ^{2}), 8.55 (t, ^{3}J = 6.3 Hz, 2H, NH, ^{3}), 8.16 (d, ^{3}J = 7.8 Hz, 2H, NH, ^{4}), 8.08-8.02 (m, 4H, CH, ^{5}), 7.83 (s, 4H, aromatic, ^{6}), 7.82 (s, 4H, aromatic, ^{7}), 4.30 (s br, 2H, CH, ^{8}), 3.54 (q, ^{3}J = 6.9 Hz, 4H, CH_2, ^{9}), 1.96 (s br, 4H, CH_2, ^{10}), 1.69-1.50 (m, 8H, CH_2, ^{10}), 1.34-1.17 (m, 16H, CH_2, ^{11}).

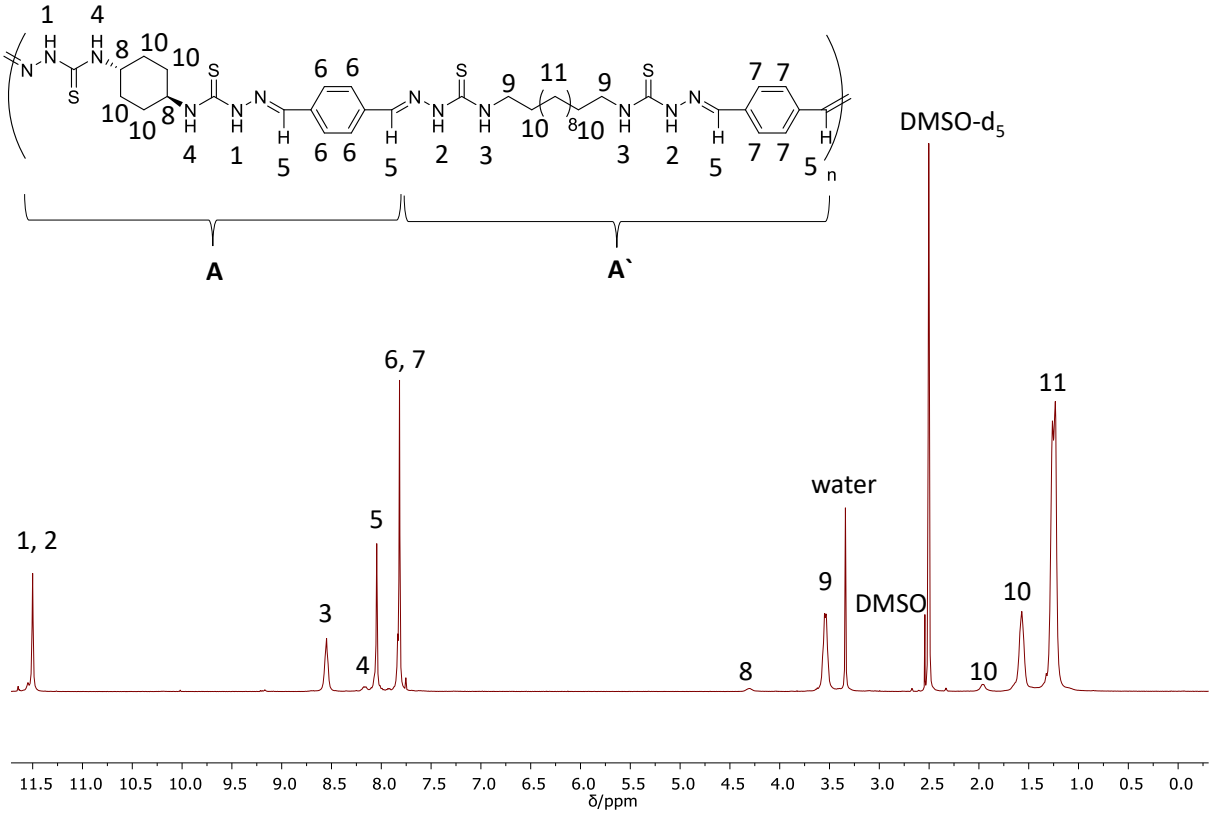

*Figure 219: Proton NMR-spectrum of **P11**.*

^{13}C-NMR (101 MHz, DMSO-d_6) δ/ppm = 176.81 (C=S), 141.08 (C=N), 135.36 (quaternary-aromatic), 127.41 (aromatic), 52.65 (CH), 43.54 (CH_2), 30.41 (CH_2), 29.05 (CH_2), 28.86 (CH_2), 26.38 (CH2).

Carbon signals arising of monomer **88** are not all visible due to low intensity, compare **P10**.

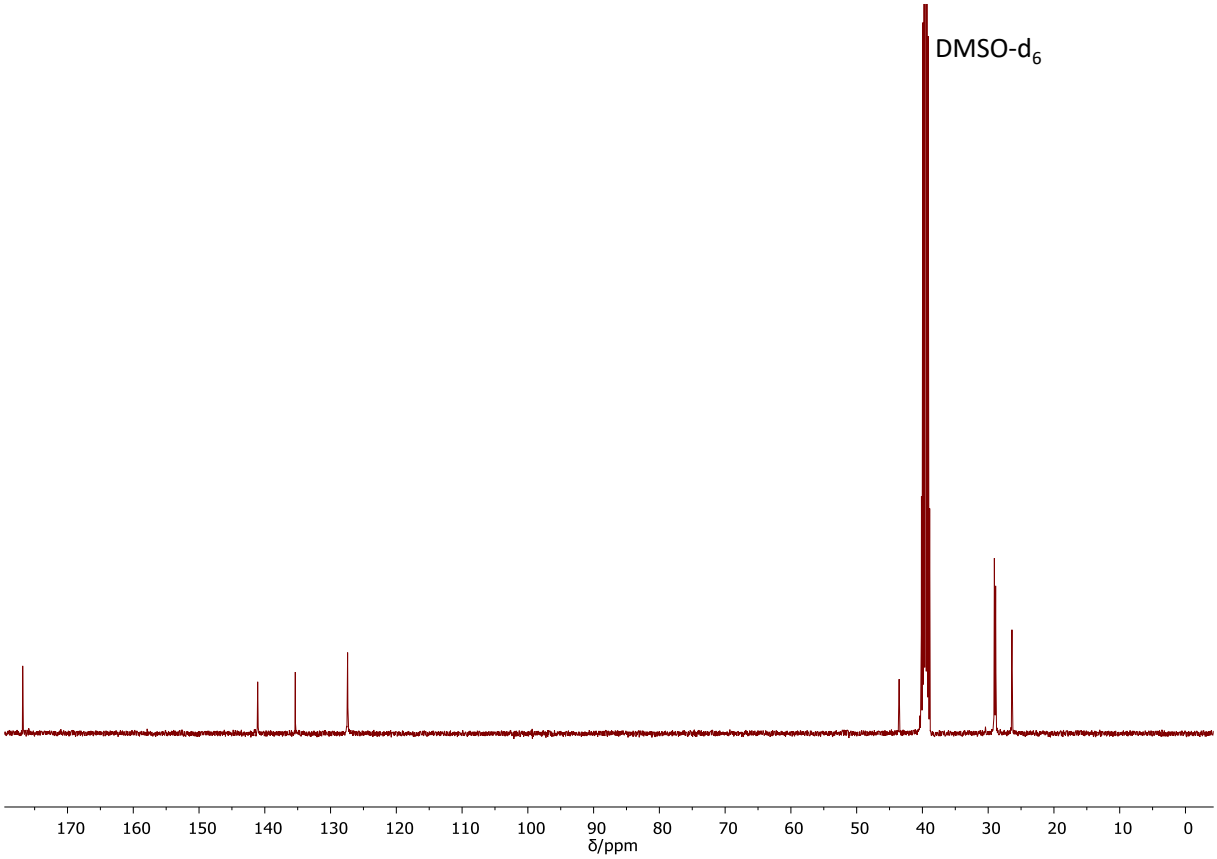

*Figure 220: Carbon NMR-spectrum of **P11**.*

IR: ν / cm^{-1} = 3345 (vw, br), 3151 (vw, br), 2923 (w), 2851 (w), 1623 (vw), 1526 (vs), 1485 (vs), 1415 (w), 1316 (w), 1288 (w), 1226 (s), 1191 (s), 1117 (w), 1096 (m), 938 (w), 827 (w), 786 (vw), 716 (vw), 640 (w), 574 (w), 535 (m), 498 (w) cm^{-1}.

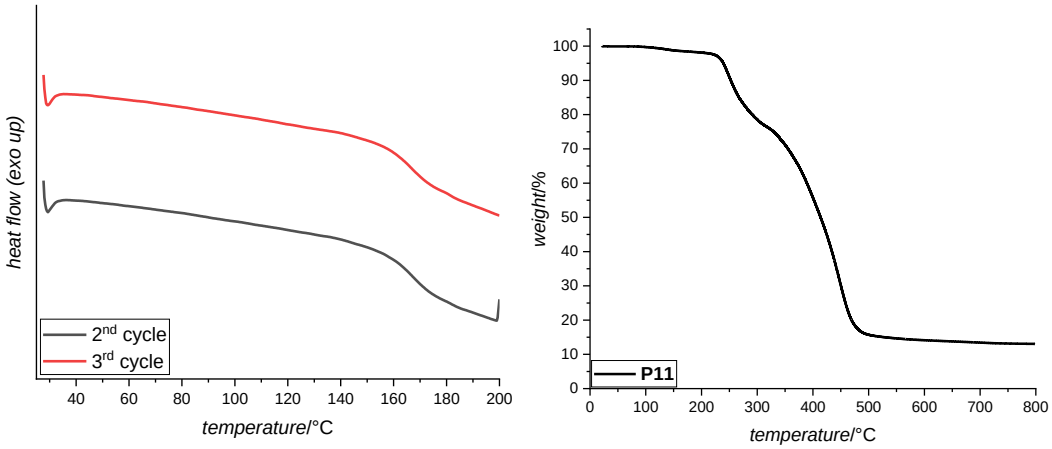

*Figure 221: Left: DSC-curve of **P11** from 25-210 °C at 30 K/min. Right: TGA-curve from 25-800 °C.*

PolyTSC P12

N,*N*'-(Dodecyl-1,12-diyl) bis(hydrazinecarbothioamide) **86** (100 mg, 287 mmol, 1.00 eq.) and biphenyl-4,4´dicarbaldehyde **92** (60.3 mg, 287 mmol, 1.00 eq.) were used in 191 µL DMSO following the general procedure. The reaction was stirred for 4 hours at room temperature and then at 100 °C and 500 mbar for 17 hours. 1.1 mL of DMSO were added to the reaction mixture for solubilizing the polymer for precipitation. After work-up, the product was obtained as yellow solid (131 mg) in a yield of 87%.

N,*N*'-(Dodecyl-1,12-diyl) bis(hydrazinecarbothioamide) **86** (1.00 g, 2.87 mol, 1.00 eq.) and biphenyl-4,4´-dicarbaldehyde **92** (603 g, 2.87 mol, 1.00 eq.) were used in 1.9 mL DMSO following the general procedure. The reaction was stirred for 4 hours at room temperature and then at 100 °C and 500 mbar for 17 hours. 5 mL of NMP were added to the reaction mixture for solubilizing the polymer for precipitation using a sonification bath (50 °C, 80 kHz) out of 400 mL of water. After work-up, the product was obtained as yellow solid (1.46 g) in a yield of 92% containing less than 2 w% of DMSO.

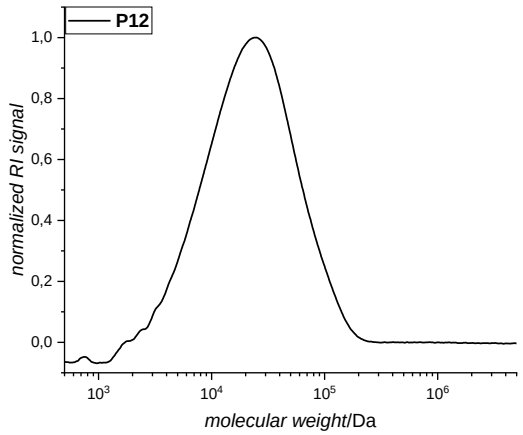

*Figure 222: SEC-trace of **P12**. M_n=17.0 kDa, M_w=30.8 kDa, Đ=1.81 (crude SEC displayed: M_n=15.4 kDa, M_w=34.9 kDa, Đ=2.27).*

^{1}H-NMR (400 MHz, DMSO-d_6) δ/ppm = 11.47 (s, 2H, NH, ^{1}), 8.54 (s br, 2H, NH, ^{2}), 8.08 (s, 2H, CH, ^{3}), 7.88 (d, ^3J = 7.9 Hz, 4H, aromatic, ^{4}), 7.75 (d, ^3J = 8.1 Hz, 4H, aromatic, ^{5}), 3.55 (q, ^3J = 7.0 Hz, 4H, CH_2, ^{6}), 1.78-1.46 (m, 4H, CH_2, ^{7}), 1.32-1.14 (m, 16H, CH_2, ^{8}).

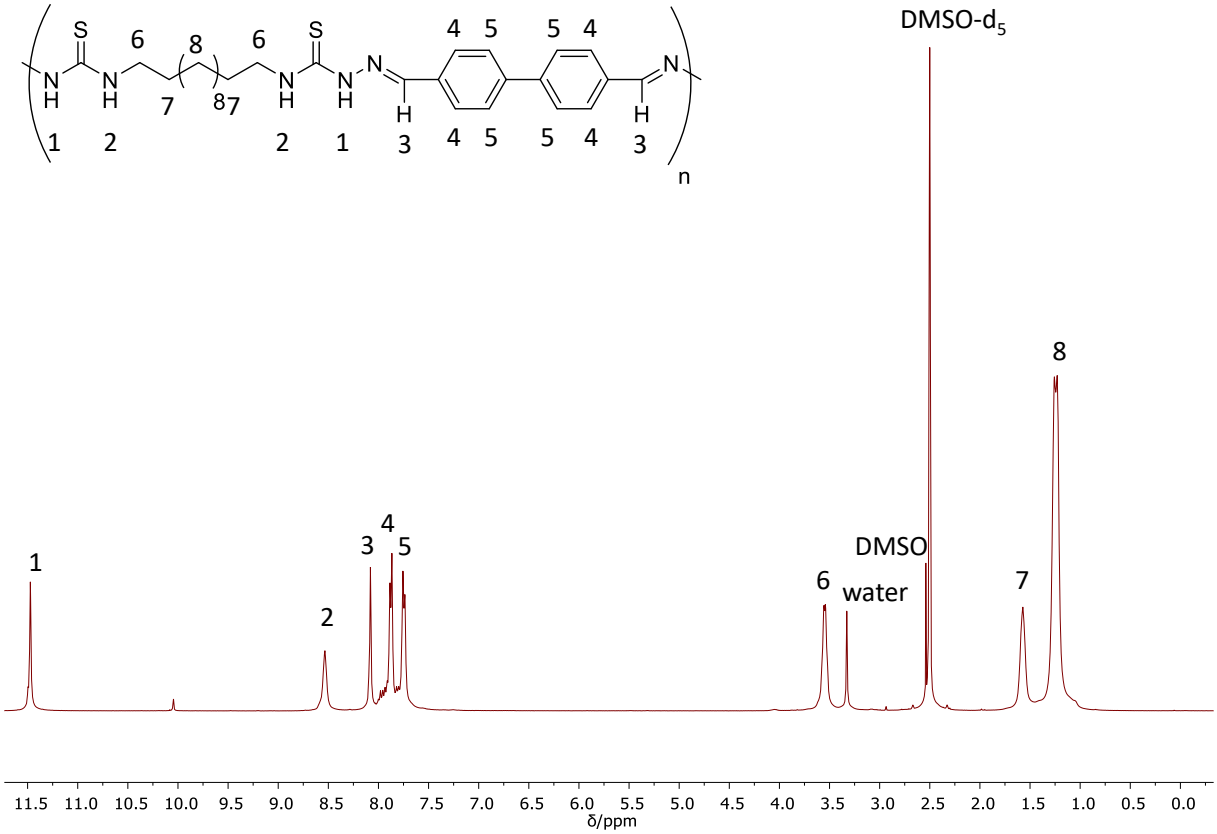

*Figure 223: Proton NMR-spectrum of **P12**.*

^{13}C-NMR (126 MHz, DMSO-d_6) δ/ppm = 176.80 (C=S), 141.22 (C=N), 140.38 (quaternary-aromatic), 133.72 (quaternary-aromatic), 127.87 (aromatic), 126.80 (aromatic), 43.53 (CH_2), 29.03 (CH_2), 28.84 (CH_2), 26.36 (CH_2).

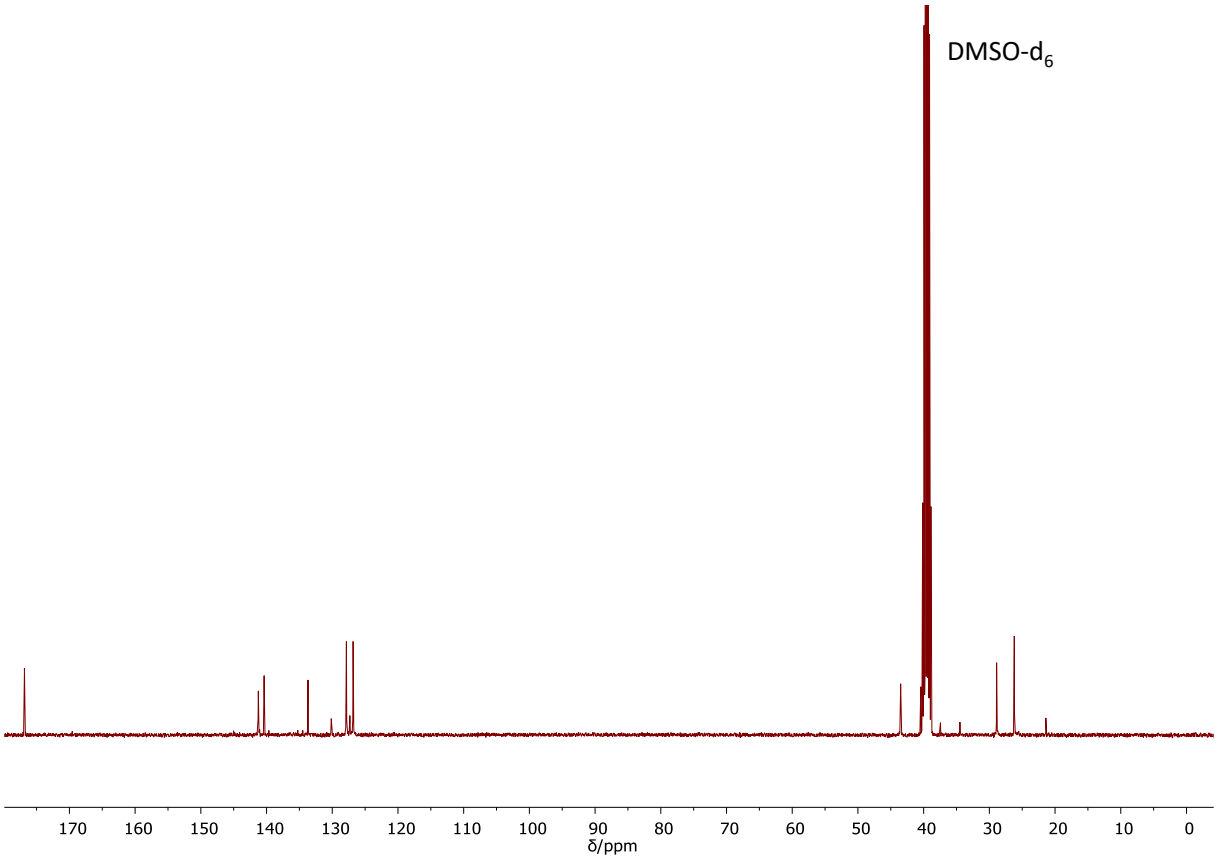

*Figure 224: Carbon NMR-spectrum of **P12**.*

IR: ν / cm^{-1} = 3320 (vw, br), 3149 (vw, br), 2921 (m), 2851 (w), 1697 (vw), 1606 (w), 1530 (vs), 1487 (vs), 1403 (vw), 1327 (w), 1288 (w), 1230 (s), 1205 (m), 1098 (m), 1004 (w), 956 (vw), 930 (vw), 819 (m), 796 (vw), 722 (vw), 640 (vw), 590 (w), 578 (w), 559 (w), 520 (w) cm^{-1}.

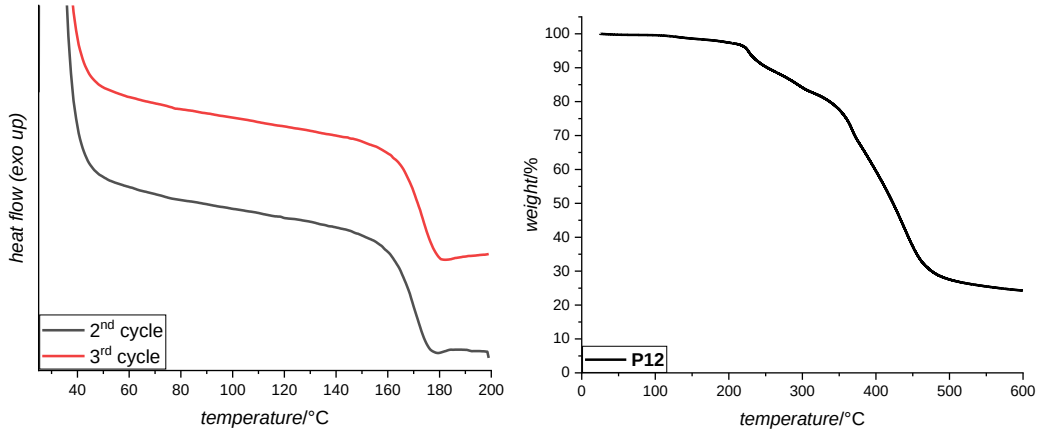

*Figure 225: Left: DSC-curve of **12** from 25-200 °C at 30 K/min. Right: TGA-curve from 25-600 °C.*

PolyTSC P13

N,*N*'-(Hexyl-1,6-diyl) bis(hydrazinecarbothioamide) **87** (100 mg, 378 mmol, 1.00 eq.) and biphenyl-4,4´-dicarbaldehyde **92** (79.5 mg, 378 mmol, 1.00 eq.) were used in 378 µL DMSO (c(dithiosemicarbazide)=1.0 M) to improve the solubility following the general procedure. The reaction was stirred for 4 hours at room temperature and then at 100 °C and 500 mbar for 17 hours. 1.1 mL of DMSO were added to the reaction mixture for solubilizing the polymer for precipitation. After work-up, the product was obtained as yellow static flakes (149 mg) in a yield of 90%.

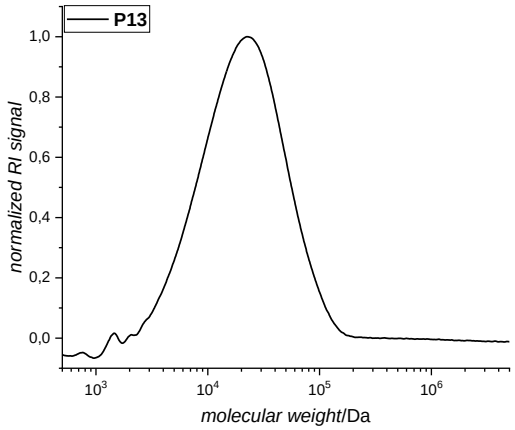

*Figure 226: SEC-trace of **P13**. M_n=16.8 kDa, M_w=28.0 kDa, Đ=1.67 (crude SEC displayed: M_n=18.8 kDa, M_w=26.3 kDa, Đ=1.40).*

^{1}H-NMR (400 MHz, DMSO-d_6) δ/ppm = 11.49 (s, 2H, NH,[1]), 8.58 (t, ^3J = 6.2 Hz, 2H, NH, [2]), 8.09 (s, 2H, CH, [3]), 7.89 (d, ^3J = 8.0 Hz, 4H, aromatic, [4]), 7.77 (d, ^3J = 8.1 Hz,4H, aromatic, [5]), 3.59 (q, ^3J = 6.9 Hz, 4H, CH_2, [6]), 1.64 (t, ^3J = 7.5 Hz, 4H, CH_2, [7]), 1.40-1.33 (m, 4H, CH_2, [8]).

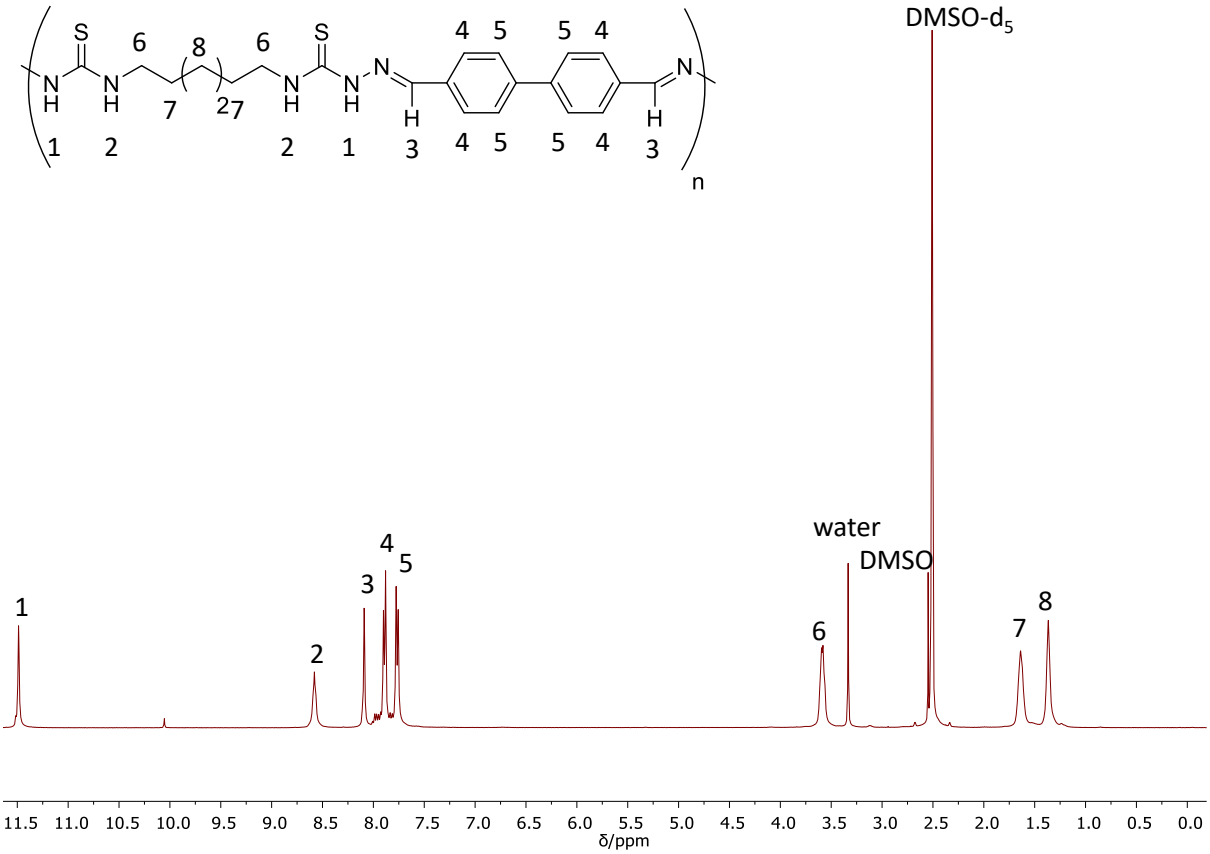

*Figure 227: Proton NMR-spectrum of **P13**.*

^{13}C-NMR (126 MHz, DMSO-d_6) δ/ppm = 176.84 (C=S), 141.27 (C=N), 140.38 (quaternary-aromatic), 133.71 (quaternary -aromatic), 127.87 (aromatic), 126.85 (aromatic), 43.51 (CH_2), 28.90 (CH_2), 26.22 (CH_2).

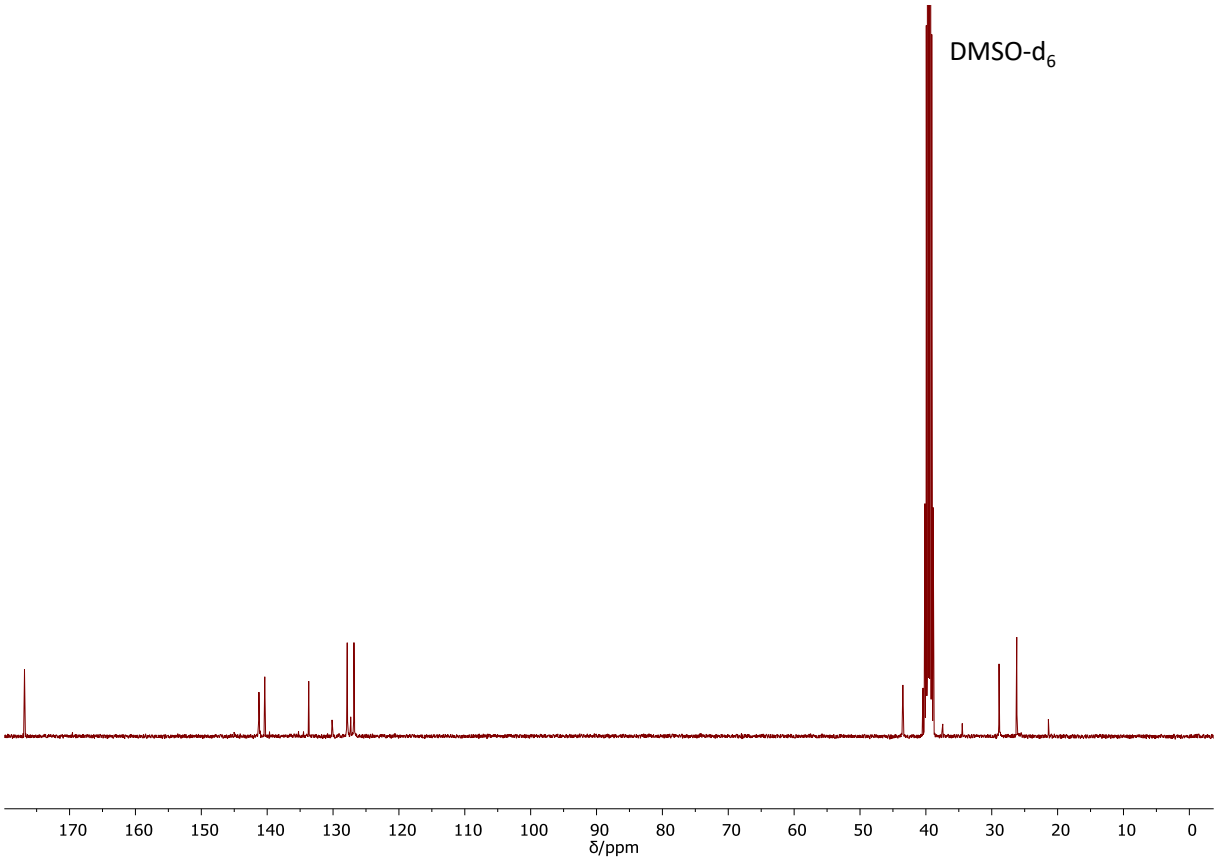

*Figure 228: Carbon NMR-spectrum of **P13**.*

IR: ν / cm^{-1} = 3324 (vw, br), 3133 (vw, br), 2929 (w), 2855 (w), 1693 (vw), 1606 (w), 1530 (vs), 1485 (vs), 1423 (w), 1401 (w), 1327 (w), 1294 (w), 1230 (s), 1212 (m), 1195 (m), 1172 (m), 1092 (s), 1016 (w), 1004 (w), 930 (w), 817 (s), 716 (vw), 588 (w), 580 (w), 557 (w), 518 (w), 467 (w) cm^{-1}.

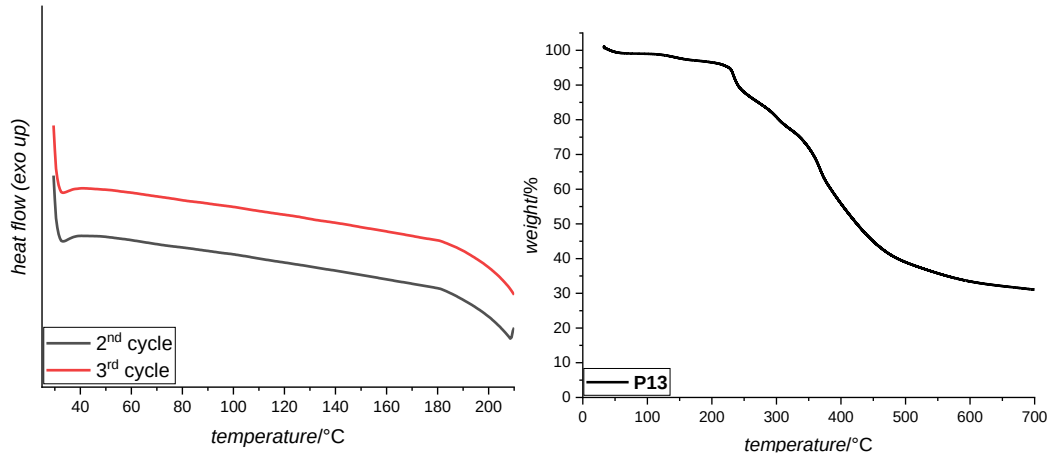

*Figure 229: Left: DSC-curve of **P13** from 25-210 °C at 30 K/min. Right: TGA-curve from 25-700 °C.*

PolyTSC P14

N,*N*'-(Dodecyl-1,12-diyl) bis(hydrazinecarbothioamide) **86** (100 mg, 287 mmol, 1.00 eq.) and 4,4'-(ethyne-1,2-diyl) dibenzaldehyde **93** (67.2 mg, 287 mmol, 1.00 eq.) were used in 287 µL DMSO (c(dithiosemicarbazide)=1.0 M) to improve the solubility following the general procedure. The reaction was stirred for 4 hours at room temperature and then at 100 °C and 500 mbar for 17 hours. 1.45 mL of DMSO were added to the reaction mixture for solubilizing the polymer for precipitation. After work-up, the product was obtained as brown solid (146 mg) in a yield of 93%.

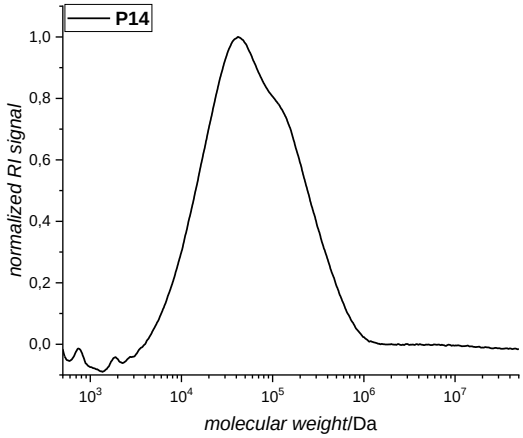

*Figure 230:SEC-trace of **P14**. M_n=38.1 kDa, M_w=91.1 kDa, Đ=2.41 (crude SEC displayed: M_n=25.7 kDa, M_w=46.6 kDa, Đ=1.81).*

^{1}H-NMR (400 MHz, DMSO-d_6) δ/ppm = 11.50 (s, 2H, NH, ^{1}), 8.58 (t, ^3J = 7.0 Hz, 2H, NH, ^{2}), 8.05 (s, 2H, CH, ^{3}), 7.85 (d, ^3J = 8.2 Hz, 4H, aromatic, ^{4}), 7.58 (d, ^3J = 8.0 Hz, 4H, aromatic, ^{5}), 3.54 (q, ^3J = 7.0 Hz, 4H, aromatic), 1.66-1.48 (m, 4H, CH_2, ^{7}), 1.32-1.12 (m, 16H, CH_2, ^{8}).

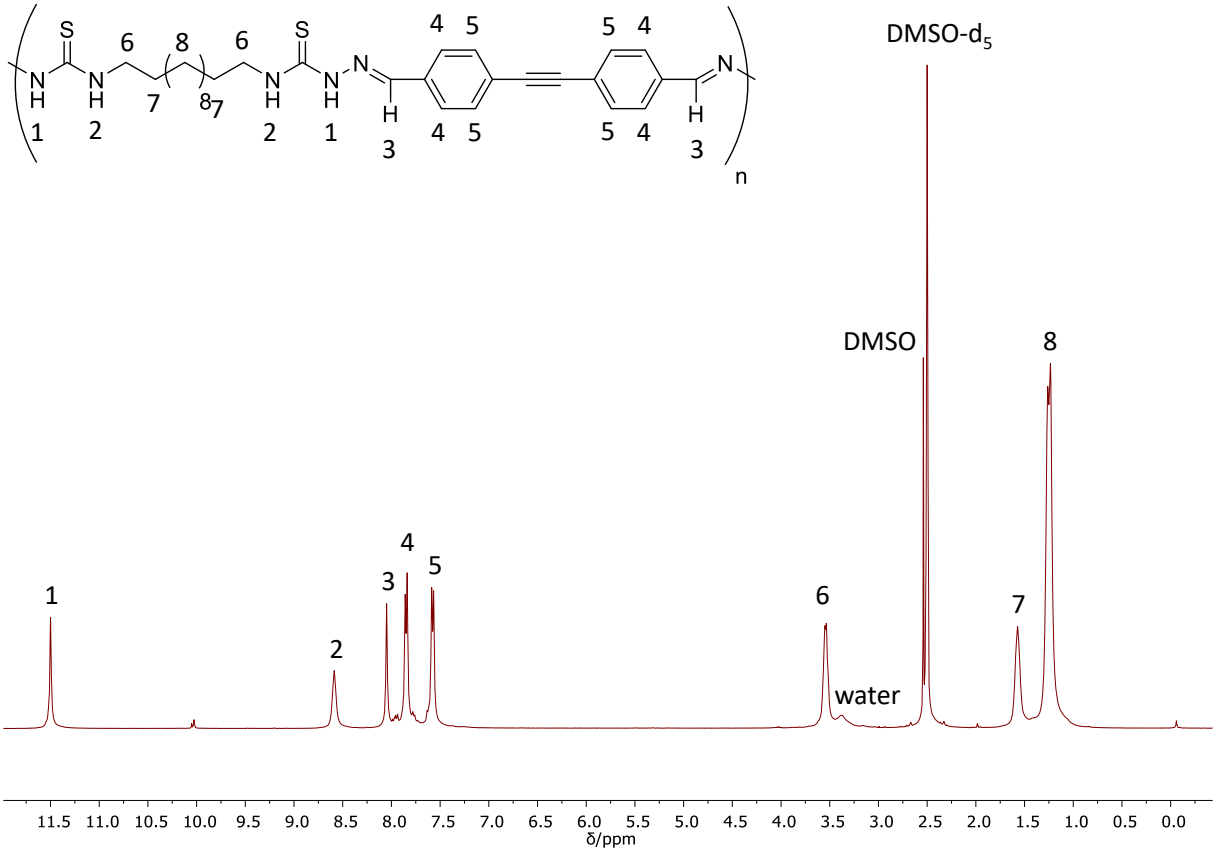

*Figure 231: Proton NMR-spectrum of **P14**.*

^{13}C-NMR (101 MHz, DMSO-d_6) δ/ppm = 176.85 (C=S), 140.67 (C=N), 134.65 (quaternary-aromatic), 131.61 (aromatic), 127.42 (aromatic), 123.00 (quaternary-aromatic), 91.01 (C≡C), 43.56 (CH_2), 29.04 (CH_2), 28.84 (CH_2), 26.37 (CH_2).

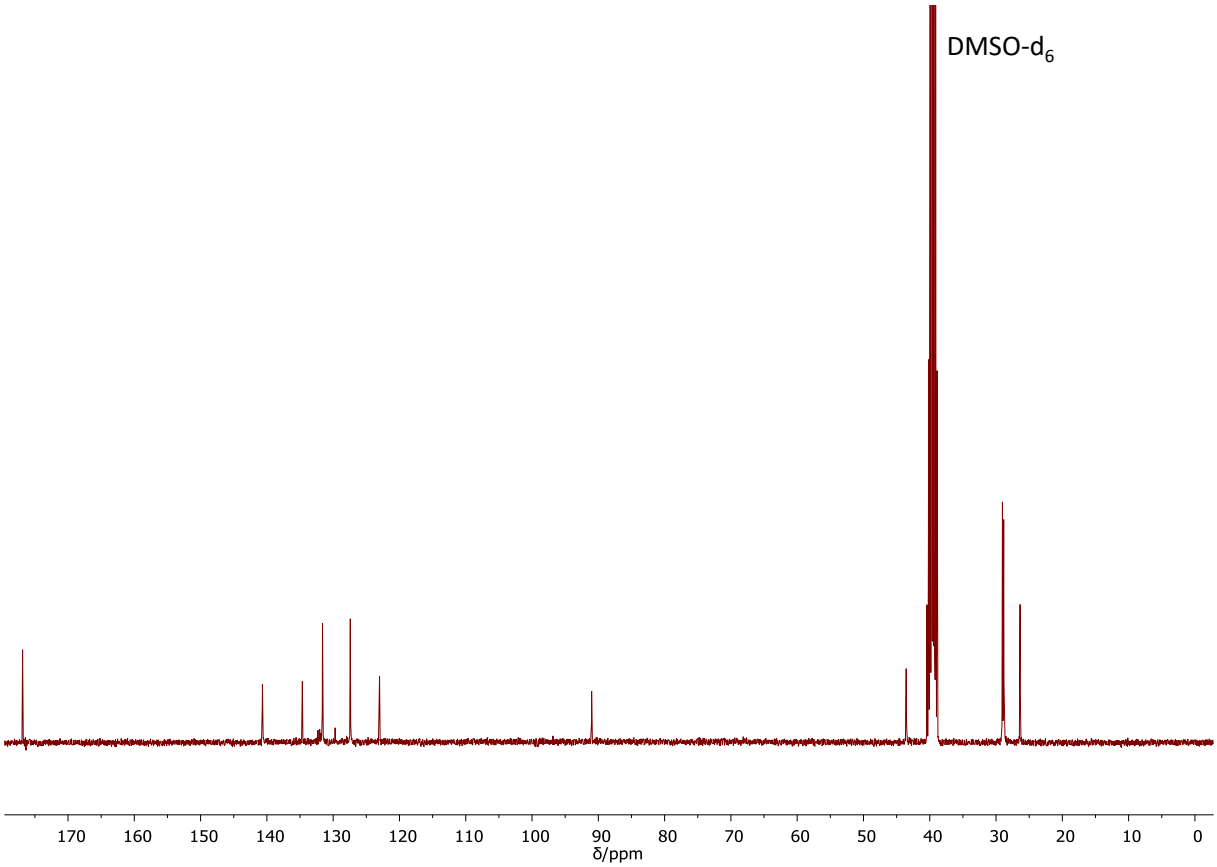

*Figure 232: Carbon NMR-spectra of **P14**.*

IR: ν / cm^{-1} = 3371 (w), 3133 (w), 2991 (w), 2919 (s), 2849 (s), 1693 (w), 1604 (w), 1528 (vs), 1512 (vs), 1487 (vs), 1409 (m), 1316 (w), 1284 (s), 1230 (vs), 1203 (vs), 1135 (m), 1113 (s), 1094 (s), 1014 (m), 926 (m), 829 (s), 802 (w), 720 (w), 627 (w), 533 (m), 502 (w) cm^{-1}.

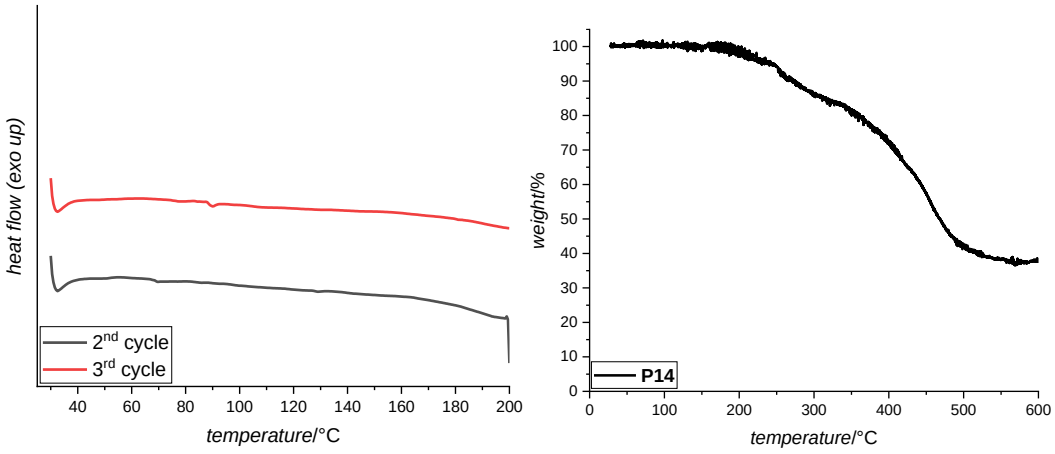

*Figure 233: Left: DSC-curve of **P14** from 25-200 °C at 30 K/min. Right: TGA-curve from 25-600 °C*

PolyTSC P15

N,*N*'-(Hexyl-1,6-diyl) bis(hydrazinecarbothioamide) **87** (100 mg, 378 mmol, 1.00 eq.) and 4,4'-(ethyne-1,2-diyl) dibenzaldehyde **93** (88.6 mg, 378 mmol, 1.00 eq.) were used in 378 µL DMSO (c(dithiosemicarbazide)=1.0 M) to improve the solubility following the general procedure. The reaction was stirred for 4 hours at room temperature and then at 100 °C and 500 mbar for 17 hours. 1.45 mL of DMSO was added to the reaction mixture for solubilizing the polymer for precipitation. After work-up, the product was obtained as brown solid (130 mg) in a yield of 74%.

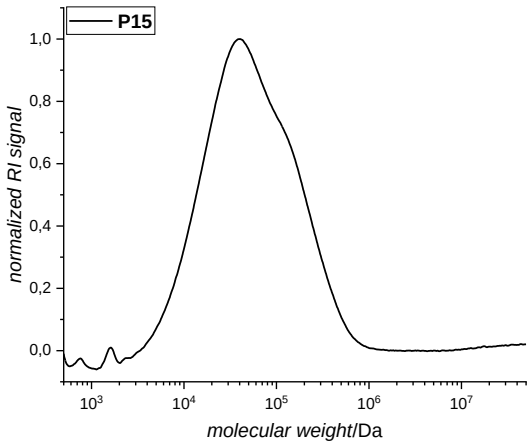

*Figure 234: SEC-trace of **P15**. M_n=33.7 kDa, M_w=76.7 kDa, Đ=2.27 (crude SEC displayed: M_n=32.0 kDa, M_w=54.8 kDa, Đ=1.71).*

^{1}H-NMR (400 MHz, DMSO-d_6) δ/ppm = 11.51 (s, 2H, NH, ^{1}), 8.61 (t, ^3J = 6.2 Hz, 2H, NH, ^{2}), 8.13-8.03 (s, 2H, CH, ^{3}), 7.86 (d, ^3J = 8.3 Hz, 4H, aromatic, ^{4}), 7.59 (d, ^3J = 8.1 Hz, 4H, aromatic, ^{5}), 3.57 (q, ^3J = 7.1 Hz, 4H, ^{6}), 1.67-1.57 (m, 4H, CH_2, ^{7}), 1.39-1.31 (m, 4H, CH_2, ^{8}).

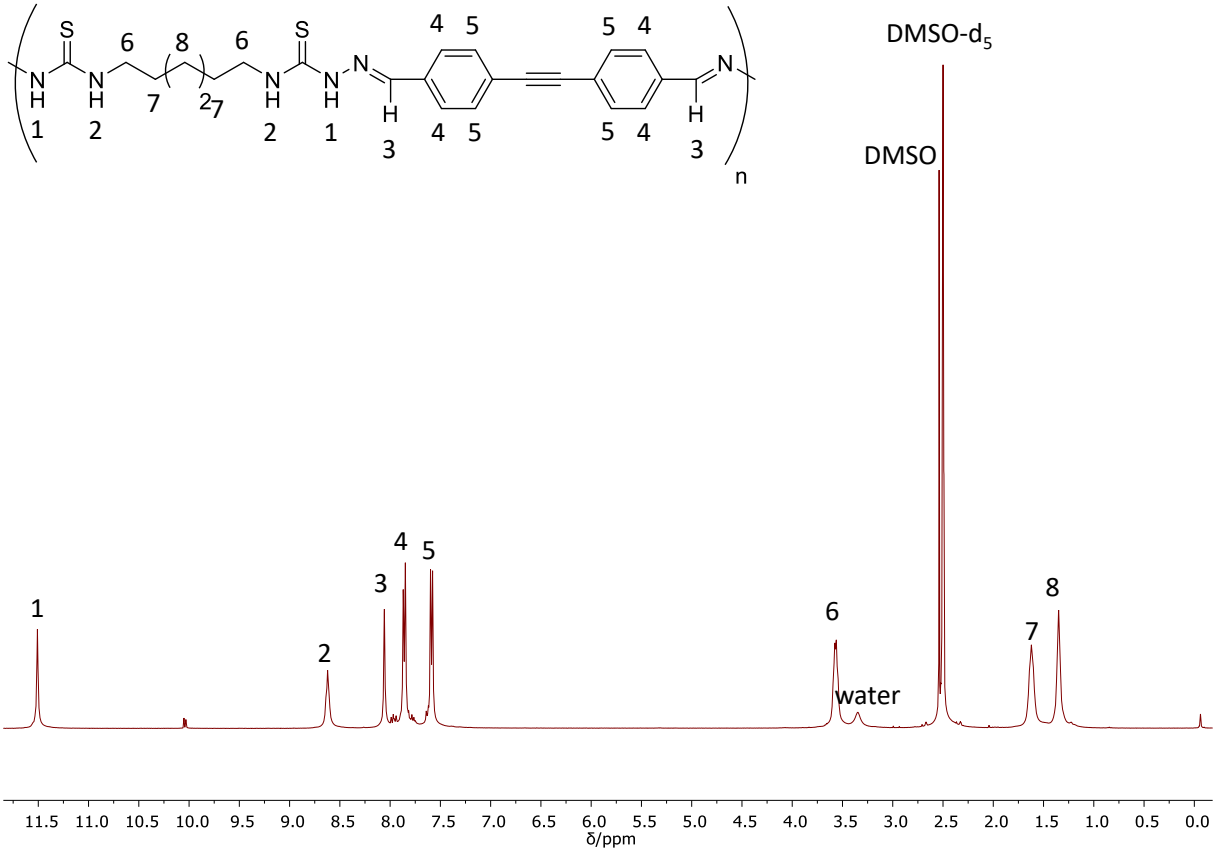

*Figure 235: Proton NMR-spectrum of **P15**.*

^{13}C-NMR (101 MHz, DMSO-d_6) δ/ppm = 176.88 (C=S), 140.74 (C=N), 134.67 (quaternary-aromatic), 131.65 (aromatic), 127.47 (aromatic), 123.01 (quaternary-aromatic), 91.04(C≡C), 43.53 (CH_2), 28.91 (CH_2), 26.23 (CH_2).

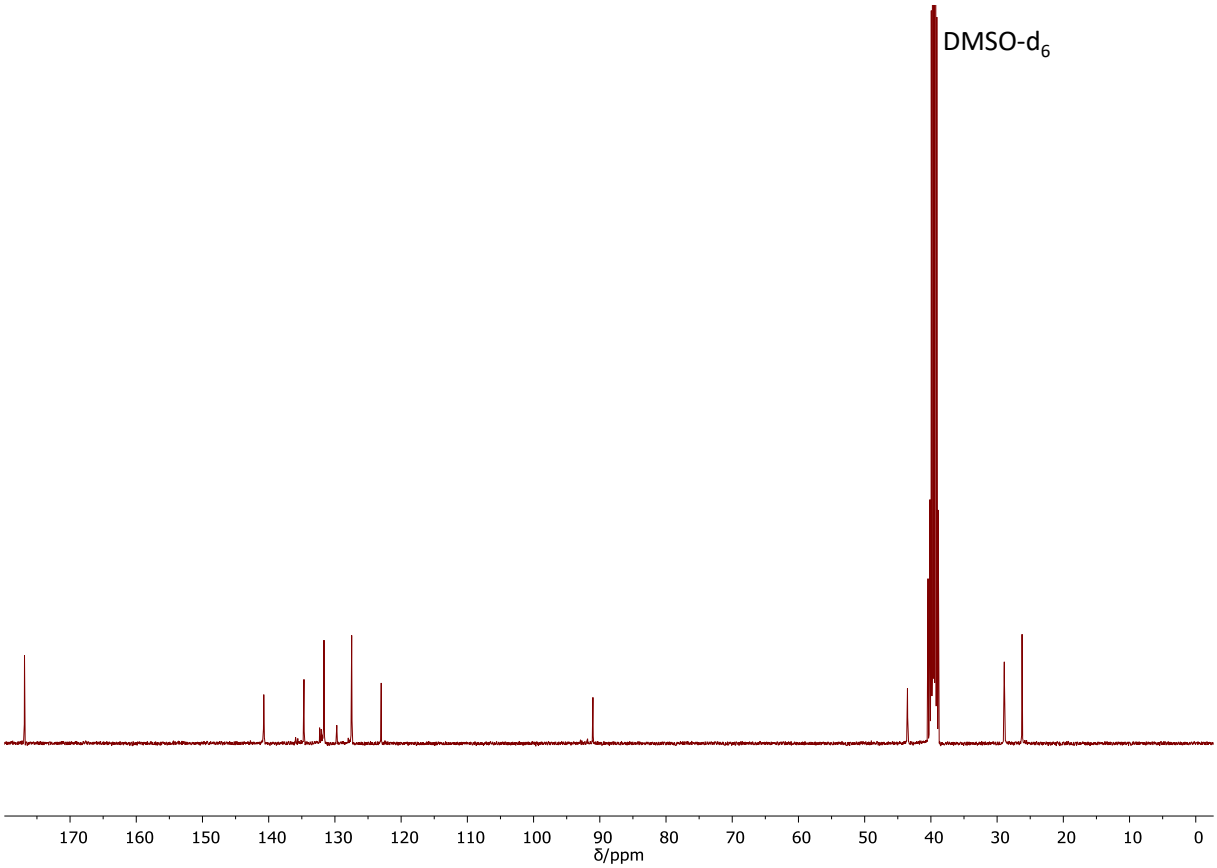

*Figure 236: Carbon NMR-spectrum of **P15**.*

IR: ν / cm^{-1} = 3254 (w, br), 3153 (w, br), 2991 (w), 2921 (w), 2849 (w), 1693 (w), 1602 (w), 1526 (vs), 1510 (vs), 1481 (vs), 1407 (s), 1372 (w), 1318 (w), 1294 (m), 1230 (vs), 1191 (s), 1164 (vs), 1111 (s), 1088 (vs), 1012 (m), 952 (w), 924 (m), 825 (s), 720 (w), 634 (vw), 580 (vw), 529 (m) cm^{-1}.

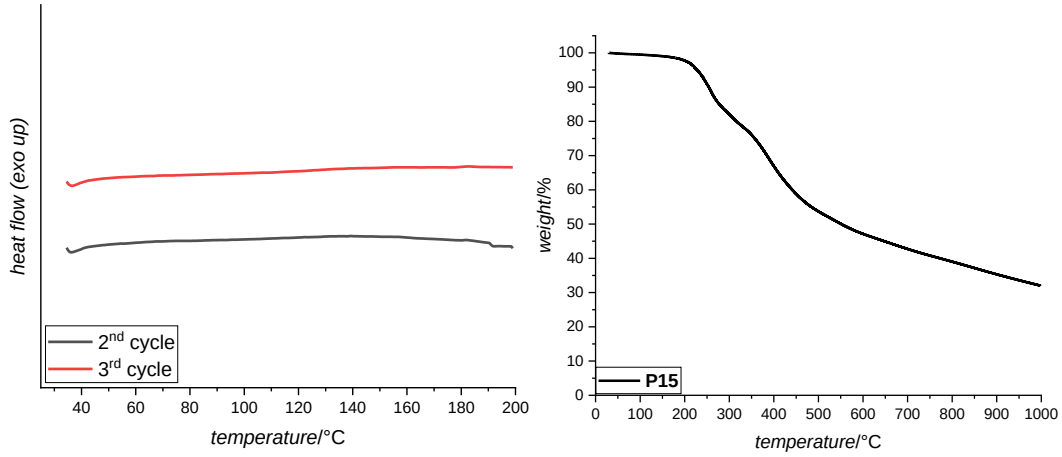

*Figure 237: Left: DSC-curve of **P15** from 25-200 °C at 30 K/min. Right: TGA-curve from 25-1000 °C.*

6.8.5 Synthesis route for dithiosemicarbazones

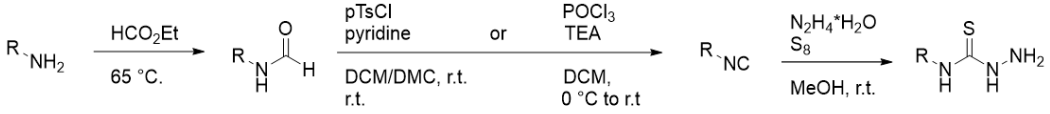

Scheme 50: Reaction scheme for the synthesis of dithiosemicarbazides.

6.8.6 Decomposition of monomer 90

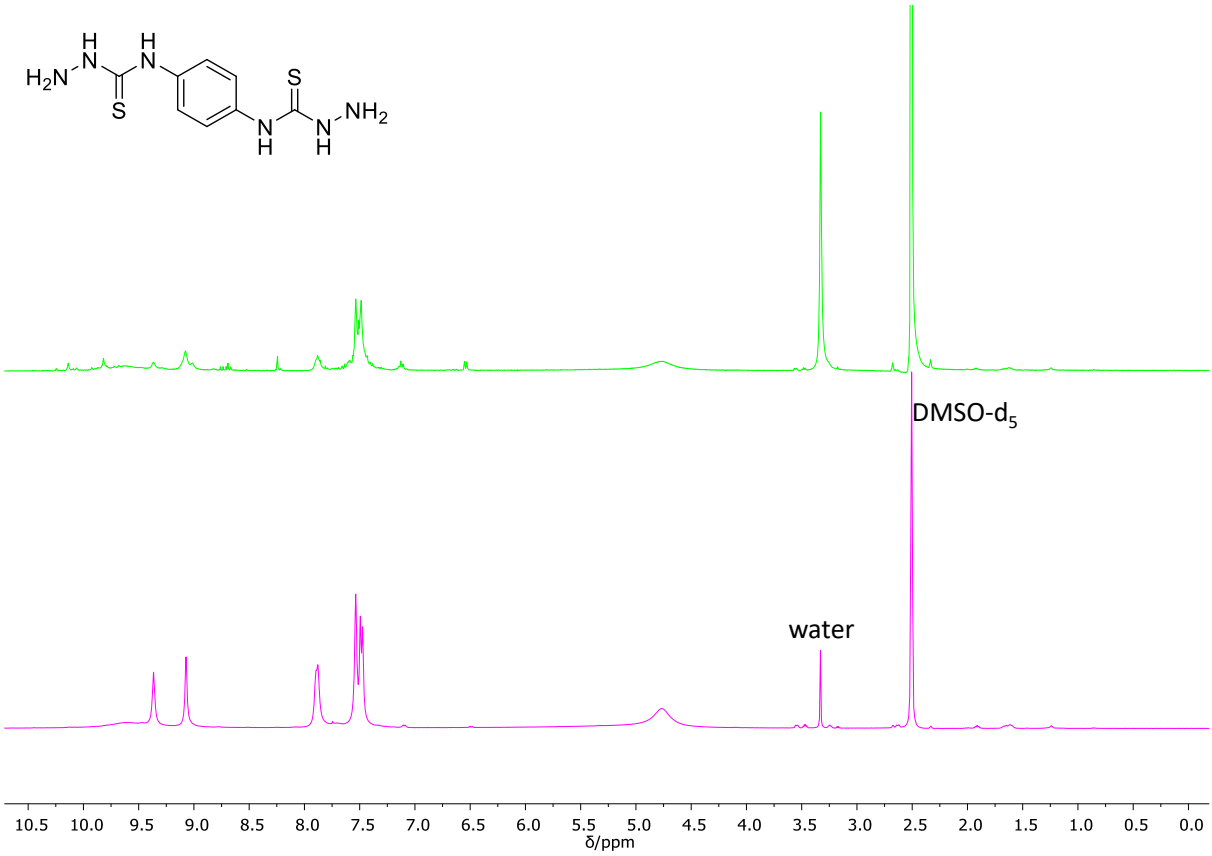

Figure 238: Comparison of proton NMR-spectra of obtained product from synthesis of monomer 90. The lower spectrum shows results from a freshly prepared sample (pink), while the upper one shows the same sample re-measured after several hours (green).

6.8.7 Optimization of poly(TSC) synthesis: reaction of monomer 86 and terephthtaldehyde 91

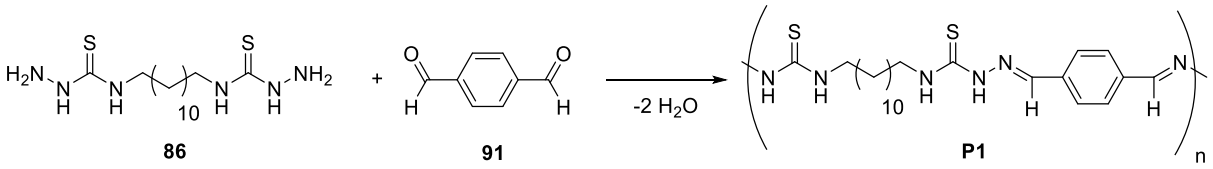

Scheme 51: Reaction chosen for optimization of poly(TSC) synthesis.

Concentrations given in the tables below correspond to monomer **86** and dialdehyde **91**, respectively. SEC-samples were taken from the reaction mixture and molecular weights and dispersities were determined by SEC using DMAc+3w% LiBr as eluent after 2 hours of reaction time, if not noted otherwise. The respective parameter yielding the highest molecular weight are highlighted in bold, final conditions are colored in green.

Solvent screening

Table 39: Solvent screening of polyTSC synthesis.

entry	solvent	*c*/M	*T*/°C	M_n/kDa	M_w/kDa	*Đ*
1[a)]	EtOH	0.083	100	12.0	2.13	1.73
2	DMF	1.0	90	15.0	32.4	2.16
3	DMAc	1.0	90	15.5	31.1	2.01
4	DMAc+3w%LiBr	1.0	90	17.1	32.7	1.91
5[b)]	**DMSO**	**1.0**	**90**	**16.5**	**34.4**	**2.08**

a) Reaction was performed in a pressure tube. Polymer precipitated already after 15 min of reaction time; b) DMSO was chosen since it exhibited the best solubility for polyTSC **P1**.

Concentration screening

Table 40: Concentration screening of polyTSC synthesis

entry	solvent	*c*/M	*T*/°C	M_n/kDa	M_w/kDa	*Đ*
1	DMSO	0.5	90	17.5	36.7	2.10
2[a)]	DMSO	1.0	90	16.5	34.4	2.08
3	**DMSO**	**1.5**	**90**	**18.2**	**41.3**	**2.27**
4	-	-	90	2.20	6.00	2.73

a) corresponds to entry 5 in table of solvent screening.

Temperature screening

Table 41: Temperature and pressure screening of polyTSC synthesis

entry	solvent	*c*/M	*T*/°C	M_n/kDa	M_w/kDa	*Đ*
1	DMSO	1.0	120	15.4	38.8	2.52
2[a)]	DMSO	1.5	90	18.2	41.3	2.27
3	DMSO	1.5	50	17.1	26.0	1.52
4	**DMSO**	**1.5**	**r.t**	**18.9**	**29.6**	**1.56**
5[b)]	**DMSO**	**1.5**	**r.t.**	**25.9**	**45.0**	**1.73**

r.t. = room temperature; a) corresponds to entry 3 in table of concentration screening; b) after work-up; c) polymer was not completely soluble in eluent but was still measured, traces of high molecular species visible in chromatogram, which was not considered.

Time screening

Note that all SEC-samples were taken out of the same reaction mixture.

Table 42: Time screening of polyTSC synthesis

entry	*t*/h[a)]	M_n/kDa	M_w/kDa	*Đ*
1	1	13.8	22.0	1.59
2[b)]	**2**	**16.2**	**24.0**	**1.48**
3	3	16.6	25.3	1.52
4	4	17.8	27.3	1.53
5	25	20.2	31.9	1.58

a) reaction was performed in DMSO (*c*(monomer **86**)=1.5 M) at r.t.; b) a further increase of molecular weight could be observed running the reaction for 25 h (entry 5), but was deemed unimportant for practical reasons of the short reaction time of 2 h.

Test of non-equimolar ratio of starting materials

TableS43: Excess test of polyTSC synthesis

entry	**86**: **91**[a)]	M_n/kDa	M_w/kDa	*Đ*
1	2:3	2.00	3.20	1.62
2	3:2	2.01	3.20	1.61

a) reaction was performed in DMSO (*c*(monomer **86**)=1.0 M) at 90 °C.

6.8.8 Comparison of IR-spectra: P3 compared to its starting material

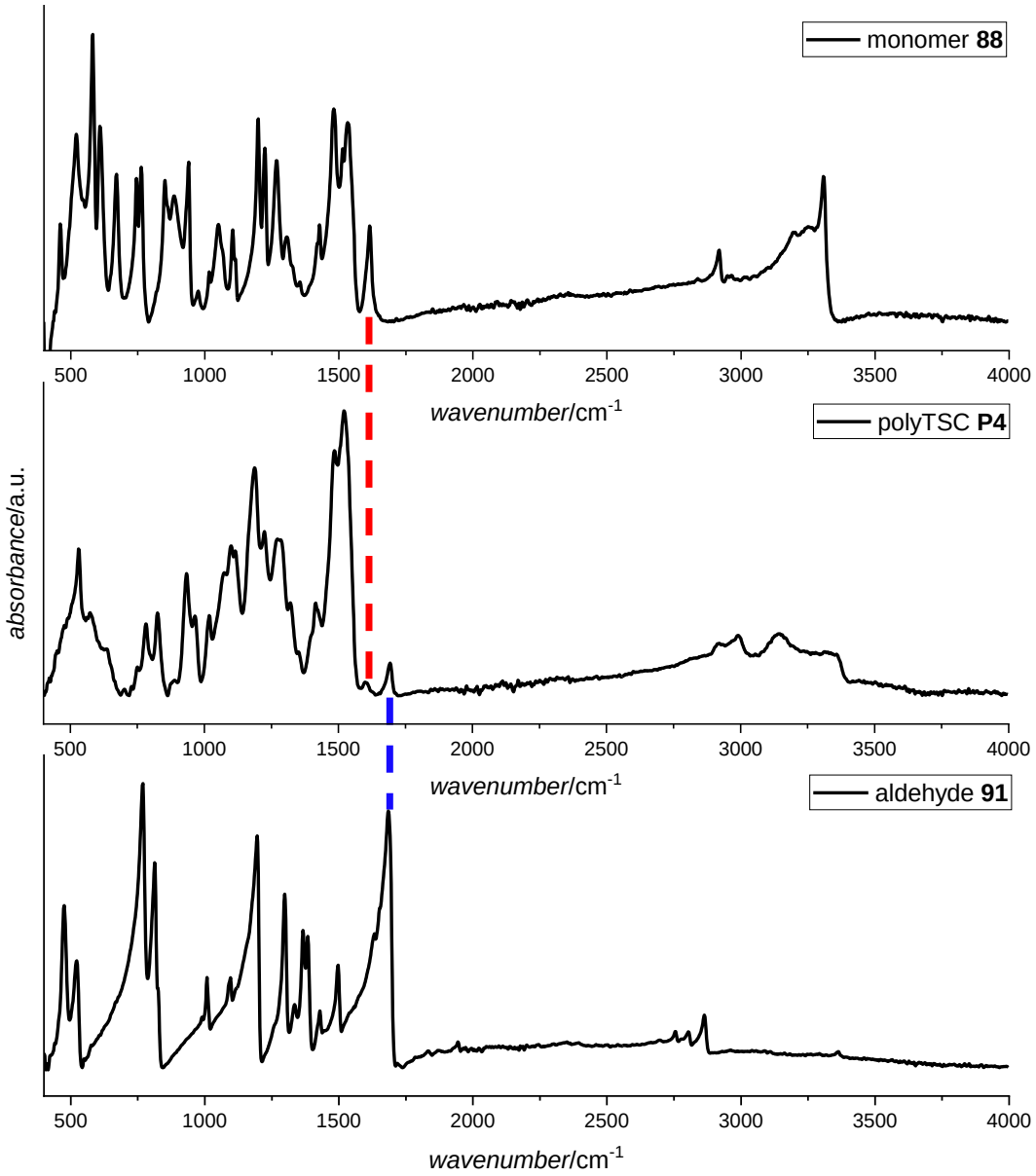

*Figure 239: Comparison of ATR-IR-absorbance spectra of monomers **88** and **91** as well as polyTSC **P3**. The red dashed line corresponds to the δ(NH_2) vibration of the thiosemicabrazide functional group, the blue dashed line to the ν(C=O) vibration of the aldehyde functional group.*

6.8.9 Comparison of IR-spectra: Intensities of end-groups of nonsoluble P3 and P4 compared to P4 and P12.

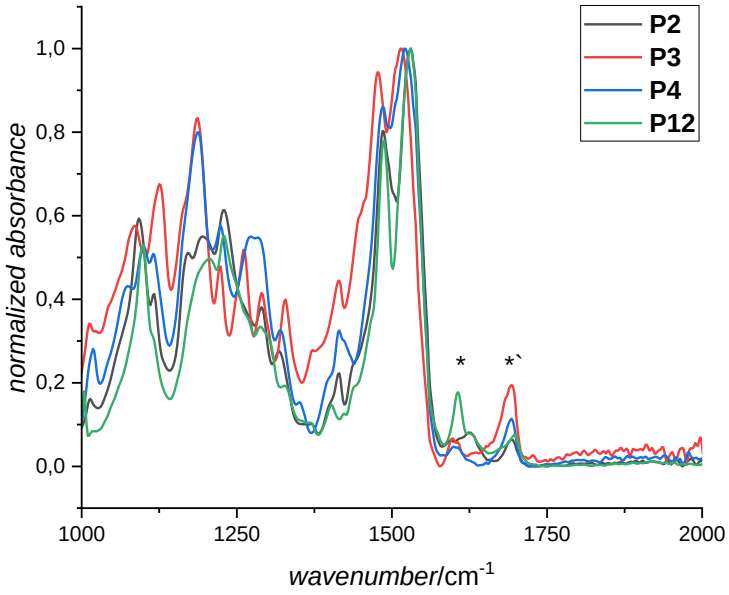

*Figure 240: Comparison of ATR-IR-absorbance spectra of **P2-4** and **P12**. Intensities of vibrations related to the end groups of **P3** and **P4** are of similar intensities than the ones of **P2** and **P12**, indicating a sufficiently high degree of polymerization (around 1615 cm^{-1} for the $\delta(NH_2)$ vibration of the thiosemicarbazide (*) and 1685 $cm^{-1}$for the $\nu(C=O)$ vibration of the aldehyde (*`)).*

6.8.10 Excess test oligomer O1

To obtain a soluble oligomer using monomer **89**, the following synthesis procedure was applied:

N,*N*'-(1,4-Phenylenebis(methylene)) bis(hydrazinecarbothioamide) **89** (75.0 mg, 264 µmol, 1.00 eq.) and an excess of terephthaldehyde **91** (53.1 mg, 396 µmol, 1.50 eq.) was added to 176 µL of DMSO (c(dithiosemicarbazide) = 1.5 M) and the reaction was stirred at r.t. for 3 hours. Subsequently, the formed oligomer was precipitated by dropping the oligomer solution in 30 ml of cold water. The oligomer was obtained after drying at 100 °C and 500 mbar for at least 20 hours as yellow powder.

Thus, SEC as well as proton and carbon NMR-spectroscopy of **O1** could be performed, further evidencing the correct chemical structure of polyTSC **P4**.

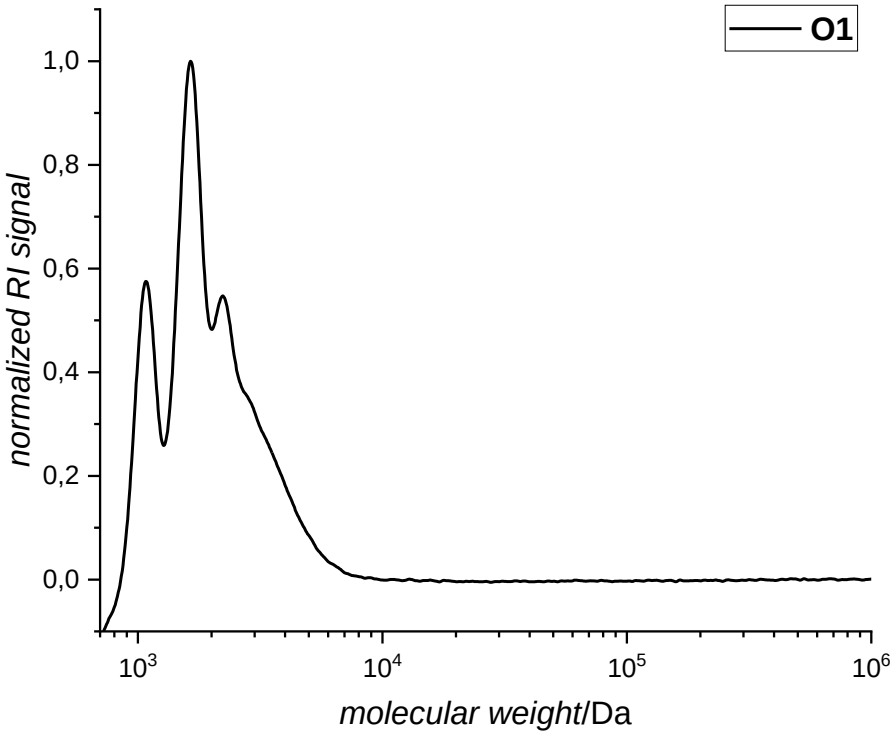

*Figure 241: SEC-trace of **O1**. M_n = 1.6 kDa, M_w = 2.2 kDa, Đ = 1.33.*

^{1}H-NMR (400 MHz, DMSO-d_6) δ/ppm = 11.79 (s, NH, ^{1*}), 11.65 (s, NH, ^{1}), 10.14-10.01 (m, CHO), 9.23 (s br, NH, ^{2*}), 9.09 (s br, NH, ^{2}), 8.15-8.10 (m, CH, ^{3*,3}), 8.08 -7.99 (m, aromatic, ^{4*}), 7.94-7.88 (m, aromatic, ^{4*}), 7.82 (s, aromatic, ^{4}), 7.31 (s, aromatic, ^{5}), 4.82 (s, CH_2, ^{6}).

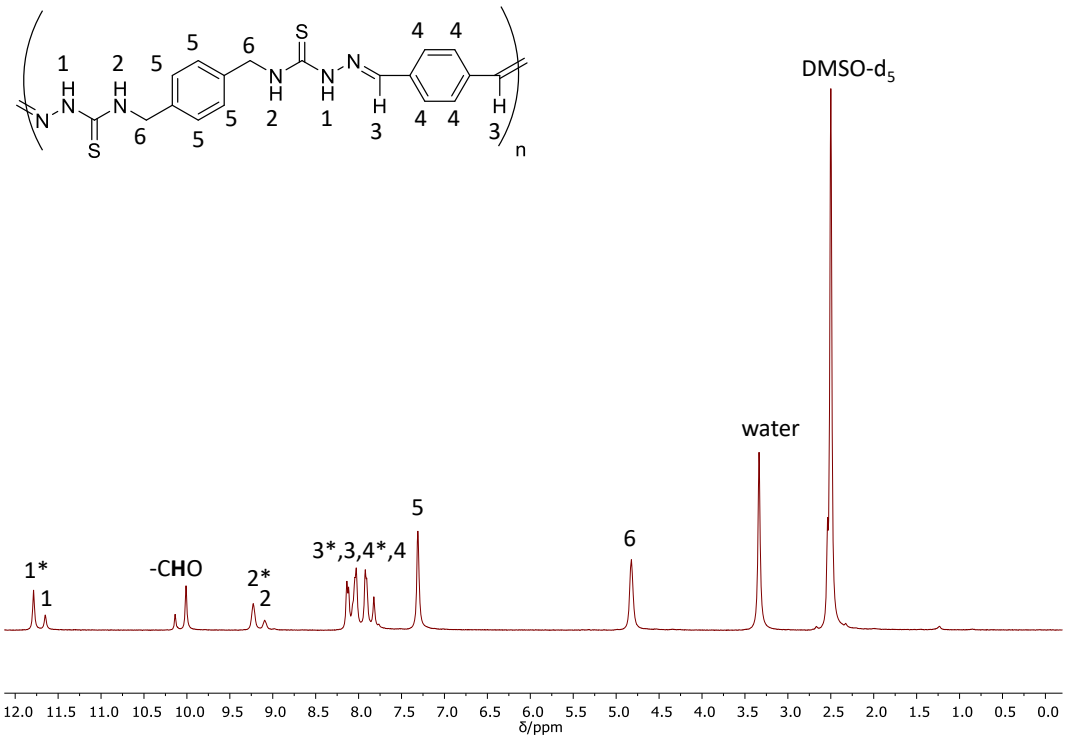

*Figure 242: Proton NMR-spectrum of **O1** in DMSO-d_6. Due to the excess of **91**, aldehyde end-group are present exclusively (signals arising du to vicinity of end-group are labeled with *).*

^{13}C-NMR (126 MHz, DMSO-d_6) δ/ppm = 193.12 (C=O), 192.67 (C=O), 177.74 (C=S), 177.53 (C=S), 140.59 (C=N), 139.86 (C=N), 139.74 (quaternary-aromatic), 137.75 (quaternary-aromatic), 136.47 (quaternary-aromatic), 129.71 (aromatic), 127.74 (aromatic), 127.09 (aromatic), 46.44 (CH_2).

6.8.11 SEC traces of P8-10

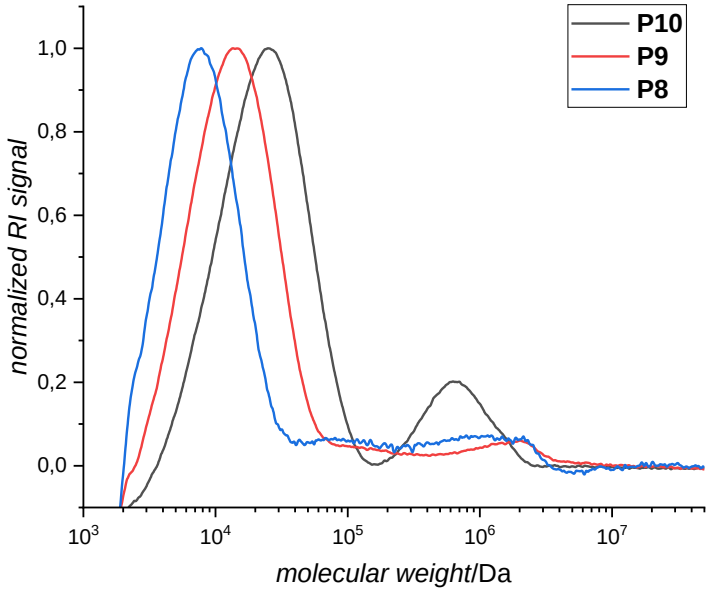

*Figure 243: SEC-traces of **P8-10**. As all SEC-samples were not completely soluble in the eluent, thus the observed distribution is falsified, and SEC-traces are depicted with the sole purpose to show the formation of a second high molecular polymer species.*

6.8.12 Purification tests

PolyTSCs could easily be precipitated from DMSO, into either water or methanol as anti-solvent. However, in both cases residual DMSO was observed. Additional purification methods were thus evaluated and are listed in Table 44.

*Table 44: Comparison of purification methods exemplarily shown for polymer **P6**. Best method is highlighted (bold).*

entry	purification	Residual DMSO/w%[a)]	Other impurities
1	100 °C+500 mbar, 20 h	2.8	yes
2	50 °C+0.05 mbar, 20 h	7.4	-
3	3x Sonification (50 °C, 37 kHz) in 30 mL water, 30 min[b)]	6.4	-
4	1x washing in 30 mL water at reflux, 45 min[b)]	2.6	
5	**3x washing in 30 mL water at reflux, 45 min[b)]**	**1.9**	-
6	3x washing min in 30 mL MeOH at reflux, 45 min[b)]	1.8	Traces of MeOH

a) determined by proton NMR-spectroscopy, comparing ratio of monomer unit and DMSO-h_6. b) Subsequently, polymer was dried at 100 °C and 12 mbar for 20 hours.

Using methanol for washing (entry 6) led to lowest residual of DMSO, however, methanol was found as a second impurity. Using water instead resulted in similar amount of DMSO (entry 5), while water itself did not remain as an impurity in the polymer after work-up. This was confirmed by comparing the water content of the polymer NMR-sample and of plain DMSO-d_6, used for NMR-sample preparation, *via* proton NMR-spectroscopy.

Applying the optimized purification method (see general procedure of polyTSC synthesis in chapter 6.8.4.) polymers in high purities were obtained in some cases with a residual amount of DMSO.

Table 45: Overview of obtained purity of polymers

polyTSC	purity/wt%[a)]
P1	>99
P2	>99
P3	>99[b)]
P4	>99[b)]
P5	>97
P6	>94
P7	>97
P10	>99
P11	>99
P12	>99
P13	>98
P14	>97
P15	>96

a) Determined by proton NMR-spectroscopy; b) determined by IR-Spectroscopy due to insolubility.

6.8.13 TGA measurements

Table 46: Overview of decomposition temperatures of all (co-) polymers with the respective weight loss as well as the residual weight.

polymer	1st decomp./°C	weight loss/w%	2nd decomp./°C	weight loss/w%	3rd decomp./°C	weight loss/w%	residual weight/w%
P1	228	19	403	65	-	-	15
P2	228	26	382	49	-	-	21
P3	224	10	290	66	-	-	24
P4[a.)]	245	17	340	41	-	-	36
P5[a.)]	237	16	360	44	-	-	34
P6[a.)]	236	18	378	51	-	-	21
P7[a.)]	238	18	391	61	-	-	15
P10	237	26	401	54	-	-	20
P11	234	22	399	64	-	-	13
P12	219	11	285	17	382	56	24
P13	226	12	290	9	369	46	30
P14	203	5	234	12	396	46	37
P15	224	19	380	47	-	-	33

a) degradation of residual amount of DMSO was visible, compare Table 45.

6.8.14 GC-MS and TGA-IR measurements- extrusion of ammonia

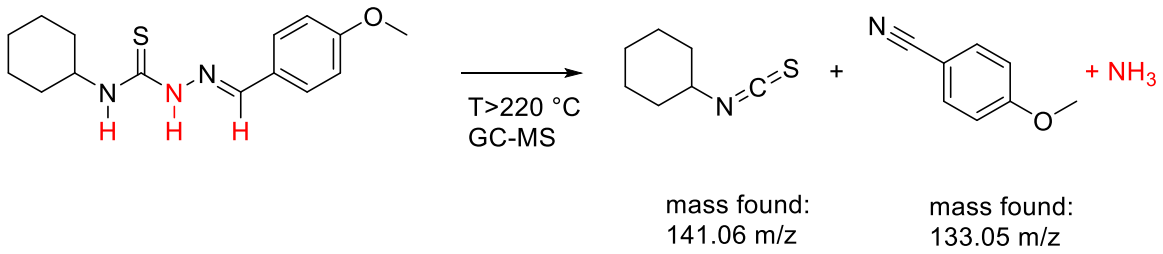

Scheme 52: Degradation of monoTSC sample in GC-MS measurement up to 300 °C resulting in extrusion of ammonia.

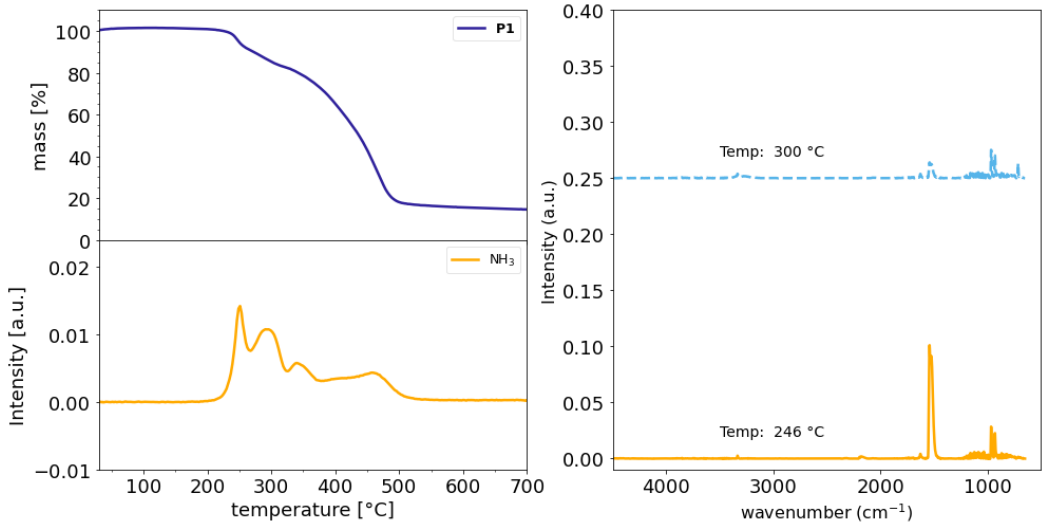

*Figure 244: TGA-IR analysis of **P1**, depicting extrusion of ammonia. The corresponding IR is shown at 246 °C and 300 °C, exemplarily.*

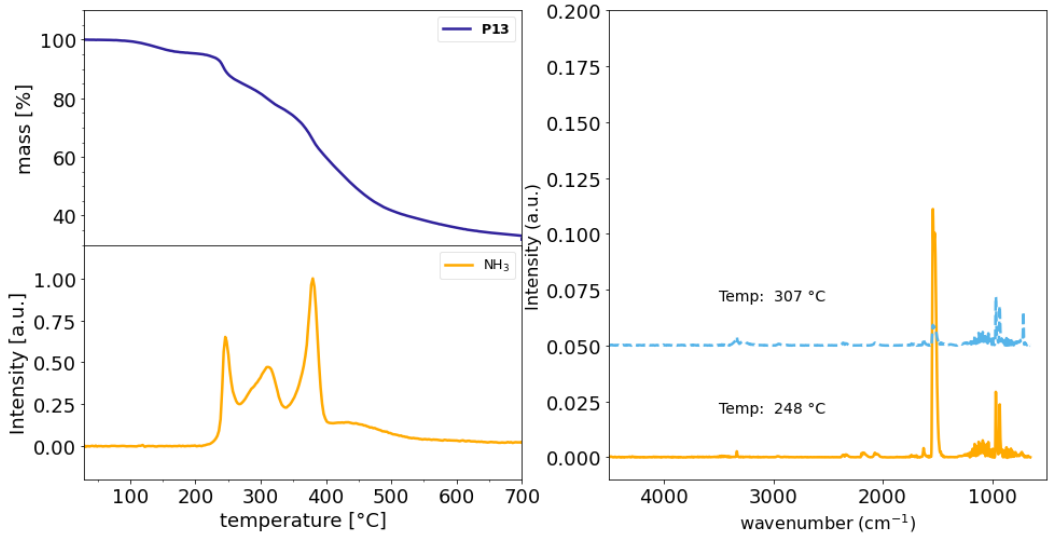

*Figure 245: TGA-IR analysis of **P13**, depicting extrusion of ammonia. The corresponding IR is shown at 248 °C and 307 °C, exemplarily*

Besides ammonia, another species was detected in the decomposition of the polyTSCs exhibiting a very strong vibration at around 1500 cm^{-1} (s. TGA-IR especially at 246 °C for **P1** and 248 °C for **P13**), which could not be assigned.

6.8.15 PH stability of polymer P1

Applying a pH of 0 was achieved by adding a 1 M aq. solution of hydrochloric acid to **P1**. Applying a pH of 14 was achieved by adding a 1 M aq. solution of sodium hydroxide to **P1**. In both cases, a suspension was obtained since the polymer was not soluble in aqueous layers and the mixture was let stay for 16 hours. In addition, the sample was put in a sonification bath (80 kHz) at 50 °C for 8 hours. Afterwards, the polymer was filtered off and dissolved in DMSO-d_6, and a proton-NMR was taken. When basic conditions were applied and the polymer was dissolved in DMSO-d_6, the remaining of sodium hydroxide on the polymer sample led to a color change from yellow to deep red by deprotonation of the most acidic proton. This is visible comparing the proton-NMR spectra of **P1** with the one having applied basic conditions, in which the signal of N-H at 11.47 ppm is missing while the second, less acidic, broadened N-H signal is shifted (from 8.53 to 8.45 ppm) as well as the aromatic signals (from 7.81 to 7.79 ppm). No degradation could be determined in acidic and basic conditions.

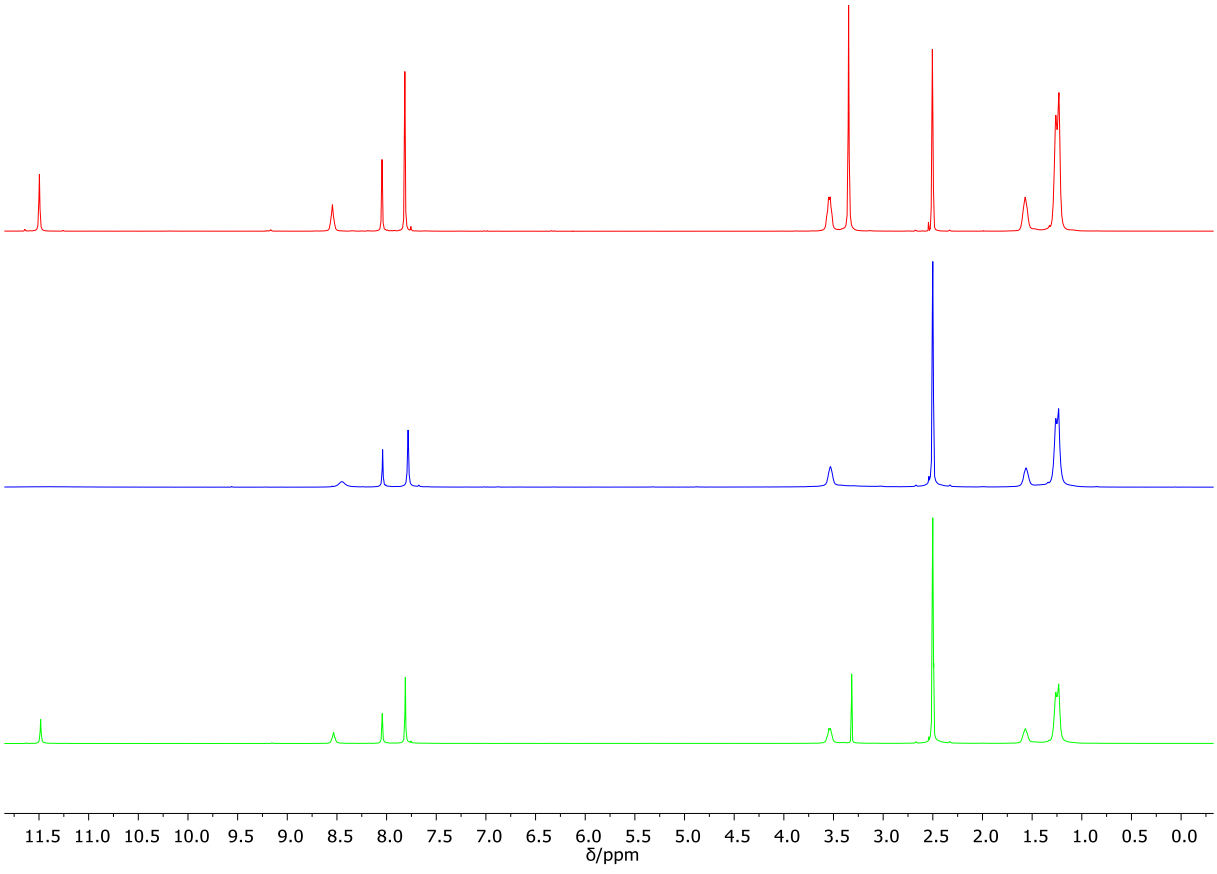

*Figure 246: Proton-NMR spectra of polymer **P1** after 24 hours in aqueous acid (pH=0, top, red) and basic (pH=14, middle, blue) conditions. Reference NMR-spectrum is given in green (bottom). Solvent was DMSO-d_6.*

6.9 Application of poly(TSC)s for membrane formation

6.9.1 Membrane formation *via* NIPS

A polymer solution containing poly(TSC) **P1** in the respective weight percentage and DSMO or NMP was prepared. Dissolution of the polymer was facilitated by stirring the solution in a roller mixer under a heated lamp (in general it took 24 hours to obtain a homogenous solution for higher weight percentage polymer solutions, in some cases heating up to 70 °C for an hour under stirring had to be applied). The NIPS process followed the proceeding shown in Figure 18: The polymer casting solution was poured on a glass plate and was spread evenly on the support by using a casting knife having a 400 µm gap. Subsequently, the polymer film with support was immersed in a coagulation batch containing one liter of Milli-Q® water for precipitation. In general, precipitation was completed after several seconds or less, for some low weight percentage polymer solution the precipitation process took several minutes. Afterwards, the membrane was washed at least three times with roughly one liter of water and was then ready to use.

6.9.2 Permeation test

Experiments were performed in an Amicon cell in a dead-end configuration:

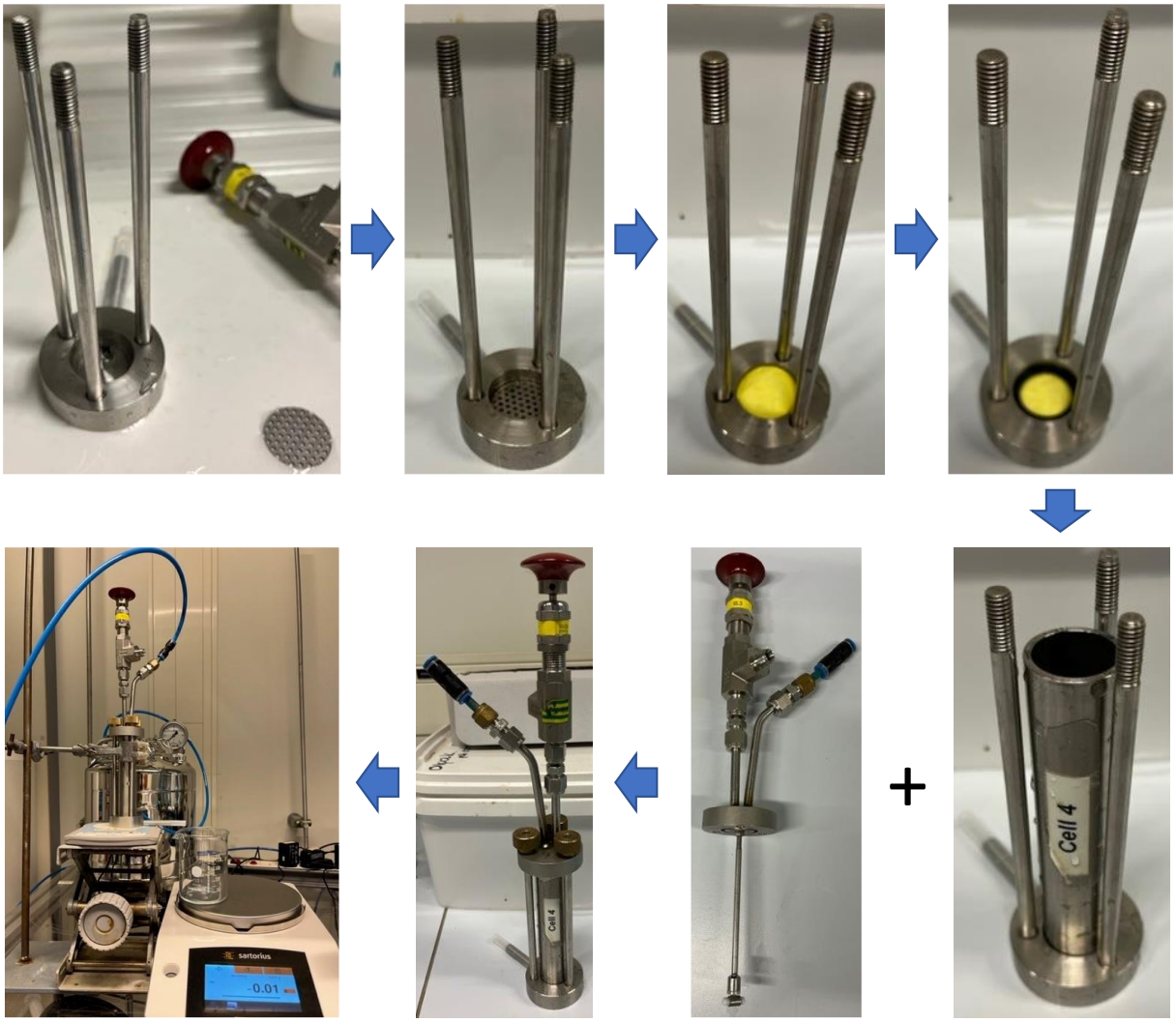

Figure 247: Set up for the permeability tests with an Amicon cell: 1.) mechanical support was put in the casing. 2.) membrane with a non-woven paper support at the bottom is placed on the top of the mechanical support. The top layer of the membrane is facing the feed solution. 3.) A rubber O-ring is placed on top of the membrane for sealing. 4.) A metal cylinder is placed on top of the rubber ring and the cylinder is closed on the top part with a cap consisting of a fixed stirring bar, a safety pressure valve and a connection for water tubing. 5.) The cap is screwed tightly on the cylinder. 6.) The Amicon cell is mounted on a magnetic stirrer and the outlet of the water tubing on the bottom of the cell is placed on top of a beaker that stands on a balance connected to a computer, see also zoom-in picture below.

The permeability test were conducted at 3 bar of applied water pressure and for every membrane at least two samples were tested, collecting at least 20 data points. A zoom in on the final set-up is given in Figure 248:

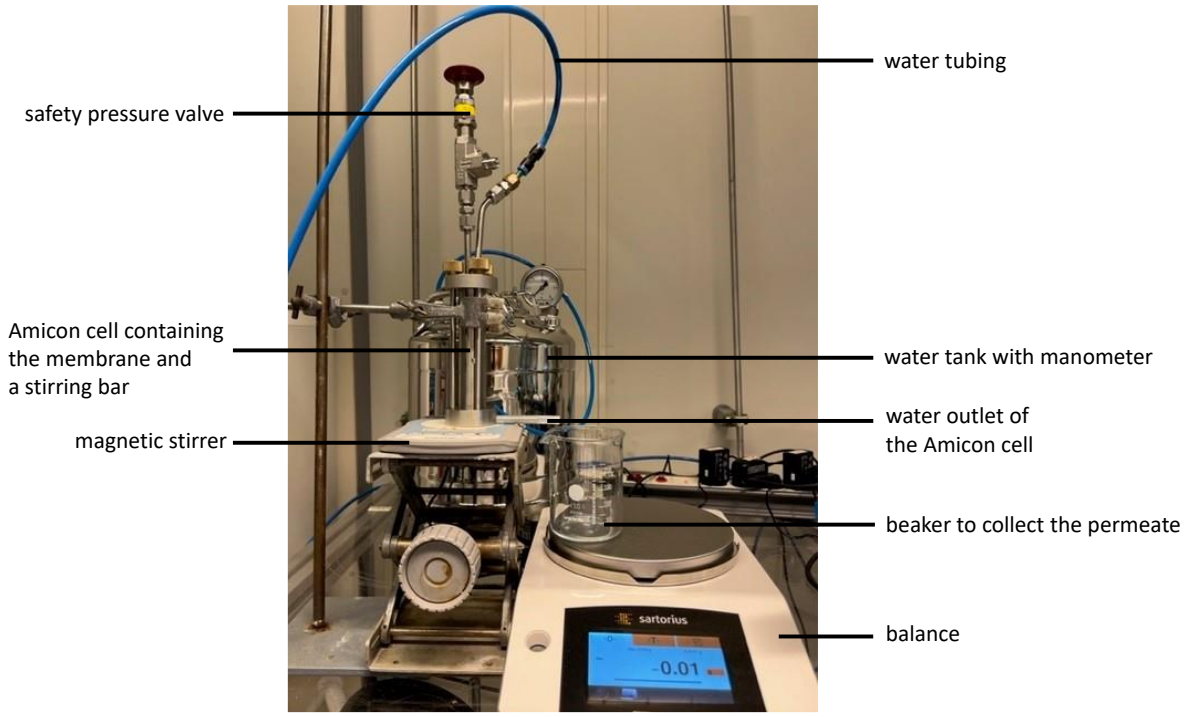

Figure 248: Overview of the the permeability and retention set-up using an Amicon cell.

6.9.3 SEM-pictures

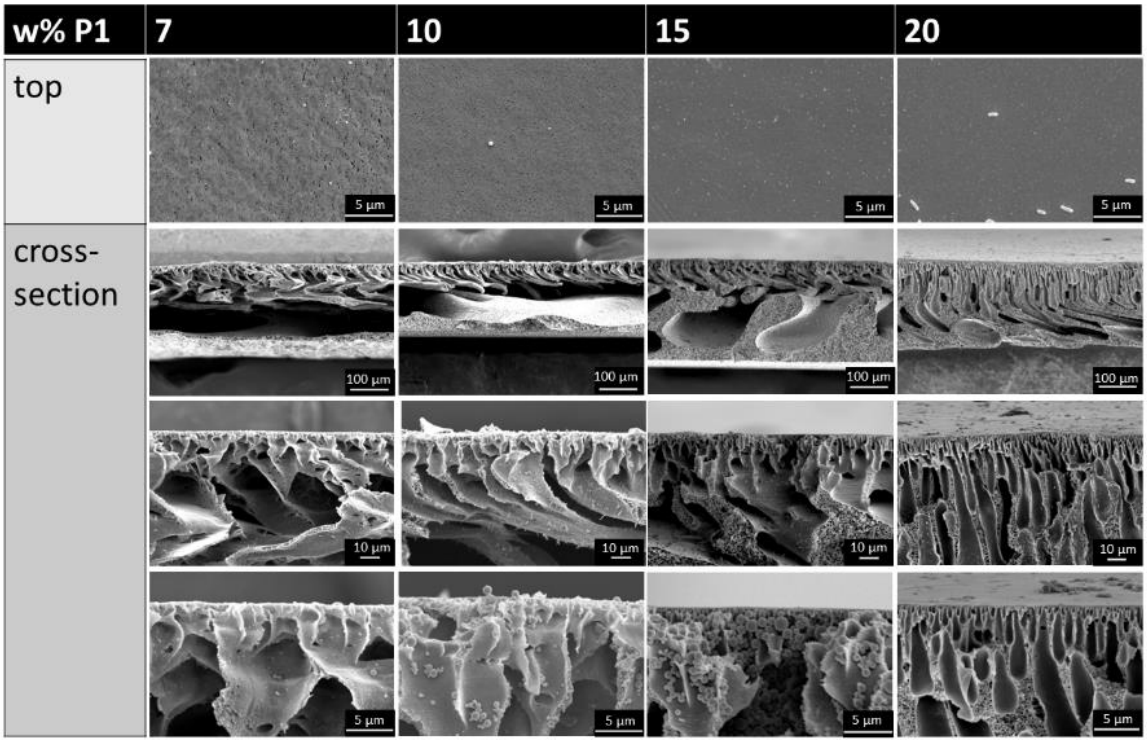

*Figure 249: SEM-pictures of membranes obtained using different weight-percentages of poly(TSC) **P1** and NMP as solvent. The top and cross sections as well as zoom-ins of the cross sections at two different magnifications are depicted. Note that for 7 and 10wt% the porous substructure is broken due to sample preparation and thus depicting a gap between bottom and top layer.*

6.9.4 MWCO experiments

An aqueous solution of PEGs with the molecular weights of 0.2, 0.4, 0.6, 1.0, 1.5 and 2.0 kDa (concentration of each PEG was 1 gL^{-1}) was prepared. Roughly 20 mL of the PEG-solution were poured in the Amicon cell and pumped through the membrane at 3 bar. The PEG solution inside the Amicon cell was stirred to reduced the effects of concentration polarization. The first milliliter of permeate was discharged and then at least one milliliter was collected. A SEC-sample was prepared of the permeate as well as the retentate and analyzed by SEC-measurement.

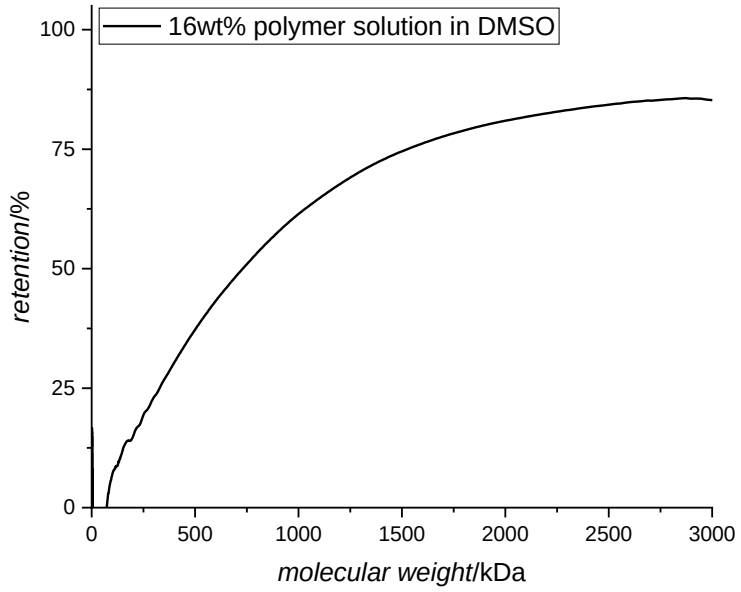

Figure 250: MWCO of a PEG-solution for a membrane obtained from a 16wt% polymer solution using DMSO. Two samples of the membrane were measured and the average is depicted. Note that the MWCO is incomplete, since the rejection saturated at 80%.

An aqueous solution of BSA (c(BSA)=0.1 gL^{-1}) was prepared in 0.1 M phosphate buffer at pH = 4. Roughly 20 mL of the BSA-solution were put in the Amicon cell and pumped through the membrane at 3 bar. The first milliliter of the permeate was discharged and then at least one milliliter was collected. The permeate and the BSA-solution were measured using UV/VIS analysis.

6.9.5 Water contact angle measurements

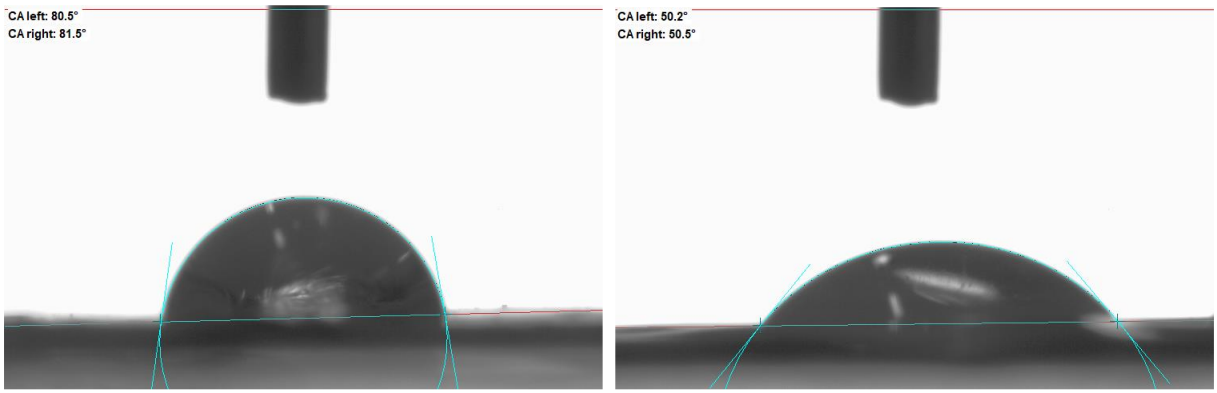

*Figure 251: Examples of water contact measurements of a membrane using a 10wt% polymer solution of **P1** in NMP (left) and a 15wt% polymer solution in DMSO (right).*

6.9.6 Batch removal experiment

The respective area needed for the removal was cut out from the membrane and put in a vial. Subsequently, the respective amount of a 1.25 mM aqueous solution of the respective metal salt ($AgNO_3$, $ZnCl_2$, $CuCl_2*2H_2O$) was added and the vial was closed. The vial was shaken for the respective amount of time and then a sample for the ion chromatography was taken. For the monitoring of the kinetic, one vial was used to prepare all samples. The removal of the respective ions was calculated as follows:

$$R(\%) = (1 - \frac{C_t}{C_{FEED}}) \times 100$$

where R is the removal of the respective ion in percentage, C_t and C_{FEED} are the integral values of the ion obtained from the ion chromatography curves of the respective sample after a certain time and the feed solution, respectively.

6.9.7 Complexation reaction of polsy(TSC) P1 with transition metals

Complexation with $AgNO_3$

Poly(TSC) **P1** (50 mg, corresponds to 224 µmol TSC groups) was dissolved in 1.12 mL DMSO. Then $AgNO_3$ (19.0 µg, 112 µmol) was added and the mixture was stirred at 80 C for 80 minutes. Subsequently, 1.12 mL DMSO was added to the suspension and further stirred at 80 °C for 2 hours. Then, 2.24 mL DMSO was added and the reaction was again stirred at 80 °C for 19 hours. The reaction mixture was cooled to room temperature and the formed precipitate was filtered off. The obtained brown solid was washed with water and dried at 80 °C overnight.

IR (ATR platinum diamond): ν/cm^{-1} = 3200 (br, vw), 2921 (s), 2851 (m), 1693 (vw), 1537 (s), 1460 (s), 1407 (m), 1353 (m), 1265 (s), 1039 (vs), 983 (m), 841 (m), 766 (m), 720 (m), 65 (w), 598 (m), 532(m).

IR-Comparison with pure poly(TSC) **P1** depicted formation of the Ag-TSC-complex:

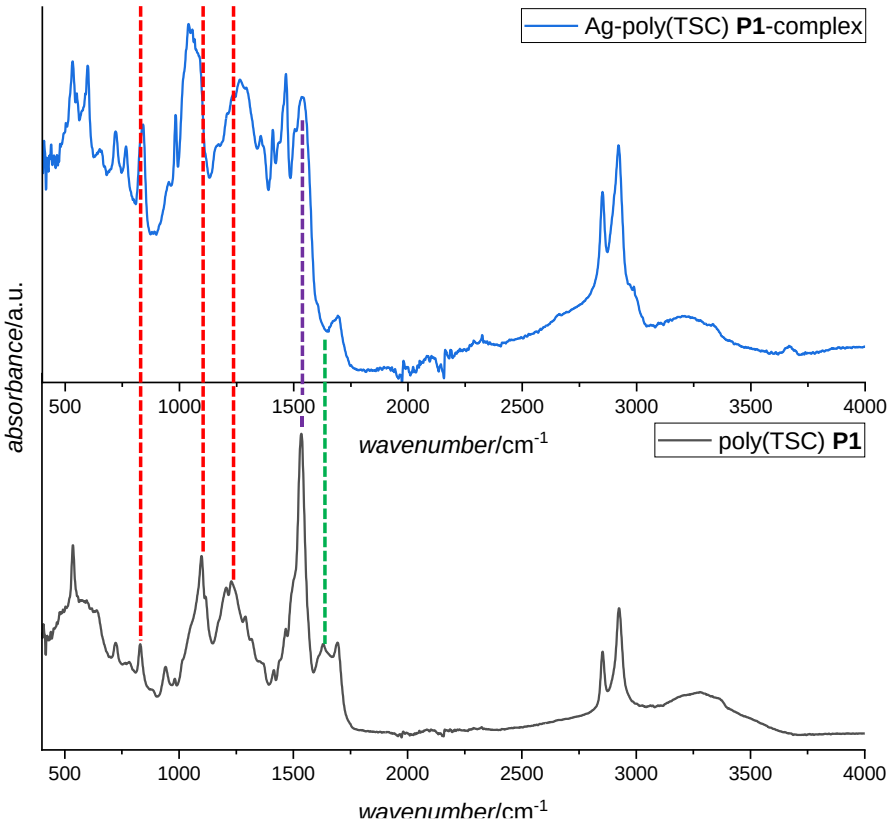

*Figure 252: IR-spectrum of poly(TSC) **P1** (bottom, black) and the obtained Ag-complex (top, blue). Shift of the three vibrational bonds of the C=S group of the TSC group is depicted (red dashed lines). In addition, the intensity of the v(C=N) vibration) is strongly reduced (purple dashed line) accompanied by an emerging signal at 1504 cm^{-1} (top). The signal of the δ(NH$_2$) vibration of the hydrazide end group is gone (green dashed line) and probably shifted into other signals at lower wavenumber. According to literature anionic metal-TSC complexes bear a lower C=S vibrational bond at 790-820 cm^{-1} and are missing one v(N-H) vibrational bond at 3260-3500 cm^{-1} compared to neutral complexes exhibiting a C=S vibrational bond at 800-850 cm^{-1} that is usually insignificantly shifted compared to the non-complexed TSC compound.[594] For the obtained complex no clear difference in the N-H region could be determined while the C=S vibrational bond was slightly shifted from 831 to 840 cm^{-1} indicating neutral bonding. Furthermore, a bond emerged at 766 cm^{-1} that could be related to the C=S vibrational bond of an anionic TSC-metal complex, even though it depicts lower wavenumber than usual.*

Complexation with $CuCl_2*2H_2O$

Poly(TSC) **P1** (50 mg, corresponds to 224 µmol TSC groups) was dissolved in 1.12 mL DMSO. Then $CuCl_2*2H_2O$ (19.1 µg, 112 µmol) was added and the mixture was stirred at 80 C for 80 minutes. Subsequently, 1.12 mL DMSO was added to the suspension and further stirred at 80 °C for 2 hours. Then, 2.24 mL DMSO was added and the reaction was again stirred at 80 °C for 19 hours. The reaction mixture was cooled to room temperature and the formed precipitate was filtered off. The obtained brown solid was washed with water and dried at 80 °C overnight.

IR (ATR platinum diamond): ν/cm^{-1} = 3255 (br, vw), 2923 (s), 2851 (m), 1695 (vw), 1668(vw), 1602 (vw), 1521 (s), 1455 (m), 1435 (m), 1406 (w), 1355 (w), 1309 (vw), 1264 (w), 1209 (w), 1162 (w), 979 (s), 834 (m), 764 (vw), 586 (m).

IR-Comparison with pure poly(TSC) **P1** depicted formation of the Cu-TSC-complex:

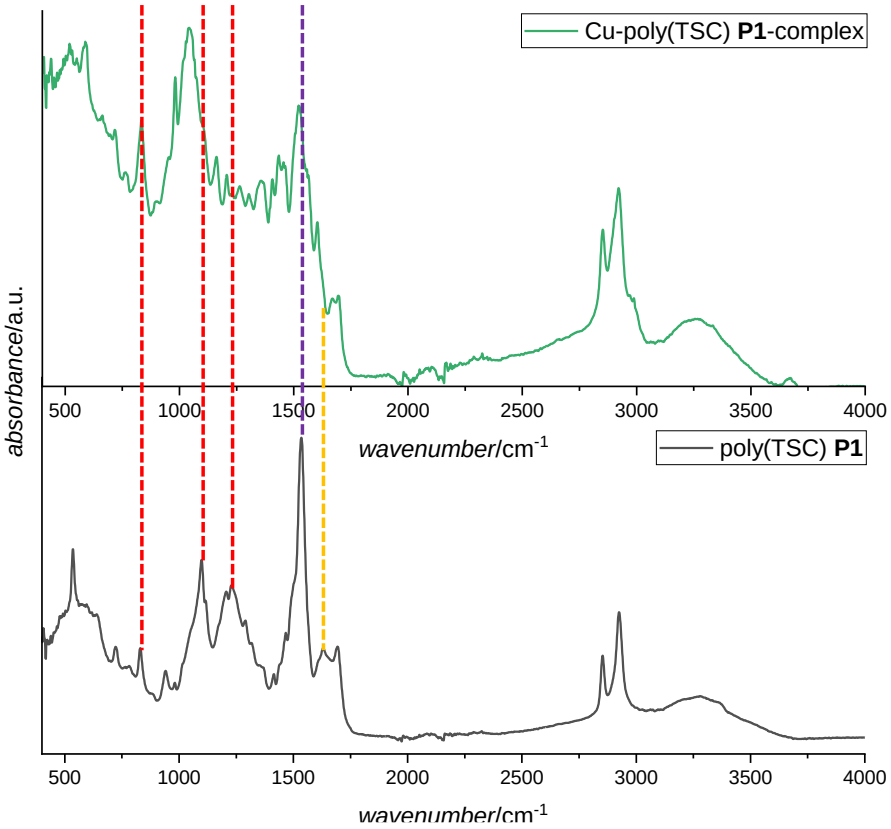

*Figure 253: IR-spectrum of poly(TSC) **P1** (bottom, black) and the obtained Cu-complex (top, green). Shift of the two vibrational bonds of the C=S group of the TSC group is depicted while one signal at 1226 cm^{-1} vanished completely (red dashed lines). In addition, the v(C=N) vibration) is slightly shifted (purple dashed line). The signal of the δ(NH_2) vibration of the hydrazide end group is gone (yellow dashed line) and probably shifted into other signals at lower wavenumber. According to literature anionic metal-TSC complexes bear a lower C=S vibrational bond at 790-820 cm^{-1} and are missing one v(N-H) vibrational bond at 3260-3500 cm^{-1} compared to neutral complexes exhibiting a C=S vibrational bond at 800-850 cm^{-1} that is usually insignificantly shifted compared to the non-complexed TSC compound.*[594] *For the obtained complex no clear difference in the N-H region could be determined while the C=S vibrational bond was slightly shifted from 831 to 834 cm^{-1} indicating neutral bonding. Furthermore, a bond emerged at 767 cm^{-1} that could be related to the C=S vibrational bond of an anionic TSC-metal complex, even though it depicts lower wavenumber than usual.*

6.9.8 Pictures of $AgNO_3$ complexation on membrane

Successful removal of $AgNO_3$ using a flow experiment was visible with the naked eye:

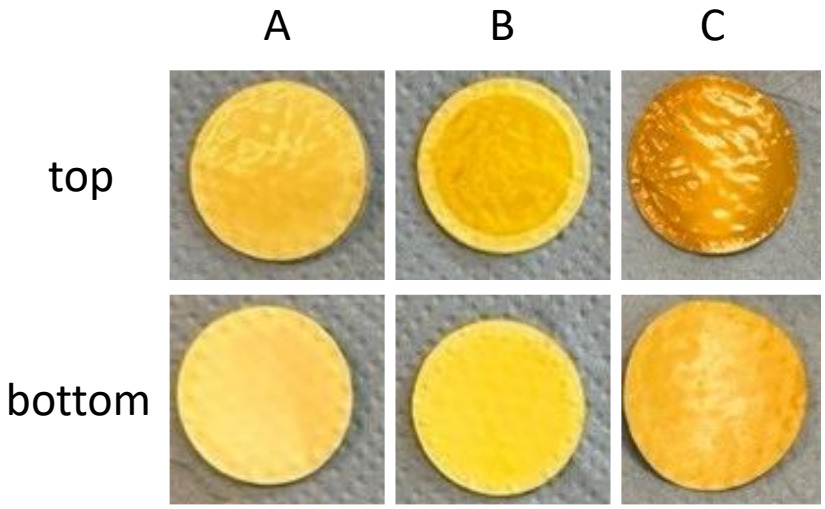

*Figure 254: Pictures of membrane samples: A: poly(TSC) **P1** membrane obtained by using 15wt%polymer solution in DMSO without further treatment. B: Sample from the same membrane depicted in A but after the dynamic removal of a 1.25 mM aqueous $AgNO_3$ solution in an Amicon cell. On the top side a darker coloration is visible (the lighter coloration on the outside of the membrane is because this part of the membrane was covered by a rubber ring). C: Sample from a poly(TSC) membrane obtained from a 16wt% polymer solution in DMSO, which was then immersed in a liter of a 17.9 mM aqueous $AgNO_3$ solution for one day. Brown coloration of the membrane is visible on the top and bottom side, since it was completely immersed in the solution.*

Complexation of $AgNO_3$ during the NIPS process was also visible by naked eye:

Figure 255: pictures of membranes and their samples: top: A: Top side of a poly(TSC) membrane obtained by using 15wt%polymer solution in DMSO without further treatment. B and C: Poly(TSC) membrane obtained by using a 16wt% polymer solution in DMSO and a 17.9 mM $AgNO_3$ aqueous solution as non-solvent in the NIPS process. Depicted is the bottom (B) and top side (C). center: Respective membrane of the sample shown in top A. bottom: respective membrane of the sample of top B and C.

6.9.9 EDX measurements

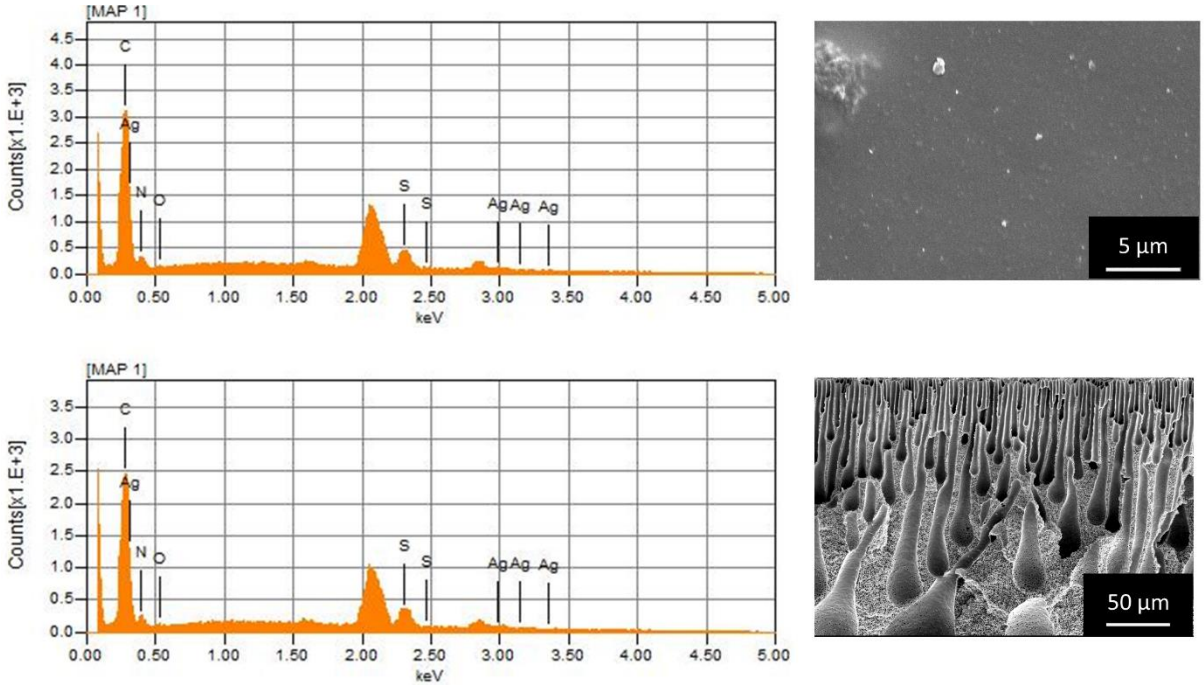

*Figure 256: EDX analysis (left) and respective SEM-picture (right) of a poly(TSC) **P1** membrane obtained by using a 16wt% casting solution in DMSO. The top layer layer (top) and the CS (bottom) are depicted.*

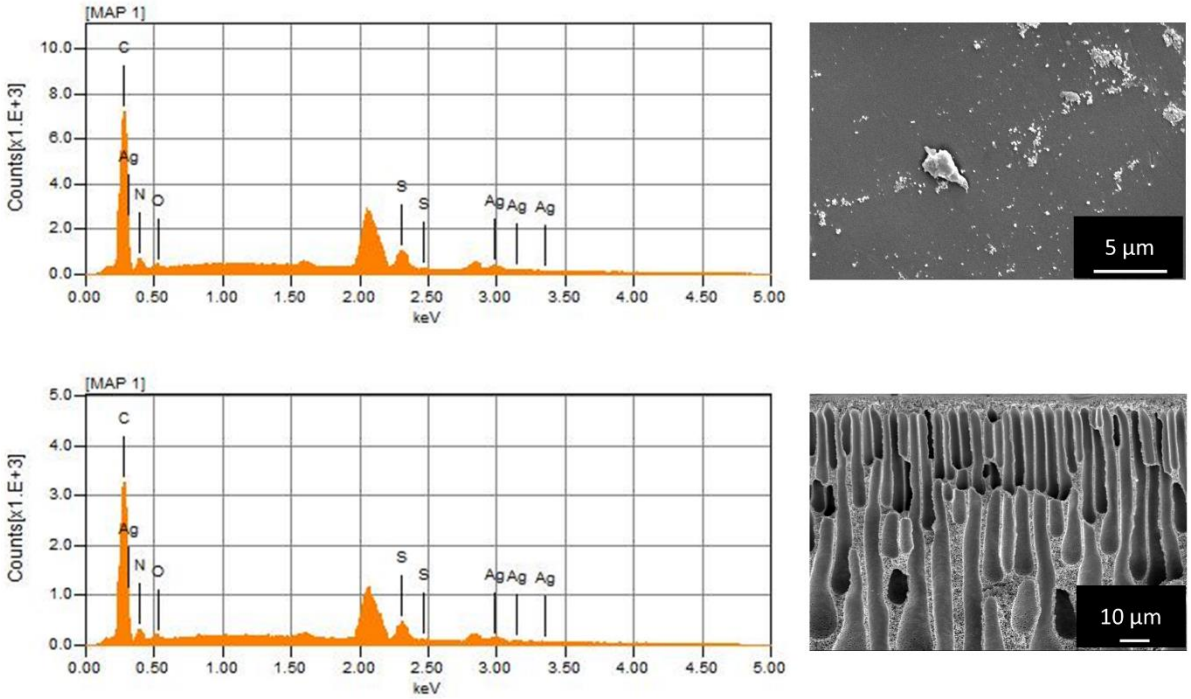

*Figure 257: EDX analysis (left) and respective SEM-picture (right) of a poly(TSC) **P1** membrane obtained by using a 16wt% casting solution in DMSO. The membrane was then used in a dead-end Amicon cell set-up for the removal of siler ions. Thus, 20 mL of a 1.25 mM aqueous $AgNO_3$ solution was pumped through the membrane. The top layer layer (top) and the CS (bottom) are depicted.*

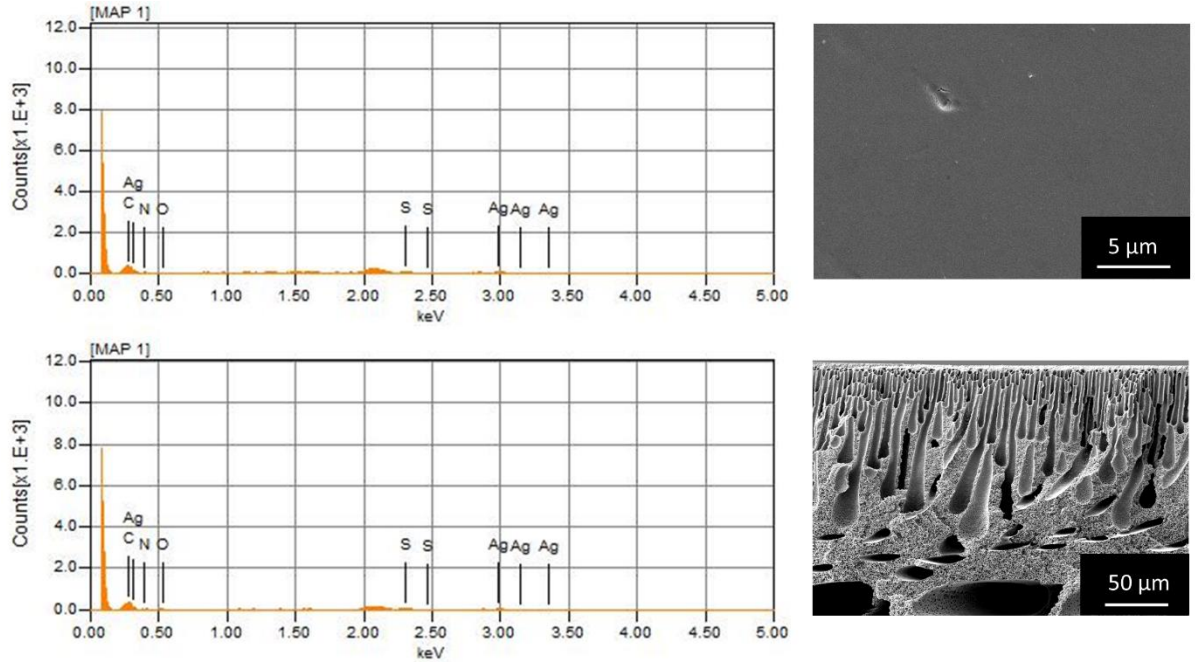

*Figure 258: EDX analysis (left) and respective SEM-picture (right) of a poly(TSC) **P1** membrane obtained by using a 16wt% casting solution in DMSO. The membrane was then immersed in 1 L of a 17.9 mM aqueous $AgNO_3$ solution for two days. The top layer layer (top) and the CS (bottom) are depicted.*

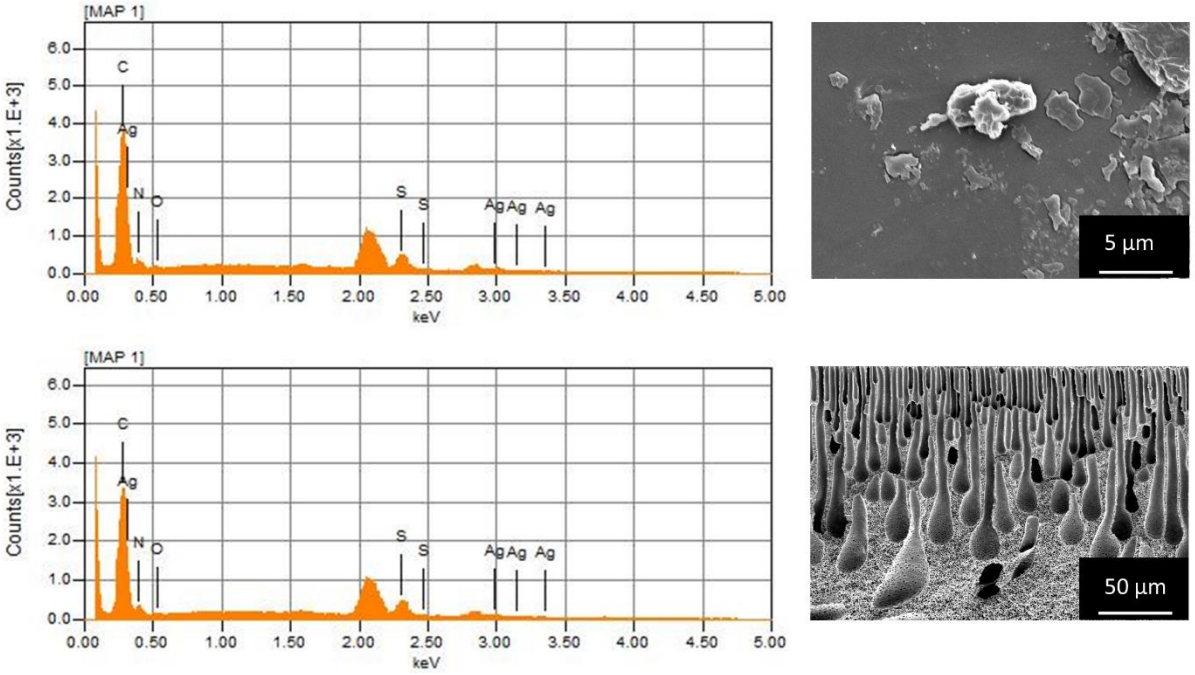

*Figure 259: EDX analysis (left) and respective SEM-picture (right) of a poly(TSC) **P1** membrane obtained by using a 16wt% casting solution in DMSO. The membrane was then used in a dead-end Amicon cell set-up for the removal of siler ions. Thus, 20 mL of a 1.25 mM aqueous $AgNO_3$ solution was pumped through the membrane. Subsequently, the membrane was immersed in ca. 5 mL of water over seven days. The water was exchanged three times over this time. The top layer layer (top) and the CS (bottom) are depicted.*

7 Appendix

7.1 Abbreviations

AAE	Actual Atom Economy
AE	Atom efficiency
AES	Auger electron spectroscopy
AM-3CR	Al-Mourabit-three component polymerization reaction
AM-3CR	Al-Mourabit-three component reaction
BINOL	1,1`-Bi-2-naphtol
BSA	Bovine Serum Albumin
CALB	*Candida Antarctica* lipase B
cEF	complete E-factor
CS	Cross-section
DBU	1,8-diazabicyclo[5.4.0]undec-7-ene
DCM	dichlormethane
DMT	dimercaptotriazine
DP	degree of polymerization
EATOS	environmental assessment tool for organic syntheses
EWG	electron-withdrawing group
GC	gas chromatography
HB	hydrogen bondingHB
IC	isocyanide
IMCR	isocyanide-based multicomponent reaction
IS	internal standard
ITC	isothiocyanate
LCA	life cycle assessment
MCR	Multi component reaction
MF	microfiltration

MOM	methoxy methyl
MWCO	molecular weight cut off
NF	nanofiltation
NIPS	non-solvent induced phase separation
NMM	*N*-Methyl morpholine
P-3CPR	Passerini-three-component polymerization reaction
PMI	process mass intensity
RME_{global}	reaction mass efficiency
RO	reverse osmosis
ROMP	ring-opening metathesis polymerization
sEF	simple E-factor
SIMS	secondary ion mass spectrometry
SMCR	sulfur-based multicomponent reaction
TBD	1,5,7-triazabycyclo[4.4.0]dec-5-ene
TEM	transmission electron microscopy
TON	turnover number
TU	thiourea
U-4CR	Ugi-four component reaction
UF	ultrafiltration
VOC	volatile organic compound
WDS	wavelength-dispersive X-ray spectroscopy
XRD	X-ray diffractometry

7.2 List of Publications

Publikationen in Fachzeitschriften als Hauptauthor

R. Nickisch, P. Conen, M. A. R. Meier* *Macromolecules*, 2022, 55, 3267.

R. Nickisch, P. Conen, S. M. Gabrielsen, M. A. R. Meier* *RSC Adv.*, 2021, 11, 3134.

R. Nickisch, S. M. Gabrielsen, M. A. R. Meier* *ChemistrySelect*, 2020, 5, 11915.

K. Waibel, R. Nickisch, N. Möhl, R. Seim, M. A. R. Meier* *Green Chem.*, 2020, 22, 933. (geteilte Erstauthorenschaft)

Publikationen in Fachzeitschriften als Nebenauthor

J. Wolfs, R. Nickisch, L. Wanner, M. A. R. Meier* *J. Am. Chem. Soc.* 2021, 143, 44, 18693.

S. T. Jung, R. Nickisch, T. Reinsperger, B. Luy, J. Podlech* *J Phys Org Chem*. 2021,34, e4165.

K. S. Wetzel, M. Frölich, S. C. Solleder, R. Nickisch, P. Treu, *Commun Chem* 2020, 3, 63.

8 Bibliography

1 T. A. Rappold and K. S. Lackner, *Energy*, 2010, **35**, 1368–1380.

2 W. J. Chung, J. J. Griebel, E. T. Kim, H. Yoon, A. G. Simmonds, H. J. Ji, P. T. Dirlam, R. S. Glass, J. J. Wie, N. A. Nguyen, B. W. Guralnick, J. Park, A. Somogyi, P. Theato, M. E. Mackay, Y.-E. Sung, K. Char and J. Pyun, *Nat. Chem.*, 2013, **5**, 518–524.

3 National Mineral Information Center, Mineral Commodity Summaries 2020.

4 E. Riedel and C. Janiak, *Anorganische Chemie*, De Gruyter, 2011.

5 D. N. Nakamura, *Oil Gas J.*, 2003, 15.

6 M. Lorenzetti, *Oil Gas J.*, 2002, **100**, 30.

7 F. Crescenzi, A. Crisari, E. D'Angel and A. Nardella, *Environ. Sci. Technol.*, 2006, **40**, 6782–6786.

8 T. B. Nguyen, *Adv. Synth. Catal.*, 2017, **359**, 1066–1130.

9 R. Nickisch, P. Conen, S. M. Gabrielsen and M. A. R. Meier, *RSC Adv.*, 2021, **11**, 3134–3142.

10 T. B. Nguyen, L. Ermolenko and A. Al-Mourabit, *Synthesis*, 2014, **46**, 3172–3179.

11 Z. Karagoz, M. Genc, E. Yılmaz and S. Keser, *Spectrosc. Lett.*, 2013, **46**, 182–190.

12 G. M. Viana, D. C. Soares, M. V. Santana, L. H. do Amaral, P. W. Meireles, R. P. Nunes, L. C. R. P. da Silva, L. C. de S. Aguiar, C. R. Rodrigues, V. P. de Sousa, H. C. Castro, P. A. Abreu, P. C. Sathler, E. M. Saraiva and L. M. Cabral, *Chem. Pharm. Bull.*, 2017, **65**, 911–919.

13 D. C. Schroeder, *Chem. Rev.*, 1955, **55**, 181–228.

14 M. R. Maddani and K. R. Prabhu, *J. Org. Chem.*, 2010, **75**, 2327–2332.

15 M. Kotke and P. R. Schreiner, *Tetrahedron*, 2006, **62**, 434–439.

16 V. Štrukil, D. Gracin, O. V Magdysyuk, R. E. Dinnebier and T. Friščić, *Angewan Chem. Int. Ed.*, 2015, **54**, 8440–8443.

17 Y. Lin, W. J. Hirschi, A. Kunadia, A. Paul, I. Ghiviriga, K. A. Abboud, R. W. Karugu, M. J. Vetticatt, J. S. Hirschi and D. Seidel, *J. Am. Chem. Soc.*, 2020, **142**, 5627–5635.

18 U. Grober, *Natur und Landschaft, 2013, 88.*

19 D. H. Meadows, D. L. Meadows, J. Randers and W. W. Behrens III, *The Limits to Growth. A Report for the CLUB OF ROME`s Project on the Predicament of Mankind*, Universe Books, New York, 1972.

20 G. C. Lebel and H. Kane, *Our common future*, New York, 1987.

21 Agenda 21, 1992, Earth Summit, https://sustainabledevelopment.un.org/content/documents/Agenda21.pdf; extracted at the 11.04.2022.

22 Abschlussbericht der Enquete-Kommission „Schutz des Menschen und der Umwelt-Ziele und Rahmenbedingungen einer nachhaltig zukunftsverträglichen Entwicklung"-Konzept Nachhaltigkeit vom Leitbild zur Umsetzung,

https://dserver.bundestag.de/btd/13/112/1311200.pdf; extracted at the 11.04.2022.

23 Transforming our World: The 2030 Agenda for Sustainable Development, https://sdgs.un.org/sites/default/files/publications/21252030 Agenda for Sustainable Development web.pdf; extracted at the 11.04.2022.

24 G. A. Olah, G. K. S. Prakash and A. Goeppert, *J. Am. Chem. Soc.*, 2011, **133**, 12881–12898.

25 IPCC, 2007: Climate Change 2007: Synthesis Report. Contribution of Working Groups I, II and III to the Fourth Assessment Report of the Intergovernmental Panel on Climate Change. [Core Writing Team, Pachauri, R. K.; Reisinger, A. (eds.)]. IPCC, Geneva, Swi.

26 Direct CO2 emissions from primary chemical production in the Net Zero Scenario, 2015-2030, https://www.iea.org/reports/chemicals; extracted at the 23.05.2022.

27 A. Albini and S. Protti, *Paradigms in Green Chemistry and Technology*, Springer Cham, 1st edn., 2016.

28 B. M. Trost, *Science*, 1991, **254**, 1471–1477.

29 P. Anastas and J. C. Warner, *Green Chemistry: Theory and Practice*, Oxford Univeristy Press, Oxford, 1998.

30 P. Anastas and N. Eghbali, *Chem. Soc. Rev.*, 2010, **39**, 301–312.

31 S. L. Y. Tang, R. L. Smith and M. Poliakoff, *Green Chem.*, 2005, **7**, 761–762.

32 R. A. Sheldon, *Green Chem.*, 2007, **9**, 1273–1283.

33 A. S. Cannon, J. L. Pont and J. C. Warner, in *Green techniques for organic synthesis and medicinal chemistry.*, ed. J. W. & Sons, New York, 2012.

34 P. T. Anastas, T. C. Williamson, D. Hjeresen and J. J. Breen, *Environ. Sci. Technol.*, 1999, **33**, 116A–9A.

35 G. Centi and S. Perathoner, *Catal. Today*, 2003, **77**, 287–297.

36 C. Cathcart, *Chem. Ind.*, 1990, **5**, 684–687.

37 P. T. Anastas and M. M. Kirchhoff, *Acc. Chem. Res.*, 2002, **35**, 686–694.

38 J. A. Linthorst, *Found. Chem.*, 2010, **12**, 55–68.

39 J. H. Clark, *Green Chem.*, 1999, **1**, 1–8.

40 S2669, Green Chemistry Research and Development Act of 2008, 2008.

41 R. A. Sheldon, *Chem. Ind.*, 1992, 903–906.

42 R. A. Sheldon, *Green Chem.*, 2017, **19**, 18–43.

43 A. P. Dicks and A. Hent, *Green Chemistry Metrics-A Guide to Determining and Evaluating Process Greenness*, Springer, 2015.

44 S. K. Ma, J. Gruber, C. Davis, L. Newman, D. Gray, A. Wang, J. Grate, G. W. Huisman and R. A. Sheldon, *Green Chem.*, 2010, **12**, 81–86.

45 A. D. Curzons, D. J. C. Constable, D. N. Mortimer and V. L. Cunningham, *Green Chem.*, 2001, **3**, 1–6.

46 D. J. C. Constable, A. D. Curzons and V. L. Cunningham, *Green Chem.*, 2002, **4**, 521–527.

47 J. Andraos, *Org. Process Res. Dev.*, 2005, **9**, 149–163.

48 C. Jimenez-Gonzalez, C. S. Ponder, Q. B. Broxterman and J. B. Manley, *Org. Process Res. Dev.*, 2011, **15**, 912–917.

49 C. Jiménez-González, D. J. C. Constable and C. S. Ponder, *Chem. Soc. Rev.*, 2012, **41**, 1485–1498.

50 F. Roschangar, R. A. Sheldon and C. H. Senanayake, *Green Chem.*, 2015, **17**, 752–768.

51 F. Tieves, F. Tonin, E. Fernández-Fueyo, J. M. Robbins, B. Bommarius, A. S. Bommarius, M. Alcalde and F. Hollmann, *Tetrahedron*, 2019, **75**, 1311–1314.

52 K. Van Aken, L. Strekowski and L. Patiny, *Beilstein J. Org. Chem.*, 2006, **2**, 3.

53 R. A. Sheldon, *Chemtech*, 1994, 38–47.

54 R. A. Sheldon, *Chem. Soc. Rev.*, 2012, **41**, 1437–1451.

55 E. Heinzle, D. Weirich, F. Brogli, V. H. Hoffmann, G. Koller, M. A. Verduyn and K. Hungerbühler, *Ind. Eng. Chem. Res.*, 1998, **37**, 3395–3407.

56 M. Eissen and J. O. Metzger, *Chem. – A Eur. J.*, 2002, **8**, 3580–3585.

57 EATOS-software, http://www.metzger.chemie.uni-oldenburg.de/eatos/english.htm; extracted at the 08.05.2022.

58 M. Lancaster, *Green Chemistry: an introductory text*, RSC Paperbacks, Cambridge, 2nd edn., 2010.

59 P. T. Anastas and R. L. Lankey, *Green Chem.*, 2000, **2**, 289–295.

60 A. D. Curzons, C. Jiménez-González, A. L. Duncan, D. J. C. Constable and V. L. Cunningham, *Int. J. Life Cycle Assess.*, 2007, **12**, 272.

61 R. K. Henderson, C. Jimenez-Gonzalez, D. J. C. Constable, S. R. Alston, G. G. A. Inglis, G. Fisher, J. Sherwood, S. P. Binks and A. D. Curzons, *Green Chem.*, 2011, **13**, 854–862.

62 D. Prat, O. Pardigon, H.-W. Flemming, S. Letestu, V. Ducandas, P. Isnard, E. Guntrum, T. Senac, S. Ruisseau, P. Cruciani and P. Hosek, *Org. Process Res. Dev.*, 2013, **17**, 1517–1525.

63 V. Hessel, N. N. Tran, M. R. Asrami, Q. D. Tran, N. Van Duc Long, M. Escribà-Gelonch, J. O. Tejada, S. Linke and K. Sundmacher, *Green Chem.*, 2022, **24**, 410–437.

64 C. Capello, U. Fischer and K. Hungerbühler, *Green Chem.*, 2007, **9**, 927–934.

65 D. Zou, S. P. Nunes, I. F. J. Vankelecom, A. Figoli and Y. M. Lee, *Green Chem.*, 2021, **23**, 9815–9843.

66 H. C. Kolb, M. G. Finn and K. B. Sharpless, *Angew. Chem. Int. Ed. Engl.*, 2001, **40**, 2004–2021.

67 J. Zhu and H. Bienaymé, *Multicomponent Reactions*, Wiley-VCH, Weinheim, 2005.

68 R. C. Cioc, E. Ruijter and R. V. A. Orru, *Green Chem.*, 2014, **16**, 2958–2975.

69 H. Cao, H. Liu and A. Dömling, *Chem. – A Eur. J.*, 2010, **16**, 12296–12298.

70 A. de la Hoz, A. Díaz-Ortiz and P. Prieto, in *Alternative Energy Sources for Green Chemistry*, The Royal Society of Chemistry, 2016, pp. 1–33.

71 P. H. Tran, H. T. Nguyen, P. E. Hansen and T. N. Le, *ChemistrySelect*, 2017, **2**, 571–575.

72 C. J. Ellstrom and B. Török, *Application of Sonochemical Activation in Green Synthesis*, Elsevier, 2018.

73 J.-T. Li, M.-X. Sun, G.-Y. He and X.-Y. Xu, *Ultrason. Sonochem.*, 2011, **18**, 412–414.

74 K. J. Ardila-Fierro and J. G. Hernández, *ChemSusChem*, 2021, **14**, 2145–2162.

75 T. Friščić, I. Halasz, P. J. Beldon, A. M. Belenguer, F. Adams, S. A. J. Kimber, V. Honkimäki and R. E. Dinnebier, *Nat. Chem.*, 2013, **5**, 66–73.

76 D. Gracin, V. Štrukil, T. Friščić, I. Halasz and K. Užarević, *Angew. Chemie Int. Ed.*, 2014, **53**, 6193–6197.

77 V. Canale, V. Frisi, X. Bantreil, F. Lamaty and P. Zajdel, *J. Org. Chem.*, 2020, **85**, 10958–10965.

78 A. Albini, M. Fagnoni and M. Mella, *Pure Appl. Chem.*, 2000, **72**, 1321–1326.

79 M. Oelgemöller, C. Jung and J. Mattay, *Pure Appl. Chem.*, 2007, **79**, 1939–1947.

80 A. Albini and M. Fagnoni, *Green Chem.*, 2004, **6**, 1–6.

81 S. Protti, S. Manzini, M. Fagnoni and A. Albini, in *Eco-friendly synthesis of fine chemicals*, RSC Publishing, 2009, pp. 80–111.

82 P. Esser, B. Pohlmann and H.-D. Scharf, *Angew. Chem. Int. Ed.*, 1994, **33**, 2009–2023.

83 N. Monnerie and J. Ortner, *J. Sol. Energy Eng.*, 2001, **123**, 171–174.

84 F. Hollmann, I. W. C. E. Arends and D. Holtmann, *Green Chem.*, 2011, **13**, 2285–2314.

85 J. M. Blamey, F. Fischer, H.-P. Meyer, F. Sarmiento and M. Zinn, *Enzymatic Biocatalysis in Chemical Transformations: A Promising and Emerging Field in Green Chemistry Practice*, Academic Press, 2017.

86 M. Weiß, T. Brinkmann and H. Gröger, *Green Chem.*, 2010, **12**, 1580–1588.

87 E. Juaristi and V. Soloshonok, *Enantioselective Synthesis of β-Amino Acids*, Wiley-VCH, New Jersey, 2nd edn., 2005.

88 M. A. Matthews, *Pure Appl. Chem.*, 2001, **73**, 1305–1308.

89 B. A. Frontana-Uribe, R. D. Little, J. G. Ibanez, A. Palma and R. Vasquez-Medrano, *Green Chem.*, 2010, **12**, 2099–2119.

90 E. Steckhan, T. Arns, G. Heineman, W. R. Hilt, D. Hoormann, J. Jörissen, L. Kröner, B. Lewall and H. Pütter, *Chemosphere*, 2001, **43**, 63–73.

91 Combinatorial Chemistry-an overview, https://www.sciencedirect.com/topics/chemistry/combinatorial-chemistry; extracted at 14.04.2022.

92 A. Kadam, Z. Zhang and W. Zhan, *Curr. Org. Synth.*, 2011, **8**, 295–309.

93 E. Wolf, E. Richmond and J. Moran, *Chem. Sci.*, 2015, **6**, 2501–2505.

94 *CRC Handbook of Chemistry and Physicy*, 97th edn.

95 M. Schmidt, *Chemie unserer Zeit*, 1973, **7**, 11–18.

96 C. Janiak, H.-J. Meyer, D. Gudat and P. Kurz, *Riedel Moderne Anorganische Chemie*, De Gruyter, 2018.

97 R. Prasad and Y. S. Shivay, *Proc. Natl. Acad. Sci. India Sect. B Biol. Sci.*, 2018, **88**, 429–434.

98 S. H. Lebowitz, *J. Chem. Educ.*, 1931, **8**, 1630–1633.

99 J. S. Eow, *Environ. Prog.*, 2002, **21**, 143–162.

100 B. Schreiner, *Chemie unserer Zeit*, 2008, **42**, 378–392.

101 National Mineral Information Center, Mineral Commodity Summaries 2022, https://pubs.usgs.gov/periodicals/mcs2022/mcs2022.pdf; extracted at the 22.06.2022.

102 J. Kruželák, R. Sýkora and I. Hudec, *Chem. Pap.*, 2016, **70**, 1533–1555.

103 N. Selvakumar, A. Azhagurajan and A. Suresh, *J. Therm. Anal. Calorim.*, 2013, **113**, 615–621.

104 Y.-X. Yin, S. Xin, Y.-G. Guo and L.-J. Wan, *Angew. Chemie Int. Ed.*, 2013, **52**, 13186–13200.

105 T. S. Kleine, R. S. Glass, D. L. Lichtenberger, M. E. Mackay, K. Char, R. A. Norwood and J. Pyun, *ACS Macro Lett.*, 2020, **9**, 245–259.

106 F. N. Tebbe, E. Wasserman, W. G. Peet, A. Vatvars and A. C. Hayman, *J. Am. Chem. Soc.*, 1982, **104**, 4971–4972.

107 W. Adam, R. M. Bargon and W. A. Schenk, *J. Am. Chem. Soc.*, 2003, **125**, 3871–3876.

108 W. Adam and R. M. Bargon, *Chem. Commun.*, 2001, 1910–1911.

109 M. Arisawa, T. Ichikawa and M. Yamaguchi, *Chem. Commun.*, 2015, **51**, 8821–8824.

110 G. Zhang, H. Yi, H. Chen, C. Bian, C. Liu and A. Lei, *Org. Lett.*, 2014, **16**, 6156–6159.

111 L. G. Fedenok, K. Y. Fedotov, E. A. Pritchina and N. E. Polyakov, *Tetrahedron Lett.*, 2016, **57**, 1273–1276.

112 L. Meng, T. Fujikawa, M. Kuwayama, Y. Segawa and K. Itami, *J. Am. Chem. Soc.*, 2016, **138**, 10351–10355.

113 T. Miyazaki, S. Kasai, Y. Ogiwara and N. Sakai, *European J. Org. Chem.*, 2016, **2016**, 1043–1049.

114 N. Taniguchi, *Tetrahedron*, 2016, **72**, 5818–5823.

115 M. Braun, W. Frank, G. J. Reiss and C. Ganter, *Organometallics*, 2010, **29**, 4418–4420.

116 W. S. Farrell, P. Y. Zavalij and L. R. Sita, *Angew. Chemie Int. Ed.*, 2015, **54**, 4269–4273.

117 A. Reza Kiasat, B. Mokhtari, F. Kazemi, S. Yousefi and M. Javaherian, *J. Sulfur Chem.*, 2007, **28**, 171–176.

118 G. W. Rewcastle, T. Janosik and J. Bergman, *Tetrahedron*, 2001, **57**, 7185–7189.

119 L. Yu, Y. Wu, T. Chen, Y. Pan and Q. Xu, *Org. Lett.*, 2013, **15**, 144–147.

120 M.-Q. Huang, T.-J. Li, J.-Q. Liu, A. Shatskiy, M. D. Kärkäs and X.-S. Wang, *Org. Lett.*, , DOI:10.1021/acs.orglett.0c00907.

121 S. N. Talapaneni, T. H. Hwang, S. H. Je, O. Buyukcakir, J. W. Choi and A. Coskun, *Angew. Chemie Int. Ed.*, 2016, **55**, 3106–3111.

122 F. Shibahara, R. Sugiura, E. Yamaguchi, A. Kitagawa and T. Murai, *J. Org. Chem.*, 2009, **74**, 3566–3568.

123 H. Gan, D. Miao, Q. Pan, R. Hu, X. Li and S. Han, *Chem. – An Asian J.*, 2016, **11**, 1770–1774.

124 M. A. McLaughlin and D. M. Barnes, *Tetrahedron Lett.*, 2006, **47**, 9095–9097.

125 I. Z. Kondyukov, Y. V Karpychev, P. G. Belyaev, G. K. Khisamutdinov, S. I. Valeshnii, S. P. Smirnov and V. P. Il'in, *Russ. J. Org. Chem.*, 2007, **43**, 635–636.

126 N. V Russavskaya, V. A. Grabel'nykh, E. P. Levanova, E. N. Sukhomazova and E. N. Deryagina, *Russ. J. Org. Chem.*, 2002, **38**, 1498–1500.

127 R. Umeda, H. Kouno, T. Kitagawa, T. Okamoto, K. Kawashima, T. Mashino and Y. Nishiyama, *Heteroat. Chem.*, 2014, **25**, 698–703.

128 X. Wang, P. Li, X. Yuan and S. Lu, *J. Mol. Catal. A Chem.*, 2006, **255**, 25–27.

129 T. B. Nguyen and P. Retailleau, *Adv. Synth. Catal.*, 2019, **361**, 3588–3592.

130 T. B. Nguyen, L. P. A. Nguyen and T. T. T. Nguyen, *Adv. Synth. Catal.*, 2019, **361**, 1787–1791.

131 J. Zhang, L. Hu, Y. Liu, Y. Zhang, X. Chen, Y. Luo, Y. Peng, S. Han and B. Pan, *J. Org. Chem.*, 2021, **86**, 14485–14492.

132 T. B. Nguyen, M. Q. Tran, L. Ermolenko and A. Al-Mourabit, *Org. Lett.*, 2014, **16**, 310–313.

133 A. G. Németh, B. Marlok, A. Domján, Q. Gao, X. Han, G. M. Keserű and P. Ábrányi-Balogh, *European J. Org. Chem.*, 2021, **2021**, 3587–3597.

134 L. A. Nguyen, Q. A. Ngo, P. Retailleau and T. B. Nguyen, *Green Chem.*, 2017, **19**, 4289–4293.

135 T. B. Nguyen, D. H. Mac and P. Retailleau, *J. Org. Chem.*, 2021, **86**, 9418–9427.

136 Z. Zhou, M. Liu, S. Sun, E. Yao, S. Liu, Z. Wu, J.-T. Yu, Y. Jiang and J. Cheng, *Tetrahedron Lett.*, 2017, **58**, 2571–2573.

137 Y. Zhang, Y. Liu, J. Zhang, R. Gu and S. Han, *Tetrahedron Lett.*, 2019, **60**, 151289.

138 A. G. Németh, R. Szabó, G. Orsy, I. M. Mándity, G. M. Keserű and P. Ábrányi-Balogh, *Molecules*, 2021, 26, 303–311.

139 A. G. Németh, R. Szabó, A. Domján, G. M. Keserű and P. Ábrányi-Balogh, *ChemistryOpen*, 2021, **10**, 16–27.

140 M. Saito, S. Murakami, T. Nanjo, Y. Kobayashi and Y. Takemoto, *J. Am. Chem. Soc.*, 2020, **142**, 8130–8135.

141 M. H. Klingele and S. Brooker, *European J. Org. Chem.*, 2004, **2004**, 3422–3434.

142 L. A. Nguyen, T. D. Dang, Q. A. Ngo and T. B. Nguyen, *European J. Org. Chem.*, 2020, 3818–3821.

143 A. G. Németh, G. M. Keserű and P. Ábrányi-Balogh, *Beilstein J. Org. Chem.*, 2019, **15**, 1523–1533.

144 A. Samzadeh-Kermani, *Synlett*, 2015, **26**, 643–645.

145 Y. Nishiyama, C. Katahira and N. Sonoda, *Tetrahedron*, 2006, **62**, 5803–5807.

146 J. Zhang, Q. Zang, F. Yang, H. Zhang, J. Z. Sun and B. Z. Tang, *J. Am. Chem. Soc.*, 2021, **143**, 3944–3950.

147 R. Vanjari, T. Guntreddi, S. Kumar and K. N. Singh, *Chem. Commun.*, 2015, **51**, 366–369.

148 P. Gisbert and I. M. Pastor, *European J. Org. Chem.*, 2020, **2020**, 4319–4325.

149 M. Khalaj, M. Sadeghpour, S. M. Mousavi Safavi, A. Lalegani and S. M. Khatami, *Monatshefte für Chemie - Chem. Mon.*, 2019, **150**, 1085–1091.

150 H. Jin, X. Chen, C. Qian, X. Ge and S. Zhou, *European J. Org. Chem.*, 2021, **2021**, 3403–3406.

151 N. J. Fina and J. O. Edwards, *Int. J. Chem. Kinet.*, 1973, **5**, 1–26.

152 R. Bruckner, *Organic Mechanisms-Reactions, Stereochemistry and Synthesis*, Springer-Verlag Berlin Heidelberg, 1st edn., 2010.

153 W. Cao, F. Dai, R. Hu and B. Z. Tang, *J. Am. Chem. Soc.*, 2020, **142**, 978–986.

154 T. B. Nguyen, D. H. Mac and P. Retailleau, *J. Org. Chem.*, 2020, **85**, 13508–13516.

155 K. V Belyaeva, L. V Andriyankova, L. P. Nikitina, A. G. Mal'kina, A. V Afonin, I. A. Ushakov, I. Y. Bagryanskaya and B. A. Trofimov, *Tetrahedron*, 2014, **70**, 1091–1098.

156 L. Gan, Y. Gao, L. Wei and J.-P. Wan, *J. Org. Chem.*, 2019, **84**, 1064–1069.

157 A. Samzadeh-Kermani and S. Zamenraz, *Monatshefte für Chemie - Chem. Mon.*, 2017, **148**, 1753–1760.

158 T. A. Tikhonova, N. V Ilment, K. A. Lyssenko, I. V Zavarzin and Y. A. Volkova, *Org. Biomol. Chem.*, 2020, **18**, 5050–5060.

159 T. Mizuno, J. Takahashi and A. Ogawa, *Tetrahedron*, 2003, **59**, 1327–1331.

160 T. B. Nguyen, L. Ermolenko and A. Al-Mourabit, *Org. Lett.*, 2012, **14**, 4274–4277.

161 J. M. Tinsley, in *Name reactions in heterocyclic chemistry*, eds. J. J. Li and E. J. Corey, Wiley, New York, pp. 193–198.

162 C.-K. Ran, L. Song, Y.-N. Niu, M.-K. Wei, Z. Zhang, X.-Y. Zhou and D.-G. Yu, *Green Chem.*, 2021, **23**, 274–279.

163 W. Tan, J. Wei and X. Jiang, *Org. Lett.*, 2017, **19**, 2166–2169.

164 W. Bao, C. Chen, N. Yi, J. Jiang, Z. Zeng, W. Deng, Z. Peng and J. Xiang, *Chinese J. Chem.*, 2017, **35**, 1611–1618.

165 T. B. Nguyen and P. Retailleau, *J. Org. Chem.*, 2019, **84**, 5907–5912.

166 T. Guntreddi, R. Vanjari and K. N. Singh, *Org. Lett.*, 2014, **16**, 3624–3627.

167 A. Siva Reddy and K. C. Kumara Swamy, *Org. Lett.*, 2015, **17**, 2996–2999.

168 Y. Jiang, Y. Qin, S. Xie, X. Zhang, J. Dong and D. Ma, *Org. Lett.*, 2009, **11**, 5250–5253.

169 T. Tian, R. Hu and B. Z. Tang, *J. Am. Chem. Soc.*, 2018, **140**, 6156–6163.

170 Z. Chen, P. Liang, F. Xu, Z. Deng, L. Long, G. Luo and M. Ye, *J. Org. Chem.*, 2019, **84**, 12639–12647.

171 Y. Yue, H. Shao, Z. Wang, K. Wang, L. Wang, K. Zhuo and J. Liu, *J. Org. Chem.*, 2020, **85**, 11265–11279.

172 F. Heydari-Mokarrar, R. Heydari, M.-T. Maghsoodlou and A. Samzadeh-Kermani, *J. Sulfur Chem.*, 2020, **41**, 258–270.

173 Z. Wang, C. Li, H. Huang and G.-J. Deng, *J. Org. Chem.*, 2020, **85**, 9415–9423.

174 M. Carmack, *J. Heterocycl. Chem.*, 1989, **26**, 1319–1323.

175 M. Carmack, M. Behforouz, G. A. Berchtold, S. M. Berkowitz, D. Wiesler and R. Barone, *J. Heterocycl. Chem.*, 1989, **26**, 1305–1318.

176 L. Li, Q. Chen, H.-H. Xu, X.-H. Zhang and X.-G. Zhang, *J. Org. Chem.*, 2020, **85**, 10083–10090.

177 T. Chivers and P. J. W. Elder, *Chem. Soc. Rev.*, 2013, **42**, 5996–6005.

178 K. X. Nguyen, P. H. Pham, T. T. Nguyen, C.-H. Yang, H. T. B. Pham, T. T. Nguyen, H. Wang and N. T. S. Phan, *Org. Lett.*, 2020, **22**, 9751–9756.

179 S. Jin, S.-J. Li, X. Ma, J. Su, H. Chen, Y. Lan and Q. Song, *Angew. Chemie Int. Ed.*, 2021, **60**, 881–888.

180 Safety data sheet-sodium carbonate, https://www.sigmaaldrich.com/DE/en/sds/sigald/222321; extracted 26.07.2022.

181 J. Zhu, Q. Wang and M.-X. Wang, *Multicomponent Reactions in Organic Synthesis*, Wiley-VCH Verlag GmbH & Co. KGaA, Weinheim, Germany, 2015.

182 A. Dömling and I. Ugi, *Angew. Chemie Int. Ed.*, 2000, **39**, 3168–3210.

183 A. Dömling, *Chem. Rev.*, 2006, **106**, 19.

184 I. Ugi, A. Dömling and W. Hörl, *Endeavour*, 1994, **18**, 115–122.

185 K. N. Onwukamike, S. Grelier, E. Grau, H. Cramail and M. A. R. Meier, *RSC Adv.*, 2018, **8**, 31490–31495.

186 Z. Söyler, K. N. Onwukamike, S. Grelier, E. Grau, H. Cramail and M. A. R. Meier, *Green Chem.*, 2018, **20**, 214–224.

187 E. Esen and M. A. R. Meier, *ACS Sustain. Chem. Eng.*, 2020, **8**, 15755–15760.

188 P. Slobbe, E. Ruijter and R. V. A. Orru, *Medchemcomm*, 2012, **3**, 1189–1218.

189 I. Akritopoulou-Zanze, *Curr. Opin. Chem. Biol.*, 2008, **12**, 324–331.

190 J. O. Holloway, K. S. Wetzel, S. Martens, F. E. Du Prez and M. A. R. Meier, *Polym. Chem.*, 2019, **10**, 3859–3867.

191 S. C. Solleder, K. S. Wetzel and M. A. R. Meier, *Polym. Chem.*, 2015, **6**, 3201–3204.

192 K. S. Wetzel, M. Frölich, S. C. Solleder, R. Nickisch, P. Treu and M. A. R. Meier, *Commun. Chem.*, 2020, **3**, 63.

193 S. C. Solleder, D. Zengel, K. S. Wetzel and M. A. R. Meier, *Angew. Chem. Int. Ed.*, 2016, **55**, 1204.

194 A. Strecker, *Liebigs Ann. der Chemie*, 1850, **75**, 27.

195 A. Hantzsch, *Liebigs Ann. der Chemie*, 1882, **215**, 1.

196 F. Bossert and W. Vater, *Naturwissenschaften*, 1971, **58**, 578.

197 A. Hantzsch, *Ber. Dtsch. Chem. Ges.*, 1890, **23**, 1474.

198 P. Biginelli, *Ber. Dtsch. Chem. Ges.*, 1891, **24**, 1317.

199 C. Mannich and W. Krösche, *Arch. Pharm.*, 1912, **250**, 647.

200 R. Robinson, *J. Chem. Soc.*, 1917, **111**, 876.

201 N. A. Petasis and I. Akritopoulou, *Tetrahedron Lett.*, 1993, **34**, 583–586.

202 P. Wu, M. Givskov and T. E. Nielsen, *Chem. Rev.*, 2019, **119**, 11245–11290.

203 T. A. Keating and R. W. Armstrong, *J. Org. Chem.*, 1998, **63**, 867.

204 A. Dömling, E. Herdtweck and I. Ugi, *Acta Chem. Scand.*, 1998, **52**, 107–113.

205 G. Balme, D. Bouyssi and N. Monteiro, *Multicomponent Reactions*, Wiley-VCH Verlag GmbH & Co. KGaA, Weinheim, Germany, 2005.

206 R. Braun, K. Zeitter and T. J. J. Müller, *Org. Lett.*, 2001, **3**, 3297.

207 R. Shintani and T. Yamagami, Takafumi, Hayashi, *Org. Lett.2*, 2006, **8**, 4799.

208 R. Dhawan and B. A. Arndtsen, *J. Am. Chem. Soc.*, 2004, **126**, 468.

209 M. Passerini, *Gazz. Chim. Ital.*, 1921, **51**, 126.

210 R. Ramozzi and K. Morokuma, *J. Org. Chem.*, 2015, **80**, 5652.

211 I. Ugi and R. Meyr, *Chem. Ber.*, 1961, **94**, 2229.

212 R. Neidlein, *Z. Naturforsch. B*, 1964, **19**, 1159.

213 R. Neidlein, *Arch. Pharm.*, 1966, **299**, 603.

214 A. Maleki and A. Sarvary, *RSC Adv.*, 2015, **5**, 60938–60955.

215 K. N. and K. Lämmerhirt, *Angew. Chemie Int. Ed. Engl.*, 1968, **7**, 372.

216 A. L. Chandgude and A. Dömling, *Org. Lett.*, 2016, **18**, 6396–6399.

217 T. Soeta, S. Matsuzaki and Y. Ukaji, *Chem. – A Eur. J.*, 2014, **20**, 5007–5012.

218 T. Soeta, Y. Kojima, Y. Ukaji and K. Inomata, *Org. Lett.*, 2010, **12**, 4341–4343.

219 L. El Kaim, M. Gizolme and L. Grimaud, *Org. Lett.*, 2006, **8**, 5021–5023.

220 I. Ugi, U. Fetzer and C. Steinbrückner, *Angew. Chem.*, 1959, **71**, 373.

221 N. Chéron, R. Ramozzi, L. El Kaïm, L. Grimaud and P. Fleurat-Lessard, *J. Org. Chem.*, 2012, **77**, 1361–1366.

222 I. Ugi, F. K. Rosendahl and F. Bodesheim, *Liebigs Ann. der Chemie*, 1963, **666**, 54.

223 J. W. McFarland, *J. Org. Chem.*, 1963, **28**, 2179–2181.

224 L. El Kaïm, L. Grimaud and J. Oble, *Angew. Chem. Int. Ed.*, 2005, **44**, 7961.

225 C. G. Neochoritis, T. Zhao and A. Dömling, *Chem. Rev.*, 2019, **119**, 1970–2042.

226 N. P. Tripolitsiotis, M. Thomaidi and C. G. Neochoritis, *European J. Org. Chem.*, 2020, **2020**, 6525–6554.

227 R. F. Nutt and M. M. Joullie, *J. Am. Chem. Soc.*, 1982, **104**, 5852–5853.

228 A. Katsuyama, A. Matsuda and S. Ichikawa, *Org. Lett.*, 2016, **18**, 2552–2555.

229 K. Khoury, M. K. Sinha, T. Nagashima, E. Herdtweck and A. Dömling, *Angew. Chemie Int. Ed.*, 2012, **51**, 10280–10283.

230 S. C. Solleder, K. S. Wetzel and M. A. R. Meier, *Polym. Chem.*, 2015, **6**, 3201–3204.

231 T. Zarganes-Tzitzikas and A. Dömling, *Org. Chem. Front.*, 2014, **1**, 834–837.

232 E. Ruijter and R. V. A. Orru, *Drug Discov. Today. Technol.*, 2013, **10**, e15-20.

233 E. M. M. Abdelraheem, S. Khaksar, K. Kurpiewska, J. Kalinowska-Tłuścik, S. Shaabani and A. Dömling, *J. Org. Chem.*, 2018, **83**, 1441–1447.

234 C. G. Neochoritis, T. Zarganes-Tzitzikas, M. Novotná, T. Mitríková, Z. Wang, K. Kurpiewska, J. Kalinowska-Tłuścik and A. Dömling, *European J. Org. Chem.*, 2019, **2019**, 6132–6137.

235 S. Hosokawa, K. Nakanishi, Y. Udagawa, M. Maeda, S. Sato, K. Nakano, T. Masuda and Y. Ichikawa, *Org. Biomol. Chem.*, 2020, **18**, 687–693.

236 K. Groebke, L. Weber and F. Mehlin, *Synlett*, 1998, **1998**, 661–663.

237 C. Blackburn, B. Guan, P. Fleming, K. Shiosaki and S. Tsai, *Tetrahedron Lett.*, 1998, **39**, 3635–3638.

238 H. Bienaymé and K. Bouzid, *Angew. Chem. Int. Ed. Engl.*, 1998, **37**, 2234–2237.

239 A. Boltjes and A. Dömling, *European J. Org. Chem.*, 2019, **2019**, 7007–7049.

240 C.-H. Lee, W.-S. Hsu, C.-H. Chen and C.-M. Sun, *European J. Org. Chem.*, 2013, **2013**, 2201–2208.

241 H. Olivier-Bourbigou, L. Magna and D. Morvan, *Appl. Catal. A Gen.*, 2010, **373**, 1–56.

242 T. Akbarzadeh, A. Ebrahimi, M. Saeedi, M. Mahdavi, A. Foroumadi and A. Shafiee, *Monatshefte für Chemie - Chem. Mon.*, 2014, **145**, 1483–1487.

243 N. Devi, R. K. Rawal and V. Singh, *Tetrahedron*, 2015, **71**, 183–232.

244 S. Shaaban and B. F. Abdel-Wahab, *Mol. Divers.*, 2016, **20**, 233–254.

245 O. N. Burchak, L. Mugherli, M. Ostuni, J. J. Lacapère and M. Y. Balakirev, *J. Am. Chem. Soc.*, 2011, **133**, 10058–10061.

246 S. Heck and A. Dömling, *Synlett*, 2000, **2000**, 424–426.

247 A. M. Van Leusen, J. Wildeman and O. H. Oldenziel, *J. Org. Chem.*, 1977, **42**, 1153–1159.

248 J. Sisko, A. J. Kassick, M. Mellinger, J. J. Filan, A. Allen and M. A. Olsen, *J. Org. Chem.*, 2000, **65**, 1516–1524.

249 X. Zheng, Z. Ma and D. Zhang, *Pharm.* , 2020, 13.

250 V. Gracias, A. F. Gasiecki and S. W. Djuric, *Org. Lett.*, 2005, **7**, 3183–3186.

251 R. S. Bon, C. Hong, M. J. Bouma, R. F. Schmitz, F. J. J. de Kanter, M. Lutz, A. L. Spek and R. V. A. Orru, *Org. Lett.*, 2003, **5**, 3759–3762.

252 N. Elders, E. Ruijter, F. J. J. de Kanter, M. B. Groen and R. V. A. Orru, *Chem. – A Eur. J.*, 2008, **14**, 4961–4973.

253 D. Bonne, M. Dekhane and J. Zhu, *Angew. Chemie Int. Ed.*, 2007, **46**, 2485–2488.

254 M. Lipp, F. Dallacker and I. M. zu Köcker, *Monatshefte für Chemie und verwandte Teile anderer Wissenschaften*, 1959, **90**, 41–48.

255 H. Liu, Y. Fang, S.-Y. Wang and S.-J. Ji, *Org. Lett.*, 2018, **20**, 930–933.

256 *23 isocyanides and one diisocyanide are offered on Sigma-Aldrich (purity 94-99% in smaller gram scales) 59 isocyanides and one diisocyanide are offered on abcr (in smaller gram scales, many only on request) date accessed 25.09.2019.*, .

257 O. Kreye, H. Mutlu and M. A. R. Meier, *Green Chem.*, 2013, **15**, 1431–1455.

258 K. A. Waibel, R. Nickisch, N. Möhl, R. Seim and M. A. R. Meier, *Green Chem.*, 2020, **22**, 933–941.

259 C. G. Neochoritis, S. Stotani, B. Mishra and A. Dömling, *Org. Lett.*, 2015, **17**, 2002–2005.

260 P. Patil, M. Ahmadian-Moghaddam and A. Dömling, *Green Chem.*, 2020, **22**, 6902–6911.

261 T. A. Rappold and K. S. Lackner, *Energy*, 2010, **35**, 1368.

262 C. Willgerodt, *Berichte der Dtsch. Chem. Gesellschaft*, 1987, **20**, 2467.

263 K. Kindler, *Liebigs Ann. der Chemie*, 1923, **413**, 187.

264 D. L. Priebbenow and C. Bolm, *Chem. Soc. Rev.*, 2013, **42**, 7870–7880.

265 E. V. Brown, *Synthesis*, 1975, 358.

266 R. Wegler, E. Kuhle and W. Schafer, *Angew. Chem.*, 1958, **70**, 358.

267 F. Asinger and M. Thiel, *Angew. Chem.*, 1958, **70**, 667.

268 F. Asinger and H. Offermanns, *Angew. Chem. Int. Ed. Engl.*, 1967, **79**, 953.

269 F. Asinger, A. Saus, K. Halcour, H. Triem and W. Scharfer, *Angew. Chem. Int. Ed.*, 1963, **75**, 1050.

270 H. R. Darabi, K. Aghapoor and K. Tabar-Heidar, *Monatshefte für Chemie / Chem. Mon.*, 2004, **135**, 79–81.

271 F. Durton-Woitrin, R. Merényi and H. G. Viehe, *Synthesis*, 1985, **1985**, 79–80.

272 T. S. Jagodziński, *Chem. Rev.*, 2003, **103**, 197–228.

273 R. N. Hurd and G. Delamater, *Chem. Rev.*, 1961, **61**, 45–86.

274 C. Lamberth, *Bioorg. Med. Chem.*, 2020, **28**, 115471.

275 S. K. Vujjini, V. R. K. R. Datla, K. R. Badarla, V. N. K. V. P. R. Vetukuri, R. Bandichhor, M. Kagga and P. Cherukupally, *Tetrahedron Lett.*, 2014, **55**, 3885–3887.

276 K. Shimada, M. Yamaguchi, T. Sasaki, K. Ohnishi and Y. Takikawa, *Bull. Chem. Soc. Jpn.*, 1996, **69**, 2235–2242.

277 F. Asinger, *Angew. Chem.*, 1956, **68**, 413.

278 W. Keim and H. Offermanns, *Angew. Chemie Int. Ed.*, 2007, **46**, 6010–6013.

279 N. Griboura, K. Gatzonas and C. G. Neochoritis, *ChemMedChem*, 2021, **16**, 1997–2020.

280 W. M. Weigert, H. Offermanns and P. S. Degussa, *Angew. Chemie Int. Ed. English*, 1975, **14**, 330–336.

281 J. Peisach and W. E. Blumberg, *Mol. Pharmacol.*, 1969, **5**, 200–209.

282 A. H. Hall, *Toxicol. Lett.*, 2002, **128**, 69–72.

283 A. V Camp, *Proc. R. Soc. Med.*, 1977, **70**, 67–69.

284 K. Gewald, E. Schinke and H. Böttcher, *Chem. Ber.*, 1966, **99**, 94–100.

285 R. W. Sabnis, D. W. Rangnekar and N. D. Sonawane, *J. Heterocycl. Chem.*, 1999, **36**, 333–345.

286 Y. Huang and A. Dömling, *Mol. Divers.*, 2011, **15**, 3–33.

287 X.-P. Liang, M. Luo, L. Kang, L.-X. Tang, Q. Liang, Y.-L. Liu, Z. Yang, C.-T. Zhang, C.-Y. Peng and R.-G. Fu, *Tetrahedron Lett.*, 2022, **100**, 153874.

288 T. B. Nguyen and P. Retailleau, *Green Chem.*, 2018, **20**, 387–390.

289 J. G. Rudick, *J. Polym. Sci. Part A Polym. Chem.*, 2013, **51**, 3985–3991.

290 R. Kakuchi, *Angew. Chemie Int. Ed.*, 2014, **53**, 46–48.

291 A. Sehlinger and M. A. R. Meier, ed. P. Theato, Springer International Publishing, Cham, 2015, pp. 61–86.

292 J. T. Windbiel and M. A. R. Meier, *Polym. Int.*, 2021, **70**, 506–513.

293 H. Xue, Y. Zhao, H. Wu, Z. Wang, B. Yang, Y. Wei, Z. Wang and L. Tao, *J. Am. Chem. Soc.*, 2016, **138**, 8690–8693.

294 H. Wu, Z. Wang and L. Tao, *Polym. Chem.*, 2017, **8**, 7290–7296.

295 A. Llevot, A. C. Boukis, S. Oelmann, K. Wetzel and M. A. R. Meier, *Top. Curr. Chem.*, 2017, **375**, 66.

296 O. Kreye, T. Tóth and M. A. R. Meier, *J. Am. Chem. Soc.*, 2011, **133**, 1790–1792.

297 X.-X. Deng, L. Li, Z.-L. Li, A. Lv, F.-S. Du and Z.-C. Li, *ACS Macro Lett.*, 2012, **1**, 1300–1303.

298 Y.-Z. Wang, X.-X. Deng, L. Li, Z.-L. Li, F.-S. Du and Z.-C. Li, *Polym. Chem.*, 2013, **4**, 444–448.

299 A. Sehlinger, R. Schneider and M. A. R. Meier, *Eur. Polym. J.*, 2014, **50**, 150–157.

300 L.-J. Zhang, X.-X. Deng, F.-S. Du and Z.-C. Li, *Macromolecules*, 2013, **46**, 9554–9562.

301 J. Zhang, M. Zhang, F.-S. Du and Z.-C. Li, *Macromolecules*, 2016, **49**, 2592–2600.

302 A. Sehlinger, P.-K. Dannecker, O. Kreye and M. A. R. Meier, *Macromolecules*, 2014, **47**, 2774–2783.

303 A. Sehlinger, R. Schneider and M. A. R. Meier, *Macromol. Rapid Commun.*, 2014, **35**, 1866–1871.

304 N. Gangloff, D. Nahm, L. Döring, D. Kuckling and R. Luxenhofer, *J. Polym. Sci. Part A Polym. Chem.*, 2015, **53**, 1680–1686.

305 L. Li, A. Lv, X.-X. Deng, F.-S. Du and Z.-C. Li, *Chem. Commun.*, 2013, **49**, 8549–8551.

306 Y. Cui, M. Zhang, F.-S. Du and Z.-C. Li, *ACS Macro Lett.*, 2017, **6**, 11–15.

307 W. Lin, X. Guan, T. Sun, Y. Huang, X. Jing and Z. Xie, *Colloids Surf. B. Biointerfaces*, 2015, **126**, 217–223.

308 J. Zhang, Y.-H. Wu, J.-C. Wang, F.-S. Du and Z.-C. Li, *Macromolecules*, 2018, **51**, 5842–5851.

309 B. T. Tuten, L. De Keer, S. Wiedbrauk, P. H. M. Van Steenberge, D. R. D'hooge and C. Barner-Kowollik, *Angew. Chemie Int. Ed.*, 2019, **58**, 5672–5676.

310 M. Hartweg and C. R. Becer, *Green Chem.*, 2016, **18**, 3272–3277.

311 X. Zhang, S. Wang, J. Liu, Z. Xie, S. Luan, C. Xiao, Y. Tao and X. Wang, *ACS Macro Lett.*, 2016, **5**, 1049–1054.

312 Y. Tao, Z. Wang and Y. Tao, *Biopolymers*, 2019, **110**, e23288.

313 S. Javanbakht and A. Shaabani, *ACS Appl. Bio Mater.*, 2020, **3**, 156–174.

314 Y. Zeng, Y. Li, G. Liu, Y. Wei, Y. Wu and L. Tao, *ACS Appl. Polym. Mater.*, 2020, **2**, 404–410.

315 P.-K. Dannecker, A. Sehlinger and M. A. R. Meier, *Macromol. Rapid Commun.*, 2019, **40**, 1800748.

316 K. S. Wetzel and M. A. R. Meier, *Polym. Chem.*, 2019, **10**, 2716–2722.

317 T. Kanbara, Y. Kawai, K. Hasegawa, H. Morita and T. Yamamoto, *J. Polym. Sci. Part A Polym. Chem.*, 2001, **39**, 3739–3750.

318 W. Li, X. Wu, Z. Zhao, A. Qin, R. Hu and B. Z. Tang, *Macromolecules*, 2015, **48**, 7747–7754.

319 J. Wu, Q. Shi, Z. Chen, M. He, L. Jin and D. Hu, *Molecules*, 2012, **17**, 5139–5150.

320 P. A. Yonova and G. M. Stoilkova, *J. Plant Growth Regul.*, 2004, **23**, 280–291.

321 C. P. Richter, *J. Am. Med. Assoc.*, 1945, **129**, 927–931.

322 M. H. Rosove, *West. J. Med.*, 1977, **126**, 339–343.

323 B. Masereel, D. M. Lambert, J. M. Dogné, J. H. Poupaert and J. Delarge, *Epilepsia*, 1997, **38**, 334–337.

324 B. Loev, P. E. Bender, H. Bowman, A. Helt, R. McLean and T. Jen, *J. Med. Chem.*, 1972, **15**, 1024–1027.

325 D. Quy Huong, T. Duong and P. C. Nam, *ACS Omega*, 2019, **4**, 14478–14489.

326 K. M. Dawood, *J. Heterocycl. Chem.*, 2019, **56**, 1701–1721.

327 S. Rajappa, M. D. Nair, B. G. Advani, R. Sreenivasan and J. A. Desai, *J. Chem. Soc. Perkin Trans. 1*, 1979, 1762–1764.

328 J. C. Kaila, A. B. Baraiya, A. N. Pandya, H. B. Jalani, K. K. Vasu and V. Sudarsanam, *Tetrahedron Lett.*, 2009, **50**, 3955–3958.

329 K. D. Hargrave, F. K. Hess and J. T. Oliver, *J. Med. Chem.*, 1983, **26**, 1158–1163.

330 U. Heinelt, D. Schultheis, S. Jäger, M. Lindenmaier, A. Pollex and H. S. g. Beckmann, *Tetrahedron*, 2004, **60**, 9883–9888.

331 K. Biswas and M. F. Greaney, *Org. Lett.*, 2011, **13**, 4946–4949.

332 C. A. Maryanoff, R. C. Stanzione, J. N. Plampin and J. E. Mills, *J. Org. Chem.*, 1986, **51**, 1882–1884.

333 B. R. Linton, A. J. Carr, B. P. Orner and A. D. Hamilton, *J. Org. Chem.*, 2000, **65**, 1566–1568.

334 T. Saetan, M. Sukwattanasinitt and S. Wacharasindhu, *Org. Lett.*, 2020, **22**, 7864–7869.

335 M. Khan, N. Khan, K. Ghazal, S. Shoaib, Samiullah, I. Ali, M. K. Rauf, A. Badshah, M. N. Tahir and A.-U. Rehman, *J. Coord. Chem.*, 2020, **73**, 1790–1805.

336 W. Chen, R. Li, B. Han, B.-J. Li, Y.-C. Chen, Y. Wu, L.-S. Ding and D. Yang, *European J. Org. Chem.*, 2006, **2006**, 1177–1184.

337 V. D. Schwade, L. Kirsten, A. Hagenbach, E. Schulz Lang and U. Abram, *Polyhedron*, 2013, **55**, 155–161.

338 X. Zhao, S. Zhang, C. Bai, B. Li, Y. Li, L. Wang, R. Wen, M. Zhang, L. Ma and S. Li, *J. Colloid*

Interface Sci., 2016, **469**, 109–119.

339 W. Henderson, B. K. Nicholson and E. R. T. Tiekink, *Inorg. Chim. Acta*, 2006, **359**, 204–214.

340 M. Kotke and P. R. Schreiner, in *Hydrogen Bonding in Organic Synthesis*, ed. P. M. Pihko, Wiley-VCH Verlag GmbH & Co. KGaA, Weinheim, 2009, p. 141ff.

341 P. R. Schreiner, *Chem. Soc. Rev.*, 2003, **32**, 289–296.

342 F. Ulatowski and J. Jurczak, *J. Org. Chem.*, 2015, **80**, 4235–4243.

343 S. Nishizawa, P. Bühlmann, M. Iwao and Y. Umezawa, *Tetrahedron Lett.*, 1995, **36**, 6483–6486.

344 U. Boas, A. J. Karlsson, B. F. M. de Waal and E. W. Meijer, *J. Org. Chem.*, 2001, **66**, 2136–2145.

345 U. Manna and G. Das, *Cryst. Growth Des.*, 2018, **18**, 3138–3150.

346 K. Kumamoto, Y. Misawa, S. Tokita, Y. Kubo and H. Kotsuki, *Tetrahedron Lett.*, 2002, **43**, 1035–1038.

347 M. L. Moore and F. S. Crossley, *Organic Syntheses*, John Wiley & Sons, New York, 1955.

348 B. N. Singh, *Agric. Biol. Chem.*, 1978, **42**, 1285–1286.

349 B. K. Verlinden, J. Niemand, J. Snyman, S. K. Sharma, R. J. Beattie, P. M. Woster and L.-M. Birkholtz, *J. Med. Chem.*, 2011, **54**, 6624–6633.

350 H. Sudhamani, S. K. Thaslim Basha, S. Adam, B. V. Bhaskar and C. N. Raju, *Monatsh. Chem.*, 2017, **148**, 1525–1537.

351 S. A. Elseginy, R. Hamdy, V. Menon, A. M. Almehdi, R. El-Awady and S. S. M. Soliman, *Bioorg. Med. Chem. Lett.*, 2020, **30**, 127658.

352 G. Kaupp, J. Schmeyers and J. Boy, *Tetrahedron*, 2000, **56**, 6899–6911.

353 K. Appalanaidu, T. Dadmal, N. Jagadeesh Babu and R. M. Kumbhare, *RSC Adv.*, 2015, **5**, 88063–88069.

354 M. Zhang, Y.-R. Liang, H. Li, M.-M. Liu and Y. Wang, *Bioorg. Med. Chem.*, 2017, **25**, 6623–6634.

355 H. Sugimoto, I. Makino and K. Hirai, *J. Org. Chem.*, 1988, **53**, 2263–2267.

356 V. Iashin, D. Berta, K. Chernichenko, M. Nieger, K. Moslova, I. Pápai and T. Repo, *Chem. – A Eur. J.*, 2020, **26**, 13873–13879.

357 J. B. Bream and J. Schmutz, *Helv. Chim. Acta*, 1977, **60**, 2872–2880.

358 Z. Zhang, H.-H. Wu and Y.-J. Tan, *RSC Adv.*, 2013, **3**, 16940–16944.

359 P. P. Kumavat, A. D. Jangale, D. R. Patil, K. S. Dalal, J. S. Meshram and D. S. Dalal, *Environ. Chem. Lett.*, 2013, **11**, 177–182.

360 M. Đud, O. V Magdysyuk, D. Margetić and V. Štrukil, *Green Chem.*, 2016, **18**, 2666–2674.

361 G. Wieland and G. Simchen, *Liebigs Ann. der Chemie*, 1985, **1985**, 2178–2193.

362 K. Hartke and G. Salamon, *Chem. Ber.*, 1970, **103**, 133–146.

363 A. Affrose, P. Suresh, I. A. Azath and K. Pitchumani, *RSC Adv.*, 2015, **5**, 27533–27539.

364 R. J. Herr, J. L. Kuhler, H. Meckler and C. J. Opalka, *Synthesis*, 2000, **2000**, 1569–1574.

365 K. Singh and S. Sharma, *Tetrahedron Lett.*, 2017, **58**, 197–201.

366 K. Ramadas, N. Srinivasan and N. Janarthanan, *Tetrahedron Lett.*, 1993, **34**, 6447–6450.

367 L. Ciszewski, D. Xu, O. Repič and T. J. Blacklock, *Tetrahedron Lett.*, 2004, **45**, 8091–8093.

368 X. Ran, Y. Long, S. Yang, C. Peng, Y. Zhang, S. Qian, Z. Jiang, X. Zhang, L. Yang, Z. Wang and X. Yu, *Org. Chem. Front.*, 2020, **7**, 472–481.

369 M. Kidwai, S. Bala and A. D. Mishra, *Indian J. Chem.*, 2004, **43**, 2485–2487.

370 E. Rafiee and H. Jafari, *Bioorg. Med. Chem. Lett.*, 2006, **16**, 2463–2466.

371 M. Pelckmans, T. Renders, S. Van de Vyver and B. Sels, *Bio-based amines through sustainable heterogeneous catalysis*, 2017, vol. 19.

372 B. List and K. Maruoka, *Asymmetric Organocatalysis, Vol. 1-2*, Thieme Chemistry, Stuttgart, 2012.

373 A. Antenucci, S. Dughera and P. Renzi, *ChemSusChem*, 2021, **14**, 2785–2853.

374 P. I. Dalko and L. Moisan, *Angew. Chem. Int. Ed.*, 2004, **43**, 5138–5175.

375 Y. Takemoto, *Org. Biomol. Chem.*, 2005, **3**, 4299–4306.

376 K. Morita, Z. Suzuki and H. Hirose, *Bull. Chem. Soc. Jpn.*, 1968, **41**, 2815.

377 P. R. Schreiner and A. Wittkopp, *Org. Lett.*, 2002, **4**, 217–220.

378 N. T. McDougal and S. E. Schaus, *J. Am. Chem. Soc.*, 2003, **125**, 12094–12095.

379 T. Akiyama, J. Itoh, K. Yokota and K. Fuchibe, *Angew. Chemie Int. Ed.*, 2004, **43**, 1566–1568.

380 B. M. Nugent, R. A. Yoder and J. N. Johnston, *J. Am. Chem. Soc.*, 2004, **126**, 3418–3419.

381 J. P. Malerich, K. Hagihara and V. H. Rawal, *J. Am. Chem. Soc.*, 2008, **130**, 14416–14417.

382 A. Jeppesen, B. E. Nielsen, D. Larsen, O. M. Akselsen, T. I. Sølling, T. Brock-Nannestad and M. Pittelkow, *Org. Biomol. Chem.*, 2017, **15**, 2784–2790.

383 D. J. Maher and S. J. Connon, *Tetrahedron Lett.*, 2004, **45**, 1301–1305.

384 H. Huang and E. N. Jacobsen, *J. Am. Chem. Soc.*, 2006, **128**, 7170–7171.

385 T. Okino, Y. Hoashi and Y. Takemoto, *J. Am. Chem. Soc.*, 2003, **125**, 12672–12673.

386 B. Vakulya, S. Varga, A. Csámpai and T. Soós, *Org. Lett.*, 2005, **7**, 1967–1969.

387 Y. Sohtome, A. Tanatani, Y. Hashimoto and K. Nagasawa, *Tetrahedron Lett.*, 2004, **45**, 5589–5592.

388 Y. Sohtome, N. Takemura, T. Iguchi, Y. Hashimoto and K. Nagasawa, *Synlett*, 2006, **2006**, 144–146.

389 M. Retini, F. Bartoccini, G. Zappia and G. Piersanti, *European J. Org. Chem.*, 2021, **2021**, 825.

390 Y. Wang, H. Yang, J. Yu, Z. Miao and R. Chen, *Adv. Synth. Catal.*, 2009, **351**, 3057–3062.

391 J. T. Su, P. Vachal and E. N. Jacobsen, *Adv. Synth. Catal.*, 2001, **343**, 197–200.

392 A. G. Wenzel and E. N. Jacobsen, *J. Am. Chem. Soc.*, 2002, **124**, 12964–12965.

393 D. P. Curran and L. H. Kuo, *Tetrahedron Lett.*, 1995, **36**, 6647–6650.

394 R. C. Pratt, B. G. G. Lohmeijer, D. A. Long, P. N. P. Lundberg, A. P. Dove, H. Li, C. G. Wade, R. M. Waymouth and J. L. Hedrick, *Macromolecules*, 2006, **39**, 7863–7871.

395 R. R. Knowles, S. Lin and E. N. Jacobsen, *J. Am. Chem. Soc.*, 2010, **132**, 5030–5032.

396 M. C. Etter and T. W. Panunto, *J. Am. Chem. Soc.*, 1988, **110**, 5897.

397 D. P. Curran and L. H. Kuo, *J. Org. Chem.*, 1994, **59**, 3259–3261.

398 M. S. Sigman and E. N. Jacobsen, *J. Am. Chem. Soc.*, 1998, **120**, 4901–4902.

399 M. S. Sigman, P. Vachal and E. N. Jacobsen, *Angew. Chemie Int. Ed.*, 2000, **39**, 1279–1281.

400 A. Wittkopp and P. R. Schreiner, *Chem. – A Eur. J.*, 2003, **9**, 407–414.

401 F. G. Bordwell, D. J. Algrim and J. A. Harrelson Jr, *J. Am. Chem. Soc.1*, 1988, **110**, 5903–5904.

402 A. Berkessel, F. Cleemann, S. Mukherjee, T. N. Müller and J. Lex, *Angew. Chemie*, 2005, **117**, 817–821.

403 R. P. Herrera, V. Sgarzani, L. Bernardi and A. Ricci, *Angew. Chemie Int. Ed.*, 2005, **44**, 6576–6579.

404 D. Larsen, L. M. Langhorn, O. M. Akselsen, B. E. Nielsen and M. Pittelkow, *Chem. Sci.*, 2017, **8**, 7978–7982.

405 A. Izaga, R. P. Herrera and M. C. Gimeno, *ChemCatChem*, 2017, **9**, 1313–1321.

406 M. Andreini, M. De Paolis and I. Chataigner, *Catal. Commun.*, 2015, **63**, 15–20.

407 J. Y. C. Lim, N. Yuntawattana, P. D. Beer and C. K. Williams, *Angew. Chem. Int. Ed. Engl.*, 2019, **58**, 6007–6011.

408 X. Chang, J. Zhang, Q. Zhang and C. Guo, *Angew. Chemie Int. Ed.*, 2020, **59**, 18500.

409 N. Vallavoju, S. Selvakumar, S. Jockusch, M. P. Sibi and J. Sivaguru, *Angew. Chem. Int. Ed. Engl.*, 2014, **53**, 5604–5608.

410 N. Spiliopoulou, N. Nikitas and C. G. Kokotos, *Green Chem.*, 2020, **22**, 3539–3545.

411 S. F. Pizzolato, B. S. L. Collins, T. van Leeuwen and B. L. Feringa, *Chem. – A Eur. J.*, 2017, **23**, 6174–6184.

412 S. E. Reisman, A. G. Doyle and E. N. Jacobsen, *J. Am. Chem. Soc.*, 2008, **130**, 7198–7199.

413 M. Li, S. Zhang, X. Zhang, Y. Wang, J. Chen, Y. Tao and X. Wang, *Angew. Chemie Int. Ed.*, 2021, **60**, 6003–6012.

414 R. Hrdina, C. E. Müller, R. C. Wende, K. M. Lippert, M. Benassi, B. Spengler and P. R. Schreiner, *J. Am. Chem. Soc.*, 2011, **133**, 7624–7627.

415 E. Marqués-López, A. Alcaine, T. Tejero and R. P. Herrera, *European J. Org. Chem.*, 2011, **2011**, 3700–3705.

416 Á. Madarász, Z. Dósa, S. Varga, T. Soós, A. Csámpai and I. Pápai, *ACS Catal.*, 2016, **6**, 4379–4387.

417 M. Blain, H. Yau, L. Jean-Gérard, R. Auvergne, D. Benazet, P. R. Schreiner, S. Caillol and B. Andrioletti, *ChemSusChem*, 2016, **9**, 2269–2272.

418 C. Zhao and D. Seidel, *J. Am. Chem. Soc.*, 2015, **137**, 4650–4653.

419 B. Lin and R. M. Waymouth, *J. Am. Chem. Soc.*, 2017, **139**, 1645–1652.

420 K. M. Lippert, K. Hof, D. Gerbig, D. Ley, H. Hausmann, S. Guenther and P. R. Schreiner,

European J. Org. Chem., 2012, **2012**, 5919–5927.

421 M. T. Robak, M. Trincado and J. A. Ellman, *J. Am. Chem. Soc.*, 2007, **129**, 15110–15111.

422 M. Ganesh and D. Seidel, *J. Am. Chem. Soc.*, 2008, **130**, 16464–16465.

423 Y. Fan and S. R. Kass, *Org. Lett.*, 2016, **18**, 188–191.

424 C. R. Jones, G. Dan Pantoş, A. J. Morrison and M. D. Smith, *Angew. Chemie Int. Ed.*, 2009, **48**, 7391–7394.

425 A. J. Neuvonen, T. Földes, Á. Madarász, I. Pápai and P. M. Pihko, *ACS Catal.*, 2017, **7**, 3284–3294.

426 Y. Fan and S. R. Kass, *J. Org. Chem.*, 2017, **82**, 13288–13296.

427 Z. D. Susam and C. Tanyeli, *Asian J. Org. Chem.*, 2021, **10**, 1251–1266.

428 P. Wipf and M. Grenon, *Can. J. Chem.*, 2006, **84**, 1226–1241.

429 S. Bhowmick, A. Mondal, A. Ghosh and K. C. Bhowmick, *Tetrahedron: Asymmetry*, 2015, **26**, 1215–1244.

430 S. Shirakawa, L. Wang, R. He, S. Arimitsu and K. Maruoka, *Chem. – An Asian J.*, 2014, **9**, 1586–1593.

431 M. Barbero, S. Cadamuro, S. Dughera and R. Torregrossa, *Org. Biomol. Chem.*, 2014, **12**, 3902–3911.

432 M. Barbero, S. Cadamuro and S. Dughera, *Green Chem.*, 2017, **19**, 1529–1535.

433 B. Rodríguez, T. Rantanen and C. Bolm, *Angew. Chemie Int. Ed.*, 2006, **45**, 6924–6926.

434 B. Rodríguez, A. Bruckmann and C. Bolm, *Chem. – A Eur. J.*, 2007, **13**, 4710–4722.

435 Y. Hayashi, T. Sumiya, J. Takahashi, H. Gotoh, T. Urushima and M. Shoji, *Angew. Chemie Int. Ed.*, 2006, **45**, 958–961.

436 D. Almaşi, D. A. Alonso and C. Nájera, *Adv. Synth. Catal.*, 2008, **350**, 2467–2472.

437 H. Ohtake, Y. Imada and S.-I. Murahashi, *Bull. Chem. Soc. Jpn.*, 1999, **72**, 2737–2754.

438 T. Scattolin, A. Klein and F. Schoenebeck, *Org. Lett.*, 2017, **19**, 1831–1833.

439 G. E. Veitch and E. N. Jacobsen, *Angew. Chem. Int. Ed. Engl.*, 2010, **49**, 7332–7335.

440 D. E. Fuerst and E. N. Jacobsen, *J. Am. Chem. Soc.*, 2005, **127**, 8964–8965.

441 S. B. Tsogoeva and S. Wei, *Chem. Commun.*, 2006, 1451–1453.

442 S. J. Connon, *Chem. Commun.*, 2008, 2499–2510.

443 T. Marcelli, J. H. van Maarseveen and H. Hiemstra, *Angew. Chemie Int. Ed.*, 2006, **45**, 7496–7504.

444 A. K. Barbour, M. W. Buxton, M. Stacey, J. C. Tatlow and A. G. Sharpe, in *Advances in Fluorine Chemistry*, London, 1963, pp. 181–270.

445 K. Liu, H.-F. Cui, J. Nie, K.-Y. Dong, X.-J. Li and J.-A. Ma, *Org. Lett.*, 2007, **9**, 923–925.

446 A. Carlone and L. Bernardi, *Phys. Sci. Rev.*, , DOI:doi:10.1515/psr-2018-0097.

447 P. Renzi and M. Bella, *Chem. Commun.*, 2012, **48**, 6881–6896.

448 T. Fulgheri, F. Della Penna, A. Baschieri and A. Carlone, *Curr. Opin. Green Sustain. Chem.*, 2020, **25**, 100387.

449 M. Barbero, S. Cadamuro, S. Dughera and P. Venturello, *Synthesis*, 2008, **2008**, 3625–3632.

450 M. Barbero, S. Cadamuro, S. Dughera and P. Venturello, *Synlett*, 2007, **2007**, 2209–2212.

451 M. Barbero, S. Cadamuro, S. Dughera and P. Venturello, *Synthesis*, 2008, **2008**, 1379–1388.

452 D. Vuluga, J. Legros, B. Crousse and D. Bonnet-Delpon, *Chem. – A Eur. J.*, 2010, **16**, 1776–1779.

453 D.-H. Chen, W.-T. Sun, C.-J. Zhu, G.-S. Lu, D.-P. Wu, A.-E. Wang and P.-Q. Huang, *Angew. Chemie Int. Ed.*, 2021, **60**, 8827–8831.

454 H. Miyabe, S. Tuchida, M. Yamauchi and Y. Takemoto, *Synthesis*, 2006, **19**, 3295–3300.

455 M. Liu, X. Zhang, X. Huang, G. Dhawan, J. Evans, M. Kaur, J. P. Jasinski and W. Zhang, *European J. Org. Chem.*, 2019, **2019**, 150–155.

456 T. Miura, S. Nishida, A. Masuda, N. Tada and A. Itoh, *Tetrahedron Lett.*, 2011, **52**, 4158–4160.

457 T. Jichu, T. Inokuma, K. Aihara, T. Kohiki, K. Nishida, A. Shigenaga, K. Yamada and A. Otaka, *ChemCatChem*, 2018, **10**, 3402–3405.

458 J. M. Andrés, M. González, A. Maestro, D. Naharro and R. Pedrosa, *European J. Org. Chem.*, 2017, **2017**, 2683–2691.

459 L. Tuchman-Shukron, S. J. Miller and M. Portnoy, *Chem. – A Eur. J.*, 2012, **18**, 2290–2296.

460 M. Kotke and P. Schreiner, *Synthesis*, 2007, **2007**, 779–792.

461 J. Li, G. Yang and Y. Cui, *J. Appl. Polym. Sci.*, 2011, **121**, 1506–1511.

462 J. Li, G. Yang, Y. Qin, X. Yang and Y. Cui, *Tetrahedron: Asymmetry*, 2011, **22**, 613–618.

463 J. M. Andrés, N. de La Cruz, M. Valle and R. Pedrosa, *Chempluschem*, 2016, **81**, 86–92.

464 R. Pedrosa, J. M. Andrés, D. P. Ávila, M. Ceballos and R. Pindado, *Green Chem.*, 2015, **17**, 2217–2225.

465 J. M. Andrés, A. Maestro, P. Rodríguez-Ferrer, I. Simón and R. Pedrosa, *ChemistrySelect*, 2016, **1**, 5057–5061.

466 A. Puglisi, M. Benaglia, R. Annunziata and J. S. Siegel, *ChemCatChem*, 2012, **4**, 972–975.

467 J. M. Andrés, F. González, A. Maestro, R. Pedrosa and M. Valle, *European J. Org. Chem.*, 2017, **2017**, 3658–3665.

468 Y. Luan, N. Zheng, Y. Qi, J. Tang and G. Wang, *Catal. Sci. Technol.*, 2014, **4**, 925–929.

469 Q. Wu, W. Gong and G. Li, *ACS Appl. Mater. Interfaces*, 2020, **12**, 17861–17869.

470 A. Corma, S. Iborra and A. Velty, *Chem. Rev.*, 2007, **107**, 2411–2502.

471 A. Llevot, P.-K. Dannecker, M. von Czapiewski, L. C. Over, Z. Söyler and M. A. R. Meier, *Chem. – A Eur. J.*, 2016, **22**, 11510–11521.

472 C. V. Rieker, *Sustainability Evaluation of Isocyanides Synthesis*, KIT., 2019.

473 N. D. C. L. Möhl and Bachelorthesis:, *Improving the sustainability of isocyanide synthesis*, 2019.

474 N. Fusetani, *Curr. Org. Chem.*, 1997, **1**, 127.

475 M. Passerini, *Gazz. Chim. Ital.*, 1923, **53**, 331.

476 I. Ugi, U. Fetzer and C. Steinbrückner, *Angew. Chem.*, 1959, **71**, 386.

477 T. Yamaguchi, Y. Miyake, A. Miyamura, N. Ishiwata and K. Tatsuta, *J. Antibiot.* , 2006, **59**, 729–734.

478 A. Sehlinger, O. Kreye and M. A. R. Meier, *Macromolecules*, 2013, **46**, 6031–6037.

479 A. Sehlinger, L. M. De Espinosa and M. A. R. Meier, *Macromol. Chem. Phys.*, 2013, **214**, 2821–2828.

480 Z. Zhang, Y.-Z. You, D.-C. Wu and C.-Y. Hong, *Macromolecules*, 2015, **48**, 3414–3421.

481 W. Lieke, *Liebigs Ann. der Chemie*, 1859, **112**, 316.

482 E. Meyer, *J. Prakt. Chem.*, 1866, 147.

483 P. Boullanger and G. Descotes, *Tetrahedron Lett.*, 1976, **17**, 3427–3430.

484 A. W. Hoffmann, *Ber. Dtsch. Chem. Ges.*, 1867, **144**, 114.

485 W. P. Weber, G. W. Gokel and I. K. Ugi, *Angew. Chemie*, 1972, **84**, 587.

486 P. G. Gassman and L. M. Haberman, *Tetrahedron Lett.*, 1985, **26**, 4971–4974.

487 Y. Kitano, K. Chiba and M. Tada, *Tetrahedron Lett.*, 1998, **39**, 1911–1912.

488 R. Meyr and I. Ugi, *Angew. Chemie*, 1958, **70**, 702–703.

489 G. Skorna and I. Ugi, *Angew. Chem.*, 1977, **89**, 267.

490 A. Efraty, I. Feinstein, L. Wackerle and A. Goldman, *J. Org. Chem.*, 1980, **45**, 4059–4061.

491 K. Katayama, K. Nakagawa, H. Takeda, A. Matsuda and S. Ichikawa, *Org. Lett.*, 2014, **16**, 428–431.

492 T. A. Keating and R. W. Armstrong, *J. Am. Chem. Soc.*, 1996, **118**, 2574.

493 S. M. Creedon, H. Kevin Crowley and D. G. McCarthy, *J. Chem. Soc. Perkin Trans. 1*, 1998, 1015–1018.

494 R. Appel, R. Kleistück and K. D. Ziehn, *Angew. Chem.*, 1971, **83**, 143.

495 J. E. Baldwin and I. A. O'Neil, *Synlett*, 1990, **1990**, 603–604.

496 R. E. Schuster, J. E. Scott and J. Casanova Jr., *J. Mol. Spectrosc.*, 1979, **76**, 55–70.

497 S. Abou-Shehada, P. Mampuys, B. U. W. Maes, J. H. Clark and L. Summerton, *Green Chem.*, 2017, **19**, 249–258.

498 R. Obrecht, R. Herrmann and I. Ugi, *Synthesis*, 1985, 400.

499 D. H. Barton, T. Bowles, S. Husinec, J. E. Forbes, A. Llobera, A. E. Porter and S. Z. Zard, *Tetrahedron Lett.*, 1988, **29**, 3343–3346.

500 H. Bienaymé, *Tetrahedron Lett.*, 1998, **35**, 640.

501 R. Bossio, S. Marcaccini, R. Pepino, U. Schiff, U. Firenze and V. G. Capponi, *Liebigs Ann. der Chemie*, 1990, 935.

502 X. Wang and Q. Wang, *Synthesis*, 2015, **47**, 49.

503 R. Mocci, S. Murgia, L. De Luca, E. Colacino, F. Delogu and A. Porcheddu, *Org. Chem. Front.*,

2018, **5**, 531–538.

504 I. Ugi and R. Meyr, *Angew. Chem.1*, 1958, **70**, 702.

505 K. Alfonsi, J. Colberg, P. J. Dunn, T. Fevig, S. Jennings, T. A. Johnson, H. P. Kleine, C. Knight, M. A. Nagy, D. A. Perry and M. Stefaniak, *Green Chem.*, 2008, **10**, 31–36.

506 D. Prat, J. Hayler and A. Wells, *Green Chem.*, 2014, **16**, 4546–4551.

507 R. A. Sheldon, *Chem. Ind. (London)*, 1992, 903–906.

508 C. Fahlberg and I. Remsen, *Berichte der Dtsch. Chem. Gesellschaft*, 1879, **12**, 469–473.

509 D. J. Ager, D. P. Pantaleone, S. A. Henderson, A. R. Katritzky, I. Prakash and D. E. Walters, *Angew. Chemie Int. Ed.*, 1998, **37**, 1802–1817.

510 R. K. Henderson, A. P. Hill, A. M. Redman and H. F. Sneddon, *Green Chem.*, 2015, **17**, 945–949.

511 W. Bull, One-step process for preparing diisopropylamine, US 2686811, 1954.

512 S. Shimizu, N. Watanabe, T. Kataoka, T. Shoji, N. Abe, S. Morishita and H. Ichimura, in *Ullmann's Encyclopedia of Industrial Chemistry*, Wiley-VCH, Weinheim, 2005.

513 W. Reppe and W. J. Schweckendiek, *Justus Liebigs Ann. Chem.*, 1948, **560**, 104–116.

514 K. Eller, E. Henkes, R. Rossbacher and H. Höke, in *Ullmann's Encyclopedia of Industrial Chemistry*, Wiley-VCH, Weinheim, 2005.

515 J. Eberhardt, H. Meissner, B. W. Hoffer, J.-P. Melder and E. Schwab, Process for the preparation of an amine, US20100267948A1, 2010.

516 F. Haese, J. Wulff-Döring, U. Köhler, P. Gaa, F.-F. Pape, J.-P. Melder and M. Julius, Method for the continuous production of an amine, WO2006136571A1, 2006.

517 P. Tundo and M. Selva, *Acc. Chem. Res.*, 2002, **35**, 706–716.

518 H.-J. Buysch, in *Ullmann's Encyclopedia of Industrial Chemistry*, Wiley-VCH, Weinheim, 2005.

519 K. Pérez-Labrada, I. Brouard, I. Méndez and D. G. Rivera, *J. Org. Chem.*, 2012, **77**, 4660–4670.

520 M. K. W. Mackwitz, A. Hamacher, J. D. Osko, J. Held, A. Schöler, D. W. Christianson, M. U. Kassack and F. K. Hansen, *Org. Lett.*, 2018, **20**, 3255–3258.

521 S. Sharma, R. A. Maurya, K. I. Min, G. Y. Jeong and D. P. Kim, *Angew. Chemie - Int. Ed.*, 2013, **52**, 7564–7568.

522 A. V. Gulevich, L. S. Koroleva, O. V. Morozova, V. N. Bakhvalova, V. N. Silnikov and V. G. Nenajdenko, *Beilstein J. Org. Chem.*, 2011, **7**, 1135–1140.

523 J. G. Polisar, L. Li and J. R. Norton, *Tetrahedron Lett.*, 2011, **52**, 2933–2934.

524 K. Škoch, I. Císařová and P. Štěpnička, *Chem. - A Eur. J.*, 2018, **24**, 13788–13791.

525 L. Wildersinn, *Optimization and investigation of the reaction conditions of Ugi four-component reactions*, KIT, 2019.

526 A. R. Nödling, G. Jakab, P. R. Schreiner and G. Hilt, *European J. Org. Chem.*, 2014, **2014**, 6394–6398.

527 K. M. Diemoz and A. K. Franz, *J. Org. Chem.*, 2019, **84**, 1126–1138.

528 A. Dömling and I. Ugi, *Angew. Chem. Int. Ed.*, 2000, **39**, 3168–3210.

529 Safety data sheet 1-dodecanol, https://www.sigmaaldrich.com/DE/de/sds/sigald/126799; extracted at 18.07.2022.

530 S. Sharma, *Sulfur Reports*, 1989, **8**, 327–454.

531 S. Wu, M. Luo, D. J. Darensbourg and X. Zuo, *Macromolecules*, 2019, **52**, 8596–8603.

532 R. Ma, V. Sharma, A. F. Baldwin, M. Tefferi, I. Offenbach, M. Cakmak, R. Weiss, Y. Cao, R. Ramprasad and G. A. Sotzing, *J. Mater. Chem. A*, 2015, **3**, 14845–14852.

533 Safety data sheet 1,10-decanediol, https://www.sigmaaldrich.com/DE/de/sds/aldrich/d1203; extracted 18.07.2022.

534 Safety data sheet tetraethylene glycol, https://www.sigmaaldrich.com/DE/de/sds/aldrich/110175; extracted at 18.07.2022.

535 M. Uygun, M. A. Tasdelen and Y. Yagci, *Macromol. Chem. Phys.*, 2010, **211**, 103–110.

536 A. Das and K. R. J. Thomas, *European J. Org. Chem.*, 2020, **2020**, 7214–7218.

537 S. Hafeez, V. Khatri, H. K. Kashyap and L. Nebhani, *New J. Chem.*, 2020, **44**, 18625–18632.

538 D. Limnios and C. G. Kokotos, *Adv. Synth. Catal.*, 2017, **359**, 323–328.

539 D. J. Keddie, G. Moad, E. Rizzardo and S. H. Thang, *Macromolecules*, 2012, **45**, 5321–5342.

540 A. Leitgeb, J. Wappel and C. Slugovc, *Polymer*, 2010, **51**, 2927–2946.

541 C. Barner-Kowollik, *Handb. RAFT Polym.*, 2008, 1–4.

542 J. Nicolas, Y. Guillaneuf, C. Lefay, D. Bertin, D. Gigmes and B. Charleux, *Prog. Polym. Sci.*, 2013, **38**, 63.

543 N. P. Truong, G. R. Jones, K. G. E. Bradford, D. Konkolewicz and A. Anastasaki, *Nat. Rev. Chem.*, 2021, **5**, 859–869.

544 A. F. M. Kilbinger, *Synlett*, 2019, **30**, 2051–2057.

545 S. Hilf and A. F. M. Kilbinger, *Macromolecules*, 2009, **42**, 4127–4133.

546 D. Barther and D. Moatsou, *Macromol. Rapid Commun.*, 2021, **42**, 2100027.

547 D. A. N'Guyen, V. Montembault, S. Piogé, S. Pascual and L. Fontaine, *J. Polym. Sci. Part A Polym. Chem.*, 2017, **55**, 4051–4061.

548 C. Janiak and P. G. Lassahn, *J. Mol. Catal. A Chem.*, 2001, **166**, 193–209.

549 S. Elyashiv-Barad, N. Greinert and A. Sen, *Macromolecules*, 2002, **35**, 7521–7526.

550 E. Szuromi, H. Shen, B. L. Goodall and R. F. Jordan, *Organometallics*, 2008, **27**, 402–409.

551 J. P. Kennedy and H. S. Makowski, *J. Macromol. Sci. Part A - Chem.*, 1967, **1**, 345–370.

552 C. Janiak and P. G. Lassahn, *Macromol. Rapid Commun.*, 2001, **22**, 479–493.

553 P. Conen, *Sustainable isothiocyante synthesis and some mechanistic insights*, KIT, 2020.

554 D. Prat, A. Wells, J. Hayler, H. Sneddon, C. R. McElroy, S. Abou-Shehada and P. J. Dunn, *Green Chem.*, 2016, **18**, 288–296.

555 F. Ravalico, S. L. James and J. S. Vyle, *Green Chem.*, 2011, **13**, 1778–1783.

556 J. A. Dean, *Lange´s Handbook of Chemistry*, McGRAW-HILL, INC., New York, 15th edn., 1999.

557 I. Kaljurand, A. Kütt, L. Sooväli, T. Rodima, V. Mäemets, I. Leito and I. A. Koppel, *J. Org. Chem.*, 2005, **70**, 1019–1028.

558 K. M. K. Yu, I. Curcic, J. Gabriel, H. Morganstewart and S. C. Tsang, *J. Phys. Chem. A*, 2010, **114**, 3863–3872.

559 W. Schwarz, J. Schossig, R. Rossbacher, R. Pinkos and H. Höke, *Ullmann's Encycl. Ind. Chem.*, 2019, 1–7.

560 J. Sherwood, M. De bruyn, A. Constantinou, L. Moity, C. R. McElroy, T. J. Farmer, T. Duncan, W. Raverty, A. J. Hunt and J. H. Clark, *Chem. Commun.*, 2014, **50**, 9650–9652.

561 M. Arisawa, M. Ashikawa, A. Suwa and M. Yamaguchi, *Tetrahedron Lett.*, 2005, **46**, 1727–1729.

562 W. Adam, R. M. Bargon, S. G. Bosio, W. A. Schenk and D. Stalke, *J. Org. Chem.*, 2002, **67**, 7037–7041.

563 S. Fujiwara, T. Shink-Ike, N. Sonoda, M. Aoki, K. Okada, N. Miyoshi and N. Kambe, *Tetrahedron Lett.*, 1991, **32**, 3503–3506.

564 A. Ishii, R. Ebina, M. Shibata, Y. Hayashi and N. Nakata, *J. Sulfur Chem.*, 2020, **41**, 238–257.

565 J. J. Li, *Name Reactions-A Collection of Detailed Mechanisms and Synhteitc Applications*, Springer Nature Switzerland AG, 6th edn., 2021.

566 G. Mlostoń, K. Urbaniak, K. Gębicki, P. Grzelak and H. Heimgartner, *Heteroat. Chem.*, 2014, **25**, 548–555.

567 T. Zhu, X. Wu, X. Yang, B. Sharma, N. Li, J. Huang, W. Wang, W. Xing, Z. Zhao and H. Huang, *Inorg. Chem.*, 2018, **57**, 9266–9273.

568 A. U. Augustin, M. Sensse, P. G. Jones and D. B. Werz, *Angew. Chemie Int. Ed.*, 2017, **56**, 14293–14296.

569 R. Hamera-Fałdyga, P. Grzelak, P. Pipiak and G. Mlostoń, *Phosphorus. Sulfur. Silicon Relat. Elem.*, 2017, **192**, 197–198.

570 U. Rohr, J. Schatz and J. Sauer, *European J. Org. Chem.*, 1998, **1998**, 2875–2883.

571 J. Breu, P. Höcht, U. Rohr, J. Schatz and J. Sauer, *European J. Org. Chem.*, 1998, **1998**, 2861–2873.

572 G. Mlostoń, P. Grzelak, A. Linden and H. Heimgartner, *Chem. Heterocycl. Compd.*, 2017, **53**, 518–525.

573 V. Petrov, R. J. Dooley, A. A. Marchione, E. L. Diaz and B. S. Clem, *J. Fluor. Chem.*, 2019, **225**, 1–10.

574 R. Mayer, J. Morgenstern and J. Fabian, *Angew. Chemie Int. Ed.*, 1964, **3**, 277–286.

575 Q. Zhao, Y. Chen, M. Sun, X.-J. Wu and Y. Liu, *RSC Adv.*, 2016, **6**, 50673–50679.

576 M. Stahl, U. Pidun and G. Frenking, *Angew. Chemie Int. Ed. English*, 1997, **36**, 2234–2237.

577 D. X. Zeng and Y. Chen, *Synlett*, 2006, **2006**, 490–492.

578 X.-F. Duan, J. Zeng, J.-W. Lü and Z.-B. Zhang, *J. Org. Chem.*, 2006, **71**, 9873–9876.

579 R. Bruckner, *Organic Mechanisms-Reactions, Stereochemistry and Synthesis*, Springer-Verlag Berlin Heidelberg, 1st edn., 2010.

580 J. M. Burns, T. Clark and C. M. Williams, *J. Org. Chem.*, 2021, **86**, 7515–7528.

581 R. M. Kellogg, *Acc. Chem. Res.*, 2017, **50**, 905–914.

582 J. D. E. Lane, S. N. Berry, W. Lewis, J. Ho and K. A. Jolliffe, *J. Org. Chem.*, 2021, **86**, 4957–4964.

583 S. Tamagaki, R. Ichihara and S. Oae, *Bull. Chem. Soc. Jpn.*, 1975, **48**, 355–356.

584 C. Kaepplinger, R. Beckert, G. Braunerova, L. Zahajska, A. Darsen and H. Goerls, *Sulfur Lett.*, 2003, **26**, 141–147.

585 U. Pathak, L. K. Pandey and R. Tank, *J. Org. Chem.*, 2008, **73**, 2890–2893.

586 G. Hua, Y. Li, A. M. Z. Slawin and J. D. Woollins, *Dalt. Trans.*, 2007, 1477–1480.

587 V. K. Aggarwal, E. Alonso, G. Hynd, K. M. Lydon, M. J. Palmer, M. Porcelloni and J. R. Studley, *Angew. Chemie Int. Ed.*, 2001, **40**, 1430–1433.

588 Compounds labelled as 'dicarboxaldehyde' are offered for instance from Sigma-Aldrich (13) and abcr (26)., Data extracted at 26.01.2022.

589 K. Eschliman and S. H. Bossmann, *Synthesis*, 2019, **51**, 1746–1752.

590 C. Larsen, K. Steliou and D. N. Harpp, *J. Org. Chem.*, 1978, **43**, 337–339.

591 A. J. Bloodworth, T. Melvin and J. C. Mitchell, *J. Org. Chem.*, 1986, **51**, 2612–2613.

592 R. Nickisch, S. M. Gabrielsen and M. A. R. Meier, *ChemistrySelect*, 2020, **5**, 11915–11920.

593 M. A. Metwally, S. Bondock, H. El-Azap and E.-E. M. Kandeel, *J. Sulfur Chem.*, 2011, **32**, 489–519.

594 T. S. Lobana, R. Sharma, G. Bawa and S. Khanna, *Coord. Chem. Rev.*, 2009, **253**, 977–1055.

595 D. M. Wiles, B. A. Gingras and T. Suprunchuk, *Can. J. Chem.*, 1967, **45**, 469–473.

596 R. Basri, M. Khalid, Z. Shafiq, M. S. Tahir, M. U. Khan, M. N. Tahir, M. M. Naseer and A. A. C. Braga, *ACS Omega*, 2020, **5**, 30176–30188.

597 R. Nickisch, P. Conen and M. A. R. Meier, *Macromolecules*, 2022, **55**, 3267–3275.

598 J. C. Crittenden, R. R. Trussel, D. W. Hand, K. J. Howe and G. Tchobanoglous, *Water Treatmend: Principles and Design*, John Wiley & Sons, Inc., Hoboken, NJ, 2nd edn., 2005.

599 M. Cheryan, *Ultrafiltration and Microfiltration Handbook*, Technomic, Lancaster, PA, 1998.

600 P. Eriksson, *Environ. Prog.*, 1988, **7**, 58–62.

601 A. E. Yaroshchuk, *Sep. Purif. Technol.*, 2001, **22**–**23**, 143–158.

602 P. M. Budd and N. B. McKeown, *Polym. Chem.*, 2010, **1**, 63–68.

603 G. R. Guillen, Y. Pan, M. Li and E. M. V Hoek, *Ind. Eng. Chem. Res.*, 2011, **50**, 3798–3817.

604 R. W. Baker, *Membrane Technology and Applications*, John Wiley & Sons, Ltd, 3rd edn., 2012.

605 N. Salim, A. Siddiqa, S. Shahida and S. Qaisar, *Madridge J. Nanotechnol Nanosci.*, 2019, **4**, 139–147.

606 M. Mulder, *Basic Principles of Membrane Technology*, Springer, Dordrecht, 2nd edn., 1996.

607 B. G. Carter, N. Cheng, R. Kapoor, G. H. Meletharayil and M. A. Drake, *J. Dairy Sci.*, 2021, **104**, 2465–2479.

608 M. Mulder, *Basic Principles of Membrane Technology*, Kluwer Academic Publishers, Dordrecht, 2003.

609 M. Müller and V. Abetz, *Chem. Rev.*, 2021, **121**, 14189–14231.

610 S. LOEB and S. SOURIRAJAN, in *Saline Water Conversion—II*, AMERICAN CHEMICAL SOCIETY, 1963, vol. 38, pp. 117-132 SE–9.

611 R. W. Baker, *Membrane Technology and Applications*, John Wiley & Sons, Ltd, New York, 2004.

612 M. Guillotin, C. Lemoyne, C. Noel and L. Monnerie, *Desalination*, 1977, **21**, 165–181.

613 D. M. Koenhen, M. H. V Mulder and C. A. Smolders, *J. Appl. Polym. Sci.*, 1977, **21**, 199–215.

614 H. Strathmann, K. Kock, P. Amar and R. W. Baker, *Desalination*, 1975, **16**, 179–203.

615 X. Dong, A. Al-Jumaily and I. C. Escobar, *Membranes (Basel).*, 2018, 8, 23.

616 M. Fadel, Y. Wyart and P. Moulin, *Membranes (Basel).*, 2020, 10, 271.

617 J. M. M. Peeters, M. H. V Mulder and H. Strathmann, *Colloids Surfaces A Physicochem. Eng. Asp.*, 1999, **150**, 247–259.

618 L. F. Villalobos, T. Yapici and K.-V. Peinemann, *Sep. Purif. Technol.*, 2014, **136**, 94–104.

619 R. Du, B. Gao and J. Men, *J. Chem. Technol. Biotechnol.*, 2019, **94**, 1441–1450.

620 A. Dehno Khalaji, E. Shahsavani, N. Feizi, M. Kucerakova, M. Dusek and R. Mazandarani, *Comptes Rendus Chim.*, 2017, **20**, 534–539.

621 A. I. Matesanz, I. Leitao and P. Souza, *J. Inorg. Biochem.*, 2013, **125**, 26–31.

622 Bal-Demirci, *Polyhedron*, 2008, **27**, 440–446.

623 A. Guirado, A. Zapata, J. L. Gómez, L. Trabalón and J. Gálvez, *Tetrahedron*, 1999, **55**, 9631–9640.

624 A. Ghoshal, M. D. Ambule, R. Sravanthi, M. Taneja and A. K. Srivastava, *New J. Chem.*, 2019, **43**, 14459–14474.

625 J. Spitzley, *Neue Homo-Multichromophore auf Basis der Ugi-Reaktion*, 2012.

626 X. Wang, Y. Xu, F. Mo, G. Ji, D. Qiu, J. Feng, Y. Ye, S. Zhang, Y. Zhang and J. Wang, *J. Am. Chem. Soc.*, 2013, **135**, 10330–10333.

627 H.-J. Gais and A. Böhme, *J. Org. Chem.*, 2002, **67**, 1153–1161.

628 M. Degardin, S. Wein, J.-F. Duckert, M. Maynadier, A. Guy, T. Durand, R. Escale, H. Vial and Y. Vo-Hoang, *ChemMedChem*, 2014, **9**, 300–304.

629 O. Bassas, J. Huuskonen, K. Rissanen and A. M. P. Koskinen, *European J. Org. Chem.*, 2009, **2009**, 1340–1351.

630 Z. Fu, W. Yuan, N. Chen, Z. Yang and J. Xu, *Green Chem.*, 2018, **20**, 4484–4491.

631 W. Feng and X.-G. Zhang, *Chem. Commun.*, 2019, **55**, 1144–1147.

632 T. Siatra-Papastaikoudi, A. Tsotinis, C. P. Raptopoulou, C. Sambani and H. Thomou, *Eur. J. Med. Chem.*, 1995, **30**, 107–114.

633 H. Ghosh, R. Yella, J. Nath and B. K. Patel, *European J. Org. Chem.*, 2008, **2008**, 6189–6196.

634 D. W. Carney, J. V Truong and J. K. Sello, *J. Org. Chem.*, 2011, **76**, 10279–10285.

635 Y. Xia, F. Hu, Y. Xia, Z. Liu, Y. F, Y. Zhang and W. J, *Synthesis*, 2017, **49**, 1073–1086.

636 F. Auras, L. Ascherl, A. H. Hakimioun, J. T. Margraf, F. C. Hanusch, S. Reuter, D. Bessinger, M. Döblinger, C. Hettstedt, K. Karaghiosoff, S. Herbert, P. Knochel, T. Clark and T. Bein, *J. Am. Chem. Soc.*, 2016, **138**, 16703–16710.

637 M. G. Ricardo, A. M. Ali, J. Plewka, E. Surmiak, B. Labuzek, C. G. Neochoritis, J. Atmaj, L. Skalniak, R. Zhang, T. A. Holak, M. Groves, D. G. Rivera and A. Dömling, *Angew. Chemie Int. Ed.*, 2020, **59**, 5235–5241.

638 Y. Ruan, B.-Y. Wang, J. M. Erb, S. Chen, C. M. Hadad and J. D. Badjić, *Org. Biomol. Chem.*, 2013, **11**, 7667–7675.

639 S. Koltzenburg, M. Maskos and O. Nnuyken, *Polymere: Synthese, Eigenschaften und Anwendungen*, Springer Spektrum, Heidelberg, 2014.

640 P. J. Flory, *J. Am. Chem. Soc.*, 1936, **58**, 1877–1885.

641 M. Hollauf, G. Trimmel and A.-C. Knall, *Monatshefte für Chemie - Chem. Mon.*, 2015, **146**, 1063–1080.

642 Z. Hu, D. Zhang, L. Yu and Y. Huang, *J. Mater. Chem. B*, 2018, **6**, 518–526.

643 H. W. Wanzlick, *Angew. Chemie Int. Ed. English*, 1962, **1**, 75–80.

644 E. M. Simmons and J. F. Hartwig, *Angew. Chemie Int. Ed.*, 2012, **51**, 3066–3072.

645 J. Bredt, *Justus Liebigs Ann. Chem.*, 1924, **437**, 1–13.

646 F. S. Fawcett, *Chem. Rev.*, 1950, **47**, 219–274.

647 W. Guo, H.-H. Ngo and J. Li, *Bioresour. Technol.*, 2012, **122**, 27–34.

648 R. R. Choudhury, J. M. Gohil, S. Mohanty and S. K. Nayak, *J. Mater. Chem. A*, 2018, **6**, 313–333.